

Development of Novel Carboxylation Reactions and Chemoselective Transformation of Carboxylic Acids

Thesis Submitted for the Degree of
Doctor of Philosophy (Science)

of

Jadavpur University



November 2022

By

Shantanu Nandi

(Index No.: 138/18/Chem/26)



Under supervision of

Dr. Ranjan Jana

Organic and Medicinal Chemistry Division

Indian Institute of Chemical Biology

(Council for Scientific & Industrial Research)

4, Raja S. C. Mullick Road, Jadavpur, Kolkata – 700 032
West Bengal, India



सी.एस.आई.आर-भारतीय रासायनिक जीवविज्ञान संस्थान

वैज्ञानिक तथा औद्योगिक अनुसंधान परिषद की एक इकाई
विज्ञान एवं प्रौद्योगिकी मंत्रालय के अधीन, एक स्वायत्त निकाय, भारत सरकार
4, राजा एस. सी. मुल्लिक रोड, यादवपुर, कोलकाता - 700 032



CSIR - INDIAN INSTITUTE OF CHEMICAL BIOLOGY

A Unit of Council of Scientific & Industrial Research
An Autonomous Body, under Ministry of Science & Technology, Government of India
4, Raja S. C. Mullick Road, Jadavpur, Kolkata-700 032

From:

Ranjan Jana, M.Sc., Ph.D.
Senior Principal Scientist
Organic and Medicinal Chemistry Division
CSIR-Indian Institute of Chemical Biology
4, Raja S. C. Mullick Road, Jadavpur,
Kolkata-700032, W.B., India
Phone: +91(033)24995819
Fax: +91(033)24735197
Email: rjana@iicb.res.in, janaegra@gmail.com

CERTIFICATE FROM SUPERVISOR

This is to certify that the thesis entitled "Development of Novel Carboxylation Reactions and Chemoselective Transformation of Carboxylic Acids" submitted by Mr. Shantanu Nandi who got his name registered on 30.08.2018 (Index No.: 138/18/Chem./26) for the award of Ph.D. (Science) degree of Jadavpur University, is absolutely based upon his work under my supervision and that neither this thesis nor any part of it has been submitted for any other degree/diploma or any other academic award anywhere before.

Rana
16/11/2022
(Dr. Ranjan Jana)



DR. RANJAN JANA
Principal Scientist
Organic and Medicinal Chemistry Division
CSIR-Indian Institute of Chemical Biology
4, Raja, S. C. Mullick Road, Kolkata-32



To

baba (my beloved and honoured father),

*I could never thank you enough. Stay happy
wherever you are knowing that I am here to
live your dream. And, I know I have you,
always...*

Preface

The thesis entitled “*Development of Novel Carboxylation Reactions and Chemoselective Transformation of Carboxylic Acids*” presents sustainable strategies to employ carbon dioxide (CO₂) and formic acid (HCOOH) as C-1 feedstock to synthesize carboxylic acids and subsequently to transform carboxylic acids chemo- and regioselectively to produce value-added materials.

The increasing concentration of atmospheric CO₂ is becoming a huge threat to mankind due to global warming and abnormal changes in the global climate. Therefore, there is an urgent need to utilize CO₂ and other bulk chemicals which are produced in large quantities and cause serious threats to the environment. From economic and environmental standpoints, CO₂ is an excellent C1 source; besides, other renewable and inexpensive bulk chemicals are ideal starting materials for the synthesis of value-added fine chemicals, polymer materials etc. However, from the synthetic standpoint, activation of CO₂ is still problematic and challenging because in CO₂, carbon is in the highest oxidation state which is thermodynamically stable and kinetically very inert in the many reaction conditions. As a result, most of the known studies till date used highly reactive substrates and/or very harsh and energetic reaction conditions to activate CO₂ which made those methods limited and not generalized enough to fulfill environmental or economical requirements. Particularly, in past decades, catalytic coupling of CO₂ with high energy substrates like epoxides, aziridines, carbonates etc. have been developed. To make C–C bonds with CO₂, the use of carbon nucleophiles is limited to Grignard or organolithium compounds. Currently, CO₂ is used in industries to produce bulk chemicals such as urea, salicylic acid, cyclic/poly carbonates. The reduction to methanol, CO or conversion to benzoic acid has been far less investigated as these processes require high activation energy which is unfavorable and this high energy barriers can only be overcome by the help of catalysts. In the last decade, transition-metal catalysis has shown potential to activate inert CO₂ through uphill catalysis. However, owing to its inherent kinetic and thermodynamic stability of CO₂, most of the transformations require high temperatures, high pressure, and stoichiometric amounts of organometallic reductants that leads to accidental and environmental hazards. Inspired by the natural photosynthesis and development of photoredox catalysis, photocatalytic conversion of CO₂ into value-added products has emerged as a benign and practical approach in organic synthesis. Recently, in addition to CO₂, researchers exploited its reduced form formic acid

Preface

(HCOOH) as another inexpensive, renewable, and non-toxic C-1 feedstock for carboxylation and carbonylation reactions. Intrigued by these, we have performed carboxylation/hydroxycarbonylation with these two benign C-1 source for synthesizing carboxylic acids in green and mild approach. Besides, carboxylic acids and its derivatives constitute common units in various natural products, bioactive compounds and synthetic intermediates. Upon successful attempts of producing carboxylic acids, transformation of the same would be performed using sustainable reaction conditions and new catalytic methods to produce library of pharmacophores.

Firstly, we would present a detailed general review to understand the modern sustainable modes of carboxylation reactions with CO₂ and the different strategies to convert carboxylic acids to a diverse range of important class of compounds. To circumvent the existing difficulties of carboxylation reactions with CO₂ using classical methods, photocatalysis have emerged as state-of-the-art technique for carboxylation with CO₂. In this chapter, we would chronologically portray the developments of sustainable photocarboxylation reactions to synthesize carboxylic acids. Then, the salient modes of reactions would be overviewed to convert carboxylic acids to produce value-added products. Here, we would discuss metal, metal-free, photo-, and electrocatalytic strategies for decarboxylative couplings, carboxyl group directed C–H activations, and C–H activation towards lactone formation starting from carboxylic acid substrates.

Secondly, organic photoredox-catalyzed, acylative photocarboxylation of alkene with CO₂ would be presented. The acyl radical is generated from the corresponding α -ketocarboxylic acids through decarboxylation and attaches to the β -position of the vinyl arenes, while CO₂ molecule attaches to the α -position to yield the γ -keto carboxylic acid product. Notably here, both the decarboxylation and carboxylation events would take place at single operation behaving against “Le Chatelier’s principle”.

Thirdly, a palladium catalyzed hydroxycarbonylation of aryldiazonium salt with formic acid (HCOOH) has been developed to produce aryl carboxylic acids. The method is also applicable on anilines via *in-situ* formation of diazonium salts. Here, we have been able to eliminate the high toxicity of convenient carbonyl source carbon monoxide (CO) by replacing it with commonly available HCOOH where HCOOH acts as CO-surrogate.

Lastly, we would present a copper-powder catalyzed strategy for synthesis of privileged seven-membered lactones, dibenzo[*c,e*]oxepin-5(7H)-ones through a highly

Preface

chemoselective benzylic C(sp³)-H activation from biaryl carboxylic acids. Here remarkably, the formation of widely explored six-membered lactone *via* C(sp²)-H activation has successfully been bypassed under our conditions. Here we used copper powder as catalyst along with di-tert-butyl peroxide (DTBP) as oxidant. Later, due to the potential hazards of stoichiometric DTBP, we would replace it with O₂ by coupling copper catalysis with photocatalysis. This is probably the first example of confluence between metallic copper catalysis and photocatalysis to capture gaseous O₂. A 1,5-aryl migration through Smiles rearrangement would also be discussed using similar condition. The methodology presented is scalable, applied to the total synthesis of a very important bioactive natural product Alterlactone. The catalyst is recyclable too. Very interestingly, one demonstration has been shown where the reaction has been performed without any added external catalyst in a copper-bottle. Additionally, a range of diverse reactivities *via* C-H activation of different substrates have been found with our catalytic condition.

So, the major objectives of this thesis would be concentrated on photo- and transition metal catalytic transformation of CO₂ and HCOOH to synthesize diverse range of carboxylic acids. And then it would represent copper/photocatalyzed benzylic C(sp³)-H oxidation chemistry with O₂ or peroxide to transform carboxylic acids to provide different class of compounds, which are difficult to synthesize otherwise.

Acknowledgement

I would like to take this opportunity to express my heartfelt gratitude to all the important persons/factors, who/which have filled me with utmost passion, optimism, discipline, perseverance in every step over these five years of PhD journey, helped me to sustain amid all ups and downs, celebrations and frustrations.

In the first place, my deepest gratitude and indebtedness goes to my respected advisor Dr. Ranjan Jana for his constant support and encouragement. Starting from providing me the opportunity to carry out the research under his supervision to being massively supportive as well as critical in each single research activity, he has been an incredible mentor in every sense. I would especially remain grateful to him for being patient with all my failures and shortcomings and still supporting me with full freedom, which is priceless to develop an independent and self-reliant character. His punctuality and discipline are something, from which I try to learn every single day. The motivation he instilled in me would hopefully guide me throughout my life.

I am grateful to our present director Dr. Arun Bandyopadhyay and former director Prof. Samit Chattopadhyay for giving me an opportunity to work in CSIR-Indian Institute of Chemical Biology (IICB) and providing all infrastructural support.

I would like to thank the other experts of my research advisory committee: Prof. (Dr.) Swapan Kumar Bhattacharya, Head, Department of Chemistry, Jadavpur University and Prof. (Dr.) Umasish Jana, Department of Chemistry, Jadavpur University for their insightful discussion and valuable advices.

It is of great delight that I had the pleasure to meet some of the most captivating teachers during my academic journey. Thanks to all the faculty members of Organic and Medicinal Chemistry Division, CSIR-IICB for helping me in various aspects during my research work and enlightening me with global perspective of science. I would forever remain indebted to the phenomenal teachers I came across in Jadavpur University during my undergraduate and postgraduate days. From teaching chemistry in the most fascinating way to implanting the importance of conscience, they have made me an inquisitive student of chemistry for the rest of my career. It is a must to mention my MSc project supervisor, Prof. (Dr.) Rina Ghosh, who has been utmost affectionate and continuing to stand by my side in every way possible since last eight years. All the teachers from my high school, Bhangamora

Acknowledgement

N.K.N.C.M. Institution, West Bengal have a monumental impact on my life by giving the lessons of perseverance and hard work since childhood. Specially, I want to thank my respected higher secondary chemistry teacher Mr. Sushovon Pal and english teacher Mr. Chiranjib Mondal for constantly pushing me.

I would take this opportunity to express my indebtedness to my alma mater, second home, Jadavpur University as an institution of great culture. From heartily welcoming a naïve boy to nurturing him, introducing with all the rights and wrongs, progressiveness, my university has truly shaped me to be unapologetically passionate yet empathetic.

Then, my sincere acknowledgement goes to my research institute CSIR-Indian Institute of Chemical Biology for providing me the platform, holding me up with ups and downs. I am also thankful to DST-INSPIRE, New Delhi, for providing corresponding fellowships throughout my doctoral studies.

A very special gratitude goes to all the scientific technical staffs of IICB: Dr. Tapas Sarkar, Dr. E. Padmanban, Shahfiaz Khan, Gautam Karmakar for recording NMR, Diptendu Bhattacharya, Sandip Chowdhury, Soumik Laha, and Santu Paul for LCMS analysis, Sandip Kundu for XRD. It would not be possible to work without their spontaneous help and support.

I am thankful to all my past and present lab members Suvankar da, Krishnendu da, Asik da, Manash da, Samir da, Arghya da, Pritha, Hasina, Kartic da, Varalaxmi, Subhodeep, Shuvam, Kangkan, Abdur, Animesh, and Arijit for their pleasant company, constant help, criticism and collaborative teamwork through all ebb and flow.

It is my pleasure to express heartfelt gratitude and love to all my school friends (Raj, Saikat, Kuchi, Dwai, Bubu da) for being so supportive and compassionate since childhood. I met some of the most inspiring and warm mates in university (Friends: Subarna, Deblina, Writhabrata, Anas, Supriya, Rapti, Tanmay, Kaustuv, Souradeep, Arka; Seniors: Manamohan da, Baitan da, Monalisa di, Nabamita di; Juniors: Joydip, Soumyadip, Paramita and so on) who literally kept me awake and cheerful at the darkest nights, making me confident and cultivated in all peaks and valleys. My heartiest appreciation goes to Sarita and Sikta from IACS for accompanying me so spontaneously amidst evidently busy lab schedule.

Acknowledgement

Words fall short for my partner, Subarna, who showered all her love, support, cheers in every phase of my life. Worth mentioning here, I thank her too for all the enthralling scientific discussions together about one another's research field.

I am fortunate to be born and brought up in a loving joint family. Whatever I have achieved so far is the result of their love and support. The hard work, sacrifice, simplicity of my *maa*, Swapna Nandi, and my *baba*, Subrata Nandi, are the reason why I am here today. My sincere love and respect go to my beloved *dadu-thhama* (Joydev and Sabita Nandi) for their high will and motivation towards my academics, despite them being not highly educated (so called). Any word is not enough to describe the contribution of my *jethu* (Sandip Kr. Nandi) to my life with all his hard work and honesty. I want to express my heartiest love for *jimi* (Tapati Nandi), *kakus* (Sukhen and Subir Nandi), and *kamas* (Ruma and Piali Nandi). The love and affection of my sisters –Soumi and Saheli, brothers – Subhrangsu and Srijit are something, which keeps me going through every tough time. I also offer my heartfelt love to my adorable little niece, Puchi, for being the reason of constant smile on my face.

To conclude, this journey would not have been so great without the enormous support and care from innumerable brilliant people over the years. It is a great pleasure for me to convey my sincere gratitude to each one of them after this beautiful voyage.

November, 2022

(Shantanu Nandi)

Organic and Medicinal Chemistry Division

CSIR-Indian Institute of Chemical Biology

Kolkata-700032

CONTENTS

<i>Contents</i>	<i>Pages</i>
Chapter I: Photocarboxylation Reactions with CO₂ and Transformation of Carboxylic Acids: Journey towards Sustainability	1
I.1. Introduction	3
I.2. Towards sustainable carboxylation strategies	5
I.3. Conceptual framework	7
I.4. Comparative mechanisms of transition-metal catalyzed carboxylation and photocarboxylation	8
I.5. Photocatalyzed carboxylation reactions	10
I.5.1. Transition-metal (TM) / photoredox dual catalytic carboxylation reactions with CO₂	10
I.5.1.1. Synergistic TM/photoredox catalyzed carboxylation of C–(pseudo)halide / C–O / C–N bonds	10
I.5.1.2. Dual TM/photoredox catalyzed carboxylation of C–H bonds	14
I.5.1.3. Carboxylation of unsaturated organic substrates with TM/photoredox dual catalysis	16
I.5.1.3.1. Hydrocarboxylation of alkenes/alkynes (unsaturated hydrocarbons) using dual catalysis	17
I.5.1.3.2. Carboxylative bifunctionalization of alkenes by dual catalysis	19
I.5.2. Photocarboxylation with CO₂ induced by only photocatalysts, free from synergistic TM-catalysis	20
I.5.2.1. Carboxylation of C–H bonds by photocatalysis solely	21
I.5.2.2. Carboxylation of unsaturated hydrocarbons with solely photocatalysis	24
I.5.2.2.1. Photoredox catalyzed hydrocarboxylation of alkenes/alkynes (unsaturated hydrocarbons)	24
I.5.2.2.2. Photocatalyzed carboxylative difunctionalization of alkenes	25
I.5.2.2.3. Dicarboxylation of alkenes with photocatalysis	31
I.5.2.3. Photocatalyzed hydrocarboxylation of imines	32
I.5.2.4. Photocatalytic carboxylative difunctionalization of carbonyls	34
I.5.2.5. Photocatalyzed carboxylation of C–N/O/F bonds	35

I.5.3. Catalyst-free photocarboxylation with CO₂	36
I.6. Reviewing photocarboxylation to synthesize carboxylic acids	38
I.7. Transformation of carboxylic acids	39
I.7.1. Decarboxylative reactions of carboxylic acids	40
I.7.1.1. History of decarboxylative reactions	40
I.7.1.2. Recent decarboxylative strategies: a comparative overview on transition-metal catalyzed and photocatalyzed decarboxylative reactions	42
I.7.2. Carboxy groups as directing group in C–H activation, without decarboxylation	45
I.7.3. Carboxy group as traceless directing group giving C–H functionalization and decarboxylation simultaneously	47
I.7.4. Carboxylic acid leading towards lactone formation via C-H activation	49
I.8. Conclusion	52
I.9. References	54
<i>Chapter II: Transition Metal-free, Visible Light Mediated Decarboxylative Acylation and Carboxylation of Alkenes with CO₂</i>	63
II.1. Introduction	65
II.2. Review of the previous developments	66
II.2.1. Photocatalyzed difunctionalization of alkenes with nucleophiles via carbocation intermediate	66
II.2.2. Photocatalyzed difunctionalization of alkenes with CO₂ via carbanion intermediate	68
II.3. Present work	71
II.4. Results and discussion	72
II.5. Conclusion	81
II.6. Experimental section	82
II.6.1. General information	82
II.6.2. Preparation of starting materials	82
II.6.3. Procedure for optimization of the carbocarboxylation reaction	83
II.6.4. General experimental procedures	83
II.6.5. Crystal data of 5b'	84

II.6.6. Characterization data	86
II.6.7. Product derivatization	101
II.6.8. Control experiments	101
II.7. Representative ^1H and ^{13}C spectra	105
II.8. References	142
Chapter III: One-pot Hydroxycarbonylation of Anilines via Diazonium Salt <i>en route</i> to Benzoic Acids: Formic Acid as C-1 Source	145
III.1. Introduction	147
III.2. Reviewing the previous developments	147
III.2.1. Carbonylation of C-N bonds with carbon monoxide (CO)	147
III.2.2. Carbonylation using formic acid as CO surrogate	149
III.3. Present work	152
III.4. Results and discussion	152
III.5. Conclusion	157
III.6. Experimental section	158
III.7. Characterization data	162
III.8. Representative ^1H and ^{13}C spectra	170
III.9. References	186
Chapter IV: Chemo- and Regioselective benzylic $\text{C}(\text{sp}^3)\text{-H}$ Oxidation Bridging the Gap between Hetero- and Homogeneous Copper Catalysis	189
IV.1. Introduction	191
IV.2. Reviewing the previous developments	191
IV.2.1. Developments of transition-metal catalyzed benzylic $\text{C}(\text{sp}^3)\text{-H}$ activation reactions	191
IV.2.2. Developments of intramolecular C-H activation reactions towards lactone synthesis	193
IV.2.2.1. Metal catalyzed $\text{C}(\text{sp}^2)\text{-H}$ activation for lactone synthesis	193
IV.2.2.2. Metal catalyzed $\text{C}(\text{sp}^3)\text{-H}$ activation for lactone synthesis	194
IV.2.2.3. Metal-free catalyzed C-H functionalization for lactone synthesis	195
IV.2.3. Chemoselective $\text{C}(\text{sp}^2)\text{-H}$ vs $\text{C}(\text{sp}^3)\text{-H}$ activation	196

IV.2.4. Dibenzooxepinones and their synthesis	197
IV.3. Present work	198
IV.4. Results and discussion	200
• Substrate scope	202
• Unexpected Smiles rearrangement while attempting towards 8-membered lactone	204
• Double benzylic C(sp ³)-H activation leading to dibenzooxepinones	205
• Total synthesis of Alterlactone: Demonstrating the synthetic utility of the methodology	206
• Strategic demonstration and derivatization of product	207
• Different substrates showing diverse reactivity	208
• Mechanistic study	208
• Characterization of the recovered catalyst	216
• Plausible mechanism	217
• Recyclability of the catalysts	219
IV.5. Conclusion	220
IV.6. Experimental section	221
IV.6.1. General information	221
IV.6.2. Preparation of starting materials	222
IV.6.2.1. General protocol for synthesis of 2'-alkyl-[1,1'-biphenyl]-2-carboxylic acids	222
IV.6.2.2. General protocol for the synthesis of 2-aryloxybenzoic acids	224
IV.6.2.3. Protocol for synthesis of 2-alkyl-2'-methyl-1,1'-biphenyls	224
IV.6.3. Experimental protocols for copper(0)-catalyzed chemo- and regioselective intramolecular benzylic C(sp ³)-H oxidation of 2'-alkyl-[1,1'-biphenyl]-2-carboxylic acids	225
IV.6.3.1. General "Condition A"	225
IV.6.3.2. General "Condition B"	225
IV.6.4. Experimental protocol for the copper(0)-catalyzed Smiles rearrangement of 2-phenoxybenzoic acids	226
IV.6.5. Experimental protocol for copper(0)-catalyzed double C(sp ³)-H activation of 2-alkyl-2'-methyl-1,1'-biphenyls	227
IV.6.6. Spectral data	227

Contents

IV.6.7. Step-by-step experimental protocol for total synthesis of Alterlactone	246
IV.6.8. Protocol for external catalyst-free intramolecular benzylic C(sp³)-H oxidation of 2'-methyl-[1,1'-biphenyl]-2-carboxylic acid in copper bottle	250
IV.6.9. Experimental protocol for the standard reaction with 1a in “Condition B” in gram-scale	251
IV.6.10. Product derivatization	252
IV.6.11. Representative crystal structures	253
IV.7. Representative NMR spectra	257
IV.8. References	291
Conclusion	295
• Summary of the work	297
• Scope for the future work	299
Publications/Conferences	301
• List of publications	303
• List of attended conferences	304
Reprints of Selected Publications	305

Abbreviations

AcOH	Acetic acid
AIBN	azobisisobutyronitrile
BPO	Benzoyl peroxide
bpy	2,2'-bipyridine
BQ	benzoquinone
BHT	Butylated hydroxytoluene
CDCl ₃	Deuterated chloroform
CFL	Compact fluorescent lamp
4-CzPEBN	2,3,4,6-tetra(9H-carbazol-9-yl)-5-(phenylethyl)benzonitrile
4-CzIPN	2,4,5,6-Tetrakis(9H-carbazol-9-yl)isophthalonitrile
DABCO	1,4-diazabicyclo[2.2.2]octane
DMSO	Dimethyl sulfoxide
DMSO-d ₆	Deuterated dimethyl sulfoxide
DCE	1,2-Dichloroethane
DCM	Dichloromethane
DG	Directing group
DMF	Dimethyl formamide
DTBP	Di- <i>tert</i> -Butyl peroxide
dtbpy	4,4'-Di- <i>tert</i> -butyl-2,2'-dipyridyl
4DPAIPN	1,3-Dicyano-2,4,5,6-tetrakis(diphenylamino)-benzene
DIPEA	diisopropylethylamine
HAT	Hydrogen atom transfer
HEH	Hantzsch's ester
LED	Light emitting diode
MeCN	Acetonitrile
Mes-Acr	Mesityl Acridinium
m.p.	melting point

Abbreviations

MS	Molecular sieves
NMP	<i>N</i> -Methyl-2-pyrrolidone
NMR	Nuclear magnetic resonance
PC	Photocatalyst
ppy	2-Phenylpyridine
RB	Rose bengal
SCE	Saturated calomel electrode
SET	Single electron transfer
TBAB	<i>tert</i> -butylammonium bromide
TBHP	<i>tert</i> -butylhydroperoxide
TBPB	<i>tert</i> -butylperoxybenzoate
TEM	Transmission electron microscopy
TEMPO	(2, 2, 6, 6-Tetramethylpiperidin-1-yl)oxyl
THF	Tetrahydrofuran
TM	Transition metal
UV-Vis	Ultra violet-visible
XPS	X-ray Photoelectron Spectroscopy

Chapter I

Photocarboxylation Reactions with CO_2 and Transformation of Carboxylic Acids: Journey towards Sustainability



Photocarboxylation Reactions with CO₂ and Transformation of Carboxylic Acids: Journey towards Sustainability

I.1. Introduction

Although non-toxic, being the most crucial greenhouse gas, CO₂ (carbon dioxide) is tremendously responsible for global warming.¹ The problem has been enormously accelerated since industrial revolution fossil-fuel combustion and other human activities that resulted in ever-increasing concentration of CO₂ in the environment. As, there is no possibility of giving up the industrial benefits, the realizable job to control the problem is to minimize the “carbon footprint”² in the industrial processes. Replacement of the troublesome technologies with sustainable ones and reutilization of the emitted CO₂ to produce other value-added products are the main two approaches for attaining sustainability. From the synthetic chemistry point of view, enormous effort has been dedicated to accomplish the long-cherished goal of “waste to wealth” conversion. Motivated by the strict guidelines from EPA (environment protection agencies), this field has regained upsurge lately.

“Circular carbon economy” employing CO₂ is a timely concept in today’s energy research.³ Still, as CO₂ is highly abundant, cheap and non-toxic in nature⁴, contrary to its counterpart CO (carbon monoxide), CO₂ is a potentially suitable C-1 source in the synthetic organic chemistry field. Additionally, carboxylic acids and its derivatives are prevalent in various bioactive compounds, natural products,⁵ and are commonly used as synthetic intermediates for value-added product synthesis⁶. Some significant advancement has been realized from this concept of CO₂ utilization reaction for synthesis of fine chemicals (**Figure 1**).⁷ In the last 15 years, with the advancement of transition-metal catalysis, a huge development has been executed for transition-metal catalyzed direct carboxylation reaction using CO₂ as C-1 feedstock. Here, transition-metal catalysts are used along with (super)stoichiometric amount of metal reductants, which are environmentally toxic in nature.⁸

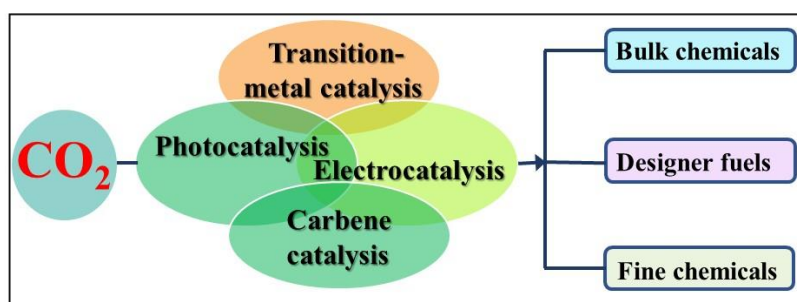


Figure 1. Utilization of Carbon Dioxide (CO₂).

So, the evident drawback lies in huge amount of toxic metal waste generation, which bars this approach for industrial use. Now, inspired by the natural photosynthesis, which uses direct solar energy for capturing and utilizing CO₂; chemists have engaged themselves to nearly mimic the technology in laboratory scale, though the advancement is still a way behind the dream.

Having said all these, the main barrier to make these goals “hard-to-achieve” is the inertness of CO₂. As CO₂ carries the carbon at the most oxidized state, it is kinetically very inert and thermodynamically stable. Thus, activating CO₂ molecule is very tough task to execute. Most of the traditional approaches are using nucleophilic organometallic reagents. As stated earlier, considerable amount of work has been performed for generating new C-C bonds using CO₂ breaking C-H, C-X (X= (pseudo)halides) or C-B bonds catalyzed by transition metals. Despite broad range of reaction scopes, the harsh and toxic nature of the requisite metal reductants and other reaction conditions makes these methods impractical in industrial scale. Additionally, plenty of substrates are incompatible in this approach for carboxylation for their instability under elevated temperature.

As the world has leaned towards green and sustainability, carboxylation approaches call for state-of-the-art technologies led by renewable energy sources. During last decade, photoredox chemistry has rapidly emerged.⁹ With this huge development of photoredox chemistry, various challenging chemical transformations have been eased to execute. As we know, natural photosynthesis deals with CO₂ fixation by plants with solar light under ambient temperature and pressure; mimicking the same inside laboratory to execute “artificial photosynthesis”¹⁰ is the most cherished goal to the scientists. If succeeded, this would change the whole dimension of the world’s need. Likewise, researchers have applied photocatalysis either solely or merging it with the transition metal (TM) catalysis to abolish the use of toxic metal reductants to afford carboxylation mostly under balloon pressure and at ambient temperature. Despite being comparatively newer in research, this strategy has been quite fruitful and explorative in this short time also. Photocatalysis has been applied for direct carboxylation reactions of unsaturated hydrocarbons such as alkenes, alkynes etc., carboxylation through the activation of C-H, C-O, C-N, or C-X (X = (pseudo)halide) bonds as well as for carboxylative difunctionalization of alkenes. This newer developments would be reviewed here and a comparative discussion between transition-metal catalyzed carboxylation

and photocarboxylation has also been made for better understanding towards availing sustainability.

Besides being prevalent in synthetic drugs, designer fuels or fine chemicals, carboxylic acids and its derivatives are very important substrates for various valuable transformations. After discussing the latest developments of state-of-the-art carboxylation techniques via photocatalysis for synthesis of diverse range of carboxylic acids, various type of reactivities of the carboxylic acids would be briefly overviewed.

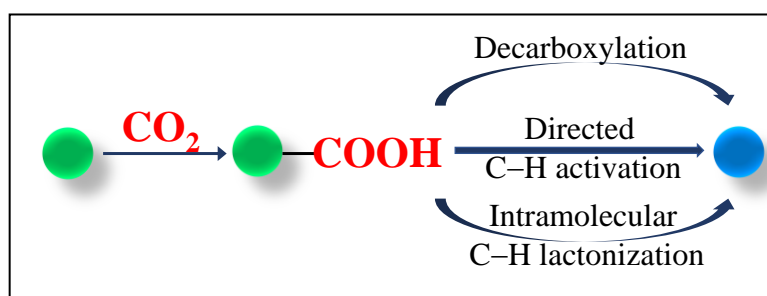


Figure 2. Transformation of carboxylic acids.

We would have a understanding on using carboxylic acids as synthons for decarboxylation reactions, carboxy group directed C–H activation and lactone ring formation via C–H activation to give privileged synthetic compounds (**Figure 2**).

I.2. Towards sustainable carboxylation strategies

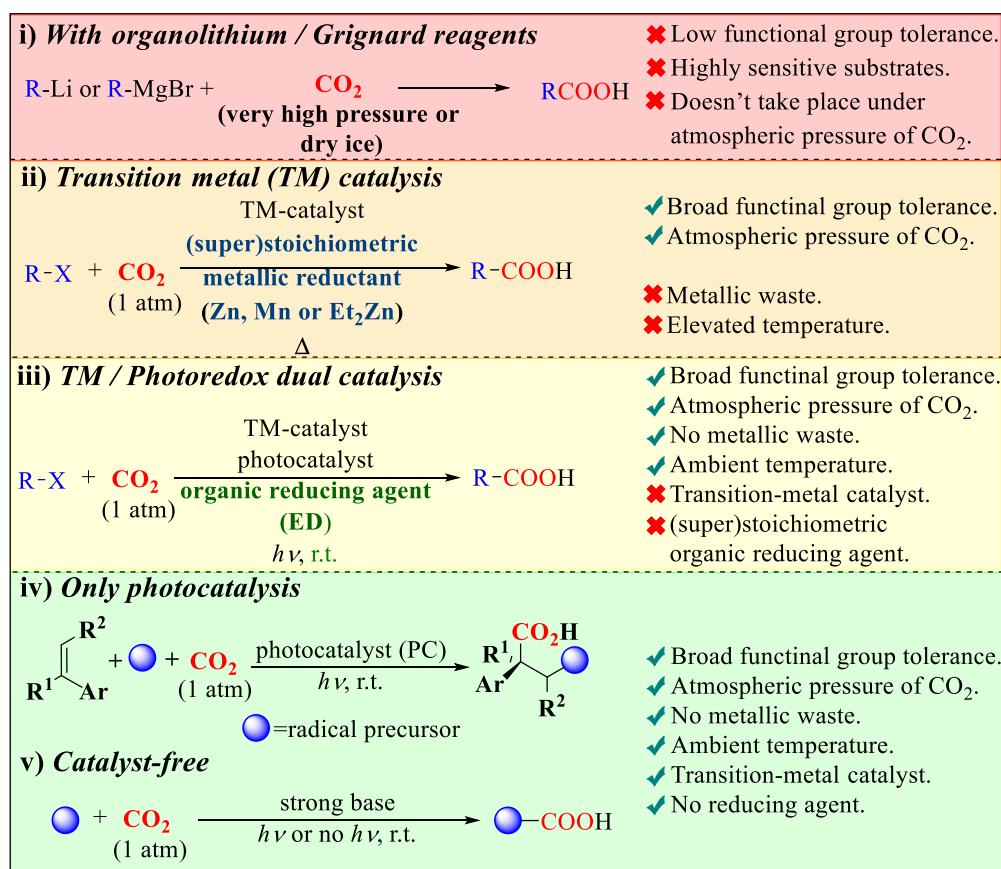
As we know, historically, the carboxylation reactions with CO₂ were developed by the involvement of Grignard or organolithium type highly nucleophilic organometallic complexes, where nucleophilic organic part combines with CO₂ molecule to provide carboxylic acids after aqueous work up. (**Scheme 1, i**). Though, this strategy is used in certain cases, very low functional group tolerance makes this process limited to very selective transformations only. Moreover, the sensitive nature of the organometallic substrates (readily decompose at aerial condition and ambient temperature) and the essential requirement of excessive high pressure of CO₂ or dry ice or super-critical CO₂ (scCO₂) make these processes to be usable only with special set-up.

Huge evolution of transition-metal catalysis in the past two decades extremely eased the carboxylation processes and also broadened its scopes to variety of substrates bearing a wide range of functional groups (**Scheme 1, ii**). Instead of using preformed organometallic

Chapter I

substrate, on use of a TM catalyst (Pd, Ni, Co, Rh, Cu etc.) along with a (super)stoichiometric metal reductant (Mn, Zn or Et₂Zn), an appropriate organometallic compound bearing low valent TM generates which executes the carboxylation mainly at elevated temperature. Besides broad functional group tolerance, here 1 atm of CO₂ mostly suffices the requirement for carboxylation. Thus, TM catalyzed carboxylation has emerged rapidly having a huge step forward to sustainability and better applicability. This approach has extensively been used for performing carboxylation of organic (pseudo)halides, alkenes, alkynes etc.

Despite immense improvement of TM-catalyzed carboxylation, the (super)stoichiometric use of hazardous metallic reducing agents make these less environmentally benign and left a huge scope for advancement.



Scheme 1. Chronological developments of carboxylation techniques towards sustainability.

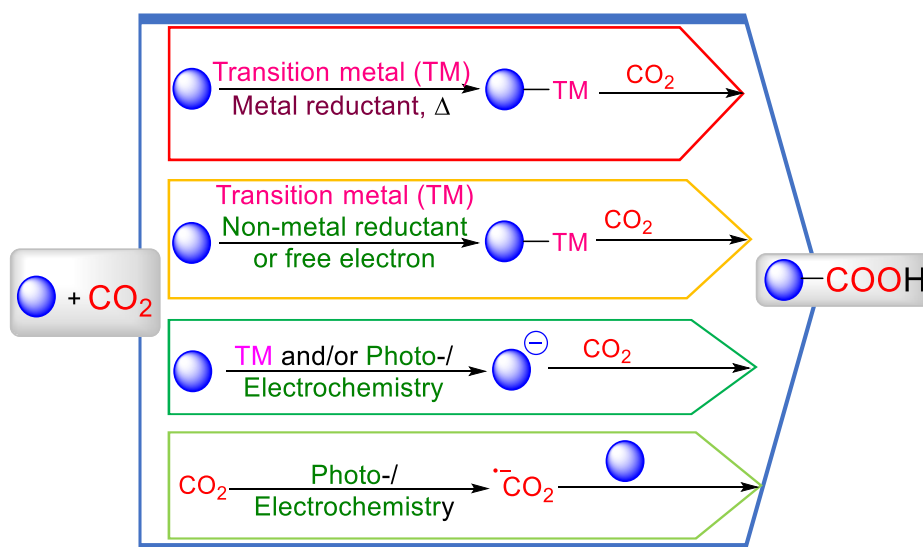
To remove the formation of toxic metal waste and simultaneously reduce the required temperature of the carboxylation processes, a state-of-the-art technique was badly necessary. Photoredox catalysis successfully served the purpose in the last few years. Firstly, it has been coupled with TM-catalysis to stop the use of metal reductants and using organic reducing agent

in their stead. Additionally, this technique has been successful to carboxylate the organic substrates with atmospheric pressure of CO₂ and at room temperature (**Scheme 1, iii**).

To attain utmost sustainability, further research on photocarboxylation has been able to be applied solely for the purpose, even without any TM catalyst. In some occasions, even no reducing agents are required at all. The photocatalyst alone can also furnish the carboxylation under balloon pressure of CO₂ and at ambient temperature with broad functional group tolerance (**Scheme 1, iv**). Even catalyst-free (photo)carboxylation techniques have started to be discovered in recent times (**Scheme 1, v**).

I.3. Conceptual framework

Due to the previously mentioned disadvantages of TM-catalysis, transforming CO₂ in more sustainable strategies under its atmospheric pressure has become an important goal to synthetic chemists. As natural photosynthesis process captures CO₂ under solar light, to take the full advantage of the recent development of photoredox catalysis, chemists turned attention to realize photo-catalyzed CO₂ utilization. Depending on the patterns of the carboxylation reactions with CO₂, a brief understanding on the mechanisms has been depicted in **Scheme 2**. As we see, vastly developed TM-catalysis essentially uses (super)stoichiometric amount of metal reducing agents, for example Mn, Zn, Et₂Zn etc. Here, in the process, active organometallic complex is formed as intermediate which captures CO₂ and insert this to the organic substrates. 2) Then, non-metallic sacrificial electron donors are used in place of the metal reductants in TM-catalysis taking synergistic assistance of photoredox catalysis.



Scheme 2. General Mechanisms for Carboxylation Reactions.

Here, intermediately formed organometallic complex carries the transformation. 3) As it is weakly electrophilic, CO₂ is susceptible to be attacked nucleophilically by an appropriate anionic intermediate as per the HSAB principle. But the main challenge resides in the fact of high kinetic inertness of CO₂. With the sole help of photocatalysis, in absence of additional TM-catalyst, stable carbanions could be formed, which react with CO₂ or a heteroatom containing organic substrate. In case of latter, nucleophilic heteroatom (N or O) attacks CO₂. 4) Making CO₂ to undergo single-electron (SET) reduction of molecule leading to ^{•-}CO₂ (radical anion) which couples with another radical which should be transient and stabilized or with unsaturated compounds to make new C–C bond. But this has been very rarely developed as CO₂ possesses extremely high negative reduction potential ($E^0 = -2.21$ V vs SCE in DMF). To surpass this high energy barrier, that too via mild approaches, photocatalytic condition or external application of high potential is on demand. To understand the developments of photocatalytic CO₂ fixation in the past decade, the discussion will be focused and classified based upon the binding modes of CO₂.

I.4. Comparative mechanisms of TM catalyzed carboxylation and photocarboxylation

As viewed in the previous section, we would now look at the detailed carboxylation mechanism associated with the conventional TM- catalysis and photocatalysis.

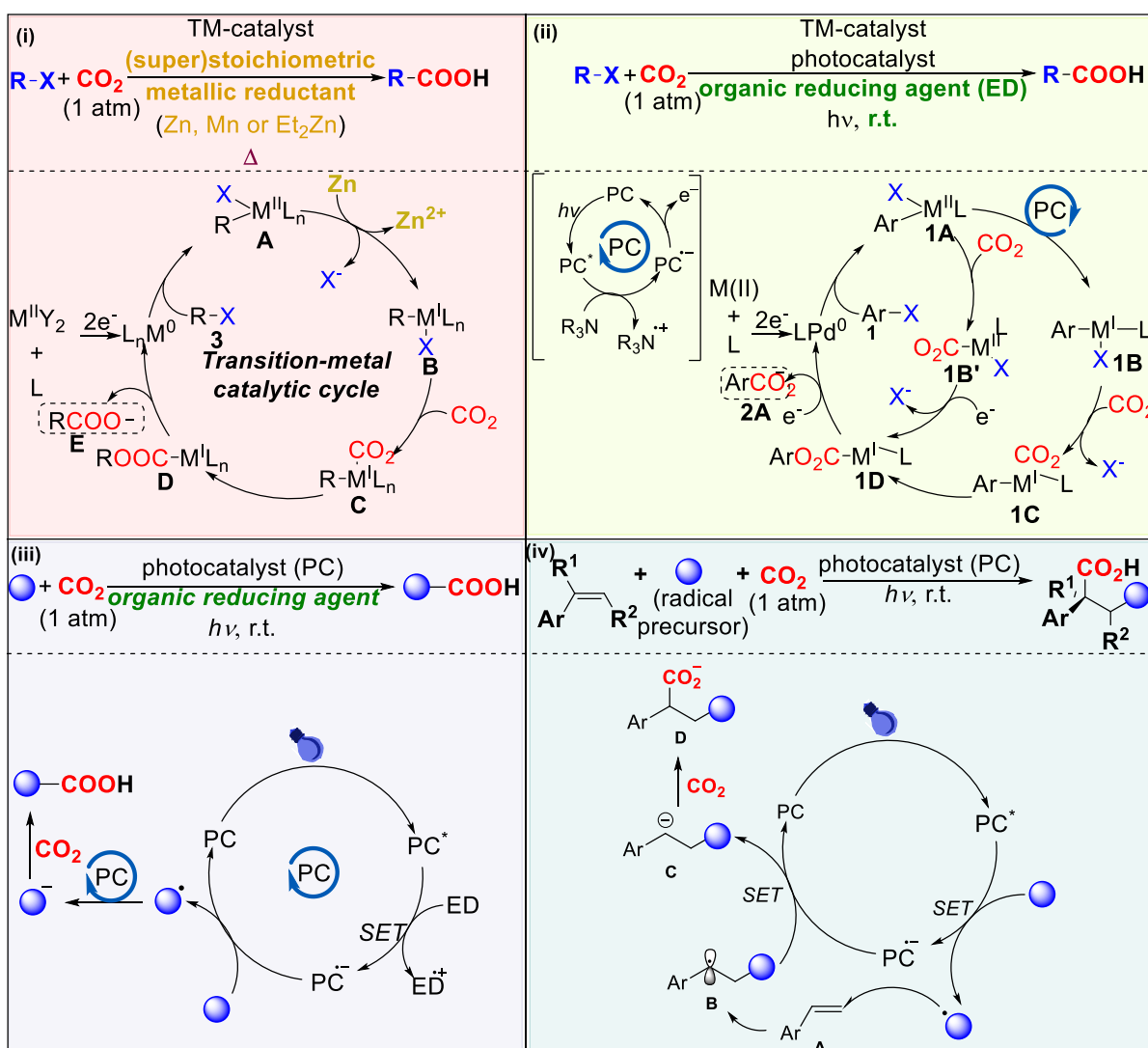
For example, during carboxylation of aryl- or alkyl- (pseudo)halides via TM-catalysis, first oxidative addition takes place by transition metal M, and the metal goes to higher oxidation state (M^{II}). As the organometallic complex having TM of higher oxidation state are not suitably nucleophilic to execute carboxylation, the metal reductant (here Zn) reduces the TM to lower oxidation state (M^I), which captures CO₂ and furnishes carboxylation (**Scheme 3, i**).

Contrastingly, when TM-catalysis is merged with photocatalysis for the same transformation, in lieu of metal reductant, photocatalysis serves the critical reduction process to step-down the oxidation state of the metal in the organometallic intermediate. Regarding photocatalysis, the photocatalyst (PC) excites by light irradiation to PC^{*}, and subsequently get reduced to PC^{•-} by organic reducing agent (commonly tertiary amines, R₃N, such as ⁱPr₂NEt, HEH etc.) This PC^{•-} reduces the oxidized transition metal (M^{II}) and itself regenerates PC (**Scheme 3, ii**).

Photocarboxylation Reactions with CO₂ and Transformation of Carboxylic Acids: Journey towards Sustainability

On sole use of photocatalysis without TM-catalysis gives carboxylation mainly via carbanion formation. Photocatalysis directly reduces the substrate to generate active carbanion which nucleophilically attack CO₂ to furnish the carboxylation. Here also, the organic reductive quencher (ED) sacrificially reduces the PC* (Scheme 3, iii)

Alternatively, some transformations involve redox neutral process, e.g., carboxylative bifunctionalization of alkenes. Here, in place of organic reducing agent one substrate itself acts as reductant and reduces the PC* to give PC⁻ itself converts to an active radical. The radical attaches to the alkene generating another alkyl radical which is reduced by PC⁻ to produce alkyl carbanion. Subsequently, the carbanion attaches to CO₂ to provide carboxylation products (Scheme 3, iv).



Scheme 3. Mechanistic pathways of various carboxylation techniques.

I.5. Photocatalyzed carboxylation reactions

Photoredox catalysis has appeared as a powerful and versatile synthetic tool to the synthetic chemists, in the last decade, strengthening the ever-growing sustainable development. This has been extensively used either by coupling with TM catalysis or solely, to fulfil a vast range of important transformations. Similarly, carboxylation reactions have also been realized by photocatalysis in similar approaches. Depending on the mode of catalysis, we would compartmentalize the developments to discuss. As stated in **Scheme 1**, photocatalysis mainly deals with three approaches for carboxylation i.e., capture of CO₂ by organometallic complex, nucleophilic addition of an anion to CO₂ and SET reduction of CO₂.

I.5.1. Transition-metal (TM) / photoredox dual catalytic carboxylation reactions with CO₂

Encouraged from the huge development of TM / photoredox dual catalysis in organic synthesis, chemists utilized the same for fixation of CO₂ in organic molecules. Handful of transformations have been realized where CO₂ has been used as C-1 source to make one or new C-C bonds from several organic compounds. As TMs have been used, the capture of CO₂ is mainly done by the organometallic complex formed in situ.

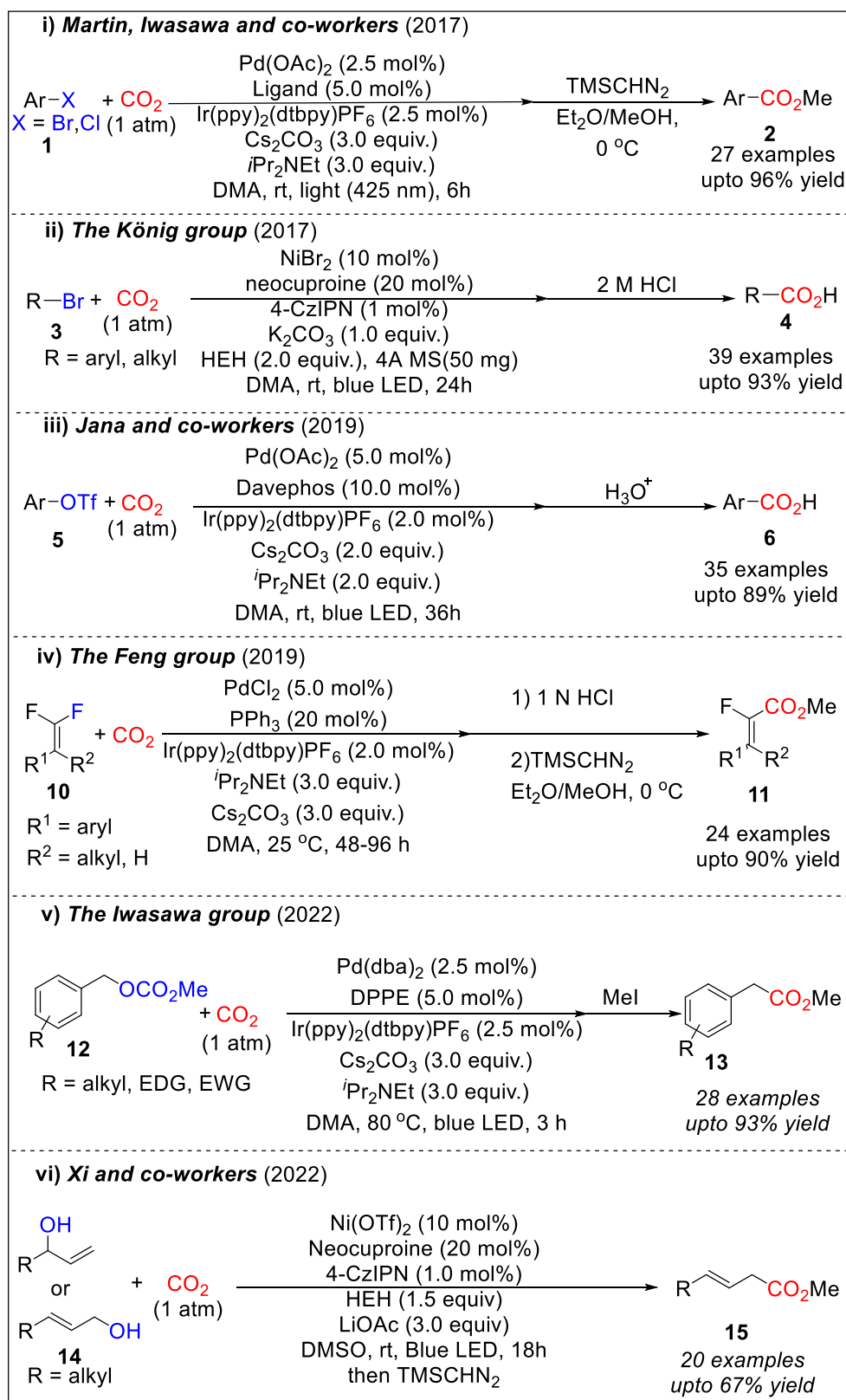
I.5.1.1. Synergistic TM/photoredox catalyzed carboxylation of C–(pseudo)halide / C–O / C–N bonds

TM catalysis has extensively been used for carboxylation of organic (pseudo)halides in the last 15 years.^{8c} Because of the discussed pitfalls, a sustainable and mild approach was call of the time.

In constant search for developing sustainable methods for carboxylation, first in 2017, Martin and Iwasawa made the breakthrough by discovering synergistic Pd/photoredox catalyzed carboxylation strategy for aryl halides (bromides / chlorides) with CO₂ (atmospheric pressure) at room temperature and under blue LED irradiation using Ir(ppy)₂(dtbpy)PF₆ as the photocatalyst (**Scheme 4, i**).¹¹ Here, they used Pd(OAc)₂ as catalyst and PhXPhos as the ligand. Additionally, ⁱPr₂NEt serves the role of reductant under photocatalytic condition instead of using metallic reducing agents. Both of the electron-rich and deficient aryl bromides yielded carboxylation products in satisfactory yields under the reaction condition. Substituting PhXPhos with another electron-donating ligand ^tBuXPhos, made the condition compatible for

Photocarboxylation Reactions with CO₂ and Transformation of Carboxylic Acids: Journey towards Sustainability

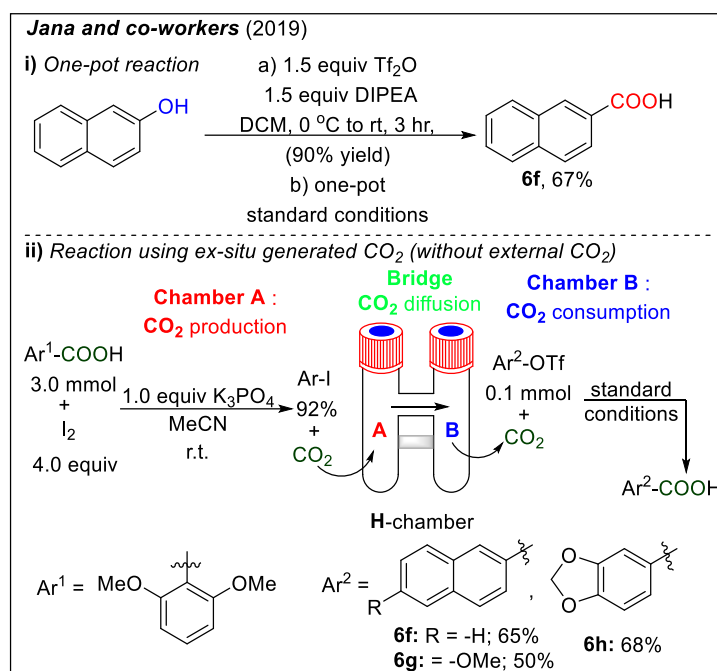
aryl chlorides also. Notably, electron deficient substrates yielded slightly higher for their facile oxidative addition to Pd.



Scheme 4. Dual catalyzed carboxylation reactions of C–(pseudo)halides.

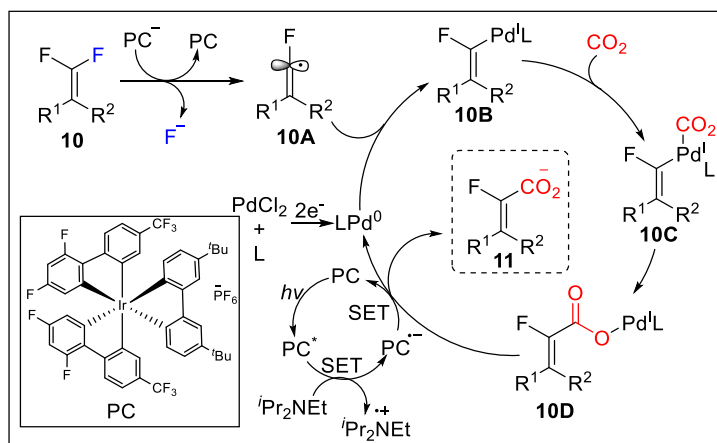
Shortly after this development, the König group realized photocarboxylation of aryl and aliphatic bromides (including 1⁰, 2⁰ and 3⁰ ones) via a mild and efficient strategy using a Nickel/photoredox dual catalysts (**Scheme 4, ii**).¹² Here, they used 4-CzIPN as organic photocatalyst and HEH (Hantzsch's ester) as the reducing agent. Notably, used base K₂CO₃ can also serve the role of carboxylation agent in addition to the externally applied CO₂ (balloon). Further, they expanded the substrate scope to aryl triflates (limited examples) for the synthesis of benzoic acids.

Encouraged by these two works, our group¹³ and Iwasawa's group¹⁴ disclosed two independent but nearly alike Pd/visible-light dual photoredox catalyzed techniques for carboxylation of aryl triflates to synthesize carboxylic acids (**Scheme 4, iii**).



Scheme 5. One-pot carboxylation of phenol and carboxylation utilizing ex situ formed CO₂.

Importantly, Iwasawa's protocol¹⁴ had been successful too for carboxylation of alkenyl triflates. Notably, we had shown diverse practical utility¹³ of this strategy like one-pot synthesis of benzoic acids directly from phenols, synthesis of commercial drug molecules e.g., Adapalene and Bexarotene, in-situ lactonization. Additionally, we demonstrated an interesting approach for reutilizing ex-situ generated CO₂ for carboxylation reaction using a H-shaped vessel (**Scheme 5**).¹³ This particular development has potential in strategic sector to transform CO₂ from fuel combustion and industrial waste to value-added products, if instead of emitting it to nature, we can bypass the released CO₂ to other carboxylation-chamber.



Scheme 6. Mechanism of defluorinative C–F carboxylation of gem-difluoroalkenes.

Notably, related to this, later, another interesting strategy for reusing in situ liberated CO₂ has been realized by Yu¹⁵ where both the incidents of carboxylation and decarboxylation reactions took place in single chamber and ended up in forming a single product (discussed in details at section I.5.2.2.2).

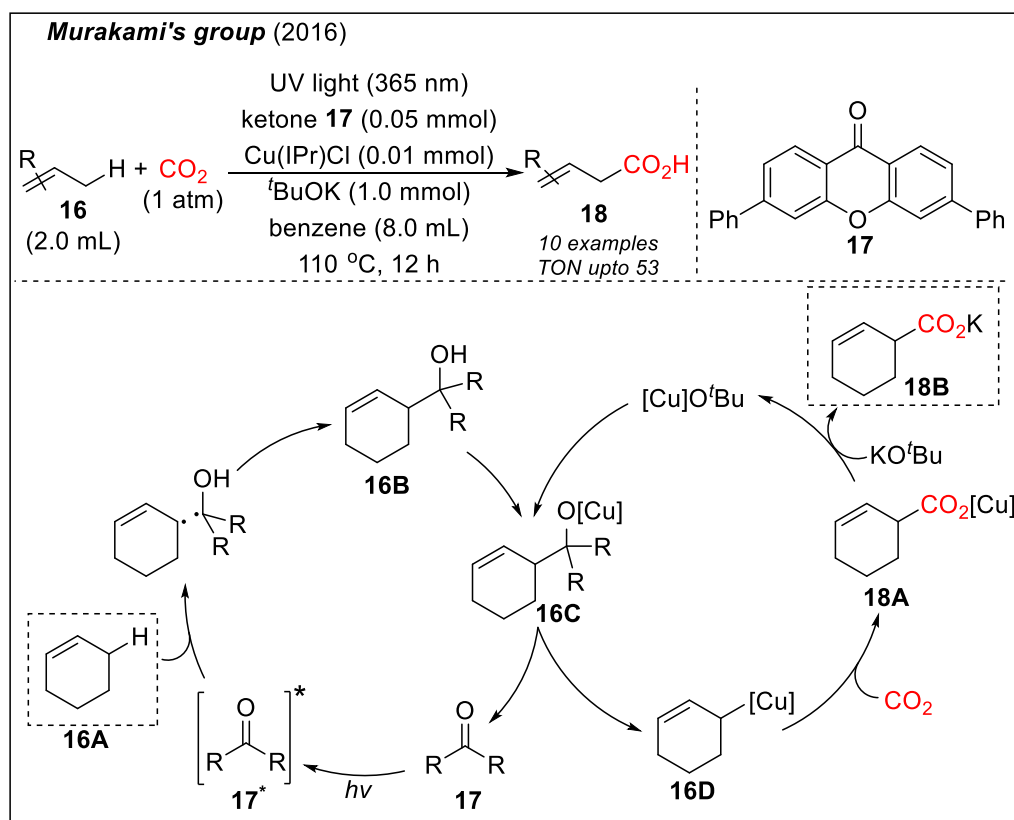
After aforementioned developments of carboxylation strategies by cleaving C–Cl, C–Br and C–O bonds, an elegant methodology to achieve defluorinative carboxylation cleaving C–F bond of *gem*-difluoroalkenes was developed by the Feng's group using Pd/photoredox dual catalysis (**Scheme 4, iv**).¹⁶ Contrary to the general ionic mechanism via oxidative addition, here at first, PC^{•-} reduces one C–F bond forming radical **10A** which complexes with LPd⁰ to generate Pd^I species **10B**. Then **10B** reacts with CO₂, successive migratory insertion generates Pd(II)-carboxyl complex **10D**. Then, **10D** gets reduced by SET from PC^{•-} to yield α -fluoroacrylic acids and to regenerate Pd(0) species. Here also, *i*Pr₂NEt acts as reductive quencher which reduces photoexcited PC to form PC^{•-} (**Scheme 6**). It is necessary to mention here that at the same time, this transformation via non-photocatalytic and copper-catalyzed methods was executed independently by the Yu¹⁷ group and Wu and Zhou¹⁸.

Up to this point, the discussed reactions led to C(sp²)-carboxylic acids only. To synthesize C(sp³)-carboxylic acids via cooperative TM/photocatalysis, Iwasawa disclosed a Pd/photoredox catalyzed approach to carboxylate benzylic alcohol derivatives (**Scheme 4, v**).¹⁹ Via their method, benzylic carbonates, acetates, pivalates and others could be transformed to substituted phenylacetic acids efficiently. In this report, they synthesized anti-inflammatory drugs (\pm)-Naproxen and Felbinac.

Lately, the Xi group reported an elegant visible light/Ni dual catalytic approach for the direct carboxylation of allylic alcohols at room temperature to form new C-C bonds (**Scheme 4, vi**).²⁰ Various aryl and alkyl allylic alcohols provided smooth result here. Hantzsch ester was used as reductant. It was found that CO₂ and the little amount of water, that Ni(OTf)₂ contains, forms carbonates from allylic alcohols to pre-activate them. Therefore, Ni(OTf)₂ generates Ni-allylic complex and then, carboxylation at terminal end is achieved.

I.5.1.2. Dual TM/photoredox catalyzed carboxylation of C–H bonds

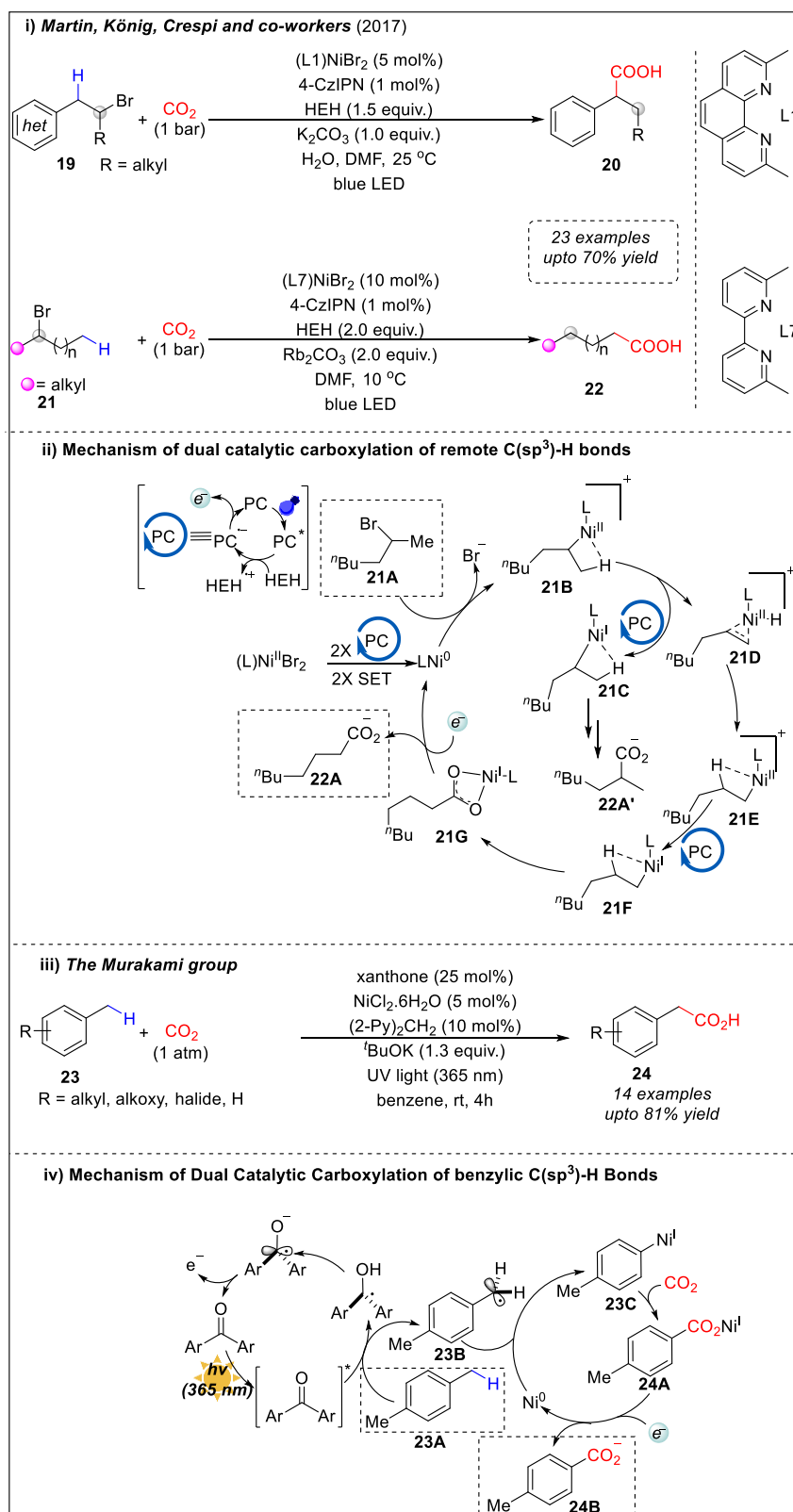
Beyond a doubt, attaining C–H carboxylation reactions directly by cleaving C–H bonds would be the most beneficial development. In this strategy, pre-functionalization of the substrates could be excluded which would improve atom-economy and minimize the number of steps.



Scheme 7. Carboxylation of allylic C(sp³)–H bonds mediated by copper / light.

Based on the previous inspiring developments²¹, Murakami and co-workers disclosed a strategy for allylic C–H carboxylation in 2016 under UV irradiation. Here, ketone was taken in catalytic amount as photosensitizer and copper complex was used as the TM-catalyst (**Scheme 7**).²² The ketone is excited by UV irradiation at first.

Photocarboxylation Reactions with CO₂ and Transformation of Carboxylic Acids: Journey towards Sustainability



Scheme 8. Dual Ni/photoredox catalyzed C(sp³)-H carboxylation.

Then, it reacts with substrate **16A** to form homoallyl alcohol **16B**. Therefore, allyl transfer takes place between **16C** and CO₂ with a C–C bond cleavage and thus copper-catalyzed carboxylation is achieved (**Scheme 7**). Though, this example is not truly of synergistic dual catalysis, it has been discussed here as photosensitizer and metal catalyst have been used together for the carboxylation reaction.

C–H carboxylation cleaving high energetic C(sp³)–H bonds remained unfulfilled for ages, even with classical TM-catalysis with metal reductants. In 2017, the Martin group broke the ice by reporting a strategy for remote C(sp³)–H carboxylation of alkyl halides using Ni-catalyzed “chain walking” reaction.²³ Here, Mn was used as the sacrificial reducing agent. Encouraged by the aforementioned findings of *ipso*-carboxylation aromatic (pseudo)halides by TM/photoredox dual catalysis¹¹⁻¹⁴, via similar Ni-catalyzed “chain walking” fashion, Martin and co-workers, in 2019, achieved remote C(sp³)–H carboxylation in an alkyl bromide using Ni/photoredox catalysis replacing their previous Ni/Mn catalytic system (**Scheme 8, i**).²⁴ They replaced stoichiometric metal reductant with organic reductant. With varying the ligands, they performed carboxylation at both terminal primary and benzylic C(sp³)–H bonds under mild conditions. Mechanistically, oxidative addition of C–Br bond takes place and generates **21B**, an alkyl-Ni complex. Then, following β-H elimination, alkene derivative forms. Successive migratory insertion, nucleophilic addition of Ni(I) species to CO₂, and SET reduction affords the carboxylated product (**Scheme 8, ii**).

Continued from their previous findings of ketone sensitized photocarboxylation reactions under UV irradiation, Murakami and co-workers expanded their strategy for benzylic C(sp³)–H carboxylation (**Scheme 8, iii**).^[24] Here, notably, primary benzylic groups furnished way better result than secondary ones. The ketone is excited and subsequently forms **23B** (benzylic radical) which is captured by Ni(0) and forms Ni(I)-complex **23C**. **23C** captures CO₂ to yield the carboxylated product **24B** (**Scheme 8, iv**).

In this same report²⁵, the authors extended their protocol for successful carboxylation of more challenging C-H bonds in saturated hydrocarbons e.g., n-pentane, cyclopentane or cyclohexane albeit the TON is low.

I.5.1.3. Carboxylation of unsaturated organic substrates with TM/photoredox dual catalysis

As alkenes are easily available abundant substrates, carboxylation has been investigated²⁶ rigorously on alkenes since long time. As far as monocarboxylation is concerned, the other end of the alkene might be functionalized with either hydrogen or another functional group. Keeping carboxylation as an integral part, the discussion has been done depending on the functionalization apart from the carboxylation.

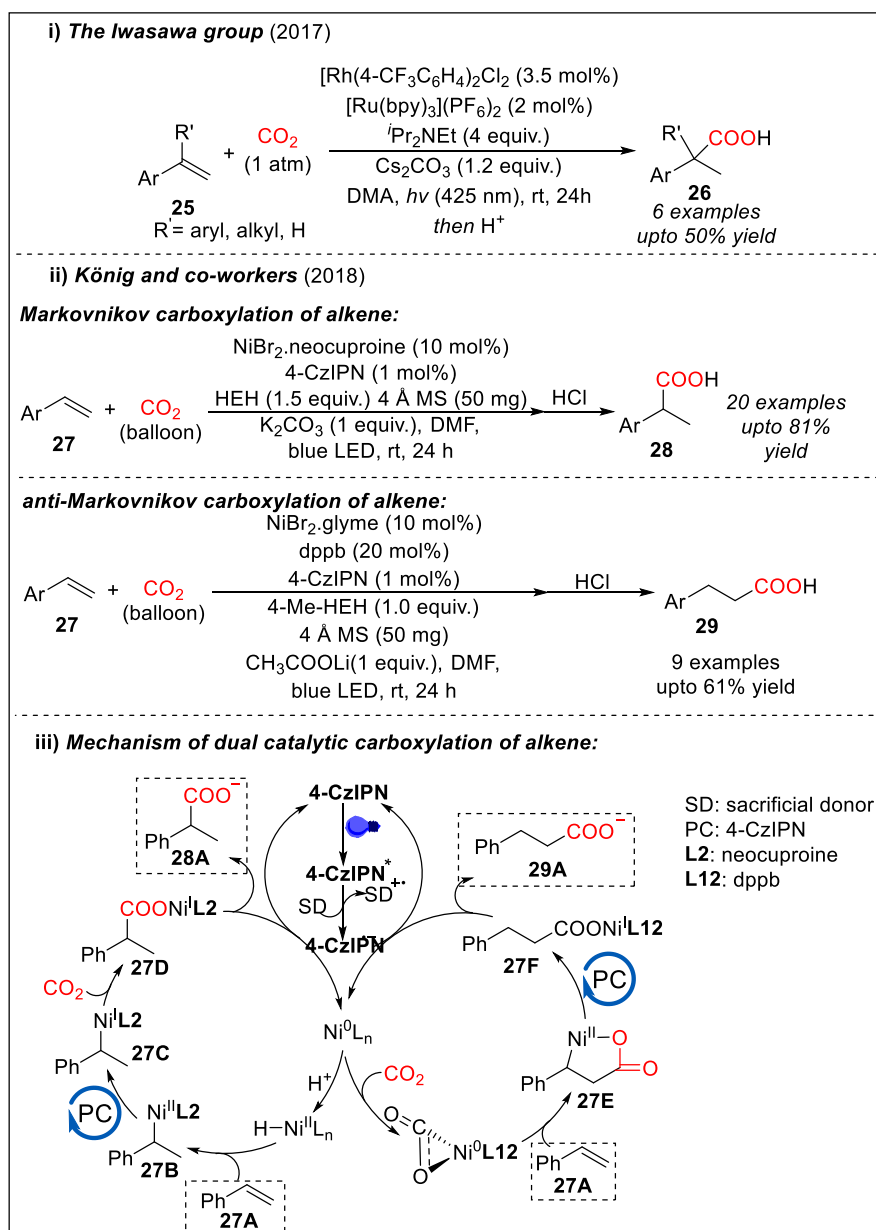
I.5.1.3.1. Hydrocarboxylation of alkenes/alkynes (unsaturated hydrocarbons) using dual catalysis

After the Lapidus group²⁷ reported an initial findings in 1978 on hydrocarboxylation of alkenes by Pd- and Rh- catalysis, several other groups including the Martin,²⁸ Tsuji,²⁹ Iwasawa,³⁰ Skrydstrup,³¹ Ma,³² Fujihara,³³ and others³⁴ contributed amply to this field. Alone transition metal catalysis using reductants like Mn, Zn or Et₂Zn has been able to meet excellent regioselectivity. Still, for the constant developments towards sustainability, chemists engaged themselves for developing milder methods removing metal reductants, which also would broaden the functional group tolerance.

First in 2017, inspired from the prior works, Iwasawa's group realized hydrocarboxylation of alkenes for synthesizing α -carboxylated products by Rh/photoredox catalysis (**Scheme 9, i**).³⁵ Here, along with Rh(I) catalyst, [Ru(bpy)₃](PF₆)₂ and ⁱPr₂NEt were used as photocatalyst and reductive quencher, respectively. Handful of electron-deficient alkenes were compatible under the reaction condition. In spite of long reaction time, moderate yields, they pioneered this field.

Driven by the drawbacks of the previous methodology, in 2019, the same group disclosed a much upgraded catalytic strategy with BI(OH)H (benzimidazoline derivative), as the sacrificial electron donor.³⁶

As we have seen, the regioselectivity guided carboxylation on α -site of the alkenes, i.e., Markovnikov carboxylation took place. Achieving anti-Markovnikov carboxylation to produce β -carboxylated product remained unreported until 2018 when the König group realized Ni/photoredox dual catalytic carboxylation following both Markovnikov and anti-Markovnikov paths controlled by ligand (**Scheme 9, ii**).³⁷ Varying the ligand from neocuproine to 1,4-bis-(diphenylphosphino)butane (dppb), the fashion of carboxylation shifted from Markovnikov to anti-Markovnikov paths.

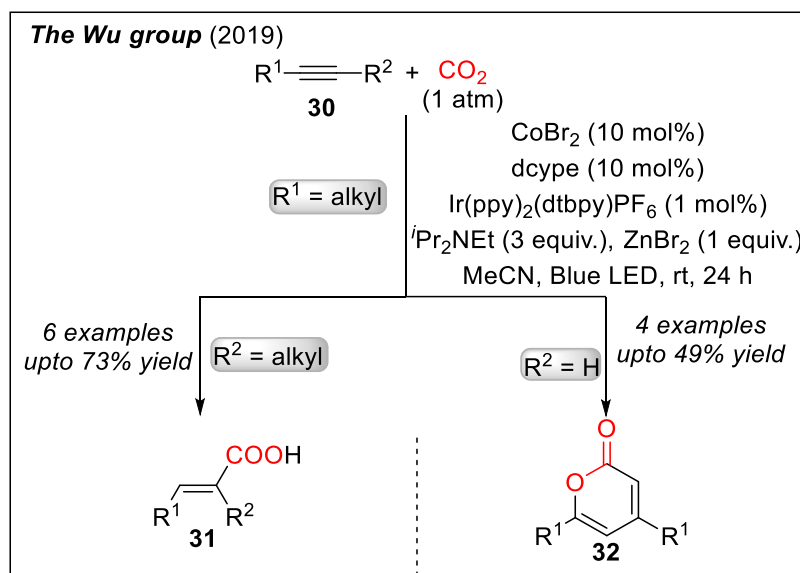


Scheme 9. Dual catalytic hydrocarboxylation of alkenes.

Irrespective of electronic nature of the substrates, the ligands successfully guided the regioselectivity by altering the mechanism. On the use of neocuproine (**L2**), formed Ni(II)-H species attaches to double bond at the α -position of alkene (**27A**) and generates Ni(II)-alkyl complex **27B**. Then Ni(I)-alkyl complex **27C** is formed by reduction of Ni(II). Therefore, **27C** undergoes nucleophilic attack irreversibly on CO_2 to give Markovnikov product **28A**. On the other hand, when dppb is used as ligand (**L12**), first Ni(0)-L complex combines with CO_2 to form stabilized 3-membered lactone. Then, the lactone complex reacts with substrate **27A** where Ni(II) goes to α -position (**27E**) of alkene and carboxylate group resides at β -position.

27E is reduced by photocatalysis and selectively yields β -carboxylated product 29A (Scheme 9, iii).

In 2019, the Wu group achieved dual Co/Ir photoredox catalyzed carboxylation of alkynes, another class of unsaturated hydrocarbon (Scheme 10).³⁸



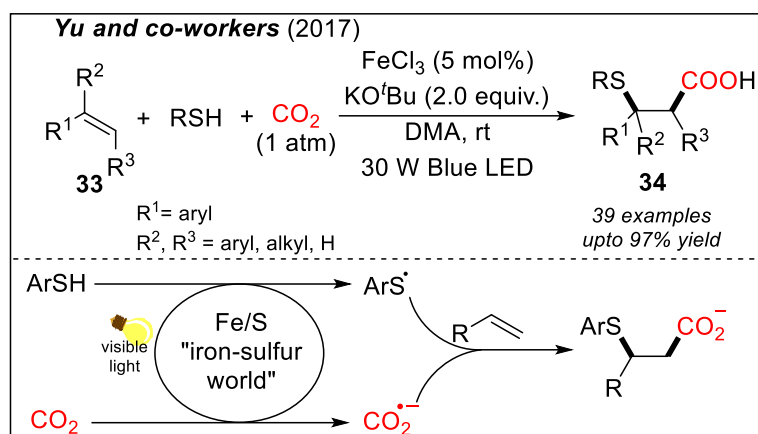
Scheme 10. Dual Co / photoredox catalyzed hydrocarboxylation of alkynes.

In this report, handful of acrylates were produced from internal alkynes by experiencing carboxylation at alkyl substituted ends, selectively. On taking terminal alkynes as substrates, [2+2+2] cycloaddition took place between one molecule of CO₂ and two molecules of alkyne resulting in formation of heterocycles. It is worth mentioning here that, Louie and co-workers previously developed a similar [2+2+2] cycloaddition reaction with CO₂ with nickel-catalysis.³⁹

I.5.1.3.2. Carboxylative bifunctionalization of alkenes by dual catalysis

Besides hydrocarboxylation reactions, a huge effort has been put to perform carboxylation and to incorporate another functional group at two ends of the olefins i.e., difunctionalization⁴⁰ with carboxylation as an integral part, at single operation. This research of bifunctionalization with selective α -carboxylation has adequately been contributed by solely photocatalysis, which would be discussed in later sections. As far as dual catalytic approach is concerned, one very interesting selective β -carboxylation strategy was developed by Yu and co-workers⁴¹ for thiocarboxylation of alkenes with CO₂ and thiols (Scheme 11) using iron promoter. Here, under the visible light irradiation, in presence of *t*BuOK, FeCl₃ combines with

thiols to form Fe/S complex and following natural “iron-sulfur world” hypothesis, under visible light, the Fe/S complex acts like electron transfer promoter. In the presence of thiol, FeCl₃, and ^tBuOK, visible light was absorbed during UV-vis spectroscopic studies and strong reduction potential peak was observed during CV measurement. Evidently, the high CO₂ to ($E^0 = -2.21$ V vs SCE in DMF) potential barrier was crossed by this reduction potential of -2.32 V.



Scheme 11. Fe-catalyzed thiocarboxylation of alkenes.

Therefore, the formed $\text{CO}_2^{\bullet-}$ combines with the styrenes at β -end, forming the stabilized benzylic radical. And the combination of the benzyl radical and thiol radical yields the thiocarboxylated product (**Scheme 11**). This report shows one very rare strategy of achieving SET reduction of CO₂ to form $\text{CO}_2^{\bullet-}$ under visible light.

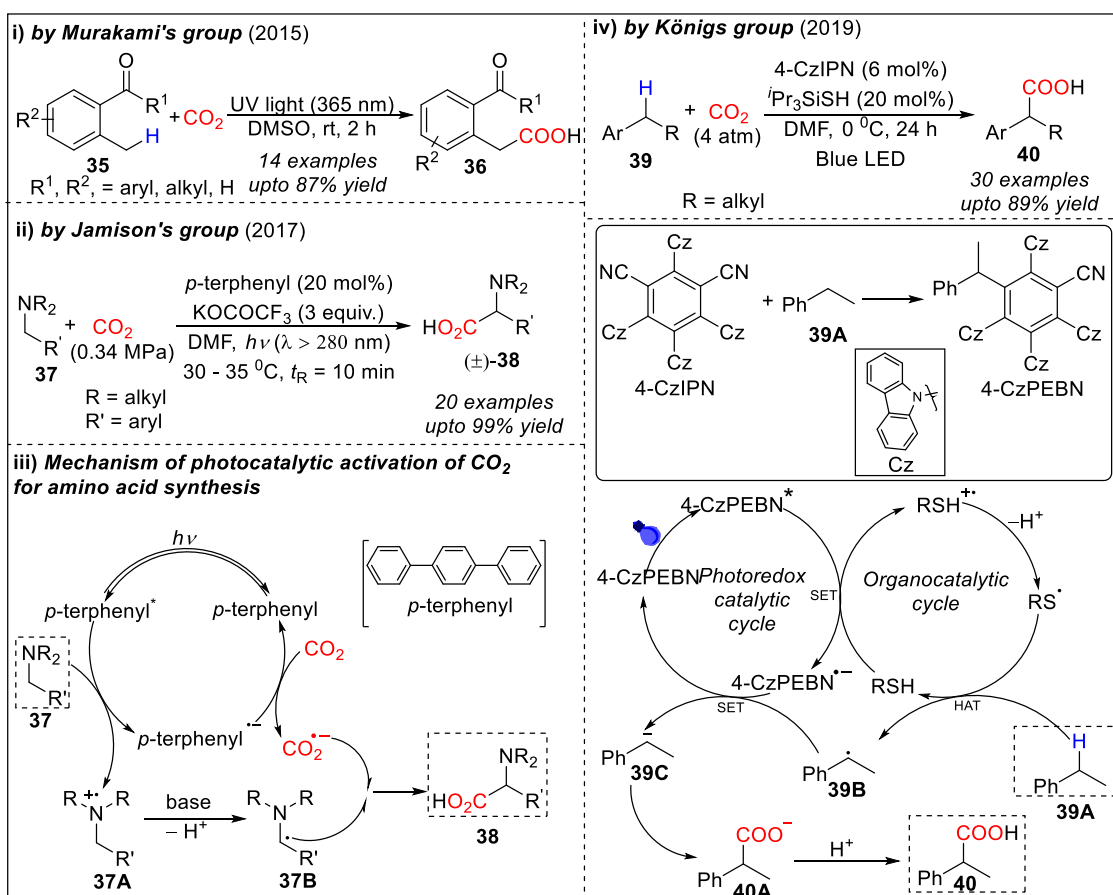
I.5.2. Photocarboxylation with CO₂ induced by only photocatalysts, free from synergistic TM-catalysis

The developed synergistic TM/photoredox dual catalytic carboxylation reactions have successfully omitted the use of (super)stoichiometric metal reductants, and the field is continuously emerging. Additionally, to reach more sustainability and energy efficiency, excluding the use of any TM (transition metal) catalyst by using photocatalysis is another daunting challenge to chemists. Contrary to the dual catalytic approach where mainly the low-valent TM-complex captured CO₂ to afford carboxylation, here, as TM is not present the strategy has to find a different mechanism. So, the main mechanisms those would play crucial role here are a) generation of one carbanion which nucleophilically attacks on CO₂ or b) formation of $\text{CO}_2^{\bullet-}$ from CO₂ by SET reduction and subsequent addition of the $\text{CO}_2^{\bullet-}$ to unsaturated bonds or another suitable radical (**Scheme 2**).

I.5.2.1. Carboxylation of C–H bonds by photocatalysis solely

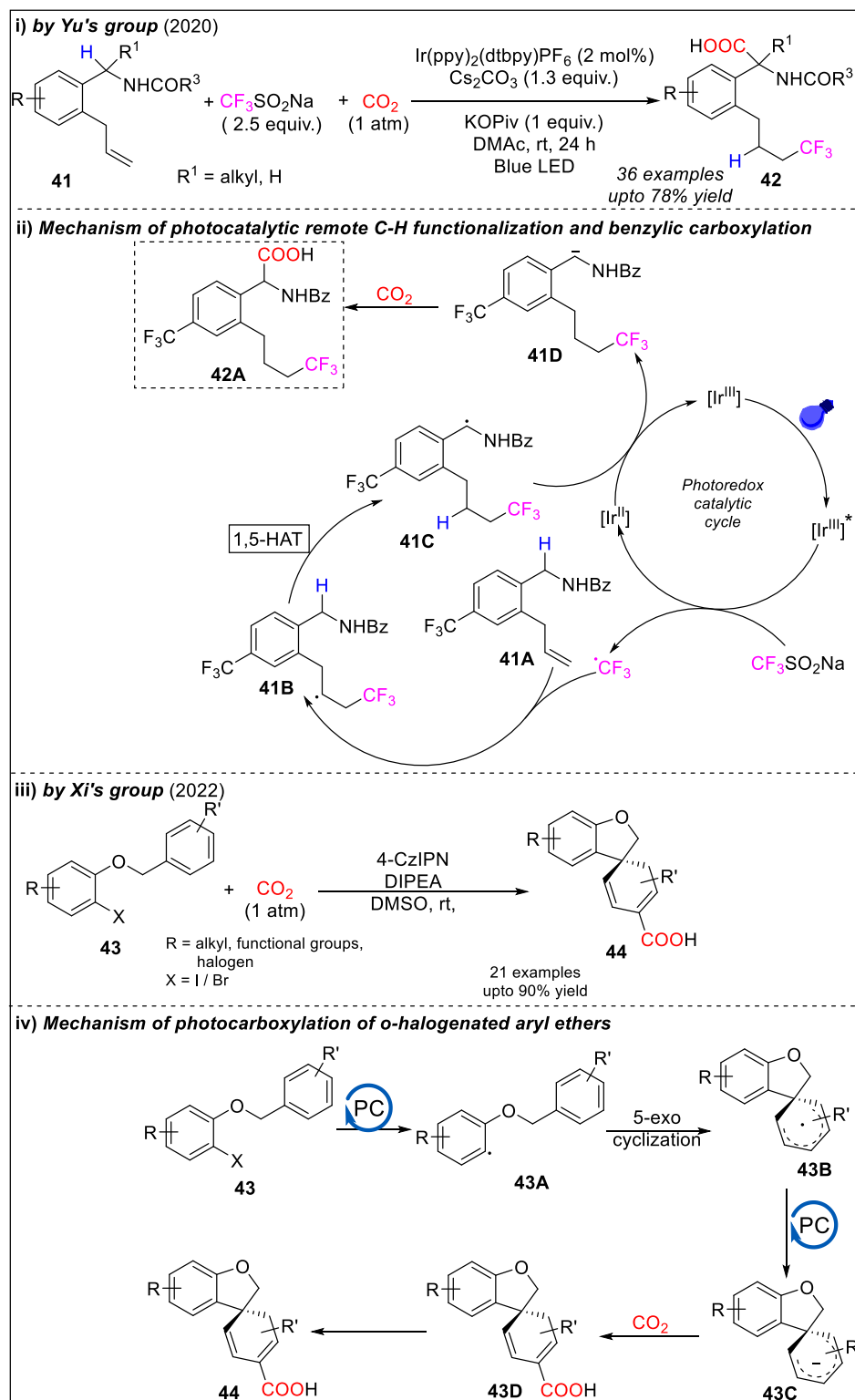
In 2015, the Murakami group was first able to directly carboxylate benzylic C(sp³)-H bonds of *o*-alkylphenyl ketones under UV or solar irradiation without using any external catalyst under 1 atm of CO₂ (Scheme 12, i).²¹ On irradiation by UV, the benzophenone is excited via photoenolization and followed by [4+2] cycloaddition between *o*-quinodimethanes and CO₂, benzylic carboxylation was achieved.

As discussed earlier, developing a general strategy for CO₂ to ⁻CO₂ SET reduction is worth searching for, owing to its very high reduction potential barrier. Jamison and co-workers, in 2017, utilized non-metallic organic compound *p*-terphenyl as photosensitizer under UV light. They performed carboxylation of C(sp³)-H in amines with CO₂ (0.34 MPa) to synthesize α -amino acids in continuous-flow (Scheme 12, ii).⁴² As we have seen, commonly used TM containing photocatalysts are not capable to cross the high potential barrier for SET reduction of CO₂. On the other hand, organic photosensitizer *p*-terphenyl ($E^0 = -2.63$ V vs SCE in DMF) is used to reduce CO₂ for HCOOH synthesis under UV irradiation.



Scheme 12. TM free photocatalytic C–H carboxylation.

The authors judiciously chose to use *p*-terphenyl instead of more common Ru- or Ir- photocatalysts for their anticipated transformation via photoreduction of CO₂ to produce ^{-•}CO₂.



Scheme 13. Photocatalytic remote C–H carboxylation.

On α -carboxylation of *N*-benzylpiperidine, α -amino acid was afforded in 92% yield after 10 min in continuous flow. In contrast, when the same reaction was performed in the batch with continuous CO₂ bubbling instead of continuous flow, even after 2 h, only 30% product was formed. As stated in the mechanism, under UV irradiation, excited to *p*-terphenyl* forms from *p*-terphenyl. Then, *p*-terphenyl* gets reduced to *p*-terphenyl⁻ by SET from the tertiary amine **37** and amine radical cation **37A** is generated. Then, *p*-terphenyl⁻ performs SET reduction on CO₂ to produce and regenerates *p*-terphenyl in the ground state. CF₃COOK acts as base and abstracts one proton from **37A** to produce **37B**, a stable benzylic radical. **37B** combines with ⁻CO₂ to afford α -amino acid **38** (Scheme 12, iii).

In 2019, independently, the Murakami group²⁵ on benzylic C(sp³)-H bonds carboxylation by Ni/photoredox dual catalysis under UV, was also revealed by the König⁴³ group, which appeared as another elegant and practical approach for the same transformation by 4-CzIPN induced visible light catalysis (Scheme 12, iv). Contrary to Murakami's protocol, König's strategy is better applicable to afford carboxylation at 2⁰-benzylic positions to afford 2-arylpropionic acids. Here, triisopropylsilanethiol was used as HAT catalyst along with the organic photocatalyst 4-CzIPN. With this methodology, various bio-active compounds e.g., fenpropfen, naproxen, flurbiprofen were successfully synthesized. As per proposed mechanism (Scheme 12, iv), one CN group of 4-CzIPN is substituted by ethylbenzene **39A** under light with the help of thiol that acts as HAT catalyst and 2,3,4,6-tetra(9H-carbazol-9-yl)-5-(phenylethyl)benzotrile (4-CzPEBN) is produced. This 4-CzPEBN enters to the catalytic cycle. RSH (triisopropylsilanethiol) reduces the excited 4-CzPEBN* to form 4-CzPEBN⁻ and converts to RSH⁺. Therefore, electrophilic thiyl radical is formed via deprotonation from RSH⁺ (BDE(S-H) = 88.2 kcal mol⁻¹). RS[•] takes up one proton from **39A**'s benzylic position (BDE(C-H) = 85.4 kcal mol⁻¹) to produce benzyl radical **39B** and regenerates RSH. Thereafter, **39B** is reduced by SET from 4-CzPEBN⁻ to give benzyl carbanion **39C** regenerate active 4-CzPEBN. Finally, **39C** attacks CO₂ to furnish the expected product **40A** (Scheme 12, iv).

Inspired by these precedents and other contemporary developments of photocatalytic bifunctionalization reactions of alkenes^{40a, 40c}, in 2020, Yu and co-workers reported an enthralling strategy for remote benzylic C(sp³)-H carboxylation combining remote C-H functionalization and HAT (Scheme 13, i).⁴⁴ ⁻CF₃ precursor which functionalized the pendent unactivated olefin and subsequently, carboxylation took place at remote benzylic C(sp³)-H bonds to furnish library of amino acids. Mechanistically, ⁻CF₃ attaches to pendent alkene **41A**

at the terminal position and forms radical **41B**. Therefore, 1,5-HAT takes place and gives rise to **41C**, more stable benzyl radical. ^-PC reduces **41C** to form benzylic carbanion **41D** which attacks to give rise to the expected carboxylated product **42A** (Scheme 13, ii).

Very recently, the Xi group reported an interesting approach to synthesize spirocyclic carboxylic acids from CO_2 and benzyl *o*-halogenated aryl ethers via sequential dearomatization/carboxylation reaction under room temperature (Scheme 13, iii).⁴⁵ 4-CzIPN was used as the photocatalyst along with reductive quencher DIPEA in DMSO solvent. A variety of functional groups tolerated the reaction condition to yield satisfactorily. According to the proposed mechanism, DIPEA reduces the excited photocatalyst (4-CzIPN^{*}) to generate and then aryl halide **43** gets reduced by PC^- to form aryl radical **43A**. Then **43A** undergoes intramolecular 5-exo radical cyclization to produce dearomatized and cyclized intermediate **43B** which is reduced again by photocatalysis to give rise to aryl anion **43C**. Nucleophilic attack on CO_2 by **43C** followed isomerization afforded the carboxylated product **44** (Scheme 13, iv).

I.5.2.2. Carboxylation of unsaturated hydrocarbons with solely photocatalysis

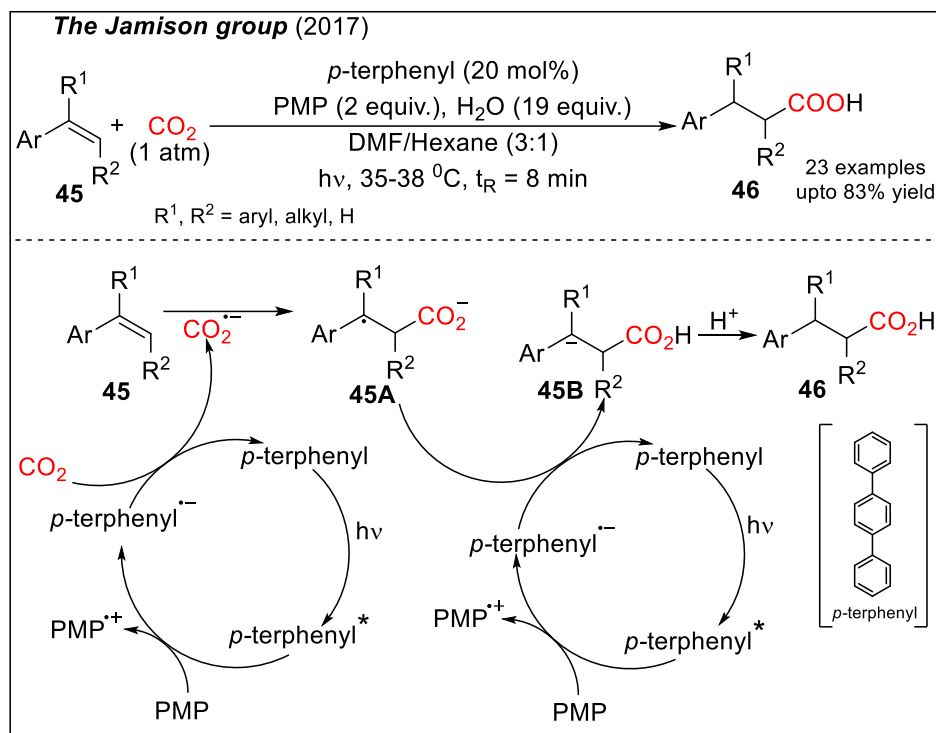
Here also, based on the chronology, the discussions would be done based on two modes i.e., hydrocarboxylation or carboxylative bifunctionalization (other than protonation) of alkenes.

I.5.2.2.1. Photoredox catalyzed hydrocarboxylation of alkenes/alkynes (unsaturated hydrocarbons)

In previous sections, we have witnessed some Markovnikov i.e., α -carboxylation³⁵⁻³⁶ and only one β -carboxylation (albeit lower yield)³⁷ of olefin by TM/photoredox dual catalysis.

Delightedly, the sole use of photocatalysis without any TM-catalyst has been able to achieve β -carboxylation of alkene in continuous flow by the Jamison group, in 2017. They utilized their pioneering discovery⁴² of *para*-terphenyl photosensitized SET reduction of CO_2 under UV light to realize anti-Markovnikov β -carboxylation (Scheme 14).⁴⁶ Here also, UV irradiation excites *p*-terphenyl to *p*-terphenyl^{*}. Thereafter, as discussed earlier, *p*-terphenyl^{*} reduces CO_2 by SET to produce $^-\text{CO}_2$ which subsequently attaches to the styrene **45** at the β -position and forms stable benzylic radical **45A**. On protonation by the added water, selectively the expected anti-Markovnikov monocarboxylated product **46** is yielded. Deuteration experiment proved water to be the main proton source (Scheme 14). Both α - and β - substituted

styrenes provided fair yields under this condition and various functional groups were also tolerated.



Scheme 14. Direct β -selective carboxylation of styrenes by solely photocatalysis.

I.5.2.2.2. Photocatalyzed carboxylative difunctionalization of alkenes

As alkene bifunctionalization allows us to increase molecular complexity just by a single operation, this field is experiencing huge attention to synthetic chemistry community.⁴⁷ Getting insight from the prior developments of photocatalyzed bifunctionalization of alkenes, carboxylation reactions have been integrated here successfully as one of the two functionalizations.

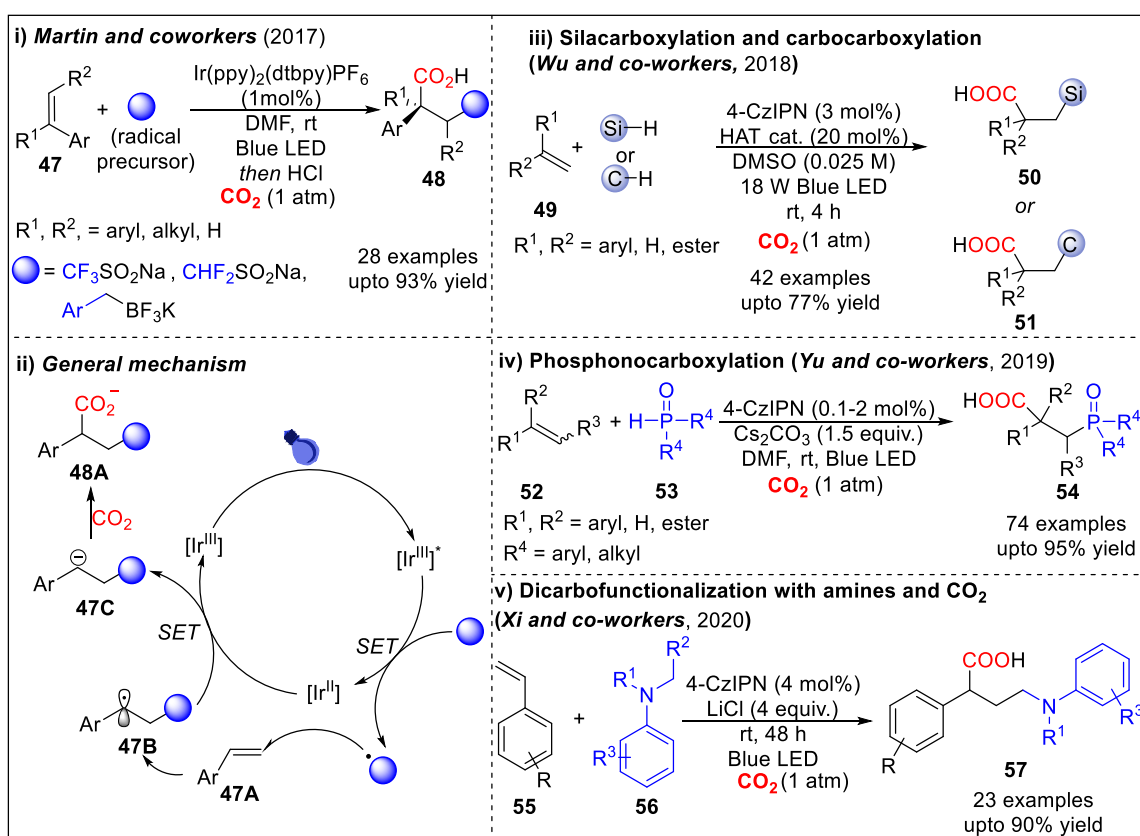
In 2017, the Martin group, reported a redox-neutral protocol for photocatalyzed carboxylative dicarbofunctionalization of styrene substrates with several C centred radical and CO₂ (**Scheme 15, i**).⁴⁸ Mainly, CF₃SO₂Na was used as $\cdot\text{CF}_3$ precursor and [Ir(ppy)₂(dtbpy)]PF₆ was taken as photocatalyst.

To demonstrate the mechanism, on photo-excitation the photocatalyst (PC) goes to PC* i.e., here Ir(III) converts to Ir(III)* which is reduced to Ir(II) by SET from the radical precursor CF₃SO₂Na to generate $\cdot\text{CF}_3$. Then $\cdot\text{CF}_3$ combines with the β -terminal of the styrene **47A** and stabilized radical at benzylic position (**47B**) is formed. **47B** is then reduced by SET from Ir(II)

and benzylic carbanion **47C** is formed along with regeneration the Ir(III) catalyst. As a result, the benzylic carbanion **47C** undergoes nucleophilic addition to CO₂ to furnish the difunctionalized product with β-carboxylation. They had also used cesium oxalates, ArCH₂BF₃K and CHF₂Na as other radical precursors (**Scheme 15, ii**).

Following Martin's work, using conceptually similar strategies several other groups⁴⁹ developed carboxylative bifunctionalization of activated alkenes or styrenes with CO₂ taking suitable photocatalysts under visible light. Mechanistically, the examples followed the similar path as depicted in **Scheme 15 ii**, just changing the radical precursor and appropriate PC in each case. The formation of benzylic carbanion is the key step for carboxylation and carbanion has been confirmed by coupling with other electrophiles e.g., ketones instead of CO₂.

In 2018, the Wu group developed 4-CzIPN catalyzed light mediated carbocarboxylation and silacarboxylation of activated alkenes (**Scheme 15, iii**).^{49a}



Scheme 15. Various difunctionalizing carboxylation of Alkenes.

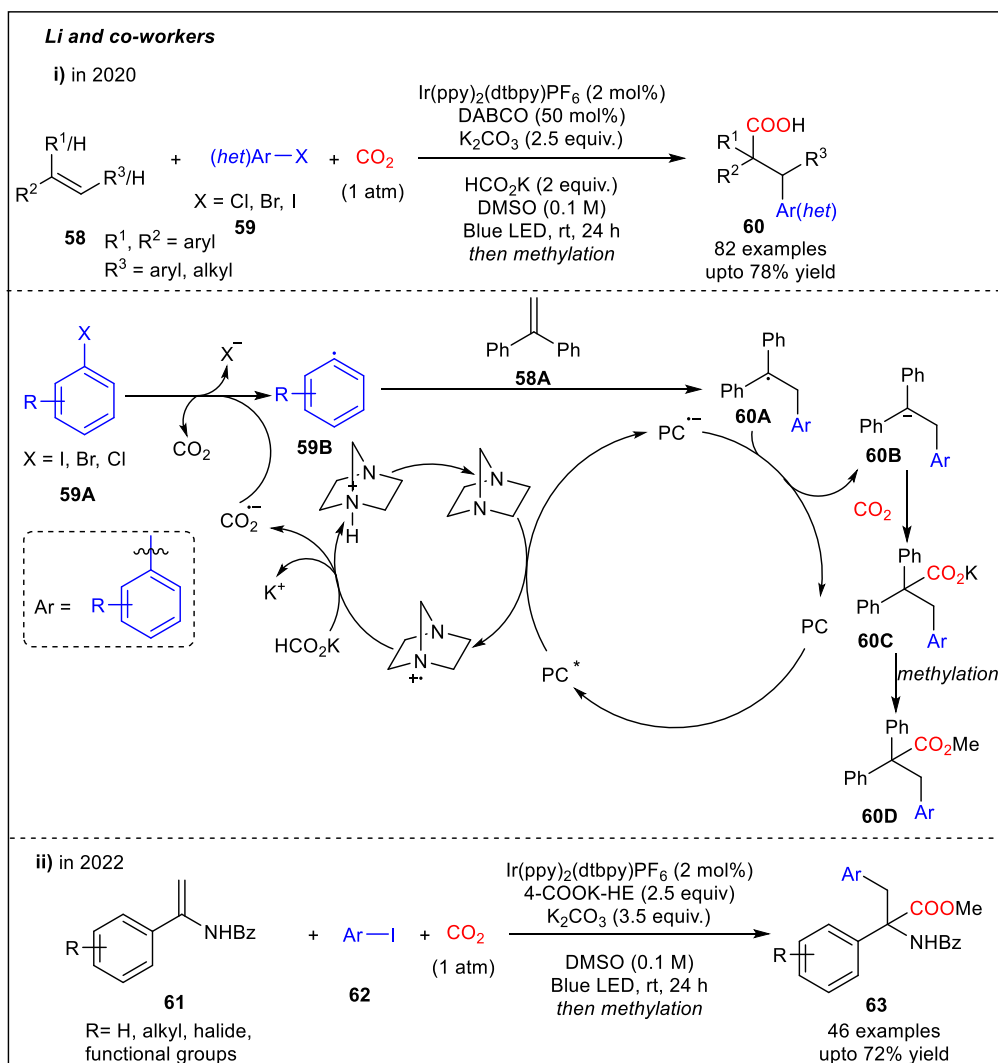
In 2019, the Yu group developed photocatalyzed phosphonocarboxylation enamides i.e., activated alkenes using 4-CzIPN as organic photocatalyst (**Scheme 15, iv**).^{49b} From phosphites

Photocarboxylation Reactions with CO₂ and Transformation of Carboxylic Acids: Journey towards Sustainability

and phosphene oxide, phosphorus centred radicals form and accomplish phosphonocarboxylation under CO₂ atmosphere.

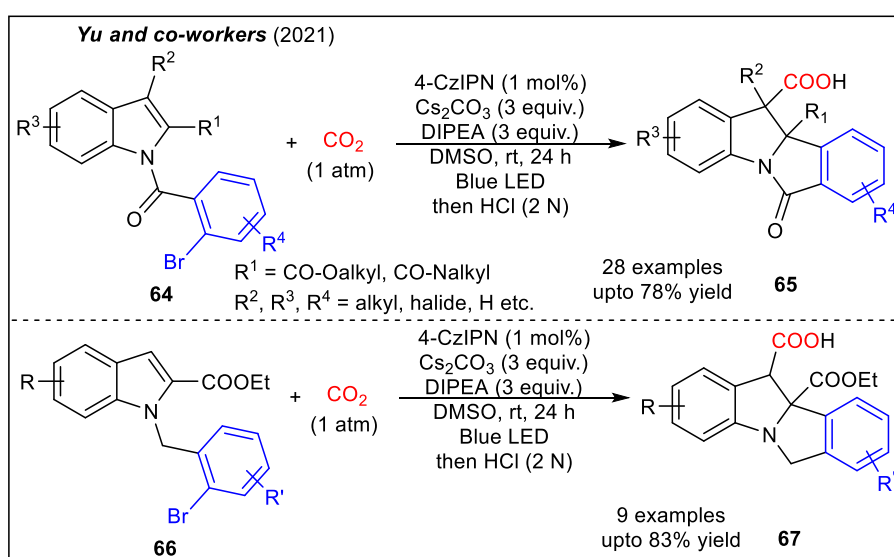
In 2020, the Xi group, synthesized several γ -amino acids from styrenes by photocatalyzed dicarbofunctionalization with CO₂ and amines (**Scheme 15, v**).^{49c}

Though aryl halides are easily available and of low-cost, use of same as aryl group precursor in photocatalyzed bifunctionalization reactions have scarcely been reported because of aryl halide's high value of reduction potential. In 2020, the Li group successfully used aryl halides as aryl radical precursor for Meerwein-arylation type photocatalyzed carbocarboxylation of styrenes with CO₂ (**Scheme 16, i**).⁵⁰ Here DABCO and HCO₂K were used as HAT reagent and low-cost sacrificial reductant, respectively.



Scheme 16. Photocatalyzed carbocarboxylation of alkenes.

As per proposed mechanism, from HCO_2K , DABCO produces $\cdot\text{CO}_2^-$, which is a strong reductant which efficiently reduce aryl halide (even aryl chlorides) **59A** to produce aryl radical (**59B**). **59B** combines with to styrene **58A** at its β -position to give benzylic radical **60A**. By the aforementioned path, under photocatalysis, α -carboxylated product **60C** is achieved (**Scheme 16, i**). Notably, when aryl halides remained absent, 24% of dicarboxylated product formed where mono-carboxylated product was achieved in 10%, which intimates the involvement of $\cdot\text{CO}_2^-$. In 2022, the same group extended this strategy to functionalize enamides for carbocarboxylation with CO_2 and aryl iodides (**Scheme 16, ii**).⁵¹

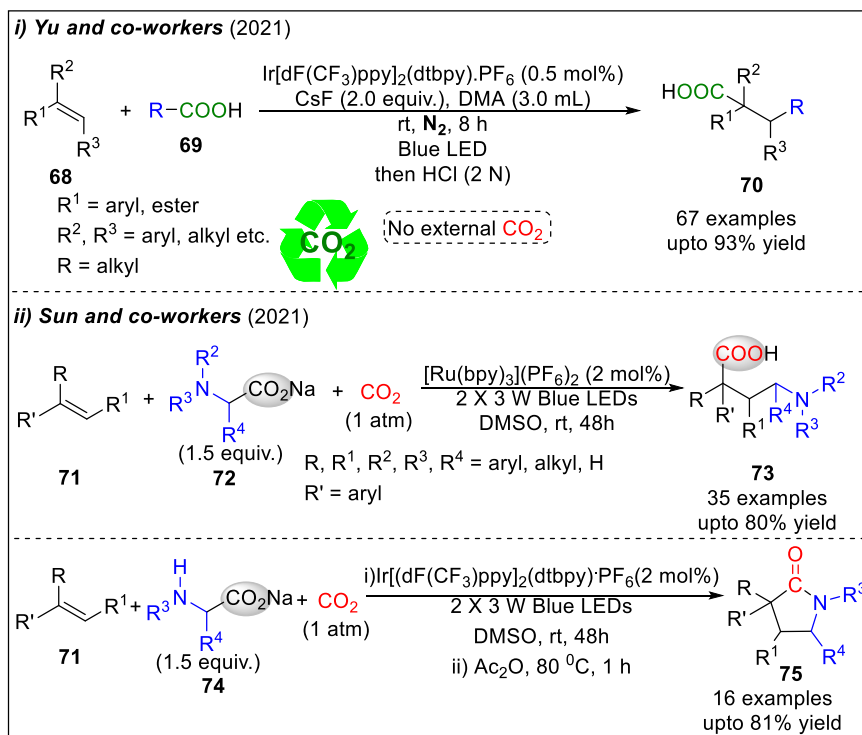


Scheme 17. Photocatalyzed dearomative arylcarboxylation of indoles.

In 2020, Yu and co-workers reported an elegant photocatalytic approach to achieve difficult-to-synthesize indoline-3-carboxylic acids from indoles and CO_2 by dearomative arylcarboxylation (**Scheme 17**).⁵² Here, the aryl bromide moiety in the substrate acted as aryl radical precursor intramolecularly. As here dearomatization is integrated with bifunctionalization, it is more challenging than the prior reports of olefin bifunctionalizations.

Yu and co-workers, recently in 2021, very interestingly reutilized in situ liberated CO_2 via decarboxylation of one acid for another carboxylation reaction under Ar atmosphere without any external CO_2 , via photocatalysis by Ir(III) catalyst (**Scheme 18, i**).¹⁵ They realized carbocarboxylation of styrenes, where in situ formed CO_2 acts as carboxylating source and another functionalizing agent is a C-centred radical that originates from the decarboxylation of various acids such as alkyl carboxylic acids, α -amino acids, and peptides, following the same

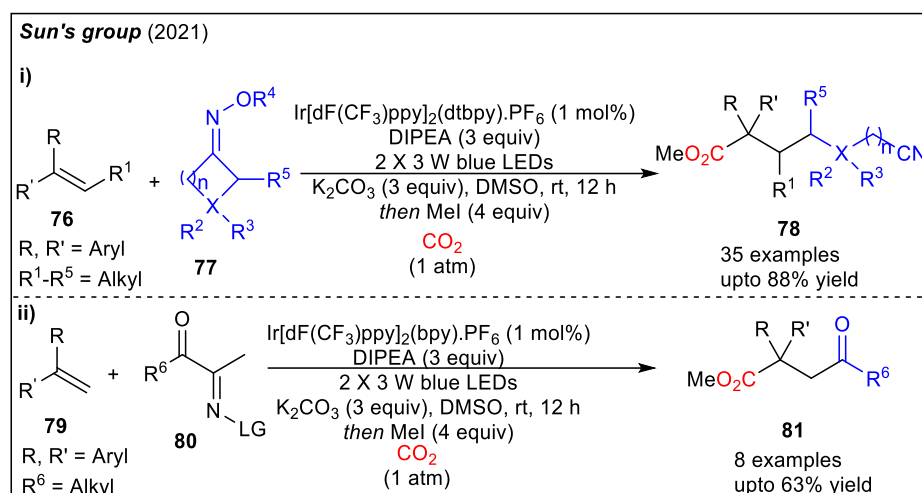
general mechanism (Scheme 15, ii). The only difference here is that despite having low P_{CO_2} (partial pressure), the in situ formed CO₂ sufficiently performs carboxylation reaction.



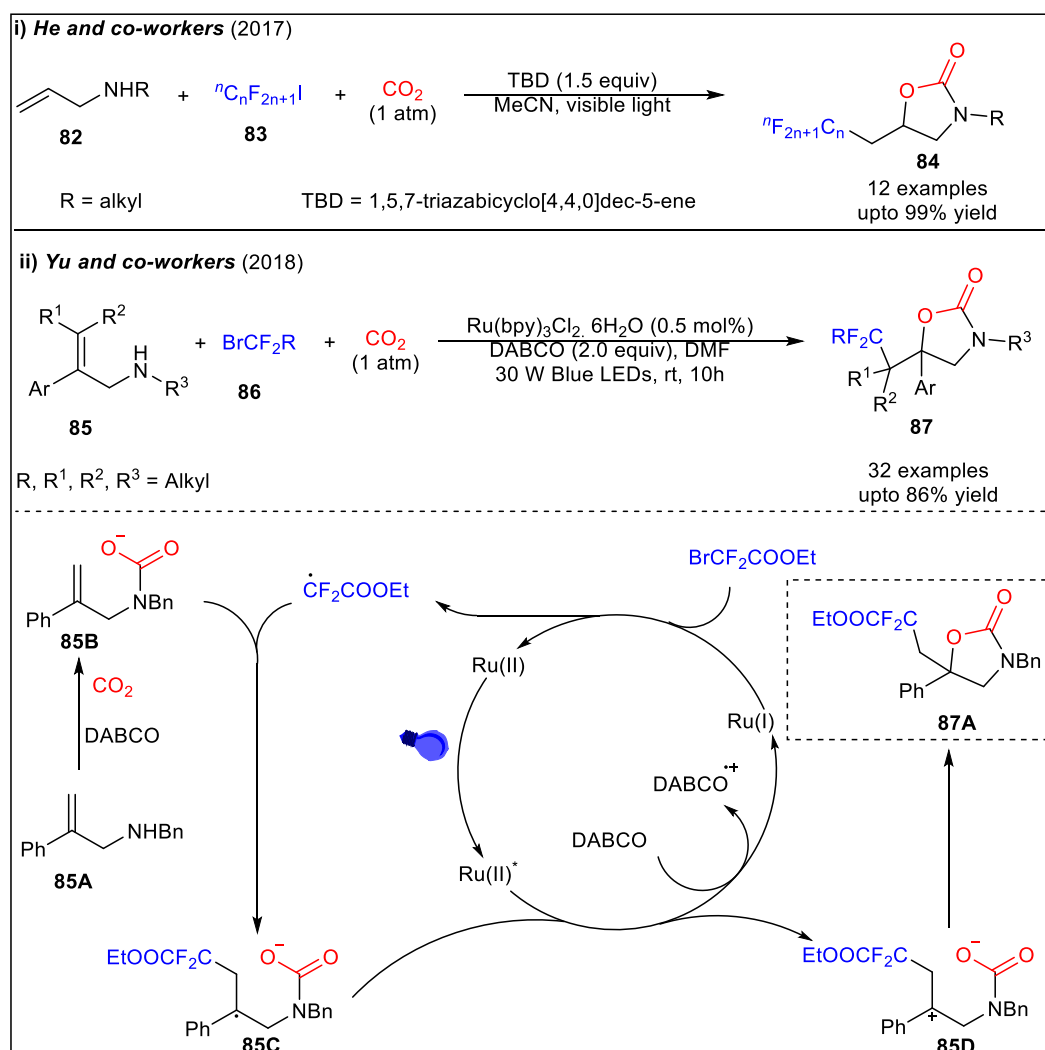
Scheme 18. Carboxylation of alkenes with carboxylic acid/esters and in situ or external CO₂.

Subsequently, the Sun group reported another carboxylative bifunctionalization reaction of styrene combining decarboxylation and carboxylation in the same reaction condition of Ru(III) photocatalysis to synthesize variety of γ -lactams and α,α -disubstituted γ -amino acids (Scheme 18, ii).⁵³ Here, they used sodium glycinate as the decarboxylative agent which give rise to the C-centred radical that attaches to styrene at the β -position. Contrary to Yu's report, here the in situ generated CO₂ was not sufficient to provide satisfactory yield, hence applying external CO₂ (balloon) was necessary.

Soon after this report, the same group bifunctionalized styrenes with commercially available n-membered (n = 4, 5 or 6) cyclic ketone oximes and CO₂ under Ir-photocatalysis to synthesize ϵ -, ζ -, η -cyanocarboxylic acids (Scheme 19, i).⁵⁴ Besides, they used acyclic ketone oximes in place of cyclic ones which afforded γ -keto acids in satisfactory yields (Scheme 19, ii).



Scheme 19. Photocatalyzed carboxylative bifunctionalization of styrenes with CO₂ and ketone oximes.



Scheme 20. Photocatalyzed oxy-difluoroalkylation of allylamines with CO₂.

In the same line, He's interesting work from 2017 for carboxylative cyclization combining allylamines, perfluoroalkyl iodides, and CO₂ is worth mentioning here (**Scheme 20, i**).⁵⁵ Perfluoroalkyl iodides acted as radical source and along with the CO₂, construct the cyclized oxazolidinone.

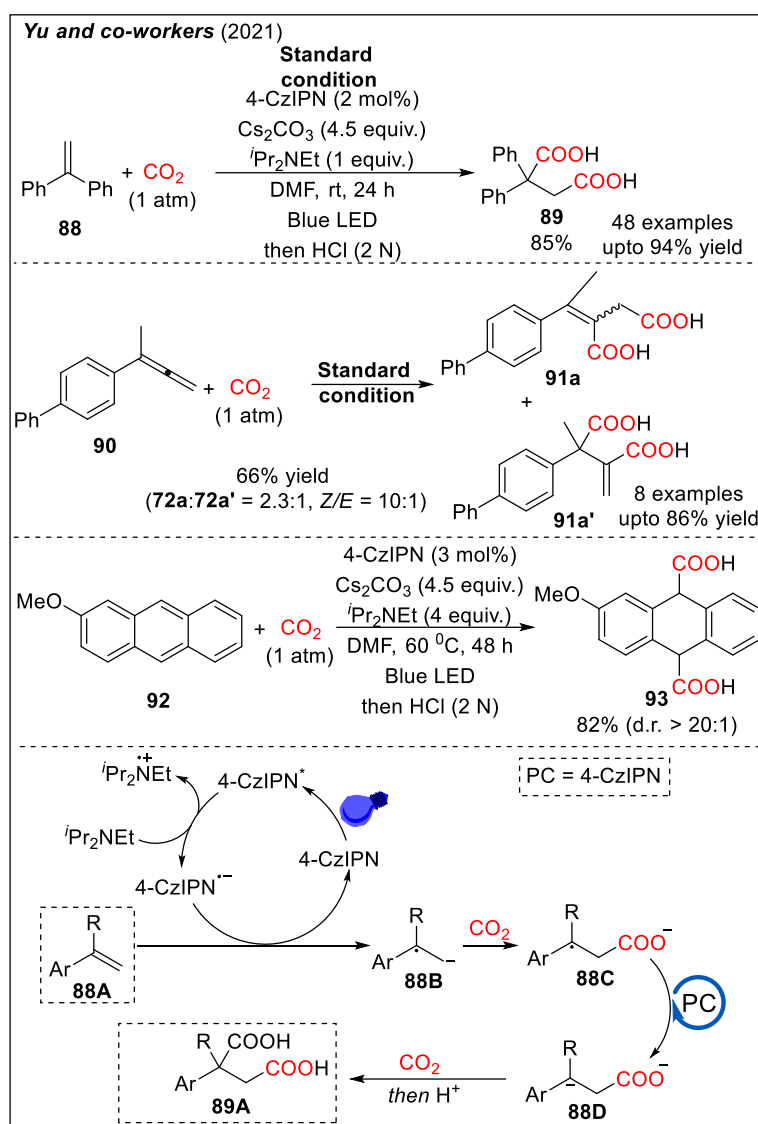
In 2018, the Yu group, performed light mediated oxy-difluoroalkylation of allylamines with difluoroalkyl bromides and CO₂ using Ru-photocatalyst to synthesize variety of difluoroalkylated 2-oxazolidinones (**Scheme 20, ii**).⁵⁶ As the proposed mechanism, first, CO₂ is captured by the nucleophilic amine **85A** to generate carbamate **85B**. DABCO reduces the excited Ru(II) photocatalyst to form Ru(I) that reduces BrCF₂COOEt to give [•]CF₂COOEt, then it adds to β -position of the double bond of **85B** and generates stable benzylic radical **85C**. Oxidation of by photoexcited Ru(II) oxidizes **85C** and produces benzylic carbocation **85D**. Then the product **87A** forms via subsequent cyclization (**Scheme 20, ii**).

As we discussed in this section, generation and involvement of benzylic carbanions or carbanions stabilized by adjacent EWGs is the essential event for the carboxylation reaction (**Scheme 15, ii**) and the chemoselectivity is also guided mainly by the substrates' electronic nature. Without help of TM-catalysis, carboxylation of unbiased alkenes has not been successful till date, as reducing an unbiased carbon radical to generate carbanion is very difficult. So, crossing this difficulty to utilize photocarboxylation techniques for unbiased simple alkenes are the upcoming challenge that demands further studies.

I.5.2.2.3. Dicarboxylation of alkenes with photocatalysis

As we discussed in the previous section, the carboxylation of alkene is confined to monocarboxylation mainly at α -position with a different functionalization at β -position. The dicarboxylation of alkenes would be another important reaction capable of synthesizing various fine chemicals but till date, this has merely been reported. In 2018, the Martin group developed an Ni-catalyzed strategy⁵⁷ to synthesize adipic acids via dicarboxylation of 1,3-dienes using Mn as reductant. Contrastingly, even with the help of TM-catalysis, no report is available where decarboxylation takes place at the both ends of one single double bond. To delight, in 2021, Yu came up with an elegant strategy for photocatalyzed decarboxylation of alkenes, (hetero)arenes or allenes with balloon pressure of CO₂, two equivalent of which with respect to the olefin substrate would be required for the reaction. They used 4-CzIPN along with DIPEA as the organic photocatalyst and the sacrificial electron donor, respectively (**Scheme**

21).⁵⁸ Mechanistically, PC is photoexcited PC* and is reduced to PC⁻ by SET from DIPEA. Then, alkene **88A** is reduced to give alkene radical anion **88B** which attacks electrophilic CO₂ and forms stable benzylic radical **88C**.



Scheme 21. Photocatalyzed Dicarboxylation of Alkenes.

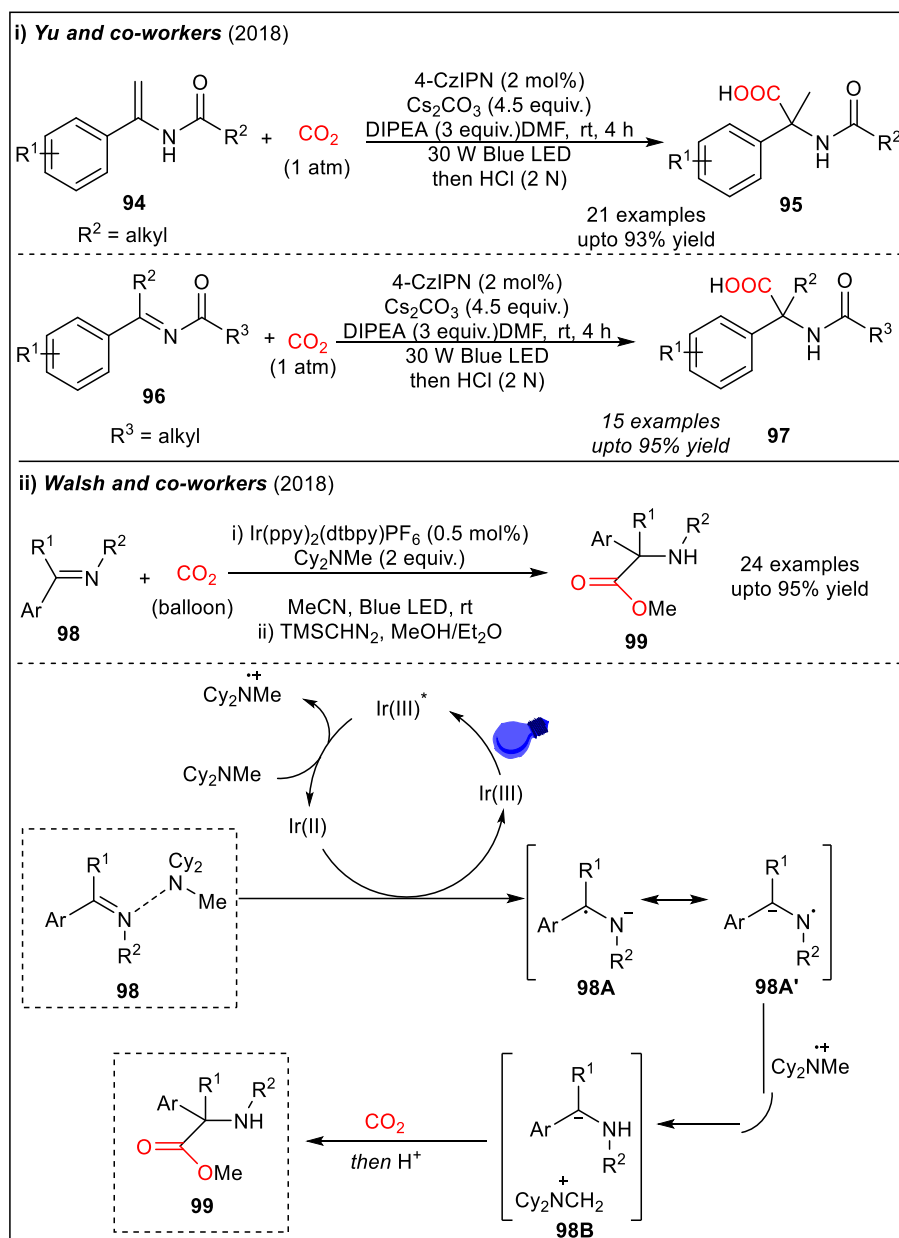
From here, photocatalysis generates benzylic carbanion **88D** and another carboxylation takes place to furnish the dicarboxylated product **89A** (**Scheme 21**).

I.5.2.3. Photocatalyzed hydrocarboxylation of imines

Capturing and utilizing CO₂ to synthesize α -amino acids would be of great interest in bioorganic chemistry.⁵⁹ As we witnessed the development of alkene hydrocarboxylation, the same strategies have great potential to be extended to imines. Thus, the Yu group extended the

Photocarboxylation Reactions with CO₂ and Transformation of Carboxylic Acids: Journey towards Sustainability

TM-free photocatalyzed alkene hydrocarboxylation technique to afford imine hydrocarboxylation, enamides yielding α , α -disubstituted α -amino acids (**Scheme 22, i**).⁶⁰ Here, 4-CzIPN and ⁱPr₂NEt were used as the photocatalyst and the sacrificial organic reducing agent, respectively. As shown in the general mechanism with alkenes, here α -amino benzylic carbanions formed and furnishes carboxylation.



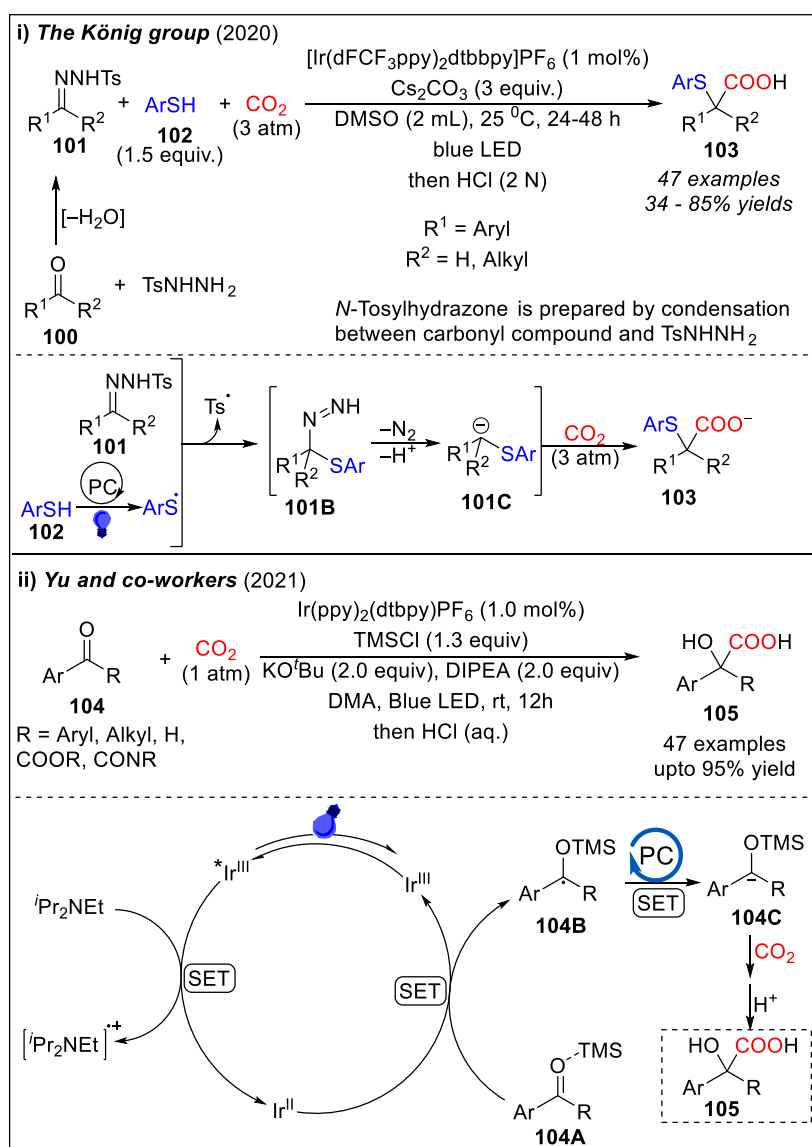
Scheme 22. Hydrocarboxylation of imines.

Almost at the same time, independently Walsh and co-workers performed Ir(III)-photocatalyzed imine hydrocarboxylation to synthesize α , α -disubstituted α -amino acids (**Scheme 22, ii**).⁶¹ Here they took primarily as electron donor and additionally, Cy₂NMe

protected the formed carboxylated product from decarboxylation and made it isolable by simple filtration.

I.5.2.4. Photocatalytic carboxylative difunctionalization of carbonyls

In 2020, the König group performed carboxylative bifunctionalization of carbonyl compounds under 3 atm CO₂ (Scheme 23, i).⁶² Interestingly here, Wolff-Kishner (WK) reaction merging with photocatalytic radical generation gave the alkyl carbanions with α -functionalization, which are the prime intermediate to afford carboxylation.



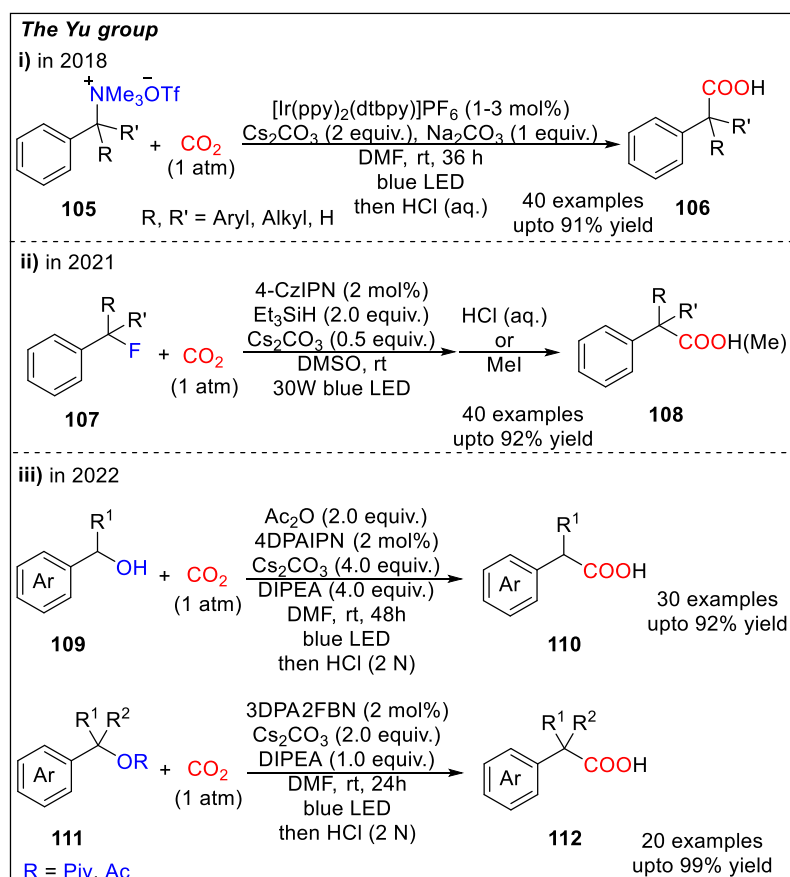
Scheme 23. Umpolung carboxylation of carbonyl compounds.

Following this, the Yu group reported an elegant approach for synthesis of plethora of α -hydroxycarboxylic acids by performing umpolung carboxylation by Ir(III)-photocatalysis

directly from carbonyl compounds (**Scheme 23, ii**).⁶³ Here, they used chlorosilanes which are Lewis acidic, to protect/activate the carbonyl groups. Performing Stern-Volmer experiment and other detailed control experiments, mechanism was proposed. First, DIPEA reduce the photoexcited Ir(III) photocatalyst to give Ir(II). Carbonyl group gets protected and activated by TMSCl forming **104A** and as reduction potential is decreased than that of carbonyl, Ir(II) reduces **104A** forming α -siloxybenzyl radical (**104B**) and regenerates Ir(III). Again, another photoredox catalytic cycle reduces **104B** to form **104C**, a benzyl carbanion. **104C** combines with CO₂ and affords the carboxylated product **105** (**Scheme 23, ii**).

I.5.2.5. Photocatalyzed carboxylation of C–N/O/F bonds

Being stable and crystalline, chemists have used organoammonium salts as electrophiles in TM-catalysis⁶⁴ and for direct C–N carboxylation⁶⁵ for affording expected products along with amines as side-product.



Scheme 24. Photocarboxylation of benzylic alcohols.

Very judiciously, in 2018, for Ir-photocatalyzed carboxylation of organoammonium salt, the Yu group reutilized the *in situ* formed amine and bypassed the use of external (super)stoichiometric organic sacrificial electron donor, commonly DIPEA or HEH (**Scheme 24, i**).⁶⁶ They have been able to reuse the *in situ* released amine even it was in very low concentration, for the carboxylation of primary, secondary, tertiary, and allylic ammonium salts. In 2021, the same group realized benzylic C(sp³)-F photocarboxylation cleaving C-F bond (**Scheme 24, ii**).⁶⁷ Here, they used 4-CzIPN as photocatalyst and Et₃SiH as reducing agent.

Almost parallelly with Iwasawa's Pd/photoredox dual catalytic carboxylation¹⁹ to synthesize C(sp³)-carboxylic acids from benzylic alcohol, independently Yu reported another solely photocarboxylation strategy for the same transformation catalyzed by 3DPA2BFN or 4-DPAIPN (**Scheme 24, iii**).⁶⁸

I.5.3. Catalyst-free photocarboxylation with CO₂

With rapid development of photocatalyst induced photocarboxylation reactions, investigation to develop the technique even without any photocatalyst has also been started. As discussed, photocatalyst induced technique mainly deals with carbanion formation followed by nucleophilic attack on CO₂, but the SET reduction of CO₂ has not been utilized widely. EDA (electron-donor and acceptor) or visible-light induced CTC (charge-transfer-complex) could lead to SET activation of CO₂, hypothetically.

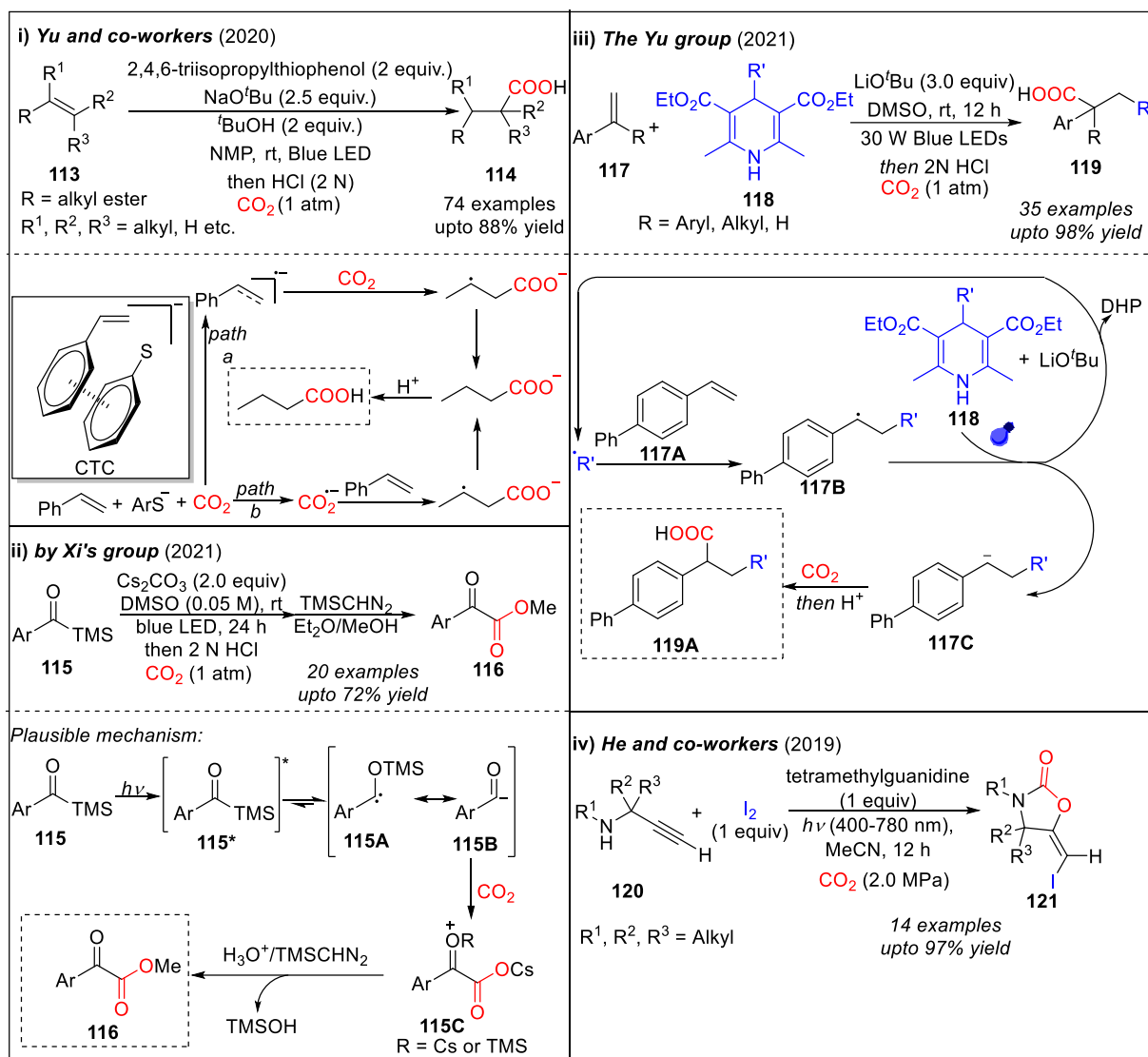
Encouraged by their own findings of photocatalyzed thiocarboxylation of alkenes, in 2020, for the first time, the Yu group developed visible light induced but TM (transition metal) and PC (photocatalyst)-free hydrocarboxylation of activated alkenes or styrenes with CO₂ to give challenging β-carboxylation in anti-Markovnikov fashion (**Scheme 25, i**).⁶⁹ Here, CTC is formed under blue LED irradiation between the aromatic thiol taken in 2.0 equiv and the styrene. Then either of the styrene and CO₂ undergoes SET reduction by the formed CTC and respective radical anion is obtained which executes carboxylation at β-position of alkene anti-Markovnikov fashion (**Scheme 25, i**).

In 2021, Xi and co-workers synthesized plethora of α-ketocarboxylic acids by directly carboxylating acyl silanes under catalyst-free photocatalysis (**Scheme 25, ii**).⁷⁰ As they proposed the mechanism, the acyl silane **115** excites under light and goes to its singlet state. Then 1,2-silyl shift takes place from **115*** to generate siloxycarbene **115A** as an intermediate

Photocarboxylation Reactions with CO₂ and Transformation of Carboxylic Acids: Journey towards Sustainability

and **115A** remains in the resonance with **115B** which attacks CO₂ and forms cesium carboxylate **115C**. On hydrolysis of **115C**, the ketocarboxylate (**116**) is afforded (**Scheme 25, ii**).

In 2021, Yu disclosed external photocatalyst free photocatalytic strategy for carbocarboxylation of styrenes (**Scheme 25, iii**).⁷¹



Scheme 25. Visible-light mediated carbocarboxylation of styrenes by external photocatalyst-free photocatalysis.

Wisely, 4-alkyl DHP was utilized as photoexcited reductants as well as the alkyl radical precursor. As per mechanism, with the help of base, alkyl radical ('R') is produced from **118** (4-alkyl DHP) under light irradiation. 'R' attaches to styrene **117A** at its β -position and forms one stabilized benzyl radical. Photoexcited 4-alkyl DHP reduces **117B** to give the **117C**

(benzylic carbanion). **117C** nucleophilically attack CO₂ to yield the difunctionalized product **119A** (Scheme 25, iii).

Though not for synthesis of carboxylic acids, in 2019, He's work to synthesize exo-iodo-methylene 2-oxazolidinones by a metal-free approach via photocatalytic carboxylative cyclization of propargylic amines with CO₂ and I₂ demands mention here (Scheme 25, iv).⁷² Further, the iodine-substituted 2-oxazolidinones could be transformed to produce other hard-to-achieve value-added chemicals.

I.6. Reviewing photocarboxylation to synthesize carboxylic acids

To conclude, a detailed description of the modern carboxylation technique via photocatalysis has been presented. With the progress of civilization and ever-growing pollution, the world has leaned towards using renewable energy sources. Being the most viable energy source, visible or solar light is being utilized profoundly in organic synthesis. Therefore, plenty of photocarboxylation techniques have been developed utilizing CO₂ as C-1 feedstock. Unlike typical TM catalyzed techniques, use of (super)stoichiometric metal reducing agents have completely been stopped here. And mostly, 1 atm pressure of CO₂ is sufficient and could be done at room temperature. Handful of challenging carboxylation reactions have been executed using these photocatalytic strategies.

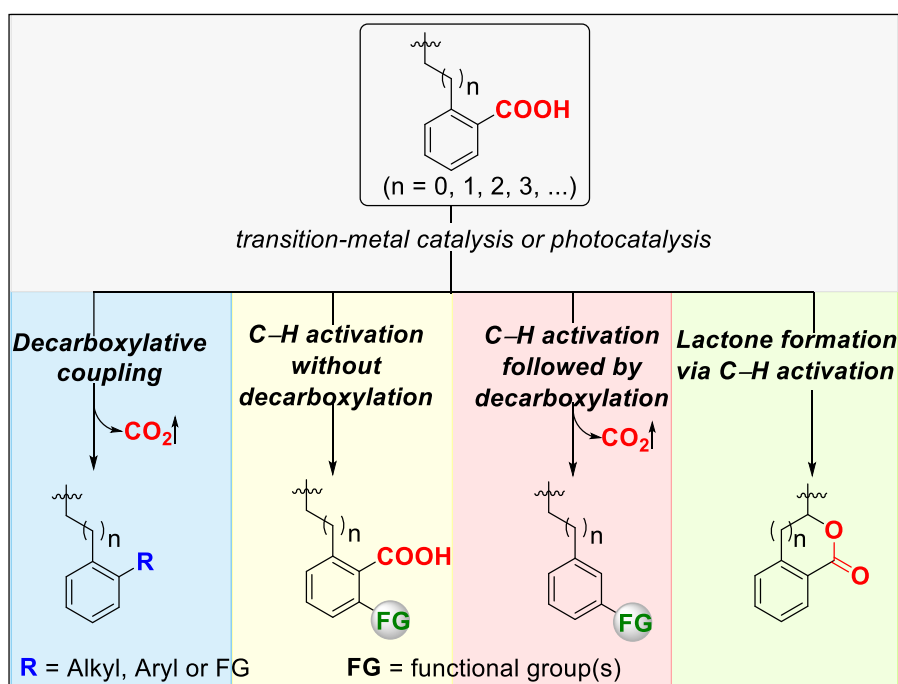
Despite significant growth, photocarboxylation techniques are still at budding stage and suffer from various pitfalls. Firstly, in comparison with TM catalyzed C–X carboxylation, the substrate variation still remains narrow. Specifically, most of carboxylation of the C–X bonds took place either with the C(sp²)- or benzylic C(sp³)- center which is a stabilized one; on the contrary, carboxylation cleaving unbiased C(sp³)–X bonds has not been developed yet. Secondly, direct carboxylation breaking unactivated C–H bonds has hardly been developed. With simultaneous development of the photocatalyzed directing group (DG)-assisted or DG-free C–H activation reactions, this major field of unbiased C–H carboxylation drew attention. Thirdly, in spite of noteworthy discoveries on carboxylation reactions of alkenes, the substrates are mostly limited to styrenes or activated alkenes, as the intermediate radicals or anions at benzylic or α -position are stabilized. So far, the normal unbiased alkenes have never been used for the same. Selective carboxylation of unbiased alkenes demands further improvements and remains a long-cherished goal. Fourthly, SET activation of CO₂ has seldom been executed compared to two-electron activation of substrate. Though, the former is achievable with

photocatalysis in selective cases, finding a general method and a wide use of the same has not been discovered till date. Last but not the least, after all these photocatalytic developments, the techniques are still at developing age as of now, so they are only apt for bench scale synthesis and far from industrial use. Few times, continuous-flow techniques have shown the potential to be applicable in large scale. Attention nowadays also is devoted towards further improvement of the strategies so that these could be implemented in strategic sector.

In brief, notable breakthroughs for sustainable photocatalytic carboxylation have been discovered in the past few years which strengthened the effort of green and sustainable developments. Despite the need of immense improvements to be accepted in strategic sector, the developments definitely paved the path. To achieve “low-carbon economy”, this modern technique would obviously widen the scopes and once it is apt for industrial scale, the real essence of “waste to wealth” transformation would be experienced to accomplish the synthesis of value-added materials from waste greenhouse gas CO₂.

I.7. Transformation of carboxylic acids

As discussed earlier, carboxylic acids are ubiquitous in various natural products, fine chemicals, and synthetic drugs. Besides, carboxylic acids (both aliphatic and aromatic) are very important building blocks in organic synthesis to conduct variety of transformations to produce diverse range of compounds.



Scheme 26. Transformation of carboxylic acid via different reaction modes.

Being readily available and non-toxic, carboxylic acids are often used as starting materials, substrate precursor, synthetic intermediates. Industrially also, carboxylic acids are used as bulk chemical to synthesize solvents, pharmaceuticals, or agrochemicals. In addition to commonly established text-book methodologies, carboxylic acids can be obtained from reaction between available substrates and gaseous CO₂ utilizing the photocatalytic strategies, as we discussed in detail and further could be used as versatile substrate to afford new C–C bond formations. If we summarize the recent developments of transformations from carboxylic acids, it could be distinguished as following divisions based on the nature of reactivity. Those are, a) carboxy group acting as chemo- and regioselective leaving group in the form of traceless gaseous CO₂ via decarboxylation giving rise to new C–C bonds (decarboxylative cross-coupling reactions), b) carboxy group acting as directing group for selective C–H functionalization, without decarboxylation, c) carboxy group as traceless directing group giving C–H functionalization and decarboxylation simultaneously, and d) carboxylic acid leading towards lactone formation via C–H activation or iodolactonization with alkene (**Scheme 26**). As substantial work has been executed in each field, we would briefly discuss these to get an overall understanding.

I.7.1. Decarboxylative reactions of carboxylic acids

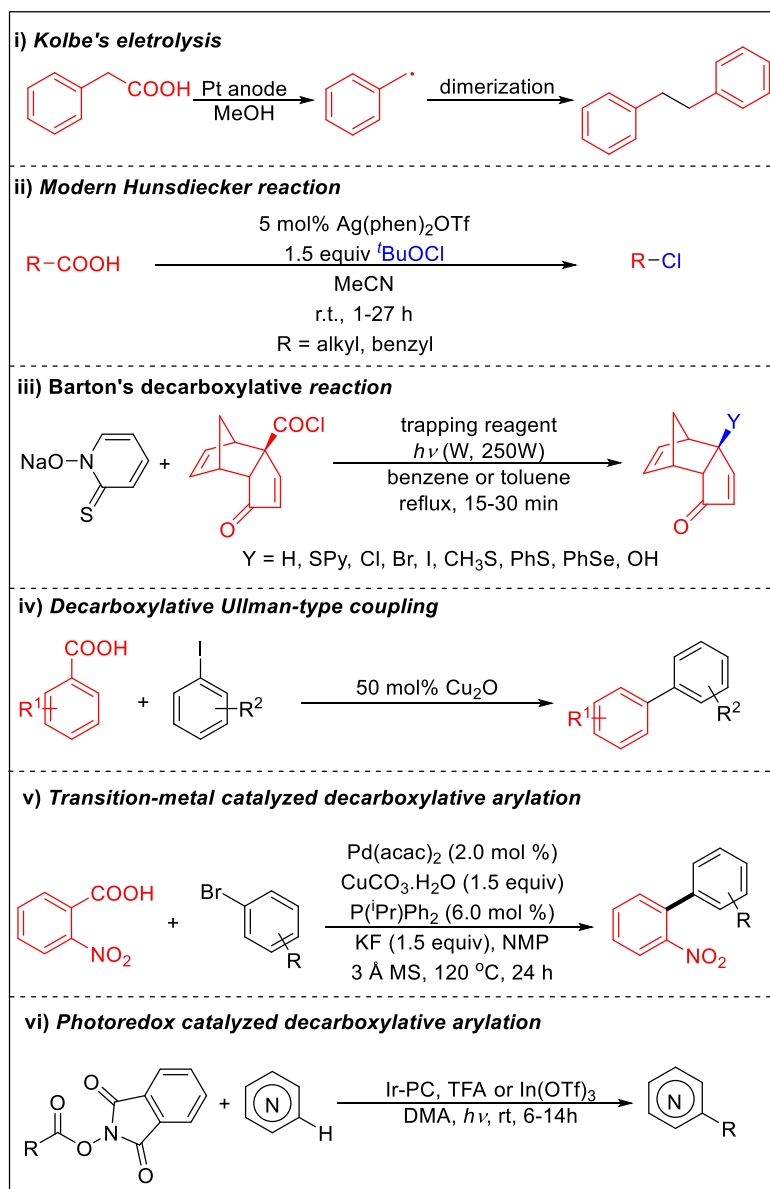
Carboxylic acids have been extensively used as synthons for new C–C bond formation via decarboxylation methods.⁷³ As mentioned earlier, easily removable by-product i.e., gaseous CO₂ which is non-toxic too, makes these approach user-friendly and practical. We would like to take an overview of the developments of decarboxylation reactions over the years.

I.7.1.1. History of decarboxylative reactions

Historically, Kolbe electrolysis from 1848 is the oldest decarboxylative reaction for C–C bond formation.⁷⁴ Here, on electrochemical condition, radicals are generated via decarboxylation of carboxylic acids and subsequent dimerization gives the product (**Scheme 27, i**).⁷⁵ In addition to the requirement of specialized laboratory equipment for the reaction, the scope of the reactions is restricted to only homocouplings. Therefore, executing cross-couplings via electrolysis is hardly achievable only in selected cases. Hunsdiecker reaction is another classic decarboxylative reaction where oxidative decarboxylation is enabled by stoichiometric amount of silver salt giving rise to alkyl radicals and those are trapped by halides.⁷⁶ Recent progresses have shown that catalytic amount of metal salts can lead to decarboxylative halogenation (**Scheme 27, ii**).⁷⁷ Therefore, Barton decarboxylation is another

Photocarboxylation Reactions with CO₂ and Transformation of Carboxylic Acids: Journey towards Sustainability

example to give decarboxylative reduction of carboxylic acids.⁷⁸ Here, activators (such as N-hydroxypyridine-2-thione, AIBN) are required to activate carboxy groups and toxic tin hydrides are used as H[•] source.⁷⁹



Scheme 27. History of decarboxylation reactions.

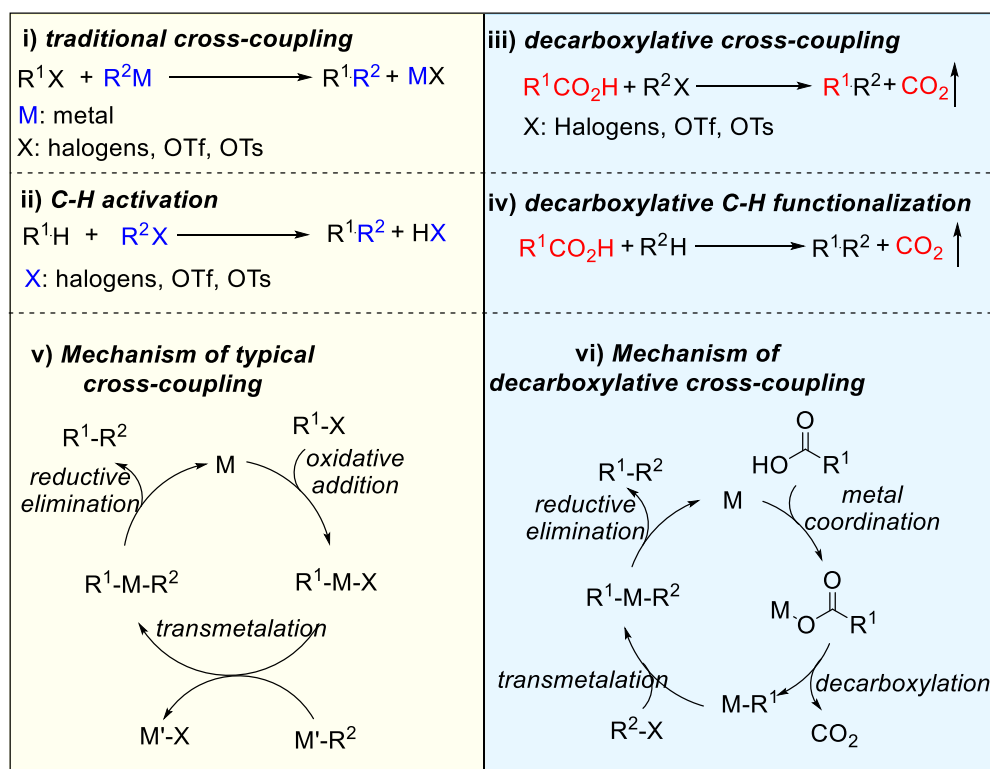
This method is mainly used in the last defunctionalization step at the end of any natural product synthesis (**Scheme 27, iii**). Copper-catalyzed Ullman decarboxylative cross-coupling discovered by Nilsson in 1966 for C(sp²)-C(sp²) bond formations paved the way for modern TM catalyzed decarboxylation reactions (**Scheme 27, iv**).⁸⁰ From the beginning of twenty first century, with huge surge of TM catalysis, decarboxylative cross-coupling have been performed with TM catalysis at elevated temperature (**Scheme 27, v**).^{73a, 73b, 73d} Decarboxylative Heck-

type olefinations⁸¹ or Suzuki reactions^{73c, 82} have extensively been studied. Owing to the pitfalls of this method and with the development of photoredox catalysis, photochemical decarboxylative cross-couplings have been developed in the last few years (Scheme 27, vi).⁸³

In the successive section, we would have a comparative discussion of these two recent strategies.

I.7.1.2. Recent decarboxylative strategies: a comparative overview on TM catalyzed and photocatalyzed decarboxylative reactions

As stated earlier, in the last two decades, huge research has been performed for the development of TM catalyzed decarboxylative cross-couplings and emerged as a modern strategy alternative to regular cross-coupling or C–H functionalization reactions (Scheme 28, iii). Here, in place of aryl halides (Scheme 28, i), aryl carboxylic acids give rise to formation of organometallic species (Scheme 28, vi). Here, unlike the cross-coupling or C–H activation, a mechanistically distinct decarboxylative metalation occurs in lieu of oxidative addition or transmetalation to form organometallic species which subsequently couple with electrophiles affording the desired products after reductive elimination (Scheme 28, vi).



Scheme 28. Comparative overview on TM catalyzed and photocatalyzed decarboxylative reactions.

However, these approaches are usually limited to aryl carboxylic acids; alkyl acids which are more abundant in biomass, does not satisfy these conditions. Besides, requirement of high temperatures and use of metal catalysts leave these methods with ample scope of improvements.

To fulfil the voids, therefore, photochemical alternatives for decarboxylative cross-couplings have been emerged rapidly. Using light over conventional heat as the energy source delivers milder reaction conditions. Despite developments of some UV-light mediated decarboxylation reactions, decomposition issue of various substrates and formation of several bi products are major drawbacks. Nowadays, radicals are formed from carboxylic acids under visible-light photocatalysis. Contrary to TM catalyzed strategy, this strategy mainly deals with radical mechanism where no organometallic species is involved. And, mainly for this reason, photocatalytic strategy is apt for decarboxylative couplings from alkyl acids as their corresponding radicals are more stabilized than the aryl ones. On the other hand, metal-catalyzed strategy is the best one for aryl carboxylic acids.

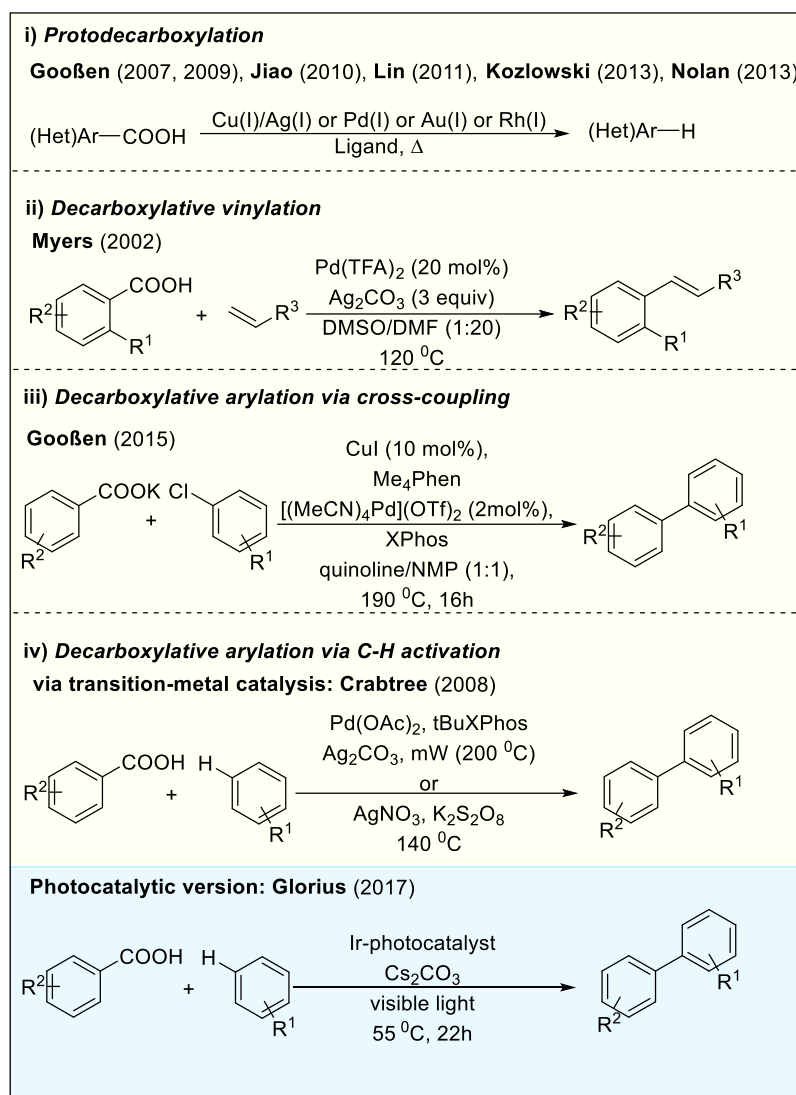
For example, different type of decarboxylative transformations have been shown schematically for both aromatic and aliphatic carboxylic acids.

Aromatic carboxylic acids

As discussed, aromatic carboxylic acids mainly undergo decarboxylation under TM catalyzed conditions. Representative examples of different types of transformations have been presented here with respective years of discovery. As we see, protodecarboxylation of aryl carboxylic acid was discovered by Gooßen⁸⁴, Lin⁸⁵, Kozłowski⁸⁶, Nolan⁸⁷, Jiao⁸⁸ groups with different metals (**Scheme 29, i**). Decarboxylative Heck type vinylation was discovered by the Myers group (**Scheme 29, ii**).⁸⁹ When it comes to decarboxylative arylation by cross-coupling approach, Gooßen's work⁹⁰ is notably important (**Scheme 29, iii**). Decarboxylative arylation by direct C-H activation was performed firstly by Crabtree in 2008 (**Scheme 29, iv**),⁹¹ where the photocatalytic version of this under lower temperature and milder condition was first discovered by the Glorius group⁹² in 2017 (**Scheme 29, iv**).

Alkyl carboxylic acids

As per the reports available, decarboxylation of aliphatic carboxylic acids has been developed more by photoredox catalysis.



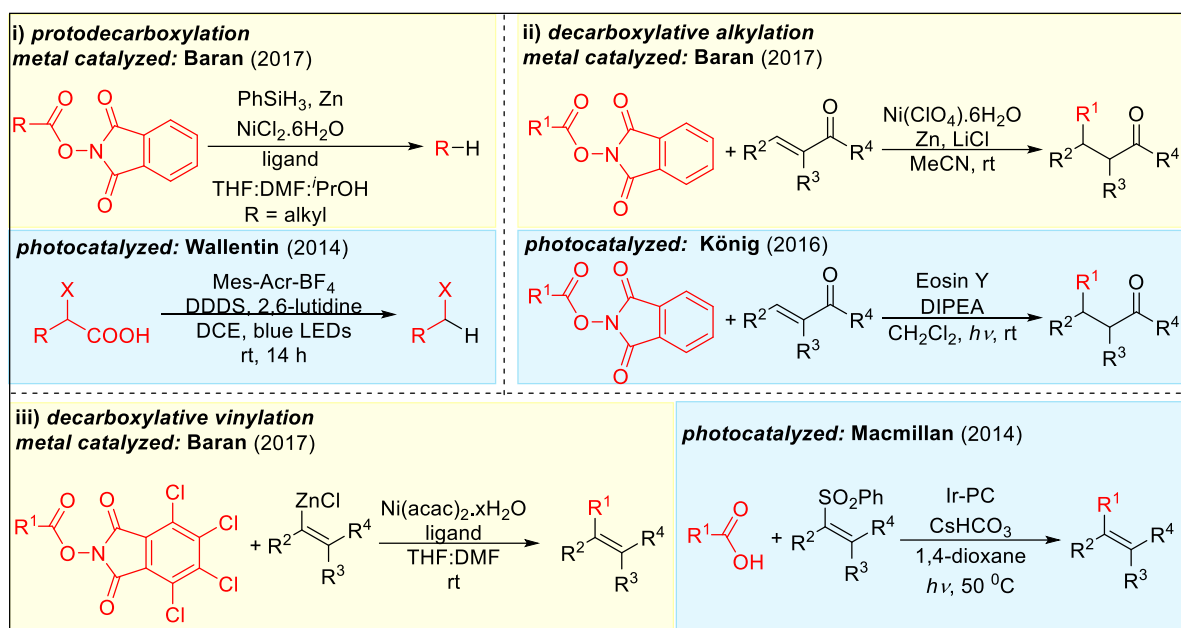
Scheme 29. Decarboxylative reactions of aromatic carboxylic acids.

Some of the representative examples have been shown here. For protodecarboxylation, the metal-catalyzed version is by the Baran group⁹³ whereas Wallentin⁹⁴ showed the photochemical path (**Scheme 30, i**). Similarly, alkylation was performed both by metal-⁹³ and photoredox⁹⁵ catalyzed methods (**Scheme 30, ii**). An example of decarboxylative alkenylation is given where Baran group⁹⁶ performed by via metal catalysis, whereas Macmillan⁹⁷ developed the photocatalytic path (**Scheme 30, iii**).

***α*-keto carboxylic acids**

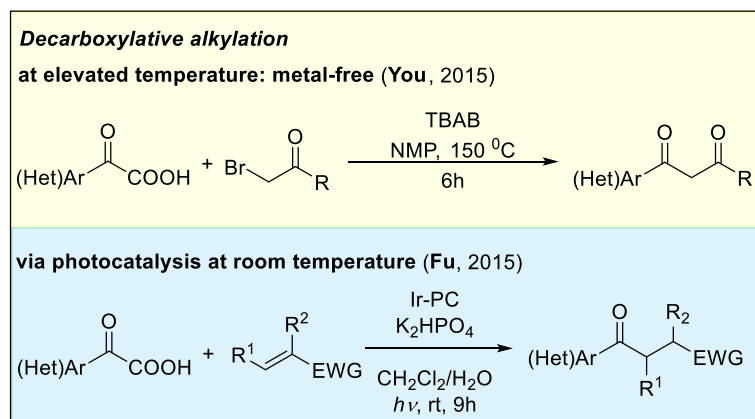
α-keto carboxylic acids are the other type which has extensively used for decarboxylative transformations. As these are very prone towards decarboxylation, additional to of metal catalyzed methods, photocatalytic or metal-free methods have also been developed successfully. For example, decarboxylative alkylation with *α*-keto carboxylic acids have been

Photocarboxylation Reactions with CO₂ and Transformation of Carboxylic Acids: Journey towards Sustainability



Scheme 30. Decarboxylative reactions of alkyl carboxylic acids.

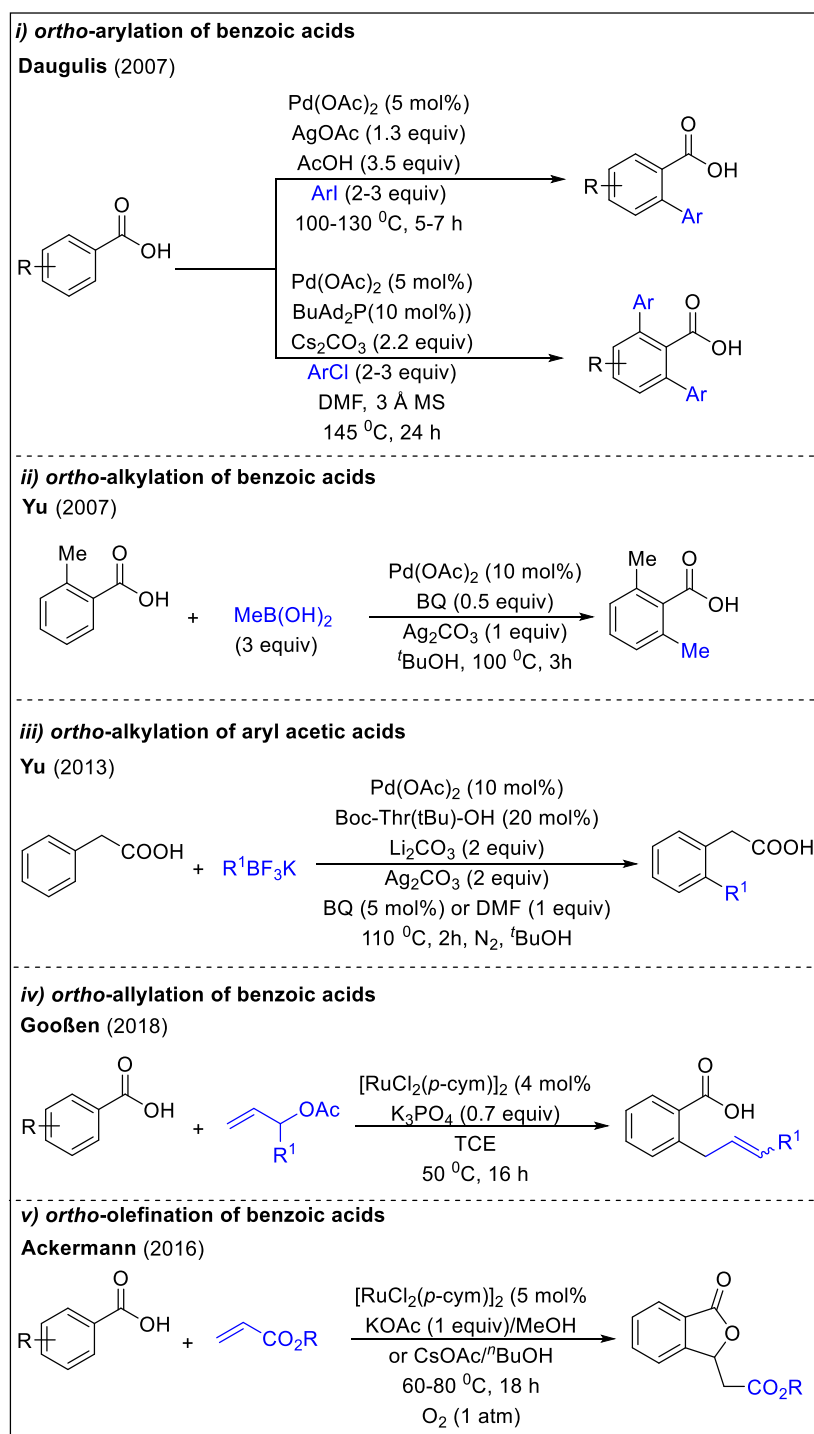
performed by metal-free condition in very high temperature (**Scheme 31**).⁹⁸ The same has been performed by reaction between the acid and activated alkene via photocatalysis (**Scheme 31**).⁹⁹ More examples of this type would be discussed in Chapter IV.



Scheme 31. Decarboxylative reactions of α -keto carboxylic acids.

I.7.2. Carboxy groups as directing group in C–H activation, without decarboxylation

Directly functionalizing carbon–hydrogen bonds are always sought-after target for increasing structural complexity.¹⁰⁰ Due to the inertness and high bond energy of C–H bonds and difficulty to achieve regio- and chemoselectivity between similar C–H bonds, the process did not meet high success till 2000. Over the last two decades, a huge improvement has been performed in C–H activation field.¹⁰¹



Scheme 32. Carboxy groups as directing group in C–H activation, without decarboxylation.

When it comes to using carboxylic acids as synthons, there are many electrophilic and nucleophilic displacement reactions, which essentially depend on the inherent reactivity of the functional group. With the development of C–H activation, the same has been efficiently applied for functionalizing carboxylic acids.¹⁰² Contrary to classical approaches, prefucionalization step can be completely avoided in C–H activation and provides a more

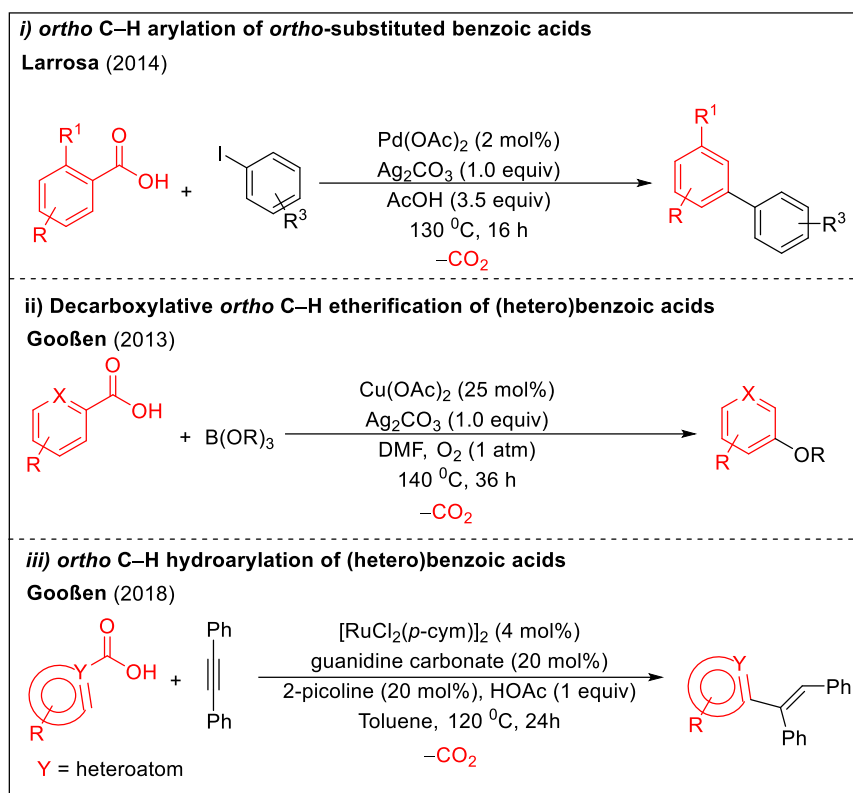
atom-efficient and straightforward approach in the field of organic synthesis. To improve chemo- and regioselectivity between two otherwise indistinguishable C–H bonds, installation of directing groups (DG), which coordinate with TMs and invites the appropriately positioned C–H bond to be activated, are required. Carboxylic acids also have been protected with various directing groups and different functional moieties have been incorporated at different positions of carboxylic acid. But, as far as directing groups are concerned, there also two additional steps are required i.e., i) DG incorporation before C–H activation, ii) postfunctionalization DG removal. Alternatively, carboxylic acids have directly been used where the carboxy group itself acted as directing groups for selective C–H functionalization. Here, aryl carboxy group coordinates with the transition metal catalysts and mostly the *ortho* C–H group is activated to provide *ortho*-substituted aryl carboxylic acid. Some representative examples have been shown in the **Scheme 32**, those are, *ortho*-arylation of benzoic acids by Daugulis¹⁰³ (**Scheme 32, i**), *ortho*-alkylation of benzoic acids¹⁰⁴ (**Scheme 32, ii**) and aryl acetic acids(**Scheme 32, iii**)¹⁰⁵ by Yu, *ortho*-allylation by Gooßen¹⁰⁶ (**Scheme 32, iv**), and *ortho*-olefination by Ackermann¹⁰⁷ (**Scheme 32, iv**).

I.7.3. Carboxy group as traceless directing group giving C-H functionalization and decarboxylation simultaneously

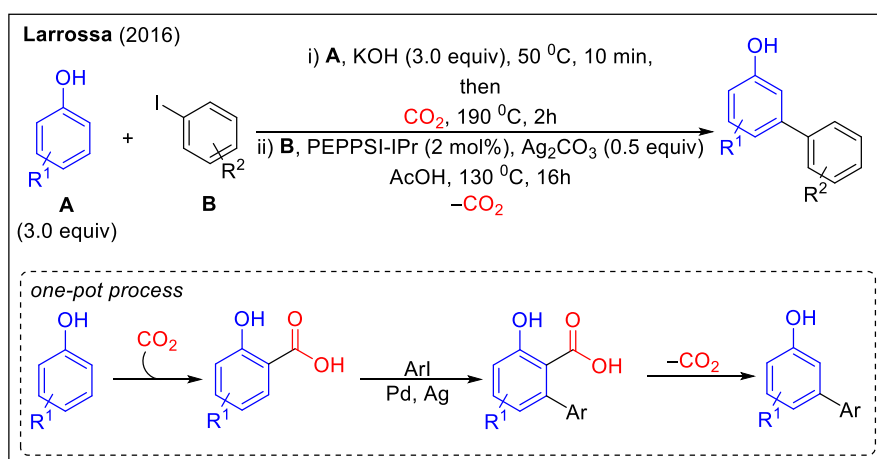
Continuing with previous section, recently carboxylic acids have been exploited many times as traceless directing groups, where after the anticipated transformation by carboxylate-directed C–H activation, the carboxy group leaves via decarboxylation. First, Larrosa performed *ortho*-arylation of 2-substituted aryl carboxylic acids via Pd catalysis with Ag₂CO₃ as the oxidant (**Scheme 33, i**).¹⁰⁸ Another two examples have been shown where Gooßen group executed *ortho*-etherification (**Scheme 33, ii**)¹⁰⁹ and olefination (**Scheme 33, iii**)¹¹⁰ with Cu and Ru catalysis, respectively.

Larrosa and co-workers extended their methodology to develop a very interesting approach for *meta*-arylation of phenols with help of carboxylic acid as traceless directing group. They in situ formed salicylic acids via base mediated reaction with gaseous CO₂(**Scheme 34**).¹¹¹ And then in one-pot fashion, they performed *ortho*-arylation of salicylic acid via carboxy group directed PEPPSI-IPr catalyzed C–H activation with successive protodecarboxylation furnishing the *meta*-arylated. Thus, carboxy group can deliver distal C–H activation indirectly

with the help of its intrinsic property to undergo protodecarboxylation under metal-catalyzed conditions.



Scheme 33. Carboxy group as traceless directing group giving C–H functionalization and decarboxylation simultaneously.



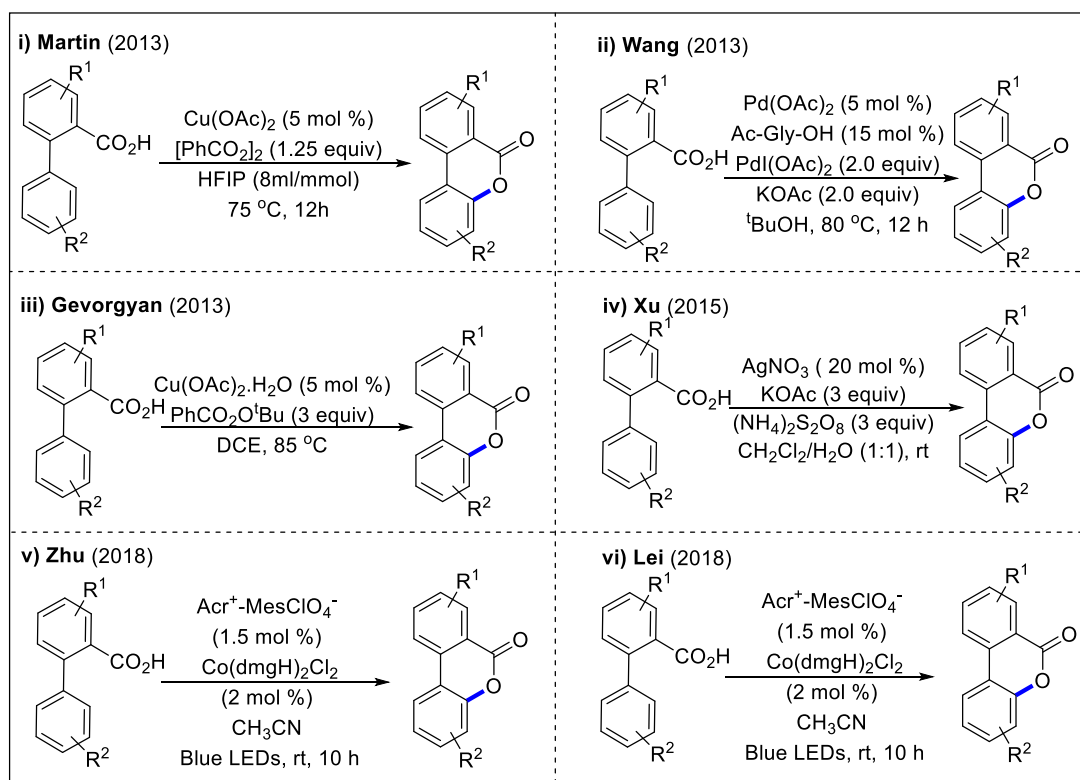
Scheme 34. meta-arylation of phenols by employing carboxy group as traceless directing group.

I.7.4. Carboxylic acid leading towards lactone formation via C-H activation

In the last decade, with the huge development of C–H activation, carboxylic acids have extensively been used as nucleophile or radical precursor for synthesizing lactones via intramolecular C–H activation of a pendant C–H bond.

Transition-metal catalyzed C(sp²)–H lactonization

Biaryl lactone derivatives are used as precursor of many natural products and found as key structural motifs in many pharmaceuticals and natural products. Martin first developed copper-catalyzed method for carboxyl group directed C–O cyclization via C–H activation to construct biaryl lactone with using benzoyl peroxide (BPO) as oxidant (**Scheme 35, i**).¹¹² Almost at the similar time, Wang developed Pd(II)/Pd(IV)-catalyzed method (**Scheme 35, ii**)¹¹³, Gevorgyan reported similar Cu-catalyzed method (**Scheme 35, iii**).¹¹⁴ The Xu group in



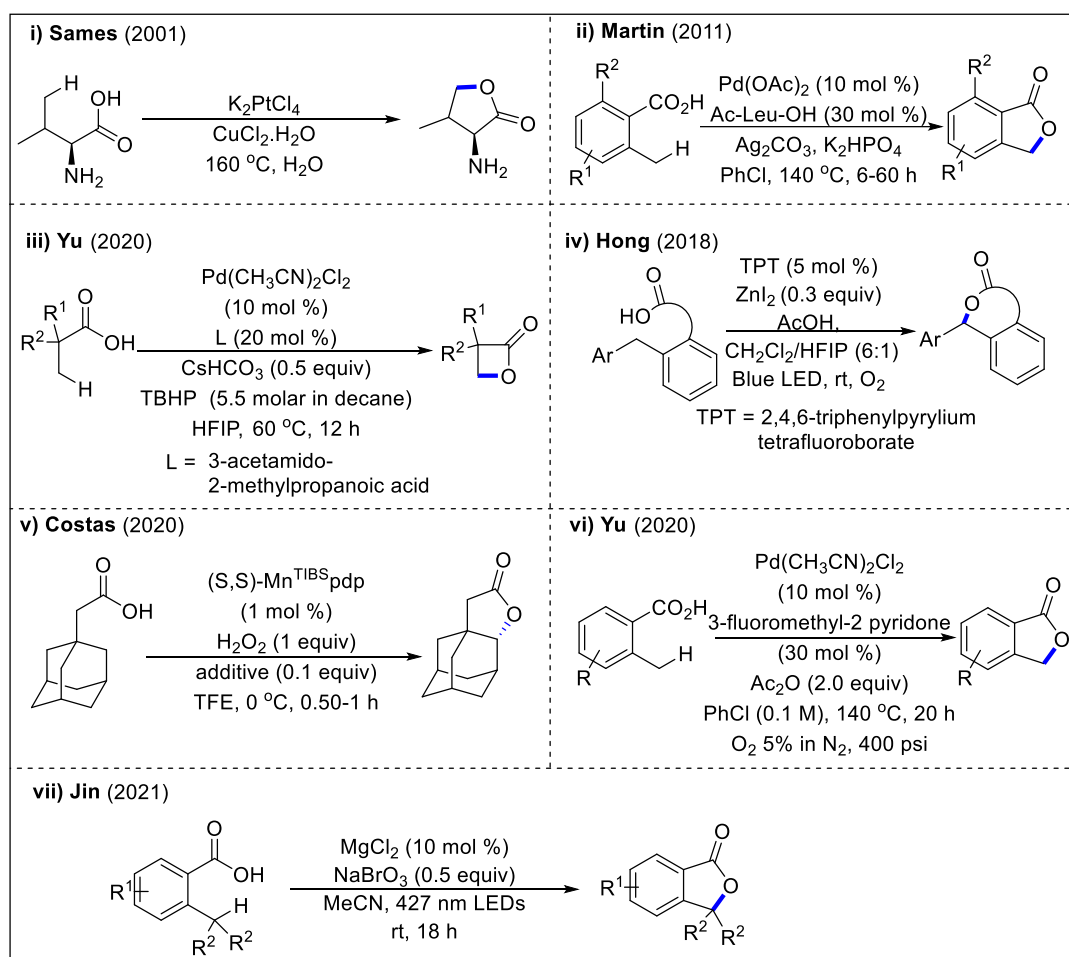
Scheme 35. Metal catalyzed C(sp²)–H lactonization.

2015, disclosed C(sp²)–H activation for same transformation in presence of silver catalyst and (NH₄)₂S₂O₈ as oxidant in open flask condition at room temperature (**Scheme 35, iv**).¹¹⁵ Subsequently, Zhu reported external oxidant free, mild, efficient Co/photoredox dual catalytic methodology (**Scheme 35, v**).¹¹⁶ At the same time, independently Lei group also reported

exactly same strategy via Co/photoredox dual catalysis (**Scheme 35, vi**).¹¹⁷ Several other reports are also available for this transformation under metal catalysis.

Metal catalyzed C(sp³)-H lactonization

The Sames group in 2001, synthesized lactone from L-valine in presence of aqueous K₂PtCl₄ and stoichiometric CuCl₂ as oxidant (**Scheme 36, i**).¹¹⁸ In 2011, Martin *et al.* reported Pd catalyzed, *N*-acyl protected amino acid assisted benzolactone formation from 2-alkyl benzoic acid derivatives (**Scheme 36, ii**).¹¹⁹ In 2020, Yu *et al.* developed lactonization of aliphatic acids through β-C(sp³)-H activation (**Scheme 36, iii**).¹²⁰ Visible light mediated γ-/δ-lactonization was disclosed by Hong *et al.* using 2,4,6-triphenylpyrylium tetrafluoroborate as



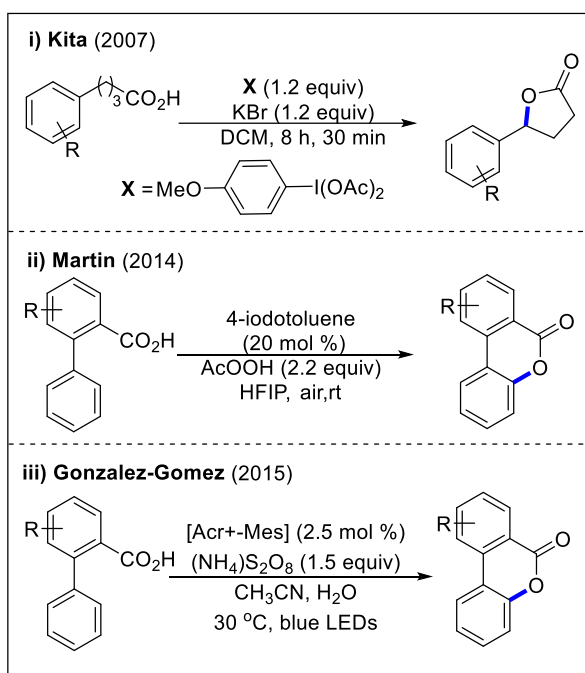
Scheme 36. Metal catalyzed C(sp³)-H lactonization.

photocatalyst (**Scheme 36, iv**).¹²¹ The Costas group reported Mn-catalyzed carboxylic acid directed γ-C-H oxidation to construct γ-lactone in high enantiomeric excess (up to 99%) (**Scheme 36, v**).¹²² The Yu group in 2020, reported lactonization of 2-methyl benzoic acid through Pd(II)/Pd(0) catalysis (**Scheme 36, vi**).¹²³ Recently a practical, mild, visible light

mediated magnesium catalyzed C(sp³)-H lactonization protocol from easily available 2-alkyl benzoic acid has been developed by the Jin group (**Scheme 36, vii**).¹²⁴

Metal free lactonization

In 2007, the Kita group synthesized aryl lactones from benzoic acids and carboxylic acids using combination of hypervalent iodine with KBr (**Scheme 37, i**).¹²⁵ Continuing with their own metal-catalyzed lactonization, the Martin's group reported a mild, metal free protocol to synthesis of benzolactones from 2-aryl benzoic acids with using 4-iodotoluene as catalyst and stoichiometric amount of AcOOH as oxidant in HFIP solvent (**Scheme 37, ii**).¹²⁶ A metal free, photocatalyzed dehydrogenative lactonization was reported by Gonzalez-Gomez (**Scheme 37, iii**).¹²⁷

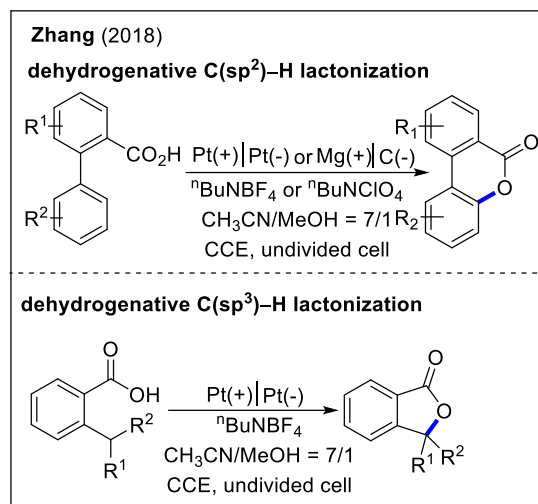


Scheme 37. Metal free lactonization.

Electrochemical lactonization

In 2018, the Zhang group disclosed an electrochemical strategy toward synthesis of dibenzolactones from 2-aryl benzoic acids via C(sp²)-H activation and 5-membered lactone from 2-alkyl benzoic acids via C(sp³)-H activation (**Scheme 38**). They used metal free, oxidant free electrocatalytic condition with Pt as both the electrodes and ⁿBuNBF₄ as redox-mediator.¹²⁸

As electrocatalysis is experiencing a renaissance during present days in the synthetic organic chemistry field, a lot more developments on single electron activation of carboxylic acids, some acylation reactions are expected to come down the line.



Scheme 38. Electrochemical lactonization.

I.8. Conclusion

As we have discussed in this chapter, carboxylic acids could be synthesized from organic substrates using gaseous CO₂, which is a widely abundant, non-toxic, cheap waste material evolved from fossil fuel combustion and the industries. Substituting the available TM catalytic methods in high temperature, photocatalysis has been able to afford carboxylation under atmospheric or balloon pressure of CO₂ via milder techniques by removing toxic metal wastes and under ambient temperature. Diverse range of carboxylic acids have been prepared from different types of substrates cleaving C–H/heteroatom bonds with photocatalysis. A chronological development has been portrayed here to reach toward more sustainable methodology. First, the TM catalysis has been merged with photoredox catalysis to remove the use of toxic metal reductants (Zn, Mn, Et₂Zn) by using organic non-toxic reductants (HEH, DIPEA etc.) and to lower the reaction temperature to room temperature. Secondly, use of TM catalysts has also been stopped with sole use of photoredox catalysis with using just the photocatalysts, where sometimes even the organic reducing agents are also not required. Thirdly, any type of catalyst-free photocatalysis for carboxylation reactions has been discussed. Upon successful synthesis of carboxylic acids via these mild carboxylation approaches, we have briefly reviewed the reactivities of carboxylic acids towards diverse directions. Many valuable organic transformations have been performed via decarboxylative coupling of

carboxylic acids. Here also, a comparative and critical analysis has been done between TM catalyzed and photocatalyzed decarboxylation techniques. Then, carboxy groups have been used as directing groups in C–H activation where two types of reaction have been observed, one is synthesis of *ortho*-substituted aryl carboxylic acids and another one is subsequent removal of carboxy group via decarboxylation instantaneously after the C–H activation. Finally, lactone formation following different techniques via C–H activation has been discussed where metal catalyzed, metal-free, photo- and electrocatalyzed techniques have been shown as examples.

I.9. References

- (1) (a) Cassia, R.; Nocioni, M.; Correa-Aragunde, N.; Lamattina, L. *Front. Plant Sci.* **2018**, *9*; (b) Anderson, T. R.; Hawkins, E.; Jones, P. D. *Endeavour* **2016**, *40*, 178-187; (c) Lamb, W. F.; Wiedmann, T.; Pongratz, J.; Andrew, R.; Crippa, M.; Olivier, J. G. J.; Wiedenhofer, D.; Mattioli, G.; Khourdajie, A. A.; House, J.; Pachauri, S.; Figueroa, M.; Saheb, Y.; Slade, R.; Hubacek, K.; Sun, L.; Ribeiro, S. K.; Khennas, S.; de la Rue du Can, S.; Chapungu, L.; Davis, S. J.; Bashmakov, I.; Dai, H.; Dhakal, S.; Tan, X.; Geng, Y.; Gu, B.; Minx, J. *Environ. Res. Lett.* **2021**, *16*, 073005.
- (2) Durojaye, O.; Laseinde, T.; Oluwafemi, I. In *A Descriptive Review of Carbon Footprint*, Human Systems Engineering and Design II, Cham, 2020//; Ahram, T., Karwowski, W., Pickl, S., Taiar, R., Eds. Springer International Publishing: Cham, 2020; pp 960-968.
- (3) (a) Navarro-Jaén, S.; Virginie, M.; Bonin, J.; Robert, M.; Wojcieszak, R.; Khodakov, A. Y. *Nat. Rev. Chem.* **2021**, *5*, 564-579; (b) Tackett, B. M.; Gomez, E.; Chen, J. G. *Nat. Catal.* **2019**, *2*, 381-386; (c) Xie, S.; Zhang, W.; Lan, X.; Lin, H. *ChemSusChem* **2020**, *13*, 6141-6159; (d) Porosoff, M. D.; Yan, B.; Chen, J. G. *Energy Environ. Sci.* **2016**, *9*, 62-73; (e) Arakawa, H.; Aresta, M.; Armor, J. N.; Barteau, M. A.; Beckman, E. J.; Bell, A. T.; Bercaw, J. E.; Creutz, C.; Dinjus, E.; Dixon, D. A.; Domen, K.; DuBois, D. L.; Eckert, J.; Fujita, E.; Gibson, D. H.; Goddard, W. A.; Goodman, D. W.; Keller, J.; Kubas, G. J.; Kung, H. H.; Lyons, J. E.; Manzer, L. E.; Marks, T. J.; Morokuma, K.; Nicholas, K. M.; Periana, R.; Que, L.; Rostrup-Nielson, J.; Sachtler, W. M. H.; Schmidt, L. D.; Sen, A.; Somorjai, G. A.; Stair, P. C.; Stults, B. R.; Tumas, W. *Chem. Rev.* **2001**, *101*, 953-996; (f) Hull, J. F.; Himeda, Y.; Wang, W.-H.; Hashiguchi, B.; Periana, R.; Szalda, D. J.; Muckerman, J. T.; Fujita, E. *Nature Chemistry* **2012**, *4*, 383-388.
- (4) (a) Federsel, C.; Jackstell, R.; Beller, M. *Angew. Chem. Int. Ed.* **2010**, *49*, 6254-6257; (b) Yu, K. M. K.; Curcic, I.; Gabriel, J.; Tsang, S. C. E. *ChemSusChem* **2008**, *1*, 893-899; (c) Hicks, J. C.; Drese, J. H.; Fauth, D. J.; Gray, M. L.; Qi, G.; Jones, C. W. *J. Am. Chem. Soc.* **2008**, *130*, 2902-2903; (d) Banerjee, R.; Phan, A.; Wang, B.; Knobler, C.; Furukawa, H.; O'Keeffe, M.; Yaghi Omar, M. *Science* **2008**, *319*, 939-943; (e) Fiorani, G.; Guo, W.; Kleij, A. W. *Green Chem.* **2015**, *17*, 1375-1389; (f) Grignard, B.; Gennen, S.; Jérôme, C.; Kleij, A. W.; Detrembleur, C. *Chem. Soc. Rev.* **2019**, *48*, 4466-4514.

- (5) Maag, H. In *Prodrugs: Challenges and Rewards Part 1*, Stella, V. J., Borchardt, R. T., Hageman, M. J., Oliyai, R., Maag, H., Tilley, J. W., Eds. Springer New York: New York, NY, 2007; pp 703-729.
- (6) (a) Hu, X.-Q.; Liu, Z.-K.; Hou, Y.-X.; Gao, Y. *iScience* **2020**, *23*, 101266; (b) Manna, K.; Begam, H. M.; Samanta, K.; Jana, R. *Org. Lett.* **2020**, *22*, 7443-7449; (c) Nandi, S.; Mondal, S.; Jana, R. *iScience* **2022**, *25*, 104341; (d) Begam, H. M.; Nandi, S.; Jana, R. *Chem. Sci.* **2022**, *13*, 5726-5733.
- (7) (a) Modak, A.; Bhanja, P.; Dutta, S.; Chowdhury, B.; Bhaumik, A. *Green Chem.* **2020**, *22*, 4002-4033; (b) Artz, J.; Müller, T. E.; Thenert, K.; Kleinekorte, J.; Meys, R.; Sternberg, A.; Bardow, A.; Leitner, W. *Chem. Rev.* **2018**, *118*, 434-504; (c) Davies, J.; Lyonnet, J. R.; Zimin, D. P.; Martin, R. *Chem* **2021**, *7*, 2927-2942.
- (8) (a) Tsuji, Y.; Fujihara, T. *Chem. Commun.* **2012**, *48*, 9956-9964; (b) Yu, D.; Teong, S. P.; Zhang, Y. *Coord. Chem. Rev.* **2015**, *293-294*, 279-291; (c) Börjesson, M.; Moragas, T.; Gallego, D.; Martin, R. *ACS Catal.* **2016**, *6*, 6739-6749; (d) Tortajada, A.; Juliá-Hernández, F.; Börjesson, M.; Moragas, T.; Martin, R. *Angew. Chem. Int. Ed.* **2018**, *57*, 15948-15982; (e) Yan, S.-S.; Fu, Q.; Liao, L.-L.; Sun, G.-Q.; Ye, J.-H.; Gong, L.; Bo-Xue, Y.-Z.; Yu, D.-G. *Coord. Chem. Rev.* **2018**, *374*, 439-463; (f) Ran, C.-K.; Liao, L.-L.; Gao, T.-Y.; Gui, Y.-Y.; Yu, D.-G. *Curr. Opin. Green Sustain. Chem.* **2021**, *32*, 100525.
- (9) (a) Twilton, J.; Le, C.; Zhang, P.; Shaw, M. H.; Evans, R. W.; MacMillan, D. W. C. *Nat. Rev. Chem.* **2017**, *1*, 0052; (b) Chatterjee, T.; Iqbal, N.; You, Y.; Cho, E. J. *Acc. Chem. Res.* **2016**, *49*, 2284-2294; (c) Majek, M.; Jacobi von Wangelin, A. *Acc. Chem. Res.* **2016**, *49*, 2316-2327; (d) Goddard, J.-P.; Ollivier, C.; Fensterbank, L. *Acc. Chem. Res.* **2016**, *49*, 1924-1936; (e) Fabry, D. C.; Rueping, M. *Acc. Chem. Res.* **2016**, *49*, 1969-1979; (f) Millet, A.; Cesana, P. T.; Sedillo, K.; Bird, M. J.; Schlau-Cohen, G. S.; Doyle, A. G.; MacMillan, D. W. C.; Scholes, G. D. *Acc. Chem. Res.* **2022**, *55*, 1423-1434; (g) Golden, D. L.; Suh, S.-E.; Stahl, S. S. *Nat. Rev. Chem.* **2022**, *6*, 405-427; (h) Ryu, K. A.; Kaszuba, C. M.; Bissonnette, N. B.; Oslund, R. C.; Fadeyi, O. O. *Nat. Rev. Chem.* **2021**, *5*, 322-337; (i) Romero, N. A.; Nicewicz, D. A. *Chem. Rev.* **2016**, *116*, 10075-10166; (j) Prier, C. K.; Rankic, D. A.; MacMillan, D. W. C. *Chem. Rev.* **2013**, *113*, 5322-5363; (k) Pitre, S. P.; Overman, L. E. *Chem. Rev.* **2022**, *122*, 1717-1751; (l) Corbin, D. A.; Miyake, G. M. *Chem. Rev.* **2022**, *122*, 1830-1874.
- (10) Barber, J.; Tran, P. D. *J. R. Soc. Interface* **2013**, *10*, 20120984.

- (11) Shimomaki, K.; Murata, K.; Martin, R.; Iwasawa, N. *J. Am. Chem. Soc.* **2017**, *139*, 9467-9470.
- (12) Meng, Q.-Y.; Wang, S.; König, B. *Angew. Chem. Int. Ed.* **2017**, *56*, 13426-13430.
- (13) Bhunia, S. K.; Das, P.; Nandi, S.; Jana, R. *Org. Lett.* **2019**, *21*, 4632-4637.
- (14) Shimomaki, K.; Nakajima, T.; Caner, J.; Toriumi, N.; Iwasawa, N. *Org. Lett.* **2019**, *21*, 4486-4489.
- (15) Liao, L.-L.; Cao, G.-M.; Jiang, Y.-X.; Jin, X.-H.; Hu, X.-L.; Chruma, J. J.; Sun, G.-Q.; Gui, Y.-Y.; Yu, D.-G. *J. Am. Chem. Soc.* **2021**, *143*, 2812-2821.
- (16) Zhu, C.; Zhang, Y.-F.; Liu, Z.-Y.; Zhou, L.; Liu, H.; Feng, C. *Chem. Sci.* **2019**, *10*, 6721-6726.
- (17) Yan, S.-S.; Wu, D.-S.; Ye, J.-H.; Gong, L.; Zeng, X.; Ran, C.-K.; Gui, Y.-Y.; Li, J.; Yu, D.-G. *ACS Catal.* **2019**, *9*, 6987-6992.
- (18) Xie, S.-L.; Cui, X.-Y.; Gao, X.-T.; Zhou, F.; Wu, H.-H.; Zhou, J. *Org. Chem. Front.* **2019**, *6*, 3678-3682.
- (19) Jin, Y.; Toriumi, N.; Iwasawa, N. *ChemSusChem* **2022**, *15*, e202102095.
- (20) Fan, Z.; Chen, S.; Zou, S.; Xi, C. *ACS Catal.* **2022**, *12*, 2781-2787.
- (21) Masuda, Y.; Ishida, N.; Murakami, M. *J. Am. Chem. Soc.* **2015**, *137*, 14063-14066.
- (22) Ishida, N.; Masuda, Y.; Uemoto, S.; Murakami, M. *Chem. Eur. J.* **2016**, *22*, 6524-6527.
- (23) Juliá-Hernández, F.; Moragas, T.; Cornella, J.; Martin, R. *Nature* **2017**, *545*, 84-88.
- (24) Sahoo, B.; Bellotti, P.; Juliá-Hernández, F.; Meng, Q.-Y.; Crespi, S.; König, B.; Martin, R. *Chem. Eur. J.* **2019**, *25*, 9001-9005.
- (25) Ishida, N.; Masuda, Y.; Imamura, Y.; Yamazaki, K.; Murakami, M. *J. Am. Chem. Soc.* **2019**, *141*, 19611-19615.
- (26) (a) Bruckmeier, C.; Lehenmeier, M. W.; Reichardt, R.; Vagin, S.; Rieger, B. *Organometallics* **2010**, *29*, 2199-2202; (b) Lejkowski, M. L.; Lindner, R.; Kageyama, T.; Bódizs, G. É.; Plessow, P. N.; Müller, I. B.; Schäfer, A.; Rominger, F.; Hofmann, P.; Futter, C.; Schunk, S. A.; Limbach, M. *Chem. Eur. J.* **2012**, *18*, 14017-14025; (c) Plessow, P. N.; Weigel, L.; Lindner, R.; Schäfer, A.; Rominger, F.; Limbach, M.; Hofmann, P. *Organometallics* **2013**, *32*, 3327-3338; (d) Hendriksen, C.; Pidko, E. A.; Yang, G.; Schäffner, B.; Vogt, D. *Chem. Eur. J.* **2014**, *20*, 12037-12040; (e) Huguet, N.; Jevtovikj, I.; Gordillo, A.; Lejkowski, M. L.; Lindner, R.; Bru, M.; Khalimon, A. Y.; Rominger, F.; Schunk, S. A.; Hofmann, P.; Limbach, M. *Chem. Eur. J.* **2014**, *20*,

- 16858-16862; (f) Tanaka, S.; Watanabe, K.; Tanaka, Y.; Hattori, T. *Org. Lett.* **2016**, *18*, 2576-2579.
- (27) Lapidus, A. L.; Pirozhkov, S. D.; Koryakin, A. A. *Russ Chem Bull* **1978**, *27*, 2513-2515.
- (28) Gaydou, M.; Moragas, T.; Juliá-Hernández, F.; Martin, R. *J. Am. Chem. Soc.* **2017**, *139*, 12161-12164.
- (29) Fujihara, T.; Horimoto, Y.; Mizoe, T.; Sayyed, F. B.; Tani, Y.; Terao, J.; Sakaki, S.; Tsuji, Y. *Org. Lett.* **2014**, *16*, 4960-4963.
- (30) Takaya, J.; Iwasawa, N. *J. Am. Chem. Soc.* **2008**, *130*, 15254-15255.
- (31) Juhl, M.; Laursen, S. L. R.; Huang, Y.; Nielsen, D. U.; Daasbjerg, K.; Skrydstrup, T. *ACS Catal.* **2017**, *7*, 1392-1396.
- (32) Cao, T.; Yang, Z.; Ma, S. *ACS Catal.* **2017**, *7*, 4504-4508.
- (33) Tani, Y.; Fujihara, T.; Terao, J.; Tsuji, Y. *J. Am. Chem. Soc.* **2014**, *136*, 17706-17709.
- (34) (a) Kawashima, S.; Aikawa, K.; Mikami, K. *Eur. J. Org. Chem.* **2016**, *2016*, 3166-3170; (b) Hayashi, C.; Hayashi, T.; Kikuchi, S.; Yamada, T. *Chem. Lett.* **2014**, *43*, 565-567; (c) Ostapowicz, T. G.; Schmitz, M.; Krystof, M.; Klankermayer, J.; Leitner, W. *Angew. Chem. Int. Ed.* **2013**, *52*, 12119-12123.
- (35) Murata, K.; Numasawa, N.; Shimomaki, K.; Takaya, J.; Iwasawa, N. *Chem. Commun.* **2017**, *53*, 3098-3101.
- (36) Murata, K.; Numasawa, N.; Shimomaki, K.; Takaya, J.; Iwasawa, N. *Front. Chem.* **2019**, *7*.
- (37) Meng, Q.-Y.; Wang, S.; Huff, G. S.; König, B. *J. Am. Chem. Soc.* **2018**, *140*, 3198-3201.
- (38) Hou, J.; Ee, A.; Feng, W.; Xu, J.-H.; Zhao, Y.; Wu, J. *J. Am. Chem. Soc.* **2018**, *140*, 5257-5263.
- (39) Louie, J.; Gibby, J. E.; Farnworth, M. V.; Tekavec, T. N. *J. Am. Chem. Soc.* **2002**, *124*, 15188-15189.
- (40) (a) Koike, T.; Akita, M. *Acc. Chem. Res.* **2016**, *49*, 1937-1945; (b) Courant, T.; Masson, G. *J. Org. Chem.* **2016**, *81*, 6945-6952; (c) Koike, T.; Akita, M. *Chem* **2018**, *4*, 409-437; (d) Pitzer, L.; Schwarz, J. L.; Glorius, F. *Chem. Sci.* **2019**, *10*, 8285-8291; (e) Xu, S.; Chen, H.; Zhou, Z.; Kong, W. *Angew. Chem. Int. Ed.* **2021**, *60*, 7405-7411.
- (41) Ye, J.-H.; Miao, M.; Huang, H.; Yan, S.-S.; Yin, Z.-B.; Zhou, W.-J.; Yu, D.-G. *Angew. Chem. Int. Ed.* **2017**, *56*, 15416-15420.

- (42) Seo, H.; Katcher, M. H.; Jamison, T. F. *Nat. Chem.* **2017**, *9*, 453-456.
- (43) Meng, Q.-Y.; Schirmer, T. E.; Berger, A. L.; Donabauer, K.; König, B. *J. Am. Chem. Soc.* **2019**, *141*, 11393-11397.
- (44) Song, L.; Fu, D.-M.; Chen, L.; Jiang, Y.-X.; Ye, J.-H.; Zhu, L.; Lan, Y.; Fu, Q.; Yu, D.-G. *Angew. Chem. Int. Ed.* **2020**, *59*, 21121-21128.
- (45) Yi, Y.; Xi, C. *Chinese J. Catal.* **2022**, *43*, 1652-1656.
- (46) Seo, H.; Liu, A.; Jamison, T. F. *J. Am. Chem. Soc.* **2017**, *139*, 13969-13972.
- (47) (a) Derosa, J.; Apolinar, O.; Kang, T.; Tran, V. T.; Engle, K. M. *Chem. Sci.* **2020**, *11*, 4287-4296; (b) Qi, X.; Diao, T. *ACS Catal.* **2020**, *10*, 8542-8556; (c) Badir, S. O.; Molander, G. A. *Chem* **2020**, *6*, 1327-1339.
- (48) Yatham, V. R.; Shen, Y.; Martin, R. *Angew. Chem. Int. Ed.* **2017**, *56*, 10915-10919.
- (49) (a) Hou, J.; Ee, A.; Cao, H.; Ong, H.-W.; Xu, J.-H.; Wu, J. *Angew. Chem. Int. Ed.* **2018**, *57*, 17220-17224; (b) Fu, Q.; Bo, Z.-Y.; Ye, J.-H.; Ju, T.; Huang, H.; Liao, L.-L.; Yu, D.-G. *Nat. Commun.* **2019**, *10*, 3592; (c) Zhang, B.; Yi, Y.; Wu, Z.-Q.; Chen, C.; Xi, C. *Green Chem.* **2020**, *22*, 5961-5965.
- (50) Wang, H.; Gao, Y.; Zhou, C.; Li, G. *J. Am. Chem. Soc.* **2020**, *142*, 8122-8129.
- (51) Zhang, M.; Yang, L.; Zhou, C.; Fu, L.; Li, G. *Asian J. Org. Chem.* **2022**, *n/a*, e202200087.
- (52) Zhou, W.-J.; Wang, Z.-H.; Liao, L.-L.; Jiang, Y.-X.; Cao, K.-G.; Ju, T.; Li, Y.; Cao, G.-M.; Yu, D.-G. *Nat. Commun.* **2020**, *11*, 3263.
- (53) Zhou, C.; Li, M.; Sun, J.; Cheng, J.; Sun, S. *Org. Lett.* **2021**, *23*, 2895-2899.
- (54) Bai, J.; Li, M.; Zhou, C.; Sha, Y.; Cheng, J.; Sun, J.; Sun, S. *Org. Lett.* **2021**, *23*, 9654-9658.
- (55) Wang, M.-Y.; Cao, Y.; Liu, X.; Wang, N.; He, L.-N.; Li, S.-H. *Green Chem.* **2017**, *19*, 1240-1244.
- (56) Yin, Z.-B.; Ye, J.-H.; Zhou, W.-J.; Zhang, Y.-H.; Ding, L.; Gui, Y.-Y.; Yan, S.-S.; Li, J.; Yu, D.-G. *Org. Lett.* **2018**, *20*, 190-193.
- (57) Tortajada, A.; Ninokata, R.; Martin, R. *J. Am. Chem. Soc.* **2018**, *140*, 2050-2053.
- (58) Ju, T.; Zhou, Y.-Q.; Cao, K.-G.; Fu, Q.; Ye, J.-H.; Sun, G.-Q.; Liu, X.-F.; Chen, L.; Liao, L.-L.; Yu, D.-G. *Nat. Catal.* **2021**, *4*, 304-311.
- (59) (a) Maruoka, K.; Ooi, T. *Chem. Rev.* **2003**, *103*, 3013-3028; (b) Perdih, A.; Dolenc, M. *S. Curr. Org. Chem.* **2007**, *11*, 801-832; (c) Nájera, C.; Sansano, J. M. *Chem. Rev.* **2007**, *107*, 4584-4671.

- (60) Ju, T.; Fu, Q.; Ye, J.-H.; Zhang, Z.; Liao, L.-L.; Yan, S.-S.; Tian, X.-Y.; Luo, S.-P.; Li, J.; Yu, D.-G. *Angew. Chem. Int. Ed.* **2018**, *57*, 13897-13901.
- (61) Fan, X.; Gong, X.; Ma, M.; Wang, R.; Walsh, P. J. *Nat. Commun.* **2018**, *9*, 4936.
- (62) Wang, S.; Cheng, B.-Y.; Sršen, M.; König, B. *J. Am. Chem. Soc.* **2020**, *142*, 7524-7531.
- (63) Cao, G.-M.; Hu, X.-L.; Liao, L.-L.; Yan, S.-S.; Song, L.; Chruma, J. J.; Gong, L.; Yu, D.-G. *Nat. Commun.* **2021**, *12*, 3306.
- (64) (a) Ouyang, K.; Hao, W.; Zhang, W.-X.; Xi, Z. *Chem. Rev.* **2015**, *115*, 12045-12090; (b) Wang, Q.; Su, Y.; Li, L.; Huang, H. *Chem. Soc. Rev.* **2016**, *45*, 1257-1272.
- (65) Moragas, T.; Gaydou, M.; Martin, R. *Angew. Chem. Int. Ed.* **2016**, *55*, 5053-5057.
- (66) Liao, L.-L.; Cao, G.-M.; Ye, J.-H.; Sun, G.-Q.; Zhou, W.-J.; Gui, Y.-Y.; Yan, S.-S.; Shen, G.; Yu, D.-G. *J. Am. Chem. Soc.* **2018**, *140*, 17338-17342.
- (67) Yan, S.-S.; Liu, S.-H.; Chen, L.; Bo, Z.-Y.; Jing, K.; Gao, T.-Y.; Yu, B.; Lan, Y.; Luo, S.-P.; Yu, D.-G. *Chem* **2021**, *7*, 3099-3113.
- (68) Ran, C.-K.; Niu, Y.-N.; Song, L.; Wei, M.-K.; Cao, Y.-F.; Luo, S.-P.; Yu, Y.-M.; Liao, L.-L.; Yu, D.-G. *ACS Catal.* **2022**, *12*, 18-24.
- (69) Huang, H.; Ye, J.-H.; Zhu, L.; Ran, C.-K.; Miao, M.; Wang, W.; Chen, H.; Zhou, W.-J.; Lan, Y.; Yu, B.; Yu, D.-G. *CCS Chem.* **2020**, *3*, 1746-1756.
- (70) Fan, Z.; Yi, Y.; Chen, S.; Xi, C. *Org. Lett.* **2021**, *23*, 2303-2307.
- (71) Niu, Y.-N.; Jin, X.-H.; Liao, L.-L.; Huang, H.; Yu, B.; Yu, Y.-M.; Yu, D.-G. *Sci. China Chem.* **2021**, *64*, 1164-1169.
- (72) He, X.; Yao, X.-Y.; Chen, K.-H.; He, L.-N. *ChemSusChem* **2019**, *12*, 5081-5085.
- (73) (a) Patra, T.; Maiti, D. *Chem. Eur. J.* **2017**, *23*, 7382-7401; (b) Gooßen, L. J.; Rodríguez, N.; Gooßen, K. *Angew. Chem. Int. Ed.* **2008**, *47*, 3100-3120; (c) Rodríguez, N.; Goossen, L. J. *Chem. Soc. Rev.* **2011**, *40*, 5030-5048; (d) Dzik, W. I.; Lange, P. P.; Gooßen, L. J. *Chem. Sci.* **2012**, *3*, 2671-2678.
- (74) (a) Kolbe, H. *Justus Liebigs Ann. Chem.* **1849**, *69*, 257-294; (b) Vijn, A. K.; Conway, B. E. *Chem. Rev.* **1967**, *67*, 623-664.
- (75) Fichter, F.; Stenzl, H. *Helv. Chim. Acta* **1939**, *22*, 970-978.
- (76) Hunsdiecker, H.; Hunsdiecker, C. *Ber. dtsh. Chem. Ges. A/B* **1942**, *75*, 291-297.
- (77) (a) Naskar, D.; Roy, S. *Tetrahedron* **2000**, *56*, 1369-1377; (b) Wang, Z.; Zhu, L.; Yin, F.; Su, Z.; Li, Z.; Li, C. *J. Am. Chem. Soc.* **2012**, *134*, 4258-4263.

Chapter I

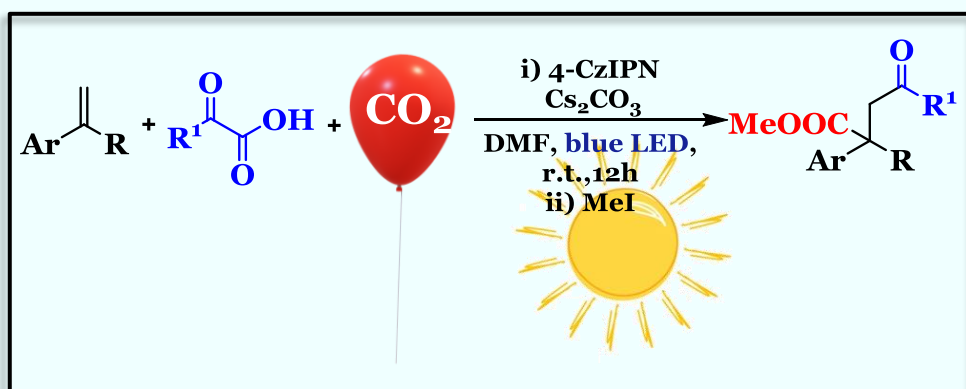
- (78) (a) Barton, D. H. R.; McCombie, S. W. *J. Chem. Soc., Perkin Trans. 1* **1975**, 1574-1585; (b) Barton, D. H. R.; Crich, D.; Motherwell, W. B. *J. Chem. Soc., Chem. Commun.* **1983**, 939-941.
- (79) Zhu, J.; Klunder, A. J. H.; Zwanenburg, B. *Tetrahedron* **1995**, *51*, 5099-5116.
- (80) Nilsson, M.; Kulonen, E.; Sunner, S.; Frank, V.; Brunvoll, J.; Bunnenberg, E.; Djerassi, C.; Records, R. J. A. C. S. *Acta Chem. Scand.* **1966**, *20*, 423-426.
- (81) (a) Dai, J.-J.; Liu, J.-H.; Luo, D.-F.; Liu, L. *Chem. Commun.* **2011**, *47*, 677-679; (b) Fromm, A.; van Wüllen, C.; Hackenberger, D.; Gooßen, L. J. *J. Am. Chem. Soc.* **2014**, *136*, 10007-10023.
- (82) Gooßen, L. J.; Deng, G.; Levy, L. M. *Science* **2006**, *313*, 662-664.
- (83) McMurray, L.; McGuire, T. M.; Howells, R. L. *Synthesis* **2020**, *52*, 1719-1737.
- (84) (a) Gooßen, L. J.; Thiel, W. R.; Rodríguez, N.; Linder, C.; Melzer, B. *Adv. Synth. Catal.* **2007**, *349*, 2241-2246; (b) Gooßen, L. J.; Linder, C.; Rodríguez, N.; Lange, P. P.; Fromm, A. *Chem. Commun.* **2009**, 7173-7175.
- (85) Xue, L.; Su, W.; Lin, Z. *Dalton Transactions* **2011**, *40*, 11926-11936.
- (86) Dickstein, J. S.; Curto, J. M.; Gutierrez, O.; Mulrooney, C. A.; Kozlowski, M. C. *J. Org. Chem.* **2013**, *78*, 4744-4761.
- (87) Dupuy, S.; Nolan, S. P. *Chem. Eur. J.* **2013**, *19*, 14034-14038.
- (88) Jia, W.; Jiao, N. *Org. Lett.* **2010**, *12*, 2000-2003.
- (89) Myers, A. G.; Tanaka, D.; Mannion, M. R. *J. Am. Chem. Soc.* **2002**, *124*, 11250-11251.
- (90) Tang, J.; Biafora, A.; Goossen, L. J. *Angew. Chem. Int. Ed.* **2015**, *54*, 13130-13133.
- (91) Voutchkova, A.; Coplin, A.; Leadbeater, N. E.; Crabtree, R. H. *Chem. Commun.* **2008**, 6312-6314.
- (92) Candish, L.; Freitag, M.; Gensch, T.; Glorius, F. *Chem. Sci.* **2017**, *8*, 3618-3622.
- (93) Qin, T.; Malins, L. R.; Edwards, J. T.; Merchant, R. R.; Novak, A. J. E.; Zhong, J. Z.; Mills, R. B.; Yan, M.; Yuan, C.; Eastgate, M. D.; Baran, P. S. *Angew. Chem. Int. Ed.* **2017**, *56*, 260-265.
- (94) Cassani, C.; Bergonzini, G.; Wallentin, C.-J. *Org. Lett.* **2014**, *16*, 4228-4231.
- (95) Schwarz, J.; König, B. *Green Chem.* **2016**, *18*, 4743-4749.
- (96) Edwards, J. T.; Merchant, R. R.; McClymont, K. S.; Knouse, K. W.; Qin, T.; Malins, L. R.; Vokits, B.; Shaw, S. A.; Bao, D.-H.; Wei, F.-L.; Zhou, T.; Eastgate, M. D.; Baran, P. S. *Nature* **2017**, *545*, 213-218.
- (97) Noble, A.; MacMillan, D. W. C. *J. Am. Chem. Soc.* **2014**, *136*, 11602-11605.

- (98) He, Z.; Qi, X.; Li, S.; Zhao, Y.; Gao, G.; Lan, Y.; Wu, Y.; Lan, J.; You, J. *Angew. Chem. Int. Ed.* **2015**, *54*, 855-859.
- (99) Wang, G.-Z.; Shang, R.; Cheng, W.-M.; Fu, Y. *Org. Lett.* **2015**, *17*, 4830-4833.
- (100) Crabtree, R. H. *J. Chem. Soc., Dalton Trans.* **2001**, 2437-2450.
- (101) (a) Brückl, T.; Baxter, R. D.; Ishihara, Y.; Baran, P. S. *Acc. Chem. Res.* **2012**, *45*, 826-839; (b) Kuhl, N.; Hopkinson, M. N.; Wencel-Delord, J.; Glorius, F. *Angew. Chem. Int. Ed.* **2012**, *51*, 10236-10254; (c) Rousseau, G.; Breit, B. *Angew. Chem. Int. Ed.* **2011**, *50*, 2450-2494.
- (102) (a) Chen, X.; Engle, K. M.; Wang, D.-H.; Yu, J.-Q. *Angew. Chem. Int. Ed.* **2009**, *48*, 5094-5115; (b) Gensch, T.; Hopkinson, M. N.; Glorius, F.; Wencel-Delord, J. *Chem. Soc. Rev.* **2016**, *45*, 2900-2936; (c) Sambigiato, C.; Schönbauer, D.; Blicke, R.; Dao-Huy, T.; Pototschnig, G.; Schaaf, P.; Wiesinger, T.; Zia, M. F.; Wencel-Delord, J.; Besset, T.; Maes, B. U. W.; Schnürch, M. *Chem. Soc. Rev.* **2018**, *47*, 6603-6743; (d) Engle, K. M.; Mei, T.-S.; Wasa, M.; Yu, J.-Q. *Acc. Chem. Res.* **2012**, *45*, 788-802.
- (103) Chiong, H. A.; Pham, Q.-N.; Daugulis, O. *J. Am. Chem. Soc.* **2007**, *129*, 9879-9884.
- (104) Giri, R.; Maugel, N.; Li, J.-J.; Wang, D.-H.; Breazzano, S. P.; Saunders, L. B.; Yu, J.-Q. *J. Am. Chem. Soc.* **2007**, *129*, 3510-3511.
- (105) Thuy-Boun, P. S.; Villa, G.; Dang, D.; Richardson, P.; Su, S.; Yu, J.-Q. *J. Am. Chem. Soc.* **2013**, *135*, 17508-17513.
- (106) Trita, A. S.; Biafora, A.; Pichette Drapeau, M.; Weber, P.; Gooßen, L. J. *Angew. Chem. Int. Ed.* **2018**, *57*, 14580-14584.
- (107) Bechtoldt, A.; Tirlor, C.; Raghuvanshi, K.; Warratz, S.; Kornhaab, C.; Ackermann, L. *Angew. Chem. Int. Ed.* **2016**, *55*, 264-267.
- (108) Cornella, J.; Righi, M.; Larrosa, I. *Angew. Chem. Int. Ed.* **2011**, *50*, 9429-9432.
- (109) Bhadra, S.; Dzik, W. I.; Gooßen, L. J. *Angew. Chem. Int. Ed.* **2013**, *52*, 2959-2962.
- (110) Huang, L.; Biafora, A.; Zhang, G.; Bragoni, V.; Gooßen, L. J. *Angew. Chem. Int. Ed.* **2016**, *55*, 6933-6937.
- (111) Luo, J.; Preciado, S.; Larrosa, I. *J. Am. Chem. Soc.* **2014**, *136*, 4109-4112.
- (112) Gallardo-Donaire, J.; Martin, R. *J. Am. Chem. Soc.* **2013**, *135*, 9350-9353.
- (113) Li, Y.; Ding, Y.-J.; Wang, J.-Y.; Su, Y.-M.; Wang, X.-S. *Org. Lett.* **2013**, *15*, 2574-2577.
- (114) Wang, Y.; Gulevich, A. V.; Gevorgyan, V. *Chem. Eur. J.* **2013**, *19*, 15836-15840.

- (115) Dai, J.-J.; Xu, W.-T.; Wu, Y.-D.; Zhang, W.-M.; Gong, Y.; He, X.-P.; Zhang, X.-Q.; Xu, H.-J. *J. Org. Chem.* **2015**, *80*, 911-919.
- (116) Zhang, M.; Ruzi, R.; Li, N.; Xie, J.; Zhu, C. *Org. Chem. Front.* **2018**, *5*, 749-752.
- (117) Shao, A.; Zhan, J.; Li, N.; Chiang, C.-W.; Lei, A. *J. Org. Chem.* **2018**, *83*, 3582-3589.
- (118) Dangel, B. D.; Johnson, J. A.; Sames, D. *J. Am. Chem. Soc.* **2001**, *123*, 8149-8150.
- (119) Novák, P.; Correa, A.; Gallardo-Donaire, J.; Martin, R. *Angew. Chem. Int. Ed.* **2011**, *50*, 12236-12239.
- (120) Zhuang, Z.; Yu, J.-Q. *Nature* **2020**, *577*, 656-659.
- (121) Im, H.; Kang, D.; Choi, S.; Shin, S.; Hong, S. *Org. Lett.* **2018**, *20*, 7437-7441.
- (122) Cianfanelli, M.; Olivo, G.; Milan, M.; Klein Gebbink, R. J. M.; Ribas, X.; Bietti, M.; Costas, M. *J. Am. Chem. Soc.* **2020**, *142*, 1584-1593.
- (123) Qian, S.; Li, Z.-Q.; Li, M.; Wisniewski, S. R.; Qiao, J. X.; Richter, J. M.; Ewing, W. R.; Eastgate, M. D.; Chen, J. S.; Yu, J.-Q. *Org. Lett.* **2020**, *22*, 3960-3963.
- (124) Chen, S.; Mu, D.; Mai, P.-L.; Ke, J.; Li, Y.; He, C. *Nat. Commun.* **2021**, *12*, 1249.
- (125) Dohi, T.; Takenaga, N.; Goto, A.; Maruyama, A.; Kita, Y. *Org. Lett.* **2007**, *9*, 3129-3132.
- (126) Wang, X.; Gallardo-Donaire, J.; Martin, R. *Angew. Chem. Int. Ed.* **2014**, *53*, 11084-11087.
- (127) Ramirez, N. P.; Bosque, I.; Gonzalez-Gomez, J. C. *Org. Lett.* **2015**, *17*, 4550-4553.
- (128) Zhang, S.; Li, L.; Wang, H.; Li, Q.; Liu, W.; Xu, K.; Zeng, C. *Org. Lett.* **2018**, *20*, 252-255.

Chapter II

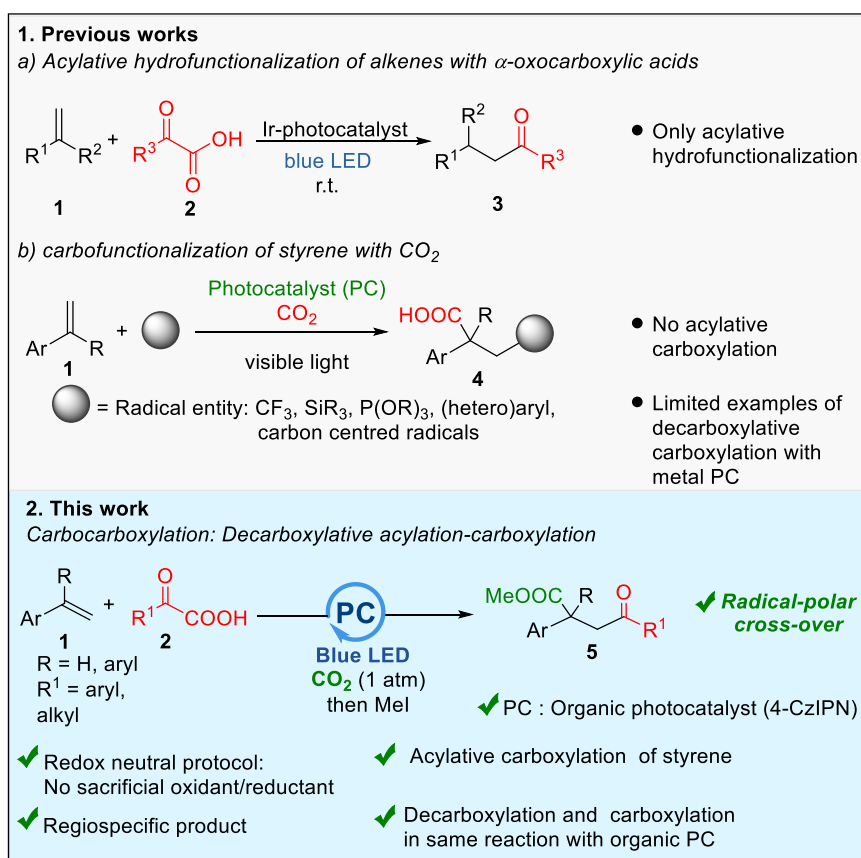
Transition Metal-free, Visible Light Mediated Decarboxylative Acylation and Carboxylation of Alkenes with CO₂



Transition Metal-free, Visible Light Mediated Decarboxylative Acylation and Carboxylation of Alkenes with CO₂

II.1. Introduction

The vicinal difunctionalisation of alkenes has emerged as a resourceful synthetic approach to get access to densely functionalized molecular framework.¹ In the past decade, extensive research has been successfully carried out categorically on hydrofunctionalisation or difunctionalisation including minimum one C–X (X = heteroatom) bond formation by transition metal or transition metal-photoredox dual catalytic systems.² Installation of two carbon subunits through the C–C double bond can rapidly increase the molecular complexity. In this line, regioselective dicarbofunctionalisation has attracted organic chemist's attention recently due to the synthetic application and associated synthetic challenges.³ In the established methods of dicarbofunctionalization, inclusion of transition metal generates problems due to β -hydride elimination, homocoupling, isomerization, or proto-demetalation. Driven by the challenges, with the upsurge of photoredox catalysis, chemists have developed solely photocatalytic difunctionalization of alkenes. Thus, acylative difunctionalization is also an interesting approach to increase molecular complexity by installing acyl functional group at one of the ends of the alkene.



Scheme 1. Photocatalyzed difunctionalization of alkenes.

Fu disclosed photocatalytic acylative hydrofunctionalization of activated alkenes where acyl group was originated from α -oxocarboxylic acids.⁴ Lei and co-workers extended this approach to hydrofunctionalization of styrenes.⁵ Intrigued by the present developments of photocatalyzed carboxylative difunctionalizations,⁶ herein, instead of hydrofunctionalization, we present acylative carboxylation of alkenes with α -oxocarboxylic acids and CO₂. Here, α -oxocarboxylic acids would undergo decarboxylation to furnish acyl functionality and CO₂ provides the carboxylation. Before going to the details about the present work, for better understanding, we would briefly discuss about the earlier developments on photocatalyzed difunctionalization reactions of alkenes.

II.2. Review of the previous developments

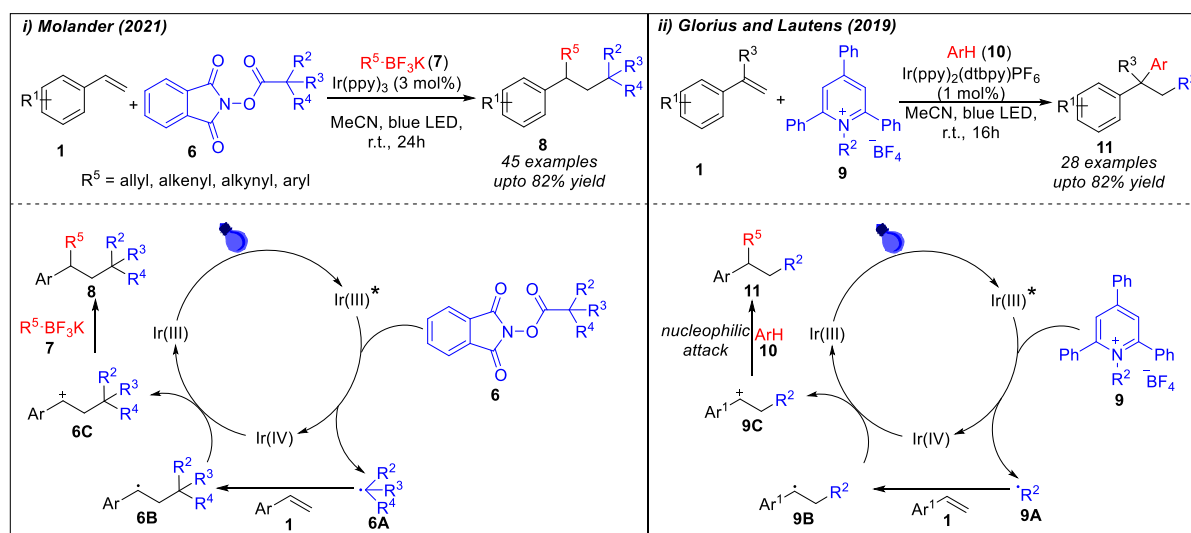
II.2.1. Photocatalyzed difunctionalization of alkenes with nucleophiles via carbocation intermediate

Molander and other groups have established photoredox/nickel dual-catalysis as a remarkable tool for alkene 1,2-difunctionalizations, the electrophilic coupling partner is mainly limited to sp²-halide systems.^{2a, 2f, 2g, 7} Recently, radical-polar crossover paradigm solely by photocatalysis has emerged as another potent concept to accomplish olefin difunctionalisation *via* ionic intermediates to accomplish reductive coupling of two electrophiles with alkene.^{2d, 8} In this approach, generally a radical attach to one end of C–C double bond of olefin gives rise to a radical at the other end which reacts with another nucleophile or electrophile in the successive steps *via* ionic intermediates. Here, we would briefly discuss the developments of difunctionalization of alkenes *via* cationic intermediate with which an incoming nucleophile would react to provide difunctionalization product.

Recently, the Molander group reported an intermolecular 1,2-dicarbofunctionalization of alkene with organotrifluoroborates **7** as carbon-centered nucleophiles and alkyl-*N*-(acyloxy)phthalimide esters **6** (redox-active) as radical precursors (**Scheme 2, i**).^{8a} Different category of organotrifluoroborates acted as amenable nucleophiles to afford carboalkynylation, carboalkenylation, carboallylation, and carboarylation *via* radical/polar crossover mechanism. A range of tertiary alkyl radicals were generated from the redox active esters which added to the olefinic double bond to furnish the dicarbofunctionalization in good yield whereas secondary alkyl radical furnished the product in lower yield. Vinyl arenes bearing no substitution, electron-donating, and electron-withdrawing groups as well as many labile and

Transition Metal-free, Visible Light Mediated Decarboxylative Acylation and Carboxylation of Alkenes with CO₂

sensitive groups at the *ortho*-, *meta*-, and *para*-positions exhibited the desired transformation with good efficiency. According to the mechanistic scenario postulated by the authors, first the Ir(III)-photocatalyst gets excited by the blue LED irradiation followed by single electron oxidation to Ir(IV) ($E_{1/2} [\text{Ir}^{\text{IV}}/\text{Ir}^{*\text{III}}] = 1.88 \text{ V vs. SCE}$) by the redox active ester **6** ($E^{\text{red}} \frac{1}{2} = 1.26 \text{ V vs. SCE}$ for 1-methylcyclohexyl-N-hydroxyphthalimide ester) induces the formation of C(sp³)-hybridized radical **6A**. It adds to the double bond to form relatively stable benzylic radical intermediate **6B** ($E^{\text{ox}} \frac{1}{2} = 0.37 \text{ V vs. SCE}$) which undergoes SET oxidation by Ir(IV) ($E_{1/2} [\text{Ir}^{\text{IV}}/\text{Ir}^{\text{III}}] = 0.77 \text{ V vs. SCE}$) to form the cationic intermediate **6C** restoring the ground state of photocatalyst. Organotrifluoroborate nucleophiles then attack **6C** to furnish the desired 1,2-dicarbonyl product **8**.



Scheme 2. Photocatalytic difunctionalization of alkenes via carbocation intermediate.

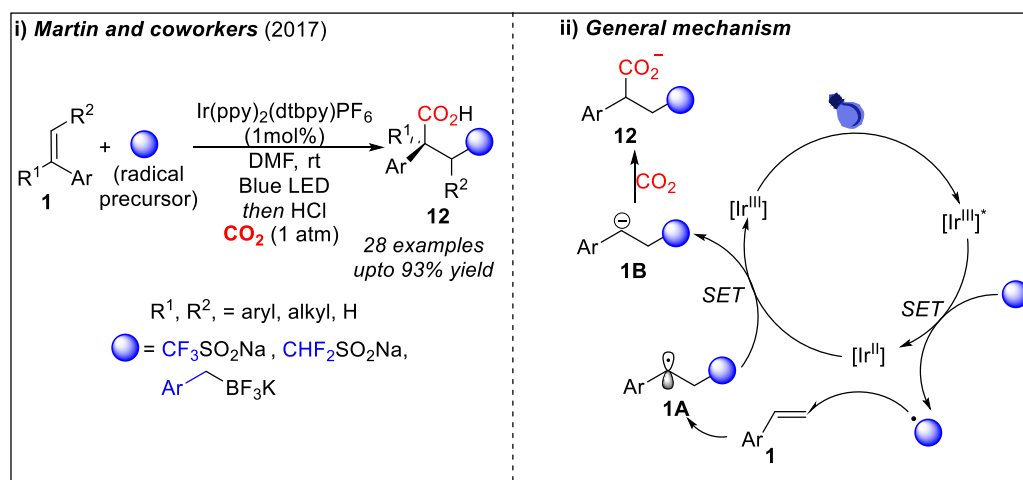
A rare example of three-component dicarbonylation of vinyl arenes by visible-light-promoted method using unbiased and unsubstituted benzylic radicals was reported by Glorius and co-workers in 2018 (**Scheme 2, ii**).⁹ The author's judiciously designed and used benzylic pyridinium salts **9** as radical precursors to unlock the potential of this strategy. Several heavily functionalized 1,1-diaryllkanes **11** were prepared by this undirected protocol by the combination of abundant styrenes **1**, benzylic amines, and electron-rich heterocycles **10**. Amino acid and dipeptide derived Katritzky salts were also well-suited for this transformation although the reaction was limited to styrene substrates. Mechanistically, the Katritzky salt undergoes photocatalysed SET process to generate the benzyl radical **9A** which adds to the double bond of styrene in anti-Markovnikov fashion. The radical intermediate **9B** undergoes

SET oxidation to form cationic intermediate **9C** followed by nucleophilic attack by arene **10** to furnish the desired polynuclear product **11**.

II.2.2. Photocatalyzed difunctionalization of alkenes with CO₂ via carbanion intermediate

Alternative to carbocation intermediate, photocatalysis has been successfully able to generate carbanion intermediates too via another radical/polar crossover, so that an incoming electrophile can react with this and increase the molecular complexity. Lately, despite being feebly electrophilic, owing to its high abundance, renewable and nontoxic nature, profound research has been directed towards utilization of CO₂ as an ideal one-carbon (C1) synthon in fine and bulk chemical synthesis by photocatalyzed methods.¹⁰ Consequently, visible-light-induced regioselective carbocarboxylation, phosphonocarboxylation, silacarboxylation, thiocarboxylation of alkenes with CO₂ have been successfully realized with various radical precursors by the Martin, Yu, and Wu groups.^{6d-f}

In 2017, the Martin group reported a redox-neutral protocol for photocatalyzed carboxylative dicarboxylation of styrene substrates with several C centred radical and CO₂ (**Scheme 3, i**).^{6d}

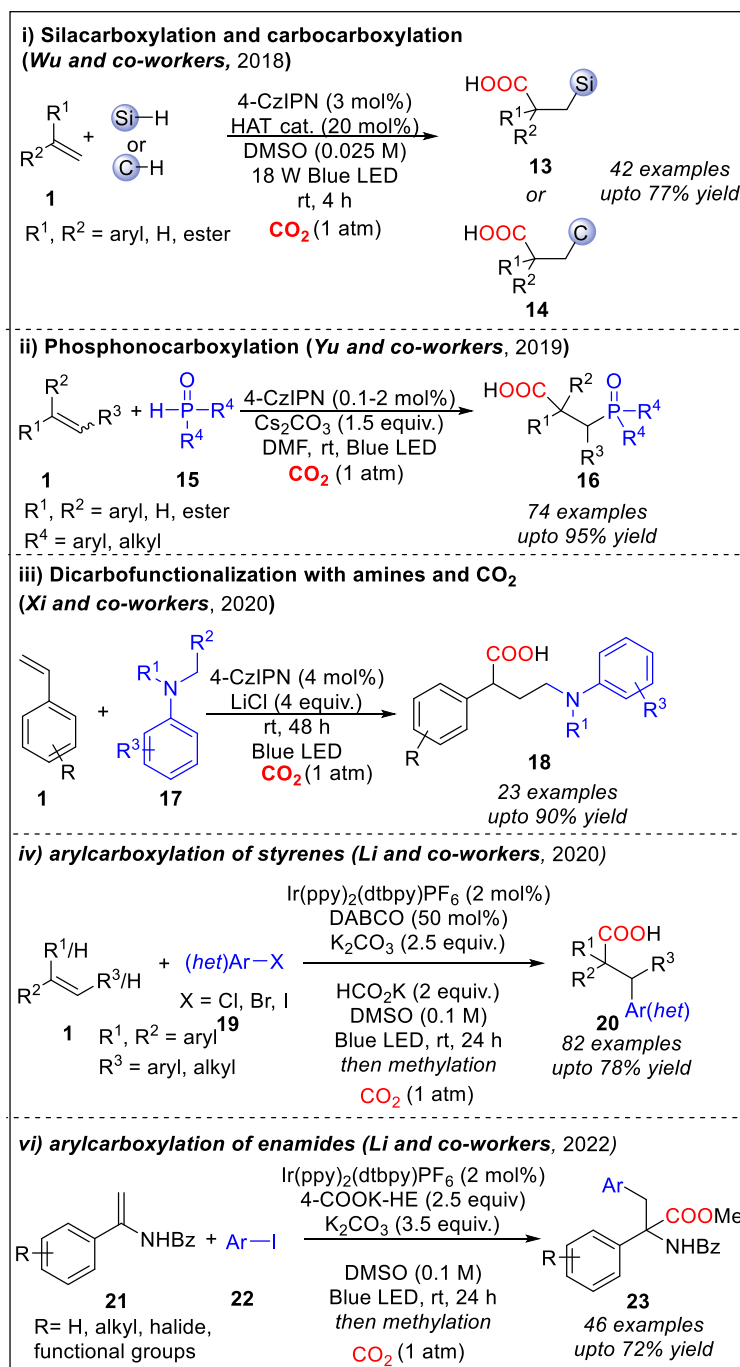


Scheme 3. Photocatalytic carbocarboxylation of styrenes and general mechanism.

Mechanistically (**Scheme 3, ii**), on photo-excitation the photocatalyst (PC) goes to PC* i.e., here Ir(III) converts to Ir(III)* which is reduced to Ir(II) by SET from the radical precursor CF₃SO₂Na to generate [•]CF₃. Then [•]CF₃ combines with the β-terminal of the styrene **1** and stabilized radical at benzylic position (**1A**) is formed. **1A** is then reduced by SET from Ir(II) and benzylic carbanion **1B** is formed along with regeneration the Ir(III) catalyst. As a result,

Transition Metal-free, Visible Light Mediated Decarboxylative Acylation and Carboxylation of Alkenes with CO₂

the benzylic carbanion **1B** undergoes nucleophilic addition to CO₂ to furnish the difunctionalized product with β-carboxylation. They had also used cesium oxalates, ArCH₂BF₃K and CHF₂Na as other radical precursors (**Scheme 3, i**). Following this work, using conceptually similar strategies, several other groups^{6c, 6e, 6f} developed carboxylative bifunctionalization of activated alkenes or styrenes with CO₂ taking suitable photocatalysts under visible light.



Scheme 4. Photocatalytic carboxylative difunctionalizations of alkenes.

Mechanistically, the examples followed the similar path as depicted in **Scheme 3 (ii)**, just changing the radical precursor and appropriate PC in each case.

The formation of benzylic carbanion is the key step for carboxylation and carbanion has been confirmed by coupling with other electrophiles e.g., ketones instead of CO₂.

In 2018, the Wu group developed 4-CzIPN catalyzed light mediated carbocarboxylation and silacarboxylation of activated alkenes (**Scheme 4, i**).^{6e}

In 2019, Yu developed photocatalyzed phosphonocarboxylation enamides i.e., activated alkenes using 4-CzIPN as organic photocatalyst (**Scheme 4, ii**).^{6f} From phosphites and phosphene oxide, phosphorus centred radicals form and accomplish phosphonocarboxylation under CO₂ atmosphere.

In 2020, the Xi group, synthesized several γ -amino acids from styrenes by photocatalyzed dicarbofunctionalization with CO₂ and amines (**Scheme 4, iii**).^{6c}

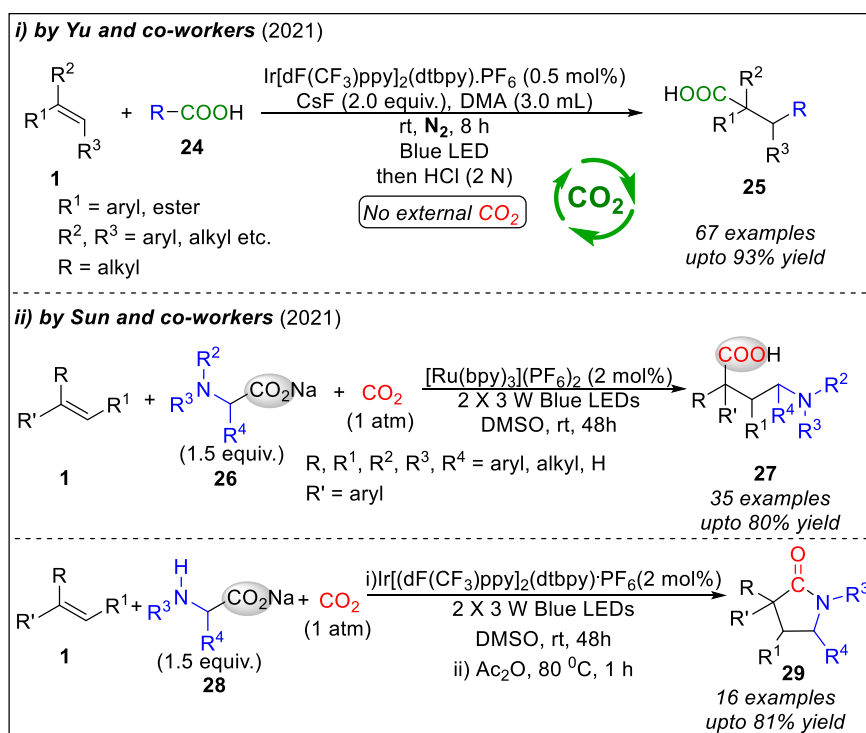
Though aryl halides are easily available and of low-cost, use of same as aryl group precursor in photocatalyzed bifunctionalization reactions has scarcely been reported because of aryl halide's high reduction potential. In 2020, the Li's group successfully used aryl halides as aryl radical precursor for the Meerwein-arylation type photocatalyzed carbocarboxylation of styrenes with CO₂ (**Scheme 4, iv**).^{6b} Notably, when aryl halides remained absent, 24% of dicarboxylated product formed where mono-carboxylated product was achieved in 10%, which intimates the involvement of $\cdot\text{CO}_2$. In 2022, the same group extended this strategy to functionalize enamides for carbocarboxylation with CO₂ and aryl iodides (**Scheme 4, iv**).¹¹

Above all these developments, the scope of carbocarboxylation is very less as per literatures.^{6b, 6c, 11} To achieve the same, one interesting strategy would be decarboxylation of carboxylic acids followed by addition to alkene and subsequent carboxylation with CO₂. Recently, in this manner, the Yu group^{6a} and the Sun group¹² separately utilized amino acids as a precursor of alkyl-radical for alkylative carboxylation of alkene with or without external carbon dioxide for the same using metal based photocatalysts. To this end, Yu and co-workers, interestingly, reutilized *in situ* liberated CO₂ via decarboxylation of one amino acid for carboxylation reaction under Ar atmosphere without any external CO₂, by Ir(III) catalyst (**Scheme 5, i**).^{6a} They realized that carbocarboxylation of styrenes, where *in situ* formed CO₂ acts as carboxylating source and another functionalizing agent is a C-centred radical that

Transition Metal-free, Visible Light Mediated Decarboxylative Acylation and Carboxylation of Alkenes with CO₂

originates from the decarboxylation of various acids such as alkyl carboxylic acids, α -amino acids, and peptides, following the same general mechanism (Scheme 3, ii). However, the major attractive feature of this methodology is that despite having low P_{CO_2} (partial pressure), the *in situ* formed CO₂ sufficiently performs carboxylation reaction offering amino acids as a bifunctional reagent.

Subsequently, the Sun group reported another carboxylative bifunctionalization reaction of styrene combining decarboxylation and carboxylation in the same reaction condition of Ru(III) photocatalysis to synthesize variety of γ -lactams and α,α -disubstituted γ -amino acids (Scheme 5, ii).¹² Here, they used sodium glycinate as the decarboxylative agent which give rise to the C-centred radical that attaches to styrene at the β -position. Contrary to Yu's report, here the *in situ* generated CO₂ was not sufficient to provide satisfactory yield, hence applying external CO₂ (balloon) was necessary.



Scheme 5. Photocatalytic decarboxylative carboxylation of alkenes.

II.3. Present work

However, decarboxylative acylation and carboxylation of alkene with carbon dioxide has never been attempted. Continuing with our constant effort¹³ to develop carboxylation reactions and using carboxylic acids as synthetic intermediates, we were intrigued to take the

challenge. With this aim we targeted acyl radical to be the primary radical component to attach to the C-C double bond. Acyl radical is a reactive nucleophilic radical with an established propensity to add to the olefinic double bond by aforesaid manner and it can be easily accessed from α -ketocarboxylic acid *via* single-electron transfer of the corresponding carboxylate by photocatalytic oxidation and successive decarboxylation.^{4-5, 14} We anticipated that addition of acyl radical to styrenyl double bond would generate the key radical intermediate which could attach to CO₂ via radical polar crossover under appropriate condition. If succeeded, we could afford carbocarboxylation/carboxyacylation of olefins from commodity chemicals with regio- and chemoselective control to generate valuable all-carbon quaternary centre. Notably, under CO₂ atmosphere, to give the decarboxylation satisfactorily and finally affording carboxylation, the system would have to behave against “Le Chatelier’s principle”¹⁵, which has been achieved here under transition-metal free mild photocatalytic condition. Remarkably, the substrates and intermediate of these protocols are redox active and are both oxidized or reduced by SET process during the redox-neutral reaction mechanism avoiding the necessity for stoichiometric external oxidants or reductants.

We report here, a practically useful methodology for the decarboxylative acylation and carboxylation of styrenyl alkenes using 1 atm gaseous CO₂ to furnish γ -keto acids (**Scheme 1**). Notably, this redox-neutral three-component alkene difunctionalization reaction underwent smoothly under the mild conditions using organic photocatalyst and without any oxidant or reductant. The extruded CO₂ from the α -ketocarboxylic acids (when taken in superstoichiometric amounts) was reused without any external CO₂ albeit in moderate yields.

II.4. Results and discussion

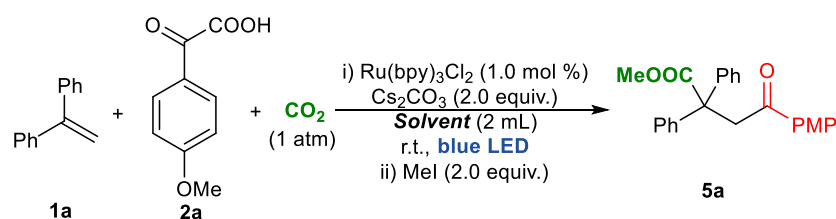
We optimized our reaction conditions taking 1,1-diphenylethylene **1a**, 4-methoxyphenylglyoxalic acid **2a** as the representative substrates (**Table 1–4**). Now, when a mixture of **1a** and **2a** were subjected under CO₂ atmosphere upon irradiation with 5W blue LED ($\lambda_{\text{max}} = 455 \text{ nm}$) in the presence of only 1 mol % of Ru(bpy)₃Cl₂·6H₂O as the photocatalyst, Cs₂CO₃ as the base in acetonitrile solvent, we pleasingly detected the formation of the desired product **5a** in 16% yield (entry 1, **Table 1**). After screening the solvents, polar solvent DMSO provided the best result (**Table 1**).

Here, during carbocarboxylation, after accomplishing decarboxylation, the reduced photocatalyst would be required to reduce the benzyl radical to produce benzylic carbanion so

Transition Metal-free, Visible Light Mediated Decarboxylative Acylation and Carboxylation of Alkenes with CO₂

that it can react with electrophilic CO₂. As the glyoxylic acid **2a** has E_{1/2}^{red} (acid/acyl radical) = -1.00 V vs SCE, we anticipated that the use of PC having similar but slightly lesser negative E_{1/2}^{red} (PC^{*}/ PC^{•-}) value than -1.00 V (vs SCE) would serve the purpose. On varying the photocatalysts, Ir(ppy)₂(dtbpy)PF₆ having E_{1/2} (Ir^{III}/Ir^{II}) = -0.31 V vs SCE, 4-CzIPN having E_{1/2} (PC^{•-} / PC) = -0.31 V vs SCE¹⁶ provided improved yield (entries 6, 7, **Table 2**).

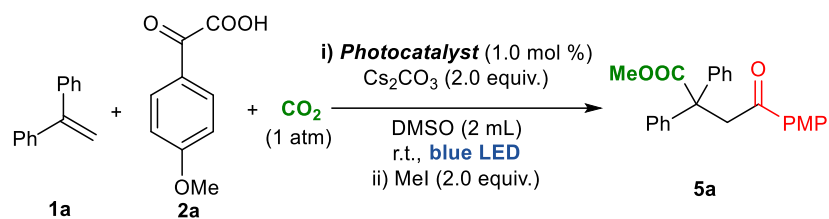
Table 1. Screening of solvents for carbocarboxylation



Entry	Solvent ^a	Yield of 5a (%)
1	MeCN	16
2	THF	25
3	DMF	31
4	DMA	28
5	DCE	trace
6	DMSO	37
7	PhCH ₃	trace
8	HFIP	10
9	NMP	trace

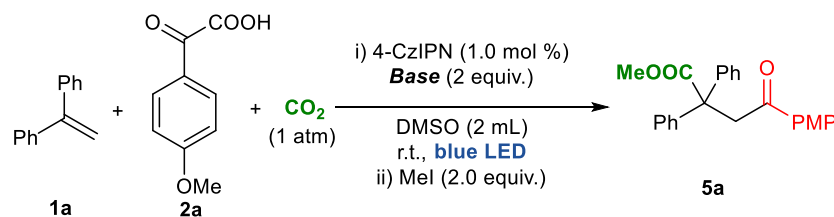
^aAll solvents are anhydrous.

On further screening of several photocatalysts, bases and solvent, it was found that irradiation with 455 nm blue LEDs for 12 h under CO₂ balloon pressure with 1.0 equivalent of **2a** in presence of 1 mol % of 4-CzIPN in DMSO solvent furnished the desired carboxylated product **5a** in 81% yield (entry 8, **Table 2**).

Table 2. Screening of photocatalysts for carbocarboxylation

Entry	Photocatalyst	Yield of 5a (%)
1	Ru(bpy) ₃ Cl ₂ ·6H ₂ O	37
2	<i>fac</i> -Ir(ppy) ₃	43
3	<i>p</i> -terphenyl	ND
4	Xanthone	ND
5	Rose bengal	trace
6	Ir(ppy) ₂ (dtbpy)PF ₆	70
7	Ir[dF(CF ₃)(ppy)] ₂ (dtbpy)PF ₆	67
8	4-CzIPN	81
9	Ru(bpy) ₃ (PF ₆) ₂	32
10	4-DPAIPN	44

Remarkably, instead of expensive Cs₂CO₃, non-carbonated base LiCl had furnished comparable yield (entry 1, **Table 3**).

Table 3. Screening of bases for carbocarboxylation

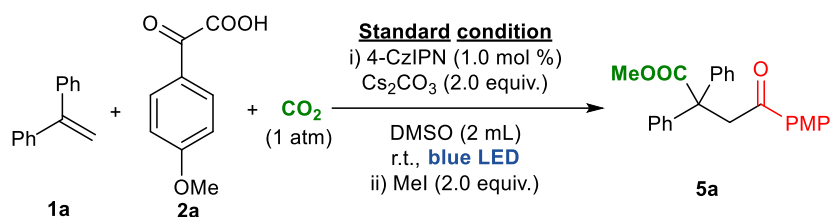
Transition Metal-free, Visible Light Mediated Decarboxylative Acylation and Carboxylation of Alkenes with CO₂

Entry	Base	Yield of 5a (%)
1	Cs ₂ CO ₃	81
2	CsF	51
3	K ₂ CO ₃	67
4	KO ^t Bu	41
5	Na ₂ CO ₃	33
6	Li ₂ CO ₃	30
7	LiCl	74
8	Et ₃ N	trace
9	ⁱ Pr ₂ NEt	trace
10	CsOAc	35
11 ^a	Cs ₂ CO ₃	78

^a3 equiv. of Cs₂CO₃.

No expected product was detected in absence of light and photocatalyst (entries 3, 4, **Table 4**). With an ambition to reutilize the released CO₂ from α -ketocarboxylic acid, the reaction was performed under argon without external CO₂ furnishing 30% yield (entry 6, **Table 4**). The partial pressure of CO₂ (P_{CO_2}) was sufficiently increased to provide 58% of the desired product using 6.0 equiv of **2a** (entry 8, **Table 4**) without addition of external CO₂. However, to approach in greener direction and minimize the wastage, use of super-stoichiometric amount of **2a** was avoided at present investigation. Reaction under O₂ atmosphere completely sieged the formation of **5a** and the phenylglyoxylic acid converted to deleterious benzoic acid rapidly (entry 7, **Table 4**).

Upto this, as entry 1, **Table 4** provided the best result, we decided to proceed with this as optimized condition. As the final reaction mixture contains remaining **2a**, product **5a** and side-product benzoic acid, for better isolation, *in-situ* esterification was performed in most of the cases with late addition of MeI into the reaction mixture.

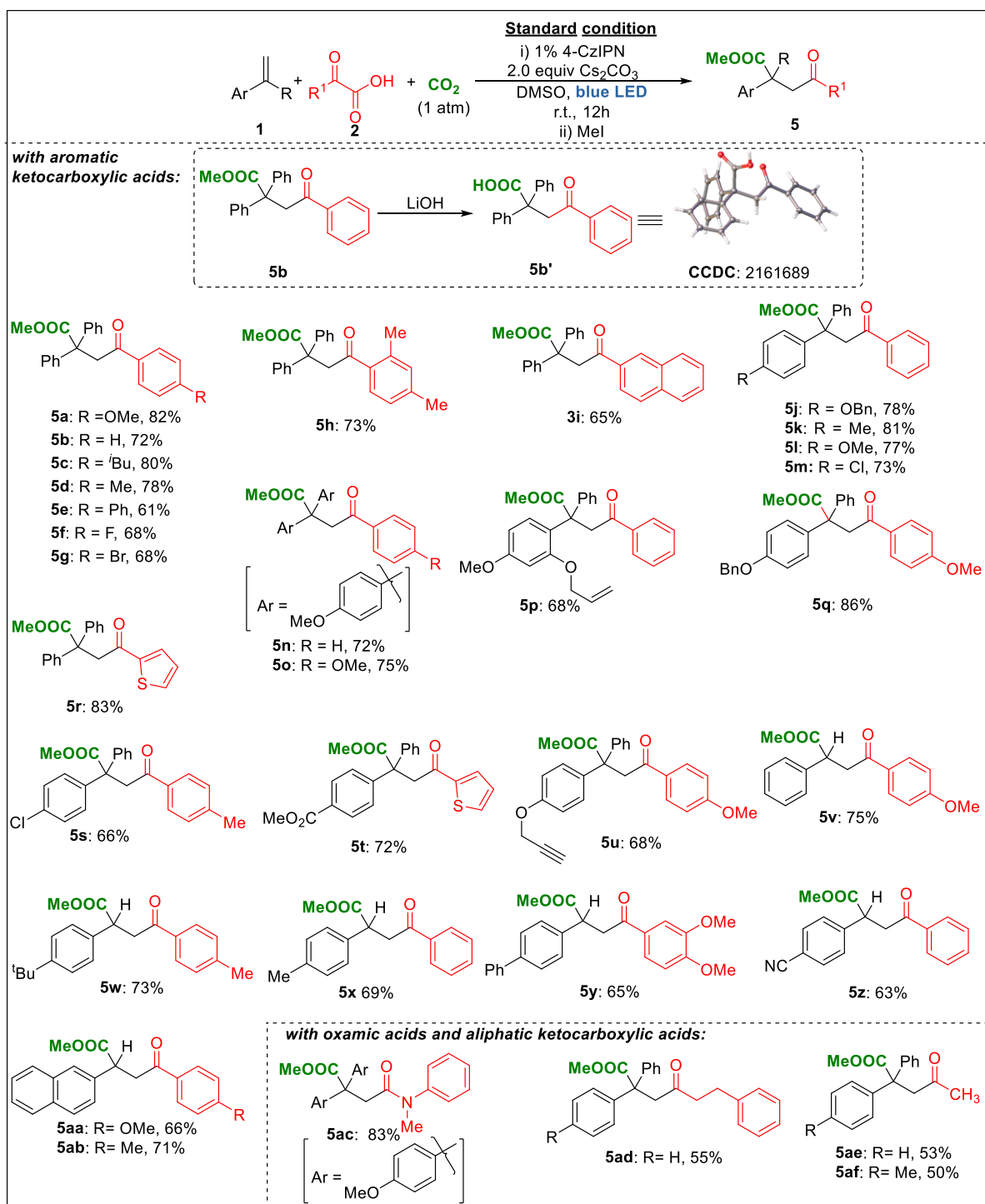
Table 4. Control experiments for carbocarboxylation

Entry	Variation from “Standard condition”	Yield of 5a (%)
1	None	81
2	Without Cs ₂ CO ₃	trace
3	Without 4-CzIPN	nd
4	Without blue LEDs	nd
5	Without 4-CzIPN, without blue LEDs	nd
6	Ar instead of CO ₂	30
7	O ₂ instead of CO ₂	nd
8	Ar instead of CO ₂ and 6 equiv. of 2a	58
9	Ar instead of CO ₂ and 6 equiv. of 2a , LiCl instead of Cs ₂ CO ₃	47

Thereafter, with the acceptable reaction condition for carboxyacylation/carboxylation in hand *i.e.*, under “standard condition”, generality of the substrates was evaluated (**Table 5**). Substituted aryl α -keto carboxylic acids containing electron-donating groups like Me, OMe, ⁱBu, Ph (**5a-5d**, **5h**, **5o**, **5q**, **5u-5y**) and withdrawing groups like F, Cl, Br (**5f**, **5g**) provided good to moderate yields under the standardized reaction condition. The formation of said product was further confirmed by x-ray structure of **5b'** (CCDC: 2161689) derived from **5b** on hydrolysis (**Table 7**).

Transition Metal-free, Visible Light Mediated Decarboxylative Acylation and Carboxylation of Alkenes with CO₂

Table 5. Substrate scope of decarboxylative acylcarboxylation of alkene under blue LED irradiation^{a,b}



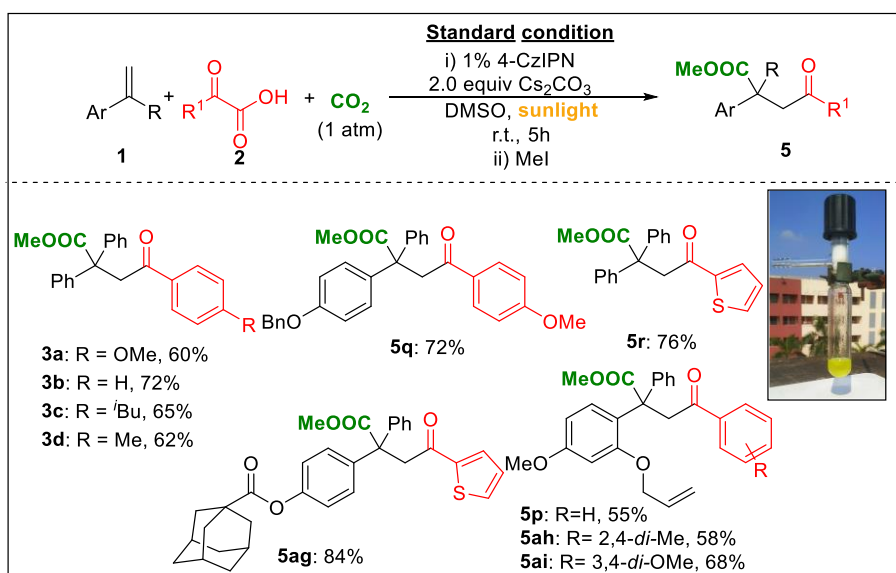
[a] Reactions were performed in 0.2 mmol scale. [b] Isolated yields have been referred.

Similarly, while styrene part was varied, α -substituted styrene having electron donating substitution such as OBn, Me, OMe (**5j-5k**, **5n-5q**) and withdrawing substitution as Cl, CO₂Me (**5m**, **5s-5t**) underwent the reaction smoothly.

Interestingly, heterocycle 2-oxo-2-(thiophen-2-yl)acetic acid furnished the desired product in high yield (**5r**, **5t**). To our delight, the styrenes without any α -substitution also provided fair yields where both donating groups as Me, ^tBu (**5w**, **5x**) and withdrawing group CN (**5z**) were compatible. Naphthyl styrene also provided satisfactory results (**5aa**, **5ab**) in our reaction condition. Interestingly, easily hydrolysable allyloxy, propargyloxy groups were well-tolerated (**5p**, **5u**) in this mild condition. To expand the scope beyond substituted phenylglyoxylic acids, the condition was applied to 2-(methyl(phenyl)amino)-2-oxoacetic acid (**5ac**). And notably, the 1° aliphatic ketocarboxylic acids provided only the expected products (**5ad-5af**) via decarboxylation. Further decarbonylation to furnish alkyl radical has not taken place unlike that comes from 2° or 3° aliphatic ketocarboxylic acids owing to the relative lesser stability of resultant 1°-alkyl radical than 2° or 3° alkyl radicals.

Therefore, to demonstrate the practical utility of the method, we checked the reaction under sunlight irradiation. To our delight, when blue LED was replaced in the “standard condition” with the sunlight irradiation (22.57° N, 88.36° E at 1100 hrs) the standard reaction between **1a**, **2a** and CO₂ provided the expected product in 60% yield within 5 h.

Table 6. Substrate scope of decarboxylative acylcarboxylation of alkene under sunlight irradiation^{a,b}

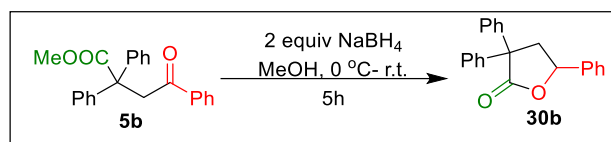


[a] Reactions were performed in 0.2 mmol scale. [b] Isolated yields have been referred.

To check the generality of this method, several substrates were prepared to react under this condition (**Table 6**). As shown in the Table 4, both the donating and withdrawing groups survived the reaction condition yielding the expected product satisfactorily (**5a-d**, **5p**, **5q**).

Heterocycle moiety is also well-tolerated (**5r**, **5ag**). Allyloxy, adamantane carboxylate substituted styrenes provided higher yields under sunlight irradiation (**5p**, **5ah-5ai**).

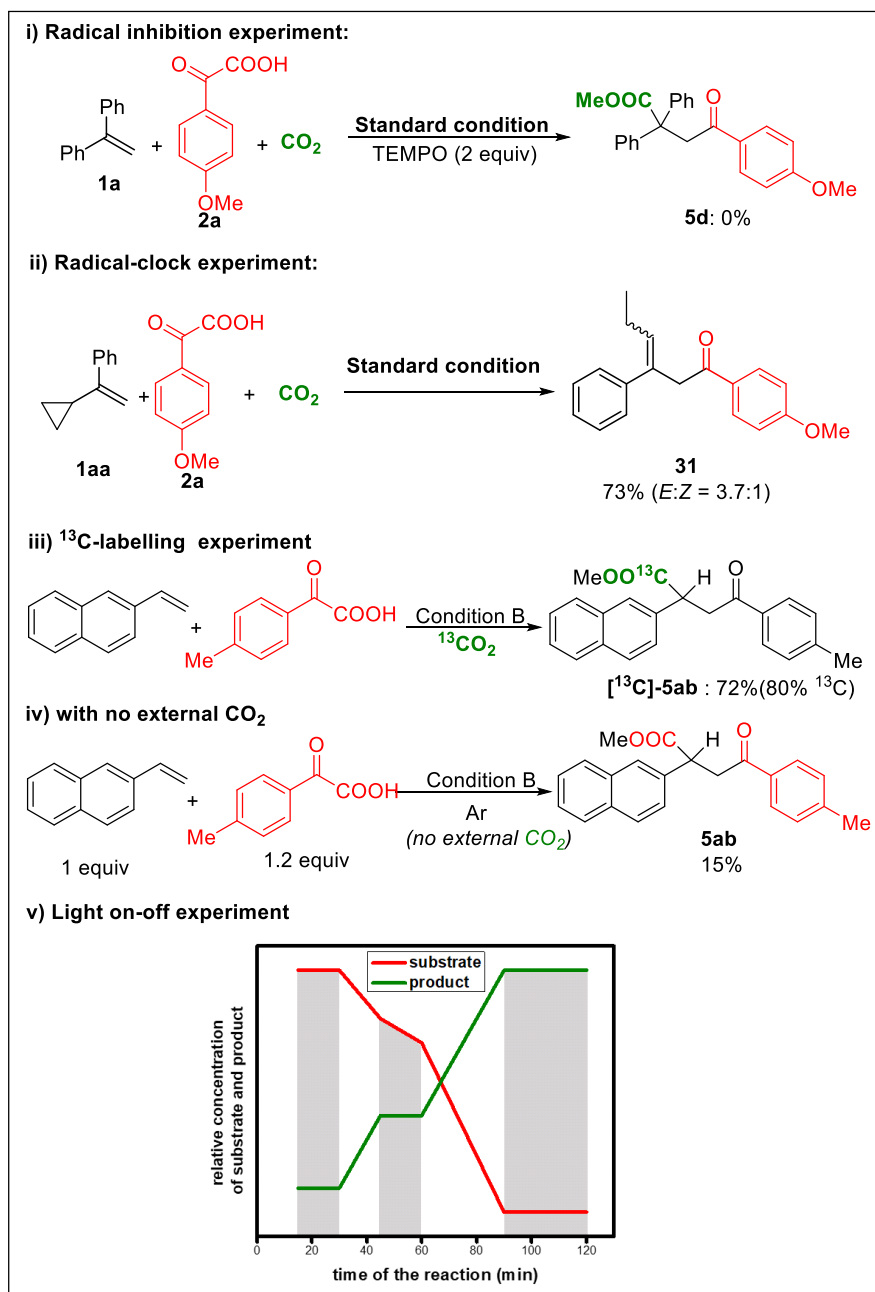
To demonstrate the utility, further transformation of the product **5b** was pursued (**Scheme 6**). On NaBH₄ reduction of **5b**, the *in situ* formed 2° alcohol reacts with the carboxylate group from the same molecule and lactonizes to form fused heterocycle **30b**.



Scheme 6. Product derivatization.

To shed light in the mechanism, we conducted several mechanistic experiments (**Scheme 7**). Radical inhibition experiment with 2.0 equiv of radical scavenger TEMPO (2,2,6,6-tetramethylpiperidin-1-yl)oxyl) completely shut down the reaction with full recovery of starting olefin which suggests that a probable radical mechanism is controlling the reaction (**Scheme 7, i**). Radical addition followed by ring opening occurs with olefin **1aa** in the radical-clock experiment to give **31** which indicates the generation of benzylic radical intermediate from styrene for carbocarboxylation (**Scheme 7, ii**). It gives further information that, no radical-radical coupling between benzylic radical and CO₂ took place and there must be a radical-polar crossover in the carboxylation process. Next, as there is possibility of carboxylation from the carbonate base, we chose to confirm the source unambiguously. As, use of LiCl instead of Cs₂CO₃ furnished comparable yield (entry 3, **Table 3**), the possibility of Cs₂CO₃ to be the main carboxylating agent could be practically excluded. To clearly understand about the carboxylating agent, we performed isotope-labeling experiment. We performed a reaction with ¹³CO₂ taking 2-vinylnaphthalene **1ab** and 4-methylphenylglyoxylic acid **2d** as formal substrates which ended up in formation of [¹³C]-**5ab** with 80% ¹³C incorporation (**Scheme 7, iii**). This provides strong evidence that the new carboxyl group is originated from the external CO₂, although a little percentage could arise from the decarboxylation of glyoxylic acid as per our result under absence of external CO₂ (Entry 6, 8, **Table 4; Scheme 7, iv**). Light on-off experiment for both of the reactions suggests that continuous light irradiation is essential for the sequential C-C bond formation although possibility of short-lived radical chains cannot be excluded (**Scheme 7, v**).

Based on the control experiments and previous literature precedence¹⁶⁻¹⁷ a probable mechanism has been portrayed in **Scheme 8**. The excited state of the photo catalyst (under Standard condition, 4-CzIPN* : $E_{1/2}^{\text{red}} = 1.35 \text{ V vs SCE}$) undergoes reduction by the carboxylate anion ($E_{1/2}^{\text{ox}} \approx +1.0 \text{ V vs. SCE}$) to produce acyl radical *via* decarboxylation.¹⁶⁻¹⁷



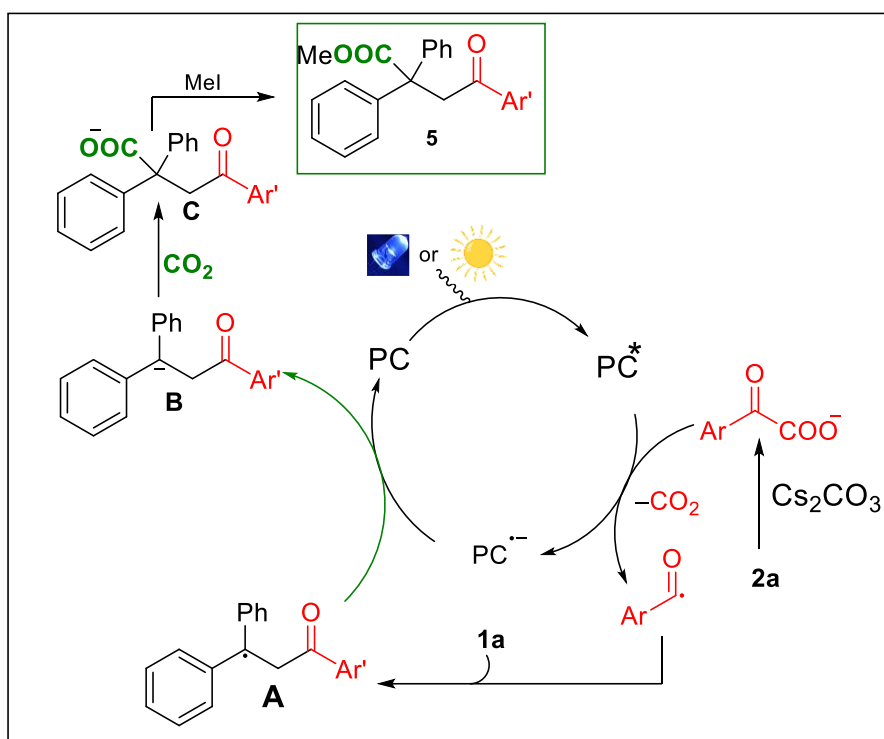
Scheme 7. Control experiments.

The reactive acyl radical promptly adds to the terminal position of styrenyl double bond to form the more stable benzylic radical intermediate **A** which is persistent in nature. Then, SET could take place between **A** and reduced photocatalyst ($\text{PC}^{\bullet-}$) ($E_{1/2}^{\text{red}} = -1.21 \text{ V vs SCE}$)

to produce carbanion **B**.¹⁸ It could attack CO₂ nucleophilically to deliver the carboxylated product **C**, which on methylation or protonation, furnishes the expected product **5**.

II.5. Conclusion

In conclusion, we have developed an organo photoredox-catalyzed, three-component acylative carboxylation of styrene from α -ketocarboxylic acid and CO₂ to afford γ -keto carboxylic acids. The carboxylation reaction takes place at 1 atm pressure following a decarboxylation process with organic photocatalyst, behaving against “Le Chatelier’s principle”.¹⁵



Scheme 8. Plausible mechanism.

This reductive coupling is initiated through the addition of acyl radical, which is generated via photoredox-mediated decarboxylation of α -ketocarboxylic acid followed by β -addition to the vinyl arenes furnishing a stabilized benzylic radical. This incipient radical is further reduced by the photocatalyst to the corresponding carbanion that attacks CO₂. Interestingly, the reaction proceeds promptly under the sunlight irradiation. The acyl radical is generated selectively from the aryl and alkyl α -ketocarboxylic acids and no aryl or alkyl radical was generated via further decarbonylation.

II.6. Experimental section

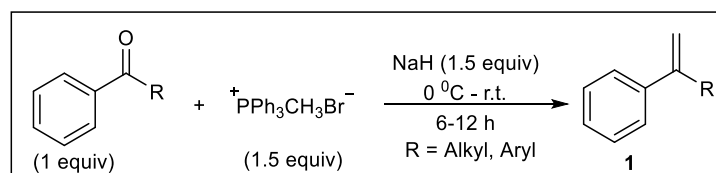
II.6.1. General information

The uncorrected melting points were measured using open end capillary tubes. On silica gel plates (Merck silica gel 60, f254), TLC was conducted out, and the spots were visualized under UV light (254 and 365 nm) and with DNP stain. X-ray of crystals was recorded in Bruker D8 Venture with a Photon-III detector instrument. ^1H NMR was recorded at 400 MHz (JEOL-JNM-ECZ400S/L1) frequency; ^{13}C NMR spectra were recorded at 100 MHz (JEOL-JNM-ECZ400S/L1) frequency in CDCl_3 , DMSO-D_6 solvent using TMS as the internal standard. Chemical shifts were evaluated in parts per million (ppm), with tetramethylsilane serving as a reference at 0.0 ppm. The acronyms s=singlet, d=doublet, t=triplet, q=quartet, and m=multiplet are used to describe multiplicities. In Hertz unit, coupling constants, J, were reported (Hz). Utilizing the ESI (Q-TOF, positive ion) technique, HRMS (m/z) were measured. All commercial reagents were used without further purification, unless otherwise noted.

II.6.2. Preparation of starting materials

General procedure for preparation of substituted olefins (**1**)

Slightly modifying a literature protocol¹⁹, these were prepared by Wittig reaction as follows.



A clean and oven-dried round-bottom flask was charged with $\text{CH}_3\text{PPh}_3\text{Br}$ (1.5 equiv.) and THF (carbonyl substrate concentration = 0.2 M), NaH (1.5 equiv.) was added in portion to the suspension at $0\text{ }^\circ\text{C}$. The resulting mixture was warmed up to ambient temperature and stirred for 1 h. The yellow suspension was cooled to $0\text{ }^\circ\text{C}$ again followed by addition of the carbonyl substrate (1 equiv.). The mixture was then given one to twelve hours of additional stirring at room temperature. After the reaction was completed, the solvent was evaporated under reduced pressure, and then the reaction mixture was extracted with EtOAc (40 mL), deionized water ($20\text{ mL} \times 2$) followed by washing the resulting organic layer with brine (20 mL), and finally the combined organic layer was passed through anhydrous Na_2SO_4 for drying and the mixture was concentrated by evaporating the solvent under reduced pressure. Then, the crude product was purified with column chromatography (eluting with petroleum ether/ethyl acetate) to afford the substituted olefin substrates **1**.

Synthesis of α -oxocarboxylic acid

The α -oxocarboxylic acids were prepared from oxidation of corresponding methyl ketones by SeO₂ according to the reported procedure.²⁰

II.6.3. Procedure for optimization of the carbocarboxylation reaction

An oven-dried Schlenk tube (10 mL) was charged with **2a** (43.2 mg, 0.24 mmol, 1.2 equiv), photocatalyst and a stirring magnet-bar. Therefore, it was transferred to glovebox, where the base was to added. The tube was then taken out of the glove box, evacuated and back-filled with CO₂ successively for three times. Therefore, under continuous CO₂ flow, solvent and **1a** (35 μ L, 1.0 equiv., 0.2 mmol) were added with syringe and subsequently the tube is sealed. The reaction was stirred for 12 hours with irradiating with a 30 W blue LED lamp (set at a distance of 3 cm, and a cooling fan was set up to hold the reaction temperature constant at 25~30 °C). After 12 hours, the light was switched off, the Schlenk tube was opened and to the mixture, methyl iodide (24.9 μ L, 0.4 mmol, 2.0 equiv.) was added and continued to stir at room temperature for additional 4 hours. Then, the reaction mixture was extracted with EtOAc (30 mL), water (10 mL \times 2), followed by washing the resulting organic layer with brine (20 mL), and finally the combined organic layer was passed through anhydrous Na₂SO₄ for drying and the mixture was concentrated by evaporating the solvent under reduced pressure. By column chromatography (SiO₂, eluting with hexane/ethyl acetate 93:7), the crude product was purified to provide the desired product **5a**.

II.6.4. General experimental procedures

General experimental procedures for carbocarboxylation under blue LED irradiation (Table 3).

An oven-dried Schlenk tube (10 mL) with a stirring bar inside was charged with **1** (0.2 mmol, 1.0 equiv, if solid), 4-CzIPN (1.5 mg, 0.002 mmol, 1.0 mol %), **2** (0.24 mmol, 1.2 equiv) and taken into glovebox where Cs₂CO₃ (130.3 mg, 0.4 mmol, 2.0 equiv) was added. The tube was then taken out, evacuated, and subsequently refilled with CO₂ for three times. Therefore, under continuous CO₂ flow, anhydrous DMSO (3.0 mL) and **1** (if liquid) were added with syringe and subsequently the tube is sealed. The reaction was stirred for 12 hours with irradiating with a 30 W blue LED lamp (set at a distance of 3 cm, and a cooling fan was set up to hold the reaction temperature constant at 25~30 °C). After 12 hours, the light was switched off, the Schlenk tube was opened and to the mixture, methyl iodide (24.9 μ L, 0.4 mmol, 2.0 equiv.) was added and continued to stir at room temperature for additional 4 hours. Then, the

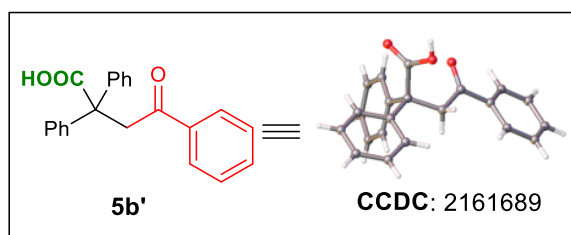
reaction mixture was extracted with EtOAc (30 mL), deionized water (10 mL × 2), followed by washing the resulting organic layer with brine (20 mL), and finally the combined organic layer was passed through anhydrous Na₂SO₄ for drying and the mixture was concentrated by evaporating the solvent under reduced pressure. By column chromatography (SiO₂, eluting with hexane/ethyl acetate), the crude product was purified by to provide the desired product.

General Procedure for Carbocarboxylation Under Sunlight Irradiation (Table 3)

An oven-dried Schlenk tube (10 mL) with a stirring bar inside was charged with **1** (0.2 mmol, 1.0 equiv, if solid), 4-CzIPN (1.5 mg, 0.002 mmol, 1.0 mol %), **2** (0.24 mmol, 1.2 equiv) and taken into glovebox where Cs₂CO₃ (130.3 mg, 0.4 mmol, 2.0 equiv) was added. The tube was then taken out, evacuated and subsequently refilled with CO₂ for three times. Therefore, under continuous CO₂ flow, anhydrous DMSO (3.0 mL) and **1** (if liquid) were added with syringe and subsequently the tube is sealed. The reaction was stirred under direct sunlight (at Kolkata, 22.57° N, 88.36° E from 1100 hrs in December) for 5 hours. After completion, the light was switched off, the Schlenk tube was opened and to the mixture, methyl iodide (24.9 μL, 0.4 mmol, 2.0 equiv.) was added and continued to stir at room temperature for additional 4 hours. Then, the reaction mixture was extracted with EtOAc (30 mL), deionized water (10 mL × 2), followed by washing the resulting organic layer with brine (20 mL), and finally the combined organic layer was passed through anhydrous Na₂SO₄ for drying and the mixture was concentrated by evaporating the solvent under reduced pressure. By column chromatography (SiO₂, eluting with hexane/ethylacetate), the crude product was purified by to provide the desired product.

II.6.5. Crystal data of 5b'

The crystal of compound **5b'** were grown in chloroform-hexane solvent system by slow evaporation procedure. The crystal data was collected in X-ray spectroscopy (Bruker D8 Venture with a Photon-III detector instrument), and the data was analyzed using OLEX2 software. The structure is given below. The corresponding cif file is uploaded separately as supporting information.



Thermal ellipsoid of **5b'**. Ellipsoids are represented with 50% probability.

Table 7. Crystal data and structure refinement for 5b'.

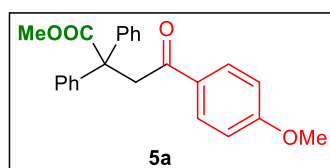
Identification code	5b'
Empirical formula	C ₄₄ H ₃₆ O ₆
Formula weight	660.73
Temperature/K	298.0
Crystal system	triclinic
Space group	P-1
a/Å	8.9980(2)
b/Å	11.5521(2)
c/Å	18.5351(4)
α/°	79.7640(10)
β/°	84.2930(10)
γ/°	67.4670(10)
Volume/Å ³	1750.20(6)
Z	2
ρ _{calc} /cm ³	1.254
μ/mm ⁻¹	0.663
F(000)	696.0
Crystal size/mm ³	0.2 × 0.2 × 0.2
Radiation	CuKα (λ = 1.54178)
2θ range for data collection/°	4.848 to 136.656

Chapter II

Index ranges	$-10 \leq h \leq 10, -13 \leq k \leq 13, -22 \leq l \leq 22$
Reflections collected	59503
Independent reflections	6396 [$R_{\text{int}} = 0.0782, R_{\text{sigma}} = 0.0395$]
Data/restraints/parameters	6396/0/453
Goodness-of-fit on F^2	1.098
Final R indexes [$I \geq 2\sigma(I)$]	$R_1 = 0.0684, wR_2 = 0.1755$
Final R indexes [all data]	$R_1 = 0.0788, wR_2 = 0.1871$
Largest diff. peak/hole / $e \text{ \AA}^{-3}$	0.27/-0.38

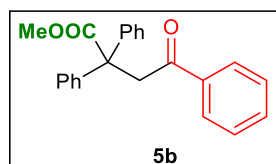
II.6.6. Characterization data

4-(4-methoxyphenyl)-4-oxo-2,2-diphenylbutanoic acid (5a)



This was synthesized following the optimized protocol and purified in column chromatography (Stationary medium is SiO_2 , and eluting solvent is 90:10 hexane/ethyl acetate) affording as white solid (61.3 mg, 82%). $^1\text{H NMR}$ (400 MHz, CDCl_3): δ 7.92 (d, $J = 8.8$ Hz, 2H), 7.30-7.26 (m, 8H), 7.23-7.20 (m, 2H), 6.90 (d, $J = 8.8$ Hz, 2H), 4.17 (s, 2H), 3.85 (s, 3H); $^{13}\text{C NMR}$ (100 MHz, CDCl_3): δ 196.3, 176.4, 164.0, 142.6, 130.7, 129.6, 128.7, 128.1, 127.1, 113.9, 57.7, 55.6, 47.3; HRMS (ESI, m/z) calcd. For $\text{C}_{23}\text{H}_{20}\text{O}_4$ $[\text{M}]^+$: 360.1362; found: 360.1359.

Methyl 4-oxo-2,2,4-triphenylbutanoate (5b)

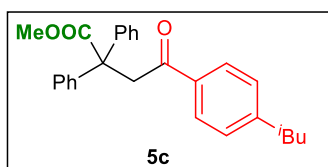


This was synthesized following the optimized protocol and purified in column chromatography (Stationary medium is SiO_2 , and eluting solvent is 90:10 hexane/ethyl acetate) affording as white solid (51.6 mg, 72%). $^1\text{H NMR}$ (400 MHz, CDCl_3): δ 7.95-7.92 (m, 2H), 7.54 (t, $J = 7.2$

**Transition Metal-free, Visible Light Mediated Decarboxylative Acylation and
Carboxylation of Alkenes with CO₂**

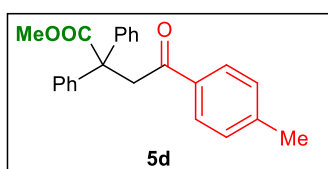
Hz, 1H), 7.43 (t, $J = 8$ Hz, 2H), 7.32-7.29 (m, 4H), 7.27-7.18 (m, 6H), 4.20 (s, 2H), 3.74 (s, 3H); ¹³C NMR (100 MHz, CDCl₃): δ 196.5, 173.7, 143.2, 136.9, 133.3, 128.8, 128.6, 128.0, 128.0, 126.9, 51.1, 52.5, 48.3; HRMS (ESI, m/z) calcd. For C₂₃H₂₁O₃ [M+H]⁺: 345.1491; found: 345.1494.

Methyl 4-(4-isobutylphenyl)-4-oxo-2,2-diphenylbutanoate (5c)



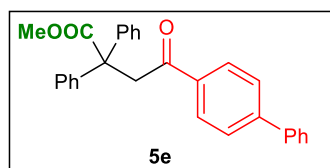
This was synthesized following the optimized protocol and purified in column chromatography (Stationary medium is SiO₂, and eluting solvent is 90:10 hexane/ethyl acetate) affording as yellowish white solid (64.0 mg, 80%). ¹H NMR (400 MHz, CDCl₃): δ 7.85 (d, $J = 8$ Hz, 2H), 7.32-7.25 (m, 7H), 7.23-7.18 (m, 5H), 4.18 (s, 1H), 3.73 (s, 3H), 2.51 (d, $J = 7.6$ Hz, 2H), 1.87 (sept., $J = 6.8$ Hz, 1H), 0.90 (s, 3H), 0.88 (s, 3H); ¹³C NMR (100 MHz, CDCl₃): δ 196.14, 173.85, 147.85, 143.30, 134.68, 129.38, 128.81, 128.06, 128.00, 126.88, 57.07, 52.51, 48.30, 45.46, 30.20, 22.39; HRMS (ESI, m/z) calcd. For C₂₇H₂₉O₄ [M+H]⁺: 401.2117; found: 401.2112.

Methyl 4-oxo-2,2-diphenyl-4-(p-tolyl)butanoate (5d)



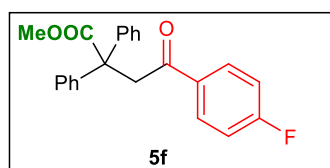
This was synthesized following the optimized protocol and purified in column chromatography (Stationary medium is SiO₂, and eluting solvent is 90:10 hexane/ethyl acetate) affording as white solid (55.8 mg, 78%). ¹H NMR (400 MHz, CDCl₃): δ 7.83 (d, $J = 8$ Hz, 2H), 7.31 – 7.25 (m, 7H), 7.23 – 7.17 (m, 5H), 4.17 (s, 2H), 3.74 (s, 3H), 2.39 (s, 3H); ¹³C NMR (100 MHz, CDCl₃): δ 196.10, 173.84, 144.13, 143.29, 134.45, 129.33, 128.80, 128.20, 128.00, 126.89, 57.11, 52.52, 48.26, 21.72; HRMS (ESI, m/z) calcd. For C₂₄H₂₃O₃ [M+H]⁺: 359.1647; found: 359.1648.

Methyl 4-([1,1'-biphenyl]-4-yl)-4-oxo-2,2-diphenylbutanoate (5e)



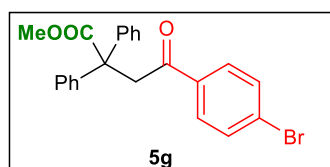
This was synthesized following the optimized protocol and purified in column chromatography (Stationary medium is SiO₂, and eluting solvent is 90:10 hexane/ethyl acetate) affording as white solid (51.2 mg, 61%). ¹H NMR (400 MHz, CDCl₃): δ 8.02-8.00 (m, 2H), 7.66-7.64 (m, 2H), 7.61-7.59 (m, 2H), 7.48-7.44 (m, 2H), 7.41-7.39 (m, 1H), 7.34-7.26 (m, 8H), 7.23-7.19 (m, 2H), 4.23 (s, 2H), 3.75 (s, 3H); ¹³C NMR (100 MHz, CDCl₃): δ 196.08, 173.80, 146.02, 143.22, 139.90, 135.60, 129.05, 128.81, 128.68, 128.36, 128.04, 127.35, 127.32, 126.95, 57.16, 52.56, 48.39; HRMS (ESI, m/z) calcd. For C₂₉H₂₅O₃ [M+H]⁺: 421.1804; found: 421.1799.

Methyl 4-(4-fluorophenyl)-4-oxo-2,2-diphenylbutanoate (5f)



This was synthesized following the optimized protocol and purified in column chromatography (Stationary medium is SiO₂, and eluting solvent is 90:10 hexane/ethyl acetate) affording as brown solid (49.2 mg, 68%). ¹H NMR (400 MHz, CDCl₃): δ ¹H NMR (400 MHz, Chloroform-*d*) δ 7.97-7.93 (m, 2H), 7.30-7.25 (m, 7H), 7.24-7.18 (m, 3H), 7.09 (t, *J* = 8.4 Hz, 2H), 4.15 (s, 2H), 3.74 (s, 3H); ¹³C NMR (100 MHz, CDCl₃): δ 194.98, 173.70, 165.88 (d, *J* = 254 Hz), 143.07, 133.36 (d, *J* = 3 Hz), 130.72 (d, *J* = 9 Hz), 128.76, 128.05, 126.99, 115.76 (d, *J* = 22 Hz), 57.19, 52.58, 48.21; HRMS (ESI, m/z) calcd. For C₂₄H₂₃O₃ [M+H]⁺: 359.1647; found: 359.1647.

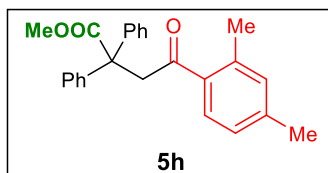
Methyl 4-(4-bromophenyl)-4-oxo-2,2-diphenylbutanoate (5g)



This was synthesized following the optimized protocol and purified in column chromatography (Stationary medium is SiO₂, and eluting solvent is 90:10 hexane/ethyl acetate) affording as yellow solid (57.4 mg, 68%). ¹H NMR (400 MHz, CDCl₃): δ 7.57 (d, *J* = 4.8 Hz, 2H), 7.36-

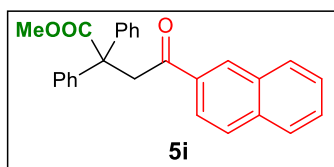
7.34 (m, 3H), 7.28-7.22 (m, 3H), 7.16-7.12 (m, 3H), 7.02 (s, 1H), 6.65 (d, $J = 8$ Hz, 2H), 3.70 (s, 2H), 3.67 (s, 3H); ¹³C NMR (100 MHz, CDCl₃): δ 192.72, 173.79, 154.19, 142.85, 142.44, 141.50, 139.17, 136.33, 131.05, 129.85, 129.25, 128.63, 128.49, 128.40, 128.07, 128.02, 127.85, 127.12, 124.28, 62.04, 52.39, 44.52; HRMS (ESI, m/z) calcd. For C₂₃H₂₀BrO₃ [M+H]⁺: 423.0596; found: 423.0602.

Methyl 4-(2,4-dimethylphenyl)-4-oxo-2,2-diphenylbutanoate (5h)



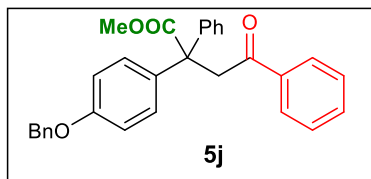
This was synthesized following the optimized protocol and purified in column chromatography (Stationary medium is SiO₂, and eluting solvent is 90:10 hexane/ethyl acetate) affording as white solid (54.3 mg, 73%). ¹H NMR (400 MHz, CDCl₃): δ 7.49 (d, $J = 8$ Hz, 2H), 7.32-7.26 (m, 6H), 7.25-7.18 (m, 4H), 7.03-7.02 (m, 2H), 4.11 (s, 2H), 3.76 (s, 3H), 2.34 (s, 3H), 2.32 (s, 3H); ¹³C NMR (100 MHz, CDCl₃): δ 200.08, 173.88, 143.29, 141.99, 138.52, 135.22, 132.87, 128.81, 128.51, 128.01, 126.89, 126.30, 57.26, 52.48, 51.06, 21.43, 21.16; HRMS (ESI, m/z) calcd. For C₂₅H₂₅O₃ [M+H]⁺: 373.1804; found: 373.1800.

Methyl 4-(naphthalen-2-yl)-4-oxo-2,2-diphenylbutanoate (5i)

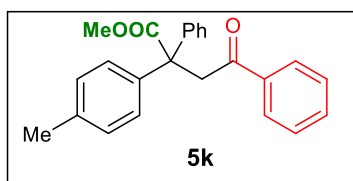


This was synthesized following the optimized protocol and purified in column chromatography (Stationary medium is SiO₂, and eluting solvent is 90:10 hexane/ethyl acetate) affording as yellowish white solid (51.2 mg, 65%). ¹H NMR (400 MHz, CDCl₃): δ 8.46 (s, 1H), 7.99 (dd, $J_1 = 8.4$ Hz, $J_2 = 1.6$ Hz, 1H), 7.94 (d, $J = 7.2$ Hz, 1H), 7.87-7.84 (m, 2H), 7.61-7.52 (m, 2H), 7.36-7.34 (m, 4H), 7.30-7.26 (m, 4H), 7.23-7.19 (m, 2H), 4.34 (s, 2H), 3.76 (m, 3H); ¹³C NMR (100 MHz, CDCl₃): δ 196.48, 173.83, 143.24, 135.70, 134.24, 132.52, 129.68, 129.63, 128.84, 128.63, 128.55, 128.06, 127.86, 126.96, 126.93, 123.86, 57.28, 52.59, 48.44; HRMS (ESI, m/z) calcd. For C₂₇H₂₃O₃ [M+H]⁺: 395.1647; found: 395.1645.

Methyl 2-(4-(benzyloxy)phenyl)-4-oxo-2,4-diphenylbutanoate (5j)

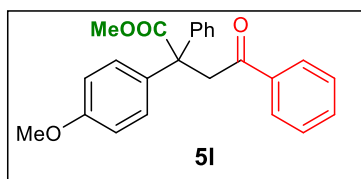


This was synthesized following the optimized protocol and purified in column chromatography (Stationary medium is SiO₂, and eluting solvent is 90:10 hexane/ethyl acetate) affording as white solid (70.2 mg, 78%). ¹H NMR (400 MHz, CDCl₃): δ 7.95-7.93 (m, 2H), 7.55 (t, *J* = 8 Hz, 1H), 7.46-7.26 (m, 12H), 7.23-7.21 (m, 2H), 6.89-6.86 (m, 2H), 5.02 (s, 2H), 4.19 (s, 2H), 3.74 (s, 3H); ¹³C NMR (100 MHz, CDCl₃): δ 196.59, 174.00, 157.63, 143.49, 137.07, 136.97, 135.52, 133.29, 130.04, 128.67, 128.07, 127.61, 126.93, 114.22, 70.08, 56.49, 52.54, 48.50; HRMS (ESI, *m/z*) calcd. For C₃₀H₂₇O₄ [M+H]⁺: 451.1909; found: 451.1911.

Methyl 4-oxo-2,4-diphenyl-2-(*p*-tolyl)butanoate (5k)

This was synthesized following the optimized protocol and purified in column chromatography (Stationary medium is SiO₂, and eluting solvent is 90:10 hexane/ethyl acetate) affording as white solid (58.0 mg, 81%). ¹H NMR (400 MHz, CDCl₃): δ 7.95-7.93 (m, 2H), 7.54 (t, *J* = 7.6 Hz, 1H), 7.43 (m, 2H), 7.33-7.30 (m, 2H), 7.27-7.25 (m, 1H), 7.24-7.17 (m, 4H), 4.19 (s, 2H), 3.73 (s, 3H), 2.29 (s, 3H); ¹³C NMR (100 MHz, CDCl₃): δ 196.55, 173.92, 143.36, 140.24, 136.97, 136.60, 133.25, 128.80, 128.76, 128.66, 128.60, 128.08, 127.98, 126.86, 56.78, 52.51, 48.41, 21.01; HRMS (ESI, *m/z*) calcd. For C₂₄H₂₃O₃ [M+H]⁺: 359.1647; found: 359.1634.

Methyl 2-(4-methoxyphenyl)-4-oxo-2,4-diphenylbutanoate (5l)

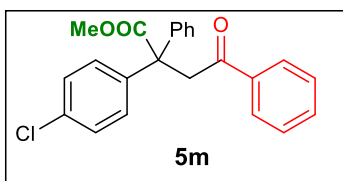


This was synthesized following the optimized protocol and purified in column chromatography (Stationary medium is SiO₂, and eluting solvent is 90:10 hexane/ethyl acetate) affording as

Transition Metal-free, Visible Light Mediated Decarboxylative Acylation and Carboxylation of Alkenes with CO₂

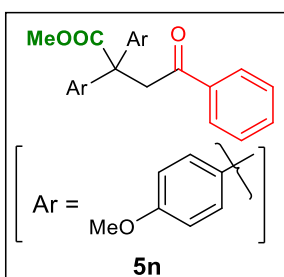
yellow gel (57.6 mg, 77%). ¹H NMR (400 MHz, CDCl₃): δ 7.95-7.92 (m, 2H), 7.54 (t, *J* = 7.6 Hz, 1H), 7.45-7.41 (m, 2H), 7.34-7.31 (m, 2H), 7.28-7.26 (m, 2H), 7.24-7.18 (m, 3H), 6.81-6.77 (m, 2H), 4.18 (s, 2H), 3.76 (s, 3H), 3.73 (s, 3H); ¹³C NMR (100 MHz, CDCl₃): δ 196.58, 174.01, 158.32, 143.51, 136.97, 135.23, 133.27, 129.99, 128.68, 128.07, 128.04, 126.90, 113.33, 56.46, 55.27, 52.51, 48.49; HRMS (ESI, *m/z*) calcd. For C₂₄H₂₃O₄ [M+H]⁺: 375.1596; found: 375.1588.

Methyl 2-(4-chlorophenyl)-4-oxo-2,4-diphenylbutanoate (5m)



This was synthesized following the optimized protocol and purified in column chromatography (Stationary medium is SiO₂, and eluting solvent is 90:10 hexane/ethyl acetate) affording as white solid (55.2 mg, 73%). ¹H NMR (400 MHz, CDCl₃): δ 7.94-7.91 (m, 2H), 7.55 (t, *J* = 7.6 Hz, 1H), 7.44 (t, *J* = 7.6 Hz, 2H), 7.30-7.25 (m, 5H), 7.24-7.19 (m, 4H), 4.17 (AB_q, *J* = 49.6 Hz, 2H), 3.73 (s, 3H); ¹³C NMR (100 MHz, CDCl₃): δ 196.27, 173.45, 142.89, 141.61, 136.74, 133.45, 132.81, 130.62, 128.73, 128.38, 128.33, 128.07, 127.99, 127.28, 56.64, 52.66, 48.25; HRMS (ESI, *m/z*) calcd. For C₂₃H₂₀ClO₃ [M+H]⁺: 379.1101; found: 379.1094.

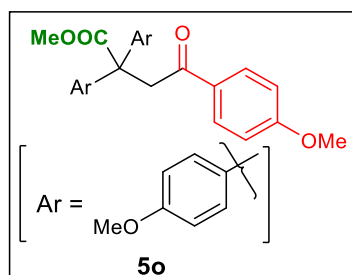
Methyl 2,2-bis(4-methoxyphenyl)-4-oxo-4-phenylbutanoate (5n)



This was synthesized following the optimized protocol and purified in column chromatography (Stationary medium is SiO₂, and eluting solvent is 90:10 hexane/ethyl acetate) affording as yellowish white solid (58.2 mg, 72%). ¹H NMR (400 MHz, CDCl₃): δ 7.94-7.91 (m, 2H), 7.53 (t, *J* = 7.8 Hz, 1H), 7.44-7.40 (m, 2H), 7.25-7.22 (m, 3H), 7.18 (d, *J* = 9.2 Hz), 6.81-6.78 (m, 4H), 4.14 (s, 2H), 3.76 (s, 6H), 3.72 (s, 3H); ¹³C NMR (100 MHz, CDCl₃): δ 196.66, 174.22,

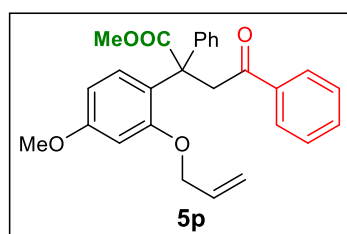
158.29, 137.01, 135.52, 133.24, 129.87, 129.72, 128.66, 128.06, 113.36, 113.33, 55.79, 55.28, 52.48, 48.60; HRMS (ESI, m/z) calcd. For $C_{25}H_{25}O_5$ $[M+H]^+$: 405.1624; found: 405.1623.

Methyl 2,2,4-tris(4-methoxyphenyl)-4-oxobutanoate (5o)



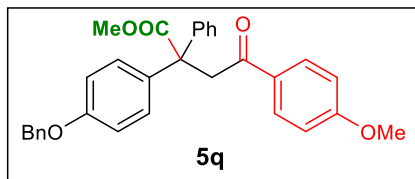
This was synthesized following the optimized protocol and purified in column chromatography (Stationary medium is SiO_2 , and eluting solvent is 90:10 hexane/ethyl acetate) affording as white solid (65.1 mg, 75%). 1H NMR (400 MHz, $CDCl_3$): δ 7.91 (d, $J = 8.8$ Hz, 2H), 7.22 (d, $J = 8.8$ Hz, 4H), 6.89 (d, $J = 8.8$ Hz, 2H), 6.78 (d, $J = 8.8$ Hz, 4H), 4.08 (s, 2H), 3.84 (s, 3H), 3.76 (s, 6H), 3.72 (s, 3H); ^{13}C NMR (100 MHz, $CDCl_3$): δ 195.15, 174.32, 163.61, 158.23, 135.66, 130.34, 130.10, 129.87, 113.77, 113.29, 55.81, 55.57, 55.27, 52.44, 48.26; HRMS (ESI, m/z) calcd. For $C_{26}H_{27}O_6$ $[M+H]^+$: 435.1808; found: 435.1820.

Methyl 2-(2-(allyloxy)-4-methoxyphenyl)-4-oxo-2,4-diphenylbutanoate (5p)



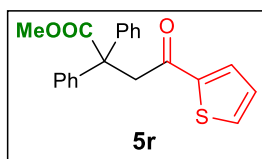
This was synthesized following the optimized protocol and purified in column chromatography (Stationary medium is SiO_2 , and eluting solvent is 90:10 hexane/ethyl acetate) affording as yellowish white solid (58.5 mg, 68%). 1H NMR (400 MHz, $CDCl_3$): δ 7.93-7.90 (m, 2H), 7.53-7.49 (m, 1H), 7.42-7.38 (m, 4H), 7.29-7.26 (m, 2H), 7.24-7.20 (m, 2H), 6.42 (dd, $J_1 = 8.8$ Hz, $J_2 = 2.4$ Hz, 1H), 6.35 (d, $J = 2.4$ Hz, 1H), 5.85-5.75 (m, 1H), 5.28-5.17 (m, 2H), 4.38-4.31 (m, 4H), 3.74 (s, 3H), 3.64 (s, 3H); ^{13}C NMR (100 MHz, $CDCl_3$): δ 197.28, 174.76, 159.79, 156.72, 140.26, 137.68, 132.97, 132.84, 132.00, 128.83, 128.48, 128.04, 127.81, 126.89, 124.00, 117.46, 103.80, 100.14, 69.29, 56.02, 55.31, 52.46, 42.90; HRMS (ESI, m/z) calcd. For $C_{26}H_{25}O_4$ $[M+H]^+$: 401.1753; found: 401.1760.

Methyl 2-(4-(benzyloxy)phenyl)-4-(4-methoxyphenyl)-4-oxo-2-phenylbutanoate (5q)



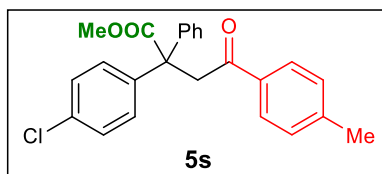
This was synthesized following the optimized protocol and purified in column chromatography (Stationary medium is SiO₂, and eluting solvent is 90:10 hexane/ethyl acetate) affording as yellow gum (82.6 mg, 86%). ¹H NMR (400 MHz, CDCl₃): δ 7.94-7.91 (m, 2H), 7.42-7.19 (m, 12H), 6.92-6.85 (m, 4H), 5.01 (s, 2H), 4.14-4.13 (m, 2H), 3.85 (s, 3H), 3.74 (s, 3H); ¹³C NMR (100 MHz, CDCl₃): δ 195.11, 174.12, 163.66, 157.59, 143.66, 137.10, 135.68, 130.38, 130.06, 130.05, 128.71, 128.67, 128.04, 127.61, 126.87, 114.18, 113.81, 70.07, 56.52, 55.59, 52.50, 48.17; HRMS (ESI, m/z) calcd. For C₃₁H₂₉O₅ [M+H]⁺: 481.2015; found: 481.2022.

Methyl 4-oxo-2,2-diphenyl-4-(thiophen-2-yl)butanoate (5r)



This was synthesized following the optimized protocol and purified in column chromatography (Stationary medium is SiO₂, and eluting solvent is 90:10 hexane/ethyl acetate) affording as yellow solid (58.1 mg, 83%). ¹H NMR (400 MHz, CDCl₃): δ 7.68 (dd, *J*₁ = 3.6 Hz, *J*₂ = 1.2 Hz, 1H), 7.58 (dd, *J*₁ = 5.2 Hz, *J*₂ = 1.2 Hz, 1H), 7.33-7.26 (m, 7H), 7.25-7.19 (m, 3H), 7.08-7.06 (m, 1H), 4.13 (s, 2H), 3.74 (s, 3H); ¹³C NMR (100 MHz, CDCl₃): δ 189.46, 173.60, 144.08, 142.97, 133.72, 131.85, 128.80, 128.12, 128.06, 127.02, 57.26, 52.63, 48.63; HRMS (ESI, m/z) calcd. For C₂₁H₁₉O₃S [M+H]⁺: 351.1055; found: 351.1055.

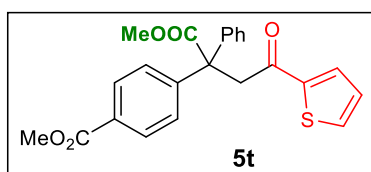
Methyl 2-(4-chlorophenyl)-4-(4-methoxyphenyl)-4-oxo-2-phenylbutanoate (5s)



This was synthesized following the optimized protocol and purified in column chromatography (Stationary medium is SiO₂, and eluting solvent is 90:10 hexane/ethyl acetate) affording as

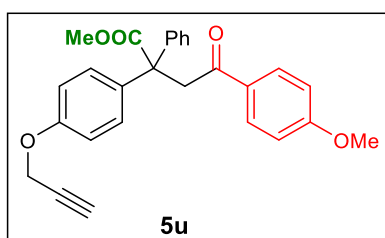
colourless gum (51.7 mg, 66%). ^1H NMR (400 MHz, CDCl_3): δ 7.86-7.83 (m, 2H), 7.53 (dd, $J_1 = 5.6$ Hz, $J_2 = 2.0$ Hz, 1H), 7.39-7.35 (m, 2H), 7.31-7.25 (m, 4H), 7.23-7.16 (m, 4H), 4.48 (AB_q, $J = 18.8$ Hz, 2H), 3.70 (s, 3H), 2.39 (s, 3H); ^{13}C NMR (100 MHz, CDCl_3): δ 196.09, 173.67, 144.03, 139.70, 134.69, 133.85, 133.12, 130.91, 129.31, 128.82, 128.51, 128.18, 128.10, 127.28, 125.92, 58.33, 52.86, 43.16, 21.70; HRMS (ESI, m/z) calcd. For $\text{C}_{24}\text{H}_{21}\text{ClO}_3$ $[\text{M}+\text{H}]^+$: 393.1257; found: 393.1249.

Methyl 4-(1-methoxy-1,4-dioxo-2-phenyl-4-(thiophen-2-yl)butan-2-yl)benzoate (5t)



This was synthesized following the optimized protocol and purified in column chromatography (Stationary medium is SiO_2 , and eluting solvent is 90:10 hexane/ethyl acetate) affording as white solid (58.8 mg, 72%). ^1H NMR (400 MHz, CDCl_3): δ 7.57 (dd, $J_1 = 4$ Hz, $J_2 = 1.2$ Hz, 1H), 7.52 (dd, $J_1 = 5.2$ Hz, $J_2 = 1.2$ Hz, 1H), 7.39 (dd, $J_1 = 4.8$ Hz, $J_2 = 0.8$ Hz, 1H), 7.33-7.31 (m, 3H), 7.11 (dd, $J_1 = 4$ Hz, $J_2 = 1.2$ Hz, 1H), 7.01 (dd, $J_1 = 5.2$ Hz, $J_2 = 4$ Hz, 1H), 6.83-6.80 (m, 4H), 4.14 (s, 2H), 3.76 (s, 6H); ^{13}C NMR (100 MHz, CDCl_3): δ 192.71, 189.65, 158.60, 144.88, 143.24, 133.61, 133.48, 132.56, 131.68, 130.83, 129.87, 127.99, 127.32, 113.61, 61.95, 55.28, 50.25; HRMS (ESI, m/z) calcd. For $\text{C}_{23}\text{H}_{21}\text{O}_5\text{S}$ $[\text{M}+\text{H}]^+$: 411.1266; found: 411.1269.

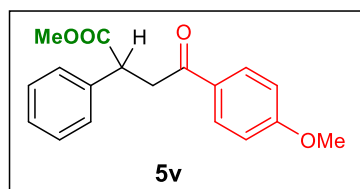
Methyl 4-(4-methoxyphenyl)-4-oxo-2-phenyl-2-(4-(prop-2-yn-1-yloxy)phenyl)butanoate (5u)



This was synthesized following the optimized protocol and purified in column chromatography (Stationary medium is SiO_2 , and eluting solvent is 90:10 hexane/ethyl acetate) affording as colourless gum (58.3 mg, 68%). ^1H NMR (400 MHz, CDCl_3): δ 7.92-7.90 (m, 2H), 7.31-7.27 (m, 3H), 7.24-7.19 (m, 4H), 6.91-6.83 (m, 4H), 4.62 (d, $J = 7.2$ Hz, 2H), 4.11 (s, 2H), 3.85 (s, 3H), 3.73 (s, 3H), 2.49 (t, $J = 2.4$ Hz, 1H); ^{13}C NMR (100 MHz, CDCl_3): δ 195.03, 174.02,

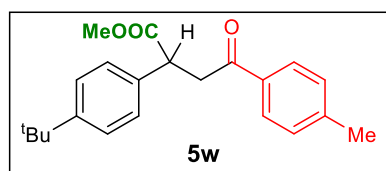
163.65, 156.33, 143.54, 136.29, 130.35, 130.09, 130.01, 128.63, 128.04, 126.89, 114.16, 113.79, 78.67, 75.57, 56.51, 55.86, 55.57, 52.50, 48.13; HRMS (ESI, m/z) calcd. For C₂₇H₂₅O₅ [M+H]⁺: 429.1702; found: 429.1689.

Methyl 4-oxo-2,4-diphenylbutanoate (5v)



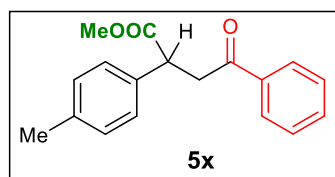
This was synthesized following the optimized protocol and purified in column chromatography (Stationary medium is SiO₂, and eluting solvent is 90:10 hexane/ethyl acetate) affording as brown solid (44.7 mg, 75%). ¹H NMR (400 MHz, CDCl₃): δ 7.96-7.92 (m, 2H), 7.34-7.26 (m, 5H), 6.92-6.89 (m, 2H), 4.27 (dd, *J*₁ = 10.4 Hz, *J*₂ = 4 Hz, 1H), 3.95-3.88 (m, 1H), 3.85 (s, 3H), 3.21 (dd, *J*₁ = 17.6 Hz, *J*₂ = 4 Hz, 1H); ¹³C NMR (100 MHz, CDCl₃): δ 196.19, 174.05, 163.73, 138.59, 132.75, 130.45, 129.61, 128.98, 127.92, 127.59, 113.82, 55.56, 52.39, 46.51, 42.56; HRMS (ESI, m/z) calcd. For C₁₈H₁₉O₄ [M+H]⁺: 299.1283; found: 299.1287.

Methyl 2-(4-(tert-butyl)phenyl)-4-oxo-4-(p-tolyl)butanoate (5w)



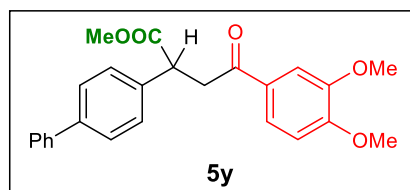
This was synthesized following the optimized protocol and purified in column chromatography (Stationary medium is SiO₂, and eluting solvent is 90:10 hexane/ethyl acetate) affording as colourless gum (49.3 mg, 73%). ¹H NMR (400 MHz, CDCl₃): δ 7.87-7.85 (m, 2H), 7.36-7.34 (m, 2H), 7.29-7.26 (m, 2H), 7.23 (d, *J* = 8 Hz, 2H), 4.26 (dd, *J*₁ = 10.4 Hz, *J*₂ = 4 Hz, 1H), 3.91 (dd, *J*₁ = 18 Hz, *J*₂ = 10.4 Hz, 1H), 3.69 (s, 3H), 3.23 (dd, *J*₁ = 18 Hz, *J*₂ = 4 Hz, 1H), 2.39 (s, 3H), 1.31 (s, 9H); ¹³C NMR (100 MHz, CDCl₃): δ 197.48, 174.18, 150.48, 144.17, 135.42, 134.07, 129.35, 128.30, 127.52, 125.91, 52.35, 45.97, 42.90, 34.57, 31.40, 21.74; HRMS (ESI, m/z) calcd. For C₂₂H₂₇O₃ [M+H]⁺: 339.1960; found: 339.1969.

Methyl 4-oxo-4-phenyl-2-(p-tolyl)butanoate (5x)



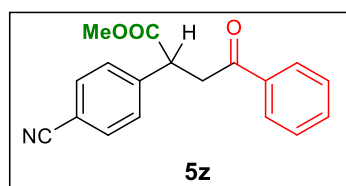
This was synthesized following the optimized protocol and purified in column chromatography (Stationary medium is SiO₂, and eluting solvent is 90:10 hexane/ethyl acetate) affording as white crystalline solid (38.9 mg, 69%). ¹H NMR (400 MHz, CDCl₃): δ 7.97-7.95 (m, 2H), 7.55 (tt, *J*₁ = 7.2 Hz, *J*₂ = 1.2 Hz, 1H), 7.44 (t, *J* = 8 Hz, 2H), 7.23 (d, *J* = 8 Hz, 2H), 7.15 (d, *J* = 8 Hz, 2H), 4.26 (dd, *J*₁ = 10 Hz, *J*₂ = 4 Hz, 1H), 3.92 (dd, *J*₁ = 17.2 Hz, *J*₂ = 9.6 Hz, 1H), 3.68 (s, 3H), 3.24 (dd, *J*₁ = 18 Hz, *J*₂ = 4 Hz, 1H), 2.33 (s, 3H); ¹³C NMR (100 MHz, CDCl₃): δ 197.81, 174.11, 137.37, 136.52, 135.43, 133.37, 129.69, 128.68, 128.17, 127.77, 52.40, 46.02, 42.93, 21.14; HRMS (ESI, m/z) calcd. For C₁₈H₁₉O₃ [M+H]⁺: 283.1334; found: 283.1326.

Methyl 2-([1,1'-biphenyl]-4-yl)-4-(3,4-dimethoxyphenyl)-4-oxobutanoate (5y)



This was synthesized following the optimized protocol and purified in column chromatography (Stationary medium is SiO₂, and eluting solvent is 90:10 hexane/ethyl acetate) affording as white solid (52.5 mg, 65%). ¹H NMR (400 MHz, CDCl₃): δ 7.61 (dd, *J*₁ = 8 Hz, *J*₂ = 2 Hz, 1H), 7.57 (m, 4H), 7.52 (d, *J* = 2 Hz, 1H), 7.44-7.41 (m, 4H), 7.34 (tt, *J*₁ = 7.2 Hz, *J*₂ = 2 Hz, 1H), 6.86 (d, *J* = 8.4 Hz, 1H), 4.33 (dd, *J*₁ = 10.0 Hz, *J*₂ = 4 Hz, 1H), 3.95-3.88 (m, 7H), 3.72 (s, 3H), 3.29 (dd, *J*₁ = 18 Hz, *J*₂ = 4.4 Hz, 1H); ¹³C NMR (100 MHz, CDCl₃): δ 196.26, 174.06, 153.59, 149.12, 140.65, 137.54, 129.73, 128.88, 128.36, 127.71, 127.48, 127.13, 122.92, 110.21, 110.12, 56.16, 56.06, 52.48, 46.27, 42.44; HRMS (ESI, m/z) calcd. For C₂₅H₂₅O₅ [M+H]⁺: 405.1702; found: 405.1702.

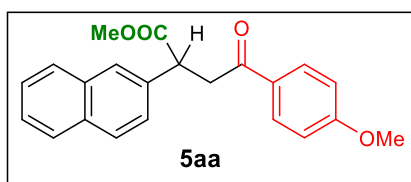
Methyl 2-(4-cyanophenyl)-4-oxo-4-phenylbutanoate (5z)



Transition Metal-free, Visible Light Mediated Decarboxylative Acylation and Carboxylation of Alkenes with CO₂

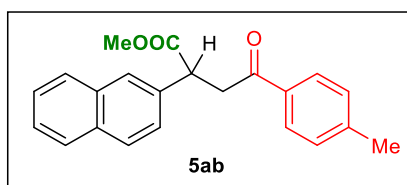
This was synthesized following the optimized protocol and purified in column chromatography (Stationary medium is SiO₂, and eluting solvent is 90:10 hexane/ethyl acetate) affording as white solid (36.9 mg, 63%). ¹H NMR (400 MHz, CDCl₃): δ 7.96-7.92 (m, 2H), 7.64-7.61 (m, 2H), 7.56 (tt, *J*₁ = 8 Hz, *J*₂ = 1.2 Hz, 1H), 7.48-7.43 (m, 4H), 4.36 (q, *J* = 4.4 Hz, 1H), 3.90 (q, *J* = 9.2 Hz, 1H), 3.69 (s, 3H), 3.30 (dd, *J*₁ = 18 Hz, *J*₂ = 4.8 Hz, 1H); ¹³C NMR (100 MHz, CDCl₃): δ 197.4, 163.2, 148.0, 138.1, 131.4, 130.9, 130.2, 128.2, 127.8, 127.5, 126.1, 126.0, 113.4, 55.5, 49.7, 43.8, 42; HRMS (ESI, *m/z*) calcd. For C₁₈H₁₆O₃ [M+H]⁺: 294.1130; found: 294.1133.

Methyl 4-(4-methoxyphenyl)-2-(naphthalen-2-yl)-4-oxobutanoate (5aa)



This was synthesized following the optimized protocol and purified in column chromatography (Stationary medium is SiO₂, and eluting solvent is 90:10 hexane/ethyl acetate) affording as reddish white solid (45.9 mg, 66%). ¹H NMR (400 MHz, CDCl₃): δ 7.97-7.94 (m, 2H), 7.83-7.80 (m, 4H), 7.48-7.45 (m, 3H), 6.92-6.90 (m, 2H), 4.45 (dd, *J*₁ = 6 Hz, *J*₂ = 4 Hz, 1H), 3.98 (dd, *J*₁ = 18 Hz, *J*₂ = 10.4 Hz, 1H), 3.85 (s, 3H), 3.69 (s, 3H), 3.30 (dd, *J*₁ = 18 Hz, *J*₂ = 4 Hz, 1H); ¹³C NMR (100 MHz, CDCl₃): δ 196.13, 174.06, 163.76, 135.99, 133.57, 132.78, 130.47, 129.62, 128.73, 127.89, 127.74, 126.76, 126.42, 126.10, 125.91, 113.84, 55.56, 52.45, 46.62, 42.54; HRMS (ESI, *m/z*) calcd. For C₂₂H₂₁O₄ [M+H]⁺: 349.1440; found: 349.1444.

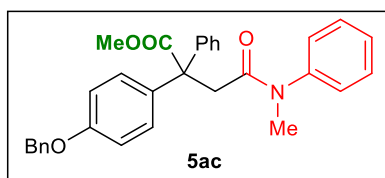
Methyl 2-(naphthalen-2-yl)-4-oxo-4-(p-tolyl)butanoate (5ab)



This was synthesized following the optimized protocol and purified in column chromatography (Stationary medium is SiO₂, and eluting solvent is 90:10 hexane/ethyl acetate) affording as white solid (47.2 mg, 71%). ¹H NMR (400 MHz, CDCl₃): δ 7.89-7.87 (m, 2H), 7.83-7.80 (m, 4H), 7.49-7.44 (m, 3H), 7.24-7.23 (m, 2H), 4.46 (dd, *J*₁ = 10.0 Hz, *J*₂ = 4.0 Hz, 1H), 4.02 (dd, *J*₁ = 18.0 Hz, *J*₂ = 10.0 Hz, 1H), 3.70 (s, 3H), 3.33 (dd, *J*₁ = 18.0 Hz, *J*₂ = 4.0 Hz, 1H), 2.39 (s,

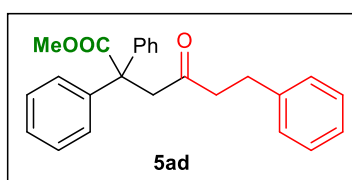
3H); ^{13}C NMR (100 MHz, CDCl_3): δ 197.28, 174.01, 144.26, 135.93, 134.03, 133.57, 132.79, 129.38, 128.75, 128.31, 127.90, 127.74, 126.77, 126.43, 126.12, 125.90, 52.47, 46.57, 42.76, 21.74; HRMS (ESI, m/z) calcd. For $\text{C}_{22}\text{H}_{20}\text{O}_3$ $[\text{M}+\text{H}]^+$: 332.1412; found: 332.1413.

Methyl 2-(4-(benzyloxy)phenyl)-4-(methyl(phenyl)amino)-4-oxo-2-phenylbutanoate (5ac)



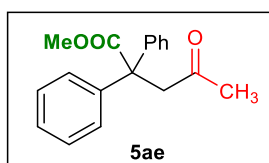
This was synthesized following the optimized protocol and purified in column chromatography (Stationary medium is SiO_2 , and eluting solvent is 90:10 hexane/ethyl acetate) affording as yellow solid (71.9 mg, 83%). ^1H NMR (400 MHz, CDCl_3): δ 7.43-7.27 (m, 8H), 7.26-7.18 (m, 4H), 6.90-6.86 (m, 2H), 5.03 (s, 2H), 3.73 (s, 3H), 3.55 (s, 3H), 3.46 (s, 2H); ^{13}C NMR (100 MHz, CDCl_3): δ 173.65, 171.22, 157.80, 142.67, 137.01, 134.74, 129.86, 128.67, 128.54, 128.08, 127.62, 127.14, 114.26, 57.03, 52.65, 51.75, 43.88; HRMS (ESI, m/z) calcd. For $\text{C}_{31}\text{H}_{30}\text{NO}_5$ $[\text{M}+\text{H}]^+$: 480.2175; found: 480.2169.

Methyl 4-oxo-2,2,6-triphenylhexanoate (5ad)



This was synthesized following the optimized protocol and purified in column chromatography (Stationary medium is SiO_2 , and eluting solvent is 90:10 hexane/ethyl acetate) affording as white gum (40.9 mg, 55%). ^1H NMR (400 MHz, CDCl_3): δ 7.26-7.16 (m, 13H), 7.08-7.06 (m, 2H), 3.68 (s, 3H), 3.58 (s, 2H), 2.79 (t, $J = 7.6$ Hz, 1H), 2.62 (t, $J = 7.6$ Hz, 1H); ^{13}C NMR (100 MHz, CDCl_3): δ 206.42, 173.61, 142.92, 140.91, 128.69, 128.52, 128.37, 128.04, 126.99, 126.15, 57.12, 52.51, 52.10, 44.88, 29.54; HRMS (ESI, m/z) calcd. For $\text{C}_{25}\text{H}_{24}\text{O}_3$ $[\text{M}+\text{H}]^+$: 373.1804; found: 373.1801.

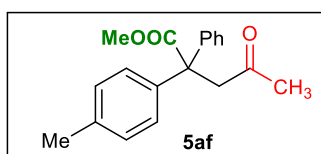
Methyl 4-oxo-2,2-diphenylpentanoate (5ae)



Transition Metal-free, Visible Light Mediated Decarboxylative Acylation and Carboxylation of Alkenes with CO₂

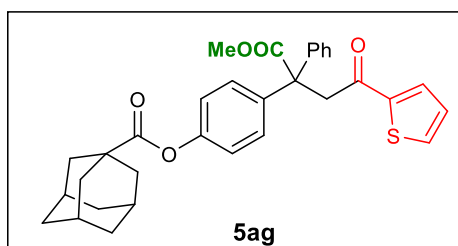
This was synthesized following the optimized protocol and purified in column chromatography (Stationary medium is SiO₂, and eluting solvent is 90:10 hexane/ethyl acetate) affording as colourless gummy liquid (29.9 mg, 53%). ¹H NMR (400 MHz, CDCl₃): δ 7.28-7.20 (m, 10 H), 3.71 (s, 3H), 3.64 (s, 2H), 2.07 (s, 3H); ¹³C NMR (100 MHz, CDCl₃): δ 205.02, 173.64, 142.99, 128.69, 128.04, 127.00, 57.05, 52.54, 30.72; HRMS (ESI, m/z) calcd. For C₁₈H₁₈O₃ [M+H]⁺: 283.1334; found: 283.1334.

Methyl 4-oxo-2-phenyl-2-(p-tolyl)pentanoate (5af)



This was synthesized following the optimized protocol and purified in column chromatography (Stationary medium is SiO₂, and eluting solvent is 90:10 hexane/ethyl acetate) affording as colourless gummy liquid (29.6 mg, 50%). ¹H NMR (400 MHz, CDCl₃): δ 7.26-7.19 (m, 5H), 7.13-7.11 (m, 2H), 7.07-7.05 (m, 2H), 3.70 (s, 3H), 3.61 (d, *J* = 2.4 Hz, 2H), 2.30 (s, 3H), 2.07 (s, 3H); ¹³C NMR (100 MHz, CDCl₃): δ 205.10, 173.77, 143.14, 139.99, 136.66, 128.76, 128.69, 128.51, 127.98, 126.92, 56.73, 52.71, 52.50, 30.74, 21.02; HRMS (ESI, m/z) calcd. For C₁₉H₂₀O₃ [M+H]⁺: 297.1491; found: 297.1499.

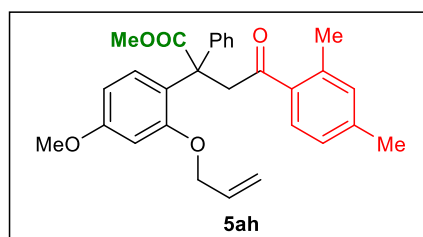
4-(1-methoxy-1,4-dioxo-2-phenyl-4-(thiophen-2-yl)butan-2-yl)phenyl (3r,5r,7r)-adamantane-1-carboxylate (5ag)



This was synthesized following the optimized protocol and purified in column chromatography (Stationary medium is SiO₂, and eluting solvent is 90:10 hexane/ethyl acetate) affording as ash coloured solid (88.7 mg, 84%). ¹H NMR (400 MHz, CDCl₃): δ 7.67 (dd, *J*₁ = 4.0 Hz, *J*₂ = 1.2 Hz, 1H), 7.59 (dd, *J*₁ = 4.8 Hz, *J*₂ = 0.8 Hz, 1H), 7.32-7.26 (m, 6H), 7.24-7.21 (m, 1H), 7.09-7.07 (m, 1H), 6.96-6.93 (m, 2H), 4.15-4.05 (m, 2H), 3.73 (s, 3H), 2.06-2.01 (m, 9H), 1.78-1.71 (m, 6H); ¹³C NMR (100 MHz, CDCl₃): δ 189.27, 176.10, 173.44, 149.91, 143.99, 142.78,

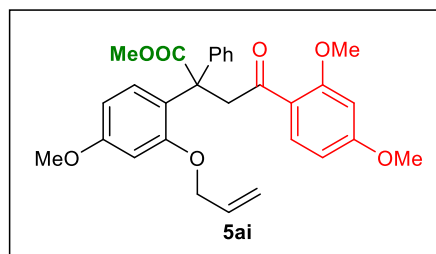
140.10, 133.76, 131.86, 129.99, 128.70, 128.14, 127.14, 120.93, 56.80, 52.66, 48.70, 41.11, 38.81, 36.53, 27.98; HRMS (ESI, m/z) calcd. For C₃₂H₃₂O₅S [M+H]⁺: 529.2049; found: 529.2061.

Methyl 2-(2-(allyloxy)-4-methoxyphenyl)-4-(2,4-dimethylphenyl)-4-oxo-2-phenylbutanoate (5ah)



This was synthesized following the optimized protocol and purified in column chromatography (Stationary medium is SiO₂, and eluting solvent is 90:10 hexane/ethyl acetate) affording as yellow gel (53.1 mg, 58%). ¹H NMR (400 MHz, CDCl₃): δ 7.50 (d, *J* = 8.0 Hz, 1H), 7.44-7.42 (m, 2H), 7.33-7.27 (m, 2H), 7.23-7.17 (m, 2H), 7.00-6.96 (m, 2H), 6.40 (dd, *J*₁ = 8.8 Hz, *J*₂ = 2.8 Hz, 1H), 6.34 (d, *J* = 2.4 Hz, 1H), 5.79-5.69 (m, 1H), 5.22-5.13 (m, 2H), 4.37-4.16 (m, 4H), 3.74 (s, 3H), 3.64 (s, 3H), 2.31 (s, 3H), 2.25 (s, 3H); ¹³C NMR (100 MHz, CDCl₃): δ 201.22, 174.69, 159.80, 156.77, 141.35, 140.68, 138.09, 136.22, 132.96, 132.59, 131.71, 128.95, 128.82, 128.52, 127.74, 126.77, 126.50, 126.11, 124.17, 117.37, 103.82, 100.28, 69.28, 56.20, 55.34, 52.40, 45.88, 21.37, 21.10; HRMS (ESI, m/z) calcd. For C₂₉H₃₀O₅ [M+H]⁺: 459.2171; found: 459.2172.

Methyl 2-(2-(allyloxy)-4-methoxyphenyl)-4-(2,4-dimethoxyphenyl)-4-oxo-2-phenylbutanoate (5ai)

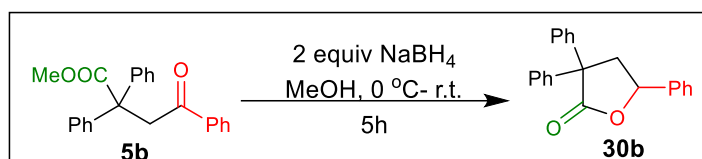


This was synthesized following the optimized protocol and purified in column chromatography (Stationary medium is SiO₂, and eluting solvent is 90:10 hexane/ethyl acetate) affording as yellow gel (66.6 mg, 68%). ¹H NMR (400 MHz, CDCl₃): δ 7.63 (dd, *J*₁ = 8.4 Hz, *J*₂ = 2.0 Hz, 1H), 7.44-7.40 (m, 3H), 7.29-7.21 (m, 4H), 6.84 (d, *J* = 8.4 Hz, 1H), 6.43 (dd, *J*₁ = 8.4 Hz, *J*₂

Transition Metal-free, Visible Light Mediated Decarboxylative Acylation and Carboxylation of Alkenes with CO₂

= 2.4 Hz, 1H), 6.37 (d, $J = 2.8$ Hz, 1H), 5.86-5.76 (m, 1H), 5.21 (qq, $J_1 = 15.6$ Hz, $J_2 = 2.0$ Hz, 2H), 4.39-4.30 (m, 4H), 3.92 (s, 3H), 3.85 (s, 3H), 3.75 (s, 3H), 3.64 (s, 3H); ¹³C NMR (100 MHz, CDCl₃): δ 195.86, 174.85, 159.76, 156.75, 153.12, 148.96, 140.37, 133.02, 132.01, 130.95, 128.85, 127.79, 126.85, 124.10, 122.52, 117.33, 110.29, 109.91, 103.80, 100.13, 69.27, 56.14, 55.99, 55.30, 52.45, 42.37; HRMS (ESI, m/z) calcd. For C₂₉H₃₀O₇ [M+H]⁺: 491.2070; found: 491.2077.

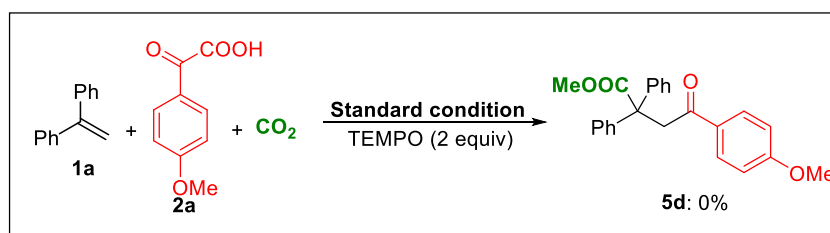
II.6.7. Product derivatization



In a clean 25 mL round bottom flask, methyl 4-oxo-2,2,4-triphenylbutanoate (**5b**) (68.8 mg, 0.2 mmol, 1 equiv.) was charged and to it 2 mL methanol was added. Therefore, the solution was set up for stirring at. At 0 °C, sodium borohydride (NaBH₄) (15.1 mg, 0.4 mmol, 2 equiv.) was added to the mixture and the flask was closed. Then, the reaction mixture was allowed to stir at room temperature for 5 hours. After that, 5 mL 2(N) HCl was added dropwise to the reaction mixture to quench the excess NaBH₄. Then, the reaction mixture was extracted with EtOAc (40 mL), deionized water (15 mL \times 2), followed by washing the resulting organic layer with brine (20 mL), and finally the combined organic layer was passed through anhydrous Na₂SO₄ for drying and the mixture was concentrated by evaporating the solvent under reduced pressure. By column chromatography (SiO₂, eluting with hexane/ethylacetate 98:2), the crude product was purified by to provide **30b** as white solid (39 mg, 61%). ¹H NMR (400 MHz, CDCl₃): δ 7.47-7.26 (m, 15H), 5.32 (q, $J = 5.2$ Hz, 1H), 3.30 (dd, $J_1 = 12.8$ Hz, $J_2 = 4.8$ Hz, 1H), 2.94 (dd, $J_1 = 12.8$ Hz, $J_2 = 10.8$ Hz, 1H); ¹³C NMR (100 MHz, CDCl₃): δ 176.96, 141.73, 139.62, 138.41, 129.18, 128.87, 128.77, 128.49, 127.97, 127.81, 127.49, 127.41, 125.76, 78.07, 58.79, 46.35; HRMS (ESI, m/z) calcd. For C₃₂H₃₂O₅S [M+H]⁺: 315.1385; found: 315.1297.

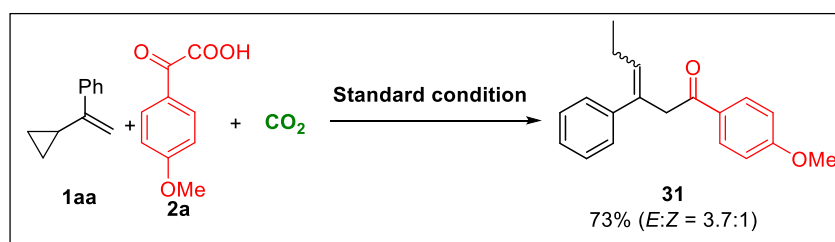
II.6.8. Control experiments

Radical inhibition experiment



An oven-dried Schlenk tube (10 mL) with a stirring bar inside was charged with **2a** (43.2 mg, 0.24 mmol, 1.2 equiv), 4-CzIPN (1.5 mg, 0.002 mmol, 1.0 mol %), **2** (0.24 mmol, 1.2 equiv), TEMPO (0.4 mmol, 62.5 mg, 2.0 equiv.) and taken into glovebox, where Cs₂CO₃ (130.3 mg, 0.4 mmol, 2.0 equiv) was added. The tube was then taken out, evacuated and subsequently refilled with CO₂ for three times. Therefore, under continuous CO₂ flow, anhydrous DMSO (3 mL) and **1a** (35 μ L, 1.0 equiv., 0.2 mmol) was added with syringe and subsequently the tube is sealed. The reaction was stirred for 12 hours with continuous irradiation from a 30 W blue LED lamp (kept at a distance of 3 cm, and a cooling fan was set to keep the reaction temperature constant at 25~30 °C). After 12 hours, the light was switched off, the shlenk tube was opened and to the mixture, methyl iodide (24.9 μ L, 0.4 mmol, 2.0 equiv.) was added and continued to stir at room temperature for additional 4 hours. Then, TLC was checked which showed no formation of expected product **5a**.

Radical-clock Experiment

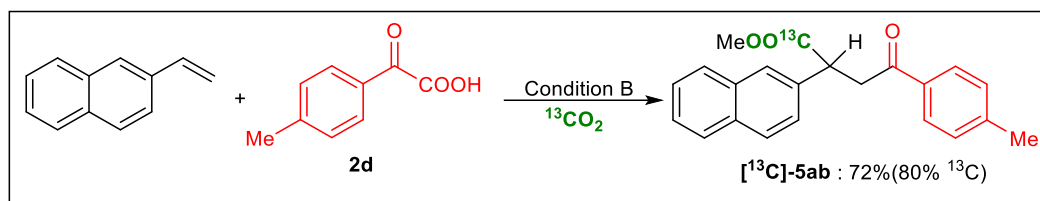


An oven-dried Schlenk tube (10 mL) with a stirring bar inside was charged with **2a** (43.2 mg, 0.24 mmol, 1.2 equiv), 4-CzIPN (1.5 mg, 0.002 mmol, 1.0 mol %) and taken into glovebox, where Cs₂CO₃ (0.4 mmol, 130.3 mg, 2.0 equiv) was added. The tube was then taken out, evacuated and subsequently refilled with CO₂ for three times. Therefore, under continuous CO₂ flow, anhydrous DMSO (3.0 mL) and radical-clock substrate **1aa** (0.2 mmol, 1.0 equiv., 28.8 mg) were added with syringe and subsequently the tube is sealed. The reaction was stirred for 12 hours with continuous irradiation from a 30 W blue LED lamp (kept at a distance of 3 cm, and a cooling fan was set to keep the reaction temperature constant at 25~30 °C). After 12 hours, the light was switched off, the shlenk tube was opened and to the mixture, methyl iodide (24.9 μ L, 0.4 mmol, 2.0 equiv.) was added and continued to stir at room temperature for additional 4 hours. After that, TLC was checked which showed no formation of expected product **5a**, instead ring opening product **31** was achieved with column chromatography (eluting with petroleum ether/ethyl acetate 97:3) as colourless liquid (25.3 mg, 73%). ¹H NMR (400 MHz, CDCl₃): δ 7.98-7.94 (m, 2H), 7.31-7.23 (m, 5H), 6.93-6.91 (m, 2H), 5.99 (t, *J* = 7.2

Transition Metal-free, Visible Light Mediated Decarboxylative Acylation and Carboxylation of Alkenes with CO₂

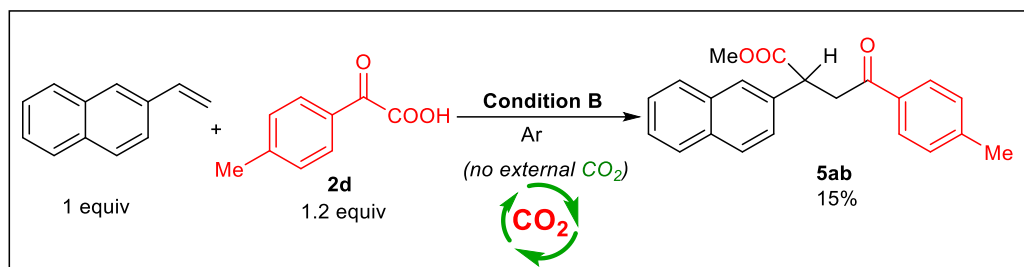
Hz, 1H), 4.13 (s, 2H), 3.85 (s, 3H), 2.18 (pent., $J = 7.6$ Hz, 2H), 1.07 (t, $J = 7.6$ Hz, 3H); ¹³C NMR (100 MHz, CDCl₃): δ 196.86, 195.78, 163.56, 163.43, 143.02, 140.65, 134.39, 133.95, 132.81, 130.81, 130.58, 130.07, 128.51, 128.35, 128.17, 126.83, 126.75, 126.11, 126.10, 113.79, 113.69, 55.56, 55.51, 48.48, 40.45, 22.65, 22.62, 14.45, 14.03; HRMS (ESI, m/z) calcd. For C₃₂H₃₂O₅S [M+H]⁺: 281.1542; found: 281.1544.

¹³C-labelling experiment for carbocarboxylation



An oven-dried Schlenk tube (10 mL) with a stirring bar inside was charged with 2-vinylnaphthalene (30.8 mg, 0.20 mmol, 1.0 equiv.), **2d** (39.4 mg, 0.24 mmol, 1.2 equiv), 4-CzIPN (1.5 mg, 0.002 mmol, 1.0 mol %) and taken into glovebox, where Cs₂CO₃ (0.4 mmol, 130.3 mg, 2.0 equiv) was added. The tube was then taken out, evacuated and subsequently refilled with ¹³CO₂ for three times. Therefore, under continuous ¹³CO₂ flow, anhydrous DMSO (3.0 mL) was added with syringe and subsequently the tube was sealed. The reaction was stirred for 12 hours with continuous irradiation from a 30 W blue LED lamp (kept at a distance of 3 cm, and a cooling fan was set to keep the reaction temperature constant at 25~30 °C). After 12 hours, the light was switched off, the shlenk tube was opened and to the mixture, methyl iodide (24.9 μL, 0.4 mmol, 2.0 equiv.) was added and continued to stir at room temperature for additional 4 hours. Then, the reaction mixture was extracted with EtOAc (40 mL), deionized water (15 mL × 2), followed by washing the resulting organic layer with brine (20 mL), and finally the combined organic layer was passed through anhydrous Na₂SO₄ for drying and the mixture was concentrated by evaporating the solvent under reduced pressure. By column chromatography (SiO₂, eluting with hexane/ethylacetate 97:3), the crude product was purified to provide the desired product [¹³C]-**5ab** as white solid (47.9 mg, 72% with 80% ¹³C incorporation). ¹H NMR (400 MHz, CDCl₃): δ 7.89-7.87 (m, 2H), 7.83-7.80 (m, 4H), 7.49-7.44 (m, 3H), 7.23-7.22 (m, 2H), 4.48-4.43 (m, 1H), 4.01 (qd, $J_1 = 10.0$ Hz, $J_2 = 2.8$ Hz, 1H), 3.69 (d, $J = 4$ Hz, 3H), 3.33 (dq, $J_1 = 18.0$ Hz, $J_2 = 4.0$ Hz, 1H), 2.39 (s, 3H); ¹³C NMR (100 MHz, CDCl₃): δ 197.28, 174.01, 144.26, 135.93, 134.03, 133.57, 132.79, 129.38, 128.75, 128.31, 127.90, 127.74, 126.78, 126.43, 126.12, 125.89, 52.47, 46.55 (d, $J = 57$ Hz, 46.27, 42.76, 21.75; HRMS (ESI, m/z) calcd. For C₂₂H₂₀O₃ [M+H]⁺: 333.1491; found: 333.1389.

Carboxylation reaction under argon (Ar) atmosphere

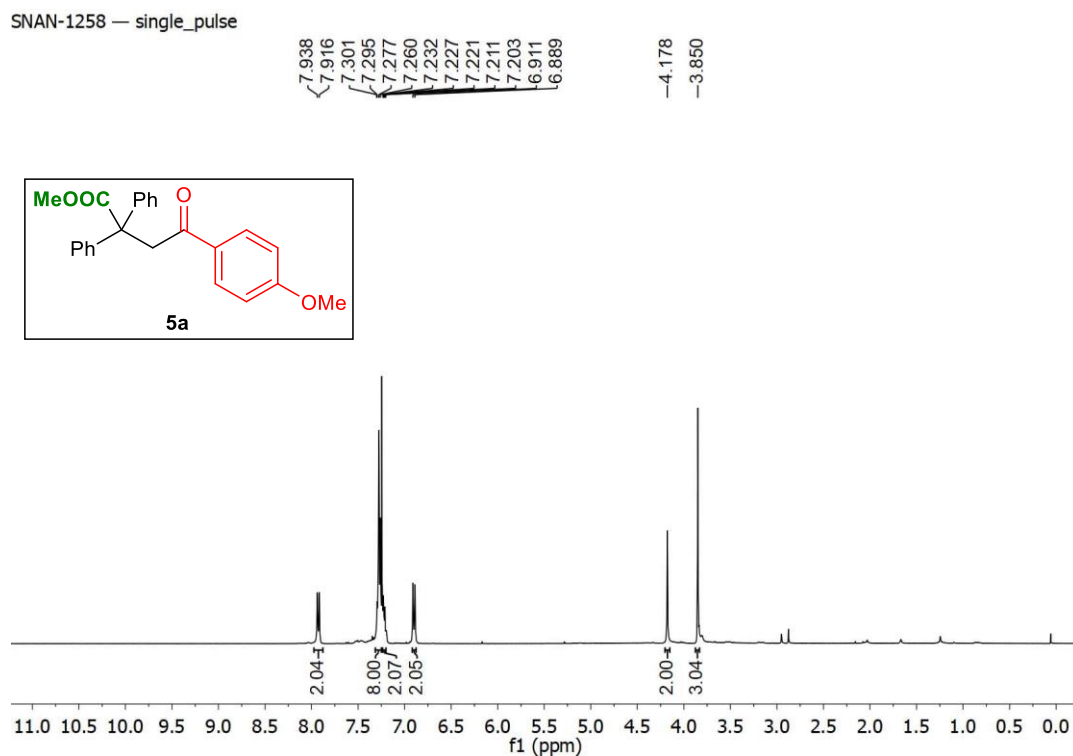


An oven-dried Schlenk tube (10 mL) with a stirring bar inside was charged with 2-vinylnaphthalene (30.8 mg, 0.20 mmol, 1.0 equiv.), **2d** (39.4 mg, 0.24 mmol, 1.2 equiv), 4-CzIPN (1.5 mg, 0.002 mmol, 1.0 mol %) and taken into glovebox, where Cs₂CO₃ (0.4 mmol, 130.3 mg, 2.0 equiv) was added. The tube was then taken out, evacuated and subsequently refilled with Ar for three times. Therefore, under continuous Ar flow, anhydrous DMSO (3.0 mL) was added with syringe and subsequently the tube is sealed. The reaction was stirred for 12 hours with continuous irradiation from a 30 W blue LED lamp (kept at a distance of 3 cm, and a cooling fan was set to keep the reaction temperature constant at 25~30 °C). After 12 hours, the light was switched off, the shlenk tube was opened and to the mixture, methyl iodide (24.9 μL, 0.4 mmol, 2.0 equiv.) was added and continued to stir at room temperature for additional 4 hours. Then, the reaction mixture was extracted with EtOAc (40 mL), deionized water (15 mL × 2), followed by washing the resulting organic layer with brine (20 mL), and finally the combined organic layer was passed through anhydrous Na₂SO₄ for drying and the mixture was concentrated by evaporating the solvent under reduced pressure. By column chromatography (SiO₂, eluting with hexane/ethylacetate 97:3), the crude product was purified to provide the desired carboxylated product **5ab** as white solid (10.0 mg, 15%).

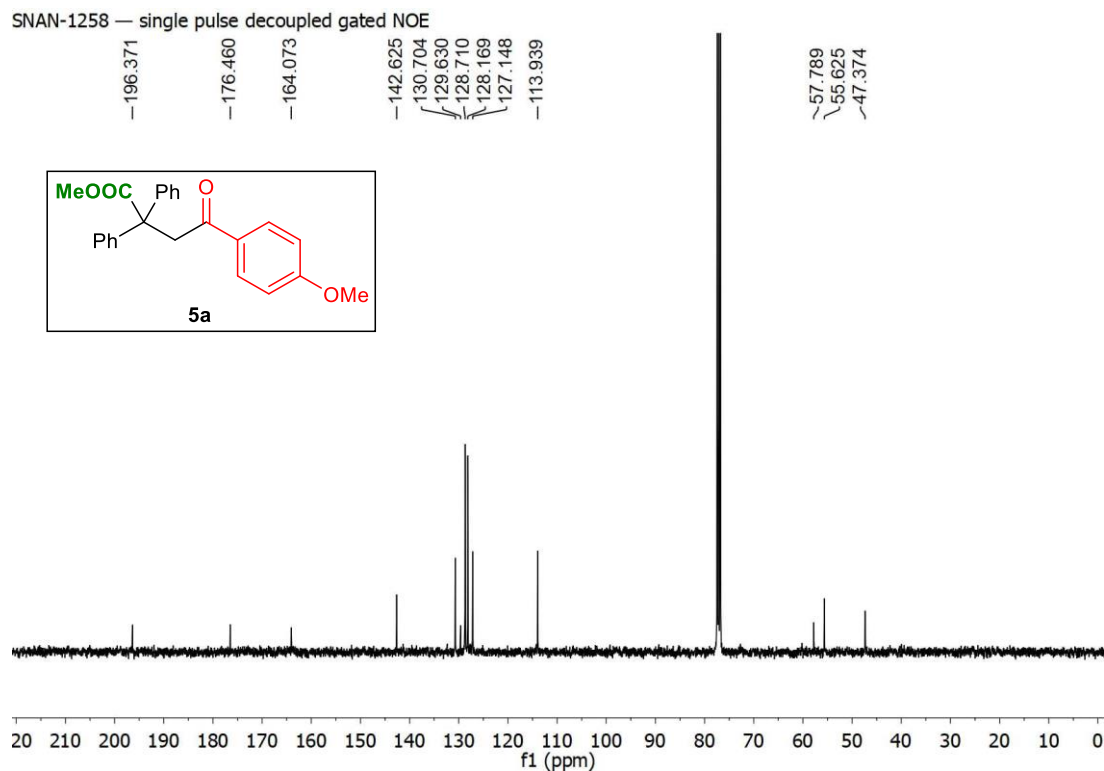
Light On-Off Experiment

Here, the standard reaction was set-up and stirred sequentially under light and in dark with a certain interval. The corresponding increase of product and decrease of starting material concentration was monitored using 1,2,3,4,5-pentafluoro-6-methylbenzene as internal standard. The relative concentration of the substrates and the corresponding product were calculated and presented graphically (**Scheme 7, v**).

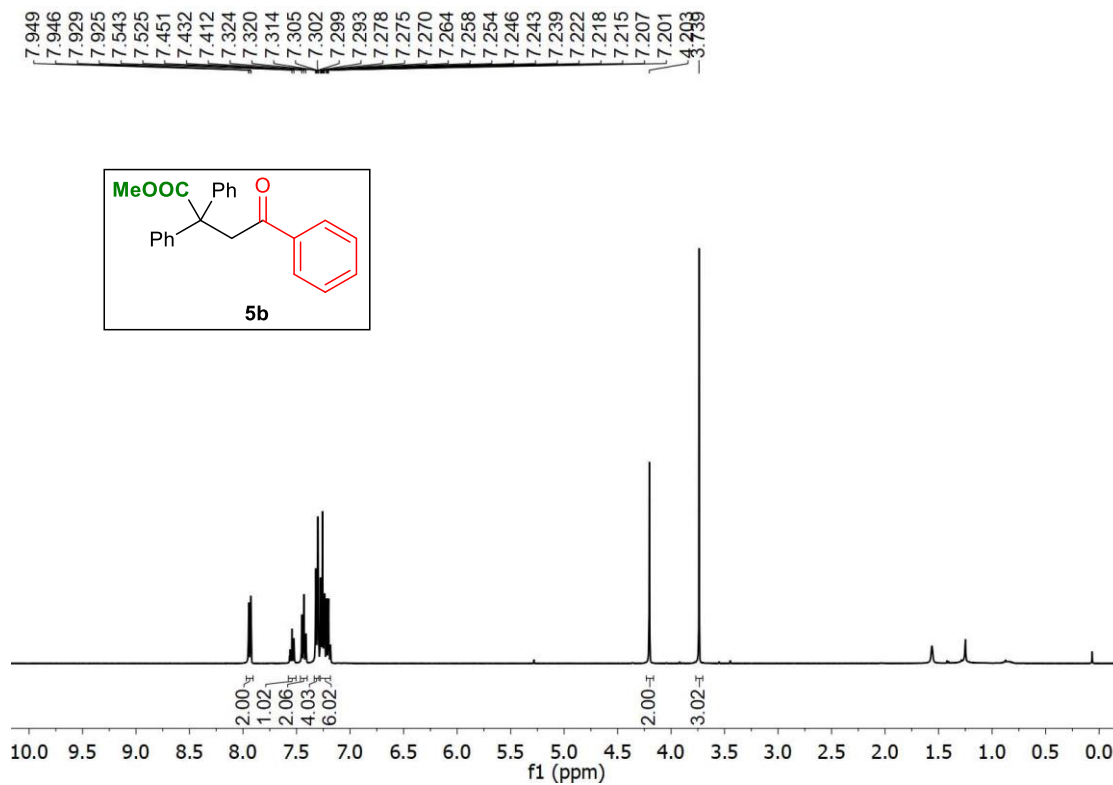
II.7. Representative ¹H and ¹³C spectra



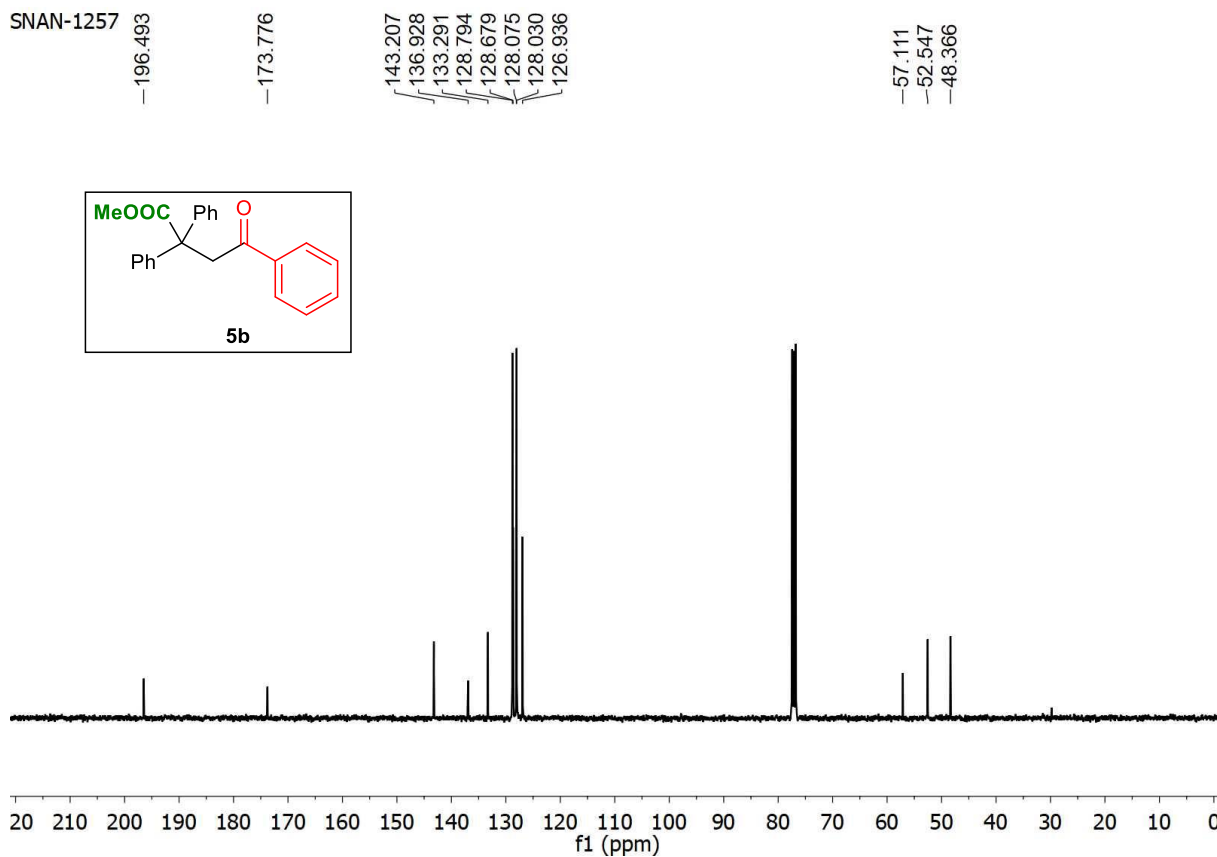
¹H spectra of **5a**



¹³C spectra of **5a**



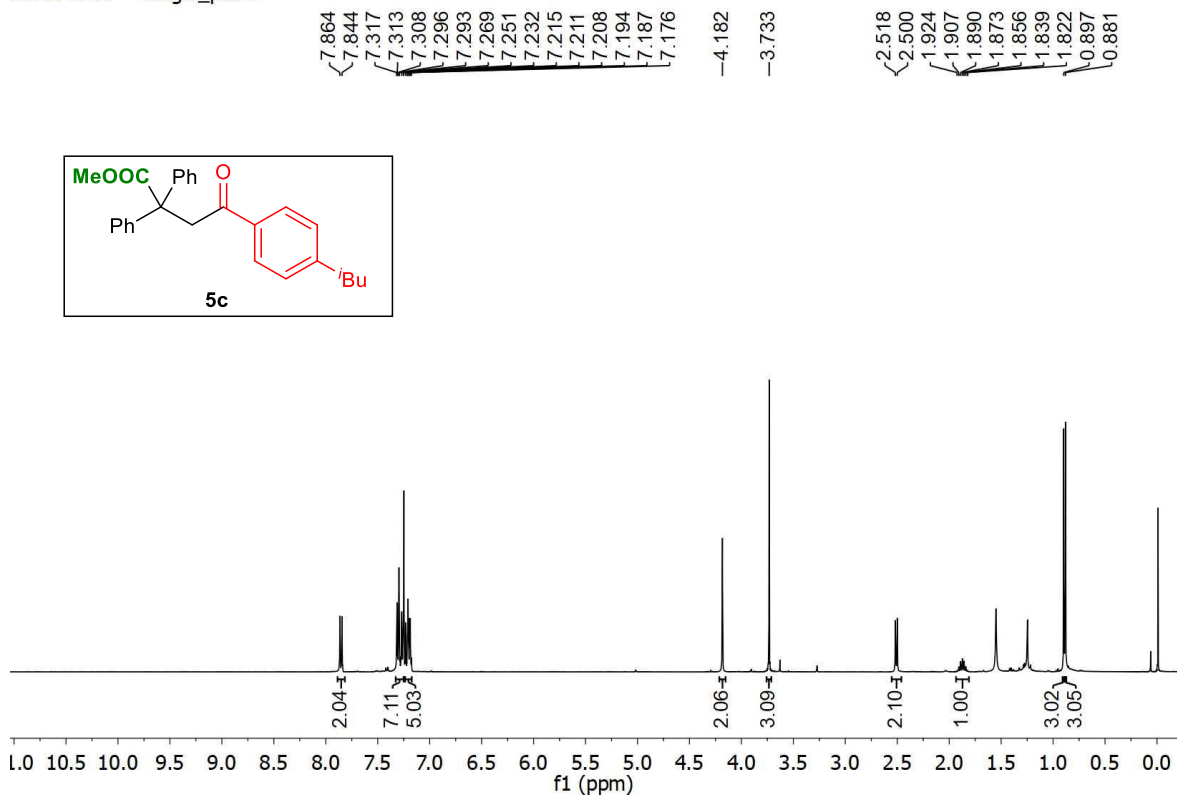
¹H spectra of **5b**



¹³C spectra of **5b**

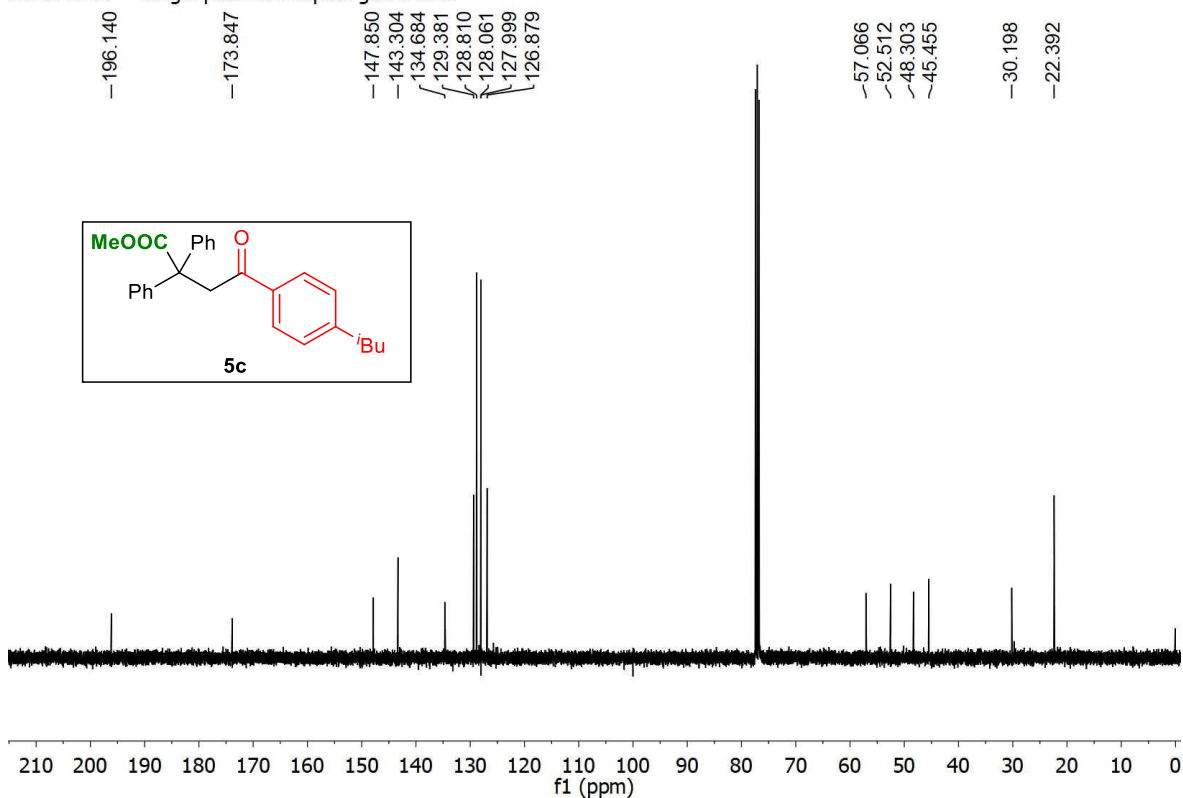
Transition Metal-free, Visible Light Mediated Decarboxylative Acylation and Carboxylation of Alkenes with CO₂

SNAN-1299 — single_pulse



¹H spectra of **5c**

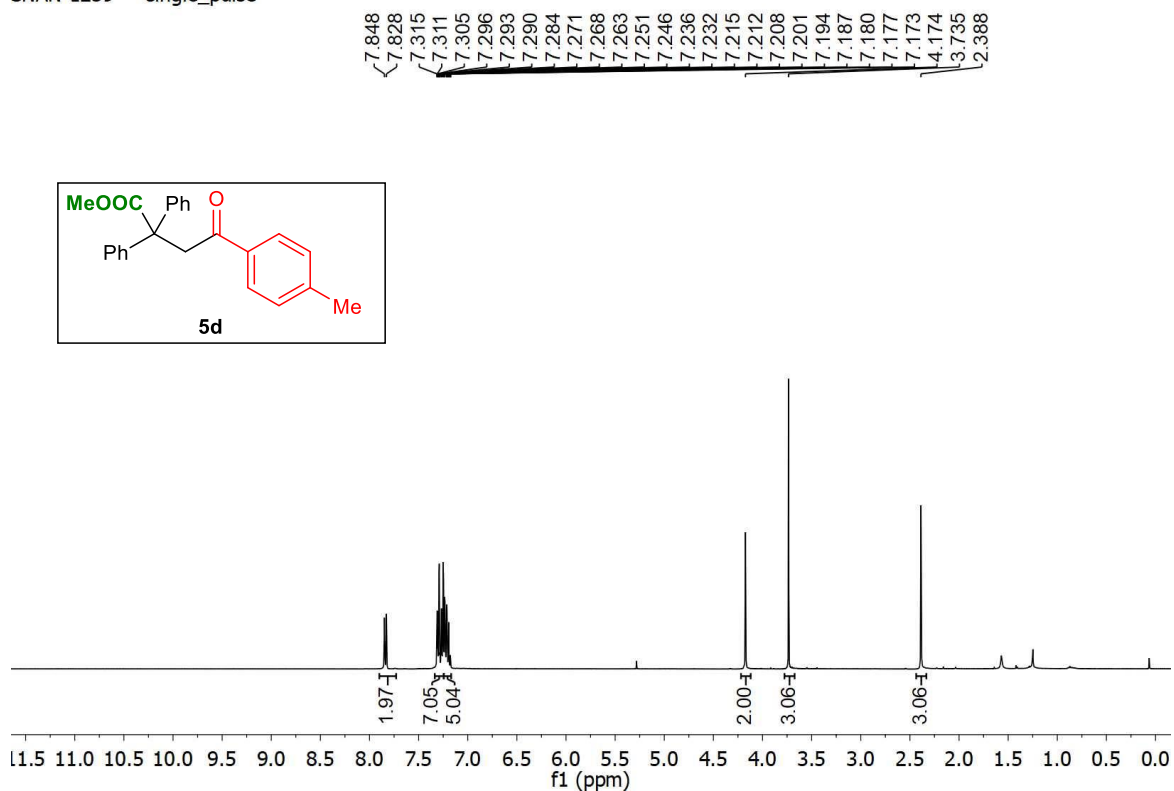
SNAN-1299 — single pulse decoupled gated NOE



¹³C spectra of **5c**

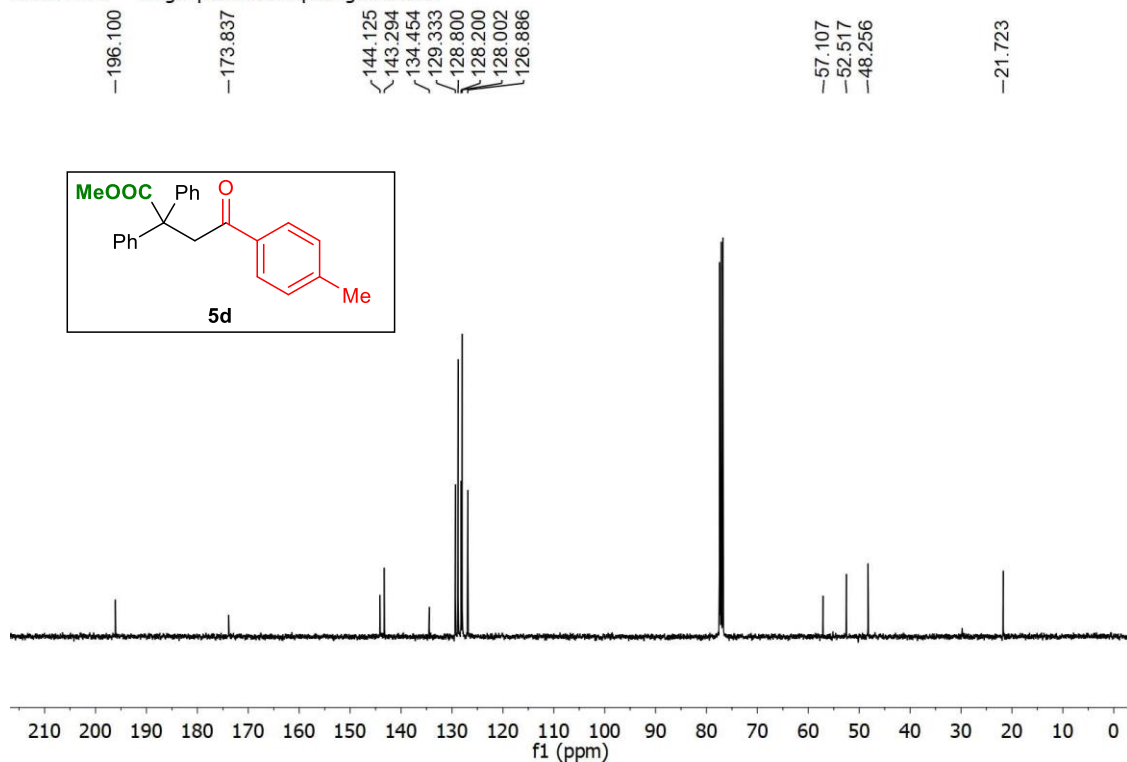
Chapter II

SNAN-1259 — single_pulse



¹H spectra of **5d**

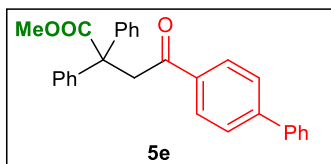
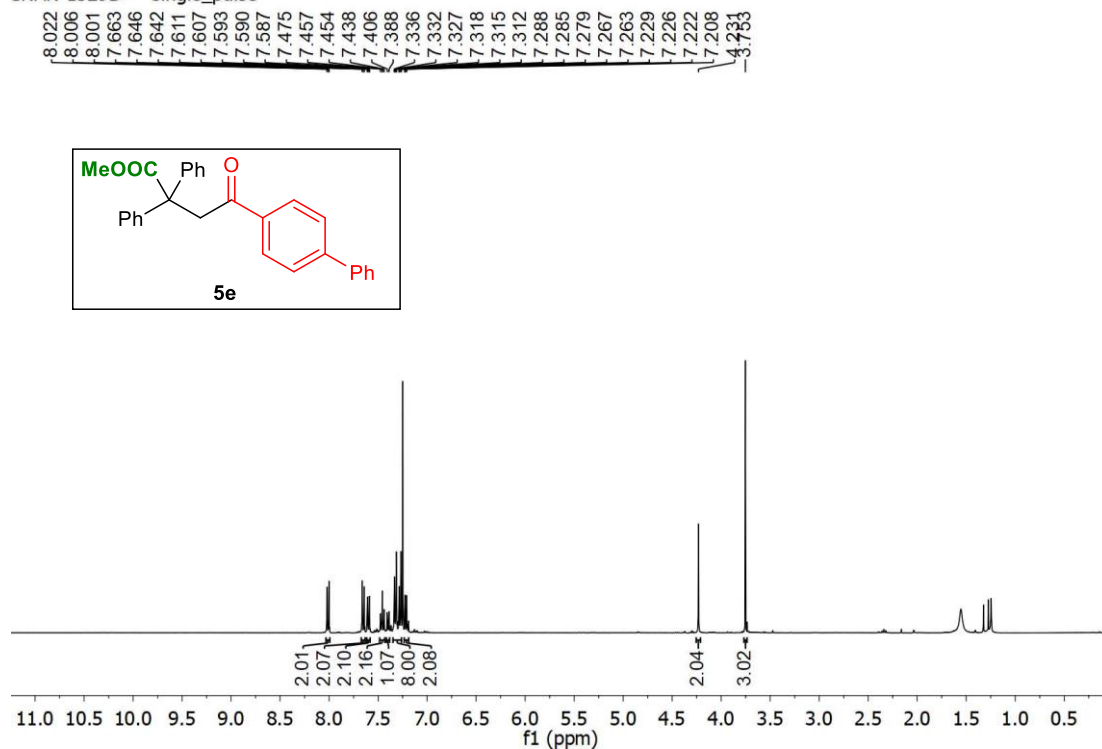
SNAN-1259 — single pulse decoupled gated NOE



¹³C spectra of **5d**

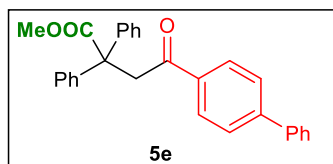
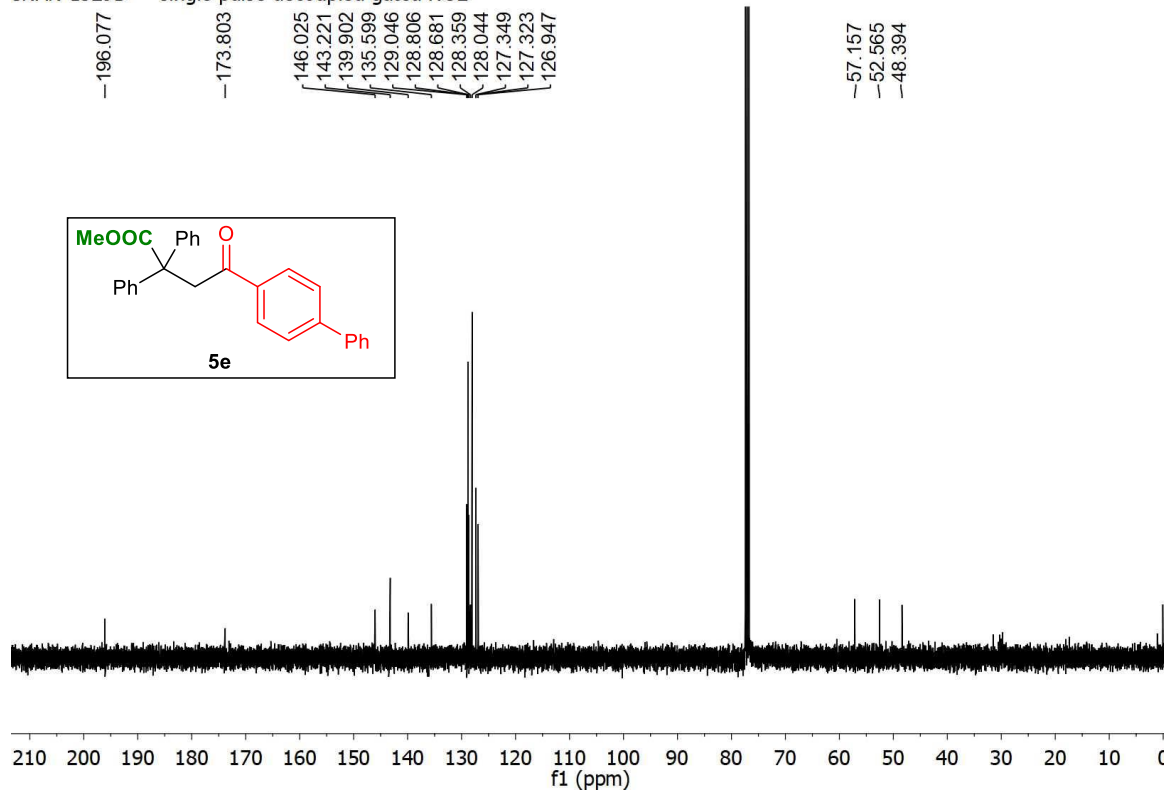
Transition Metal-free, Visible Light Mediated Decarboxylative Acylation and Carboxylation of Alkenes with CO₂

SNAN-1329D — single_pulse



¹H spectra of **5e**

SNAN-1329D — single_pulse decoupled gated NOE

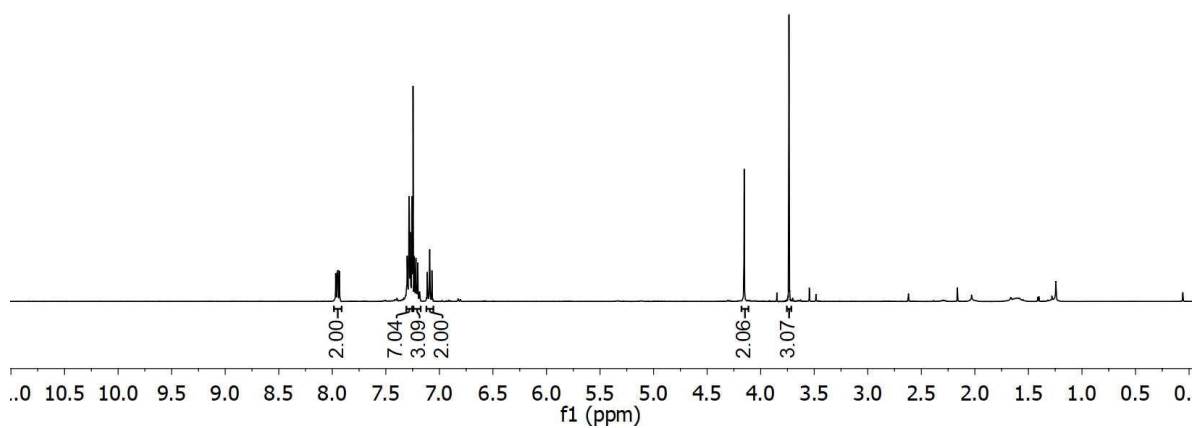
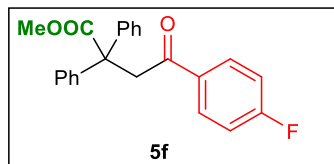


¹³C spectra of **5e**

Chapter II

SNAN-1267 — single_pulse

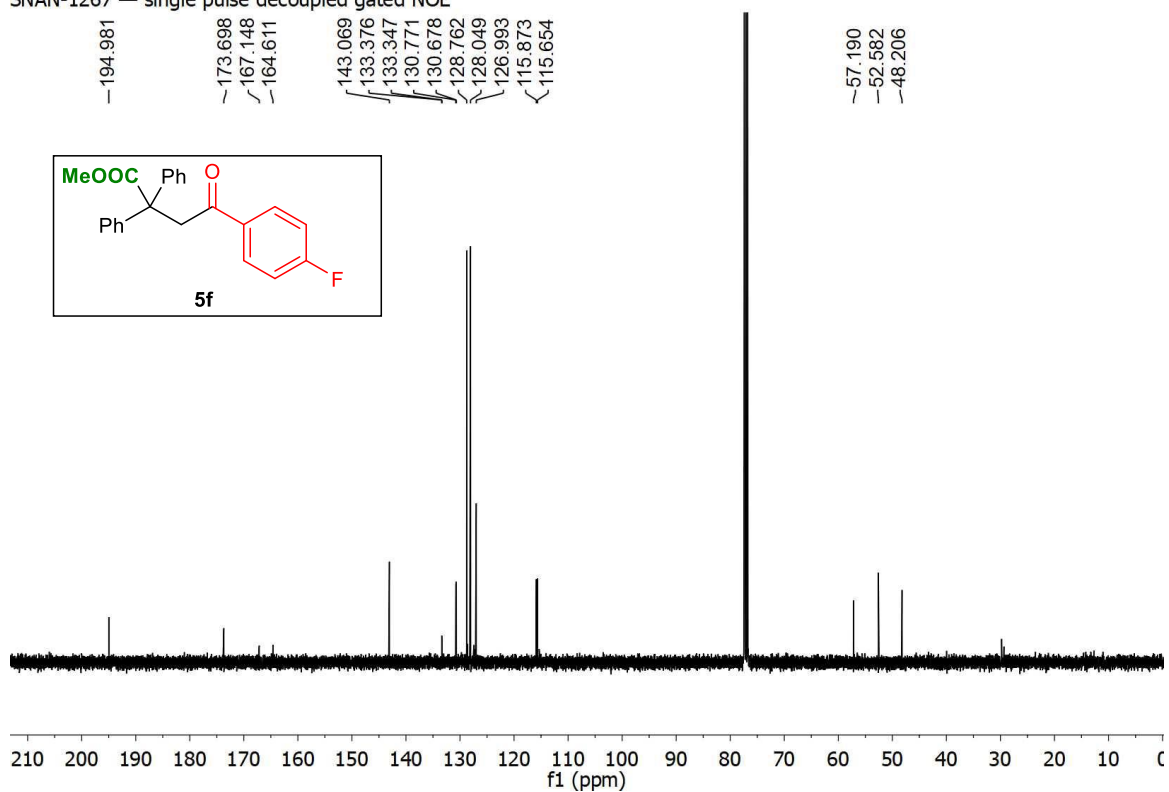
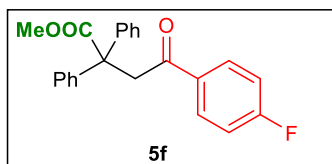
7.969
7.955
7.946
7.938
7.933
7.306
7.301
7.296
7.287
7.284
7.283
7.281
7.272
7.257
7.255
7.240
7.235
7.223
7.219
7.213
7.209
7.201
7.188
7.184
7.181
7.113
7.091
7.070
4.154
3.736



¹H spectra of **5f**

SNAN-1267 — single pulse decoupled gated NOE

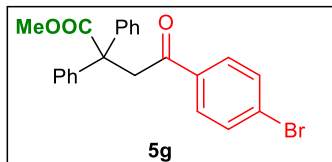
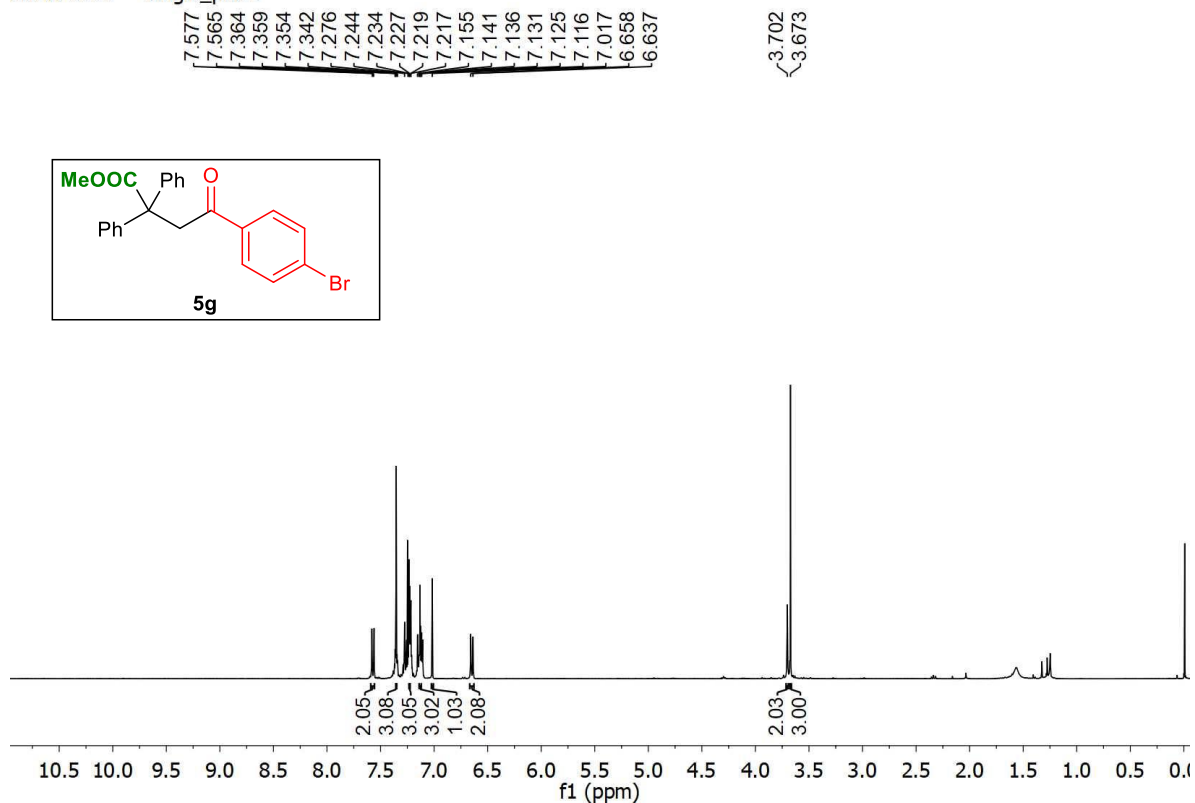
194.981
173.698
167.148
164.611
143.069
133.376
133.347
130.771
130.678
128.762
128.049
126.993
115.873
115.654
57.190
52.582
48.206



¹³C spectra of **5f**

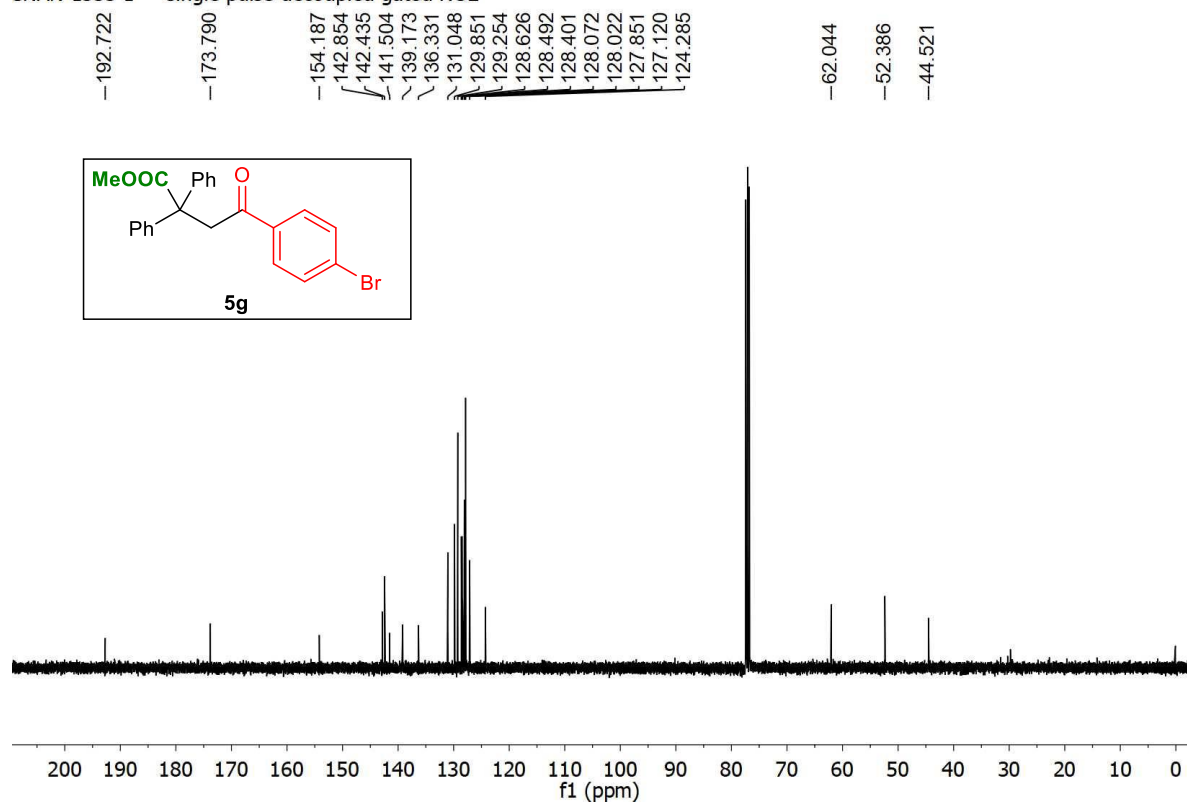
Transition Metal-free, Visible Light Mediated Decarboxylative Acylation and Carboxylation of Alkenes with CO₂

SNAN-1335 — single_pulse



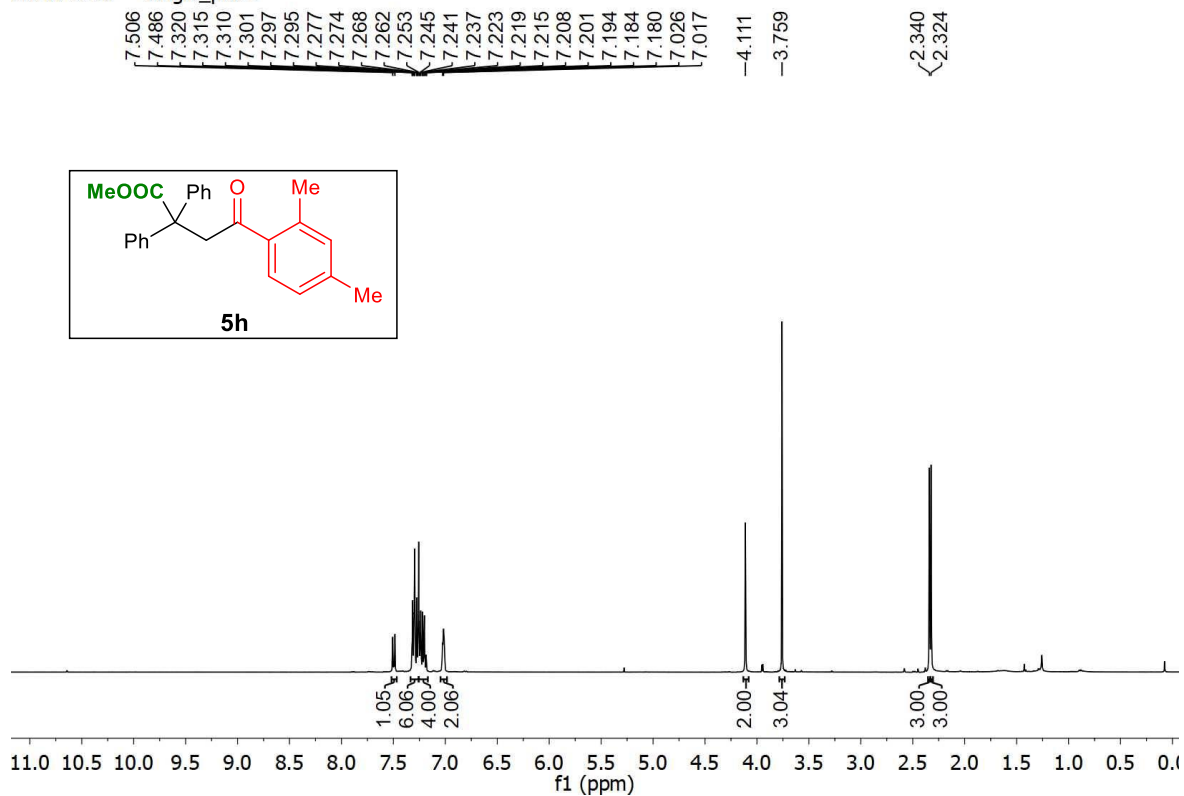
¹H spectra of **5g**

SNAN-1335 1 — single pulse decoupled gated NOE



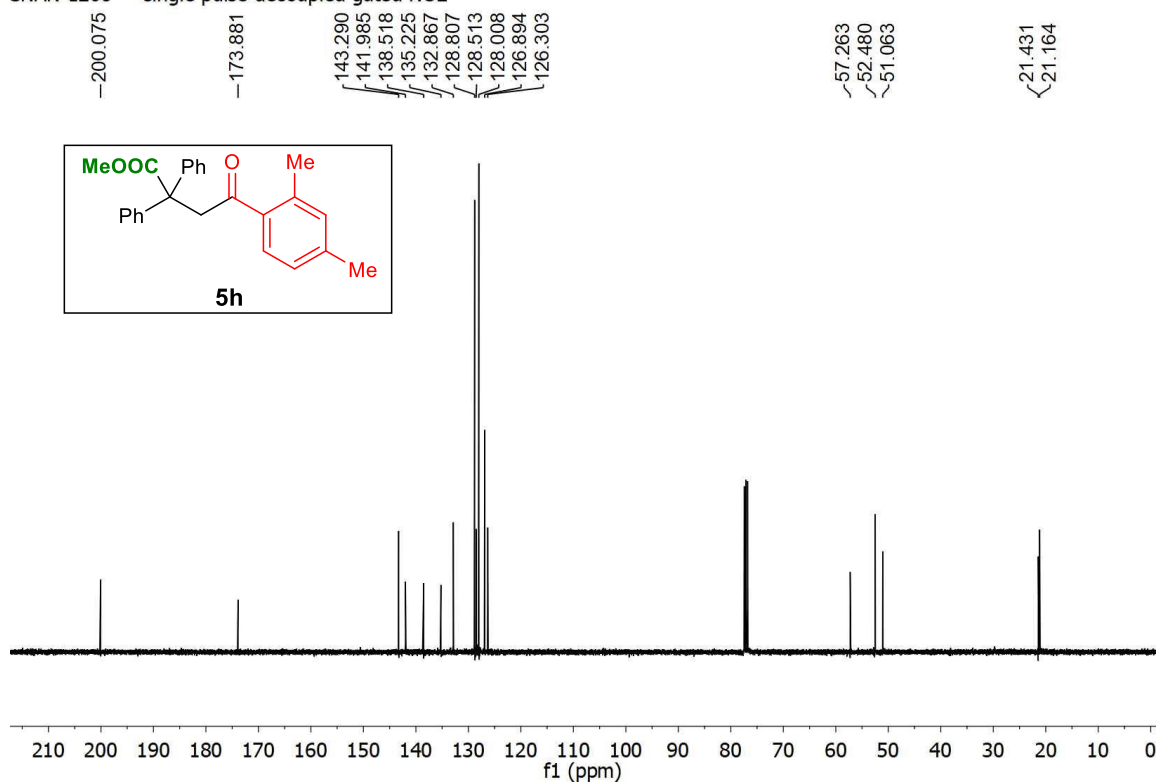
¹³C spectra of **5g**

SNAN-1268 — single_pulse



¹H spectra of 5h

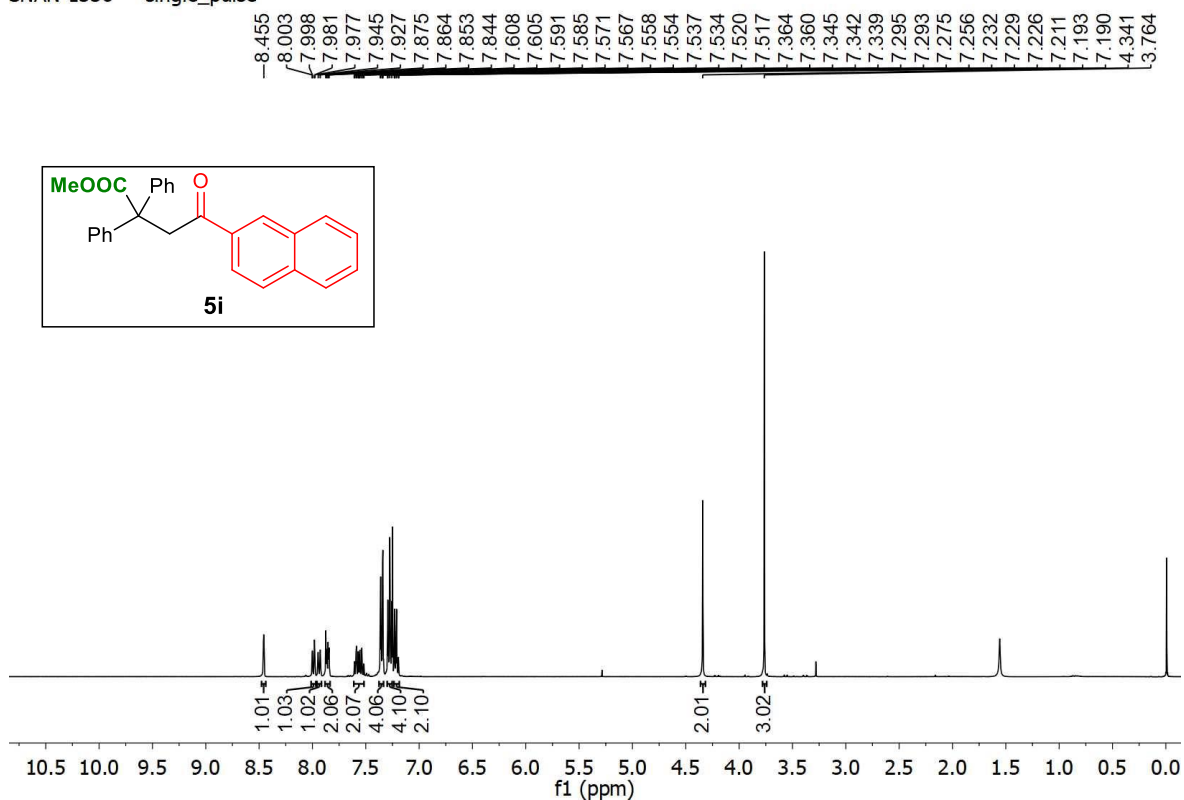
SNAN-1268 — single pulse decoupled gated NOE



¹³C spectra of 5h

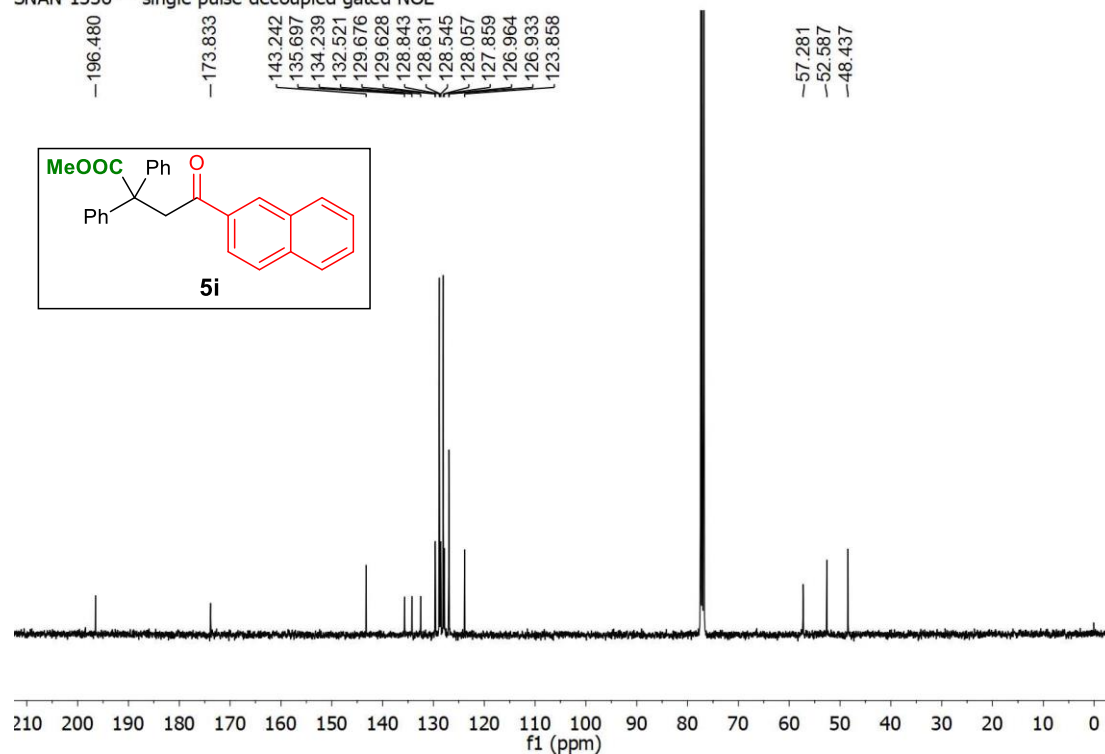
Transition Metal-free, Visible Light Mediated Decarboxylative Acylation and Carboxylation of Alkenes with CO₂

SNAN-1336 — single_pulse



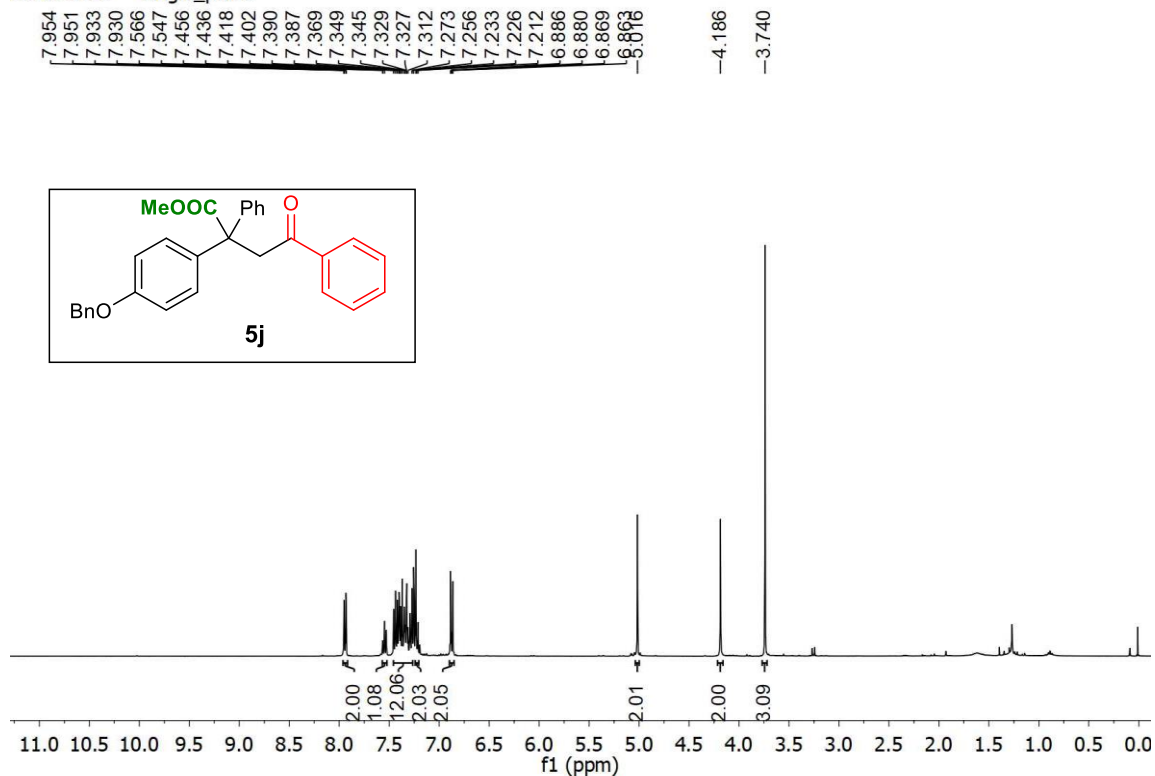
¹H spectra of **5i**

SNAN-1336 — single pulse decoupled gated NOE



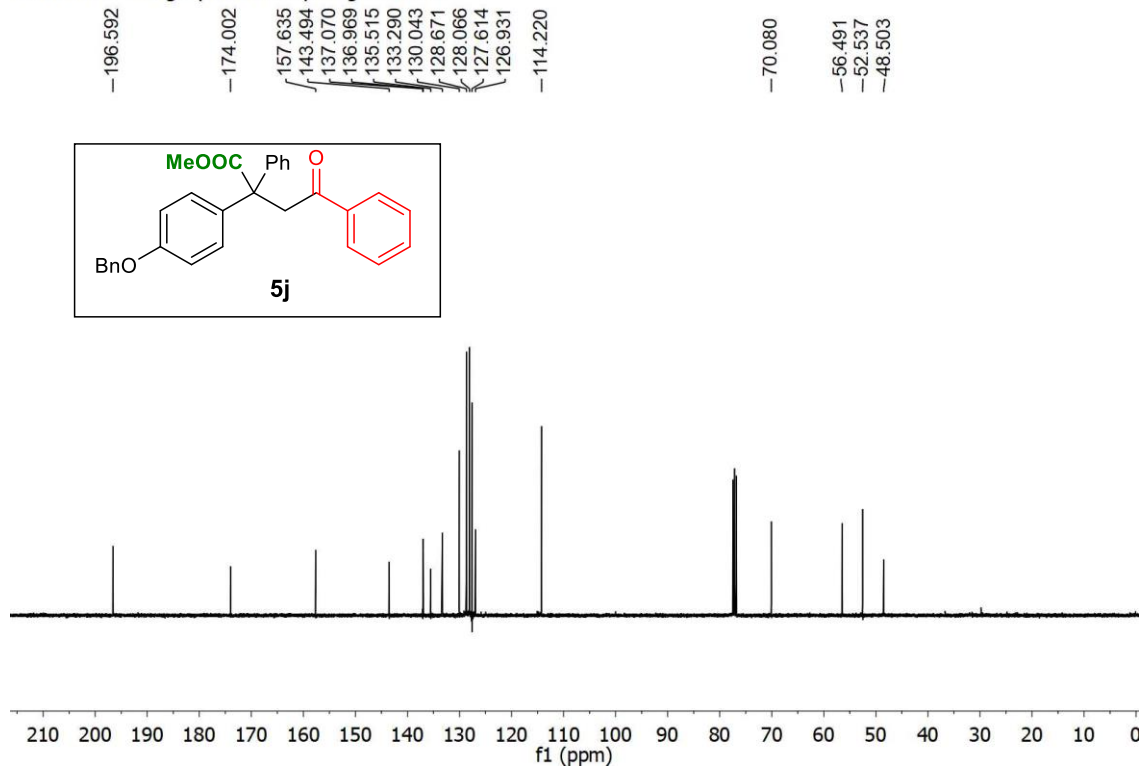
¹³C spectra of **5i**

SNAN-1323 — single_pulse



¹H spectra of **5j**

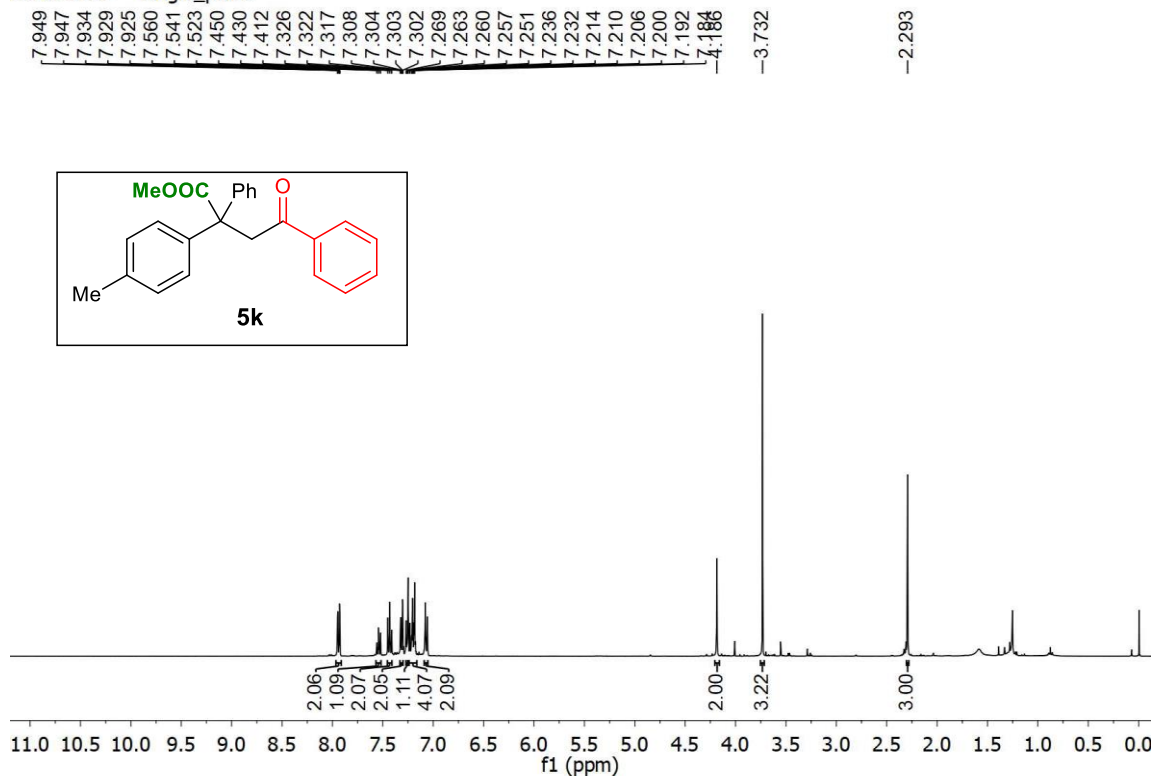
SNAN-1323 — single pulse decoupled gated NOE



¹³C spectra of **5j**

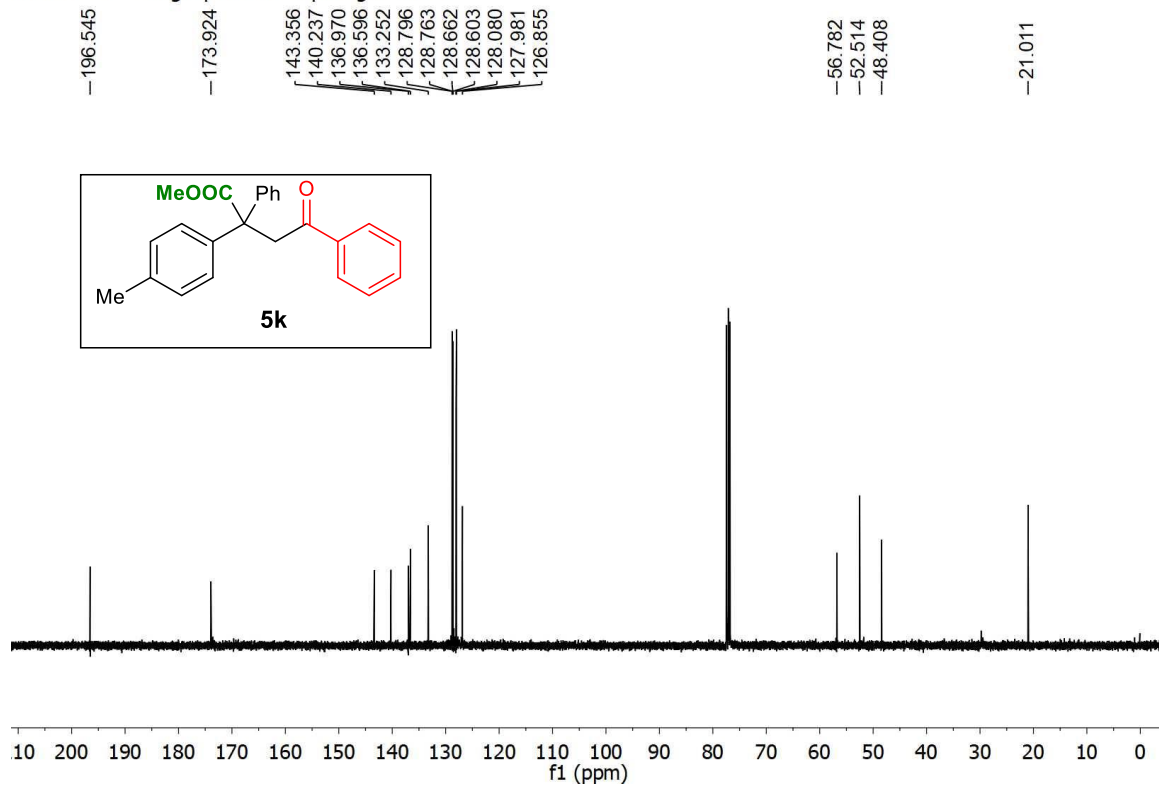
Transition Metal-free, Visible Light Mediated Decarboxylative Acylation and Carboxylation of Alkenes with CO₂

SNAN-1325 — single_pulse



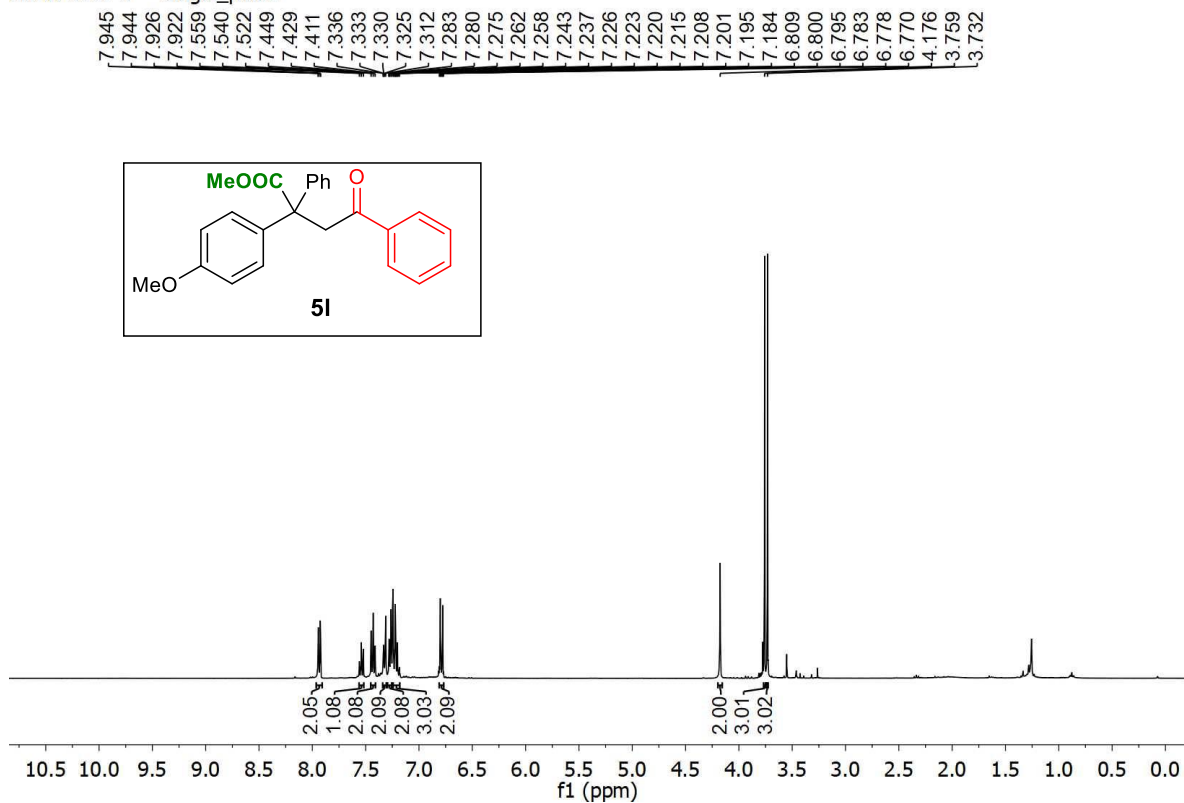
¹H spectra of **5k**

SNAN-1325 — single pulse decoupled gated NOE



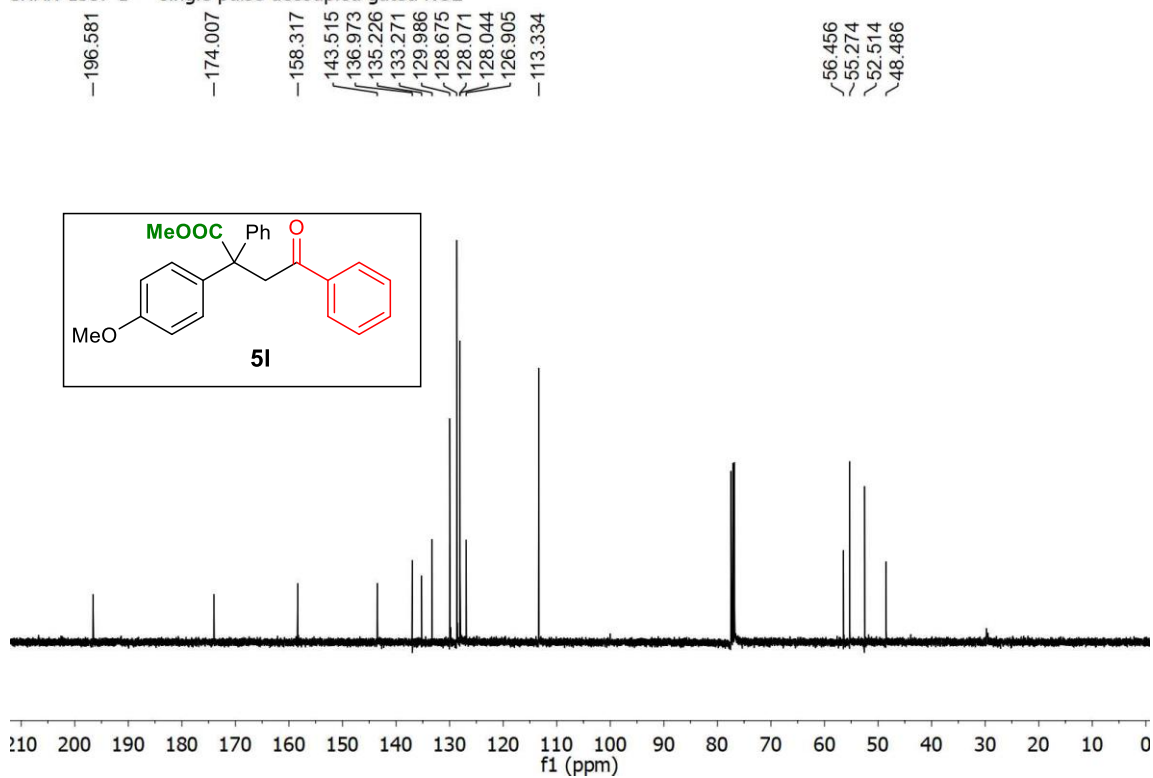
¹³C spectra of **5k**

SNAN-1337 1 — single_pulse



¹H spectra of 5I

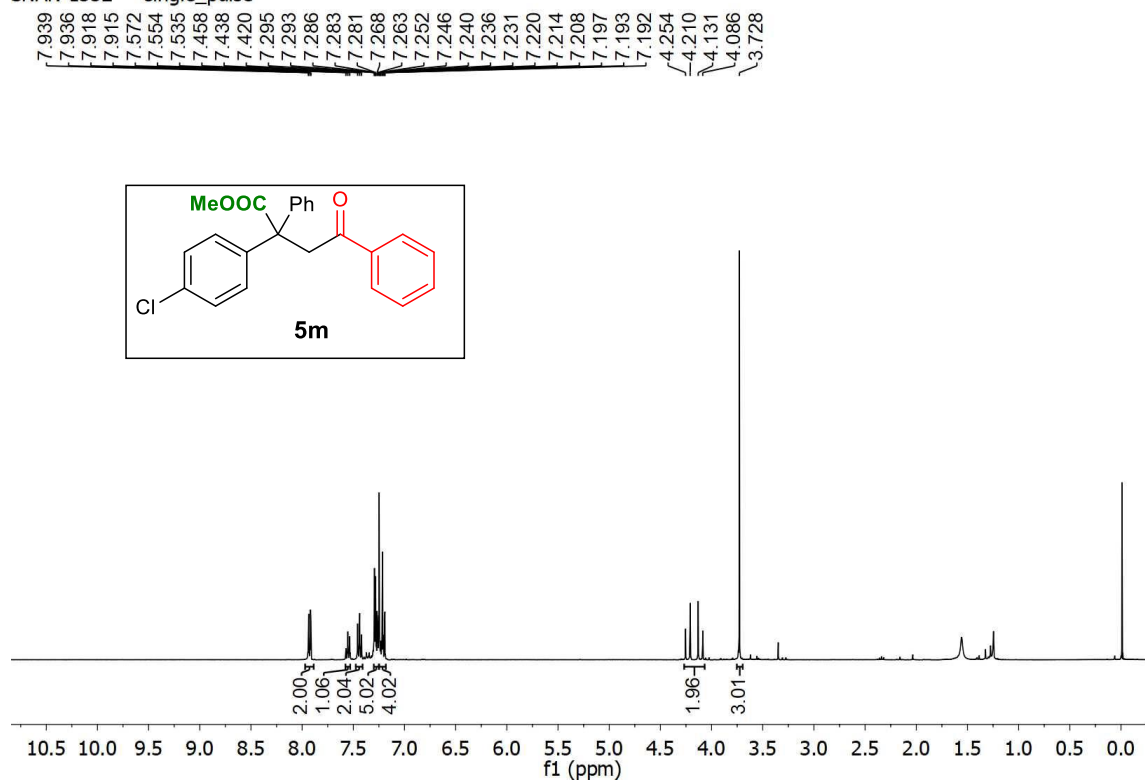
SNAN-1337 1 — single_pulse decoupled gated NOE



¹³C spectra of 5I

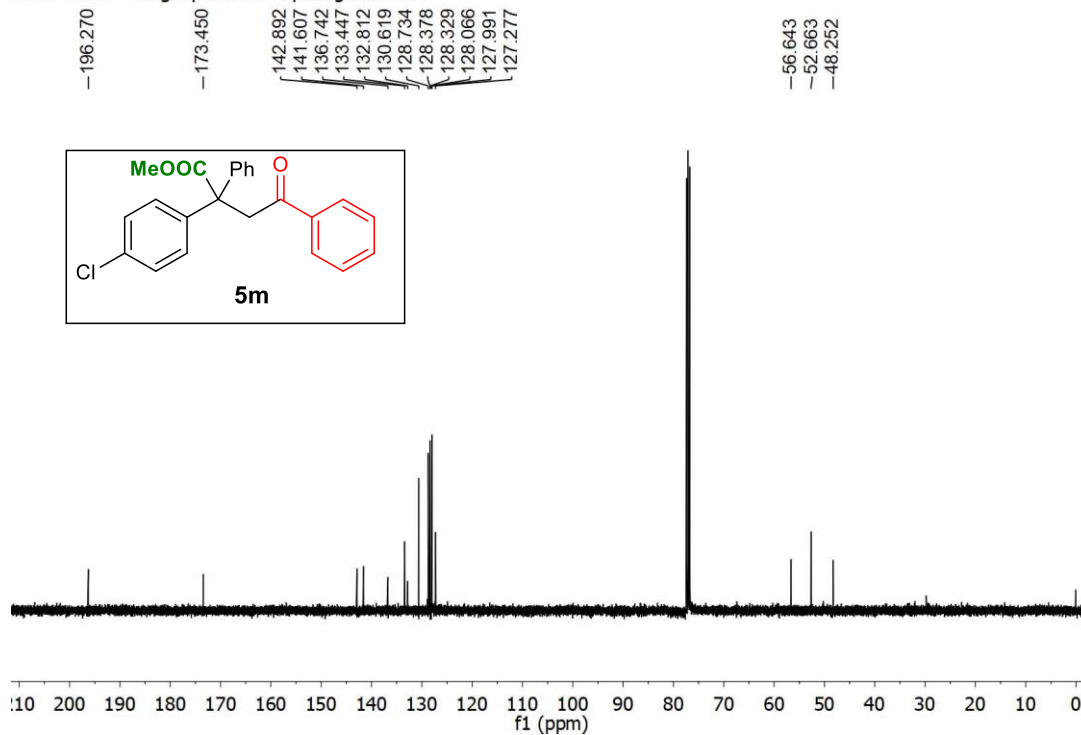
Transition Metal-free, Visible Light Mediated Decarboxylative Acylation and Carboxylation of Alkenes with CO₂

SNAN-1352 — single_pulse



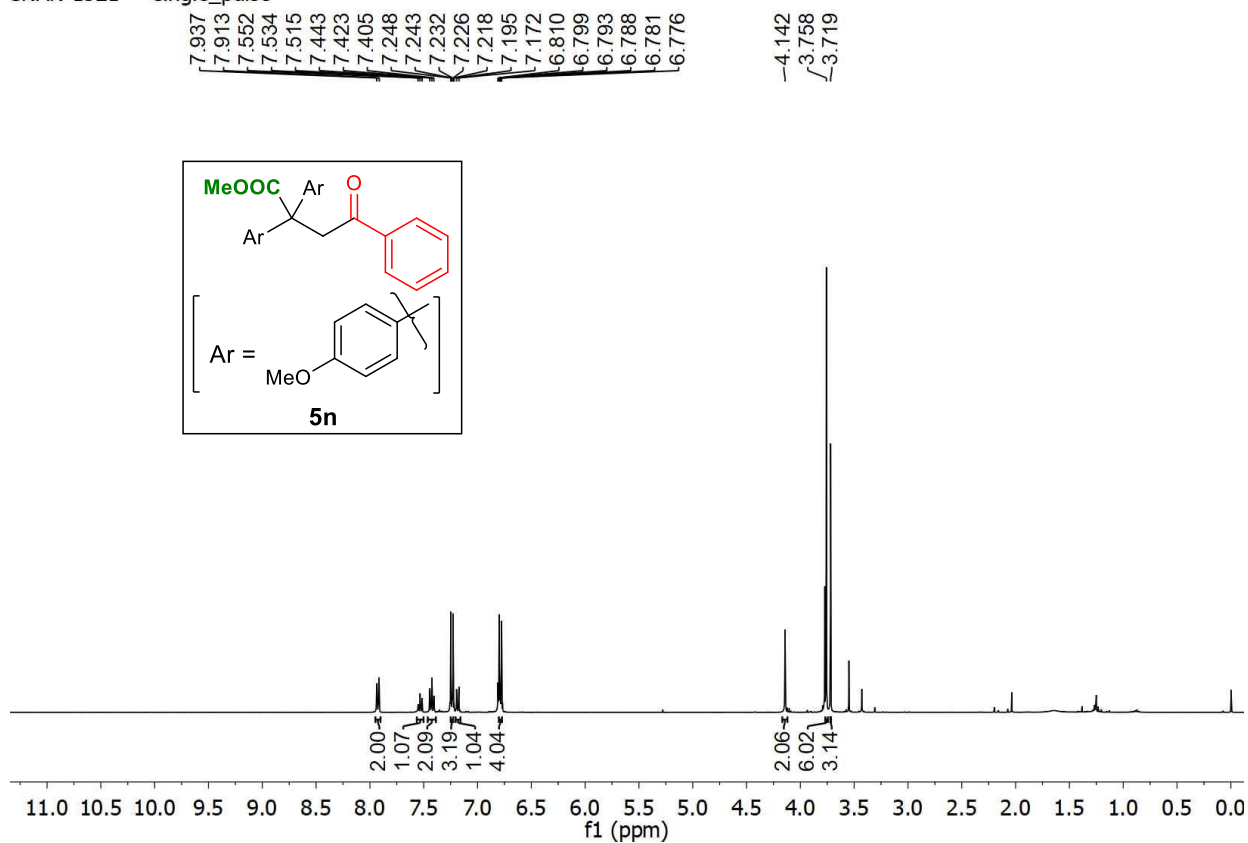
¹H spectra of **5m**

SNAN-1352 — single_pulse decoupled gated NOE

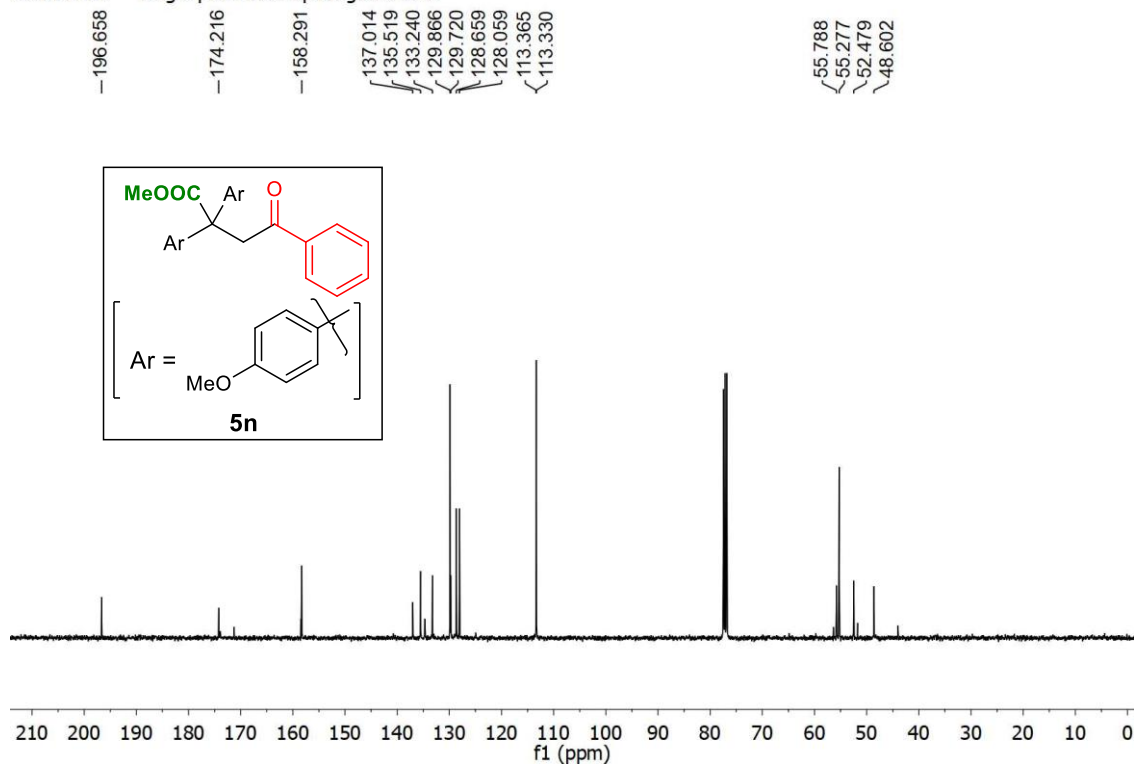


¹³C spectra of **5m**

SNAN-1321 — single_pulse

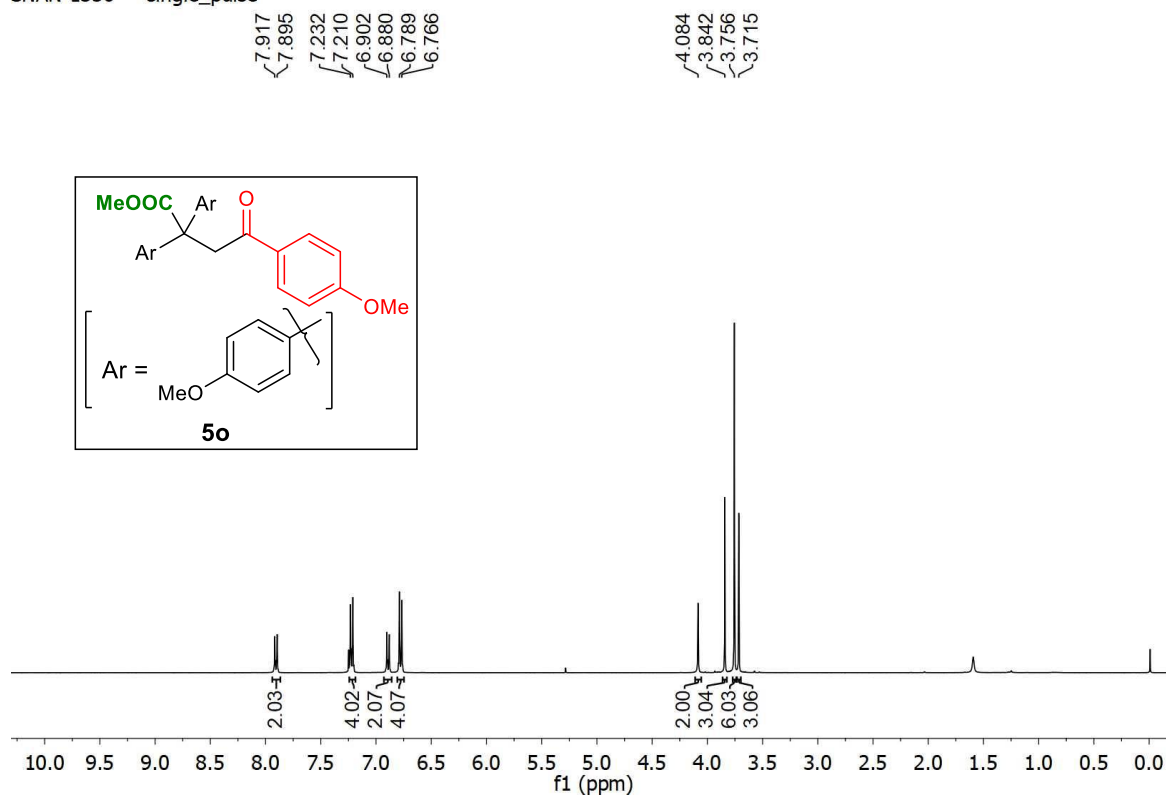
 ^1H spectra of **5n**

SNAN-1321 — single_pulse decoupled gated NOE

 ^{13}C spectra of **5n**

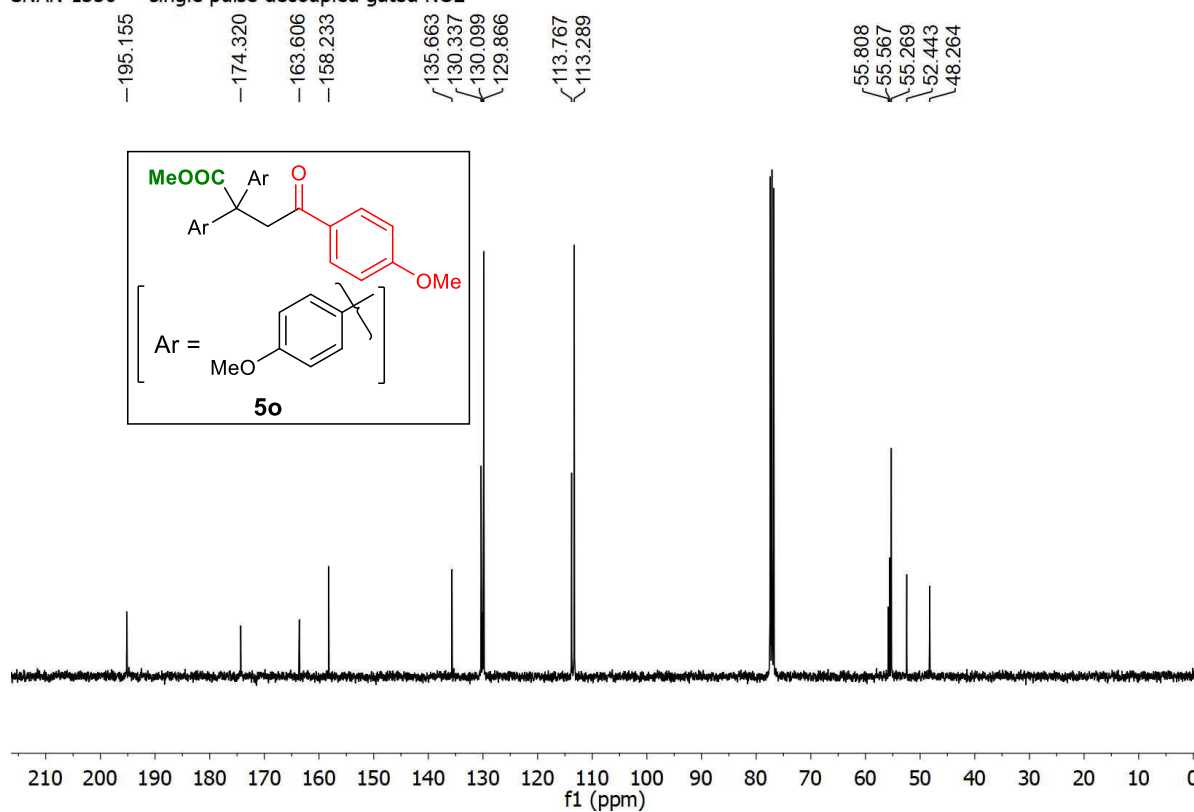
Transition Metal-free, Visible Light Mediated Decarboxylative Acylation and Carboxylation of Alkenes with CO₂

SNAN-1350 — single_pulse



¹H spectra of **5o**

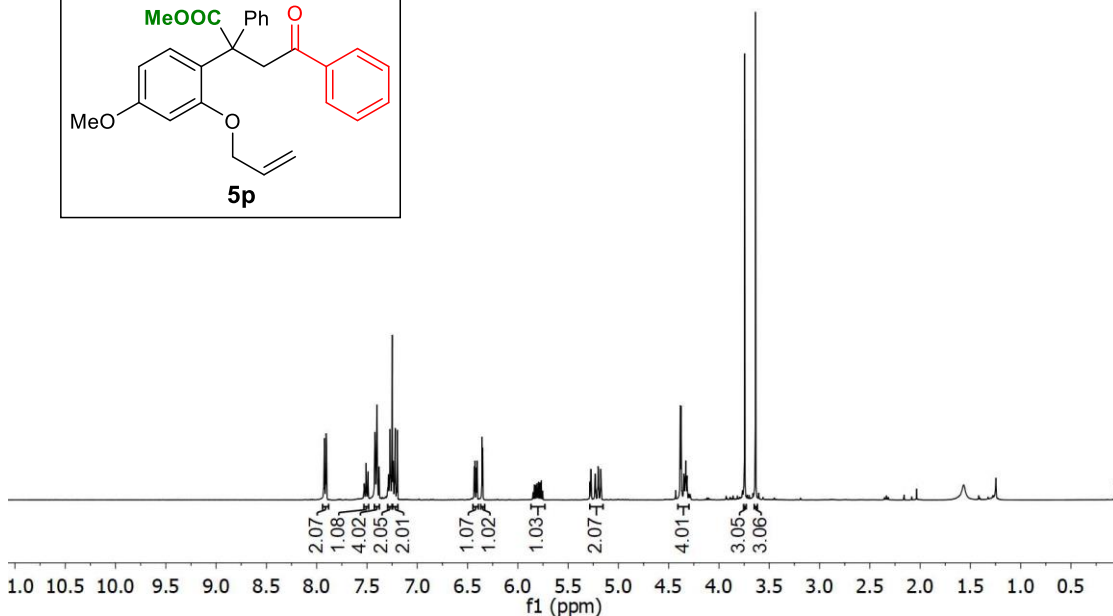
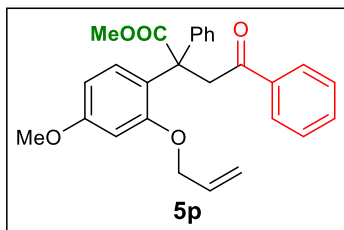
SNAN-1350 — single pulse decoupled gated NOE



¹³C spectra of **5o**

SNAN-1326 1 — single_pulse

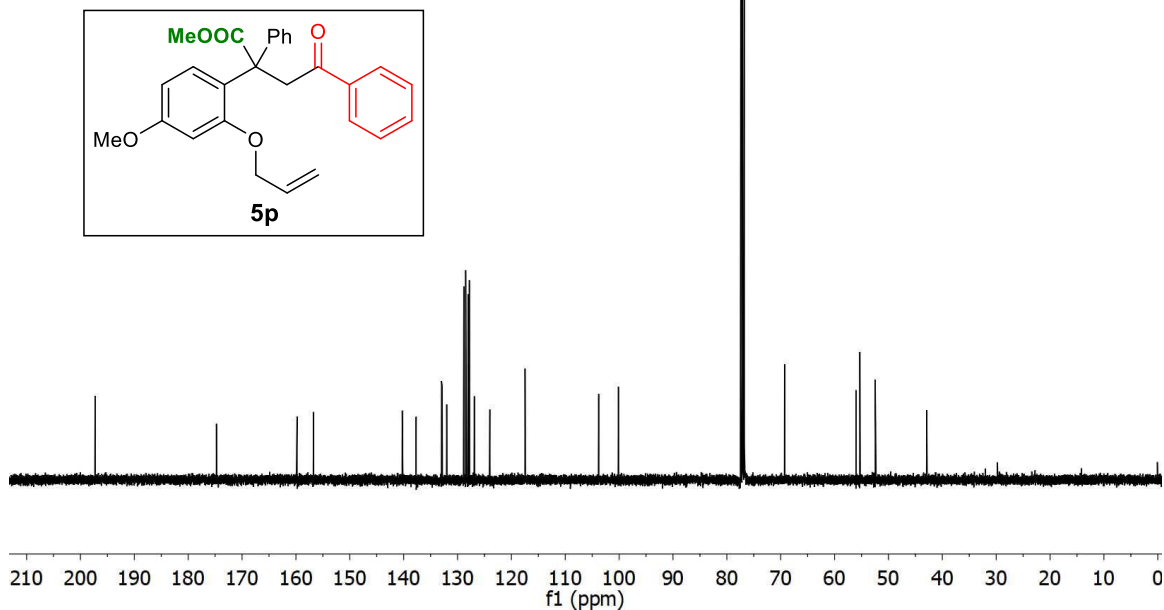
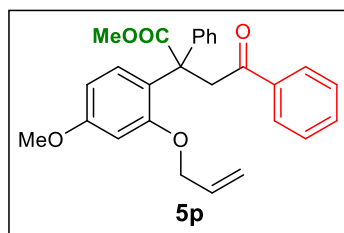
7.926
7.925
7.924
7.911
7.906
7.902
7.509
7.490
7.425
7.421
7.418
7.408
7.403
7.400
7.380
7.292
7.287
7.271
7.267
7.264
7.255
7.241
7.237
7.223
7.220
7.198
6.433
6.427
6.411
6.405
6.355
6.349
5.793
5.767
5.276
5.272
5.232
5.228
5.202
5.198
5.175
5.172
4.385
4.377
4.349
4.340
4.335
4.331
4.318
3.744
3.636



¹H spectra of **5p**

SNAN-1326 1 — single_pulse decoupled gated NOE

-197.282
-174.758
159.787
156.724
140.261
137.680
132.968
132.843
132.004
128.829
128.483
128.041
127.808
126.885
123.999
117.464
103.798
100.135
69.288
56.017
55.307
52.458
42.899

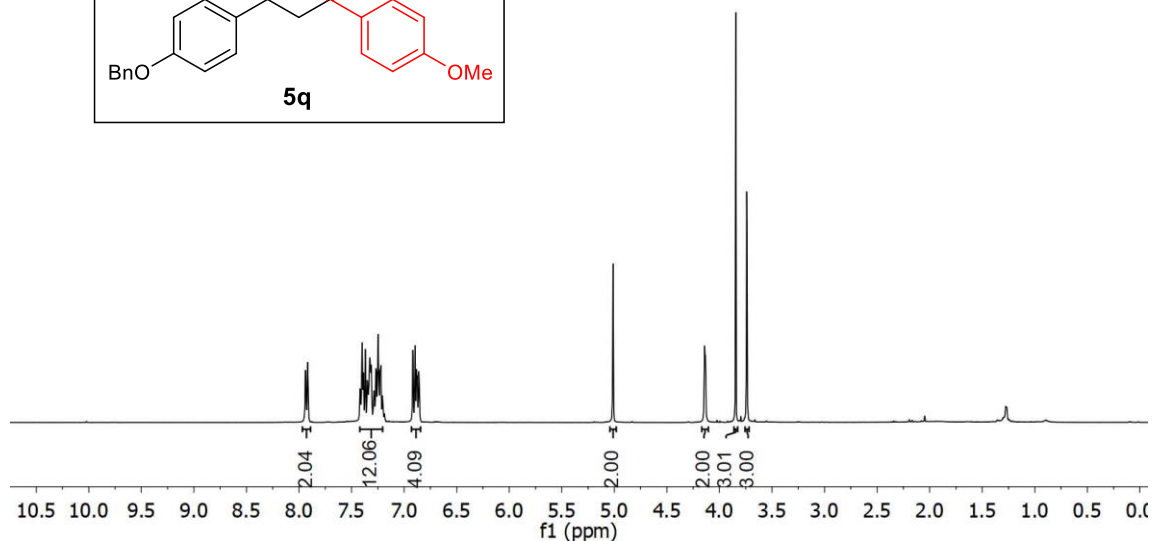
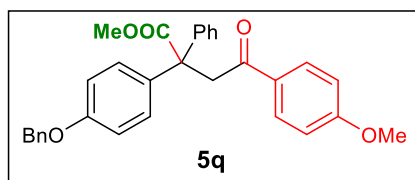


¹³C spectra of **5p**

Transition Metal-free, Visible Light Mediated Decarboxylative Acylation and Carboxylation of Alkenes with CO₂

SNAN-1341 — single_pulse

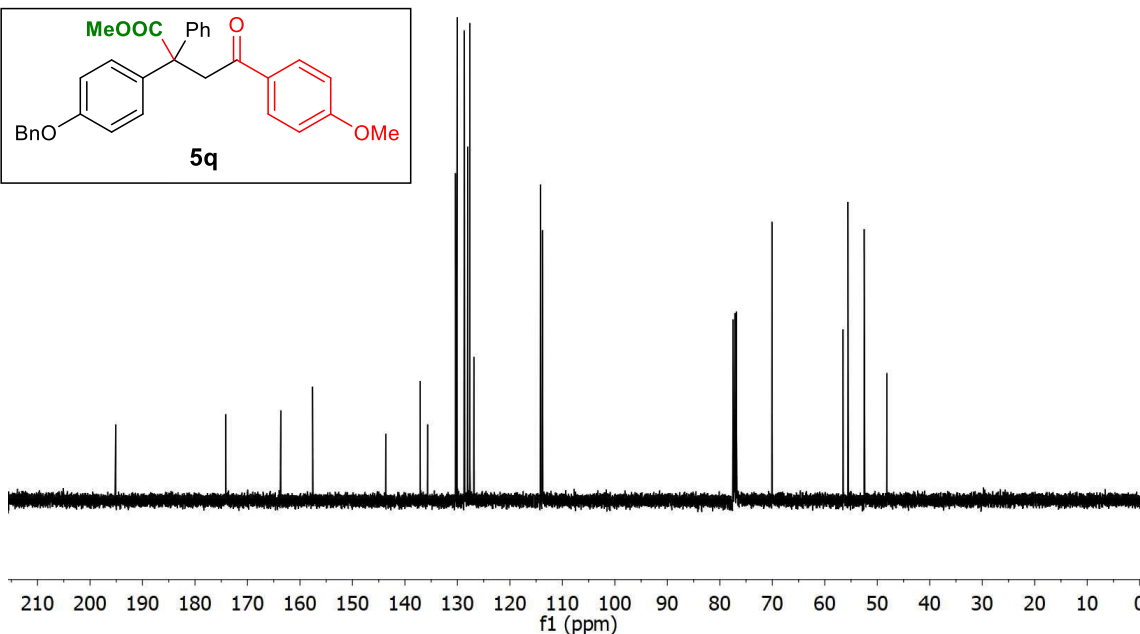
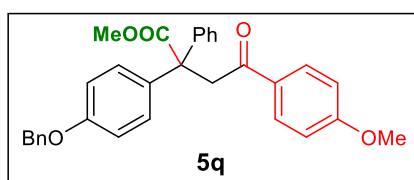
7.940
7.936
7.919
7.914
7.419
7.399
7.387
7.369
7.350
7.332
7.322
7.312
7.287
7.269
7.253
7.203
7.188
6.918
6.896
6.883
6.877
6.861
6.854
5.013
4.141
4.139
4.133
3.845
3.741



¹H spectra of **5q**

SNAN-1341 — single pulse decoupled gated NOE

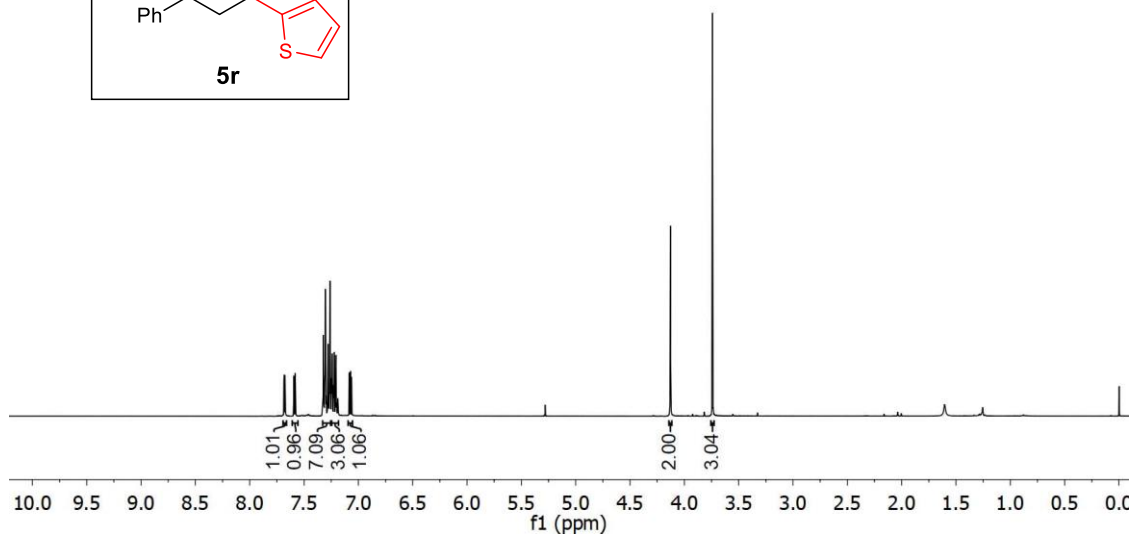
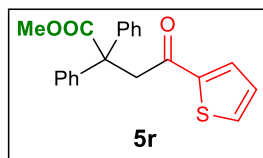
-195.110
-174.120
-163.663
-157.590
-143.656
-137.098
-135.679
-130.378
-130.061
-130.051
-128.708
-128.670
-128.037
-127.615
-126.868
-114.183
-113.811
-70.072
-56.520
-55.586
-52.498
-48.172



¹³C spectra of **5q**

SNAN-1333 — single_pulse

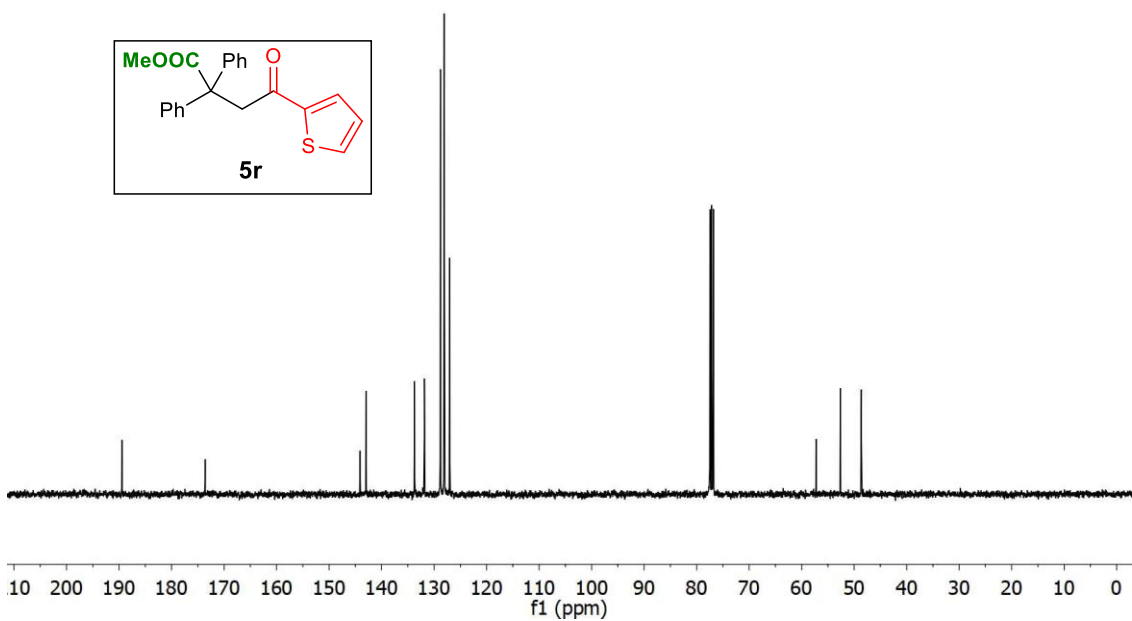
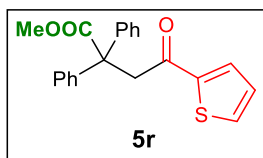
7.685
7.682
7.676
7.673
7.593
7.591
7.581
7.578
7.327
7.323
7.317
7.308
7.305
7.302
7.296
7.282
7.279
7.273
7.267
7.263
7.261
7.257
7.246
7.242
7.227
7.224
7.220
7.213
7.206
7.199
7.192
7.189
7.185
7.085
7.075
7.072
7.063
4.128
3.742



¹H spectra of **5r**

SNAN-1333 — single_pulse decoupled gated NOE

-189.460
-173.597
144.079
142.968
133.722
131.849
128.799
128.123
128.058
127.023
57.256
52.625
48.632

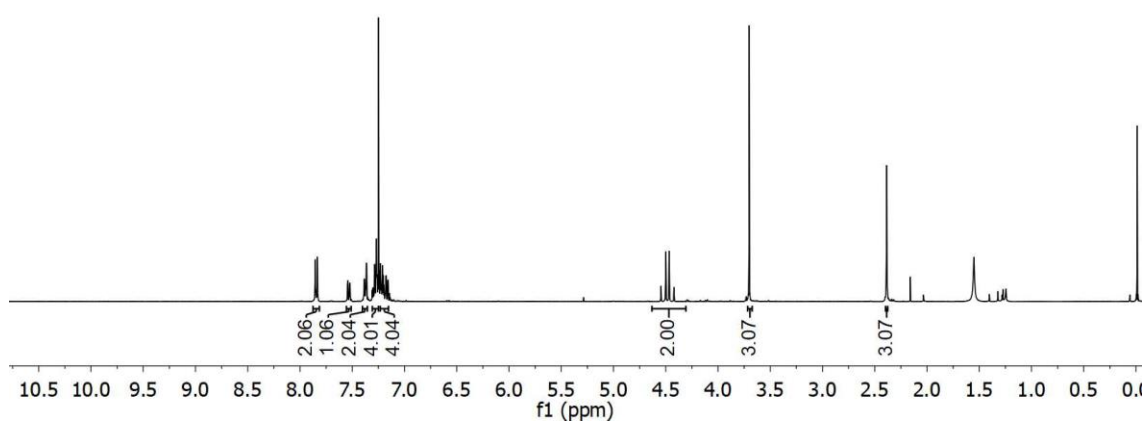
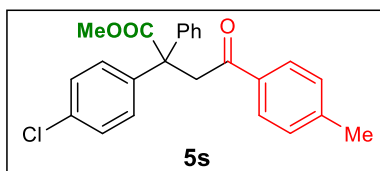


¹³C spectra of **5r**

Transition Metal-free, Visible Light Mediated Decarboxylative Acylation and Carboxylation of Alkenes with CO₂

SNAN-1442 — single_pulse

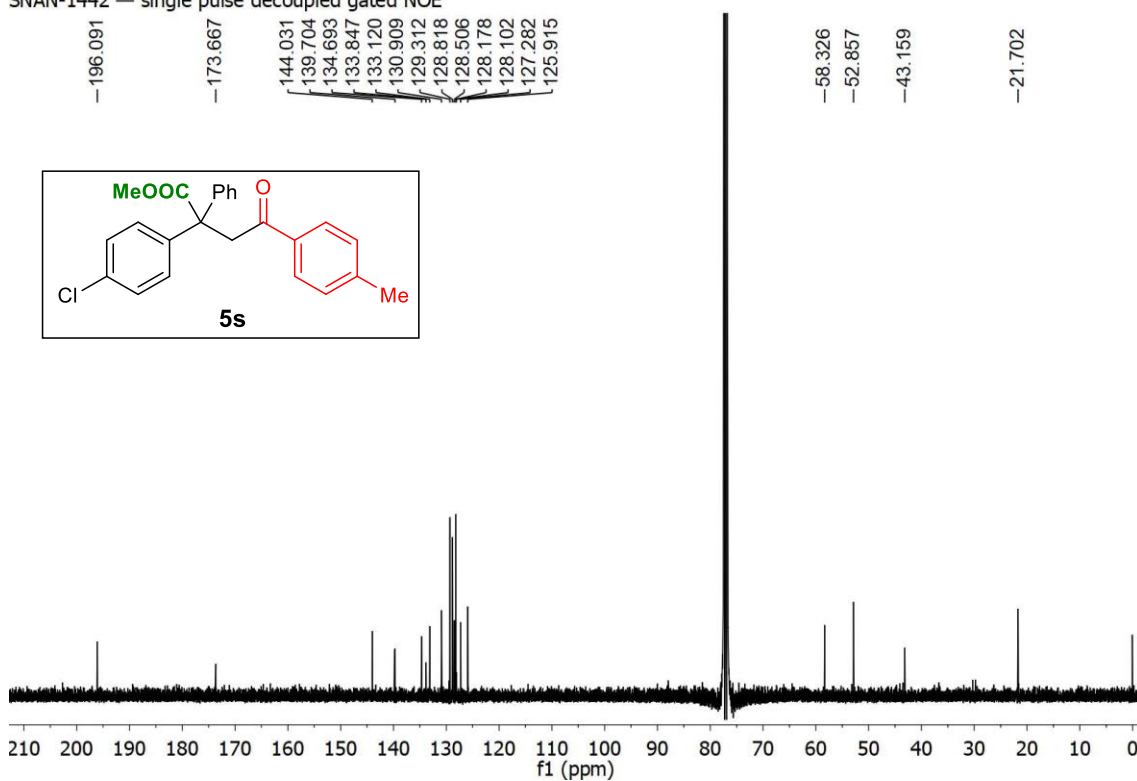
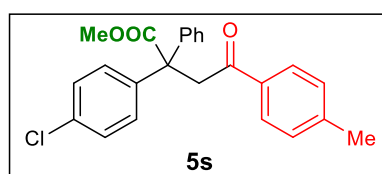
7.859
7.854
7.849
7.838
7.833
7.828
7.546
7.541
7.527
7.522
7.386
7.380
7.376
7.365
7.362
7.354
7.309
7.301
7.296
7.288
7.287
7.283
7.277
7.273
7.268
7.265
7.261
7.260
7.255
7.251
7.231
7.230
7.220
7.215
7.210
7.209
7.202
7.197
7.183
7.180
7.178
7.174
7.161
7.156
4.546
4.499
4.467
4.421
3.701
2.385



¹H spectra of **5s**

SNAN-1442 — single pulse decoupled gated NOE

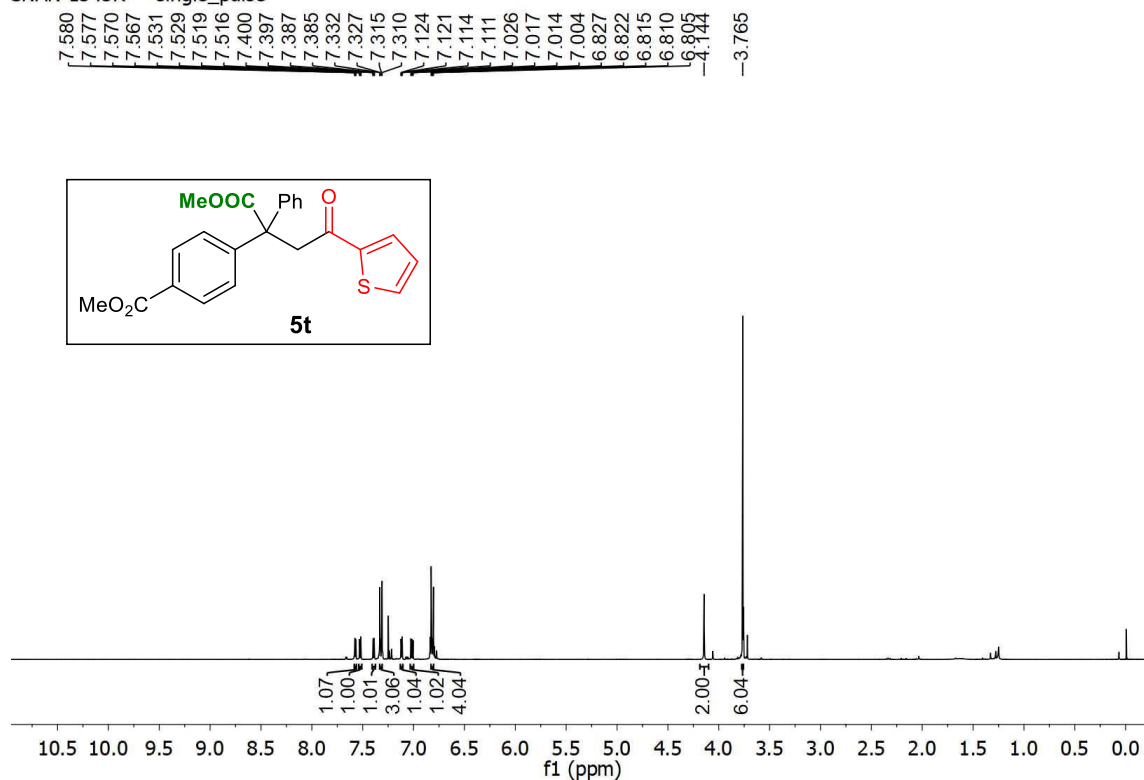
-196.091
-173.667
144.031
139.704
134.693
133.847
133.120
130.909
129.312
128.818
128.506
128.178
128.102
127.282
125.915
-58.326
-52.857
-43.159
-21.702



¹³C spectra of **5s**

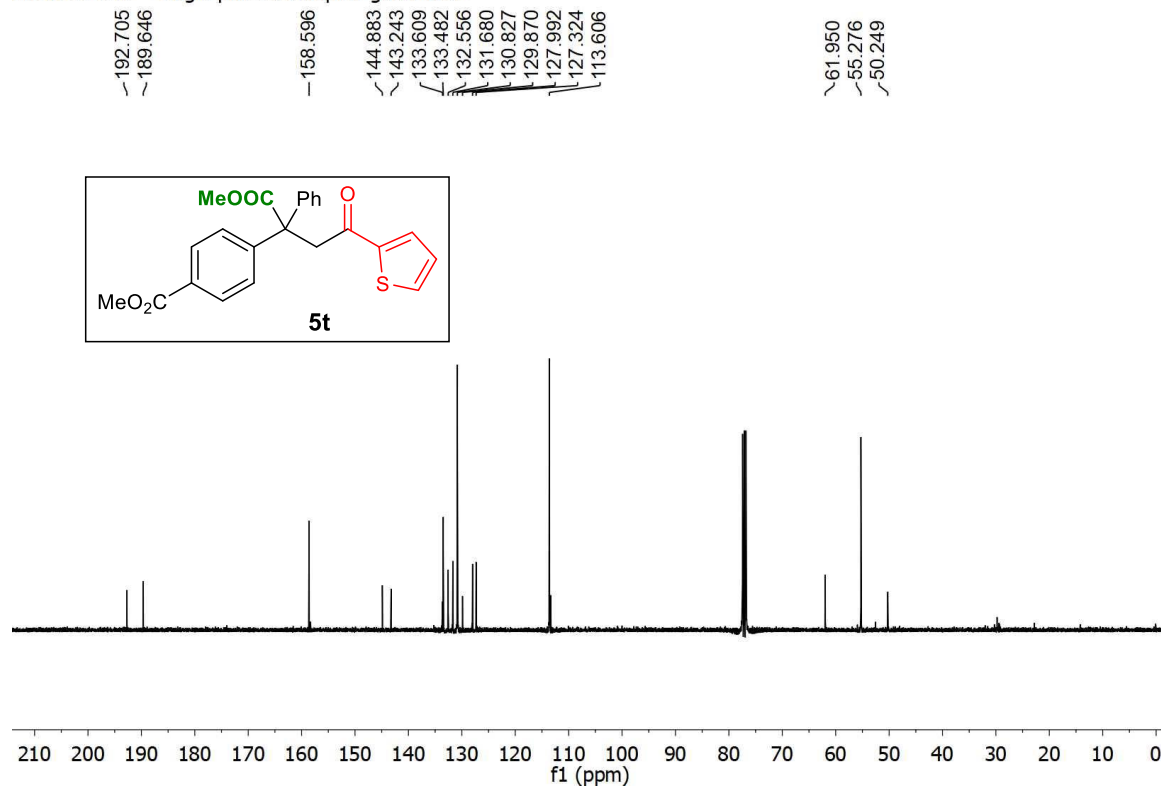
Chapter II

SNAN-1343R — single_pulse



¹H spectra of **5t**

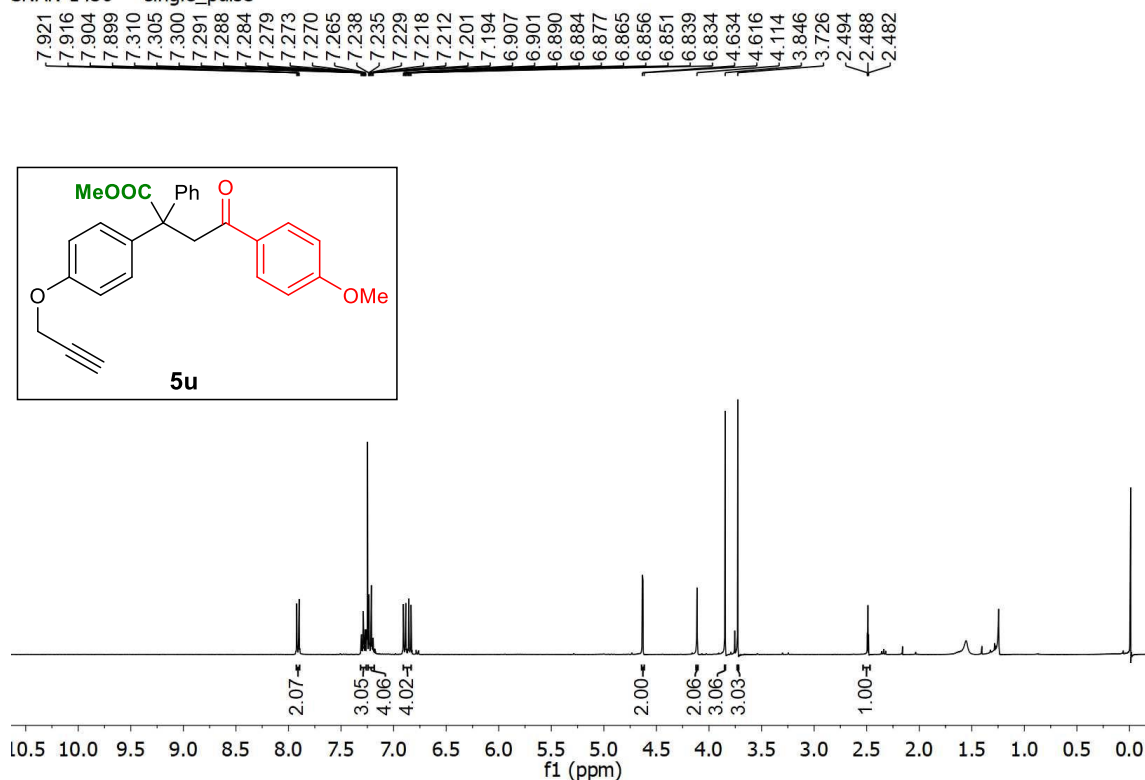
SNAN-1343R — single_pulse decoupled gated NOE



¹³C spectra of **5t**

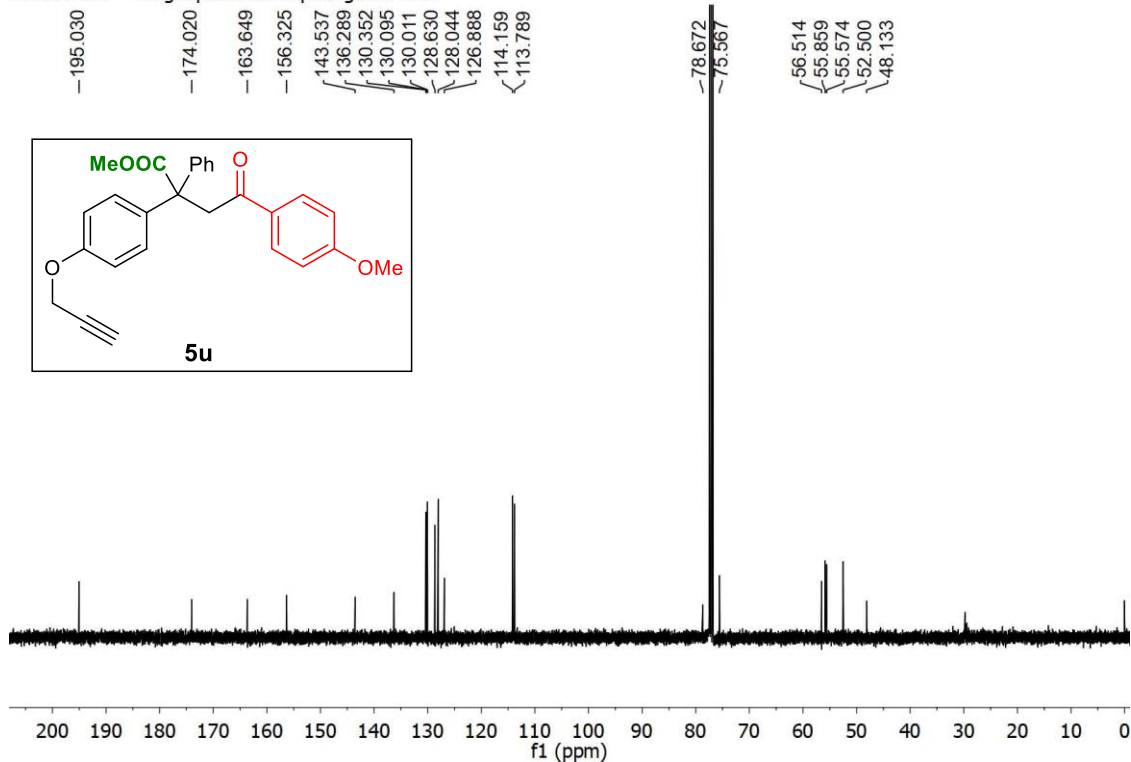
Transition Metal-free, Visible Light Mediated Decarboxylative Acylation and Carboxylation of Alkenes with CO₂

SNAN-1436 — single_pulse



¹H spectra of **5u**

SNAN-1436 — single pulse decoupled gated NOE

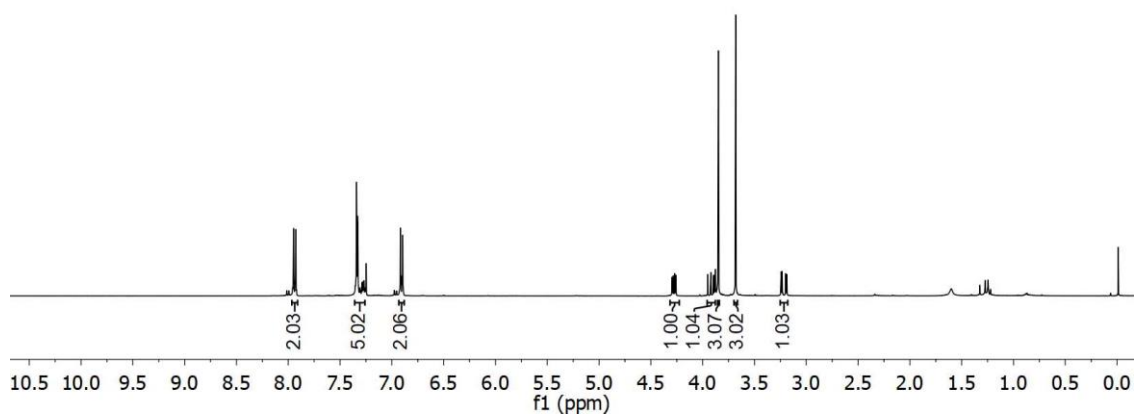
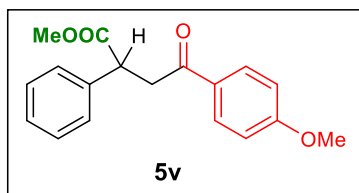


¹³C spectra of **5u**

Chapter II

SNAN-1369 — single_pulse

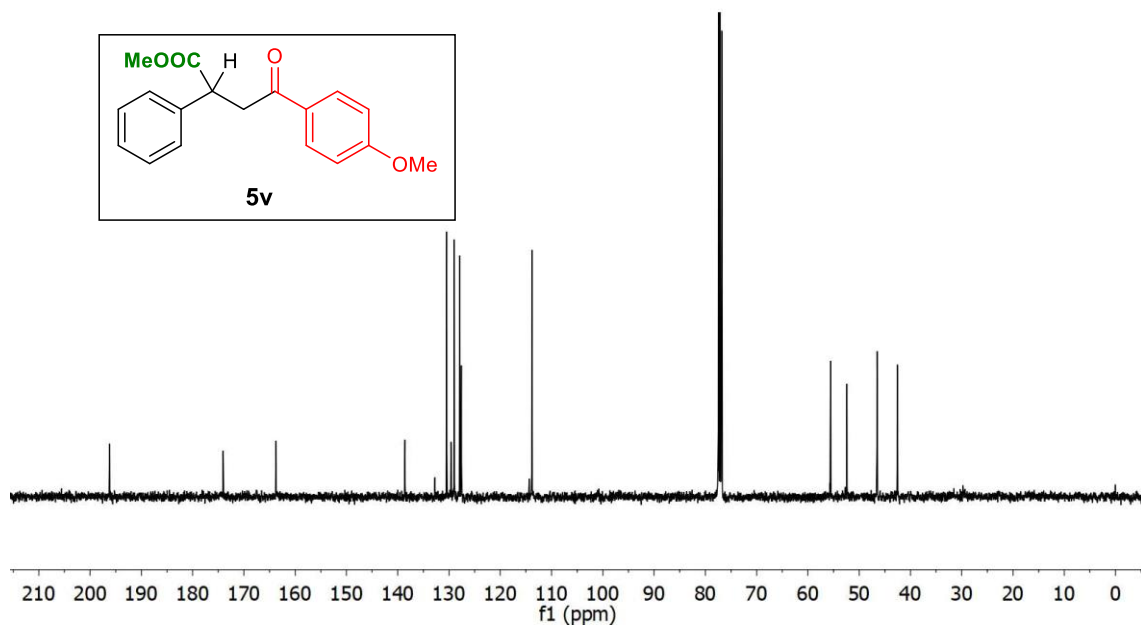
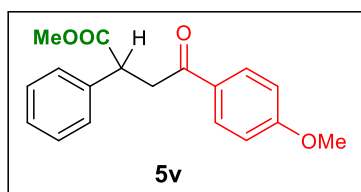
7.956
7.949
7.944
7.932
7.927
7.919
7.341
7.332
7.328
7.309
7.307
7.300
7.289
7.282
7.277
7.273
7.268
7.261
7.255
6.925
6.917
6.912
6.900
6.895
6.888
4.295
4.285
4.269
4.259
3.951
3.921
3.895
3.876
3.848
3.681
3.243
3.232
3.198
3.188



¹H spectra of **5v**

SNAN-1369 — single pulse decoupled gated NOE

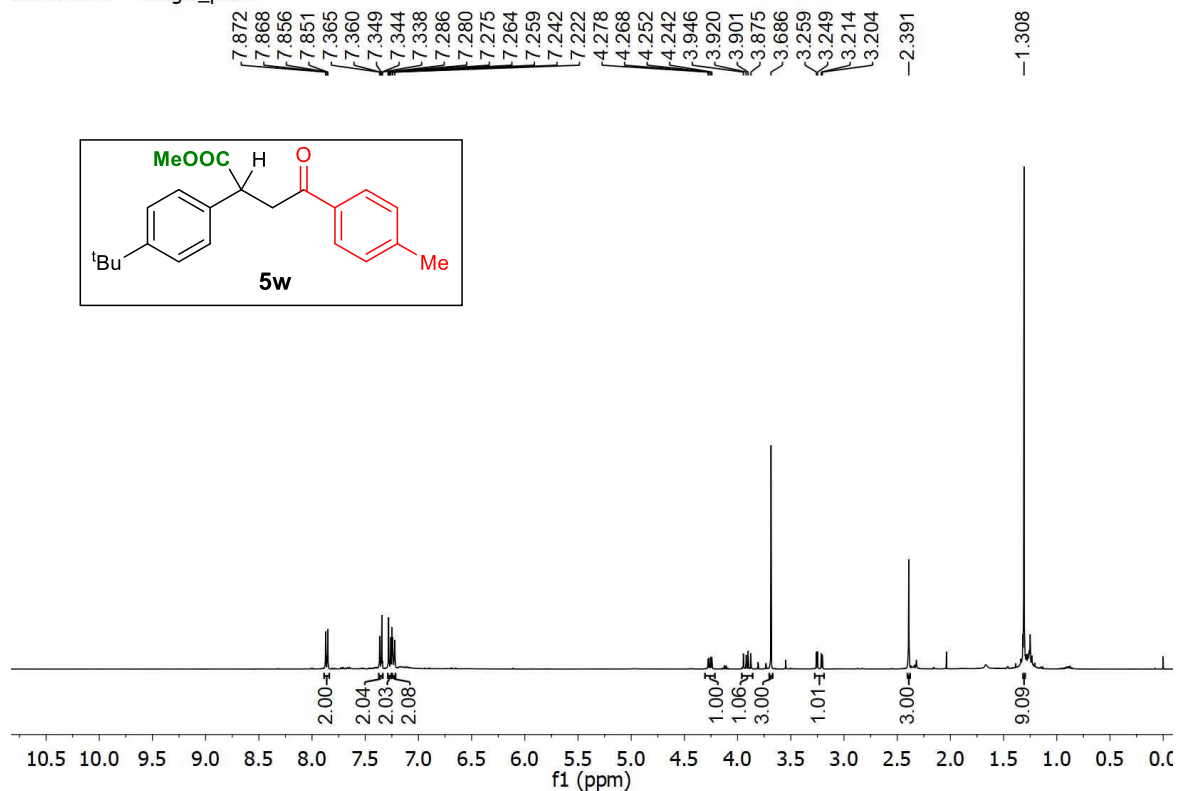
-196.192
-174.051
-163.735
138.591
132.750
130.451
129.612
128.975
127.917
127.588
-113.823
-55.556
-52.394
-46.512
-42.562



¹³C spectra of **5v**

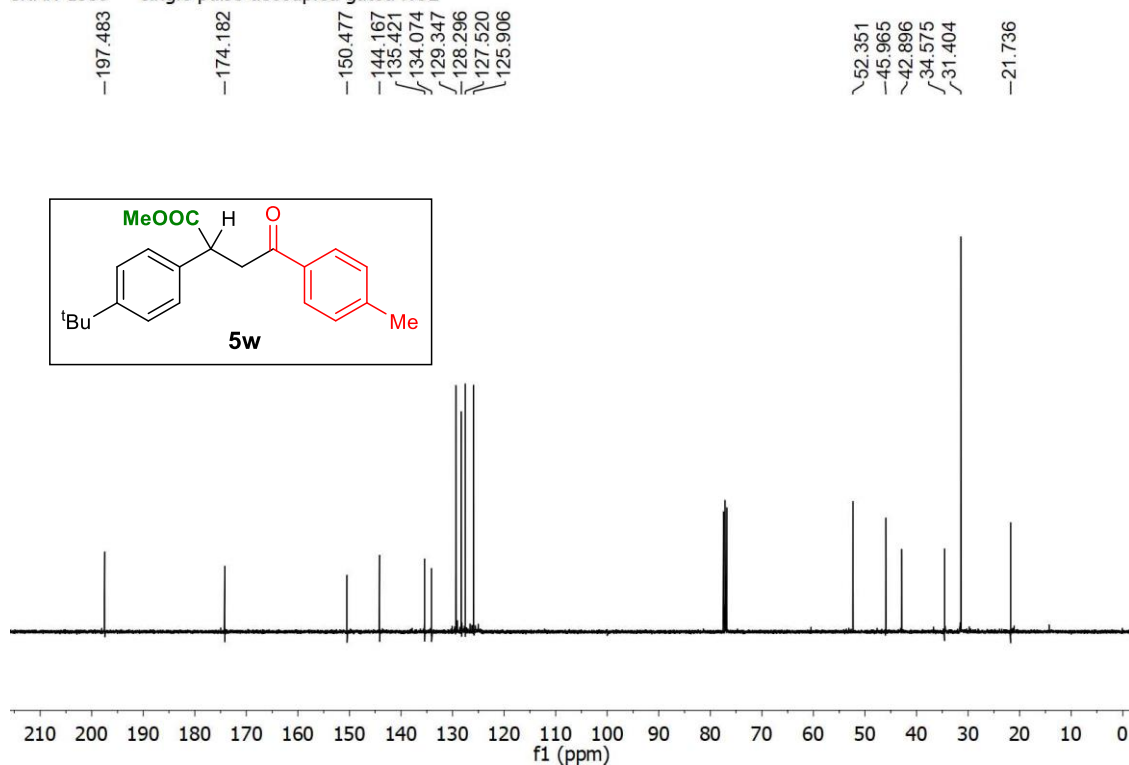
Transition Metal-free, Visible Light Mediated Decarboxylative Acylation and Carboxylation of Alkenes with CO₂

SNAN-1359 — single_pulse



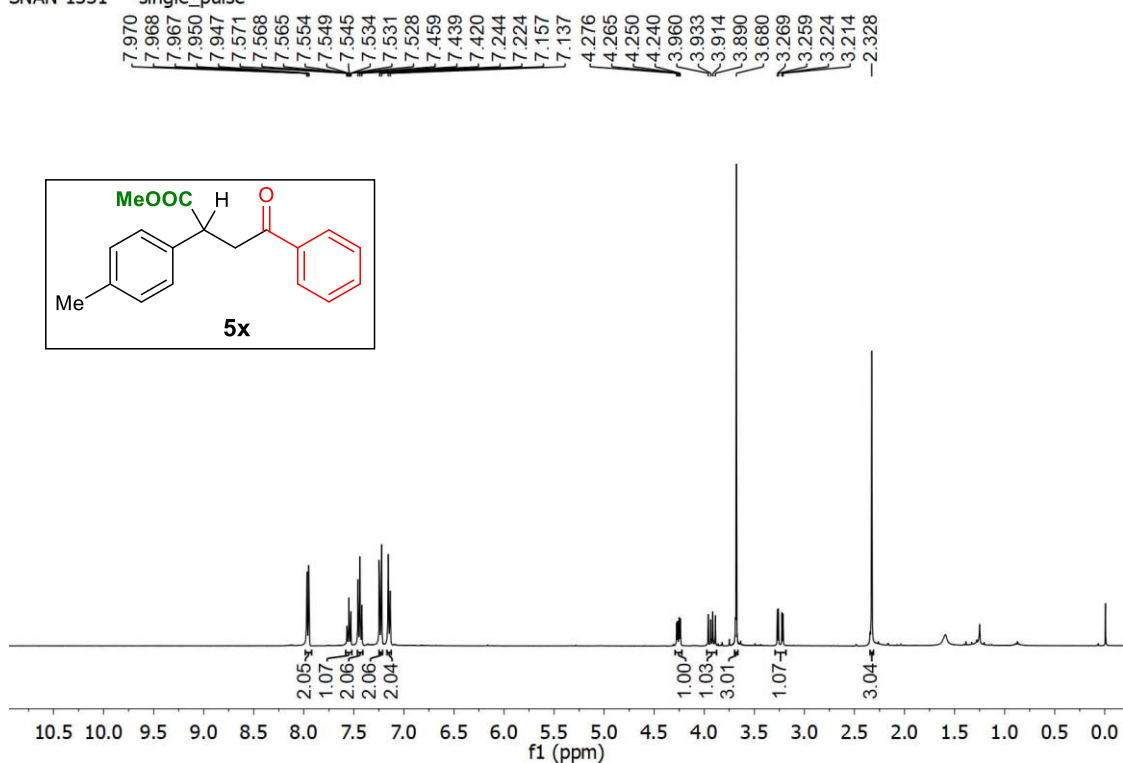
¹H spectra of **5w**

SNAN-1359 — single pulse decoupled gated NOE



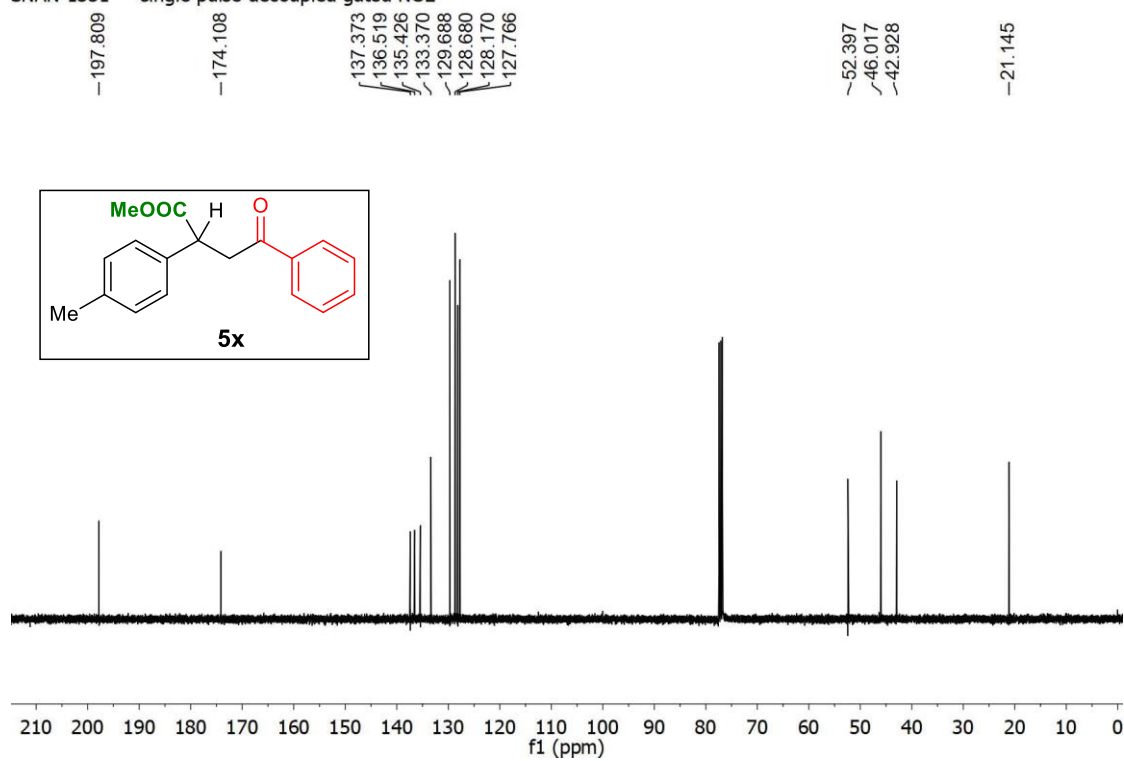
¹³C spectra of **5w**

SNAN-1331 — single_pulse



¹H spectra of **5x**

SNAN-1331 — single pulse decoupled gated NOE



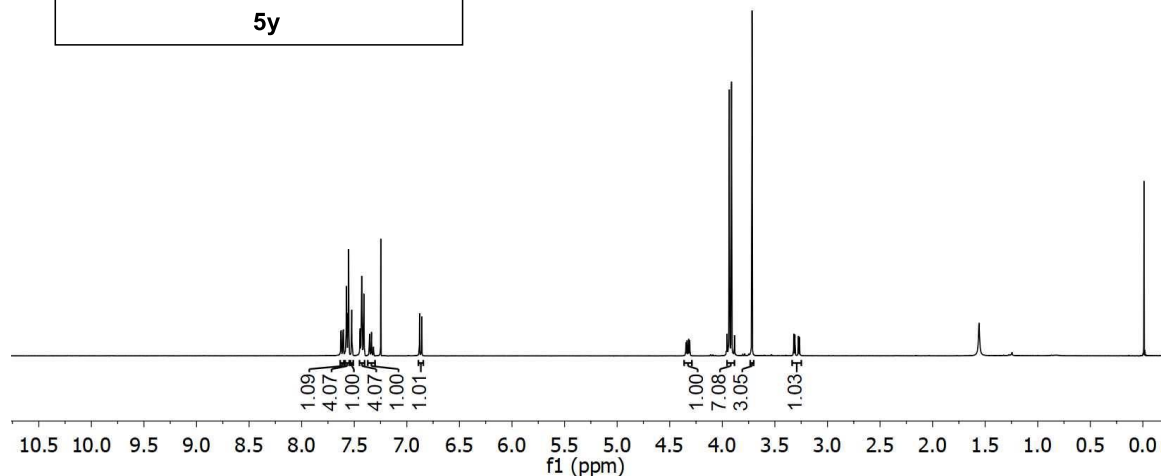
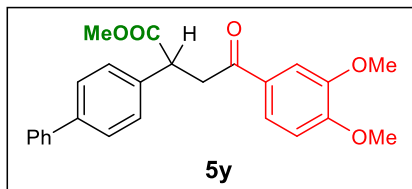
¹³C spectra of **5x**

Transition Metal-free, Visible Light Mediated Decarboxylative Acylation and Carboxylation of Alkenes with CO₂

SNAN-1366 — single_pulse

7.629
7.624
7.608
7.603
7.575
7.573
7.558
7.554
7.524
7.519
7.445
7.430
7.427
7.414
7.409
7.354
6.876
6.858

4.346
4.335
4.320
4.310
3.954
3.933
3.929
3.912
3.884
3.717
3.321
3.310
3.276
3.265

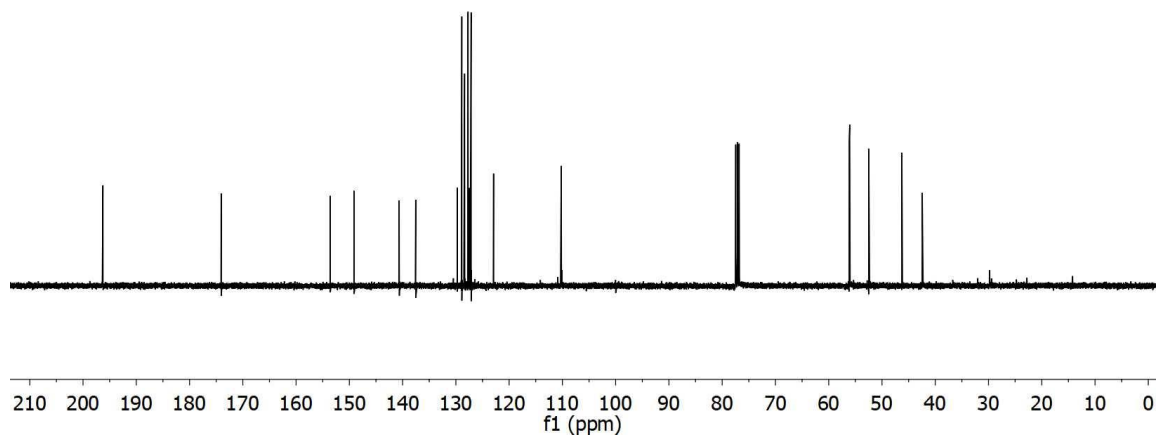
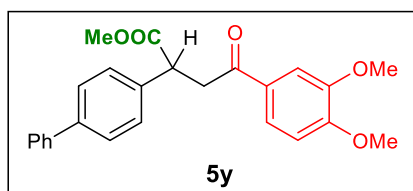


¹H spectra of **5y**

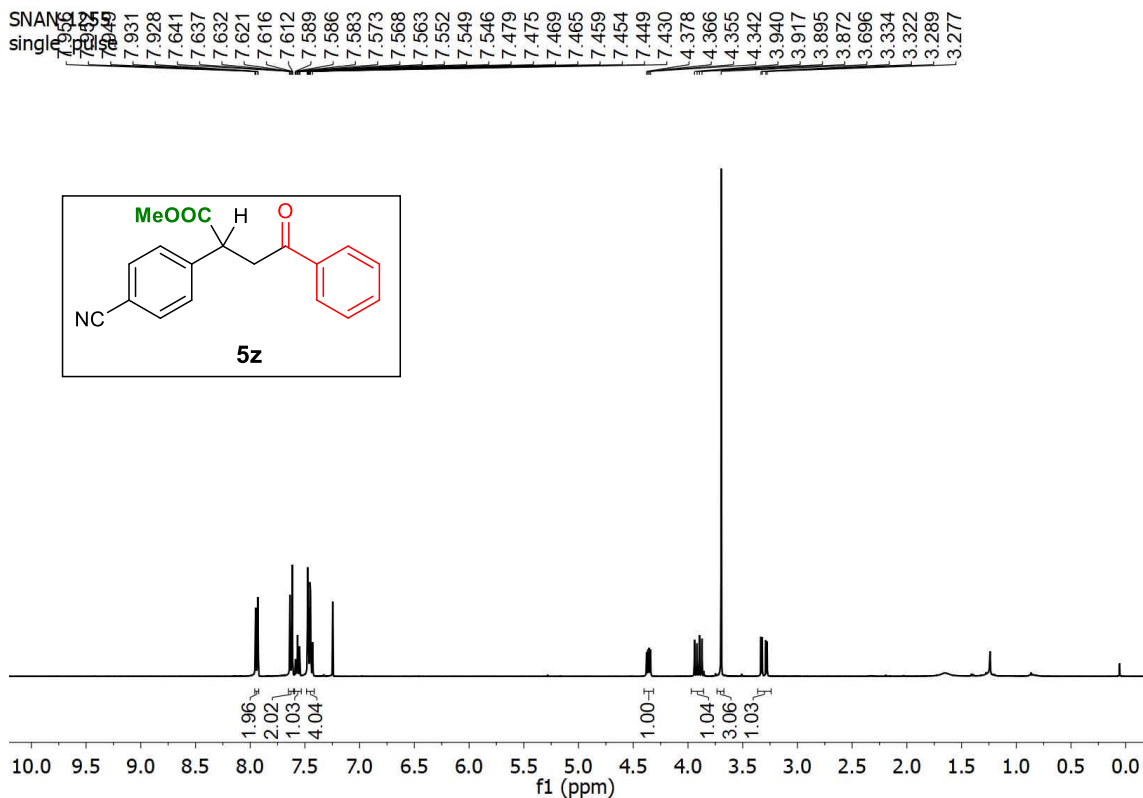
SNAN-1366 — single pulse decoupled gated NOE

196.262
174.058
153.595
149.124
140.649
137.538
129.726
128.863
128.357
127.713
127.483
127.135
122.921
110.211
110.120

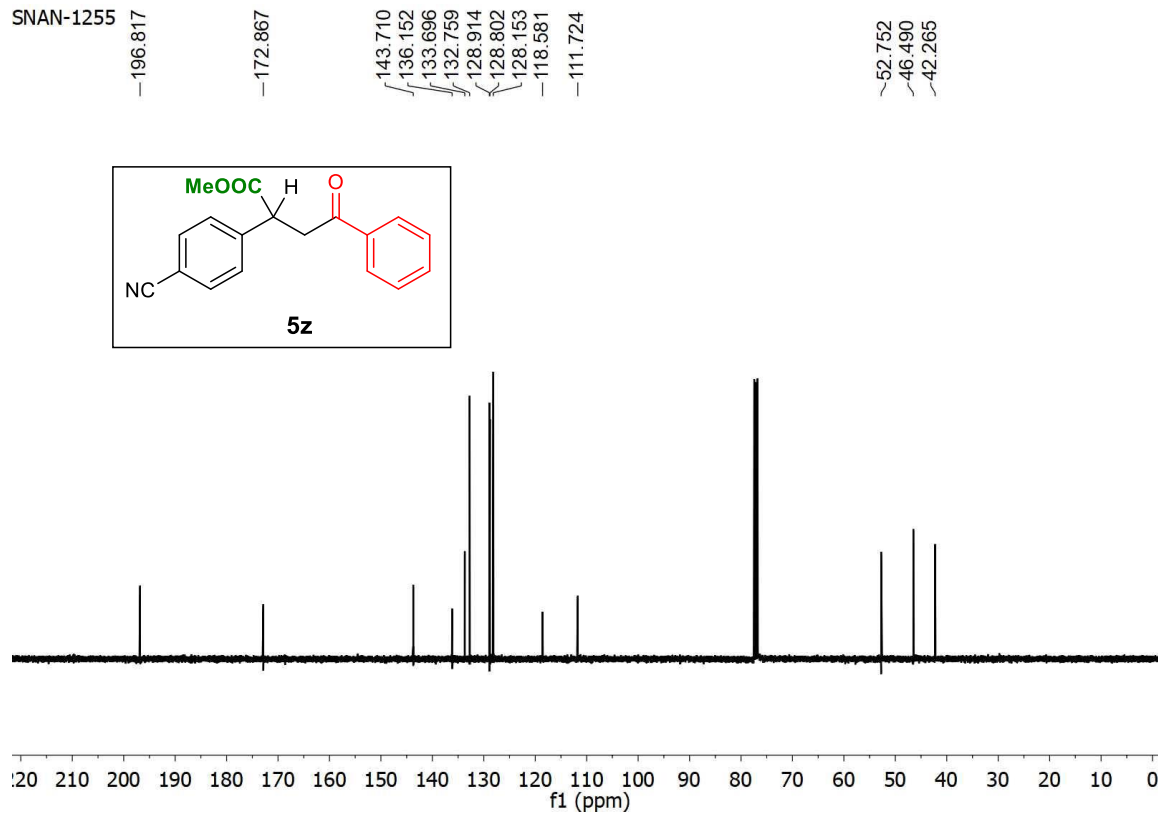
56.164
56.060
52.484
46.266
42.439



¹³C spectra of **5y**



¹H spectra of **5z**

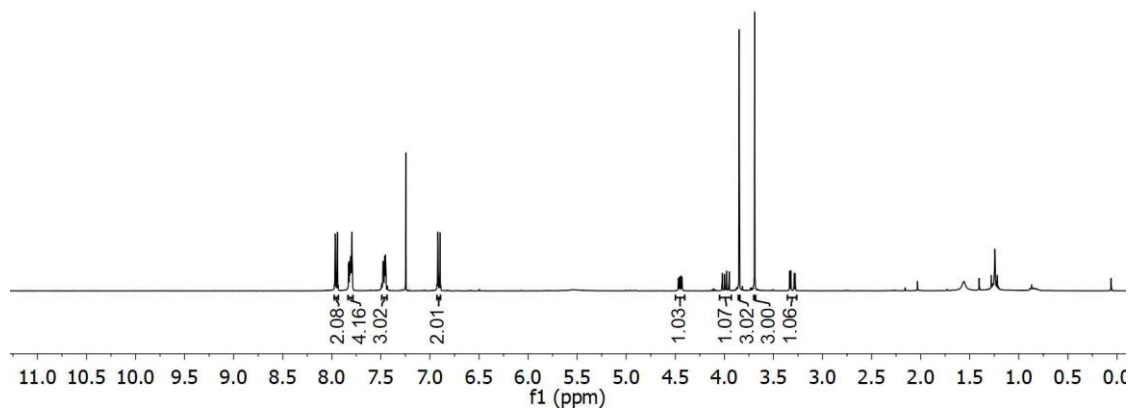
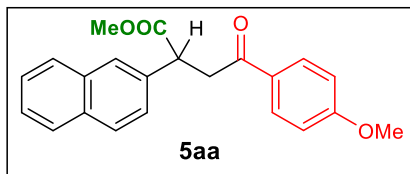


¹³C spectra of **5z**

Transition Metal-free, Visible Light Mediated Decarboxylative Acylation and Carboxylation of Alkenes with CO₂

SNAN-1269 1 — single_pulse

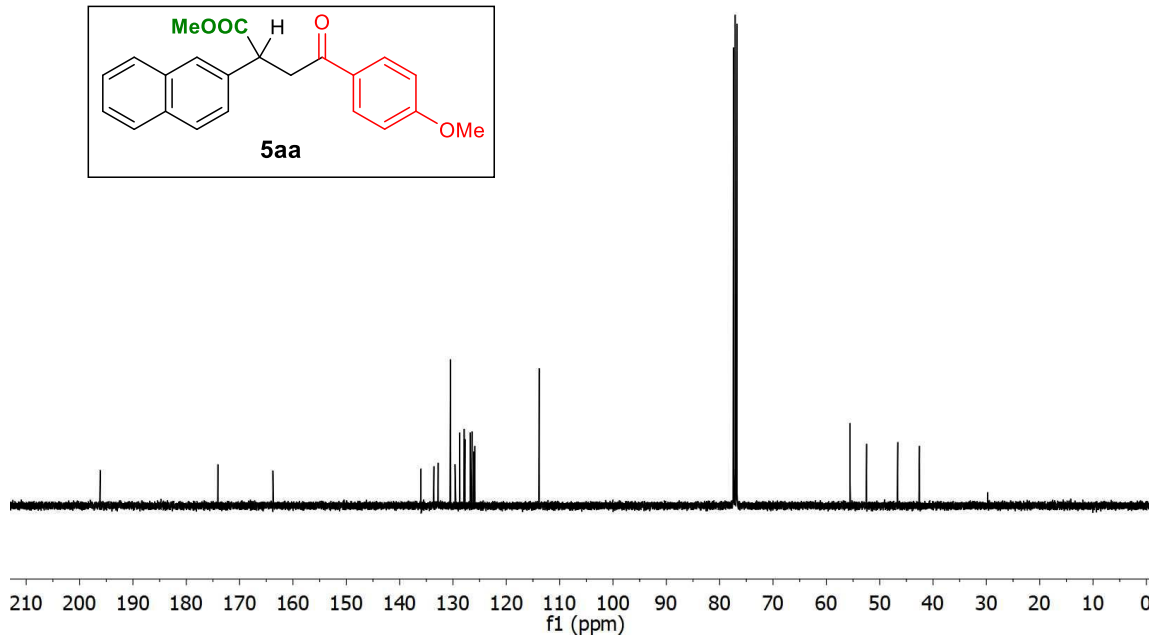
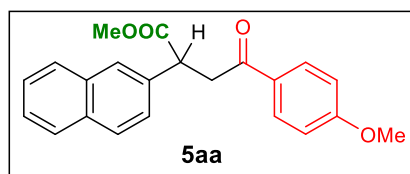
7.966
7.961
7.948
7.943
7.829
7.820
7.807
7.796
7.476
7.471
7.462
7.454
7.447
6.920
6.915
6.903
6.898
4.468
4.458
4.443
4.433
4.022
3.996
3.977
3.951
3.849
3.849
3.692
3.334
3.323
3.289
3.279



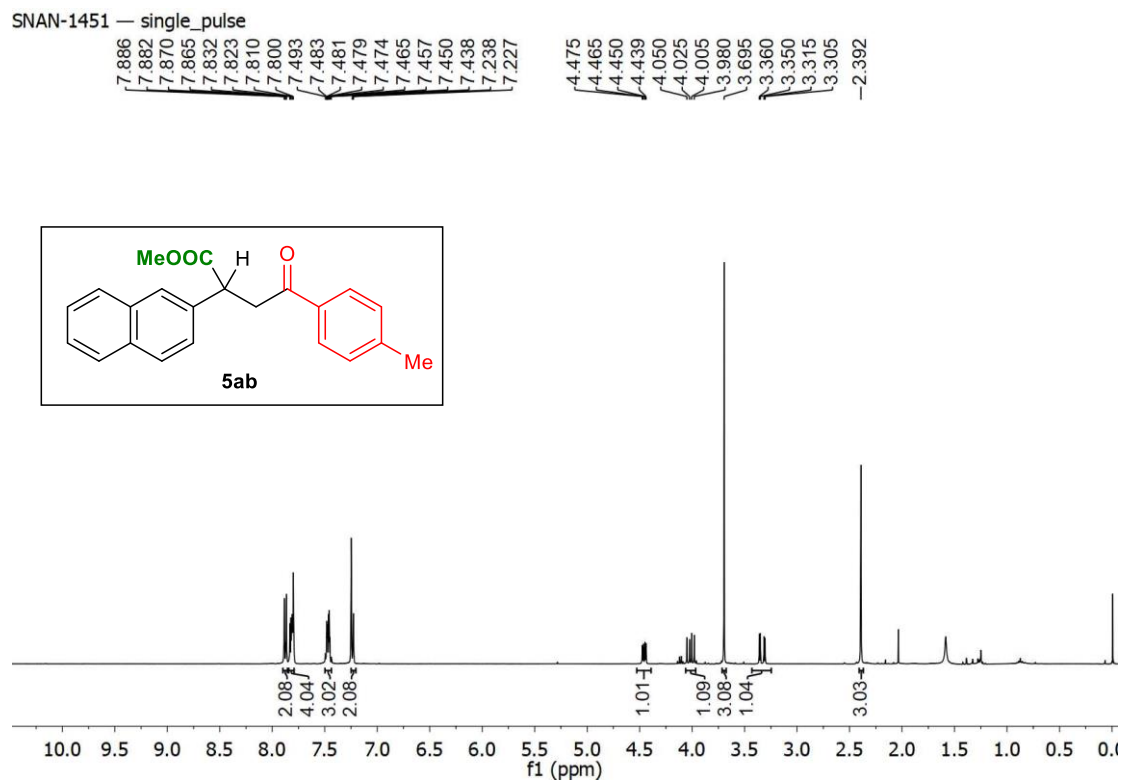
¹H spectra of 5aa

SNAN-1269 1 — single_pulse decoupled gated NOE

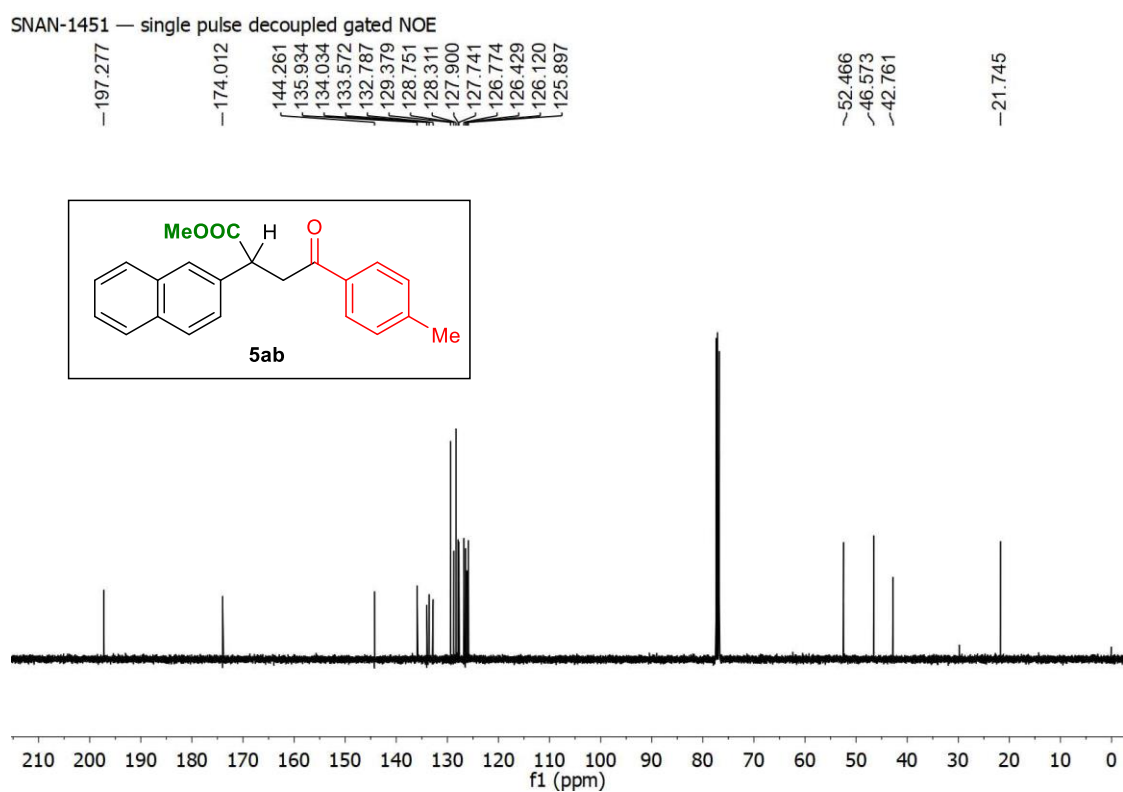
196.133
174.059
163.756
135.993
133.568
132.777
130.473
129.615
128.734
127.895
127.736
126.760
126.419
126.104
125.908
113.838
55.556
52.453
46.617
42.544



¹³C spectra of 5aa



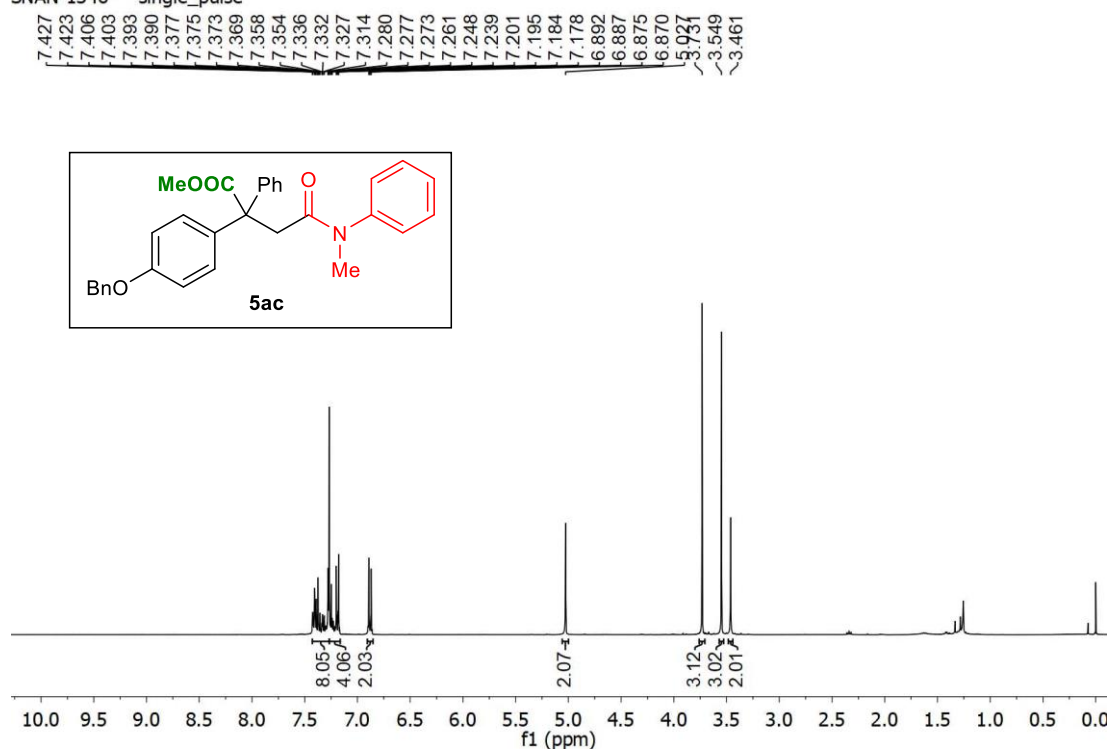
¹H spectra of **5ab**



¹³C spectra of **5ab**

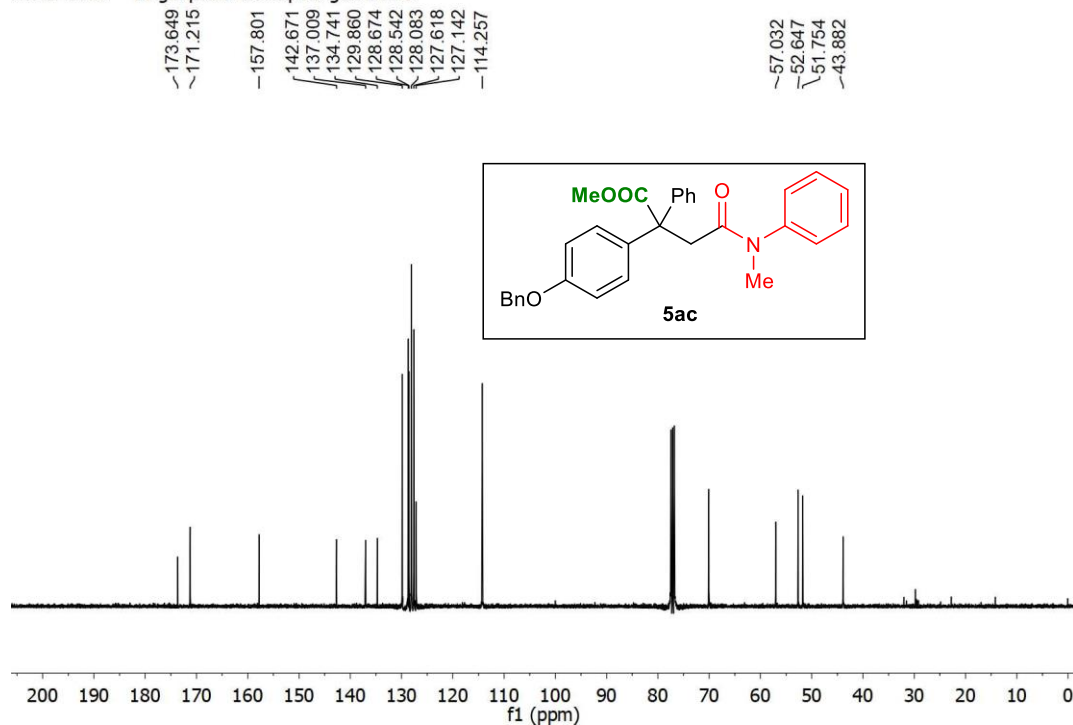
Transition Metal-free, Visible Light Mediated Decarboxylative Acylation and Carboxylation of Alkenes with CO₂

SNAN-1346 — single_pulse



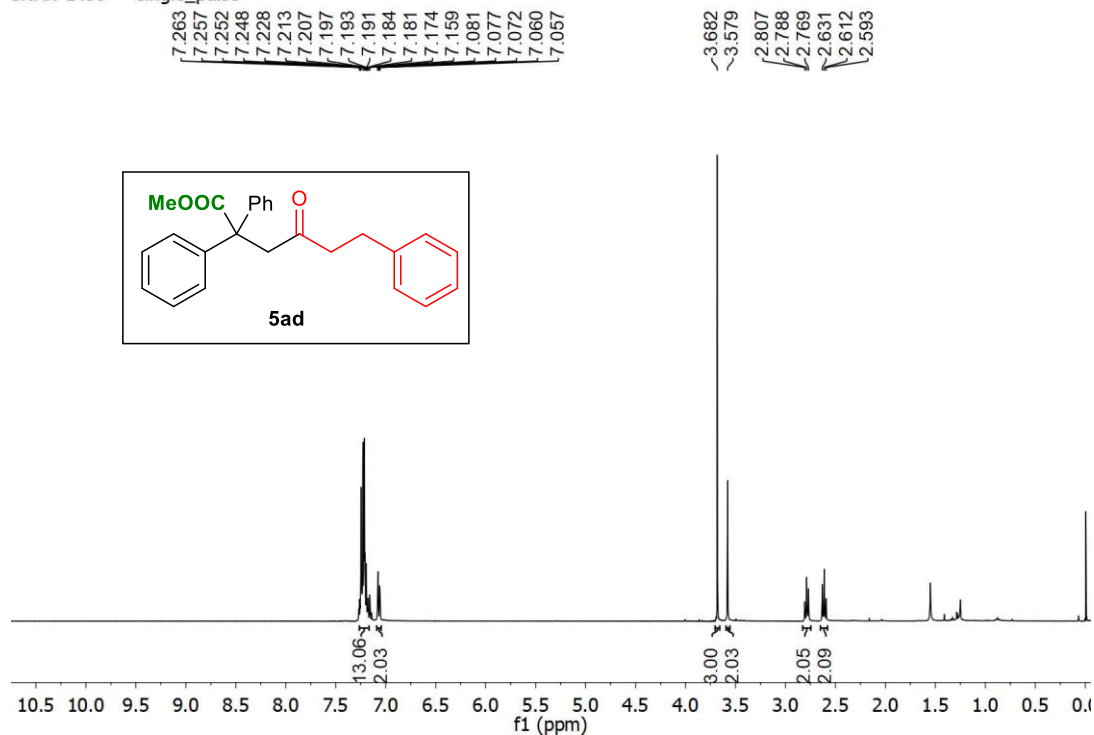
¹H spectra of **5ac**

SNAN-1346 — single pulse decoupled gated NOE



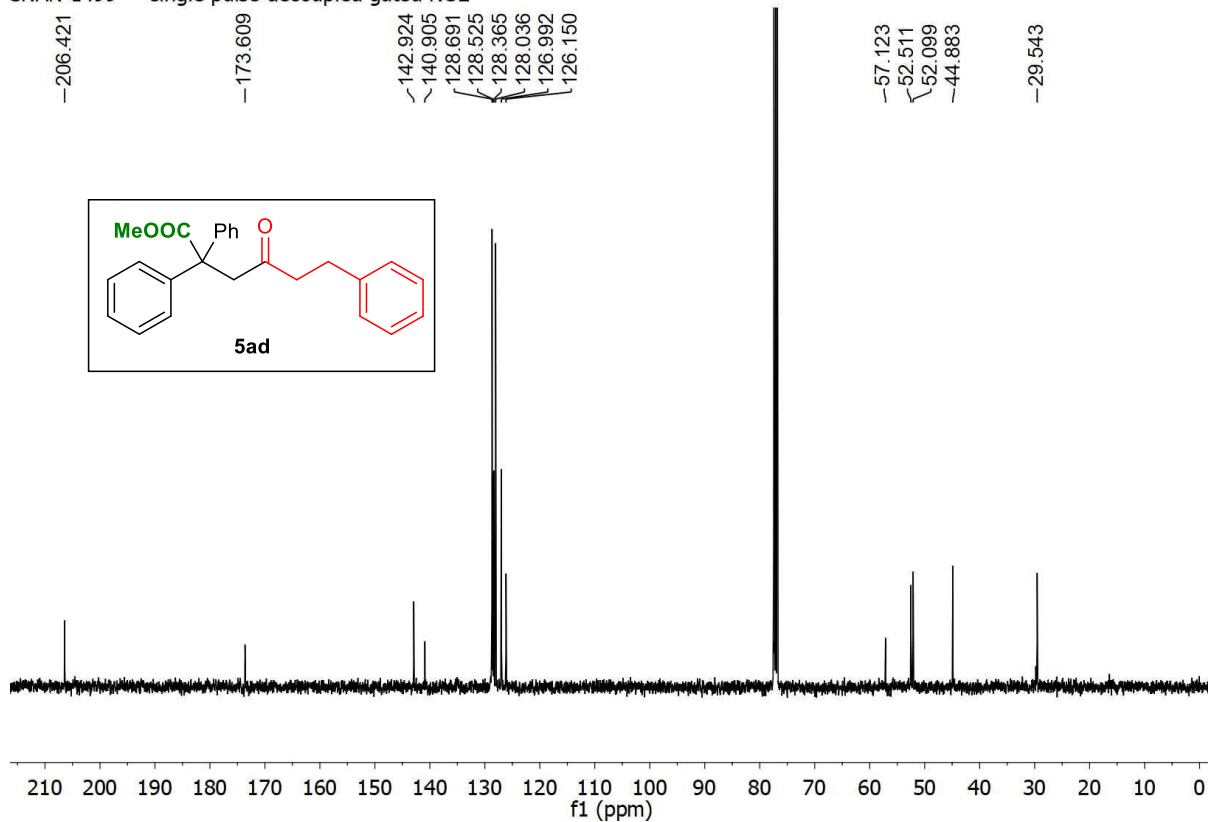
¹³C spectra of **5ac**

SNAN-1499 — single_pulse



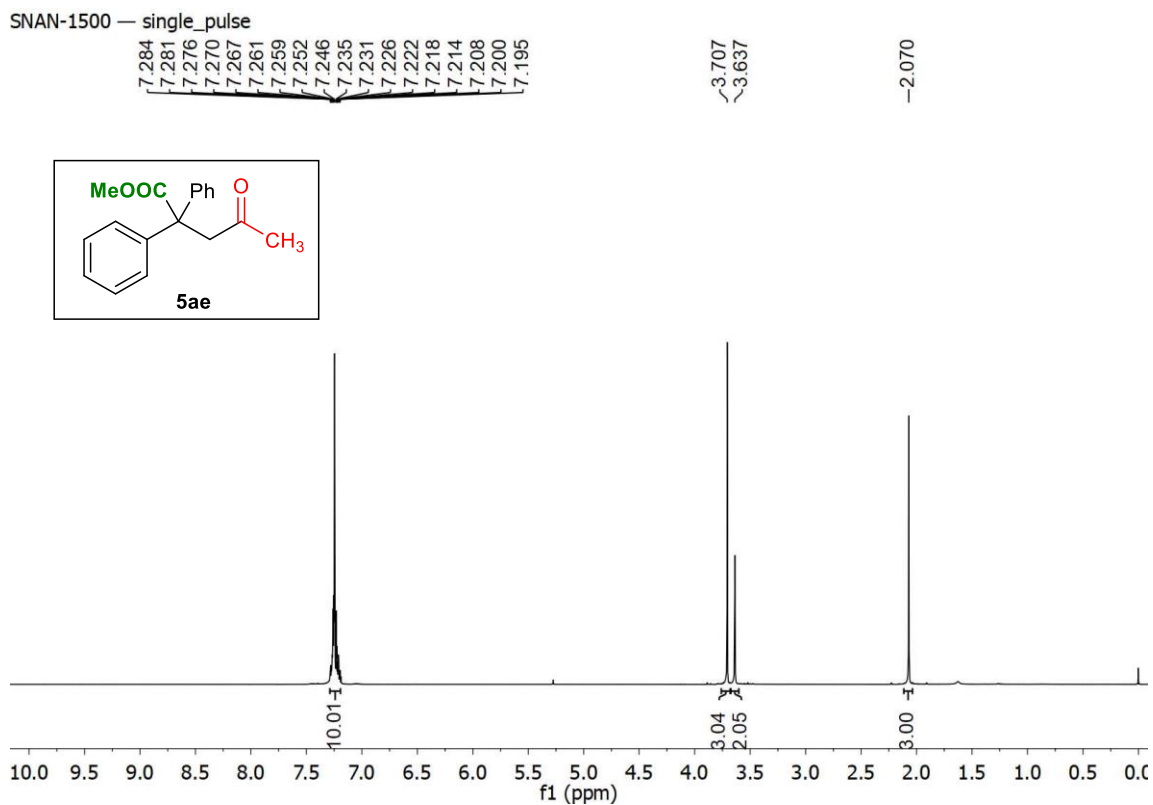
¹H spectra of **5ad**

SNAN-1499 — single pulse decoupled gated NOE

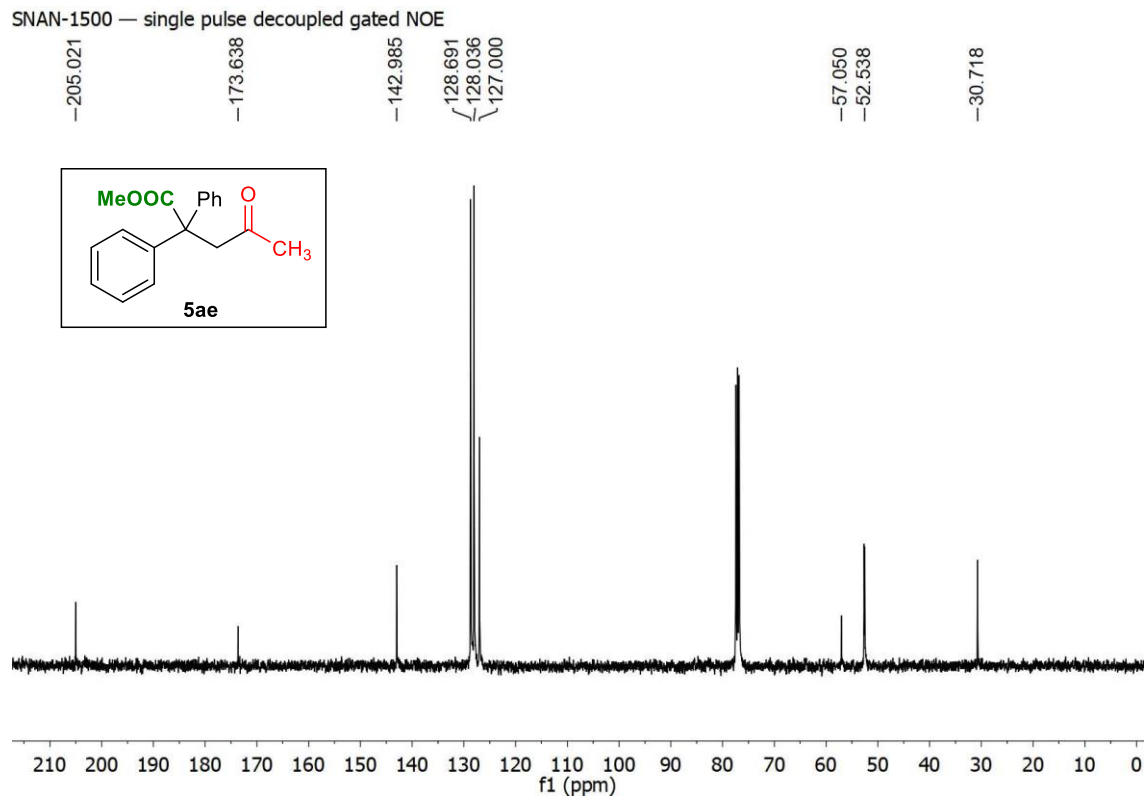


¹³C spectra of **5ad**

Transition Metal-free, Visible Light Mediated Decarboxylative Acylation and Carboxylation of Alkenes with CO₂



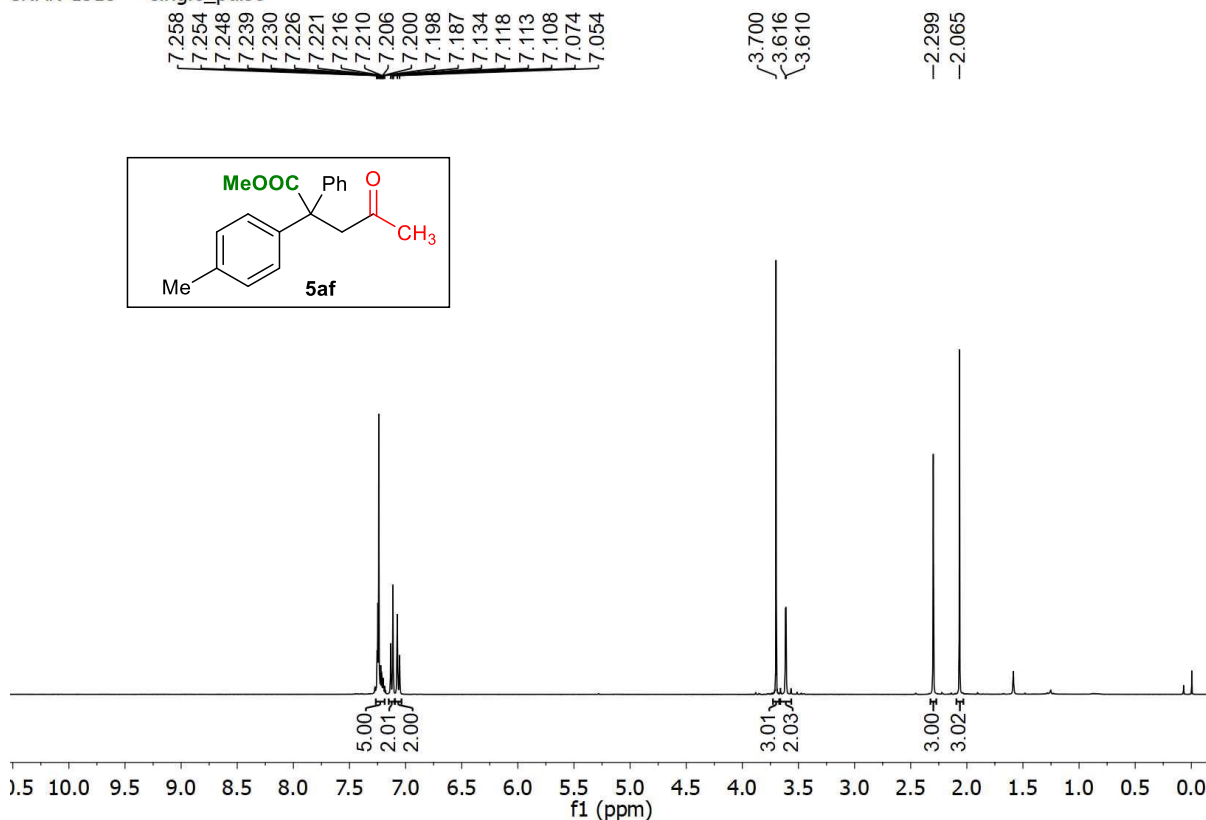
¹H spectra of **5ae**



¹³C spectra of **5ae**

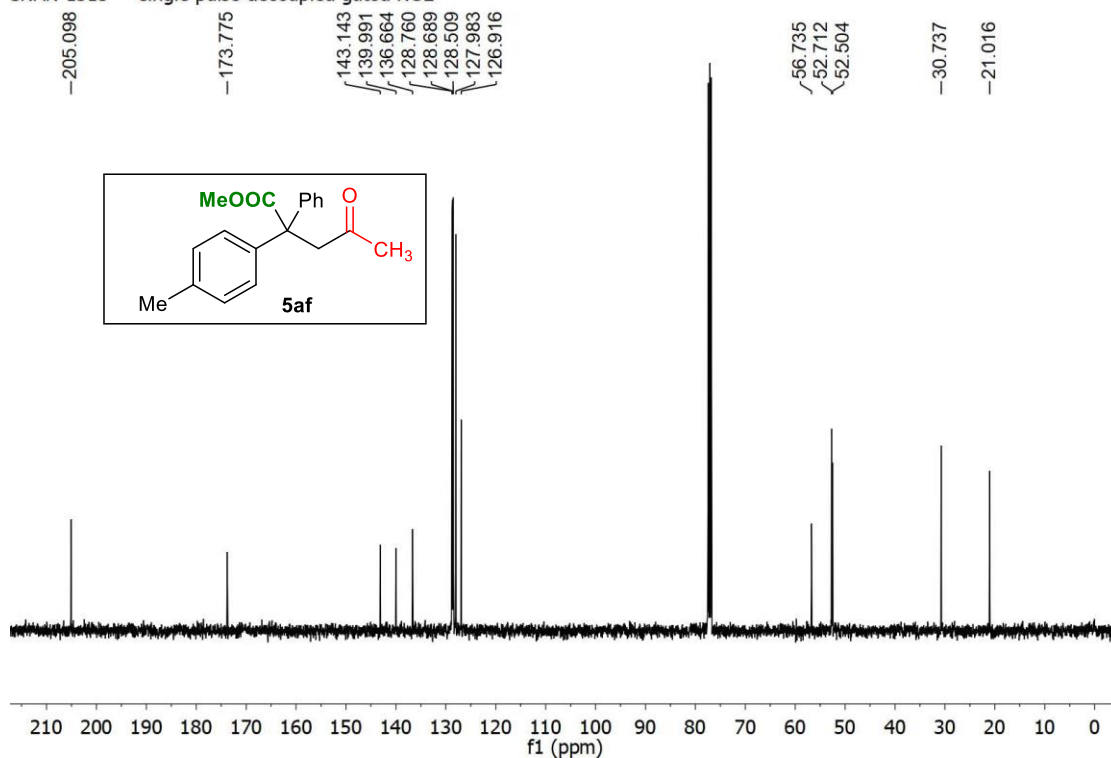
Chapter II

SNAN-1513 — single_pulse



^1H spectra of **5af**

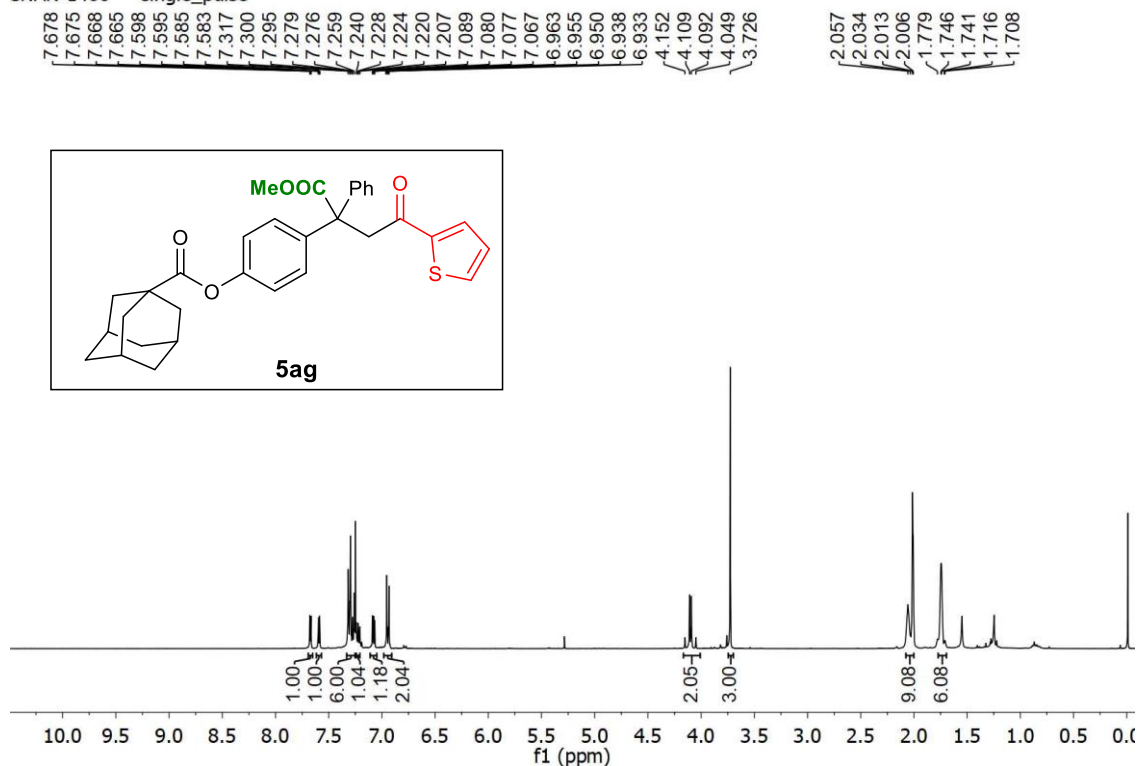
SNAN-1513 — single pulse decoupled gated NOE



^{13}C spectra of **5af**

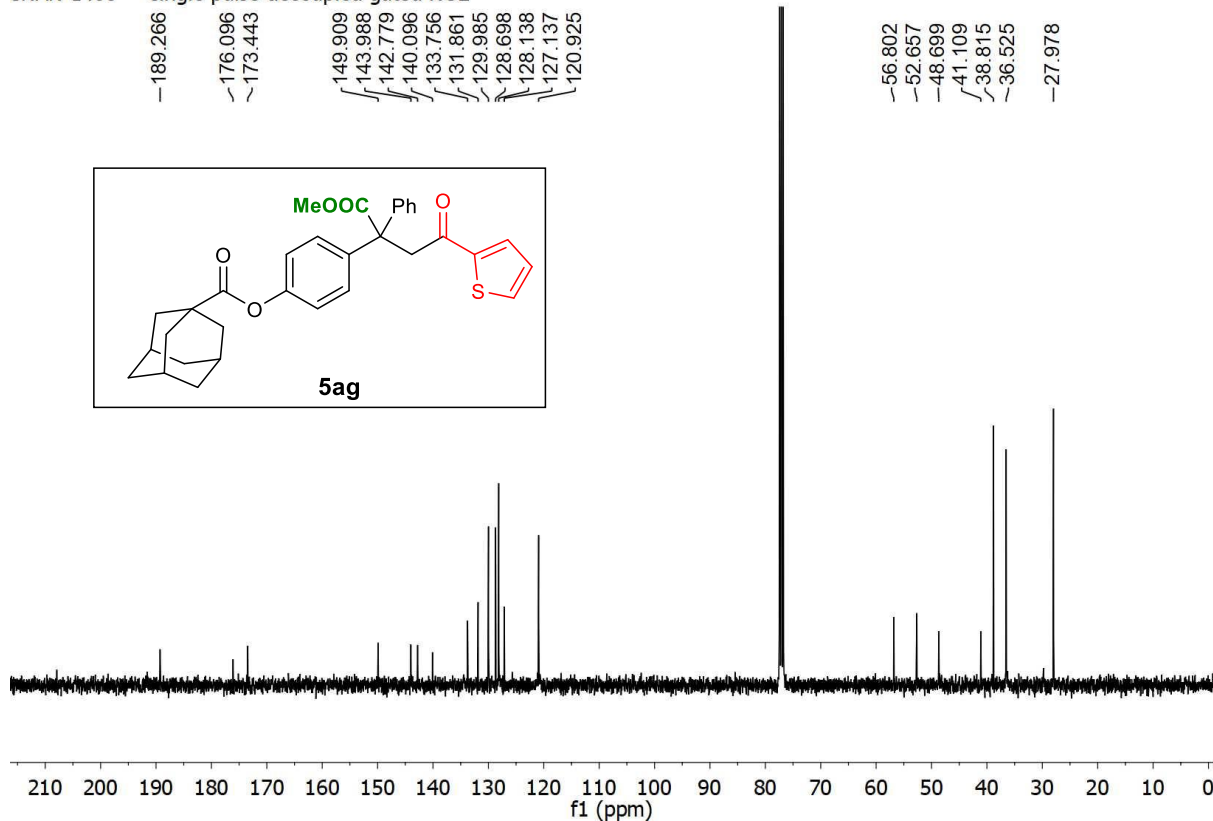
Transition Metal-free, Visible Light Mediated Decarboxylative Acylation and Carboxylation of Alkenes with CO₂

SNAN-1460 — single_pulse



¹H spectra of **5ag**

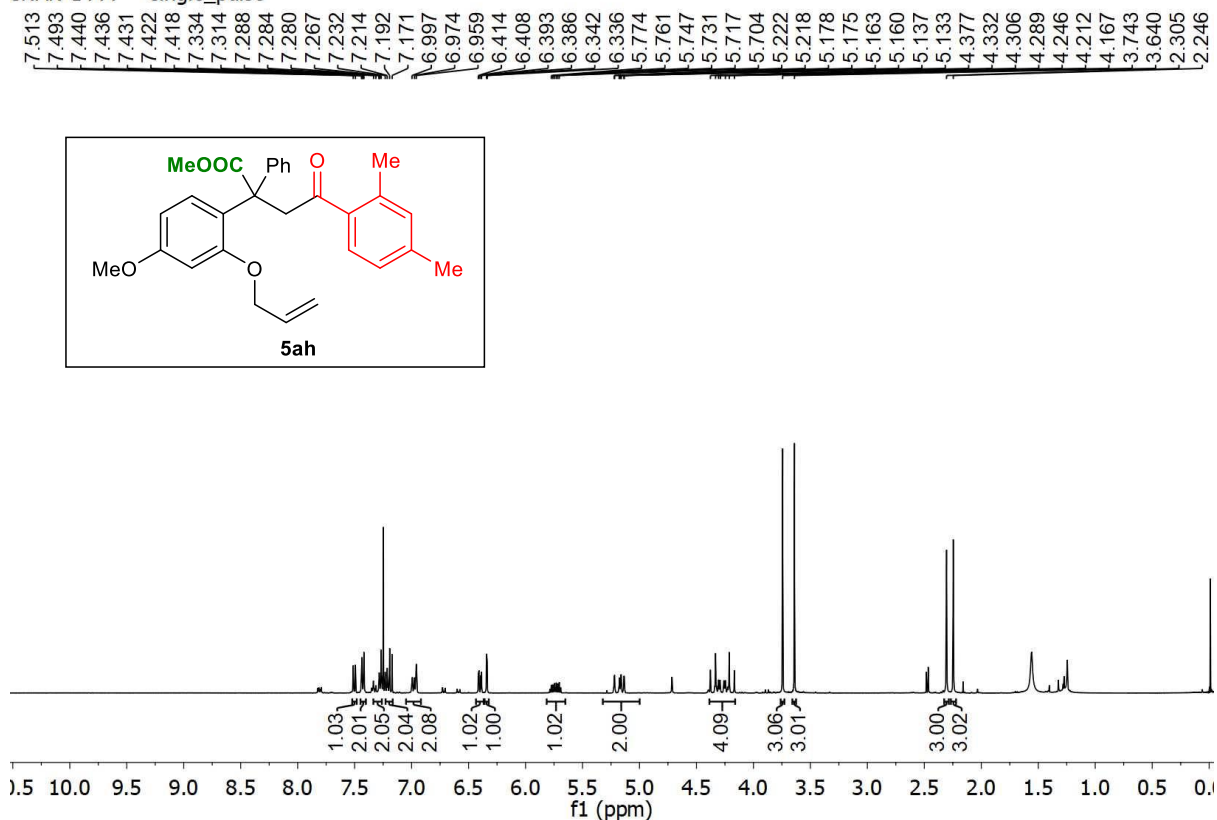
SNAN-1460 — single pulse decoupled gated NOE



¹³C spectra of **5ag**

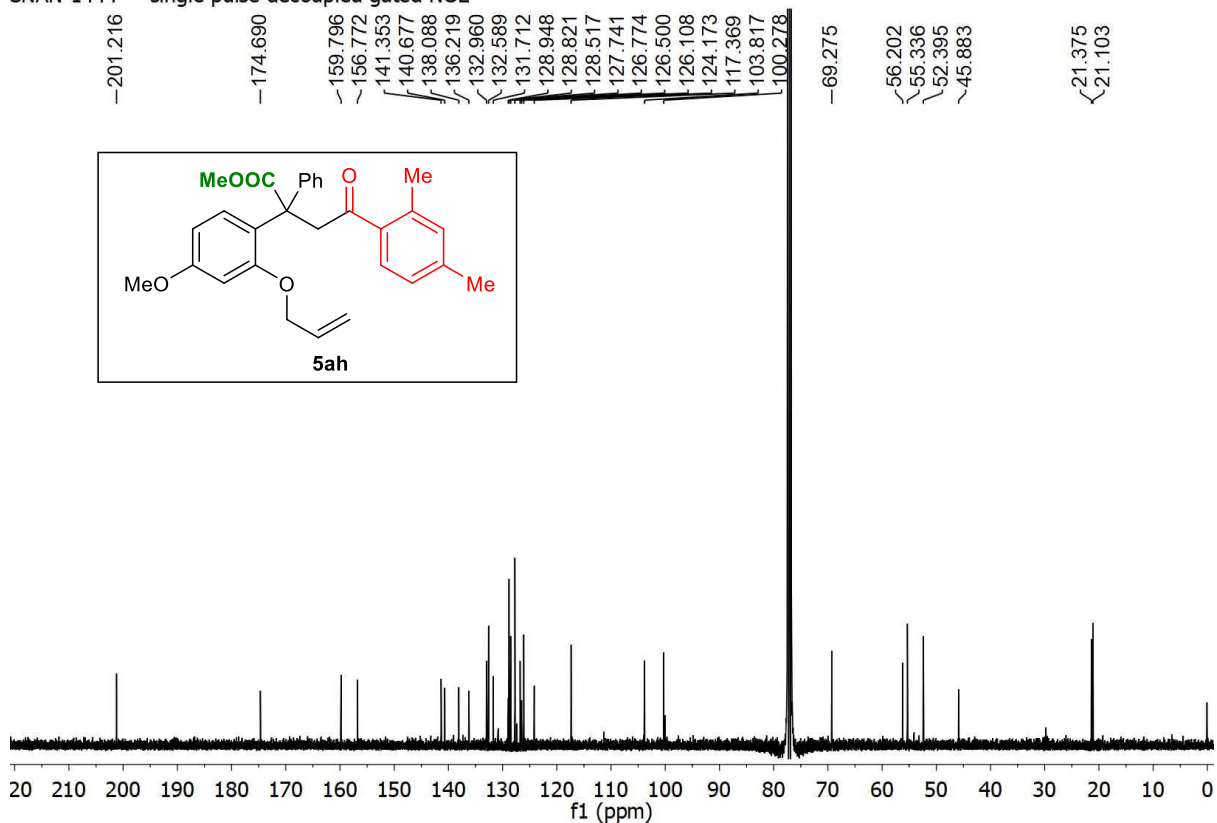
Chapter II

SNAN-1444 — single_pulse



^1H spectra of **5ah**

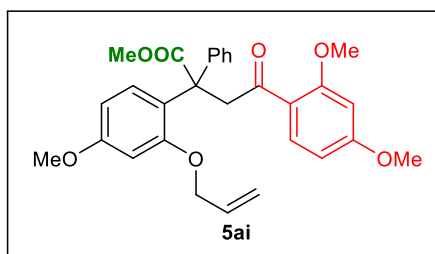
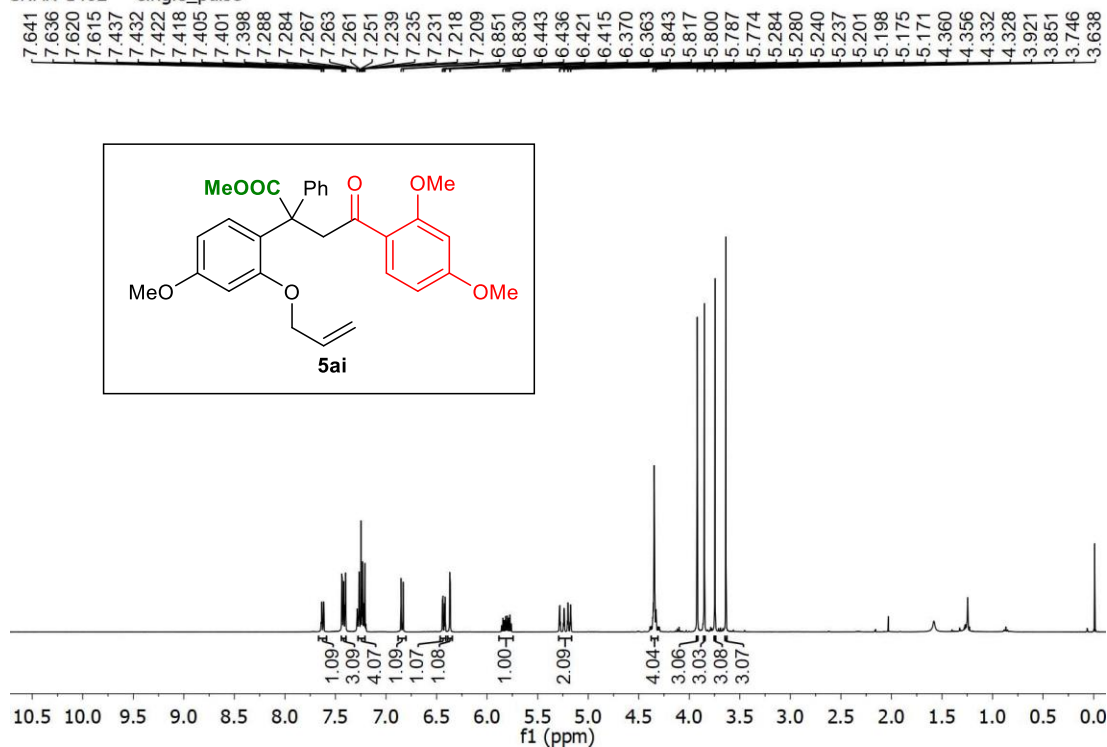
SNAN-1444 — single_pulse decoupled gated NOE



Transition Metal-free, Visible Light Mediated Decarboxylative Acylation and Carboxylation of Alkenes with CO₂

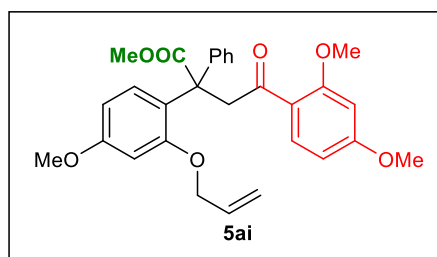
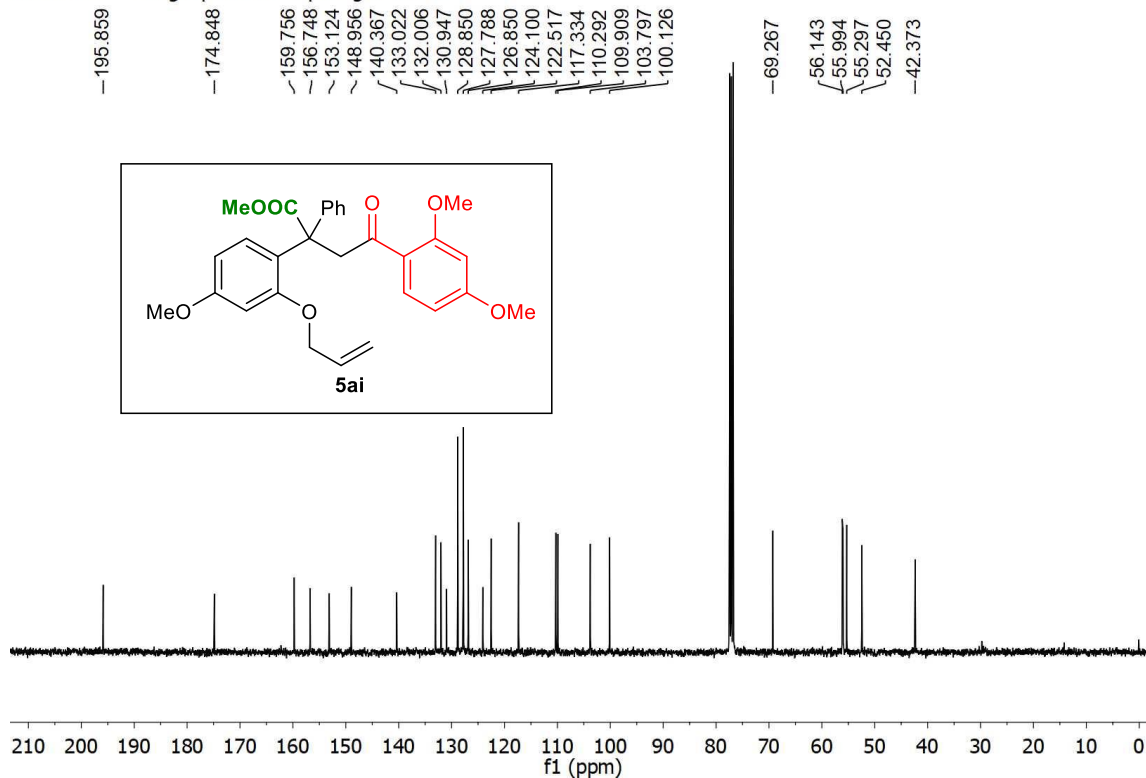
¹³C spectra of **5ah**

SNAN-1462 — single_pulse



¹H spectra of **5ai**

SNAN-1462 — single pulse decoupled gated NOE

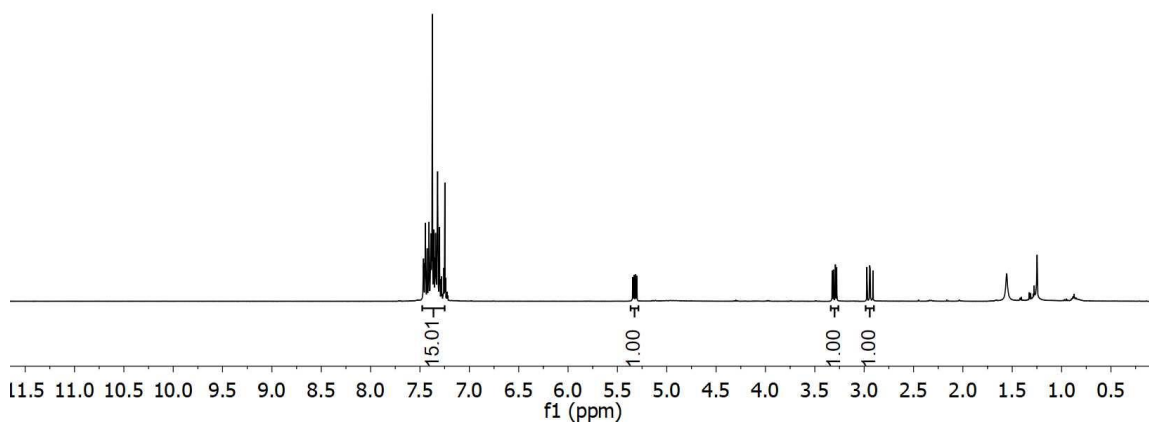
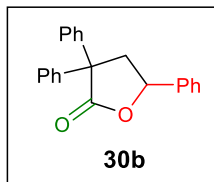


¹³C spectra of **5ai**

Chapter II

SNAN-1521 — single_pulse

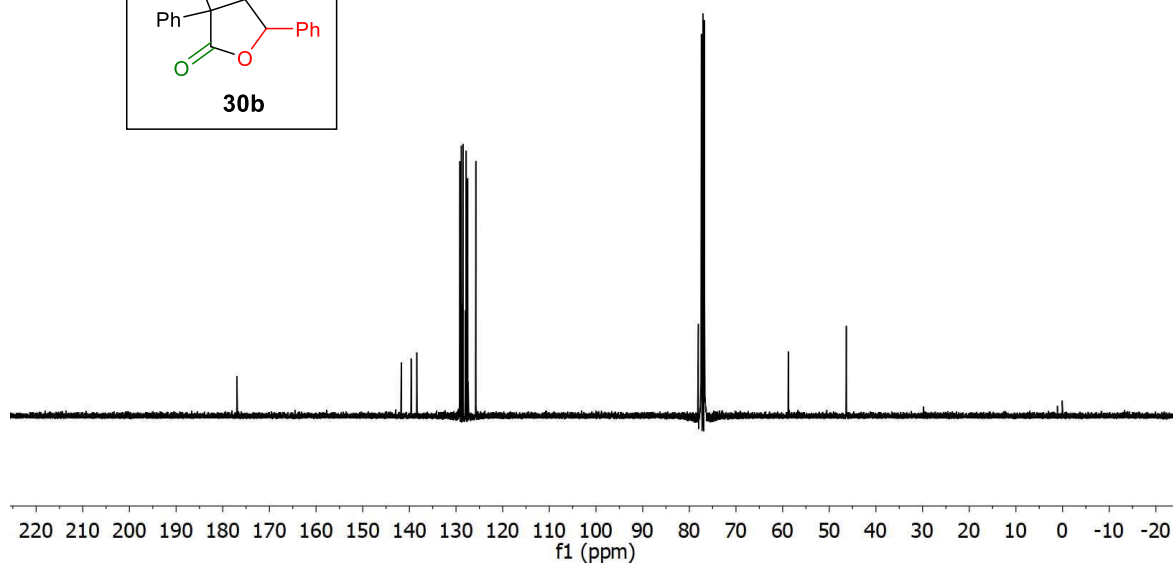
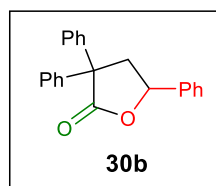
7.468
7.464
7.446
7.443
7.427
7.409
7.389
7.382
7.364
7.361
7.342
7.325
7.321
7.302
7.297
7.282
7.262
7.258
5.344
5.332
5.317
5.304
3.324
3.311
3.291
3.279
2.972
2.944
2.939
2.912



^1H spectra of **30b**

SNAN-1521 — single pulse decoupled gated NOE

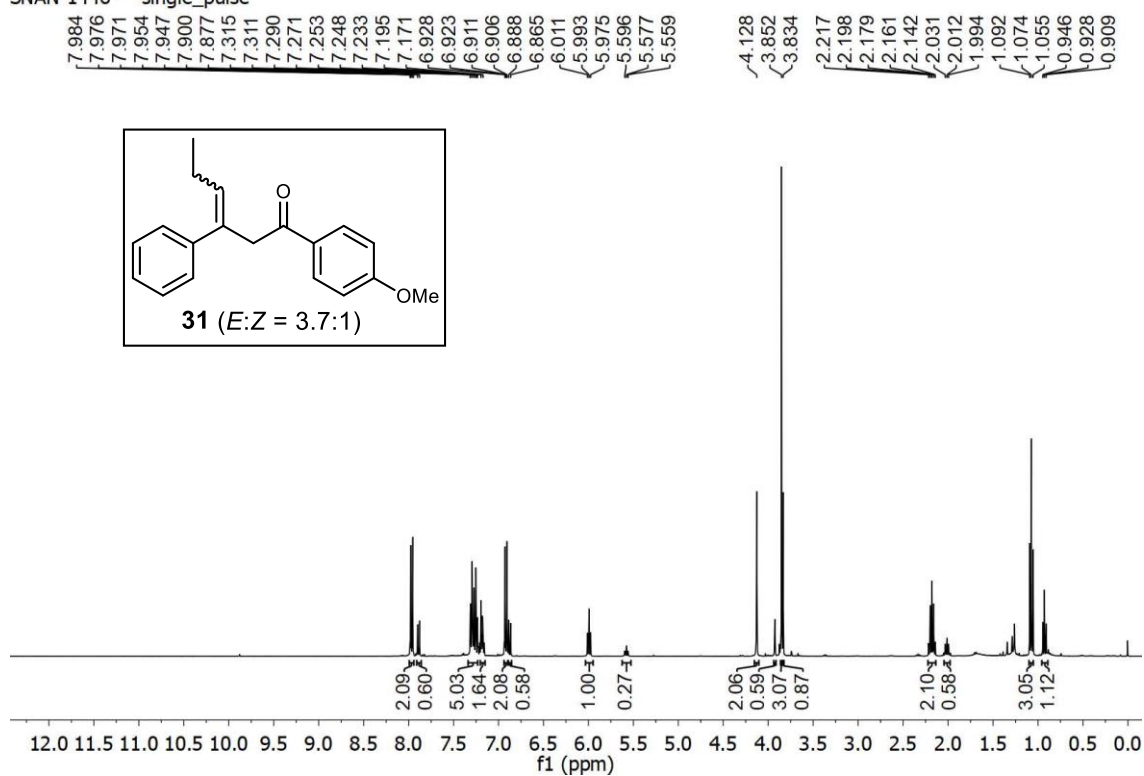
176.960
141.731
139.618
138.408
129.175
128.868
128.767
128.494
127.969
127.813
127.495
127.407
125.760
78.065
58.785
46.352



^{13}C spectra of **30b**

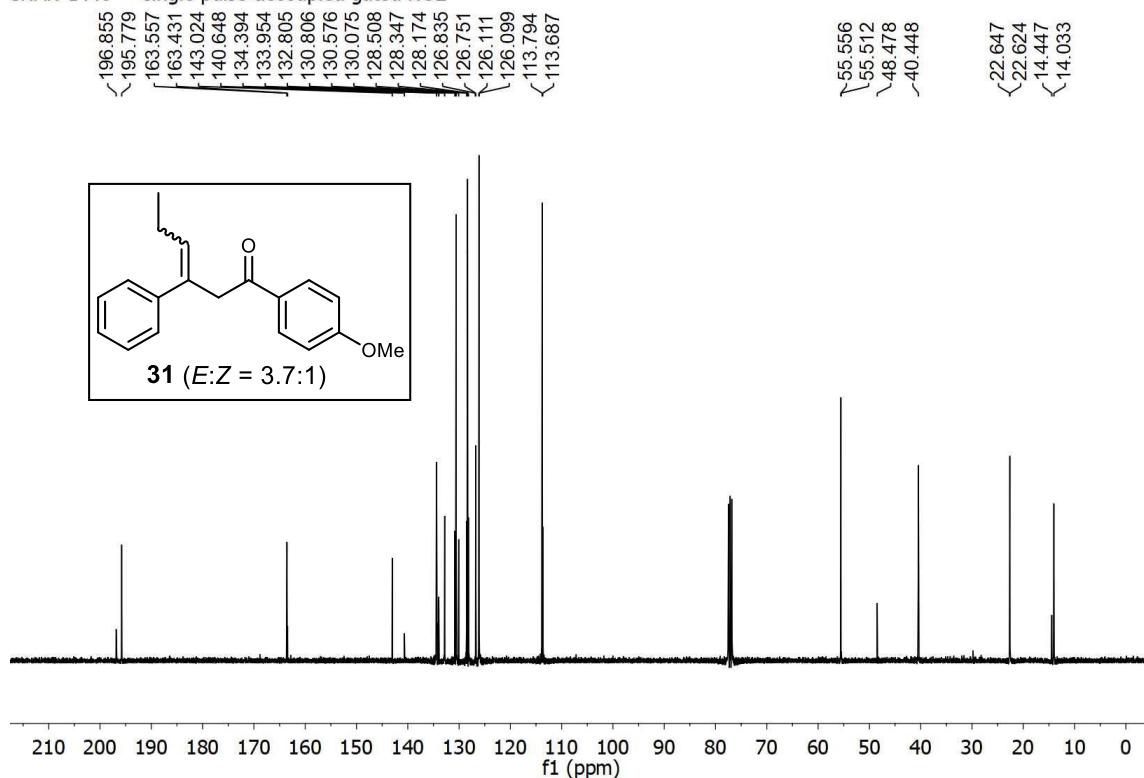
Transition Metal-free, Visible Light Mediated Decarboxylative Acylation and Carboxylation of Alkenes with CO₂

SNAN-1446 — single_pulse



¹H spectra of **31**

SNAN-1446 — single pulse decoupled gated NOE



¹³C spectra of **31**

II.8. References

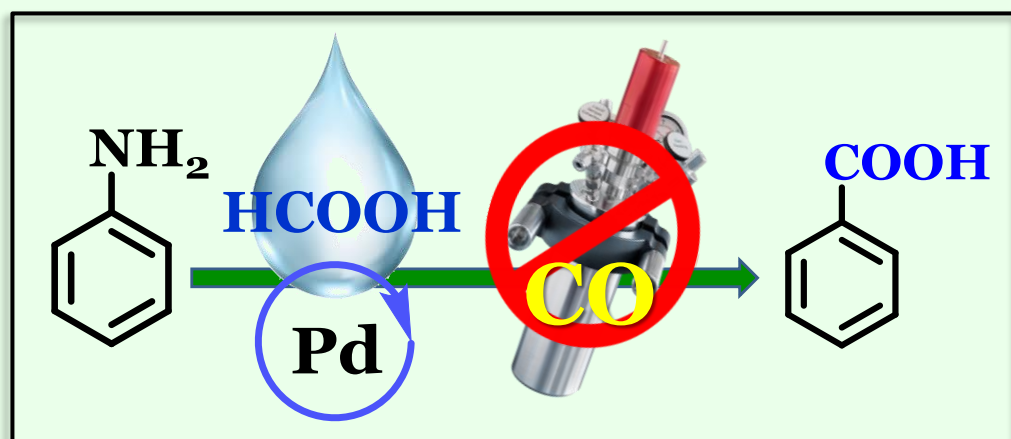
- (1) (a) Koike, T.; Akita, M. *Acc. Chem. Res.* **2016**, *49*, 1937-1945; (b) Dorn, S. K.; Brown, M. K. *ACS Catal.* **2022**, *12*, 2058-2063; (c) Chen, X.; Xiao, F.; He, W.-M. *Org. Chem. Front.* **2021**, *8*, 5206-5228; (d) Wu, Z.; Hu, M.; Li, J.; Wu, W.; Jiang, H. *Org. Biomol. Chem.* **2021**, *19*, 3036-3054; (e) Barve, B. D.; Kuo, Y.-H.; Li, W.-T. *Chem. Commun.* **2021**, *57*, 12045-12057; (f) Li, Y.; Wu, D.; Cheng, H.-G.; Yin, G. *Angew. Chem. Int. Ed.* **2020**, *59*, 7990-8003; (g) White, D. R.; Bornowski, E. C.; Wolfe, J. P. *Isr. J. Chem.* **2020**, *60*, 259-267; (h) Lin, J.; Song, R.-J.; Hu, M.; Li, J.-H. *Chem. Rec.* **2019**, *19*, 440-451.
- (2) (a) Xu, S.; Chen, H.; Zhou, Z.; Kong, W. *Angew. Chem. Int. Ed.* **2021**, *60*, 7405-7411; (b) Courant, T.; Masson, G. *J. Org. Chem.* **2016**, *81*, 6945-6952; (c) Koike, T.; Akita, M. *Chem* **2018**, *4*, 409-437; (d) Pitzer, L.; Schwarz, J. L.; Glorius, F. *Chem. Sci.* **2019**, *10*, 8285-8291; (e) Derosa, J.; Apolinar, O.; Kang, T.; Tran, V. T.; Engle, K. M. *Chem. Sci.* **2020**, *11*, 4287-4296; (f) Qi, X.; Diao, T. *ACS Catal.* **2020**, *10*, 8542-8556; (g) Badir, S. O.; Molander, G. A. *Chem* **2020**, *6*, 1327-1339; (h) Ouyang, X.-H.; Li, Y.; Song, R.-J.; Hu, M.; Luo, S.; Li, J.-H. *Sci. Adv.* *5*, eaav9839; (i) Dhungana, R. K.; Kc, S.; Basnet, P.; Giri, R. *Chem. Rec.* **2018**, *18*, 1314-1340; (j) Shu, W.; García-Domínguez, A.; Quirós, M. T.; Mondal, R.; Cárdenas, D. J.; Nevado, C. *J. Am. Chem. Soc.* **2019**, *141*, 13812-13821; (k) Ouyang, X.-H.; Song, R.-J.; Hu, M.; Yang, Y.; Li, J.-H. *Angew. Chem. Int. Ed.* **2016**, *55*, 3187-3191; (l) Liu, L.; Lee, W.; Youshaw, C. R.; Yuan, M.; Geherty, M. B.; Zavalij, P. Y.; Gutierrez, O. *Chem. Sci.* **2020**, *11*, 8301-8305; (m) Ma, X.; Zhang, G. *ACS Catal.* **2021**, *11*, 5108-5118; (n) Zhong, L.-J.; Xiong, Z.-Q.; Ouyang, X.-H.; Li, Y.; Song, R.-J.; Sun, Q.; Lu, X.; Li, J.-H. *J. Am. Chem. Soc.* **2022**, *144*, 339-348; (o) Sha, W.; Deng, L.; Ni, S.; Mei, H.; Han, J.; Pan, Y. *ACS Catal.* **2018**, *8*, 7489-7494.
- (3) (a) Pan, Q.; Ping, Y.; Wang, Y.; Guo, Y.; Kong, W. *J. Am. Chem. Soc.* **2021**, *143*, 10282-10291; (b) Dhungana, R. K.; Sapkota, R. R.; Wickham, L. M.; Niroula, D.; Giri, R. *J. Am. Chem. Soc.* **2020**, *142*, 20930-20936; (c) Li, Z.-L.; Fang, G.-C.; Gu, Q.-S.; Liu, X.-Y. *Chem. Soc. Rev.* **2020**, *49*, 32-48; (d) Tu, H.-Y.; Zhu, S.; Qing, F.-L.; Chu, L. *Synthesis* **2020**, *52*, 1346-1356; (e) Kc, S.; Dhungana, R. K.; Aryal, V.; Giri, R. *Org. Pro. Res. Dev.* **2019**, *23*, 1686-1694.
- (4) Wang, G.-Z.; Shang, R.; Cheng, W.-M.; Fu, Y. *Org. Lett.* **2015**, *17*, 4830-4833.

- (5) Chen, Z.; Lu, F.; Yuan, F.; Sun, J.; Du, L.; Li, Z.; Gao, M.; Shi, R.; Lei, A. *Sci. China Chem.* **2019**, *62*, 1497-1500.
- (6) (a) Liao, L.-L.; Cao, G.-M.; Jiang, Y.-X.; Jin, X.-H.; Hu, X.-L.; Chruma, J. J.; Sun, G.-Q.; Gui, Y.-Y.; Yu, D.-G. *J. Am. Chem. Soc.* **2021**, *143*, 2812-2821; (b) Wang, H.; Gao, Y.; Zhou, C.; Li, G. *J. Am. Chem. Soc.* **2020**, *142*, 8122-8129; (c) Zhang, B.; Yi, Y.; Wu, Z.-Q.; Chen, C.; Xi, C. *Green Chem.* **2020**, *22*, 5961-5965; (d) Yatham, V. R.; Shen, Y.; Martin, R. *Angew. Chem. Int. Ed.* **2017**, *56*, 10915-10919; (e) Hou, J.; Ee, A.; Cao, H.; Ong, H.-W.; Xu, J.-H.; Wu, J. *Angew. Chem. Int. Ed.* **2018**, *57*, 17220-17224; (f) Fu, Q.; Bo, Z.-Y.; Ye, J.-H.; Ju, T.; Huang, H.; Liao, L.-L.; Yu, D.-G. *Nat. Commun.* **2019**, *10*, 3592.
- (7) (a) Campbell, M. W.; Yuan, M.; Polites, V. C.; Gutierrez, O.; Molander, G. A. *J. Am. Chem. Soc.* **2021**, *143*, 3901-3910; (b) Zhu, C.; Yue, H.; Chu, L.; Rueping, M. *Chem. Sci.* **2020**, *11*, 4051-4064; (c) Mega, R. S.; Duong, V. K.; Noble, A.; Aggarwal, V. K. *Angew. Chem. Int. Ed.* **2020**, *59*, 4375-4379; (d) Campbell, M. W.; Compton, J. S.; Kelly, C. B.; Molander, G. A. *J. Am. Chem. Soc.* **2019**, *141*, 20069-20078; (e) García-Domínguez, A.; Mondal, R.; Nevado, C. *Angew. Chem. Int. Ed.* **2019**, *58*, 12286-12290; (f) Zheng, S.; Gutiérrez-Bonet, Á.; Molander, G. A. *Chem* **2019**, *5*, 339-352.
- (8) (a) Cabrera-Afonso, M. J.; Sookezian, A.; Badir, S. O.; El Khatib, M.; Molander, G. A. *Chem. Sci.* **2021**, *12*, 9189-9195; (b) Zhang, X.-G.; Li, X.; Zhang, C.; Feng, C. *Org. Lett.* **2021**, *23*, 9611-9615; (c) Shi, J.; Guo, L.-Y.; Hu, Q.-P.; Liu, Y.-T.; Li, Q.; Pan, F. *Org. Lett.* **2021**, *23*, 8822-8827; (d) Kosobokov, M. D.; Zubkov, M. O.; Levin, V. V.; Kokorekin, V. A.; Dilman, A. D. *Chem. Commun.* **2020**, *56*, 9453-9456; (e) Wang, S.; Cheng, B.-Y.; Sršen, M.; König, B. *J. Am. Chem. Soc.* **2020**, *142*, 7524-7531; (f) Alam, T.; Rakshit, A.; Begum, P.; Dahiya, A.; Patel, B. K. *Org. Lett.* **2020**, *22*, 3728-3733; (g) Hoque, I. U.; Chowdhury, S. R.; Maity, S. *J. Org. Chem.* **2019**, *84*, 3025-3035; (h) Oh, S. H.; Malpani, Y. R.; Ha, N.; Jung, Y.-S.; Han, S. B. *Org. Lett.* **2014**, *16*, 1310-1313; (i) Koike, T.; Akita, M. *Org. Chem. Front.* **2016**, *3*, 1345-1349.
- (9) Klauck, F. J. R.; Yoon, H.; James, M. J.; Lautens, M.; Glorius, F. *ACS Catal.* **2019**, *9*, 236-241.
- (10) (a) Cai, B.; Cheo, H. W.; Liu, T.; Wu, J. *Angew. Chem. Int. Ed.* **2021**, *60*, 18950-18980; (b) Fan, Z.; Zhang, Z.; Xi, C. *ChemSusChem* **2020**, *13*, 6201-6218; (c) Zhang, Z.; Ye, J.-H.; Ju, T.; Liao, L.-L.; Huang, H.; Gui, Y.-Y.; Zhou, W.-J.; Yu, D.-G. *ACS Catal.* **2020**, *10*, 10871-10885; (d) Zhang, G.; Cheng, Y.; Beller, M.; Chen, F. *Adv. Synth.*

- Catal.* **2021**, *363*, 1583-1596; (e) Nandi, S.; Jana, R. *Asian J. Org. Chem.* **2022**, *2022*, e202200356; (f) He, X.; Qiu, L.-Q.; Wang, W.-J.; Chen, K.-H.; He, L.-N. *Green Chem.* **2020**, *22*, 7301-7320; (g) Ran, C.-K.; Chen, X.-W.; Gui, Y.-Y.; Liu, J.; Song, L.; Ren, K.; Yu, D.-G. *Sci. China Chem.* **2020**, *63*, 1336-1351.
- (11) Zhang, M.; Yang, L.; Zhou, C.; Fu, L.; Li, G. *Asian J. Org. Chem.* **2022**, *n/a*, e202200087.
- (12) Zhou, C.; Li, M.; Sun, J.; Cheng, J.; Sun, S. *Org. Lett.* **2021**, *23*, 2895-2899.
- (13) (a) Bhunia, S. K.; Das, P.; Nandi, S.; Jana, R. *Org. Lett.* **2019**, *21*, 4632-4637; (b) Begam, H. M.; Nandi, S.; Jana, R. *Chem. Sci.* **2022**, *13*, 5726-5733; (c) Nandi, S.; Mondal, S.; Jana, R. *iScience* **2022**, *25*, 104341; (d) Manna, K.; Begam, H. M.; Samanta, K.; Jana, R. *Org. Lett.* **2020**, *22*, 7443-7449.
- (14) (a) Banerjee, A.; Lei, Z.; Ngai, M.-Y. *Synthesis* **2019**, *51*, 303-333; (b) Raviola, C.; Protti, S.; Ravelli, D.; Fagnoni, M. *Green Chem.* **2019**, *21*, 748-764; (c) Zhang, M.; Xi, J.; Ruzi, R.; Li, N.; Wu, Z.; Li, W.; Zhu, C. *J. Org. Chem.* **2017**, *82*, 9305-9311.
- (15) Miller, F. P.; Vandome, A. F.; McBrewster, J., *Le Chatelier's Principle: Chemistry, Chemical Equilibrium, Henry Louis Le Chatelier, Karl Ferdinand Braun, Concentration, Temperature, Volume, Pressure, Lenz's Law, Homeostasis, Status Quo*. Alphascript Publishing: 2009.
- (16) Holmberg-Douglas, N.; Nicewicz, D. A. *Chem. Rev.* **2022**, *122*, 1925-2016.
- (17) (a) Prier, C. K.; Rankic, D. A.; MacMillan, D. W. C. *Chem. Rev.* **2013**, *113*, 5322-5363; (b) Kalyanasundaram, K. *Coord. Chem. Rev.* **1982**, *46*, 159-244.
- (18) Romero, N. A.; Nicewicz, D. A. *Chem. Rev.* **2016**, *116*, 10075-10166.
- (19) Wan, C.; Song, R.-J.; Li, J.-H. *Org. Lett.* **2019**, *21*, 2800-2803.
- (20) Hossian, A.; Manna, K.; Das, P.; Jana, R. *ChemistrySelect* **2018**, *3*, 4315-4318.

Chapter III

One-pot
Hydroxycarbonylation of
Anilines *via* Diazonium Salt
en route to Benzoic acids:
Formic Acid as C-1 Source



III.1. Introduction

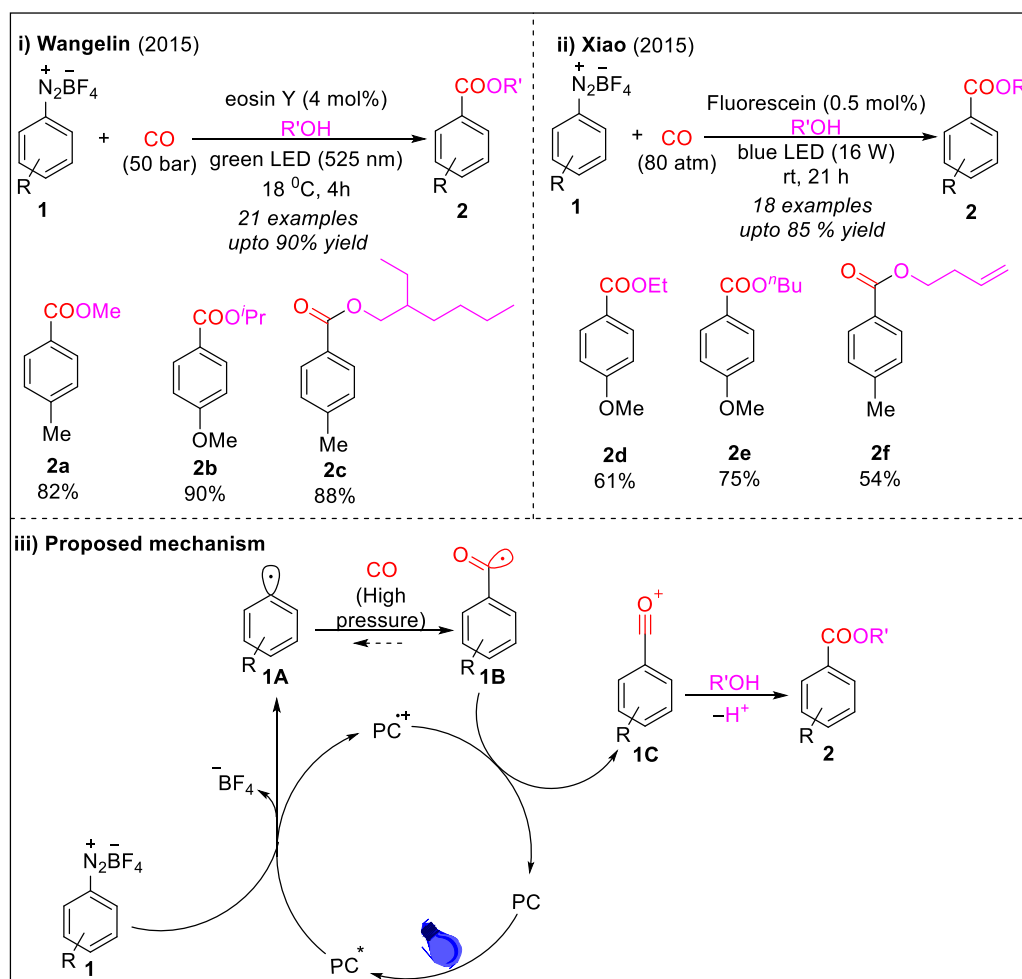
Aryl carboxylic acids or its derivatives are ubiquitous structural motifs in a plenty number of pharmaceuticals, natural products, dyes, polymers.¹ Apart from that, carboxylic acids are very important synthons for accomplishing various otherwise tough transformations.² A handful amounts of methods have already been developed for synthesizing aryl carboxylic acids since ages e.g., direct oxidation of aromatic alcohols, aldehydes or alkyl arenes.³ Carbon-monoxide has been extensively used too for the same though CO is extremely toxic and not recommended environmentally.⁴ Alternatively, CO₂ has been also used lately for direct carboxylation of organic (pseudo)halides to produce aryl carboxylic acids, though not yet extensively being used in industry.⁵ However, the essential requirement of harsh reaction condition makes these methods limited to few functional groups and sensitive to many substrates. On the other hand, anilines are widely available, low-cost organic compounds. Additionally, anilines or substituted anilines represent a large family of important structure units that exist specially in agrochemicals as well as bioactive compounds, pigments, optoelectrical materials.⁶ So, directly accessing aryl carboxylic acids from anilines i.e., to form C–C bond cleaving C–N bond, will lead to the formation of various pharmacophore or related moieties directly from agrochemicals or any other readily available sources. As the previously developed strategies have hardly been successful here, it continues to be a challenge to the chemists. In line with our constant efforts for development of mild carboxylation techniques, we wished to accomplish the same.

III.2. Reviewing the previous developments

III.2.1. Carbonylation of C-N bonds with carbon monoxide (CO)

Though the transformation of anilines to produce aryl carboxylic acids had been a long-lasting problem, in 2015, Wangelin⁷ and Xiao⁸ independently at the same time, reported two similar strategies for metal-free and photocatalytic alkoxycarbonylation of aryl diazonium salts with very high pressure of carbon monoxide (CO) (**Scheme 1, i, ii**). Wangelin⁷ used Eosin Y as the photocatalyst and under 50 bar of CO, diazonium salts underwent alkoxycarbonylation at room temperature and green LED irradiation. Xiao⁸ executed the similar reaction under blue LED irradiation and 80atm of CO with using fluorescein as organic photocatalyst. They both directly afforded range of aryl esters by performing the reaction in alcohol (MeOH, ⁱPrOH, ^tBuOH etc.) solvent. After detailed mechanistic studies, they proposed the mechanism (**Scheme**

1, iii). First, aryl diazonium salt **1** undergoes SET reduction by photoexcited photocatalyst (PC) to produce aryl radical **1A** and PC^{*+} .



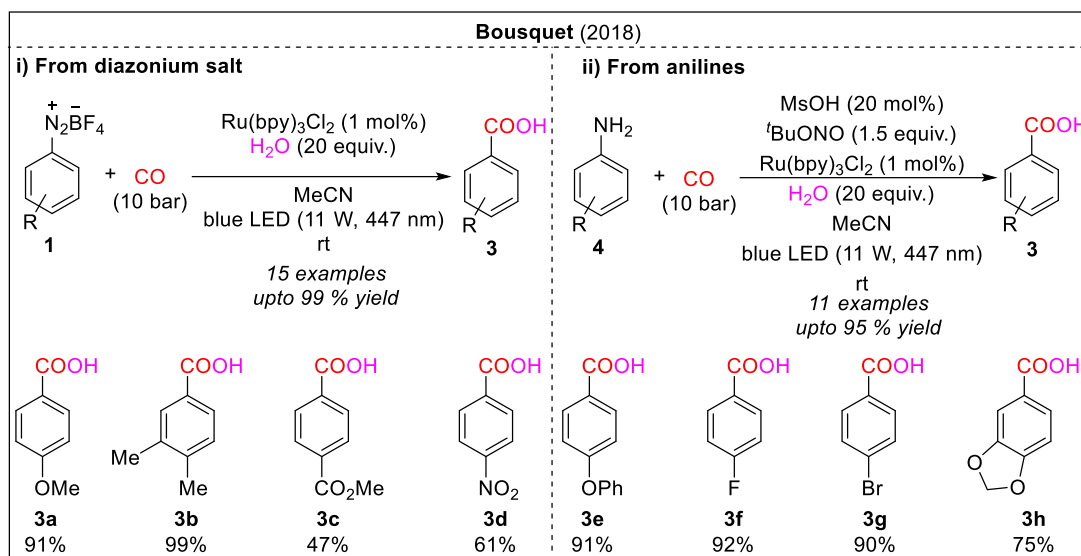
Scheme 1. Photocatalyzed alkoxy carbonylation of aryl diazonium salts.

Under high pressure of CO, **1A** captures CO and forms acyl radical adduct **1B**. Then **1B** reduces PC^{*+} to give acyl cation **1C** and regenerates PC. The alcohol which has been taken as solvent then attacks **1C** nucleophilically to furnish the aryl ester product **2**.

Subsequently, Bousquet reported another photoredox catalyzed hydroxycarbonylation method for benzoic acid synthesis from anilines via pre-isolated or in-situ generated diazonium salts (**Scheme 2**).⁹ Here, using $Ru(bpy)_3Cl_2$ as the photocatalyst and under 10 bar of CO, they had taken 20 equiv. of water which led to hydroxycarbonylation under photocatalysis following a similar mechanism. The method was satisfactorily compatible for in-situ generated diazonium salts too which provided the direct access to benzoic acids from anilines. Notably,

One-pot Hydroxycarbonylation of Anilines *via* Diazonium Salt *en route* to Benzoic Acids: Formic Acid as C-1 Source

this method requires lesser elevated pressure of CO compared to the previous alkoxycarbonylation reactions.



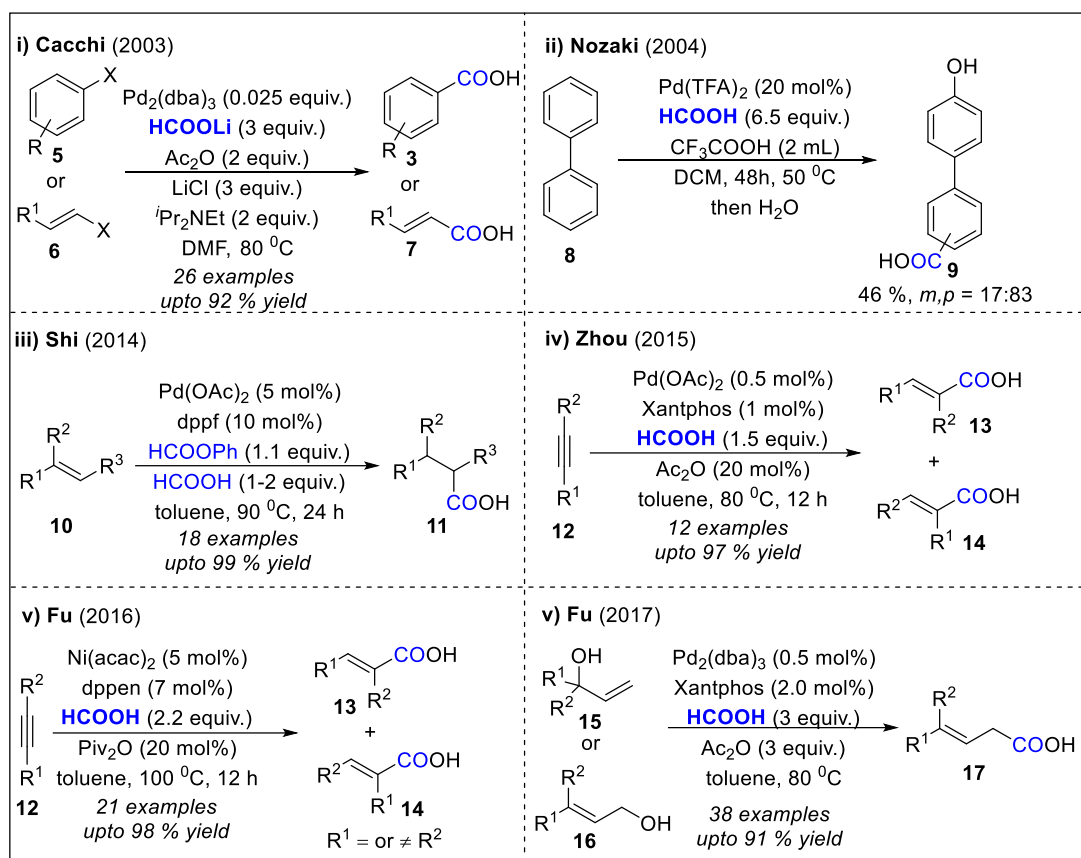
Scheme 2. Photocatalyzed hydroxycarbonylation of diazonium salts and anilines.

Despite being photocatalytic at ambient temperatures, requirement of elevated pressure (10-80 bar) of highly poisonous carbon monoxide makes these methods potentially dangerous and thus strive for further improvement. Additionally, these methods had shown limited examples to synthesize iodo/bromo group bearing benzoic acids.

III.2.2. Carbonylation using formic acid as CO surrogate

Though carbonylation reaction with carbon monoxide is a well-accepted industrial approach since the last century, lately, the chemists around the globe have been engaging themselves to investigate for more sustainable and greener C-1 source instead of CO for its high toxicity, flammability and need of specialized equipment for handling. Out of various other potential carboxylating/carbonylating sources (e.g., HCOOH, CO₂, oxalyl chloride etc.), formic acid stands out to be one of the most useful sources for its high solubility, low cost and high abundance. The first example of this kind was presented by Cacchi's group in 2003, where they used lithium formate to synthesize variety of aryl or vinyl carboxylic acids from corresponding halides or triflates via palladium-catalyzed carbonylation (**Scheme 3, i**).¹⁰ Here, they had taken acetic anhydride as activator which releases CO in situ from formate salt. Following this fashion, encouraged by the contemporary evolvement of the C-H functionalization, in 2004, Nozaki realized hydroxy-carboxylation of aromatic compounds

(Scheme 3, ii).¹¹ Here for the first time, they had been able to execute carboxylation and hydroxylation in a single reaction. Later in 2014, the Shi group reported a palladium-catalyzed

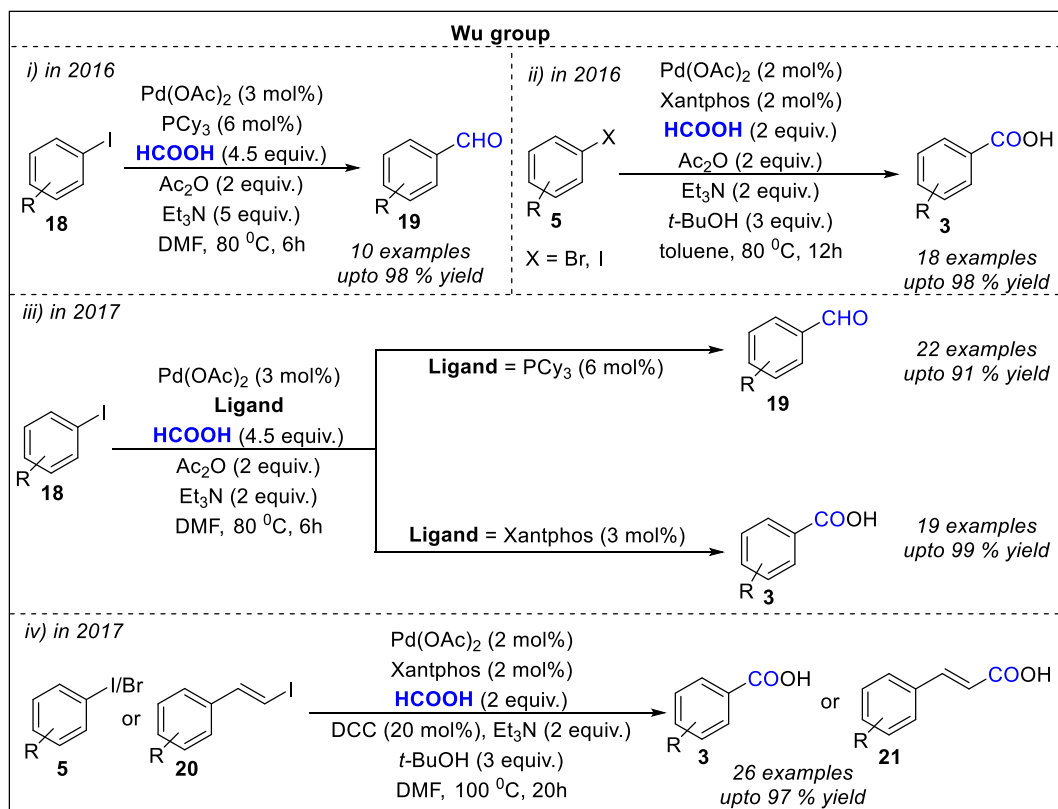


Scheme 3. Various carbonylation reactions with *in situ* generated CO from formic acids/formats.

methodology for hydroxycarbonylation of olefins using HCOOH as CO surrogate (Scheme 3, iii).¹² Subsequently in 2015, Zhou reported Pd-catalyzed hydroxycarbonylation of alkynes to synthesize various acrylic acids (Scheme 3, iv).¹³ In 2016, Fu reported the similar transformation of alkynes with Ni-catalysis (Scheme 3, v).¹⁴ In 2017, the same group realized Pd-catalyzed carbonylation of allylic alcohols to synthesize β,γ -unsaturated carboxylic acid (Scheme 3, vi).¹⁵ In 2016, the Wu group synthesized benzaldehydes from aryl iodides using HCOOH as both CO and hydride source (Scheme 4, i).¹⁶ Here also, they took help of Pd-catalysis and used Ac₂O as the activator to liberate CO from HCOOH. At the same year, they reported another work to afford Pd-catalyzed hydroxycarbonylation of aryl halides to synthesize aryl carboxylic acids (Scheme 4, ii).¹⁷ Extending these two works, the same group realized a ligand-controlled Pd-catalyzed protocol to synthesize aromatic aldehydes and carboxylic acids using HCOOH as CO precursor (Scheme 4, iii).¹⁸ They discovered that

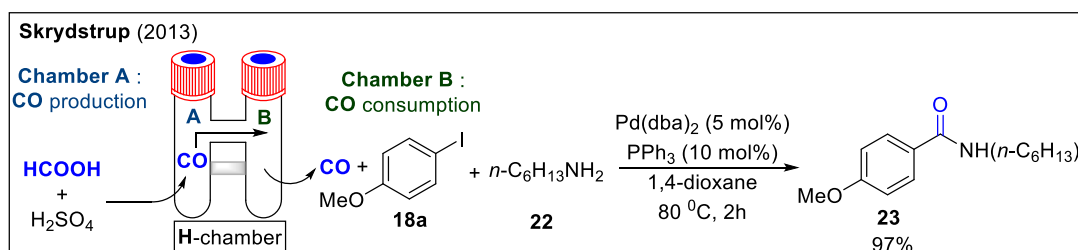
One-pot Hydroxycarbonylation of Anilines *via* Diazonium Salt *en route* to Benzoic Acids: Formic Acid as C-1 Source

monodentate ligands such as PPh₃ or PCy₃ led to aromatic aldehydes whereas bidentate ligand such as xantphos led to aromatic carboxylic acid. Here, they used DCC as the activator or dehydrating agent. Up to this, the all methods required (super)stoichiometric amount of dehydrating agent (Ac₂O, Piv₂O, DCC etc.).



Scheme 4. Carbonylation/hydroxycarbonylation of aryl halides with in situ generated CO.

The Wu group first reported a hydroxycarbonylation of vinyl iodides or aryl iodides/bromides to produce corresponding acrylic or aryl carboxylic acids using catalytic amount of DCC as activator (**Scheme 4, iv**).¹⁹



Scheme 5. Carbonylation with *ex situ* generated CO.

Besides these developments, Skrydstруп's group utilized HCOOH as *ex-situ* CO precursor for carbonylation reaction (**Scheme 5**).²⁰ Here, taking a H-shaped vessel, they

produced CO in one chamber which bypassed to another chamber via joint where the carbonylation reaction took place.

III.3. Present work

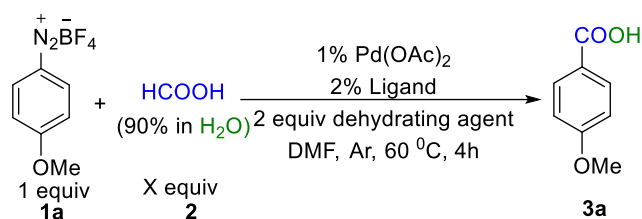
As we reviewed here, in all these strategies, a dehydrant activates the HCOOH by liberating CO *in-situ* or *ex-situ* which inserts in transition-metal catalytic cycle. Almost all the methods are requisite of very high temperature and tertiary amines where the halides are the main groups to react. However, a general method for carbonylation of aryl diazonium compounds keeping the halide groups unreacted using HCOOH as C-1 source has not been developed till date. If the hypothesis is realized, we would be able to synthesize iodo/bromo benzoic acids directly from corresponding diazonium salt in CO-free method which has not been reported earlier. Thus, continued with our effort on developing mild carboxylation techniques, we report here, a novel hydroxycarbonylation of aryl diazonium tetrafluoroborate with formic acid at palladium catalyzed method excluding tertiary amine at moderate temperature keeping halide group intact. Contrary to the related term “carboxylation” where carboxy group is installed directly, here the used term is “hydroxycarbonylation” to clearly convey that the primary transformation is carbonylation followed by hydroxylation; though both lead towards carboxylic acids.

III.4. Results and discussion

To start the investigation, 4-methoxy phenyl diazonium tetrafluoroborate **1a** was chosen as model substrate. Firstly, xantphos was used as ligand for its large bite angle giving rise to better possibility of anhydride formation and subsequent acid product. To our delight, the targeted 4-methoxybenzoic acid **3a** was yielded at 18% when mixture of **1a** and 2.0 equiv of HCOOH (90% solution in water) **2** in toluene solvent was heated with 2.0 equiv of Ac₂O as dehydrating agent, 1% of Pd(OAc)₂ as catalyst with 2% xantphos at 60 °C for 4 hours (Entry 1, **Table 1**). Encouraged by the initial result, we went on varying the dehydrating agents like DCC, Piv₂O among which DCC provided better result with 30% of **3a** (Entry 3, **Table 1**). Next, when DMF was taken as solvent, the yield of **3a** was increased to 43% (Entry 6, **Table 1**).

Table 1. Optimization of hydroxycarbonylation of diazonium salt^a

**One-pot Hydroxycarbonylation of Anilines via Diazonium Salt *en route* to Benzoic Acids:
Formic Acid as C-1 Source**



Entry	X	Ligand	Dehydrating Agent	solvent	yield (%) ^b
1	2	Xantphos	Ac ₂ O	toluene	18
2	2	Xantphos	Piv ₂ O	Toluene	15
3	2	Xantphos	DCC	Toluene	30
4	2	Xantphos	DCC	DCE	28
5	2	Xantphos	DCC	DMSO	25
6	2	Xantphos	DCC	DMF	43
7	6	Xantphos	DCC	DMF	85
8 ^c	6	Xantphos	DCC	DMF	12
9	6	X-phos	DCC	DMF	25
10	6	PCy ₃	DCC	DMF	46
11	6	Brettphos	DCC	DMF	21
12	6	dppf	DCC	DMF	27
13	7	Xantphos	DCC	DMF	82
14 ^d	6	Xantphos	DCC	DMF	73
15 ^e	6	Xantphos	DCC	DMF	68
16 ^f	6	Xantphos	DCC	DMF	83

^aReactions were performed in 0.2 mmol scale and overall isolated yields have been reported.

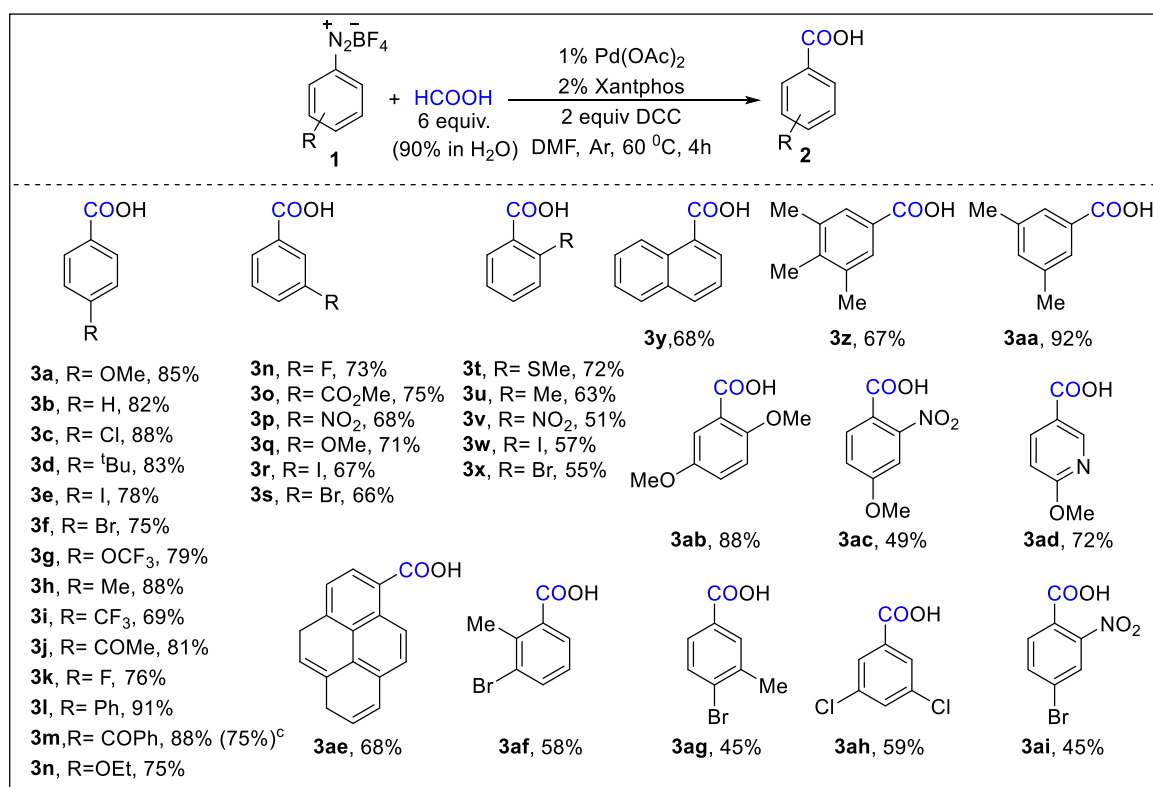
^cadditional addition of 2 equiv Et₃N. ^dat 70 °C. ^eat 80 °C. ^freaction was run for 5h.

Since, carbonylation reaction on diazonium salts require elevated pressure of CO, we thought of increasing the amount of HCOOH and DCC as well to produce CO in more efficient way and greater amount. Satisfactorily, 6 equiv. of **2** with 2 equiv of DCC furnished 85 % yield (Entry 7). Additional amount of Et₃N reduced the yield massively to 12% unlike the previous methods of hydroxycarbonylation of haloarenes (Entry 8). Further variation of other ligands exacerbated the outcome. Altering the temperature or highering the reaction time diminished

the yield of **3a** (Entry 14-16). So, the condition from entry 7 (**Table 1**) was chosen as optimized one.

With the standardized reaction condition in hand, we proceeded to evaluate the generality of the substrates. Plenty of electron donating and electron withdrawing groups survived well at *para* position (**3a-m**, **Table 2**) furnishing high yields irrespective of the electronic nature. Substrates bearing both types of electron-donating and withdrawing groups as substitution at *meta* position also yielded satisfactorily (**3n-s**, **Table 2**). Polycyclic and heterocyclic aryl benzoic acids were also synthesized successfully with this hydroxycarbonylation reaction in moderate yields (**3y**, **3ad**, **3ae**, **Table 2**). Besides, various polysubstituted aryl diazonium salts underwent the reaction providing good to moderate yields (**3z**, **3aa-ac**, **3af-ai**, **Table 2**). Most importantly, the halogens bromo and iodo groups were very

Table 2. Scope of hydroxycarbonylation of diazonium salts^a



^aReactions were performed in 0.2 mmol scale and overall isolated yields have been reported.

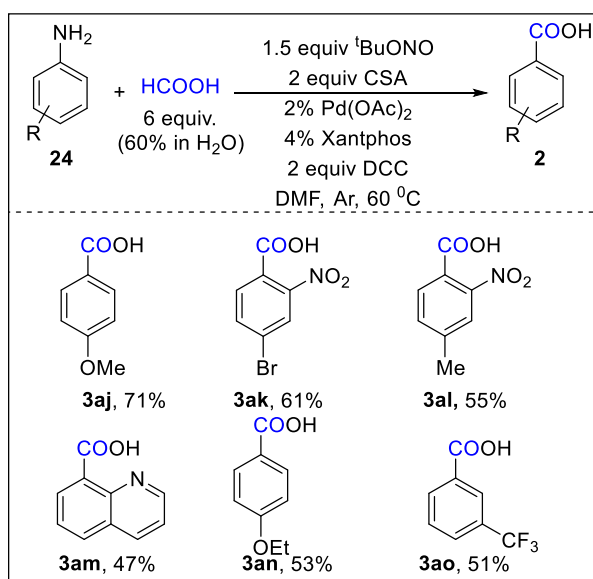
^cReaction in 10 mmol scale.

well tolerated in our reaction condition. On the contrary to previously reported procedures, where the halo groups are itself hydroxycarbonylated via similar reaction conditions, here we are successful to synthesize targeted iodo- or bromo benzoic acids in good yields.

One-pot Hydroxycarbonylation of Anilines *via* Diazonium Salt *en route* to Benzoic Acids: Formic Acid as C-1 Source

Following this substrate scope exploration, we were curious to check whether *in-situ* formed diazonium salt from primary amine would be fruitful in our reaction condition. If successful, we would be able to achieve benzoic acids directly from the aniline moieties which had been otherwise scarcely reported. Intrigued by the previously developed reactions of *in-situ* formed diazonium salts, we started the reaction taking *p*-anisidine. Therefore, taking additional amount of 2 equiv of camphor sulphonic acid (CSA) and 1.5 equiv. of *tert*-butyl nitrite in the standard reaction condition and running the reaction for 16 hours resulted in the formation of expected 4-methoxybenzoic acid **3a** in 71% yield.

Then, generality of the developed one pot hydroxycarbonylation of anilines was explored with different anilines. As shown in **Scheme 6**, the substituted anilines yielded satisfactorily irrespective of the electronic nature. Delightedly, the heterocyclic anilines furnished very good yield in this direct method (**3am**, **3an**, **Scheme 6**) whereas the corresponding diazonium salts were less compatible under the former condition.

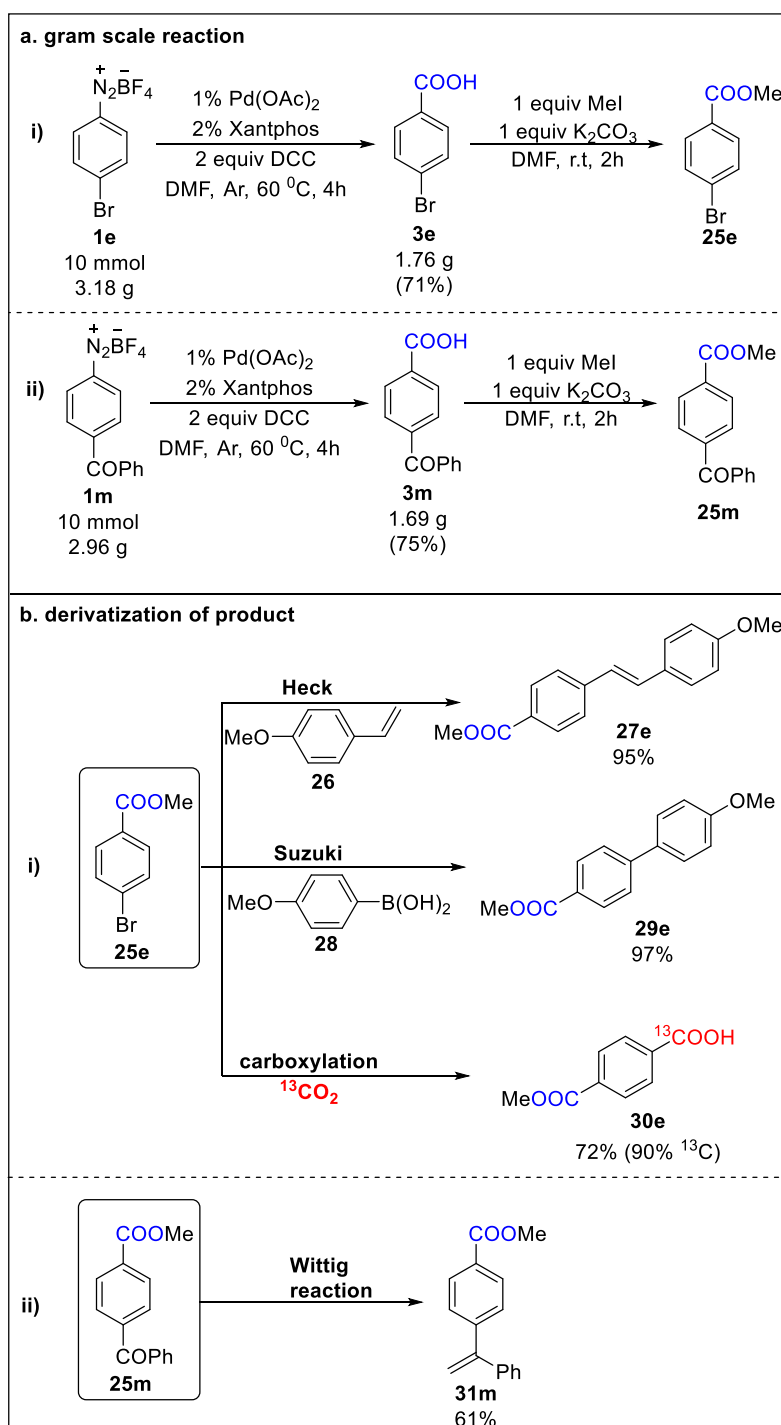


^aReactions were performed in 0.2 mmol scale and overall isolated yields have been reported.

Scheme 6. Scope of the in situ-generated diazonium salts hydroxycarbonylation.^a

To explore the practicality of the developed method, we conducted two gram-scale reactions and facile derivatization of products. First, reaction with **1e** was conducted in 10 mmol scale furnishing 71% **3e** which was subsequently converted to corresponding ester **25e** for further transformations (**Scheme 7a, i**). Heck, Suzuki reaction on **25e** afforded the corresponding products **27e** and **29e** respectively in high yields (**Scheme 7b, i**). When **25e** was subjected to photoredox catalyzed carboxylation reaction with ¹³CO₂, it ended up with

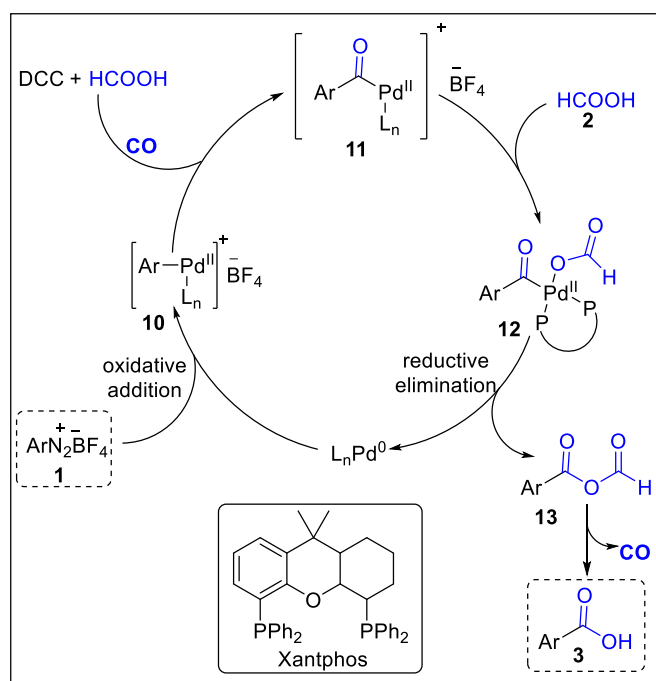
dicarboxylated product **8e** in 72% yield with 90% ^{13}C in new carboxyl group (**Scheme 7b, i**). In this way, we were able to produce dicarboxylated product with different isotopes **30e** starting from bromoaniline in just 4 steps. Next, we performed the standard reaction with **1m** in 10 mmol scale yielding 75% of **3m** (**Scheme 7a, ii**). After methylation, on performing Wittig reaction, styrene **31m** was afforded in fair yield (**Scheme 7b, ii**).



Scheme 7. Gram-scale reaction and product derivatization.

One-pot Hydroxycarbonylation of Anilines *via* Diazonium Salt *en route* to Benzoic Acids: Formic Acid as C-1 Source

From the above results and precedent reports, a plausible mechanism is proposed (**Scheme 8**). Initially, oxidative addition of *in-situ* generated Pd⁰ to C–N bond of the aryldiazonium tetrafluoroborate **1** resulted in formation of aryl palladium cationic complex **10**. Dehydrant DCC gave rise to formation of carbon monoxide (CO) from formic acid **2** and one molecule of CO inserted to aryl palladium complex **10** to deliver acylpalladium complex **11**. Subsequently, ligand exchange of BF₄[−] with another molecule of formic acid afforded complex **12**. Large bite angle of bidentate ligand xantphos forced the incoming HCOOH molecule to bind to Pd with tetrafluoroborate **1** resulted in formation of aryl palladium cationic complex **10**.



Scheme 8. Plausible Mechanism.

Dehydrant DCC gave rise to the formation of carbon monoxide (CO) from formic acid **2** and one molecule of CO inserted to aryl palladium complex **10** to deliver acylpalladium complex **11**. Subsequently, ligand exchange of BF₄[−] with another molecule of formic acid afforded complex **12**. Large bite angle of bidentate ligand xantphos forced the incoming HCOOH molecule to bind to Pd with its one oxygen atom in η¹ mode. On subsequent reductive elimination from complex **12**, benzoic formic anhydride **13** was formed and Pd⁰ is regenerated to continue the cycle. Anhydride **13** decomposed to yield desired benzoic acid **3** upon release of one molecule of CO, which took part in follow up reactions.

III.5. Conclusion

To summarize, we have successfully developed a novel palladium catalyzed strategy for direct benzoic acid synthesis from aryl diazonium salt preformed or synthesized *in situ*. Here, HCOOH acts as CO surrogate on reacting with dehydrant DCC. Interestingly, we have been able to make the halo groups intact unlike the precedent similar methods. This strategy has satisfactorily been utilized to synthesize a variety of benzoic acids directly from aryl diazonium salts or anilines with broad functional group tolerance.

III.6. Experimental section

General information

The uncorrected melting points were measured using open end capillary tubes. On silica gel plates (Merck silica gel 60, f254), TLC was conducted out, and the spots were visualized under UV light (254 and 365 nm) and with DNP stain. X-ray of crystals was recorded in Bruker D8 Venture with a Photon-III detector instrument. ¹H NMR was recorded at 400 MHz (JEOL-JNM-ECZ400S/L1) frequency; ¹³C NMR spectra were recorded at 100 MHz (JEOL-JNM-ECZ400S/L1) frequency in CDCl₃, DMSO-D₆ solvent using TMS as the internal standard. Chemical shifts were evaluated in parts per million (ppm), with tetramethylsilane serving as a reference at 0.0 ppm. The acronyms s=singlet, d=doublet, t=triplet, q=quartet, and m=multiplet are used to describe multiplicities. In Hertz unit, coupling constants, J, were reported (Hz). Utilizing the ESI (Q-TOF, positive ion) technique, HRMS (m/z) were measured. All commercial reagents were used without further purification, unless otherwise noted.

General experimental protocol (Method A) for preparation of arene diazonium salts (1)

The corresponding aniline (**24**) (20 mmol) was taken in a clean and oven-dried 100 mL round-bottom flask. Then it was cooled in an ice bath and to it, tetrafluoroboric acid solution (48 wt % in H₂O, 52 mmol, 6.8 mL) was added at 0 °C. Instantaneously, precipitate forms and minimum amount of deionized water was added to it to dissolve the precipitate. Then, sodium nitrite (NaNO₂) solution in deionized water (1.4 g, 20 mmol NaNO₂ in 4 mL water) was added dropwise with continuous stirring. After addition, it was kept on stirring for additional 30 mins at 0 °C. After that, the formed precipitate was filtered, washed with diethyl ether (Et₂O) (4 ×

40 mL). Then, the residue was dissolved in minimum amount of acetonitrile (MeCN) and was recrystallized with MeCN/Et₂O and subsequently filtered with washing to furnish the pure arene diazonium salt (**1**).

General experimental protocol (Method B) for hydroxycarbonylation of arene diazonium salts (1**) with in situ generated CO**

The aryldiazonium salt (0.2 mmol, 1 equiv.), Pd(OAc)₂ (0.5 mg, 0.002 mmol, 0.01 equiv.), Xantphos (2.3 mg, 0.004 mmol, 0.02 equiv.) and DCC (82.5 mg, 0.4 mmol, 2 equiv.) were weighed and transferred into an oven-dried 15 mL pressure tube with teflon cap. Subsequently 3 mL DMF was added to the reaction tube. Then, 90% formic acid solution in water (61.4 μL, 6 equiv.) was added via microsyringe and the tube is sealed after successfully purging with argon. After that, the mixture was heated at 60 °C with continuous stirring for 4 hours. After completion of the reaction (checked with TLC), the reaction mixture was taken in a separatory funnel and 30 mL of deionized water was added. Then it was extracted with ethyl acetate (3 × 30 mL) and the combined organic layer was washed with brine (30 mL). The combined organic layer was passed through anhydrous Na₂SO₄ for drying and the mixture was concentrated by evaporating the solvent under reduced pressure. By column chromatography (SiO₂, eluting with hexane/ethyl acetate), the crude product was purified to provide the desired benzoic acid product (**3**).

General experimental protocol for one-pot hydroxycarbonylation of anilines (24**) via in situ generation of diazonium salt**

The aniline (0.2 mmol, 1 equiv.), *tert*-butylnitrite (1.5 equiv., 0.3 mmol, 35.7 μL), camphor sulfonic acid (2 equiv., 0.4 mmol, 92.92 mg), Pd(OAc)₂ (0.01 equiv., 0.002 mmol, 0.5 mg), Xantphos (0.02 equiv., 0.004 mmol, 2.3 mg) and DCC (82.5 mg, 0.4 mmol, 2 equiv.) were successively weighed and transferred into a clean and oven-dried 15 mL pressure-tube with teflon cap. Subsequently 3 mL DMF was added to the reaction tube. Then, 90% formic acid solution in water (61.4 μL, 6 equiv.) was added via microsyringe and the tube is purged with argon and sealed. After that, this was heated at 60 °C with continuous stirring for 4 hours. Then, in a separatory funnel, the reaction mixture was extracted with EtOAc (3 × 30 mL), deionized water (2 × 10 mL), followed by washing the resulting organic layer with brine (20 mL), and finally the combined organic layer was passed through anhydrous Na₂SO₄ for drying and the mixture was concentrated by evaporating the solvent under reduced pressure. By

column chromatography (SiO₂, eluting with hexane/ethylacetate), the crude product was purified by to provide the desired product (**3**).

Experimental procedure for gram-scale synthesis of 4-bromobenzoic acid (3f) from 4-bromophenyldiazonium tetrafluoroborate

The 4-bromophenyldiazonium tetrafluoroborate (10 mmol, 1 equiv., 2.69 g), Pd(OAc)₂ (0.01 equiv., 0.1 mmol, 22.4 mg), Xantphos (0.02 equiv, 0.2 mmol, 2.3 mg) and DCC (2 equiv., 20 mmol, 4.12 g) were weighed and transferred into an oven-dried and clean 100 mL pressure-tube with teflon cap. Subsequently 20 mL DMF was added to the reaction tube. Then, 90% formic acid solution in water (3.1 mL, 6 equiv.) was added via syringe and the tube is sealed after successfully purging with argon. After that, the mixture was heated at 60 °C with continuous stirring for 4 hours. Then, the reaction mixture was extracted with EtOAc (3 × 200 mL), washing the resulting organic layer with deionized water (500 mL) and brine (100 mL), and finally the combined organic layer was passed through anhydrous Na₂SO₄ for drying and the mixture was concentrated by evaporating the solvent under reduced pressure. By column chromatography (SiO₂, eluting with hexane/ethylacetate), the crude product was purified by to provide the desired 4-bromobenzoic acid (**3f**) as white solid (1.4 g, 71%).

Experimental procedure for gram-scale synthesis of 4-benzoylbenzoic acid (3m) from 4-benzoylphenyldiazonium tetrafluoroborate

The 4-benzoylphenyldiazonium tetrafluoroborate (10 mmol, 1 equiv., 2.9 g), Pd(OAc)₂ (0.01 equiv., 0.1 mmol, 22.4 mg), Xantphos (0.02 equiv., 0.2 mmol, 2.3 mg) and DCC (2 equiv., 20 mmol, 4.12 g) were weighed and transferred into an oven-dried and clean 100 mL pressure-tube with teflon cap. Subsequently 20 mL DMF was added to the reaction tube. Then, 90% formic acid solution in water (3.1 mL, 6 equiv.) was added via syringe and the tube is sealed after successfully purging with argon. After that, the mixture was heated at 60 °C with continuous stirring for 4 hours. Then, the reaction mixture was extracted with EtOAc (3 × 200 mL), washing the resulting organic layer with deionized water (500 mL) and brine (100 mL), and finally the combined organic layer was passed through anhydrous Na₂SO₄ for drying and the mixture was concentrated by evaporating the solvent under reduced pressure. By column chromatography (SiO₂, eluting with hexane/ethylacetate), the crude product was purified by to provide the desired 4-benzoylbenzoic acid (**3m**) as white solid (1.7 g, 75%).

Product derivatization

Heck reaction between methyl 4-bromobenzoate (25e) and 4-methoxystyrene (26)

Into a 15 mL pressure tube, was added methyl 4-bromobenzoate (**25e**, 0.2 mmol, 1 equiv., 42.6 mg), 4-methoxystyrene (**26**, 1.1 equiv., 0.22 mmol, 29.5 mg), palladium acetate (0.05 equiv., 0.01 mmol, 2.24 mg), triphenylphosphine (0.1 equiv., 0.02 mmol, 5.24 mg), triethylamine (1.5 equiv., 0.3 mmol, 41.8 μ L), potassium carbonate (2 equiv., 0.4 mmol, 55.2 mg). Then, 2 mL dry DMF was added and before sealing the tube, it was flushed with argon. Therefore, the mixture was heated at 120 $^{\circ}$ C with continuous stirring for 12 h. Then, in a separatory funnel, the reaction mixture was extracted with EtOAc (3 \times 30 mL), deionized water (2 \times 10 mL), followed by washing the resulting organic layer with brine (20 mL), and finally the combined organic layer was passed through anhydrous Na₂SO₄ for drying and the mixture was concentrated by evaporating the solvent under reduced pressure. By column chromatography (SiO₂, eluting with hexane/ethylacetate), the crude product was purified by to provide methyl (*E*)-4-(4-methoxystyryl)benzoate (**27e**).

Suzuki reaction between methyl 4-bromobenzoate (25e) and 4-methoxyphenylboronic acid (28)

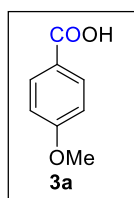
Into a 15 mL pressure tube, was added methyl 4-bromobenzoate (**25e**, 0.2 mmol, 1 equiv., 42.6 mg), 4-methoxyphenylboronic acid (**28**, 1.1 equiv, 0.22 mmol, 33.4 mg), tetrakis(triphenylphosphine)palladium(0) (0.05 equiv, 0.01 mmol, 11.5 mg), potassium carbonate (2 equiv, 0.4 mmol, 55.2 mg). Then, 2 mL dry DMF was added and before sealing the tube, it was flushed with UHP argon for 1 min. Therefore, the mixture was heated at 120 $^{\circ}$ C with continuous stirring for 20 hours. Then, in a separatory funnel, the reaction mixture was extracted with EtOAc (3 \times 30 mL), deionized water (2 \times 10 mL), followed by washing the resulting organic layer with brine (20 mL), and finally the combined organic layer was passed through anhydrous Na₂SO₄ for drying and the mixture was concentrated by evaporating the solvent under reduced pressure. By column chromatography (SiO₂, eluting with hexane/ethylacetate), the crude product was purified by to provide methyl 4'-methoxy-[1,1'-biphenyl]-4-carboxylate (**29e**).

Photocatalyzed carboxylation of methyl 4-bromobenzoate (**25e**) with $^{13}\text{CO}_2$

A DMA solution (1.0 mL) of **25e** (42.6 mg, 0.2 mmol, 1 equiv.) with palladium acetate (1.1 mg, 0.005 mmol, 2.5 mol%), PhXPhos (2.1 mg, 0.01 mmol, 5.0 mol%), Ir(ppy)₂(dtbpy)PF₆ (4.56 mg, 0.005 mmol, 2.5 mol%), additive and ¹Pr₂NEt (195.5 mg, 0.6 mmol, 3.0 equiv.) was prepared in a shlenk under a nitrogen atmosphere. Then the gas phase was replaced by atmospheric pressure of $^{13}\text{CO}_2$, and the reaction vessel was put in a water bath placed at a distance of 10 mm from light sources. The mixture was irradiated with visible light ($\lambda_{\text{irr.}} = 425$ nm) using two Kessil blue LED lamps for 6 h in the closed system. After irradiation, the reaction was quenched with water and then the mixture was extracted with ethyl acetate three times. The combined aqueous layer was acidified with 1N HCl aq., and then extracted with ethyl acetate three times. The combined organic layer was passed through anhydrous Na₂SO₄ for drying and the mixture was concentrated by evaporating the solvent under reduced pressure. By column chromatography (SiO₂, eluting with hexane/ethylacetate), the crude product was purified by to provide [^{13}C]-4-(methoxycarbonyl)benzoic acid (**30**).

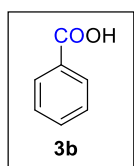
III.7. Characterization data

4-methoxy benzoic acid (**3a**)



This was synthesized following the optimized protocol 'Method A' and purified in column chromatography (Stationary medium is SiO₂, and eluting solvent is 70:30 hexane/ethyl acetate) affording as white solid (25.8 mg, 85%). ¹H NMR (400 MHz, DMSO-d₆) δ 12.63 (s, 1H), 7.90 (d, $J = 8.8$ Hz, 2H), 7.02 (dd, $J = 7.8, 2.4$ Hz, 2H), 3.84–3.81 (m, 3H). ¹³C NMR (100 MHz, DMSO-d₆) δ 167.48, 163.30, 131.81, 123.46, 114.26, 55.88.

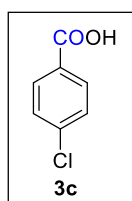
Benzoic acid (**3b**)



One-pot Hydroxycarbonylation of Anilines *via* Diazonium Salt *en route* to Benzoic Acids: Formic Acid as C-1 Source

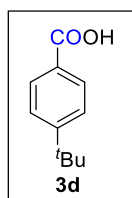
This was synthesized following the optimized protocol 'Method A' and purified in column chromatography (Stationary medium is SiO₂, and eluting solvent is 80:20 hexane/ethyl acetate) affording as white solid (20.0 mg, 82%). ¹H NMR (400 MHz, DMSO-*D*₆ + 2 drops CDCl₃): δ 12.89 (br s, 1H), 7.92-7.89 (m, 2H), 7.57 (dd, *J*₁ = 7.6 Hz, *J*₂ = 1.6 Hz, 1H), 7.47-7.43 (m, 1H); ¹³C NMR (100 MHz, DMSO-*D*₆ + 2 drops CDCl₃) δ 167.84, 133.37, 131.28, 129.78, 129.05.

4-chlorobenzoic acid (**3c**)



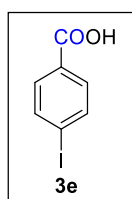
This was synthesized following the optimized protocol 'Method A' and purified in column chromatography (Stationary medium is SiO₂, and eluting solvent is 80:20 hexane/ethyl acetate) affording as white solid (27.4 mg, 88%). ¹H NMR (400 MHz, DMSO-*D*₆): δ 13.11 (br s, 1H), 7.88 (d, *J* = 8.8 Hz, 2H), 7.47 (d, *J* = 8.8 Hz, 2H); ¹³C NMR (100 MHz, DMSO-*D*₆) δ 166.97, 138.31, 131.61, 130.15, 129.18.

4-(*tert*-butyl)benzoic acid (**3d**)



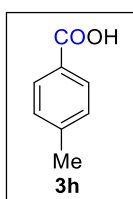
This was synthesized following the optimized protocol 'Method A' and purified in column chromatography (Stationary medium is SiO₂, and eluting solvent is 80:20 hexane/ethyl acetate) affording as white solid (29.5 mg, 83%). ¹H NMR (400 MHz, DMSO-*D*₆): δ 12.72 (br s, 1H), 7.83 (d, *J* = 8.8 Hz, 2H), 7.47 (d, *J* = 8.8 Hz, 2H), 1.25 (s, 9H); ¹³C NMR (100 MHz, DMSO-*D*₆) δ 167.77, 156.32, 129.71, 128.57, 125.88, 35.30, 31.39.

4-iodobenzoic acid (**3e**)



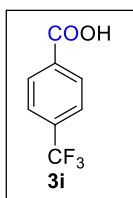
This was synthesized following the optimized protocol 'Method A' and purified in column chromatography (Stationary medium is SiO₂, and eluting solvent is 80:20 hexane/ethyl acetate) affording as white solid (38.5 mg, 78%). ¹H NMR (400 MHz, DMSO-*D*₆): δ 13.07 (br s, 1H), 7.82 (d, *J* = 7.6 Hz, 2H), 7.64 (d, *J* = 8.8 Hz, 2H); ¹³C NMR (100 MHz, DMSO-*D*₆) δ 167.42, 138.08, 131.58, 130.80, 101.65.

4-methylbenzoic acid (**3h**)



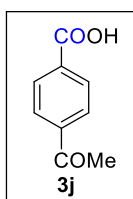
This was synthesized following the optimized protocol 'Method A' and purified in column chromatography (Stationary medium is SiO₂, and eluting solvent is 80:20 hexane/ethyl acetate) affording as white solid (23.9 mg, 88%). ¹H NMR (400 MHz, DMSO-*D*₆): δ 12.73 (br s, 1H), 7.79 (d, *J* = 8.0 Hz, 2H), 7.23 (d, *J* = 8.0 Hz, 2H), 2.30 (s, 3H); ¹³C NMR (100 MHz, DMSO-*D*₆) δ 167.83, 143.51, 129.61, 128.56, 21.61.

4-(trifluoromethyl)benzoic acid (**3i**)



This was synthesized following the optimized protocol 'Method A' and purified in column chromatography (Stationary medium is SiO₂, and eluting solvent is 80:20 hexane/ethyl acetate) affording as white solid (26.30 mg, 69%). ¹H NMR (400 MHz, CDCl₃): δ 13.43 (brs, 1H), 8.08 (d, *J* = 8.0 Hz, 2H), 7.79 (d, *J* = 8.0 Hz, 2H); ¹³C NMR (100 MHz, CDCl₃) δ 166.71, 13.10, 133.02 (q, *J* = 31.8 Hz), 130.60, 126.06-125.97 (m).

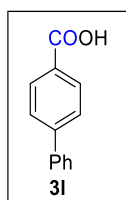
4-acetylbenzoic acid (**3j**)



One-pot Hydroxycarbonylation of Anilines *via* Diazonium Salt *en route* to Benzoic Acids: Formic Acid as C-1 Source

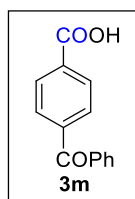
This was synthesized following the optimized protocol 'Method A' and purified in column chromatography (Stationary medium is SiO₂, and eluting solvent is 80:20 hexane/ethyl acetate) affording as white solid (26.69 mg, 81%). ¹H NMR (400 MHz, CDCl₃): δ 8.18 (d, *J* = 8.8 Hz, 2H), 7.69 (d, *J* = 8.8 Hz, 2H), 7.63 (d, *J* = 8.8 Hz, 2H); ¹³C NMR (100 MHz, CDCl₃) δ 171.09, 146.58, 139.98, 130.82, 129.04, 128.37, 128.02, 127.41, 127.26.

4-phenylbenzoic acid (**3l**)



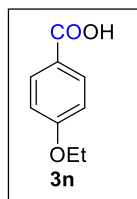
This was synthesized following the optimized protocol 'Method A' and purified in column chromatography (Stationary medium is SiO₂, and eluting solvent is 80:20 hexane/ethyl acetate) affording as white solid (39.78 mg, 88%). ¹H NMR (400 MHz, CDCl₃): δ 8.18 (d, *J* = 8.4 Hz, 2H), 7.69 (d, *J* = 8.4 Hz, 2H), 7.63 (d, *J* = 7.6 Hz, 2H), 7.47 (t, *J* = 8.0 Hz, 2H), 7.40 (t, *J* = 7.2 Hz, 2H); ¹³C NMR (100 MHz, CDCl₃) δ 171.09, 146.58, 139.98, 130.82, 129.04, 128.37, 128.02, 127.41, 127.26.

4-benzoylbenzoic acid (**3m**)



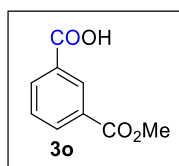
This was synthesized following the optimized protocol 'Method A' and purified in column chromatography (Stationary medium is SiO₂, and eluting solvent is 80:20 hexane/ethyl acetate) affording as white solid (39.78 mg, 88%). ¹H NMR (400 MHz, DMSO-*D*₆): δ 13.29 (br s, 1), 8.06 (d, *J* = 8.4 Hz, 2H), 7.78 (d, *J* = 8.8 Hz, 2H), 7.73-7.70 (m, 2H), 7.66 (t, *J* = 7.6 Hz, 2H), 7.53 (t, *J* = 7.6 Hz, 2H); ¹³C NMR (100 MHz, DMSO-*D*₆) δ 195.90, 167.18, 141.07, 137.03, 134.51, 133.62, 130.26, 130.15, 129.93, 129.21.

4-ethoxybenzoic acid (**3n**)



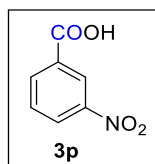
This was synthesized following the optimized protocol 'Method A' and purified in column chromatography (Stationary medium is SiO₂, and eluting solvent is 80:20 hexane/ethyl acetate) affording as white solid (24.9 mg, 75%). ¹H NMR (400 MHz, DMSO-*D*₆): δ 12.55 (brs, 1H), 7.85-7.82 (m, 2H), 6.95 (d, *J* = 8.4 Hz, 2H), 4.05 (q, *J* = 7.2 Hz, 2H), 1.30 (t, *J* = 6.8 Hz, 3H); ¹³C NMR (100 MHz, DMSO-*D*₆) δ 167.53, 162.66, 131.87, 123.32, 114.70, 63.96, 15.03.

3-(methoxycarbonyl)benzoic acid (**3o**)



This was synthesized following the optimized protocol 'Method A' and purified in column chromatography (Stationary medium is SiO₂, and eluting solvent is 80:20 hexane/ethyl acetate) affording as white solid (27.0 mg, 75%). ¹H NMR (400 MHz, DMSO-*D*₆): δ 13.26 (br s, 1), 8.44 (t, *J* = 1.6 Hz, 1H), 8.16-8.13 (m, 2H), 7.62 (t, *J* = 8.0 Hz, 1H), 3.84 (s, 3H); ¹³C NMR (100 MHz, DMSO-*D*₆) δ 166.94, 166.03, 134.25, 133.69, 131.87, 130.53, 130.25, 129.86, 52.90.

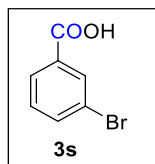
3-nitrobenzoic acid (**3p**)



This was synthesized following the optimized protocol 'Method A' and purified in column chromatography (Stationary medium is SiO₂, and eluting solvent is 80:20 hexane/ethyl acetate) affording as white solid (22.7mg, 68%). ¹H NMR (400 MHz, DMSO-*D*₆): δ 8.53-8.52

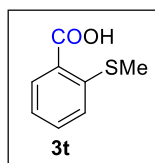
(m, 1H), 8.38-8.36 (m, 1H), 8.27-8.25 (m, 1H), 7.73 (t, $J = 8.0$ Hz, 1H); ^{13}C NMR (100 MHz, DMSO- D_6) δ 165.99, 148.32, 135.82, 132.93, 130.95, 127.75, 124.14.

3-bromobenzoic acid (**3s**)



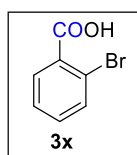
This was synthesized following the optimized protocol 'Method A' and purified in column chromatography (Stationary medium is SiO_2 , and eluting solvent is 80:20 hexane/ethyl acetate) affording as white solid (26.3mg, 66%). ^1H NMR (400 MHz, DMSO- D_6): δ 8.00-7.99 (m, 1H), 7.91-7.88 (m, 1H), 7.80-7.78 (m, 1H), 7.46-7.42 (m, 1H); ^{13}C NMR (100 MHz, DMSO- D_6) δ 166.49, 136.12, 133.61, 132.26, 131.42, 128.80, 122.24.

2-(methylthio)benzoic acid (**3t**)



This was synthesized following the optimized protocol 'Method A' and purified in column chromatography (Stationary medium is SiO_2 , and eluting solvent is 80:20 hexane/ethyl acetate) affording as white solid (24.2 mg, 72%). ^1H NMR (400 MHz, DMSO- D_6): δ 12.9 (br s, 1), 7.85 (dd, $J_1 = 8.0$ Hz, $J_2 = 1.6$ Hz, 1H), 7.49 (t, $J = 8.0$ Hz, 1H), 7.30 (d, $J = 8$ Hz, 1H), 7.15 (t, $J = 7.6$ Hz, 1H), 2.35 (s, 3H); ^{13}C NMR (100 MHz, DMSO- D_6) δ 167.89, 142.98, 132.99, 131.44, 127.87, 125.08, 123.98, 15.31.

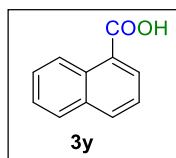
2-bromobenzoic acid (**3x**)



This was synthesized following the optimized protocol 'Method A' and purified in column chromatography (Stationary medium is SiO_2 , and eluting solvent is 80:20 hexane/ethyl acetate) affording as white solid (21.9 mg, 55%). ^1H NMR (400 MHz, DMSO- D_6): δ 7.70-7.66

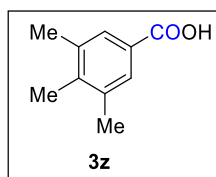
(m, 2H), 7.45-7.37 (m, 2H); ^{13}C NMR (100 MHz, $\text{DMSO-}D_6$) δ 167.89, 134.28, 133.05, 131.10, 128.24, 120.44.

1-naphthoic acid (**3y**)



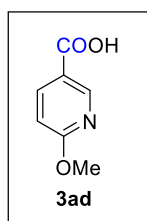
This was synthesized following the optimized protocol ‘Method A’ and purified in column chromatography (Stationary medium is SiO_2 , and eluting solvent is 80:20 hexane/ethyl acetate) affording as white solid (23.4 mg, 68%). ^1H NMR (400 MHz, CDCl_3): δ 9.10 (d, $J = 8.4$ Hz, 1H), 8.42 (dd, $J_1 = 7.2$ Hz, $J_2 = 1.2$ Hz, 1H), 8.09 (d, $J = 8.4$ Hz, 1H), 7.91 (d, $J = 8.4$ Hz, 1H), 7.68-7.64 (m, 1H), 7.56 (q, $J = 7.6$ Hz, 2H); ^{13}C NMR (100 MHz, CDCl_3) δ 173.53, 134.76, 134.04, 131.99, 131.74, 128.81, 128.21, 127.92, 126.42, 126.02, 125.70, 124.63.

3,4,5-trimethylbenzoic acid (**3z**)



This was synthesized following the optimized protocol ‘Method A’ and purified in column chromatography (Stationary medium is SiO_2 , and eluting solvent is 80:20 hexane/ethyl acetate) affording as white solid (22.0 mg, 72%). ^1H NMR (400 MHz, $\text{DMSO-}D_6$): δ 6.83 (s, 2H), 2.19 (s, 9H); ^{13}C NMR (100 MHz, $\text{DMSO-}D_6$) δ 171.37, 138.53, 134.16, 133.03, 128.50, 21.15, 19.82.

6-methoxynicotinic acid (**3ad**)

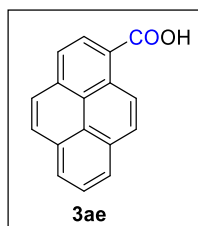


This was synthesized following the optimized protocol ‘Method A’ and purified in column chromatography (Stationary medium is SiO_2 , and eluting solvent is 80:20 hexane/ethyl

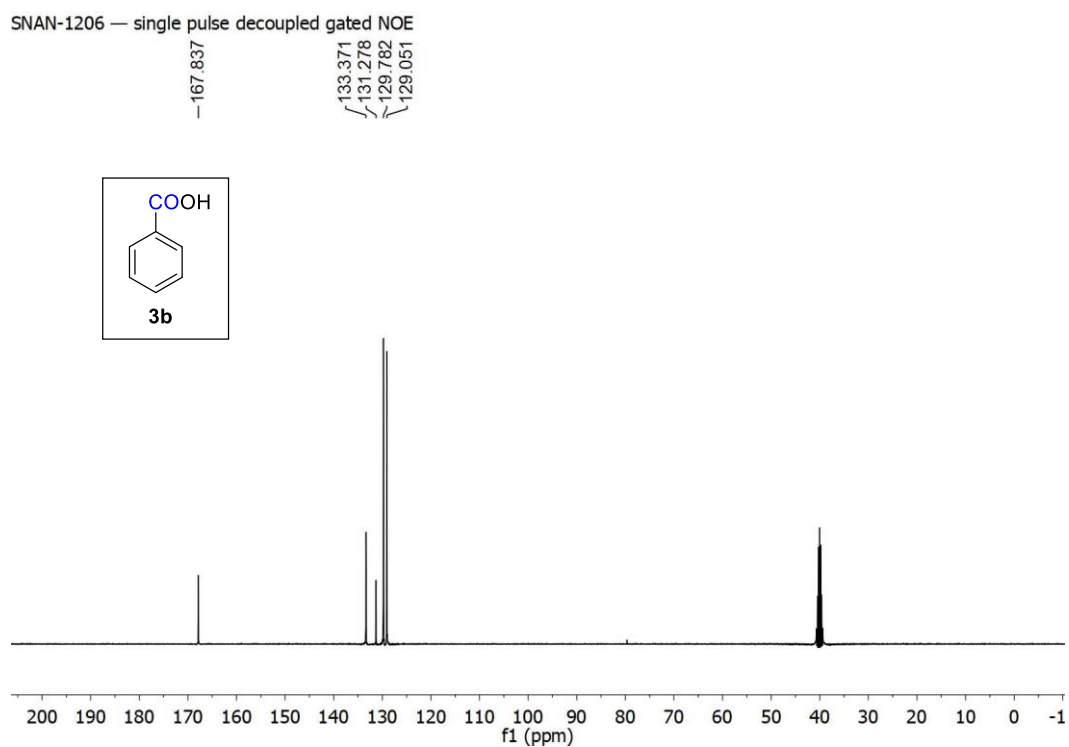
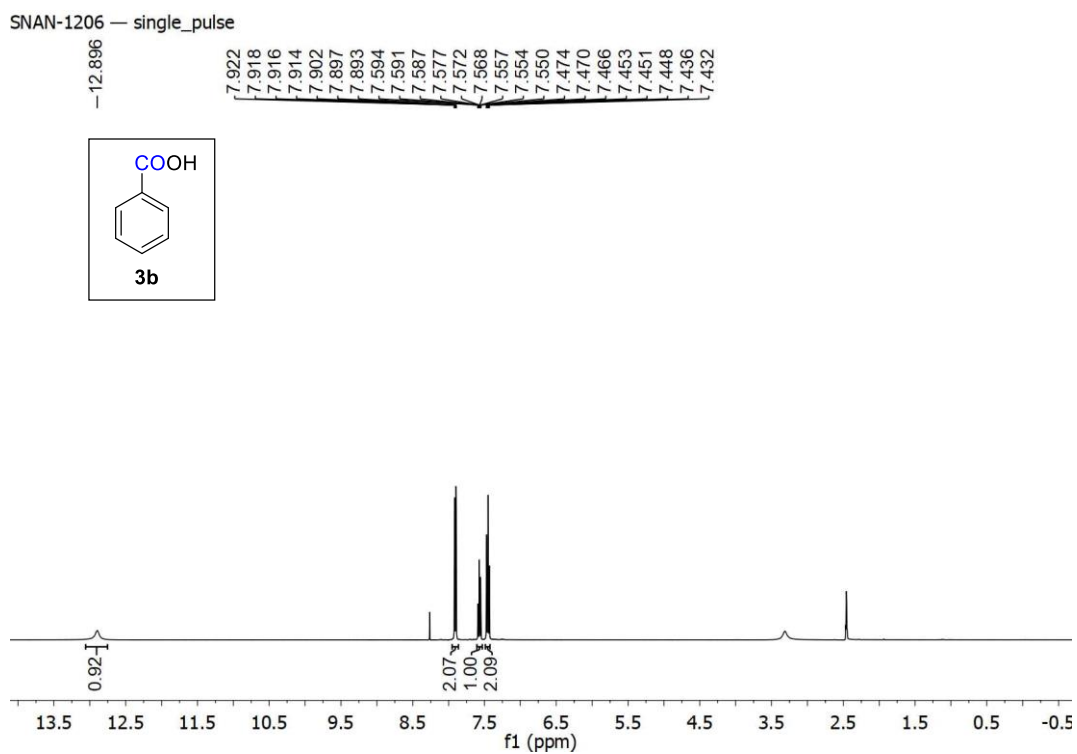
**One-pot Hydroxycarbonylation of Anilines via Diazonium Salt *en route* to Benzoic Acids:
Formic Acid as C-1 Source**

acetate) affording as white solid (22.0 mg, 72%). ^1H NMR (400 MHz, DMSO- D_6 + 2 drops CDCl_3): δ 12.99 (br s, 1H), 8.68 (dd, $J_1 = 2.4$ Hz, $J_2 = 0.4$ Hz, 1H), 8.10 (dd, $J_1 = 8.4$ Hz, $J_2 = 2.4$ Hz, 1H), 6.86 (dd, $J_1 = 8.8$ Hz, $J_2 = 0.8$ Hz, 1H), 3.88 (s, 3H); ^{13}C NMR (100 MHz, DMSO- D_6 + 2 drops CDCl_3) δ 166.68, 149.99, 140.39, 120.93, 111.05, 54.36.

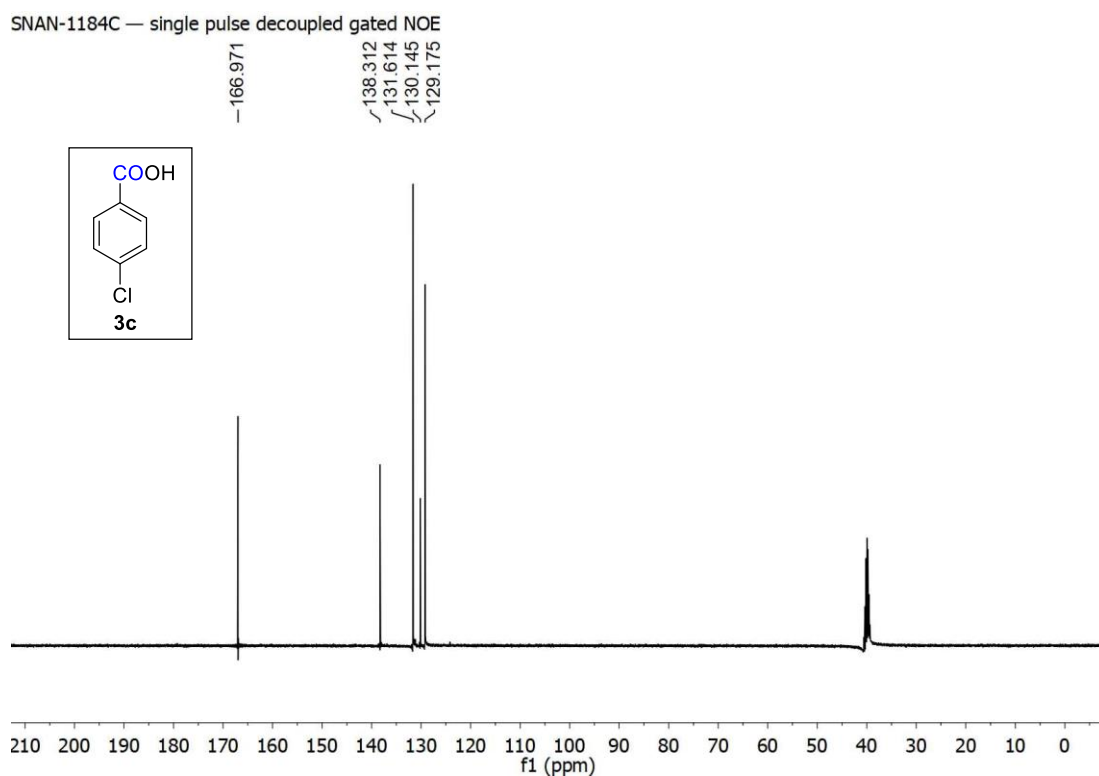
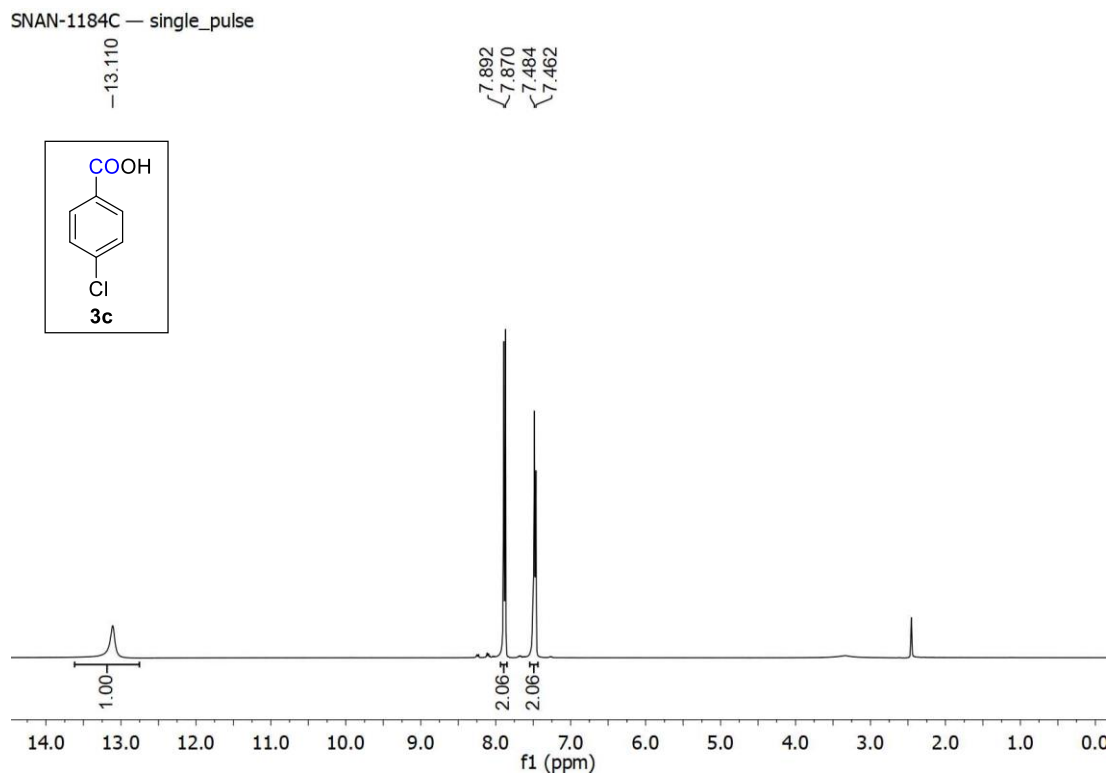
pyrene-1-carboxylic acid (**3ae**)



This was synthesized following the optimized protocol 'Method A' and purified in column chromatography (Stationary medium is SiO_2 , and eluting solvent is 80:20 hexane/ethyl acetate) affording as white solid (33.5 mg, 68%). ^1H NMR (400 MHz, DMSO- D_6 + 2 drops CDCl_3): δ 13.29 (br s, 1H), 9.19 (d, $J = 9.6$ Hz, 1H), 8.57 (d, $J = 8.0$ Hz, 1H), 8.37 (dd, $J_1 = 8.0$ Hz, $J_2 = 1.6$ Hz, 2H), 8.37-8.28 (m, 3H), 8.21 (d, $J = 8.8$ Hz, 1H), 8.10 (d, $J = 7.6$ Hz, 1H); ^{13}C NMR (100 MHz, DMSO- D_6 + 2 drops CDCl_3) δ 169.59, 134.11, 131.13, 130.62, 130.35, 129.99, 129.68, 128.95, 127.74, 127.24, 127.01, 126.72, 125.18, 124.99, 124.52, 123.94.

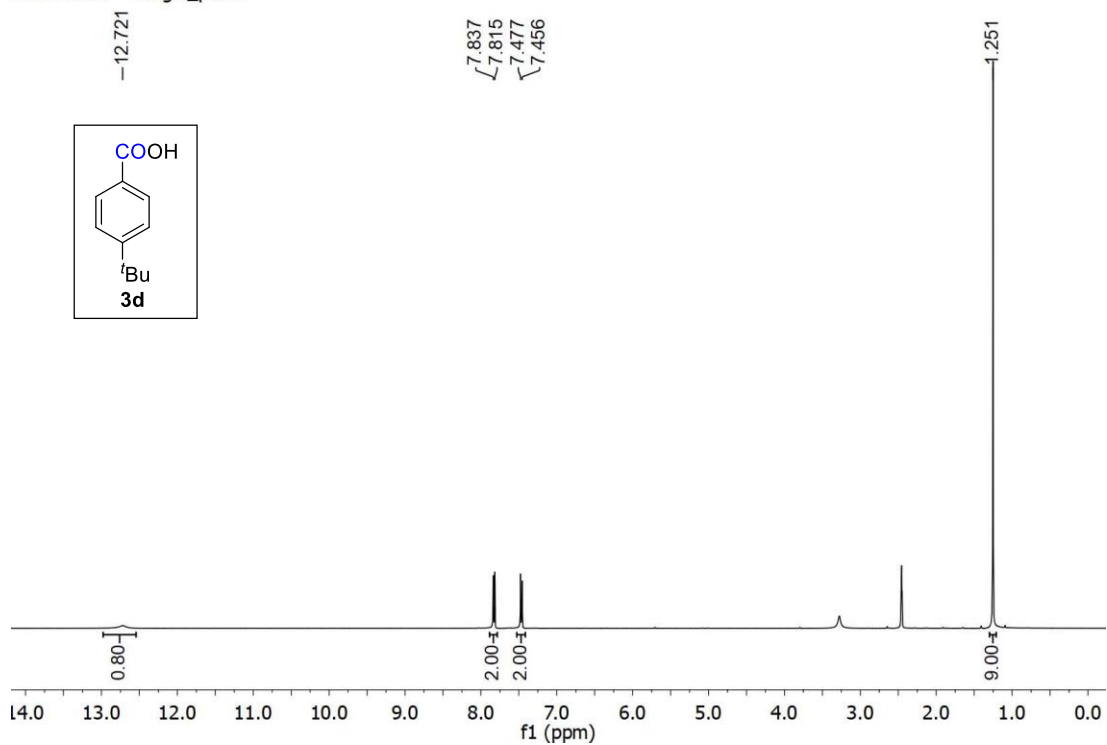
III.8. Representative ^1H and ^{13}C spectra ^1H and ^{13}C spectra of **3b**

One-pot Hydroxycarbonylation of Anilines *via* Diazonium Salt *en route* to Benzoic Acids:
Formic Acid as C-1 Source

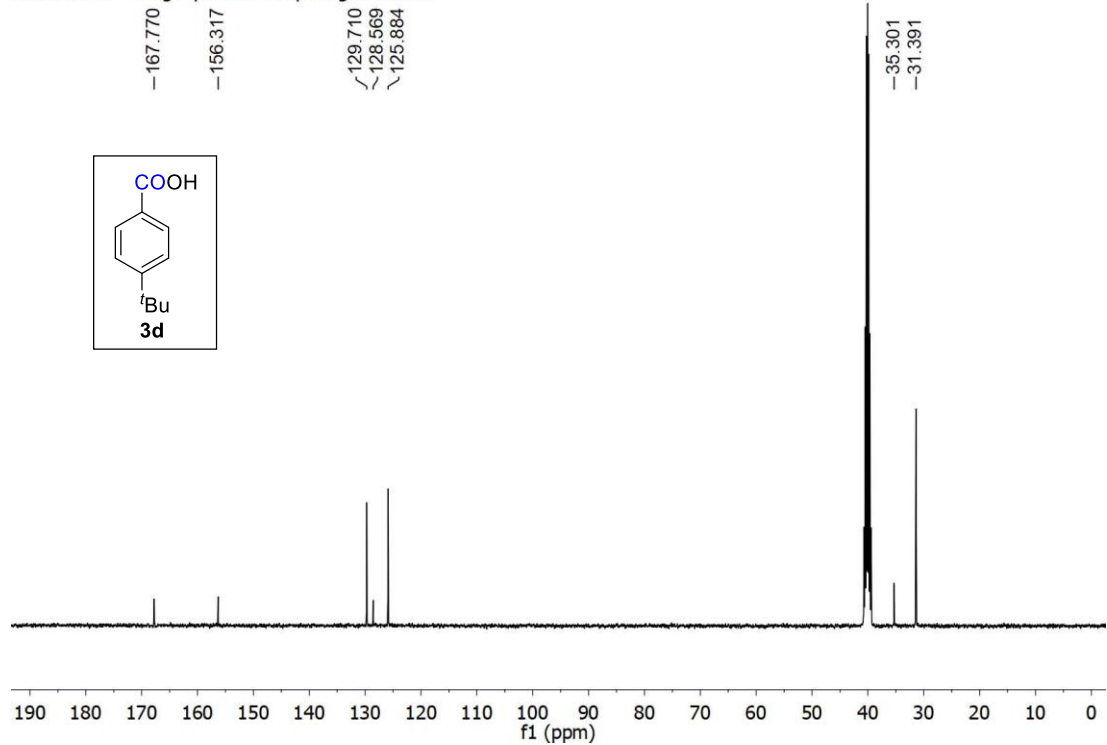


¹H and ¹³C spectra of **3c**

SNAN-1194 — single_pulse



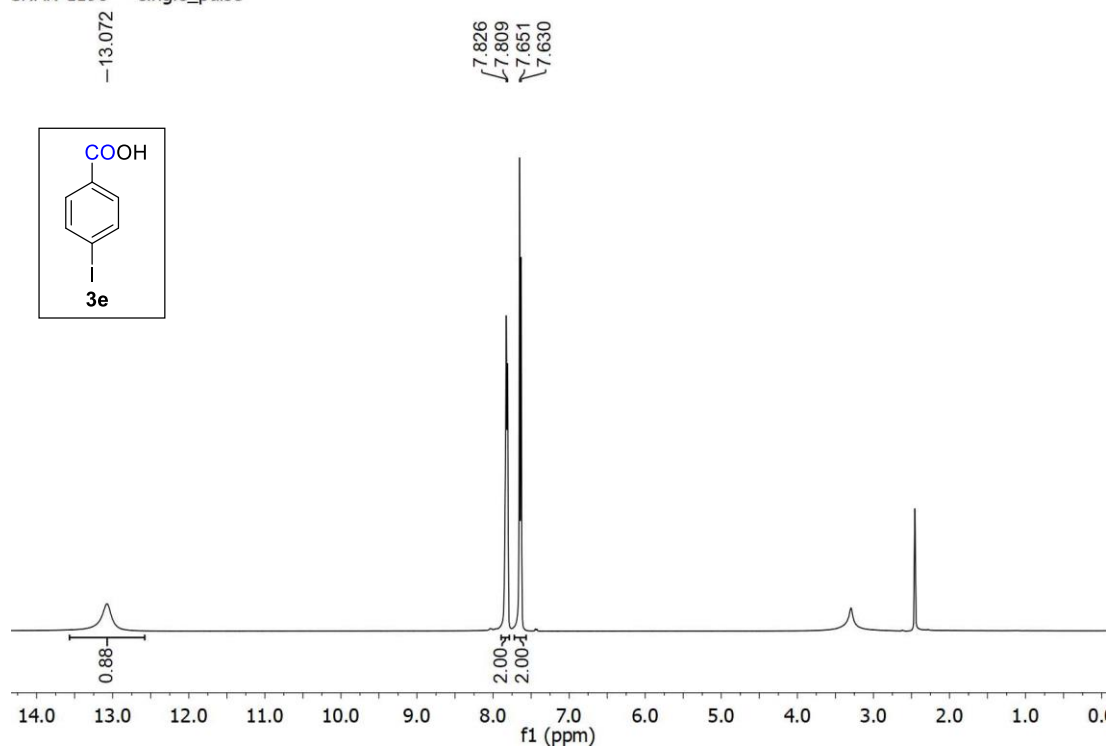
SNAN-1194 — single pulse decoupled gated NOE



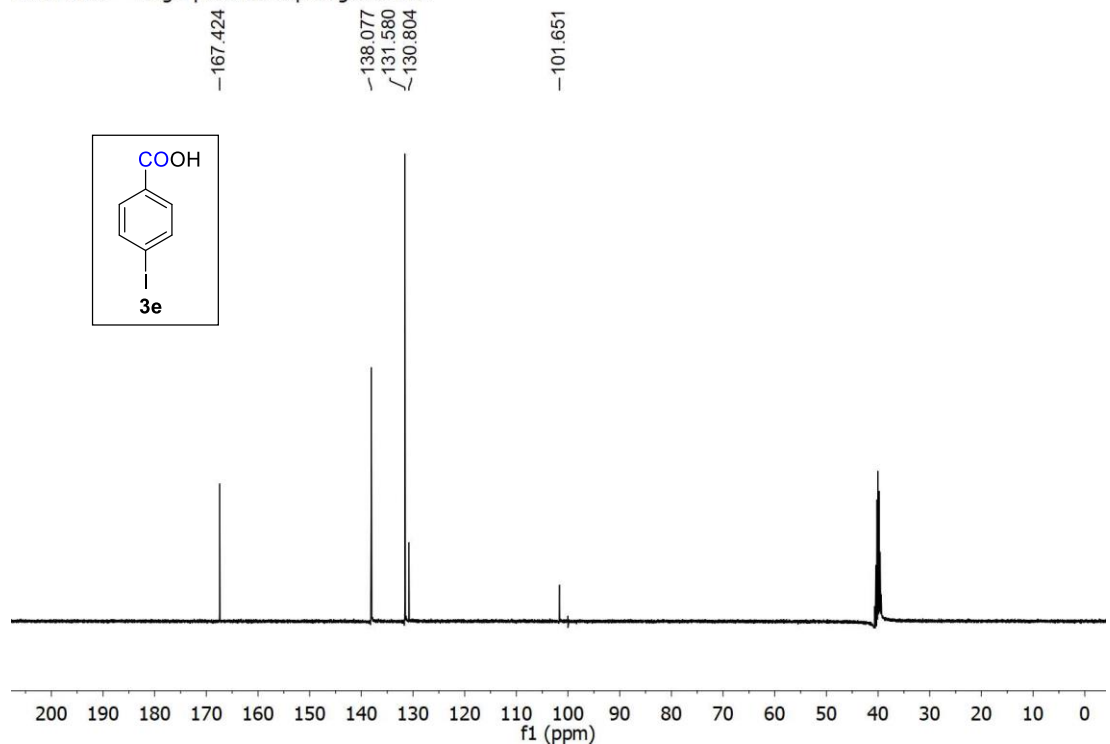
^1H and ^{13}C spectra of **3d**

One-pot Hydroxycarbonylation of Anilines *via* Diazonium Salt *en route* to Benzoic Acids:
Formic Acid as C-1 Source

SNAN-1198 — single_pulse



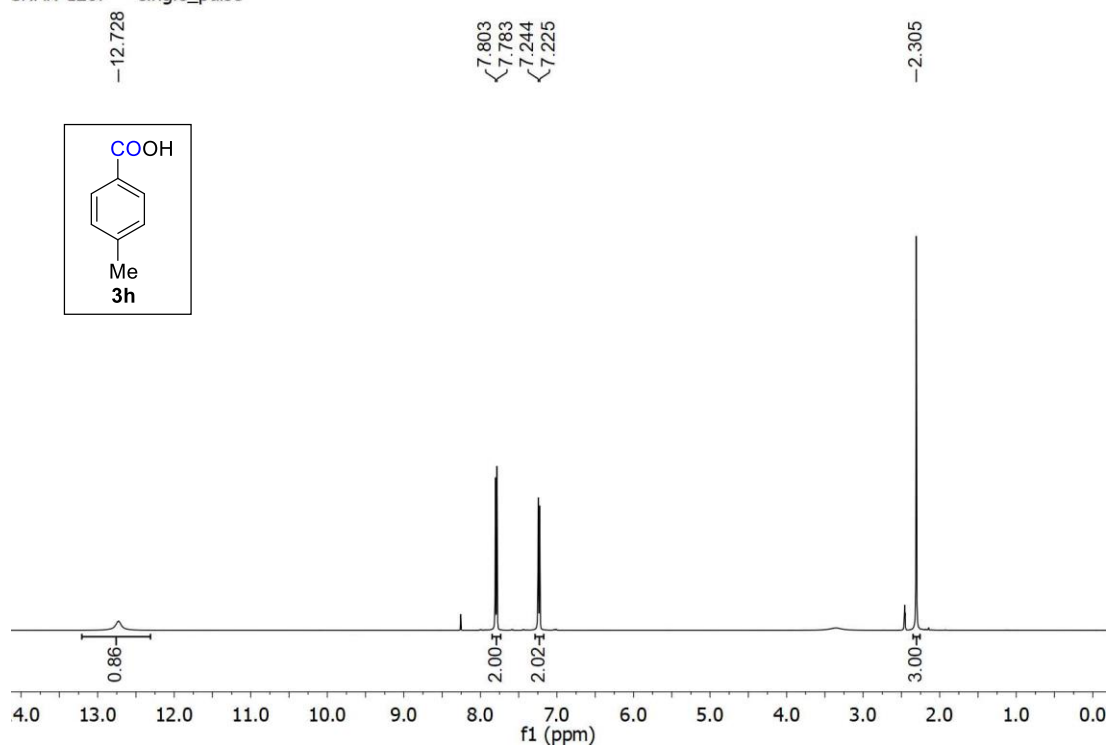
SNAN-1198 — single pulse decoupled gated NOE



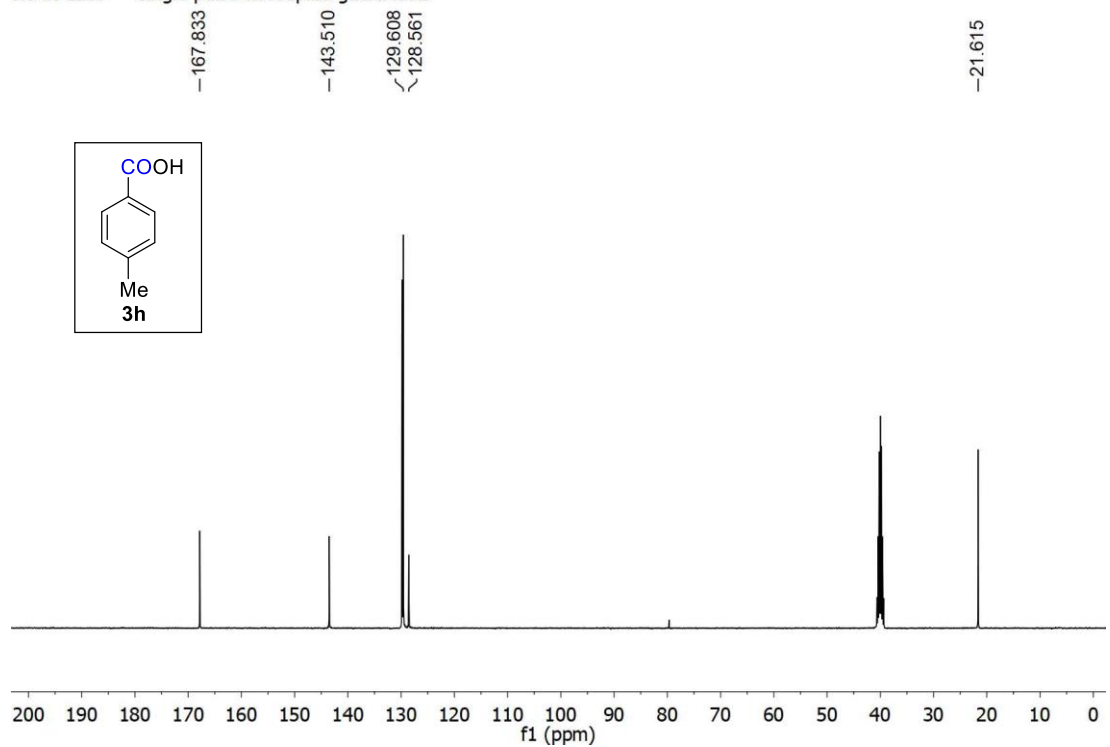
¹H and ¹³C spectra of **3e**

Chapter III

SNAN-1207 — single_pulse



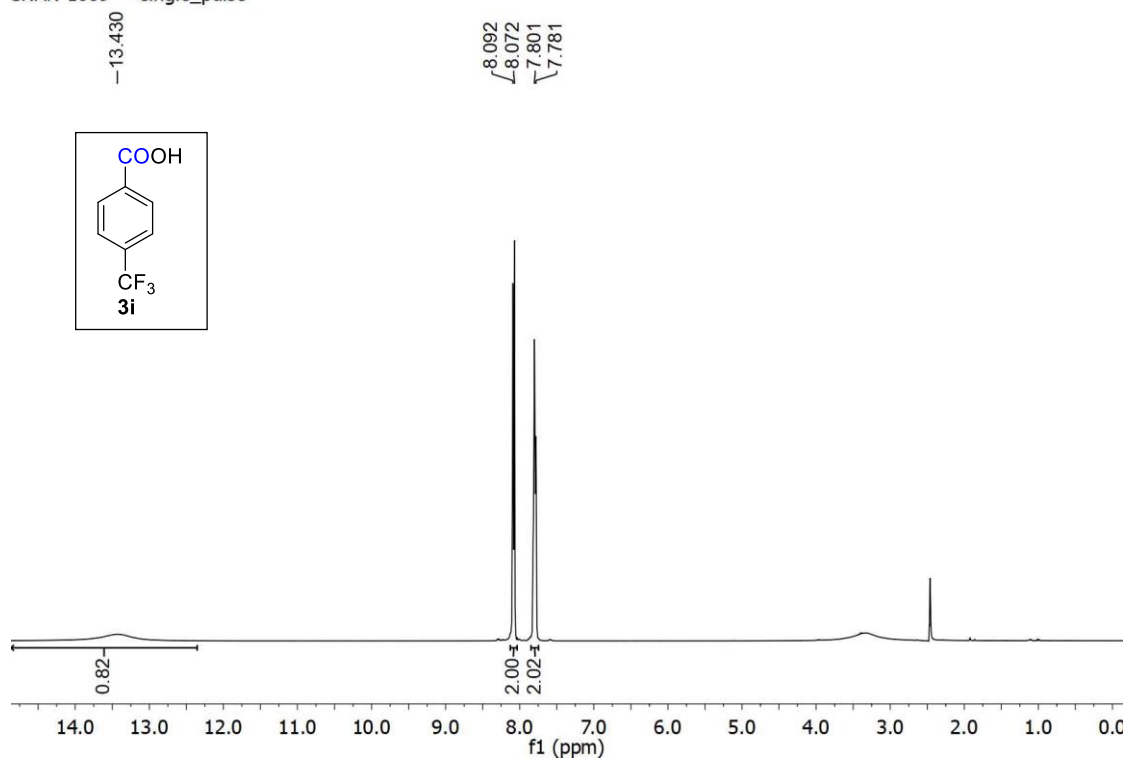
SNAN-1207 — single pulse decoupled gated NOE



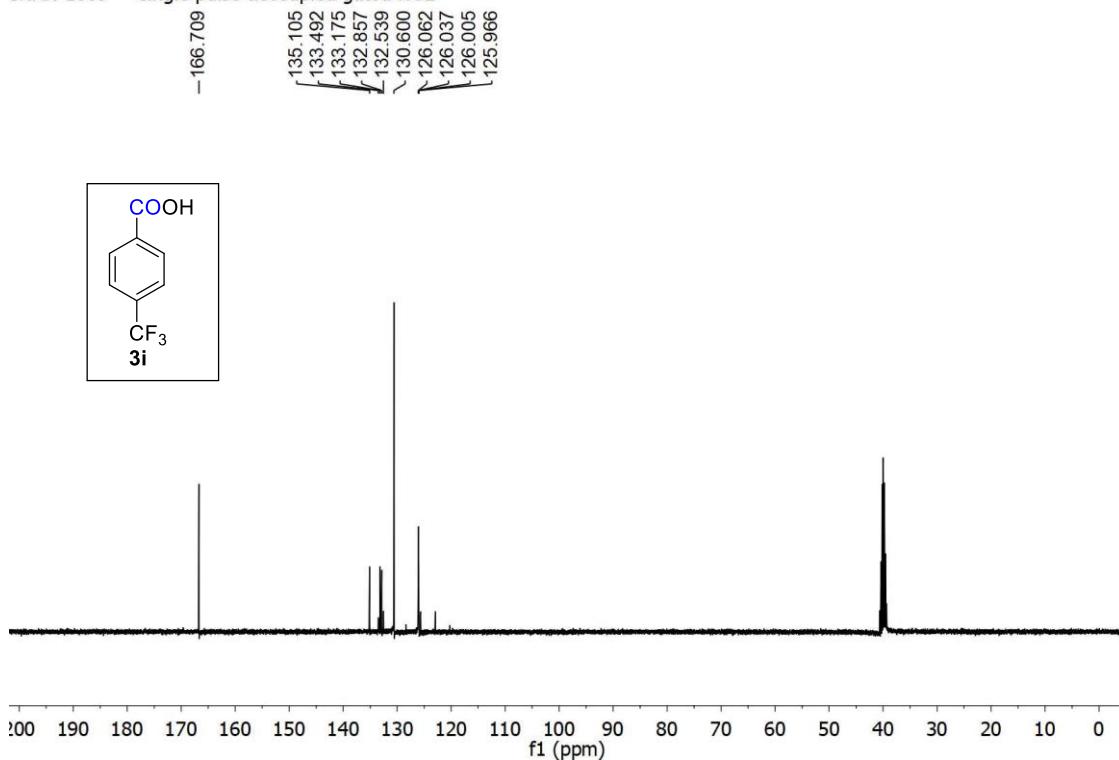
^1H and ^{13}C spectra of **3h**

One-pot Hydroxycarbonylation of Anilines *via* Diazonium Salt *en route* to Benzoic Acids:
Formic Acid as C-1 Source

SNAN-1609 — single_pulse

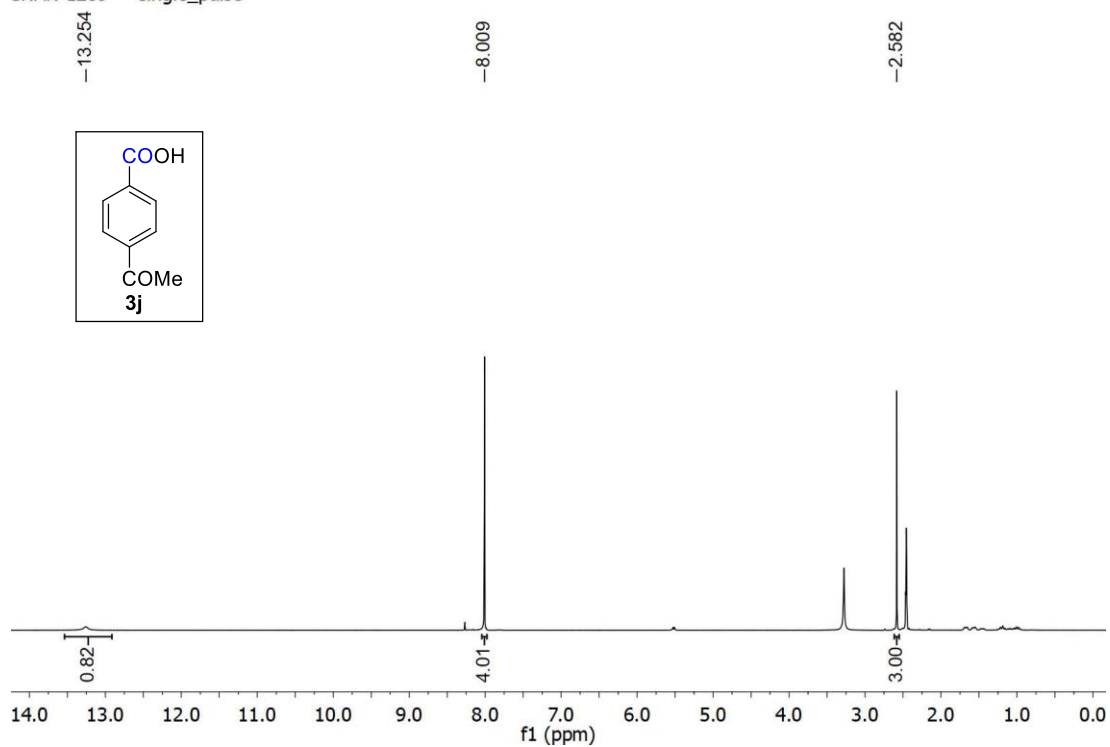


SNAN-1609 — single pulse decoupled gated NOE

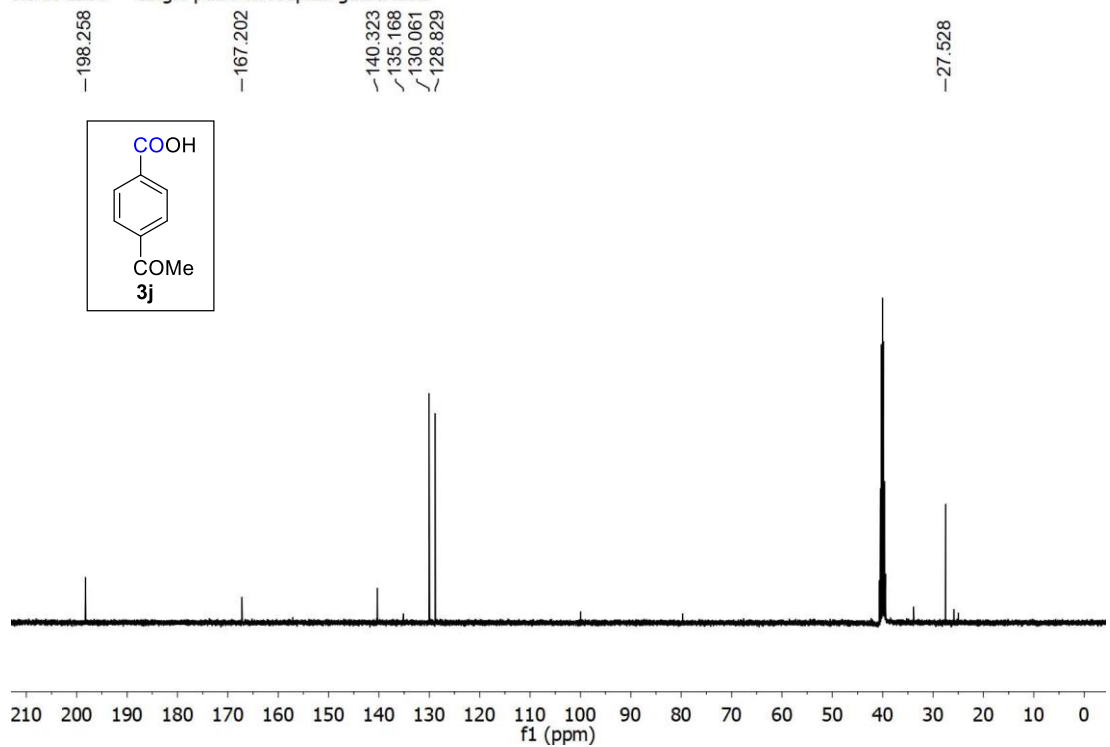


^1H and ^{13}C spectra of **3i**

SNAN-1209 — single_pulse



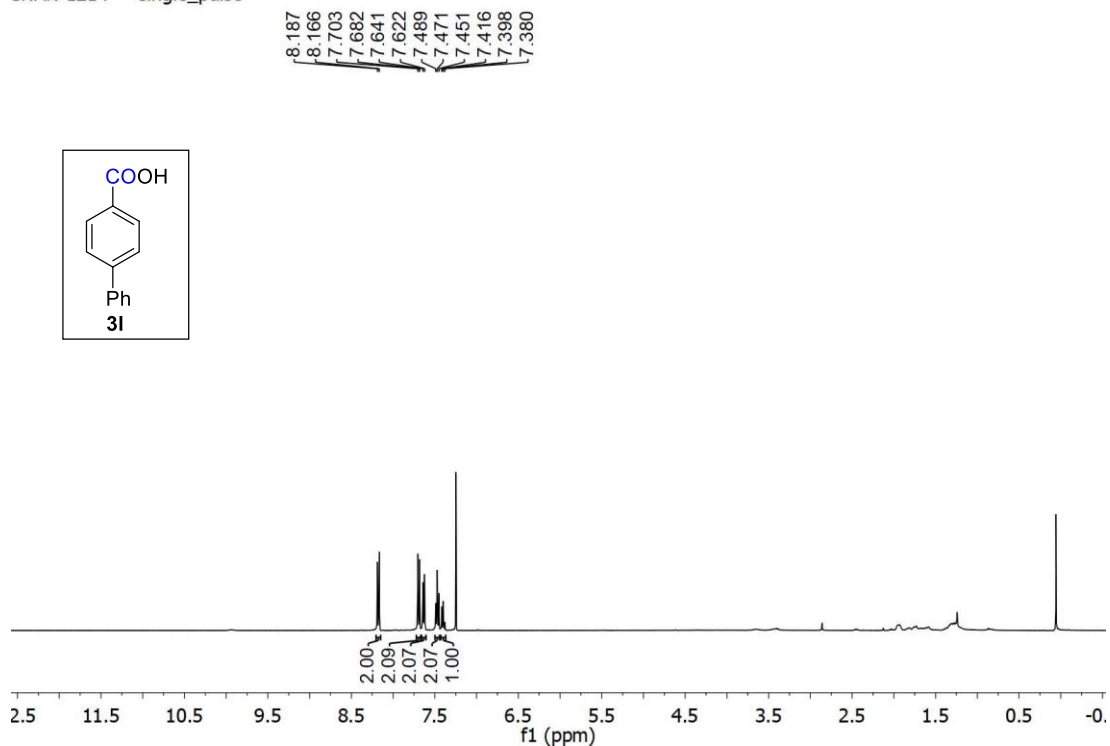
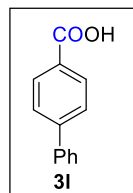
SNAN-1209 — single pulse decoupled gated NOE



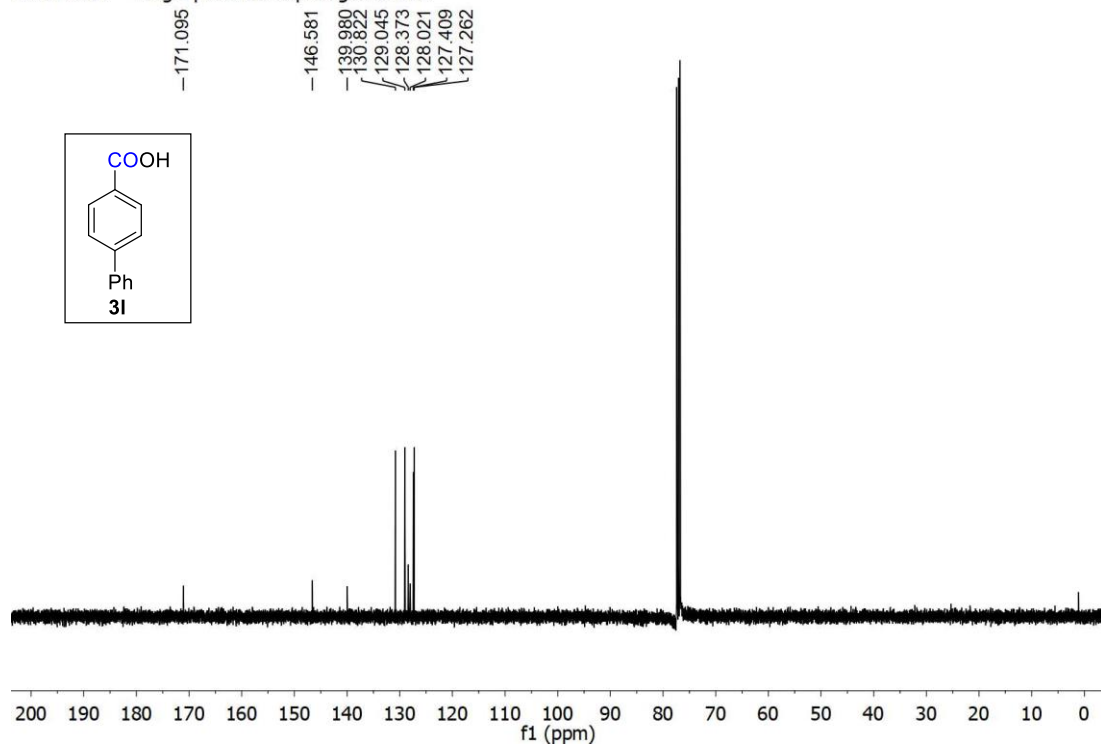
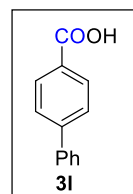
¹H and ¹³C spectra of **3j**

One-pot Hydroxycarbonylation of Anilines *via* Diazonium Salt *en route* to Benzoic Acids: Formic Acid as C-1 Source

SNAN-1214 — single_pulse



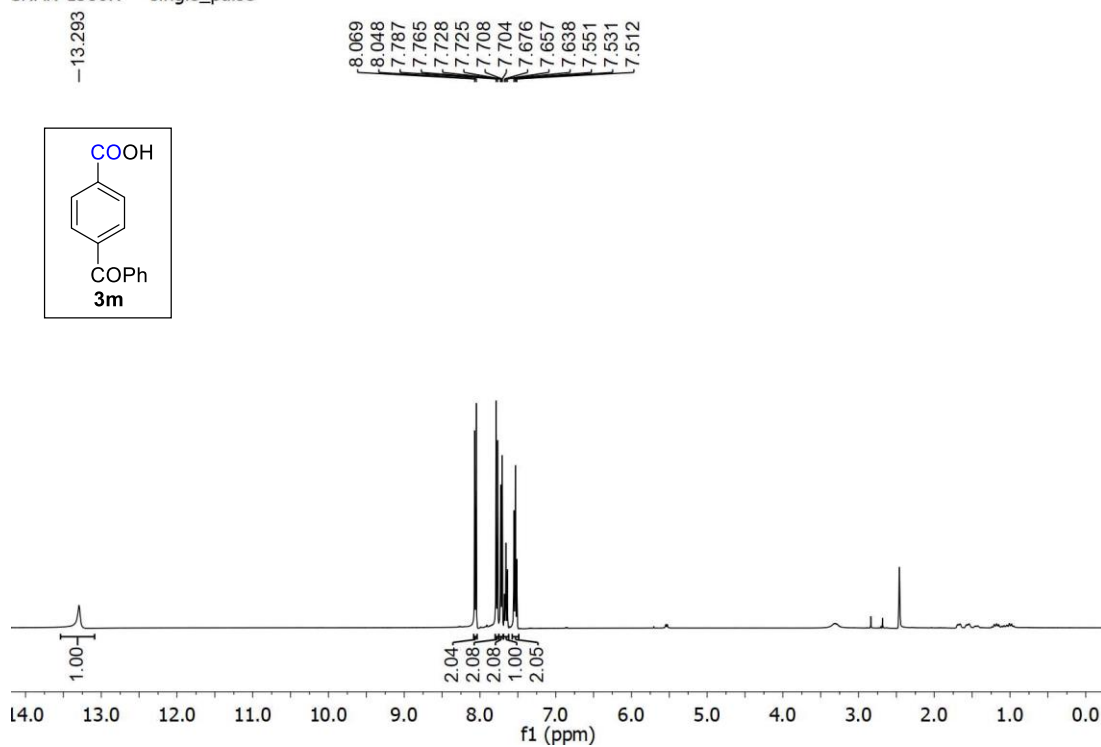
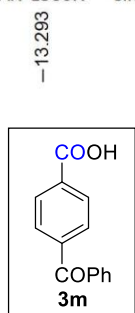
SNAN-1214 — single pulse decoupled gated NOE



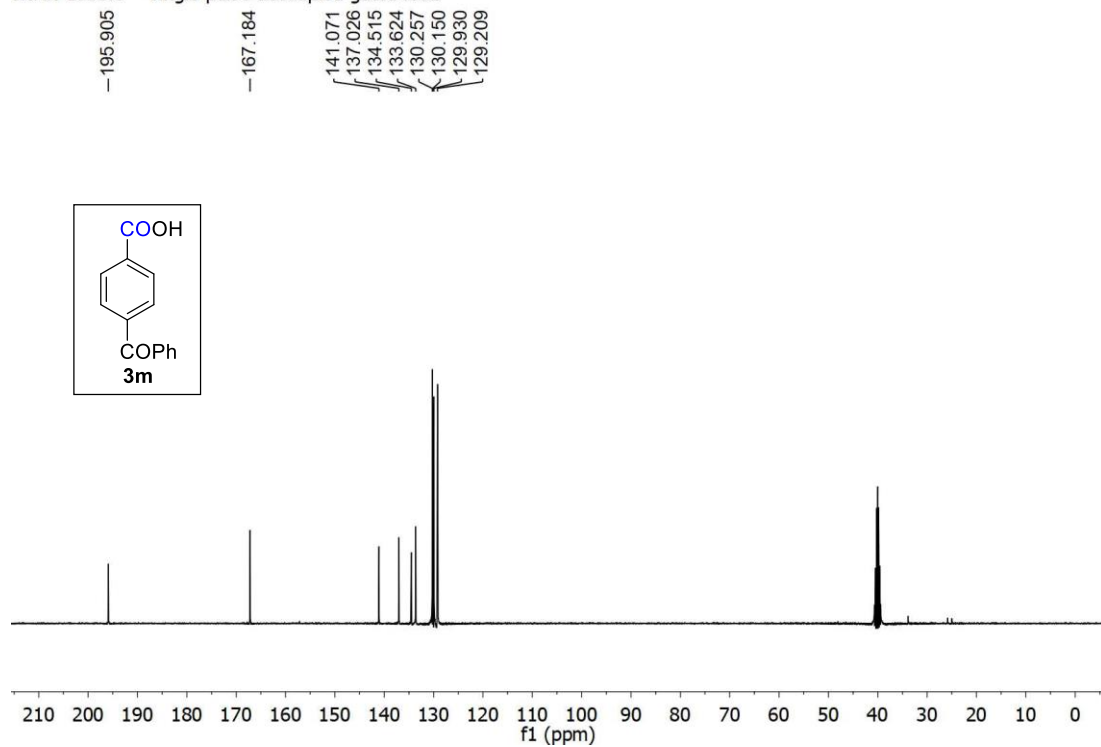
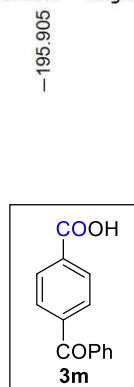
^1H and ^{13}C spectra of **3I**

Chapter III

SNAN-1380R — single_pulse



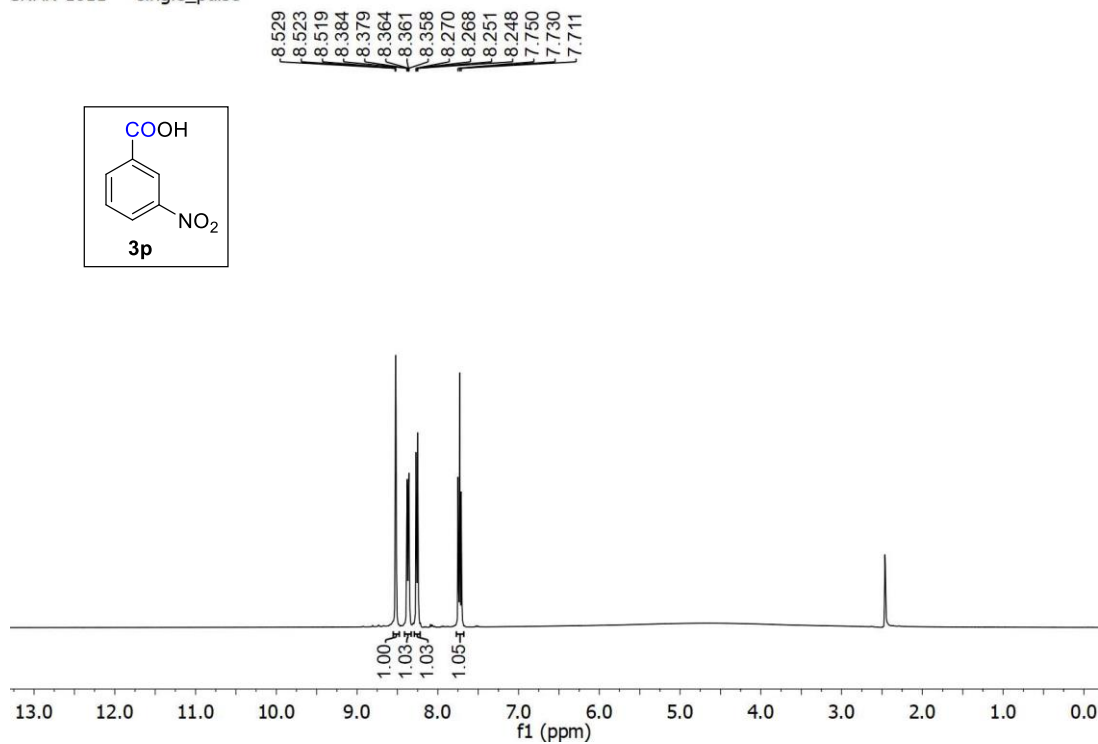
SNAN-1380R — single pulse decoupled gated NOE



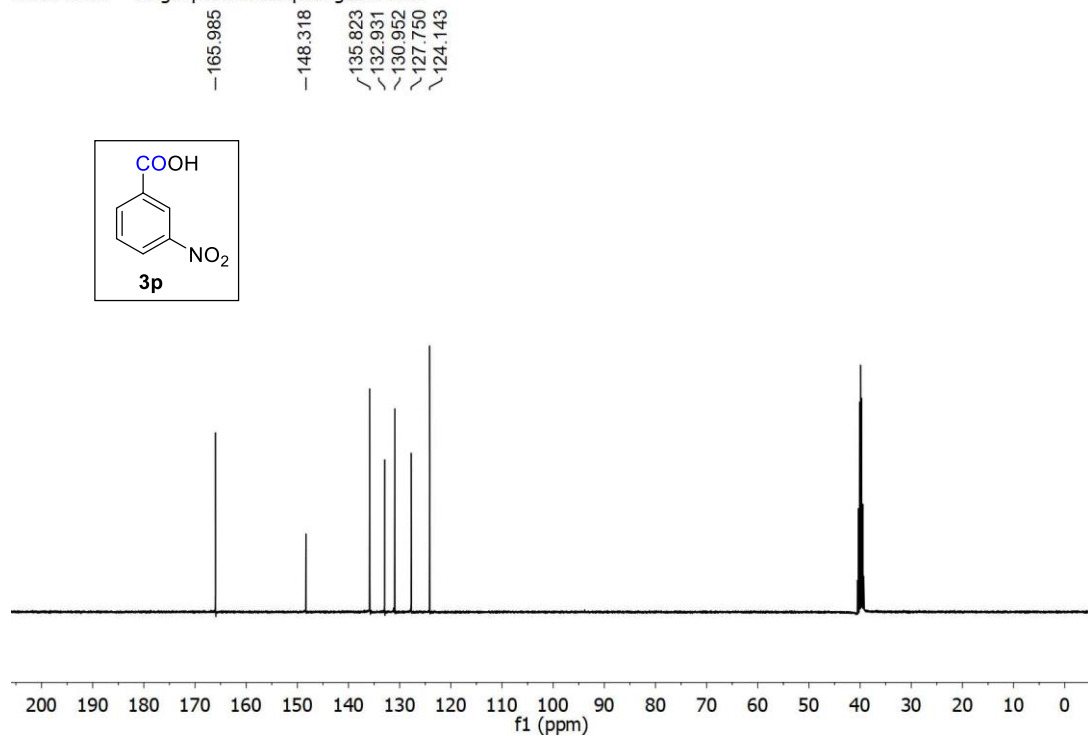
^1H and ^{13}C spectra of **3m**

One-pot Hydroxycarbonylation of Anilines *via* Diazonium Salt *en route* to Benzoic Acids: Formic Acid as C-1 Source

SNAN-1611 — single_pulse

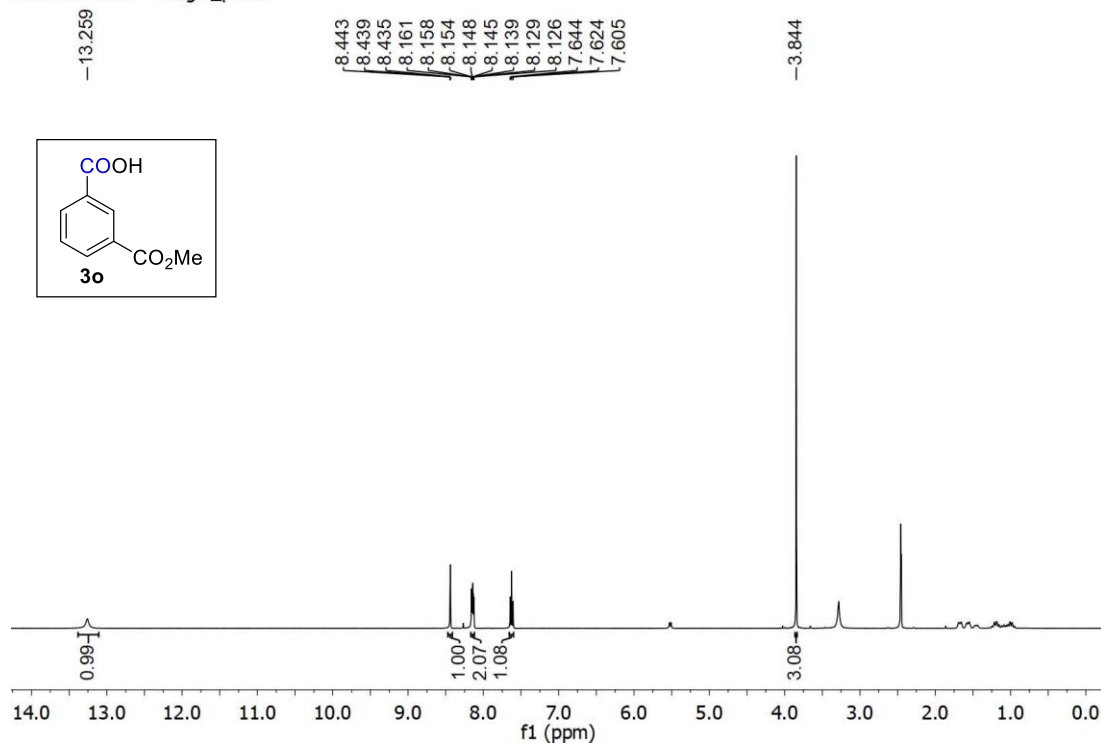


SNAN-1611 — single pulse decoupled gated NOE

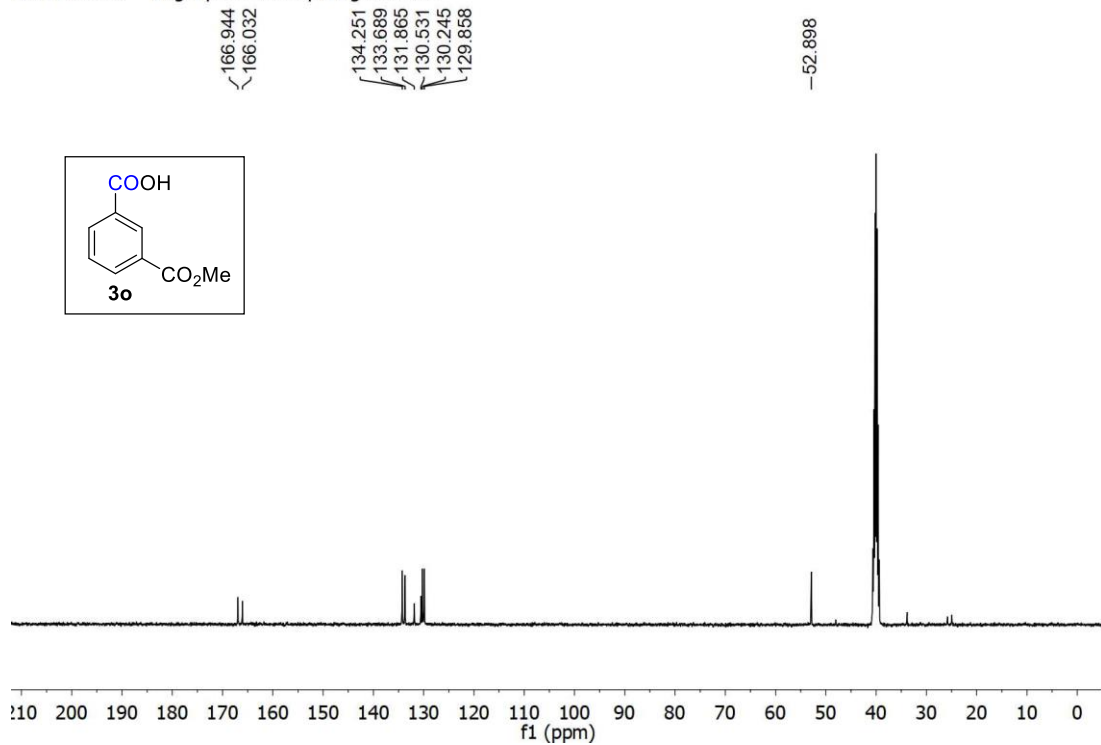


^1H and ^{13}C spectra of **3p**

SNAN-1208CR — single_pulse

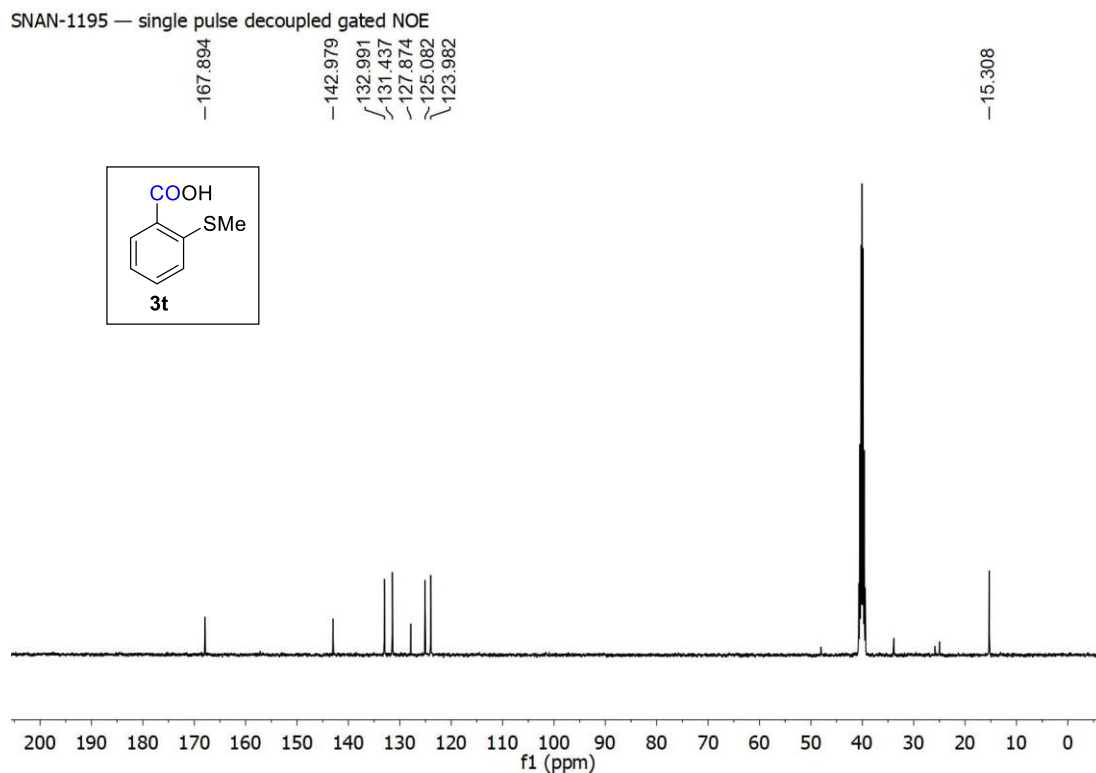
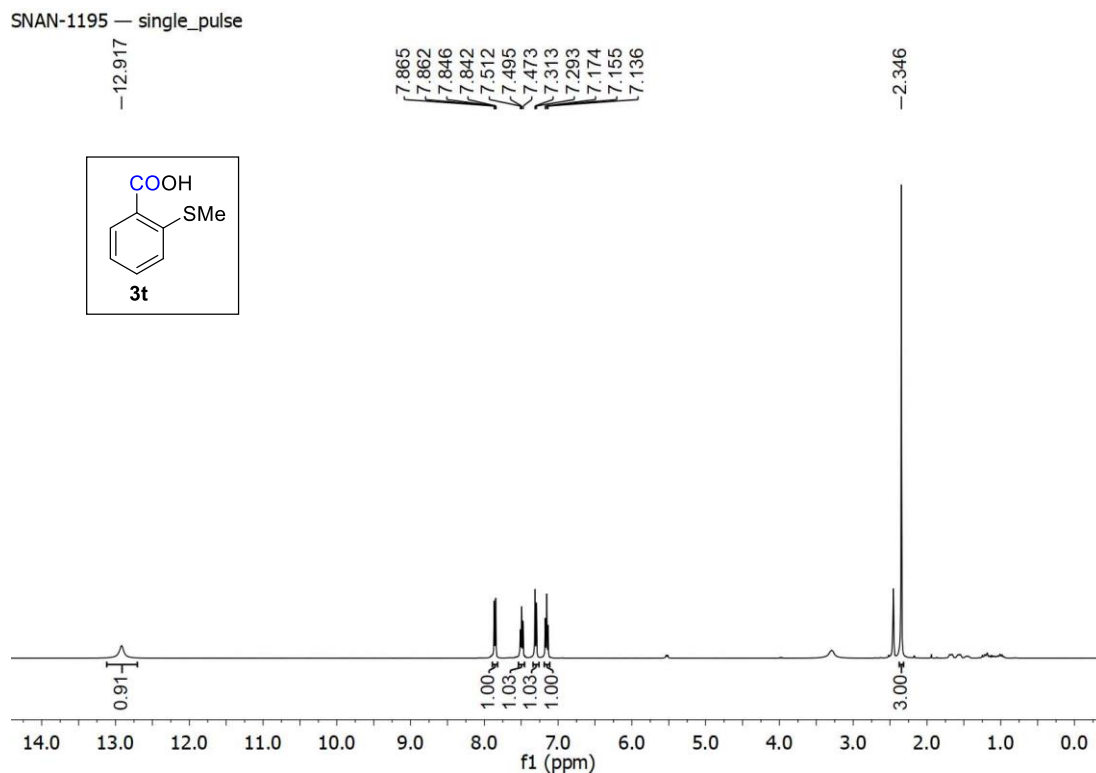


SNAN-1208R — single pulse decoupled gated NOE



¹H and ¹³C spectra of **3o**

One-pot Hydroxycarbonylation of Anilines *via* Diazonium Salt *en route* to Benzoic Acids:
Formic Acid as C-1 Source

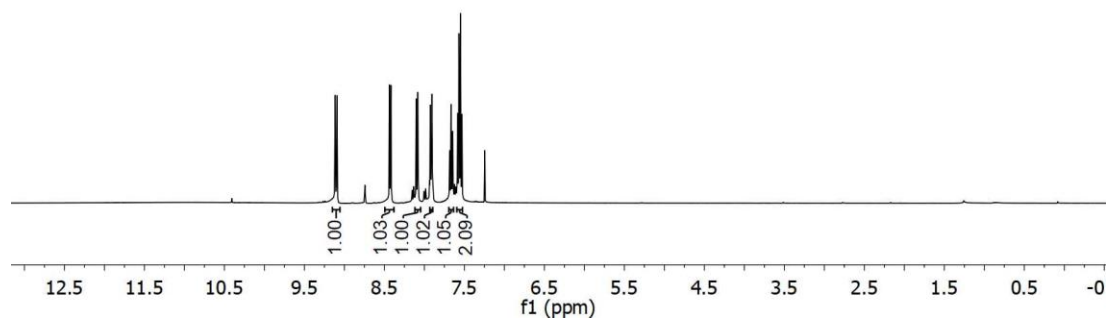
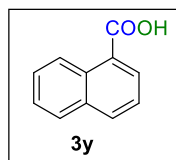


^1H and ^{13}C spectra of **3t**

Chapter III

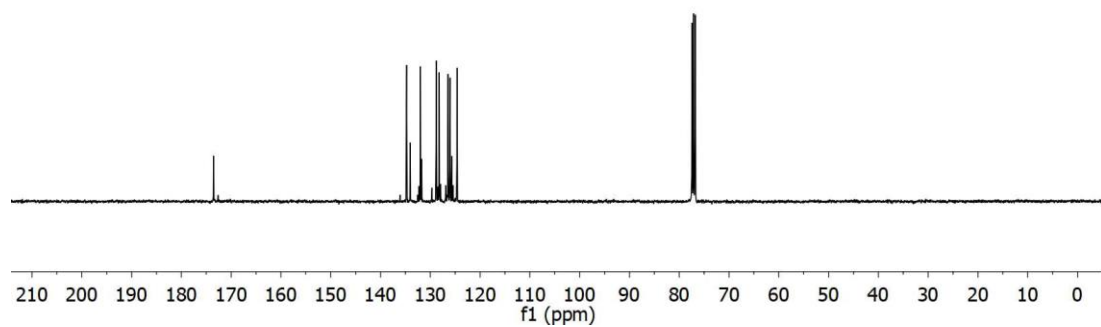
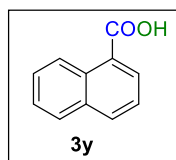
SNAN-1197 — single_pulse

9.114
9.093
8.437
8.434
8.419
8.416
8.102
8.081
7.925
7.904
7.687
7.684
7.670
7.666
7.662
7.649
7.645
7.584
7.568
7.549
7.530



SNAN-1197 — single pulse decoupled gated NOE

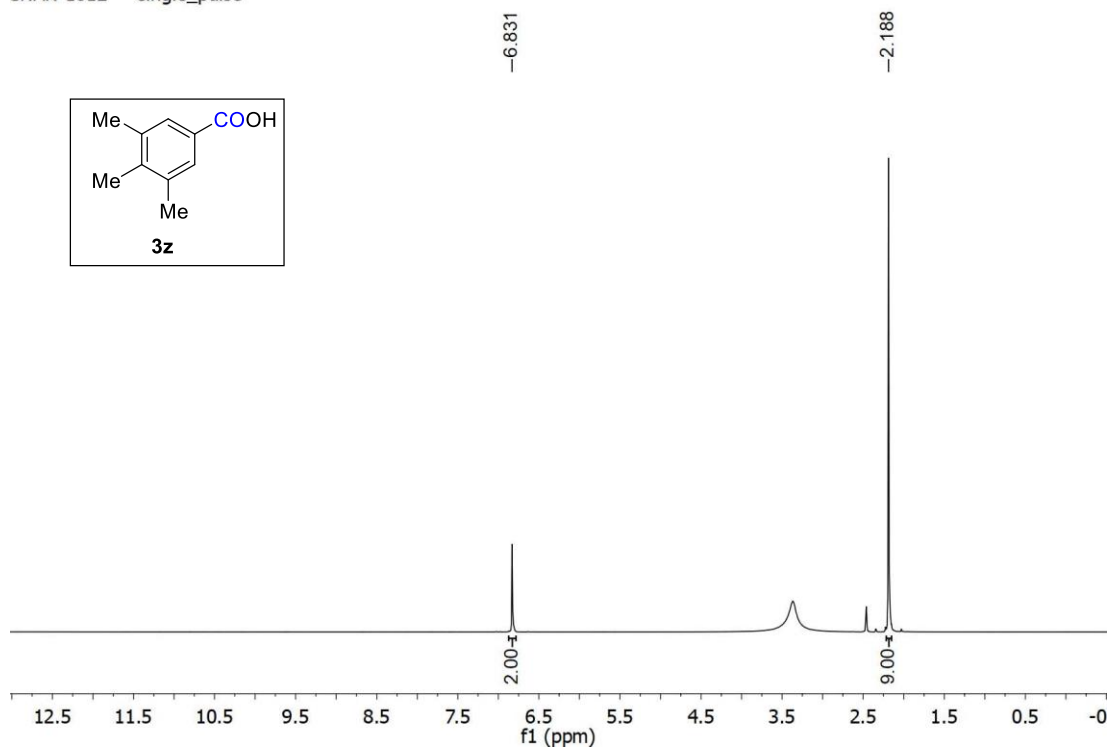
173.528
134.765
134.037
131.986
131.742
128.815
128.214
127.924
126.425
126.020
125.702
124.634



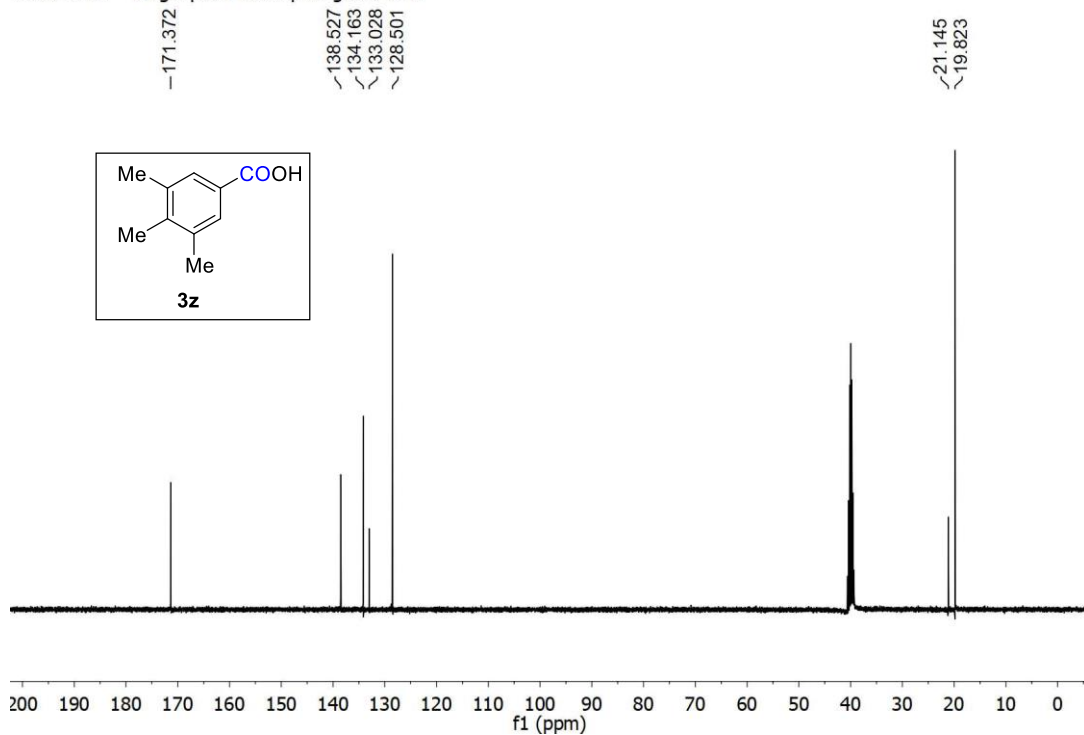
^1H and ^{13}C spectra of **3y**

One-pot Hydroxycarbonylation of Anilines *via* Diazonium Salt *en route* to Benzoic Acids:
Formic Acid as C-1 Source

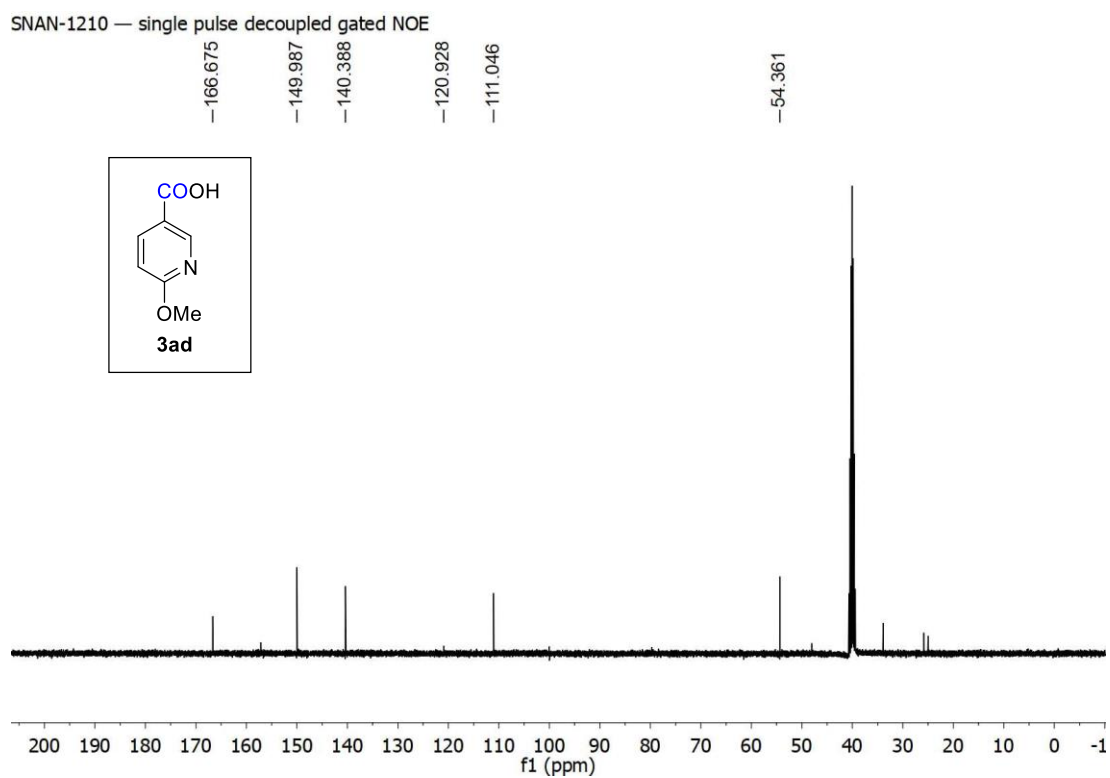
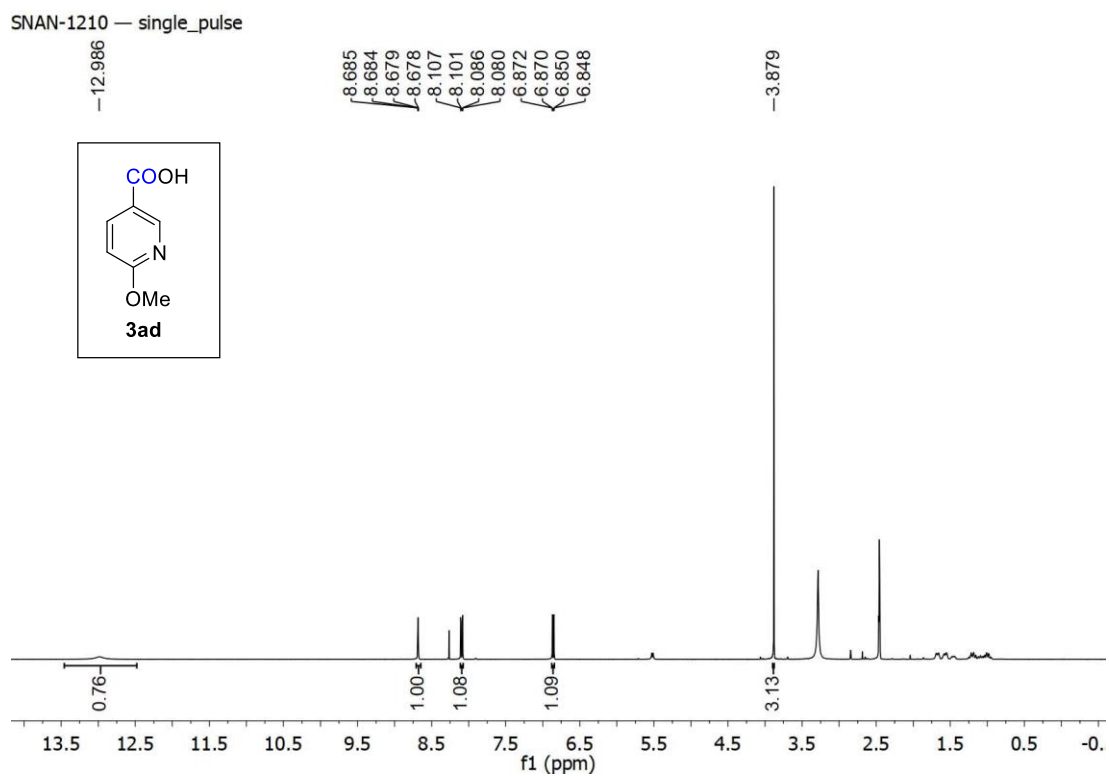
SNAN-1612 — single_pulse



SNAN-1612 — single pulse decoupled gated NOE

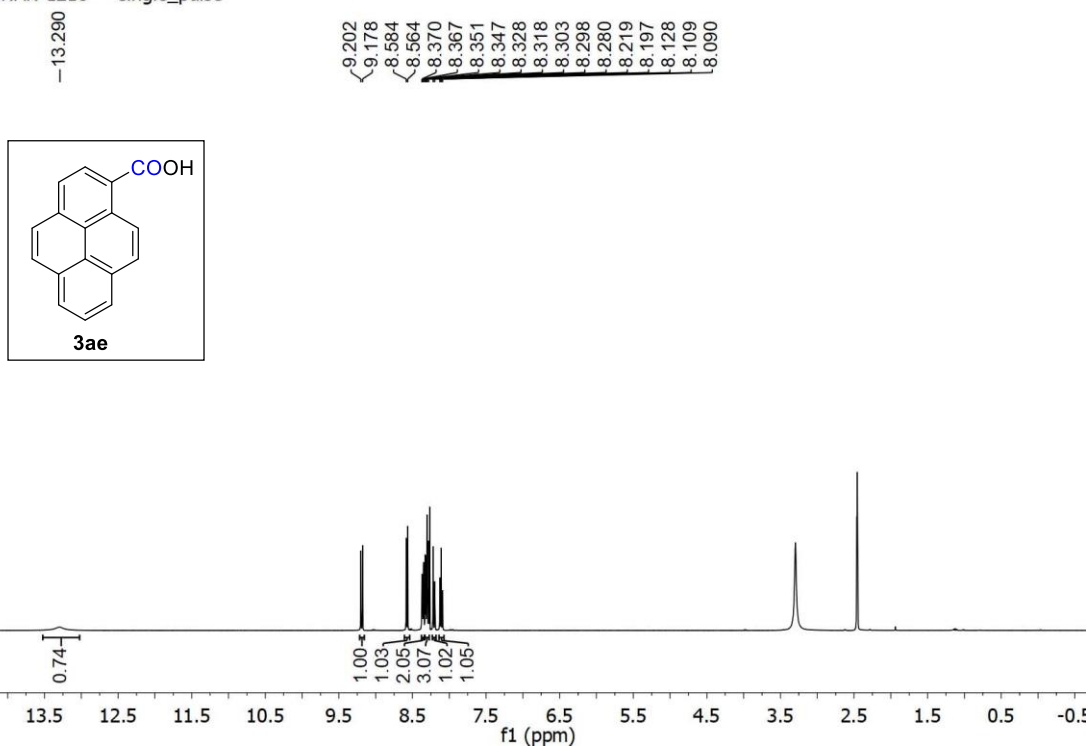


¹H and ¹³C spectra of **3z**

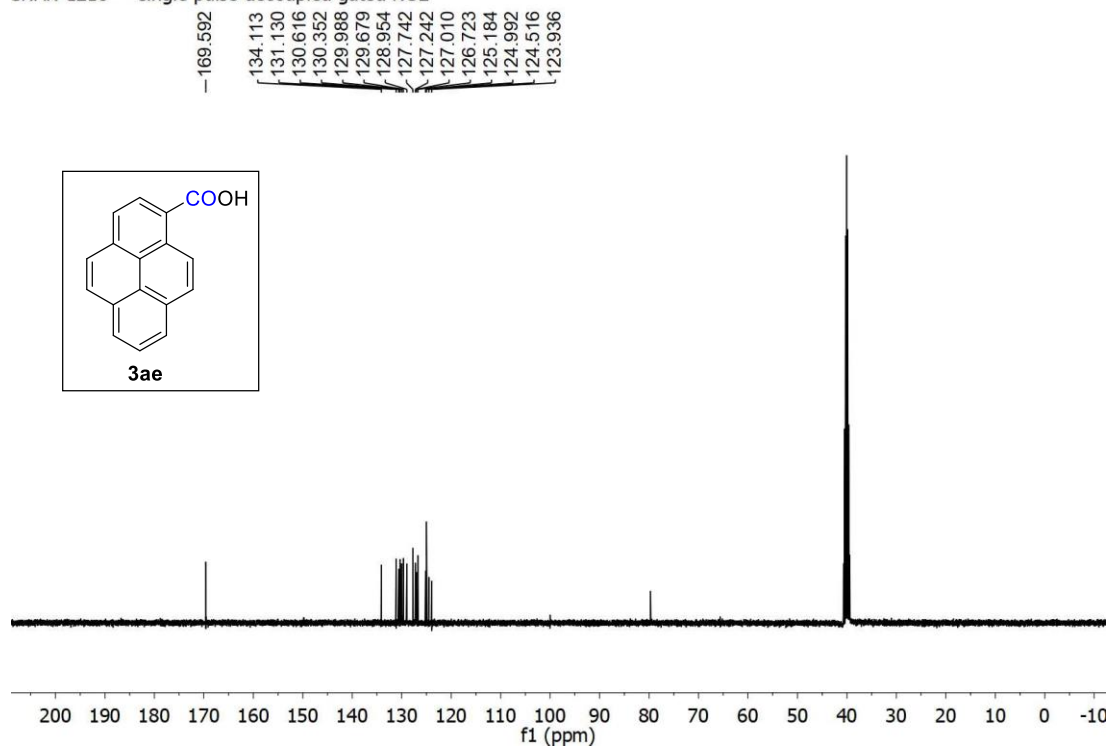
 ^1H and ^{13}C spectra of **3ad**

One-pot Hydroxycarbonylation of Anilines *via* Diazonium Salt *en route* to Benzoic Acids: Formic Acid as C-1 Source

SNAN-1218 — single_pulse



SNAN-1218 — single pulse decoupled gated NOE



¹H and ¹³C spectra of **3ae**

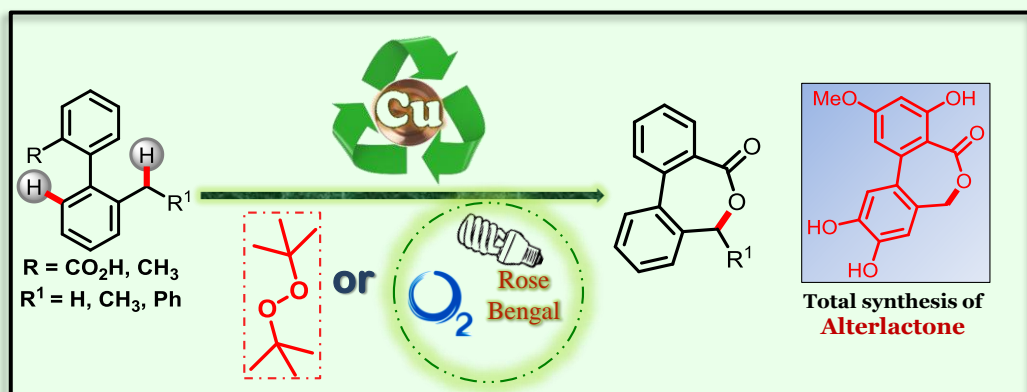
III.9. References

- (1) (a) Patai, S. In *Carboxylic Acids and Esters (1969)*, 1969; pp i-xiv; (b) Hajduk, P. J.; Bures, M.; Praestgaard, J.; Fesik, S. W. *J. Med. Chem.* **2000**, *43*, 3443-3447.
- (2) (a) Majumdar, N. *ACS Catal.* **2022**, *12*, 8291-8324; (b) Begam, H. M.; Nandi, S.; Jana, R. *Chem. Sci.* **2022**, *13*, 5726-5733; (c) Manna, K.; Begam, H. M.; Samanta, K.; Jana, R. *Org. Lett.* **2020**, *22*, 7443-7449; (d) Nandi, S.; Mondal, S.; Jana, R. *iScience* **2022**, *25*, 104341; (e) Dzik, W. I.; Lange, P. P.; Gooßen, L. J. *Chem. Sci.* **2012**, *3*, 2671-2678; (f) Rodríguez, N.; Goossen, L. J. *Chem. Soc. Rev.* **2011**, *40*, 5030-5048; (g) Gooßen, L. J.; Rodríguez, N.; Gooßen, K. *Angew. Chem. Int. Ed.* **2008**, *47*, 3100-3120; (h) Patra, T.; Maiti, D. *Chem. Eur. J.* **2017**, *23*, 7382-7401.
- (3) (a) Sam, D. J.; Simmons, H. E. *J. Am. Chem. Soc.* **1972**, *94*, 4024-4025; (b) Schmieder-van de Vondervoort, L.; Bouttemy, S.; Heu, F.; Weissenböck, K.; Alsters, Paul L. *Eur. J. Org. Chem.* **2003**, *2003*, 578-586; (c) Yamazaki, S. *Org. Lett.* **1999**, *1*, 2129-2132; (d) Wang, F.; Xu, J.; Li, X.; Gao, J.; Zhou, L.; Ohnishi, R. *Adv. Synth. Catal.* **2005**, *347*, 1987-1992; (e) Urgoitia, G.; SanMartin, R.; Herrero, M. T.; Domínguez, E. *Chem. Commun.* **2015**, *51*, 4799-4802; (f) Bastock, T. W.; Clark, J. H.; Martin, K.; Trenbith, B. W. *Green Chem.* **2002**, *4*, 615-617.
- (4) (a) Beller, M.; Wu, X.-F. *J. C. S. E. A. S.* **2013**; (b) Peng, J.-B.; Geng, H.-Q.; Wu, X.-F. *Chem* **2019**, *5*, 526-552; (c) Quintero-Duque, S.; Dyballa, K. M.; Fleischer, I. *Tetrahedron Lett.* **2015**, *56*, 2634-2650; (d) Wu, X.-F.; Fang, X.; Wu, L.; Jackstell, R.; Neumann, H.; Beller, M. *Acc. Chem. Res.* **2014**, *47*, 1041-1053; (e) Zechen Wu, C. C., Yanghui Zhang. **2021**, *41*, 2155-2174.
- (5) (a) Nandi, S.; Jana, R. *Asian J. Org. Chem.* **2022**, *2022*, e202200356; (b) Ran, C.-K.; Chen, X.-W.; Gui, Y.-Y.; Liu, J.; Song, L.; Ren, K.; Yu, D.-G. *Sci. China Chem.* **2020**, *63*, 1336-1351; (c) Matthesen, R.; Fransaer, J.; Binnemans, K.; De Vos, D. E. *Beilstein J. Org. Chem.* **2014**, *10*, 2484-2500; (d) Pradhan, S.; Roy, S.; Sahoo, B.; Chatterjee, I. *Chem. Eur. J.* **2021**, *27*, 2254-2269; (e) Zhang, G.; Cheng, Y.; Beller, M.; Chen, F. *Adv. Synth. Catal.* **2021**, *363*, 1583-1596; (f) Fan, Z.; Zhang, Z.; Xi, C. *ChemSusChem* **2020**, *13*, 6201-6218; (g) Yan, S.-S.; Fu, Q.; Liao, L.-L.; Sun, G.-Q.; Ye, J.-H.; Gong, L.; Bo-Xue, Y.-Z.; Yu, D.-G. *Coord. Chem. Rev.* **2018**, *374*, 439-463; (h) Tortajada, A.; Juliá-Hernández, F.; Börjesson, M.; Moragas, T.; Martin, R. *Angew. Chem. Int. Ed.* **2018**, *57*, 15948-15982; (i) Tsuji, Y.; Fujihara, T. *Chem. Commun.* **2012**, *48*, 9956-9964; (j) Davies, J.; Lyonnet, J. R.; Zimin, D. P.; Martin,

- R. *Chem* **2021**, *7*, 2927-2942; (k) Artz, J.; Müller, T. E.; Thenert, K.; Kleinekorte, J.; Meys, R.; Sternberg, A.; Bardow, A.; Leitner, W. *Chem. Rev.* **2018**, *118*, 434-504; (l) Grignard, B.; Gennen, S.; Jérôme, C.; Kleij, A. W.; Detrembleur, C. *Chem. Soc. Rev.* **2019**, *48*, 4466-4514; (m) Bhunia, S. K.; Das, P.; Nandi, S.; Jana, R. *Org. Lett.* **2019**, *21*, 4632-4637.
- (6) (a) Hartwig, J. F.; Shekhar, S.; Shen, Q.; Barrios-Landeros, F. In *PATAI'S Chemistry of Functional Groups*, 2009; (b) Mary, A.; Kanagathara, N.; Baby Suganthi, A. R. *Materials Today: Proceedings* **2020**, *33*, 4751-4755; (c) Leitch, J. A.; Frost, C. G. *Synthesis* **2018**, *50*, 2693-2706.
- (7) Majek, M.; Jacobi von Wangelin, A. *Angew. Chem. Int. Ed.* **2015**, *54*, 2270-2274.
- (8) Guo, W.; Lu, L.-Q.; Wang, Y.; Wang, Y.-N.; Chen, J.-R.; Xiao, W.-J. *Angew. Chem. Int. Ed.* **2015**, *54*, 2265-2269.
- (9) Gosset, C.; Pellegrini, S.; Jooris, R.; Bousquet, T.; Pelinski, L. *Adv. Synth. Catal.* **2018**, *360*, 3401-3405.
- (10) Cacchi, S.; Fabrizi, G.; Goggiamani, A. *Org. Lett.* **2003**, *5*, 4269-4272.
- (11) Shibahara, F.; Kinoshita, S.; Nozaki, K. *Org. Lett.* **2004**, *6*, 2437-2439.
- (12) Wang, Y.; Ren, W.; Li, J.; Wang, H.; Shi, Y. *Org. Lett.* **2014**, *16*, 5960-5963.
- (13) Hou, J.; Xie, J.-H.; Zhou, Q.-L. *Angew. Chem. Int. Ed.* **2015**, *54*, 6302-6305.
- (14) Fu, M.-C.; Shang, R.; Cheng, W.-M.; Fu, Y. *ACS Catal.* **2016**, *6*, 2501-2505.
- (15) Fu, M.-C.; Shang, R.; Cheng, W.-M.; Fu, Y. *Chem. Eur. J.* **2017**, *23*, 8818-8822.
- (16) Qi, X.; Li, C.-L.; Wu, X.-F. *Chem. Eur. J.* **2016**, *22*, 5835-5838.
- (17) Li, C.-L.; Qi, X.; Wu, X.-F. *ChemistrySelect* **2016**, *1*, 1702-1704.
- (18) Wu, F.-P.; Peng, J.-B.; Meng, L.-S.; Qi, X.; Wu, X.-F. *ChemCatChem* **2017**, *9*, 3121-3124.
- (19) Wu, F.-P.; Peng, J.-B.; Qi, X.; Wu, X.-F. *J. Org. Chem.* **2017**, *82*, 9710-9714.
- (20) Brancour, C.; Fukuyama, T.; Mukai, Y.; Skrydstrup, T.; Ryu, I. *Org. Lett.* **2013**, *15*, 2794-2797.

Chapter IV

Chemo- and Regioselective Benzylic C(sp³)-H Oxidation Bridging the Gap between Hetero- and Homogeneous Copper Catalysis

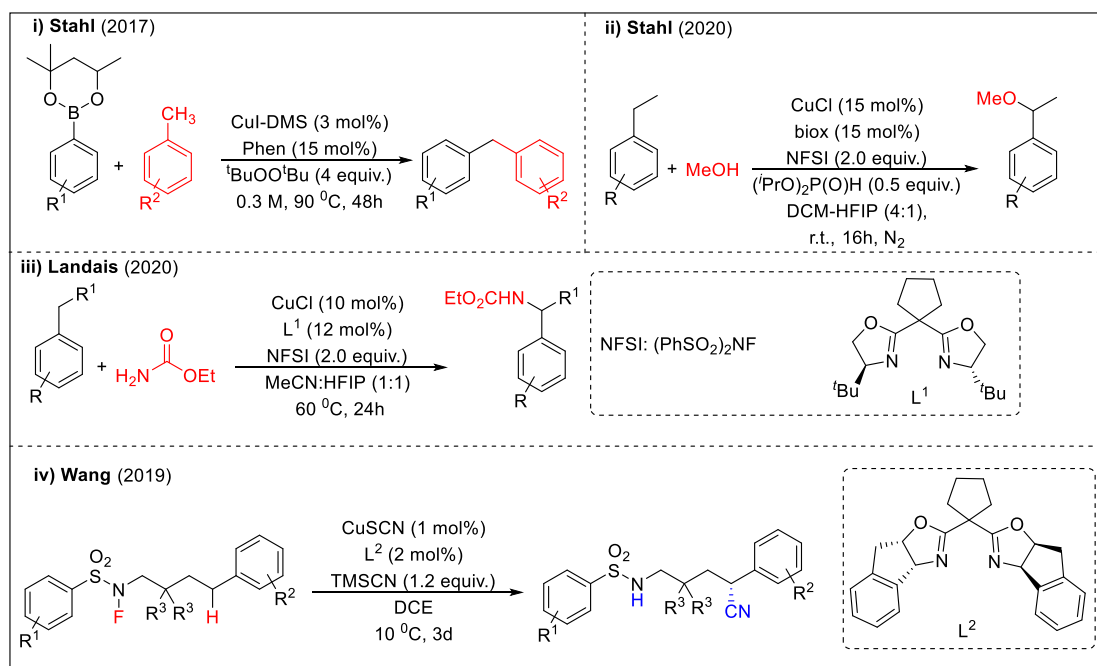


IV.1. Introduction

In spite of immense development of C–H functionalization reactions in the last two decades, attaining a particular regio-, chemo-, and stereoselective functionalization among more than one similar C–H bonds continues to be a daunting challenge.¹ So, nowadays, the foremost research area is executing chemo-, regio- and stereoselective transformation in a pool of vulnerable C–H bonds in nondirected fashion by judiciously developing the catalytic system.² In the last decade, we have witnessed several reports on intermolecular benzylic C–H acetoxylation with palladium,³ copper,⁴ iron⁵ catalysis or metal-free⁶ conditions via the formation of either an acyloxy radical species or a metal-carboxylate intermediate. Herein, we represent a benzylic C(sp³)-H benzyloxylation using a copper-catalyzed intramolecular C–H activation technique where the both benzylic C(sp³)-H and the benzoic acid moiety comes from the same substrate. Before going into detail, we would have a brief outlook on the previous developments for better understanding and present status of this field.

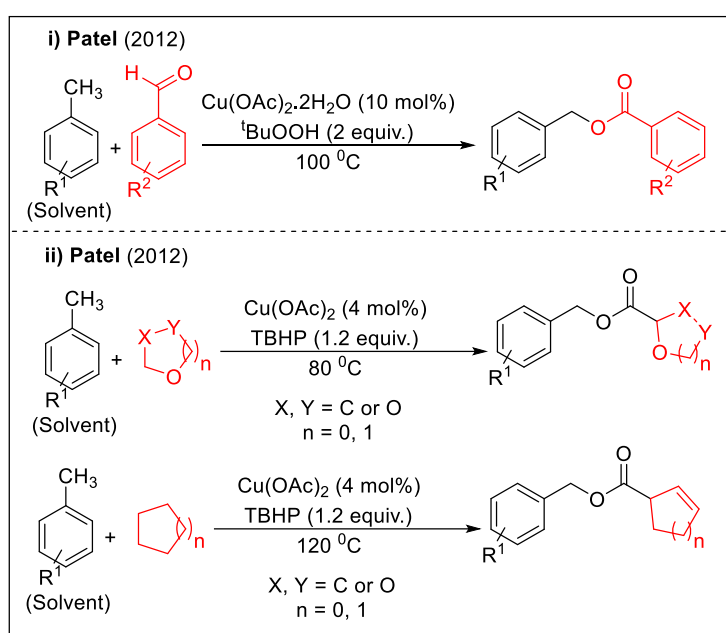
IV.2. Reviewing the previous developments

IV.2.1. Developments of transition-metal catalyzed benzylic C(sp³)-H activation reactions



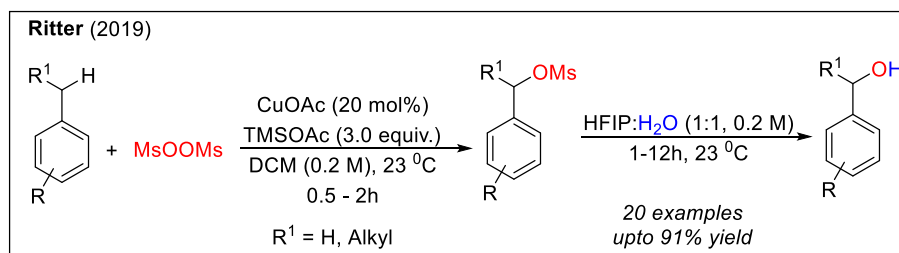
Scheme 1. Different copper-catalyzed benzylic C(sp³)-H activation reactions.

The Stahl and other groups performed intermolecular benzylic C(sp³)-H functionalization in feedstock chemicals with copper catalysis to synthesize pharmacophores (**Scheme 1**).⁷ In 2019, Stahl realized copper-catalyzed benzylic arylation from reaction between benzyl arenes and aryl boronic acids (**Scheme 1, i**). The same group, in 2020, executed benzylic etherification using alcohol as nucleophile (**Scheme 1, ii**). In similar manner, Landais realized benzylic amination from alkyl (2^o) arenes (**Scheme 1, iii**). In an interesting copper-catalyzed strategy, Wang and co-workers executed enantioselective cyanation of remote C(sp³)-H bond initiated by nitrogen-centered radical (**Scheme 1, iv**).



Scheme 2. Synthesis of benzylic esters via intermolecular C(sp³)-H activation.

The Patel group unveiled the synthesis of benzyl esters from surplus amount of methylarenes employing Cu(II)/TBHP system (**Scheme 2**).^{4, 8} In 2012, they synthesized benzylic esters from aldehydes and alkyl arenes using the latter as solvent.



Scheme 3. Access to benzylic alcohols directly from benzylic arenes.

Chemo- and Regioselective Benzylic C(sp³)-H Oxidation Bridging the Gap between Hetero- and Homogeneous Copper Catalysis

Continuing with this research, in 2014, in place of aldehydes, they used cyclic ethers or cycloalkanes to produce benzylic esters via four and six consecutive C(sp³)-H cleavages by copper catalysis. Recently, benzylic alcohols were directly synthesized from alkyl arenes by the Ritter group using bis(methanesulfonyl)peroxide as an oxidant with copper (II)-catalyst and subsequent hydrolysis (**Scheme 3**),⁹ which was a long cherished challenge to the chemists.

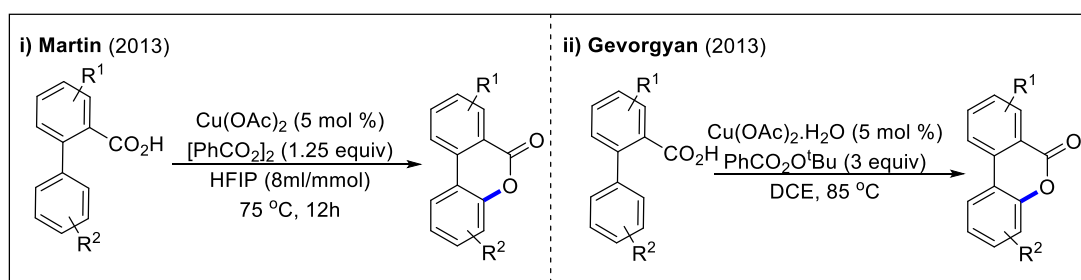
At all these developed methods, the alkyl arenes are required in large excess with respect to the other coupling partner. Still, affording selective coupling product via benzylic activation taking alkylarene in equimolar amount with the coupling partner remains very scarcely developed.

IV.2.2. Developments of intramolecular C-H activation reactions towards lactone synthesis

Alternatively, a reaction pattern has been lately emerged where starting from a substrate having a tethered carboxylic acid, intramolecular C-H oxidation is executed by using pendant carboxyl group as the coupling partner.¹⁰

IV.2.2.1. Metal catalyzed C(sp²)-H activation for lactone synthesis

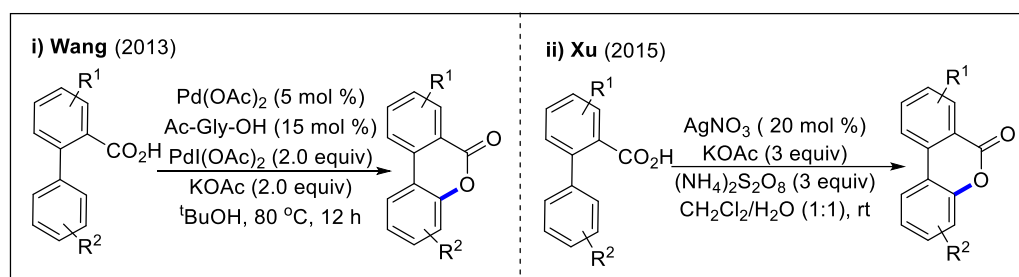
In 2013, Martin realized the intramolecular C(sp²)-H activation of *ortho*-aryl benzoic acid to synthesize six-membered lactones via copper catalysis using benzoyl peroxide (BPO) as oxidant (**Scheme 4, i**).¹¹



Scheme 4. Copper-catalyzed intramolecular C(sp²)-H activation towards 6-membered lactones.

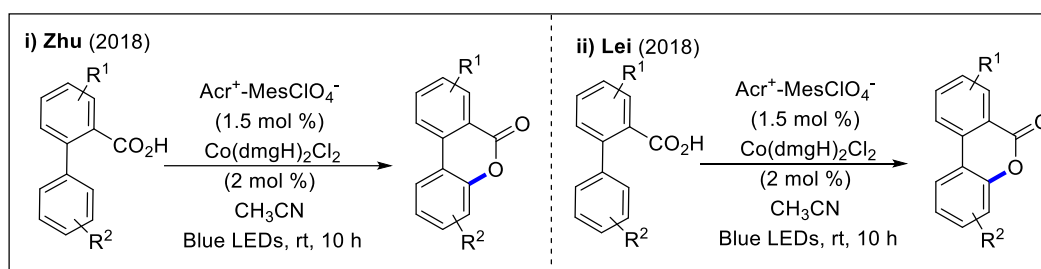
Subsequently, this protocol was extrapolated by several groups using other metals or metal-free conditions via the single electron activation of aryl carboxylic acids for the similar transformation.¹² Almost at the similar time of Martin's work, Gevorgyan reported similar Cu-catalyzed method (**Scheme 4, ii**).¹³ Pd(II)/Pd(IV)-catalyzed method (**Scheme 5, i**)^{12c} was

developed Wang. In 2015, the Xu group disclosed silver catalyzed approach with $(\text{NH}_4)_2\text{S}_2\text{O}_8$ as oxidant in open flask “Condition A” at room temperature (**Scheme 5, ii**).^{12a}



Scheme 5. Pd- and Ag-catalyzed intramolecular $\text{C}(\text{sp}^2)\text{-H}$ activation towards 6-membered lactones.

Subsequently, Zhu reported external oxidant free, mild, efficient Co/photoredox dual catalytic methodology (**Scheme 6, i**).¹²ⁱ At the same time, independently Lei group also reported similar strategy via Co/photoredox dual catalysis (**Scheme 6, ii**).^{12e} Several other reports are also available for this transformation with help of metal catalysis.



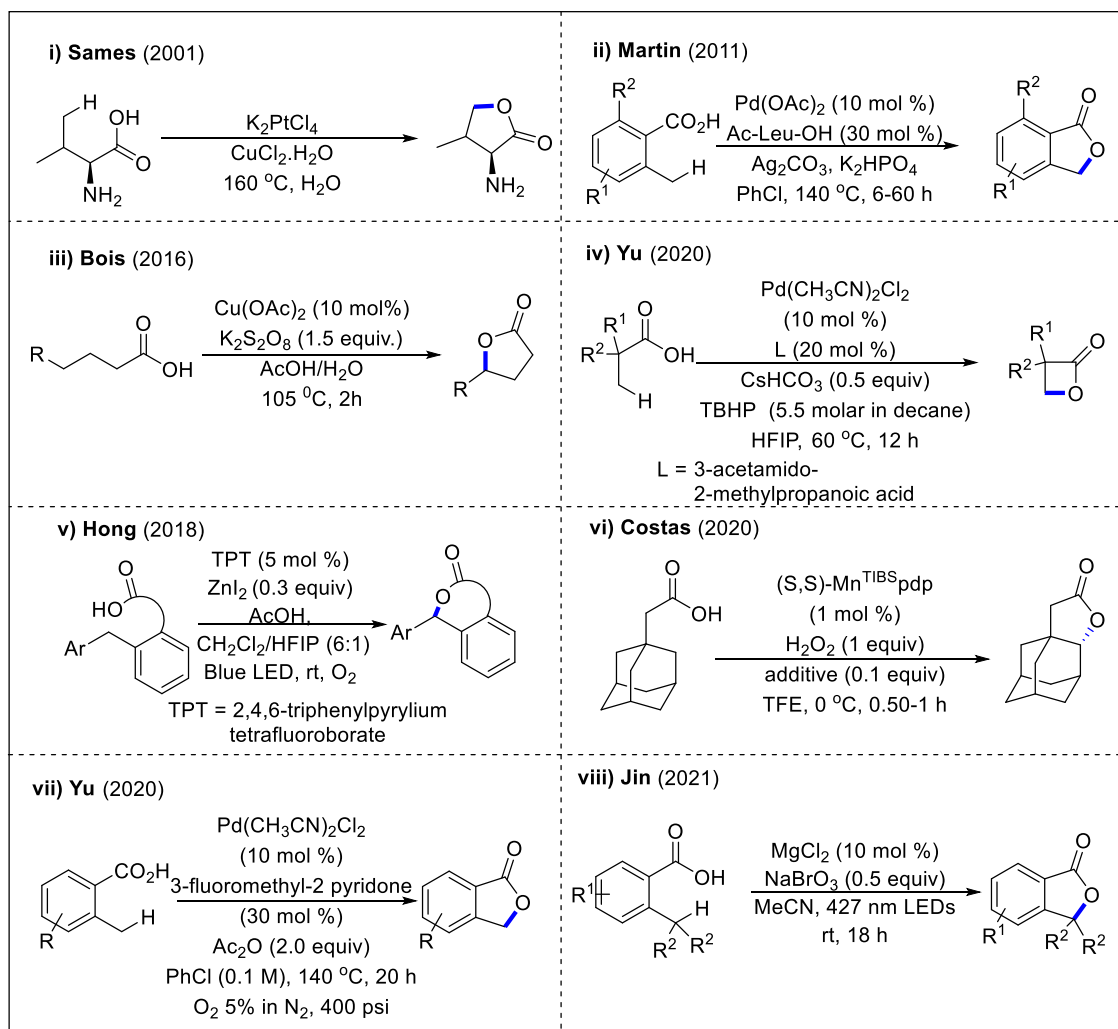
Scheme 6. Cobalt-photoredox dual catalyzed intramolecular $\text{C}(\text{sp}^2)\text{-H}$ activation towards 6-membered lactones.

IV.2.2.2. Metal catalyzed $\text{C}(\text{sp}^3)\text{-H}$ activation for lactone synthesis

The Bois group reported the synthesis of six and five-membered lactones by copper-catalyzed intramolecular benzylic C-H acetoxylation (**Scheme 7, iii**).¹⁴ The Sames group in 2001, synthesized lactone from L-valine in presence of aqueous K_2PtCl_4 and stoichiometric CuCl_2 as oxidant (**Scheme 7, i**).¹⁵ In 2011, Martin *et al.* reported Pd catalyzed, *N*-acyl protected amino acid assisted benzolactone formation from 2-alkyl benzoic acid derivatives (**Scheme 7, ii**).¹⁶ In 2020, Yu *et al.* developed lactonization of aliphatic acids through $\beta\text{-C}(\text{sp}^3)\text{-H}$ activation (**Scheme 7, iv**).^{10a} Visible light mediated γ/δ -lactonization was disclosed by Hong *et al.* using 2,4,6-triphenylpyrylium tetrafluoroborate as photocatalyst (**Scheme 7, v**).¹⁷ The Costas group reported Mn-catalyzed carboxylic acid directed $\gamma\text{-C-H}$ oxidation to construct γ -lactone in high enantiomeric excess (up to 99%) (**Scheme 7, vi**).¹⁸ Yu group in 2020, reported lactonization of

Chemo- and Regioselective Benzylic C(sp³)-H Oxidation Bridging the Gap between Hetero- and Homogeneous Copper Catalysis

2-methyl benzoic acid through Pd(II)/Pd(0) catalysis (**Scheme 7, vii**).¹⁹ Recently a practical, mild, visible light mediated magnesium catalyzed C(sp³)-H lactonization protocol from easily available 2-alkyl benzoic acid has been developed by Jin group (**Scheme 7, viii**).²⁰

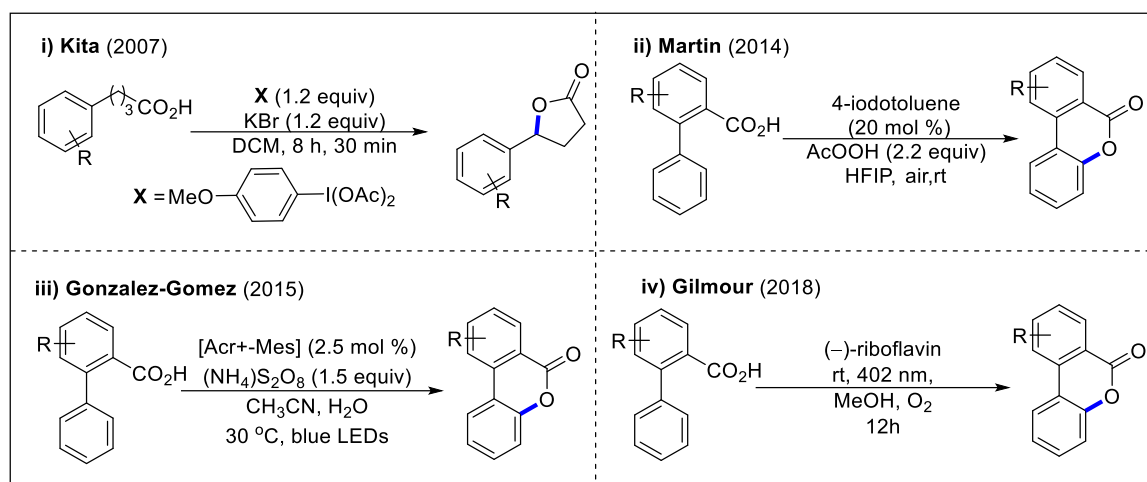


Scheme 7. Metal catalyzed C(sp³)-H activation for lactone synthesis.

IV.2.2.3. Metal-free catalyzed C-H functionalization for lactone synthesis

In 2007, the Kita group synthesized aryl lactones from benzoic acids and carboxylic acids using combination of hypervalent iodine with KBr (**Scheme 8, i**).²¹ Continuing with their own metal-catalyzed lactonization, Martin's group reported a mild, metal free protocol to synthesis of benzolactones from 2-aryl benzoic acids with using 4-iodotoluene as catalyst and stoichiometric amount of AcOOH as oxidant in HFIP solvent (**Scheme 8, ii**).²² A metal free, photocatalyzed dehydrogenative lactonization was reported by Gonzalez-Gomez (**Scheme 8, iii**).²³ In 2018, the Gilmour group developed an interesting photocatalyzed method for 6-

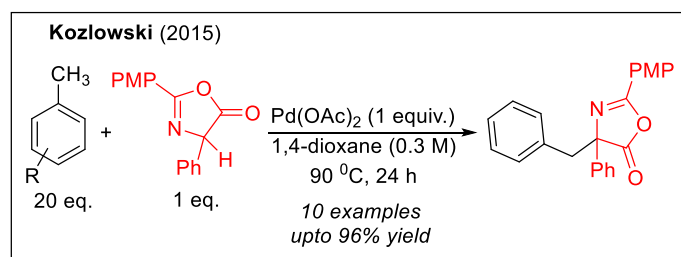
membered lactone synthesis via similar intramolecular C(sp²)-H lactonization using (-)-riboflavin as the photocatalyst (**Scheme 8, iv**).²⁴



Scheme 8. Metal-free catalyzed C-H functionalization for lactone synthesis.

IV.2.3. Chemoselective C(sp²)-H vs C(sp³)-H activation

Despite the fact that chemists have developed C-H functionalization methodologies extensively with soluble copper-complexes or CuNPs (copper-nanoparticles),²⁵ the economic use of simple copper(0) powder to achieve the same has rarely been reported, probably for the latter's poor solubility.²⁶ Besides, to achieve the cost effectiveness as well as high catalytic efficiency and selectivity, efforts are being given on the merger between homo- and heterogeneous catalysis.²⁷ Specifically, development of chemoselective sp² vs sp³ C-H activation has not been done with using inexpensive copper(0) powder as catalyst. Kozlowski group achieved this chemoselective sp² vs sp³ C-H activation in a single reaction with palladium-catalysis (**Scheme 9**).²⁸



Scheme 9. Chemoselective C(sp²)-H vs C(sp³)-H activation.

IV.2.4. Dibenzooxepinones and their synthesis

Chemo- and Regioselective Benzylic C(sp³)-H Oxidation Bridging the Gap between Hetero- and Homogeneous Copper Catalysis

Dibenzooxepinones are very important class of compounds as their analogs are prevalent in various natural products and bioactive chemicals with activity against tumors, cytotoxicity, tyrosine kinase inhibitors, and microtubules (**Figure 1**).²⁹

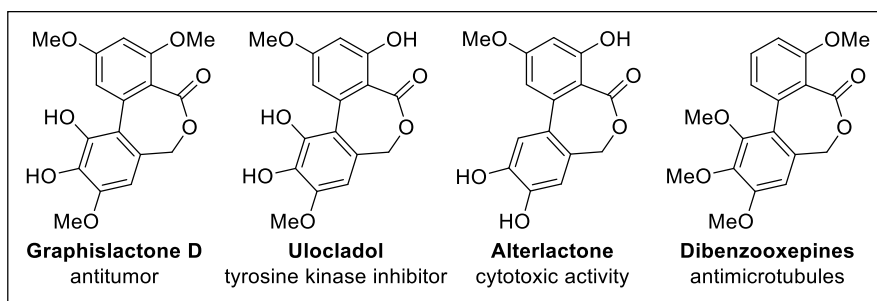
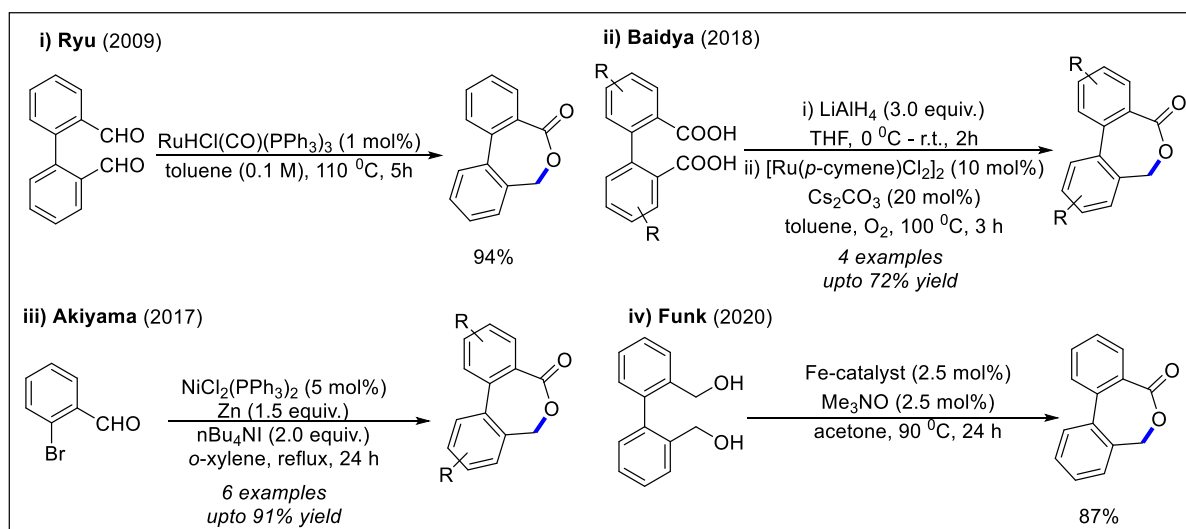


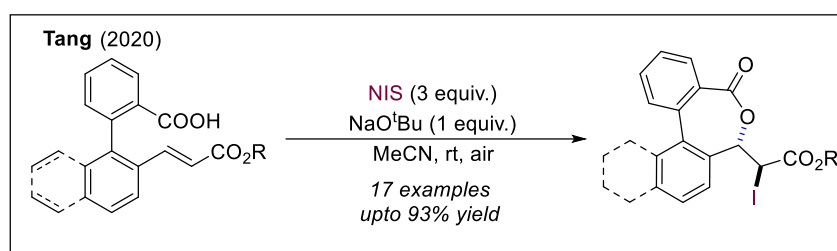
Figure 1. Naturally occurring dibenzooxepinones.

In most of the cases, this dibenzo[*c,e*]oxepin-5(7H)-one motifs are synthesized through a series of biaryl coupling and lactonization that forms C-O bonds. (Scheme 1b).³⁰ As presented in the **Scheme 10**, the procedures are limited to the oxidations of biaryl alcohols (Funk, 2020)^{30c}, aldehydes (Ryu, 2009; Akiyama, 2017)^{30b, 30d} or benzoic acids (Baidya, 2018)^{30a}. However, for lactone production, these techniques are either constrained to symmetrical biaryls or prefunctionalized benzyl alcohols.



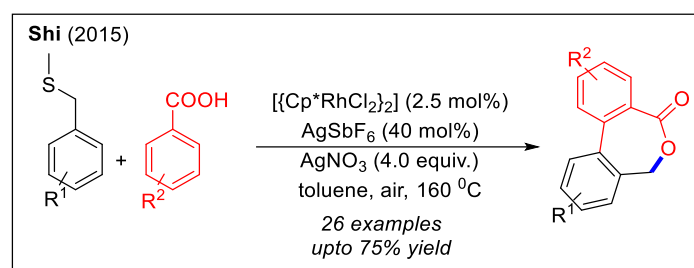
Scheme 10. Synthesis of symmetric dibenzooxepinones.

The Tang group recently revealed a elegant strategy to selectively produce 7-membered biaryl lactones where electron-deficient olefins were iodolactonized (**Scheme 11**).³¹



Scheme 11. Synthesis of symmetric dibenzooxepinones via lactonization.

In 2015, the Shi group disclosed a rhodium(III)-catalyzed method for cross-coupling between aryl carboxylic acids and benzyl thioethers to synthesize dibenzooxepinones (**Scheme 12**).³² Here, first the thioether directed C–H activation took place followed by the lactonization where the thioether group serve as a traceless directing group and is removed under the reaction condition. However, here prefuctionalization of benzylic position was required as benzyl thioethers were synthesized from the corresponding 1° benzylic bromide and the methodology was limited to 1° benzylic positions. Though, here dibenzooxepinones having different substitutions at two aryl rings are achievable, use of costly Rh catalyst, requirement of prefuctionalization and no reactivity for 2° benzylic position left this with ample scope for further improvement.



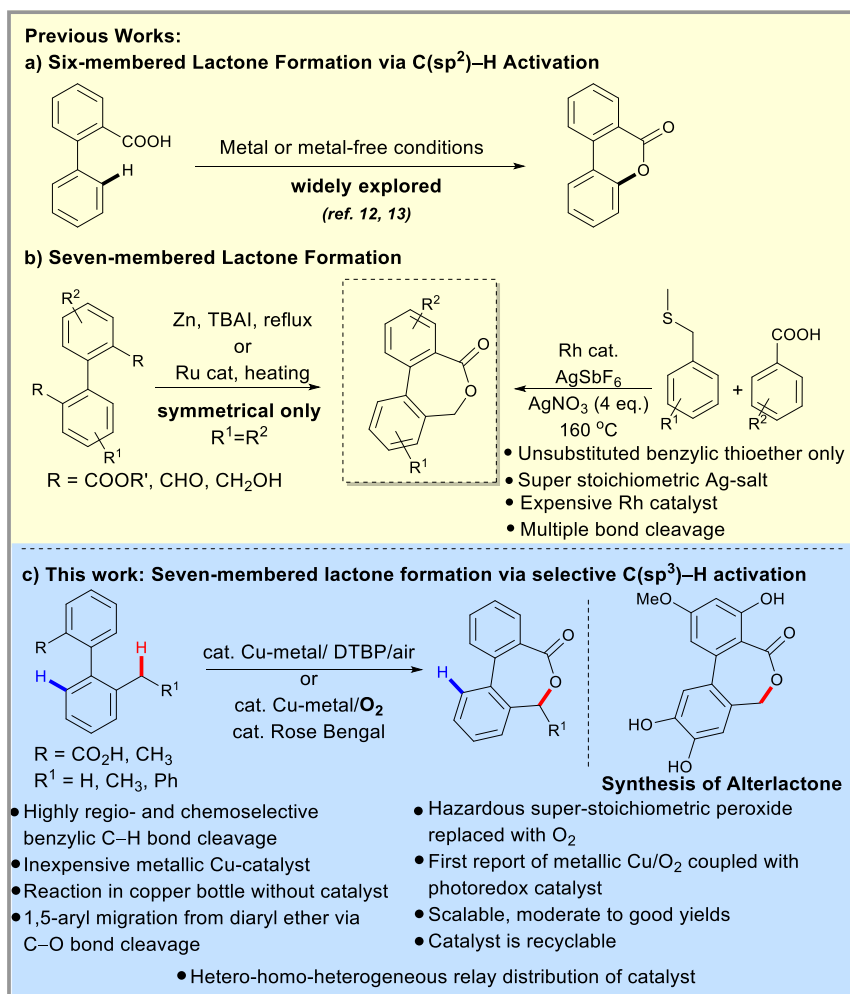
Scheme 12. Synthesis of unsymmetric dibenzooxepinones via Rh-catalyzed C–H activation.

IV.3. Present work

Surprisingly, the simple intramolecular benzylic C–H oxidation of a suitable biaryl carboxylic acid (**1**) that would result in the formation of seven-membered biaryl lactone has not been investigated. This could be possibly because of the immidiacy of unfavoured eight-membered metallacycle in case of seven-membered ring formation where six membered ring formation via arene C–H bond activation are facile for the involvement of favourable seven-membered metallacycle. However, energetically, benzylic C(sp³)–H bond (85-90 kcal/mole) is weaker than C(sp²)–H bonds (110-115 kcal/mole).^{28a, 33} Contrary to the traditional two electron approach, we hypothesized that single electron activation of the 2'-alkyl-[1,1'-biphenyl]-2-

Chemo- and Regioselective Benzylic C(sp³)-H Oxidation Bridging the Gap between Hetero- and Homogeneous Copper Catalysis

carboxylic acids followed by hydrogen atom transfer (HAT) might serve the purpose, thereby selectively supplying seven-membered lactones. If successful, this novel disconnection method might be used to synthesize a number of dibenzooxepinones, which are widely prevalent in pharmaceuticals and natural products. Intrigued by the precedents, we investigated an orthogonal reaction to produce dibenzooxepinones by intramolecularly oxidising the benzylic C(sp³)-H bonds of 2'-alkyl-[1,1'-biphenyl]-2-carboxylic acids **1** (Scheme 13).



Scheme 13. Development of intramolecular benzylic C(sp³)-H activation towards dibenzooxepinones.

Furthermore, fulfilling the hypothesis, similar dibenzo[*c,e*]oxepin-5(7H)-ones were produced from the 2,2'-dialkyl-substituted biaryls by taking advantage of the subtle difference in reactivity of the two alkyl groups from two different aryl rings. To delight, low-cost copper powder is used as an oxidant together with organic peroxide. It is fascinating that potentially dangerous peroxide has been substituted by molecular oxygen using a photocatalytic combination system of rose bengal, an organic photocatalyst, and copper powder. To the best

of our knowledge, bulk metallic copper/photocatalysis has been used for the first time here to couple O₂ in benzylic C(sp³)-H oxidation, despite their being publications for copper salt/photoredox³⁴ or copper/O₂ systems³⁵. Interestingly, the copper powder is converted into a reactive, substrate-bound, and soluble complex during the reaction to accomplish highly chemoselective sp² vs sp³ C-H oxidation (Scheme 1d). Through the cleavage of the ortho C-O bond, the corresponding biaryl ether undergoes 1,5-aryl shift with the assistance of a carboxylic acid radical. Finally, using just simple filtration, the precipitated heterogeneous catalyst is collected and reutilized for further runs, providing the advantages of both homo- and heterogeneous catalyst.

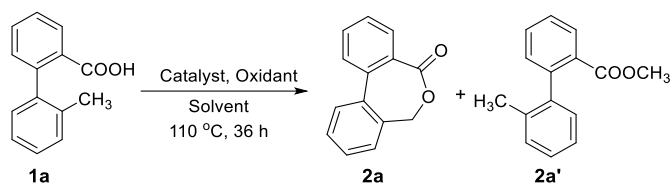
IV.4. Results and discussion

We had chosen 2'-methyl-[1,1'-biphenyl]-2-carboxylic acid **1a** as the model substrate to understand and optimize the condition for benzylic C(sp³)-H activation competing with C(sp²)-H activation (**Table 1, Part A**). Delightedly, employing catalytic CuI with 2 equiv. of DTBP (di-tert-butyl peroxide), we were able to produce 52% of our desired product **2a** as well as the 25% of corresponding methyl ester **2a'** (Entry 1).³⁶ It could be presumed that the radical-radical interaction of the carboxyl radical and the methyl radical produced from the DTBP results in the formation of **2a'**. Solvents, metal catalysts, and oxidants were rigorously studied to increase the yield of **2a** and subsequently decrease the generation of **2a'**. After optimization of the solvents, the optimum solvent was discovered to be α,α,α -trifluorotoluene. Surprisingly, we discovered that copper(II) catalysts and other oxidants including TBHP and TBPB performed worse than copper(I)/DTBP (Entry 7, 9). After that, we concentrated on using low-cost copper(0) metal as a catalyst, which finally would be oxidised *in situ* to higher oxidation states. To our delight, DTBP was successfully used with metallic copper (mesh size < 420 μ m) to produce **2a** in 82% yield along with 12% **2a'** after heating at 110 °C for 36 hours (Entry 11, **Table 1**). We hypothesised that the methyl radical may be trapped by the use of an external radical trapping agent to hinder the generation of **2a'** (**Entry 11**). According to the hypothesis, adding 2.0 equiv of TEMPO prevented the production of **2a'** while improving yields of the targeted lactone product **2a** to 83% (Entry 12). Notably, identical yields were obtained for the reaction using commercial copper nanoparticles (CuNPs) with a 25nm particle size (Entry 10). Argon or oxygen atmosphere diminished the yield (Entry 14, 15). To mention, we employed TEMPO for only a small number of substrates those yielded a substantial amount of the ester product with condition of Entry 11, since in spite of reducing the side reaction, it did not increase the yield of **2a** considerably.

Chemo- and Regioselective Benzylic C(sp³)-H Oxidation Bridging the Gap between Hetero- and Homogeneous Copper Catalysis

Up to this point, although it was possible to synthesize 7-membered lactones under acceptable synthetic conditions, one of the fundamental problems of using super stoichiometric amounts of peroxide—its explosive character in the development of large-scale processes, remains an unresolved issue. Not only that, if we are successful in getting rid of DTBP, we would be able to avoid the formation of detrimental methyl ester **2a'**.

Table 1. Optimization for intramolecular benzylic C(sp³)-H activation towards dibenzooxepinones



Entry	Catalyst (20 mol %)	Oxidant	Solvent	Yield (%) 2a/2a'
Part A. With peroxide as oxidant				
1	CuI	DTBP (2.0 eq)	DCE	52/25
2	CuI	DTBP (2.0 eq)	PhCl	60/27
3	CuI	DTBP (2.0 eq)	PhCF ₃	65/20
4	Cu(OAc) ₂	DTBP (2.0 eq)	PhCF ₃	46/35
5	Cu(OTf) ₂	DTBP (2.0 eq)	PhCF ₃	41/32
6	CuO	DTBP (2.0 eq)	PhCF ₃	35/40
7	CuI	TBHP (2.0 eq)	PhCF ₃	40/38
8	CuI	BPO (2.0 eq)	PhCF ₃	20/0
9	CuI	TBPB (2.0 eq)	PhCF ₃	38/20
10	CuNPs	DTBP (2.0 eq)	PhCF ₃	80/18
11	Cu(0)	DTBP (2.0 eq)	PhCF₃	82/12
12 ^c	Cu(0)	DTBP (2.0 eq)	PhCF ₃	83/0
13 ^d	Cu(0)	DTBP (2.0 eq)	PhCF ₃	69/0
14 ^e	Cu(0)	DTBP (2.0 eq)	PhCF ₃	75/18
15 ^f	Cu(0)	DTBP (2.0 eq)	PhCF ₃	56/27
Part B. With gaseous O₂ as oxidant				
16	Cu(0)	O ₂ (purged)	PhCF ₃	20/0
17 ^g	Cu(0)	O ₂ (purged)	PhCF ₃	20/0
18 ^h	Cu(0)	O ₂ (purged)	PhCF ₃	ND
19 ⁱ	Cu(0)	O ₂ (purged)	PhCF ₃	10/0
20 ^j	Cu(0)	O ₂ (purged)	PhCF ₃	Trace
21 ^k	Cu(0)	O ₂ (purged)	PhCF ₃	ND
22 ^l	Cu(0)	O ₂ (purged)	PhCF ₃	30/0
23 ^m	Cu(0)/EY	O ₂ (purged)	PhCF ₃	45/0
24^m	Cu(0)/RB	O₂ (purged)	PhCF₃	72/0
25 ^m	Cu(0)/ Ru(bpy) ₃ Cl ₂	O ₂ (purged)	PhCF ₃	35/0
26 ^{l,m}	Cu(0)/RB	O ₂ (purged)	PhCF ₃	50/0

^aAll reactions were carried out in 0.2 mmol scale. ^bYields refer to here are overall isolated yields. ^cadditional amount of 2 eq. TEMPO. ^dadditional 2 eq. BHT. ^eunder Ar atmosphere. ^funder O₂ atmosphere. ^gadditional 30 mol% of Et₃N. ^hadditional 30 mol% of ethylenediamine. ⁱadditional 30 mol% of pyridine. ^jadditional 30 mol% of Bpy. ^kadditional 30 mol% of terpyridine. ^ladditional 30 mol% of TMEDA was used. ^munder 32 W CFL

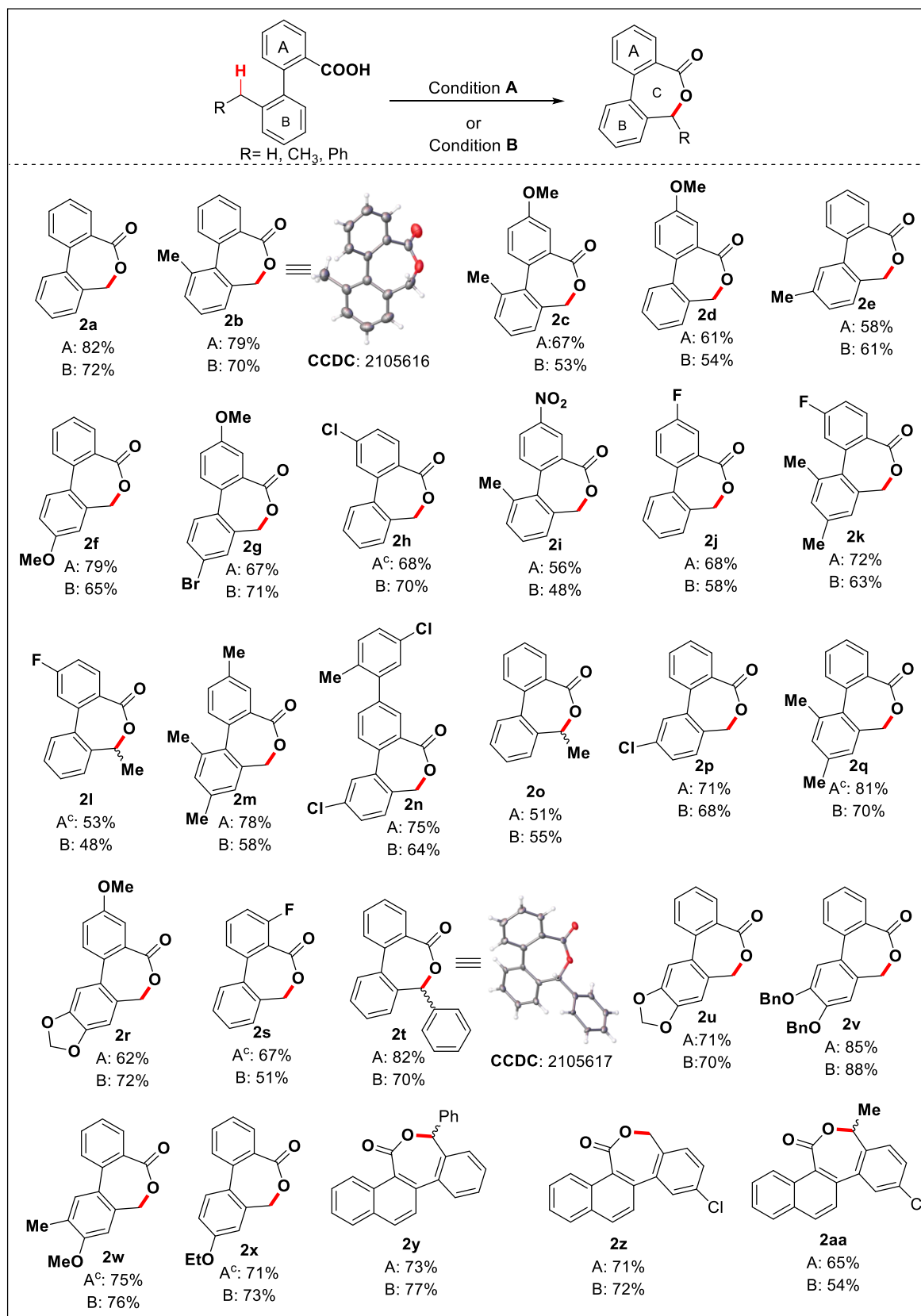
Fascinated by the intriguing works by Powers³⁷, Freakley³⁸ and others³⁹ on capturing molecular oxygen, we hypothesized that combining aerial oxygen as a terminal oxidant for this conversion would be synthetically viable and appealing (**Table 1, Part B**). During investigation, it was found that treating **1a** at 110 °C under oxygen atmosphere using catalytic copper powder in PhCF₃ produced 20% of the desired product **2a** (Entry 16). The yield was not further increased by additionally using several nitrogen-containing ligands (Entry 17-22). Rueping and others have shown how metal-catalyzed C–H activations/oxidations could be performed with molecular oxygen merging with visible light photoredox catalysis.⁴⁰ In this line, we concentrated on readjusting the reaction conditions under the light-mediated dual catalytic conditions with copper and one photosensitizer. Gratifyingly, irradiating **1a** with white CFL (46 W) at 110 °C, applying just 1 mol% eosin Y (EY) along with catalytic copper powder under oxygen atmosphere yielded **2a** in 45% (Entry 23). After systematic screening of other photocatalysts, it was found that 1 mol% rose bengal (RB) (Entry 24) increased the yield of **2a** to 72% and the unreacted substrate was recovered. We had accepted this as another optimized condition for using molecular oxygen as oxidizing agent and denoted it as “Condition B”, where the optimized condition with DTBP as oxidant was represented as “Condition A”. And with these both conditions, generality of the substrates were checked.

Substrate scope

To test the scope of this lactonization under these optimal conditions, the necessary biaryl substrates containing methyl and carboxylic acid at the 2,2'-positions were synthesized by Suzuki-Miyaura cross-coupling. Gratifyingly, the benzylic oxidation process produced seven-membered lactones in good to moderate yields from a variety of substrates, as demonstrated in **Table 2**.

Chemo- and Regioselective Benzylic C(sp³)-H Oxidation Bridging the Gap between Hetero- and Homogeneous Copper Catalysis

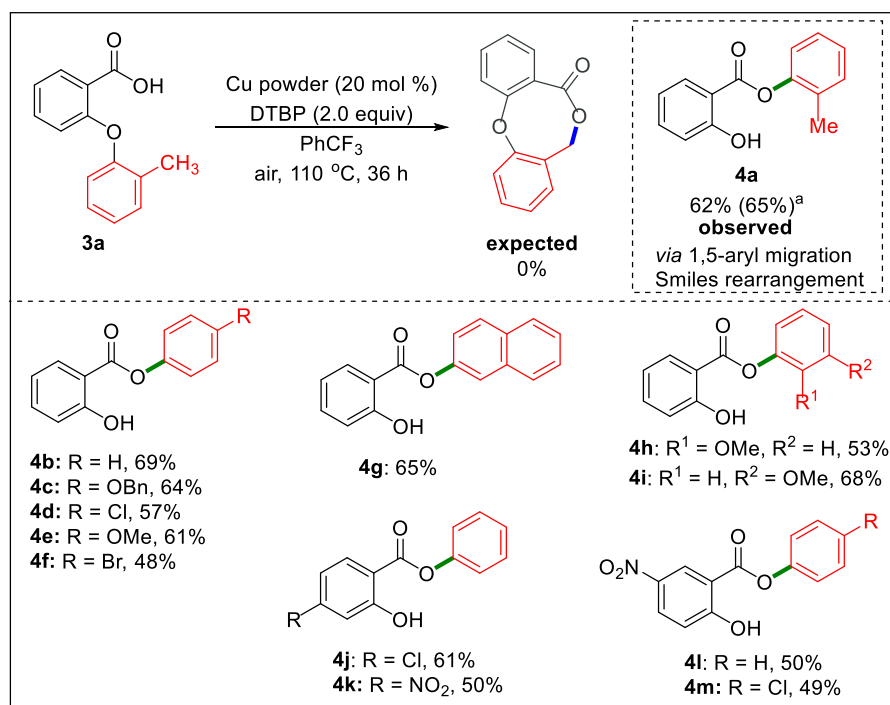
Table 2. Substrate scope of Dibenzo[*c,e*]oxepin-5(7*H*)-ones ^{a,b}



“Condition A”: 20 mol% Cu, 2.0 equiv. DTBP, PhCF₃, 110 °C, air, 36-48 h. “Condition B”: 20 mol% Cu, 1 mol% Rose Bengal, PhCF₃, 110 °C, O₂, 32 W CFL, 36-48 hrs. ^aAll reactions were carried out in 0.2 mmol scale. ^bYields refer to the overall isolated yields. ^cadditionally 2.0 equiv TEMPO was used

On both rings A and B, electron-donating groups such as Me, OMe, OEt, and OBn provided average to good yields. (2b-g, 2m, 2q, 2r, 2v-2x, Table 2). Substrates bearing electron withdrawing groups including F, Cl, and NO₂ afforded moderate to good yield of the products (2h-l, 2n, 2p, 2s, 2z, 2aa, Table 2). It's interesting to note that aryl- and ethyl-substituted diarylmethanes also underwent the expected reaction chemo- and regioselectively (2l, 2o, 2t, 2y, 2aa, Table 2), which was a shortcoming in earlier C–H activation techniques..^{30a, 32} Better yields were achieved from diarylmethanes (1t, 1y), most likely as a result of two aryl groups activating the one benzylic C–H bond. Notably, substrates with multiple methyl groups only reacted at the ortho benzyl moiety, leaving the other methyl groups unaffected (2b, 2e, 2i, 2k, 2m, 2n, 2q, 2w, Table 2).

Unexpected Smiles rearrangement while attempting towards 8-membered lactone



Condition: 20% Cu, 2 equiv DTBP, PhCF₃, 110 °C, air, 36 h. All reactions were carried out in 0.2 mmol scale. Yields refer to the overall isolated yields. ^ain 0.5 mmol scale

Scheme 14. Smiles rearrangement.

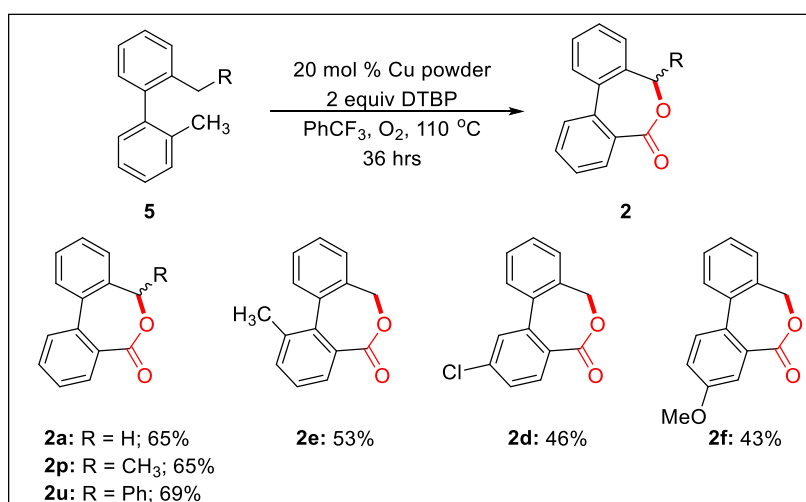
Chemo- and Regioselective Benzylic C(sp³)-H Oxidation Bridging the Gap between Hetero- and Homogeneous Copper Catalysis

Thus, carboxylic acid could play a significant role in the intramolecular benzylic C-H activation that leads to the production of the seven-membered lactone.

We synthesised the corresponding biaryl ether **3a** and tested the reaction under “Condition A” in order to discover whether the production of an 8-membered lactone was feasible. Surprisingly, contrary to the formation of anticipated product **4a'**, Smiles’ rearrangement product 2-hydroxyphenyl 2-methyl benzoate **4a** was produced in 62% yield (**Scheme 14**). Earlier, our group and others have reported that this Smiles type rearrangement produces and involves a carboxyl radical for C–O bond cleavage and 1,5-aryl migration.⁴¹ The range of 2-aryloxybenzoic acids with various substituents on both the aryl benzoic acid and phenol components was then investigated. These compounds delivered moderate to good yields under the reaction condition (**Scheme 14**). Similar yields were also obtained by reproducing the procedure at 0.5 mmol scale, which was a serious obstacle under our previous condition (**4a**, **Scheme 14**).^{41a}

Double benzylic C(sp³)-H activation leading to dibenzooxepinones

We envisaged that the 2,2'-alkyl biaryls might be converted into the same lactone product **2a** by properly regulating the reactivities between of two different alkyl moieties, where one of them would be converted into the carboxylic acid while another one would be activated selectively to give the similar reactivity as **1a** did. This led us to prepare 2,2'-dimethyl-1,1'-biphenyl (**5a**) and subjecting it to “Condition A”.



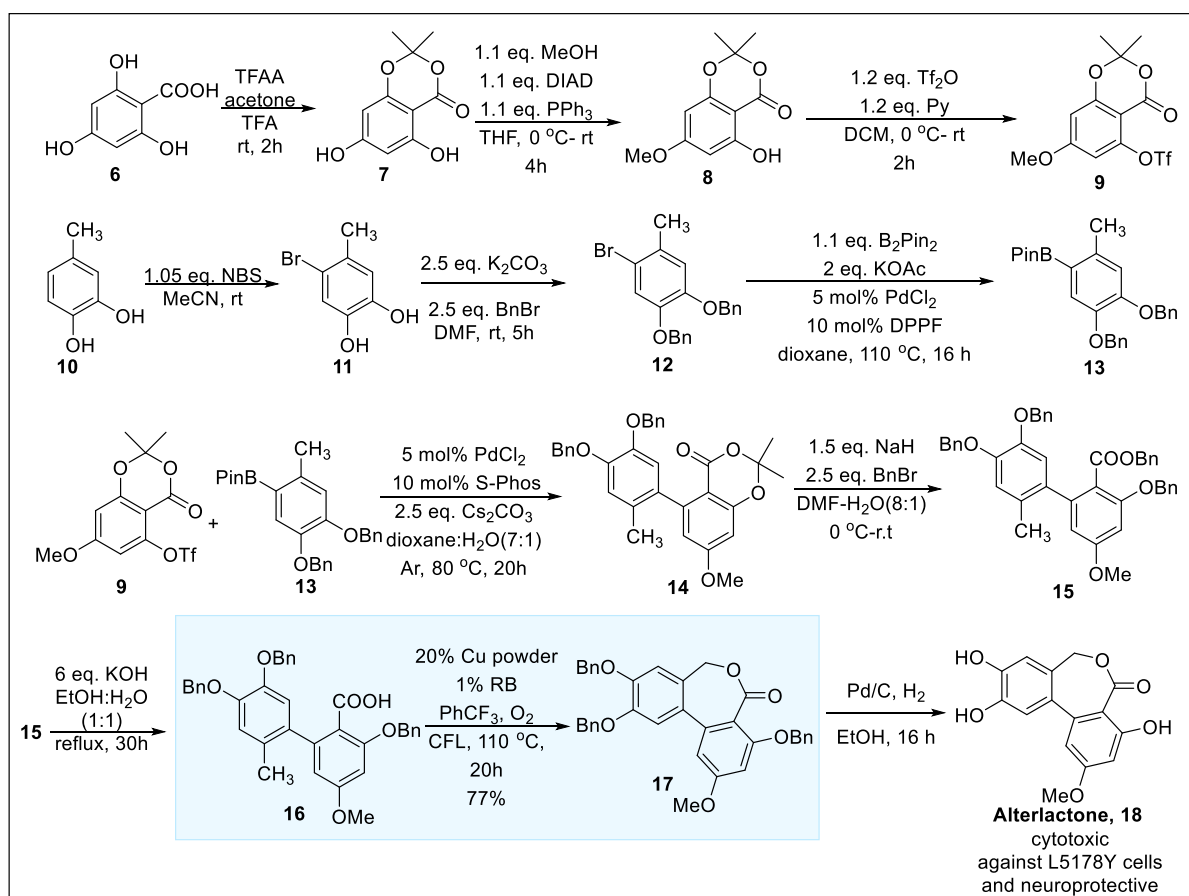
Reaction condition: 20% Cu, 2 equiv DTBP, PhCF₃, 110 °C, O₂, 36 h. All reactions were carried out in 0.2 mmol scale. Yields refer to the overall isolated yields.

Scheme 15. Lactonization through double benzylic C-H activation.

Fortunately, the anticipated 7-membered lactone **2a**—which is produced by cleaving the benzylic C–H bond four times—was obtained in 52% yield. The yield was increased even more, reaching 65% while the system was purged with O₂ (Scheme 15). In addition to unsubstituted benzyl, the desired product was also produced by the selective oxidation of methyl to carboxylic acid on phenyl- and methyl-substituted substrates. Interestingly, when unsummetrical biary substrates were taken, the corresponding lactone products were produced in modest amounts via the generation of carboxylic acid from CH₃, Cl, OMe substituted-aryl methyls (Scheme 15). Lower isolated yields were found for **5d-f** where the substrates were also could not be recovered. This is because an inseparable mixture of products probably caused by the lactonization of the other methyl group, was obtained.

Total synthesis of Alterlactone: Demonstrating the synthetic utility of the methodology

Alterlactone⁴² is a natural product comprising of dibenzooxepinones and is normally extracted from endophytic fungi *Alternaria sp.* This has been proven to be Nrf2 activator in PC12 cells, neuroprotective⁴³ cytotoxic against L5178Y cells.^{29b}



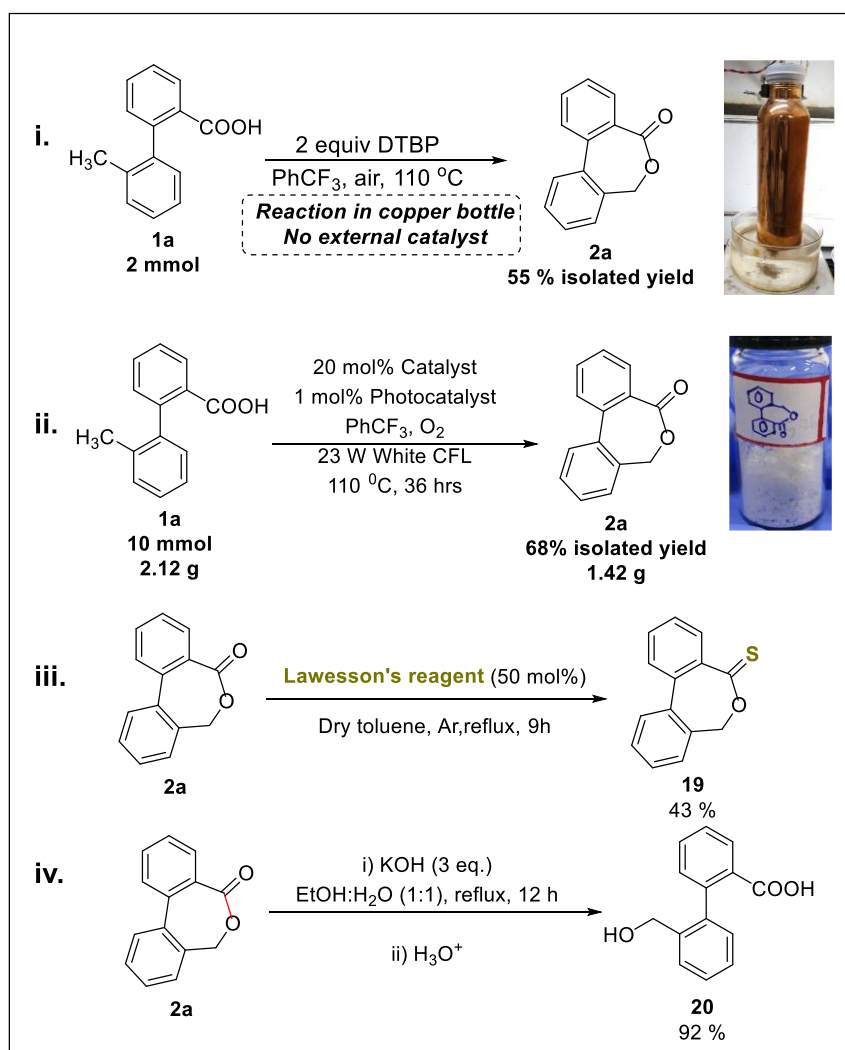
Scheme 16. Total synthesis of Alterlactone.

Chemo- and Regioselective Benzylic C(sp³)-H Oxidation Bridging the Gap between Hetero- and Homogeneous Copper Catalysis

Starting with acetal-protected phloroglucinol acid and 3,4-hydroxytoluene, we were able to synthesize Alterlactone **18** in 10 steps (Scheme 16). We used our light-mediated dual catalytic methodology in this total synthesis at a late stage, which led to the dibenzooxepinone **17** to give Alterlactone **18** on global deprotection of three benzyl groups. This method is cost effective compared to the earlier synthetic method⁴², ours is more affordable for the use of low-cost copper(0)-catalyst.

Strategic demonstration and derivatization of product

Thereafter, we had hypothesized that if the reaction was performed in a copper-vessel, it might occur even without adding any external copper-catalyst just by scratching the vessel's wall.



Scheme 17. Practical demonstration and product derivatization.

Gratifyingly, the model substrate **1a** conducted the reaction efficiently in a 2.0 mmol scale under “Condition A”, resulting in 55% isolated yield of **2a** (Scheme 17, i). The model reaction was then carried out in 10 mmol scale under “Condition B” to test the scalability. Delightedly, the reaction was robust and provided 68% of the expected product **2a** (Scheme 17, ii). Dibenzo[*c,e*]oxepin-5-thione **19**, a radical polymerization initiator⁴⁴, was produced in 43% yield by thiolating dibenzo[*c,e*]oxepin-5-one **2a** with 0.5 equiv Lawesson's reagent (Scheme 17, iii). Finally, the corresponding benzyl alcohol **20** was produced in 92% yield by base hydrolysis of compound **2a** (Scheme 17, iv).

Different substrates showing diverse reactivity

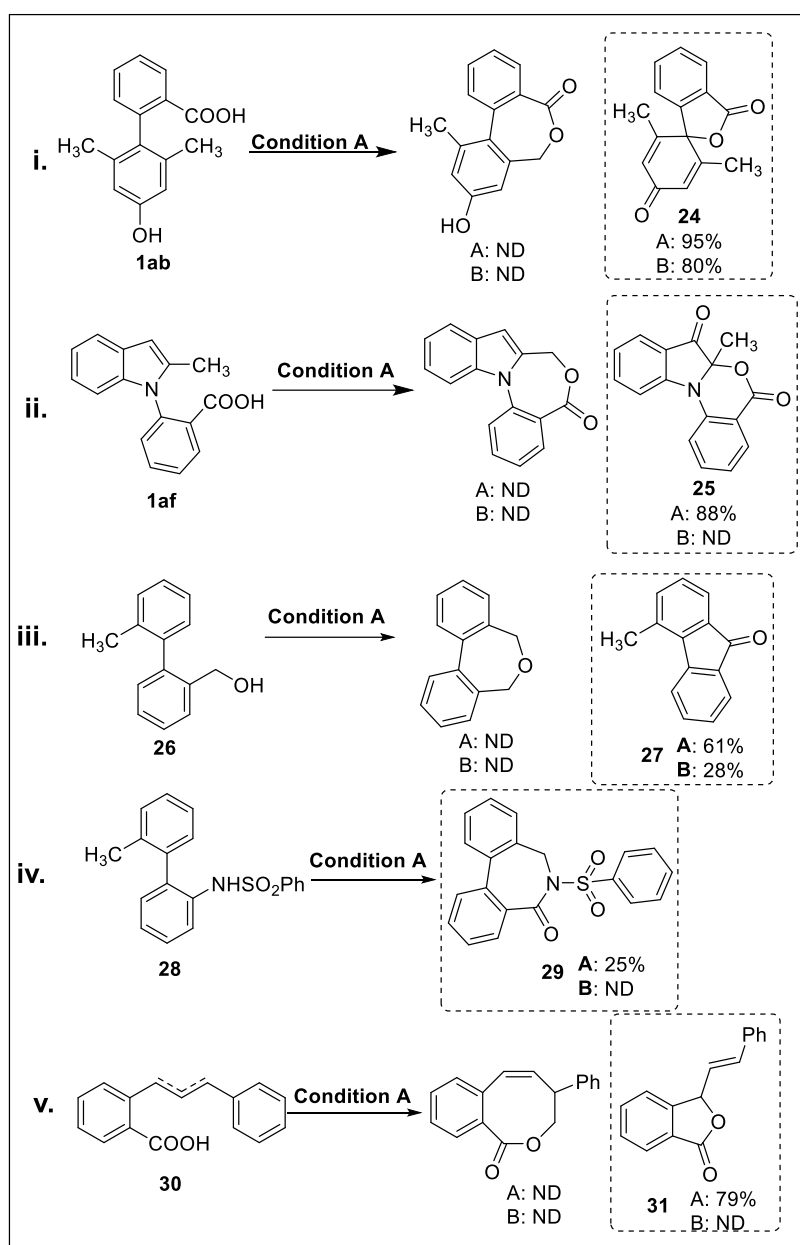
A variety of reactions were conducted to examine the compatibility of the designed catalytic systems to variously designed substrates (Scheme 18). It is interesting to note that substrate **1ab** underwent dearomatization to produce spiro lactone **24** instead of giving the desired eight membered lactone. In reaction under “Condition A” (Scheme 18, i), indole **1af** underwent activation of C(sp²)-H, which produced 6-membered indole dione **25** via subsequent oxidation at the C-3 position and dearomatization (Scheme 18, ii). When benzyl alcohol was taken in place of benzoic acid, i.e., substrate **26**, oxidation produced fluorenone **27** via C(sp²)-H activation instead of the seven membered lactone via C(sp³)-H activation (Scheme 18, iii). Intriguingly, seven membered lactam **29** was afforded from the benzenesulfonamide **28** via C(sp³)-H activation under “Condition A” (Scheme 18, iv). With our constant effort to broaden the reaction scope towards eight-membered lactone²⁰, we started with substrate **30**, but it also showed different reactivity to afford five-membered lactone **31** selectively instead of providing the desired one (Scheme 18, v). Thus, these results opened a broad arena for a diverse synthetic protocol for five and seven-membered lactone synthesis via C-H activation.

Mechanistic study

We conducted a number of control and spectroscopic studies to understand the underlying cause of the high degree of chemoselectivity.

Radical quenching experiment

During optimization, we noticed that the methyl-radical produced by the decomposition of DTBP caused methyl ester **3a**.



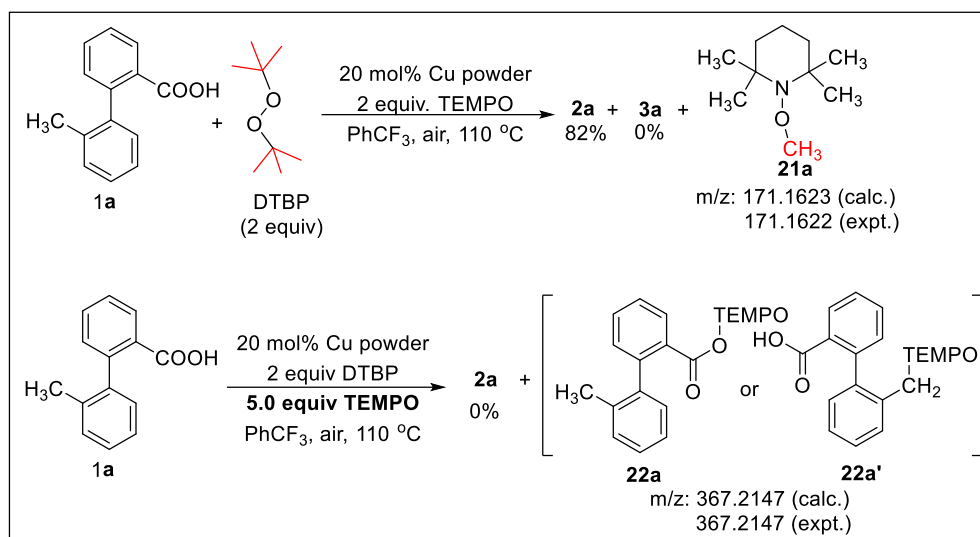
Scheme 18. Diverse reactivities.

By adding 2.0 equiv of TEMPO under optimal reaction conditions, this esterification was completely stopped, and an aliquot of the reaction mixture was taken that detected the TEMPO methyl radical adduct by ESI-MS (**Scheme 19**). A TEMPO adduct with **1a** (M+-H) at benzylic or carboxylate (**22a** or **22a'**) position was found in the ESI-MS (**Scheme 19**) and the expected reaction to give **2a** was completely suppressed.

Understanding selectivity between competitive C(sp²)-H and C(sp³)-H activation

It's interesting to note that under the Martin's reaction condition,¹¹ only the 6-membered lactone **23a** was produced in 72% by selective C(sp²)-H activation from **1a**.

Contrastingly, , we have been able to produce 7-membered lactone **2a** selectively under “Condition A” and B in 82% and 72% yields respectively (**Scheme 20, i**).



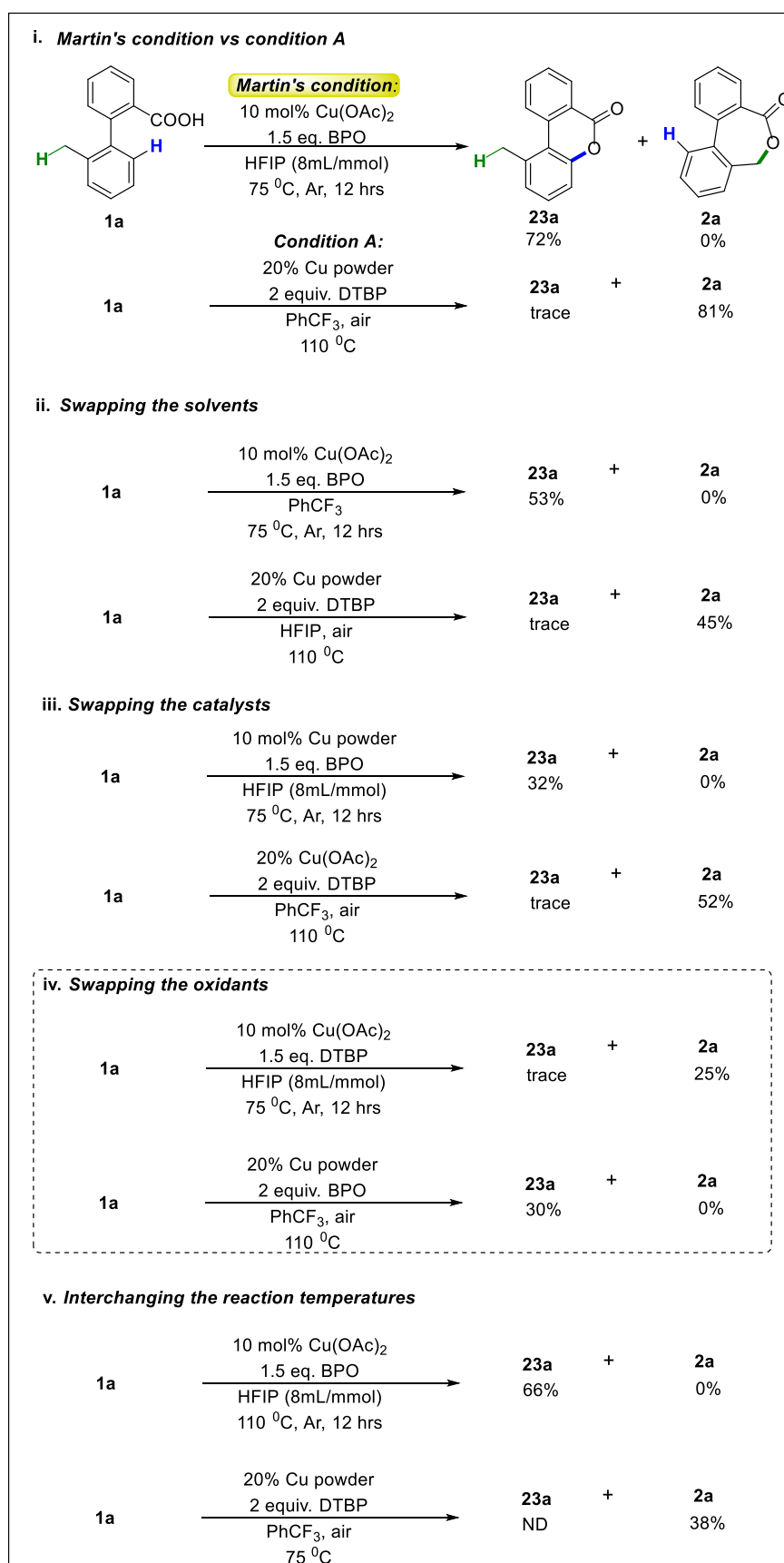
Scheme 19. Radical quenching experiment.

We observed that, for this chemoselectivity, not only the energy difference (sp^2 C–H bond vs benzylic sp^3 C–H; 110-115 vs 85-90 kcal/mole),³³ but the character of radical initiator cum oxidant might be quite important. We discovered from rigorous control investigations (**Scheme 20**) that external oxidants such as DTBP, TBHP, and TBPB those could produce at least one equivalent of methyl radical were efficient for benzylic C(sp^3)–H activation. Therefore, BPO was unsuccessful in our trial, in contrast to Martin's condition where it was an effective oxidant for activating the C(sp^2)–H bond. From here, we can conclude that the methyl radical produced by β -methyl scission of the tert-butyl oxo radical could lead to the selective weak benzylic C–H bond cleavage and methane production. While in situ produced benzoyl or phenyl radicals (through decarboxylation) likely favor C(sp^2)–H bond activation. Further investigation is necessary to understand the cause of the chemoselectivity in our established peroxide-free “Condition B”.

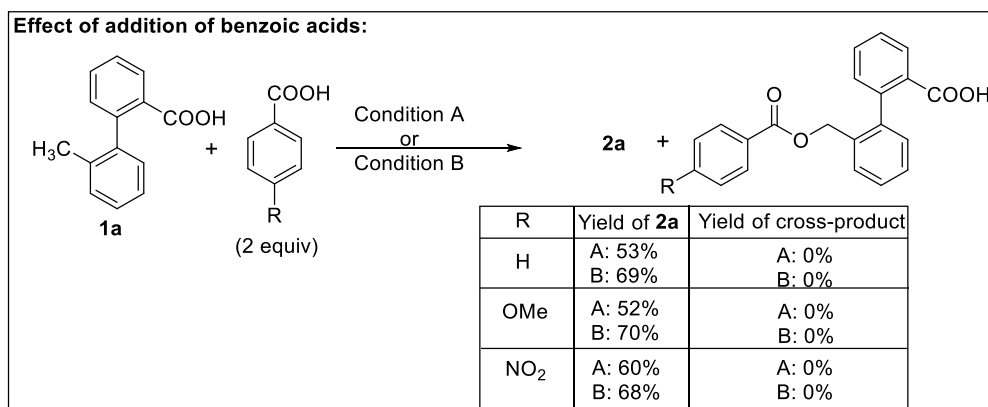
Addition of external substituted benzoic acids

Super stoichiometric (2.0 equiv) amount of benzoic acid was added to the reaction mixture under both conditions A and B to determine whether the reaction occurs via inner- or outer-sphere copper complex.

Chemo- and Regioselective Benzylic C(sp³)-H Oxidation Bridging the Gap between Hetero- and Homogeneous Copper Catalysis



Scheme 20. Competitive reactivities between C(sp²)-H and C(sp³)-H activation.



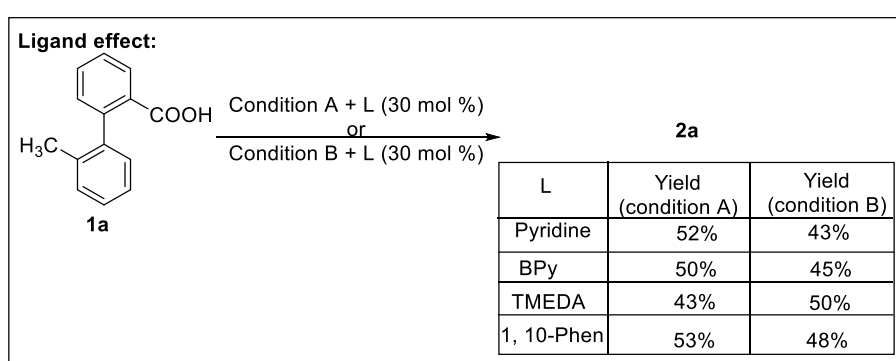
Scheme 21. Addition of external substituted benzoic acids.

Surprisingly, only the required lactonization products in modest yields were produced via intramolecular reaction and no intermolecular benzoylation compounds were detected. Similar outcomes were also achieved by electronically rich 4-methoxy or electronically poor 4-nitro benzoic acid (**Scheme 21**).

Addition of external N-containing ligands

Furthermore, common external ligands such as pyridine, bipyridine, 1,10-phenanthroline, TMEDA etc. effected negatively in the reaction outcome (**Scheme 22**) suggesting that copper

might generate an inner sphere soluble complex binding with the substrate **1a** which was further supported by the spectroscopic studies.



Scheme 22. Addition of external N-containing ligands.

Visual colour change during reaction

We were curious to understand the genesis of the active catalyst and its oxidation state as insoluble copper(0) powder was utilized as the initial catalyst. Under the “Condition A” (**Figure 2**)⁴⁵, we observed a evident colour change in the reaction medium.

Chemo- and Regioselective Benzylic C(sp³)-H Oxidation Bridging the Gap between Hetero- and Homogeneous Copper Catalysis

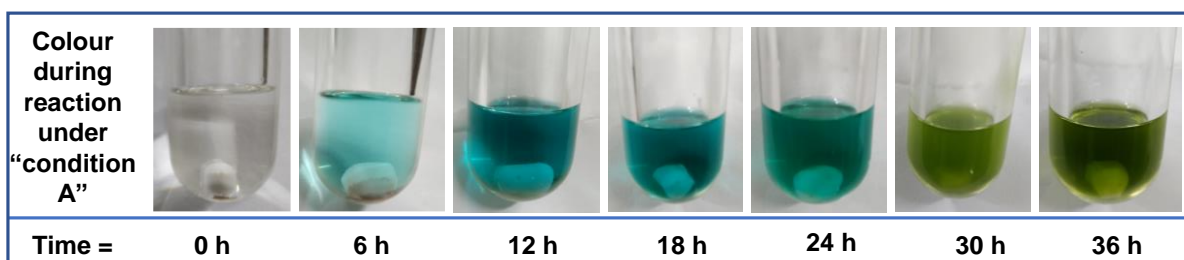


Figure 2. Visual colour change during the reaction under “Condition A”.

After 6 hours, the insoluble Cu powder visually changed into slightly suspended particles and took on a bright blue coloration. After 12 hours, it changed into an intensely blue, transparent solution, indicating the appearance of Cu(II)-species. Finally, the solution returns to being turbid and greenish.

UV-Vis experiment

“Condition A”: At 3 hour intervals, we recorded UV-Vis absorption spectra from the reaction mixture in order to unambiguously confirm the presence of Cu(II) species. After 3 hours, the distinctive Cu(II) peak at 684 nm developed, and its intensity increased as the reaction progressed (**Figure 3**)⁴⁶. The following spectra is from the standard reaction with “Condition A”. Aliquots were taken at 1h, 3h, 6h, 12h, 18h. We can visualize the formation of Cu(II) clearly from the spectra which comes at 684nm. The formation started from 1h itself and after 3h, it shows intense signature peak. We have shown the UV-Vis absorption peak of pure substrate also which comes at 274 nm and that of pure copper too which is insoluble in the solvent, hence does not show any peak.

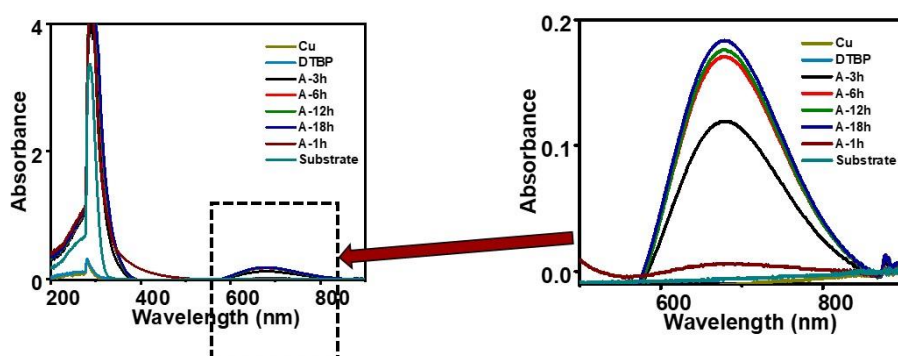


Figure 3. UV-Vis absorption spectra of standard reaction under “Condition A”.

“Condition A” excluding **1a** and DTBP (i.e., only copper): As from the above reaction it was evident that Cu(II) had been formed, now it was our conjecture that whether Cu(0) converts to Cu(II) on its own with aerial oxidation under elevated temperature.

To prove, we set up a reaction taking Cu(0) (2.54mg) in 2 mL PhCF₃ in a 15 mL pressure tube, sealed and heated with constant stirring at 100 °C. Aliquots were taken at different times as depicted in the graph. But no significant absorption had been shown at any time from which we can satisfy our conjecture. So, from here, we can easily conclude that at least alone Cu(0) cannot undergo oxidation to convert to Cu(II).

“Condition A” excluding **1a** (i.e., Cu+DTBP): To test the obvious necessity of the substrate **1a** for the formation of Cu(II) species, next reaction was set up taking a mixture of Cu (0) (2.54 mg), DTBP (36.7 μL) in 2 mL PhCF₃ in 15 mL pressure tube, sealed and heated with continuous stirring at 110 °C. Aliquots were taken at different times as depicted in the

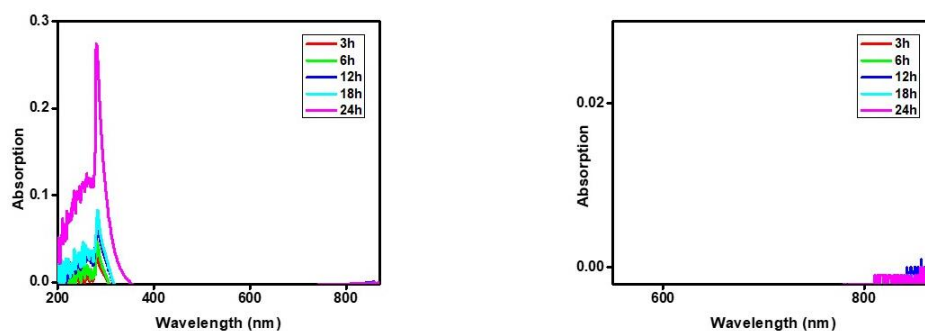


Figure 4. UV-Vis absorption spectra of reaction with “Condition A” excluding **1a**.

graph. But absolutely no significant absorption had been shown at any time to prove the formation of Cu(II) species (**Figure 4**). So, from here, we can easily conclude that the substrate is very much essential for formation of Cu(II) species. It is probable as the substrate can act as a ligand and stabilize the formed Cu(II). So, it is evident that at “Condition A”, Cu(II) is formed and stabilized, for which the substrate is essential.

“Condition B”: Similar spectral patterns were also visible in the UV-Vis spectra from “Condition B”, indicating the formation of Cu(II) species to control the process (**Figure 5**).

Chemo- and Regioselective Benzylic C(sp³)-H Oxidation Bridging the Gap between Hetero- and Homogeneous Copper Catalysis

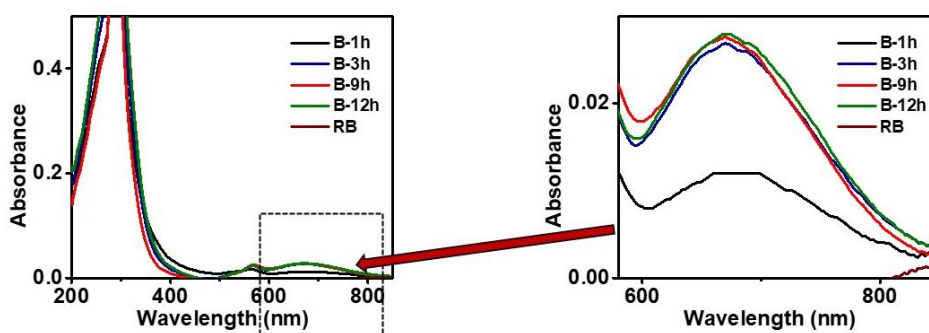


Figure 5. UV-Vis absorption spectra of standard reaction with “Condition B”.

Standard reaction was set up with **1a** substrate and aliquots were taken at different times to record UV-Vis absorption. The spectra clearly shows the formation of Cu(II) species just after 1h. And further, the intensity increases over time. We had recorded UV-Vis absorption of only rose Bengal (RB) catalyst and have shown in the diagram.

“Condition B” without **1a** (i.e. Cu+O₂+RB): Here also, like “Condition A”, to prove the necessity of substrate **1a** for the formation of Cu(II), the following experiment was performed. In a 15 mL pressure tube was taken Cu powder (1.27 mg), RB (2mg) and PhCF₃ was added. The vessel was purged with O₂ and sealed. The mixture was heated at 110 °C with continuous stirring under irradiation of white light from two white CFL each from 5cm apart. Aliquots were taken midway and UV-VIS absorption were recorded that is depicted here. It clearly shows no peak corresponding to Cu(II). So it proved that the copper (0) cannot oxidize to Cu(II) under O₂ atmosphere with photosensitizer and light without the substrate **1a**. Hence **1a** helps the formation of Cu(II) and stabilizes it which drives the forward reaction.

“Condition B” excluding RB (i.e. **1a** + O₂): Having the established fact that **1a** is essential, it is now to test the necessity the use of photosensitizer RB.

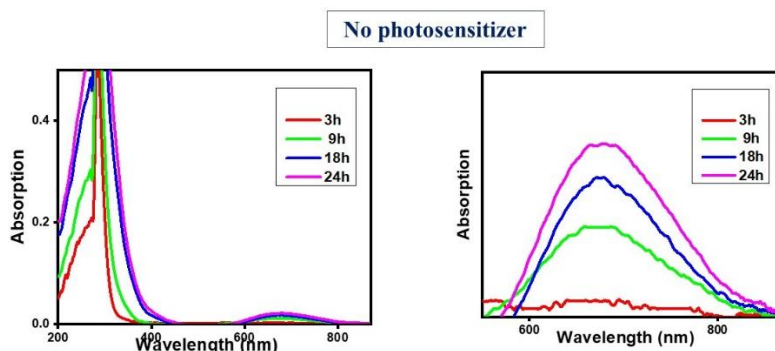


Figure 6. UV-Vis absorption spectra of reaction with “Condition B” excluding RB.

So, one reaction was set up with “Condition B” but without the addition of RB and UV-VIS absorption were recorded in situ. The result shows that Cu(II) forms after 9 hours. On the contrary Cu(II) was formed after only 1 hour in the reaction in the standard reaction with “Condition B” (**Figure 6**). So, it is evident that the use of RB facilitates the reaction in forward direction. Hence, photoredox catalyst under light irradiation may accelerate the formation of active Cu(II) catalyst by molecular oxygen.

XPS analysis

However, we did not observe the involvement of Cu(III) species under either of the two conditions. XPS analysis further validated the copper's oxidation state. And in both the reactions, similar pattern comes up. The peaks at 931.0 and 950.9 eV are assigned to Cu 2p^{3/2} and 2p^{1/2} of Cu(II). And the intense satellite peak at 942 eV confirms the presence of Cu(II) (**Figure 7**).⁴⁷

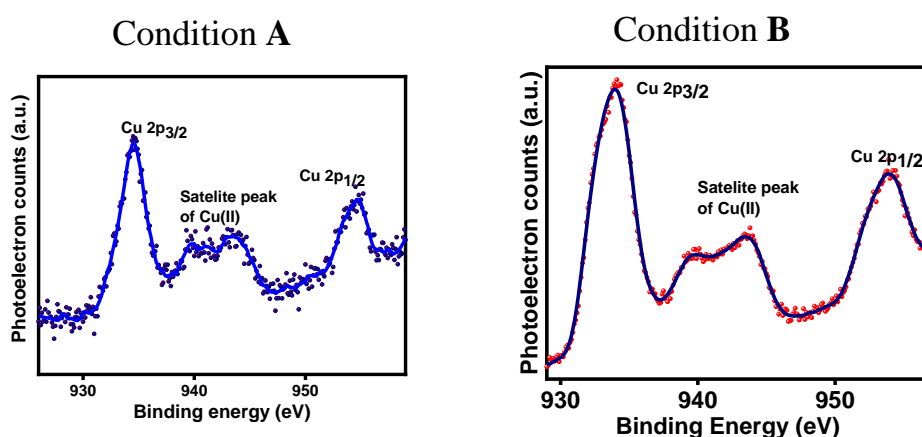


Figure 7. XPS analysis.

Characterization of the recovered catalyst

After the reaction was finished, a fairly clear blue solution turned opaque, leading us to conclude that copper (oxide or hydroxide) nanoparticles (CuNPs) might have formed. According to the transmission electron microscopic (TEM) image of both reaction mixtures, it was observed that copper nanoparticles with a diameter of 2–5 nm had formed (**Figure 8**). In fact, Entry 10, **Table 1** shows that preformed nanoparticles (CuNPs) also catalyzed the reaction. However, the particles made in situ from the copper powder may be of different sizes and not homogeneous throughout the system leaving some particles being beyond the nanometer range.

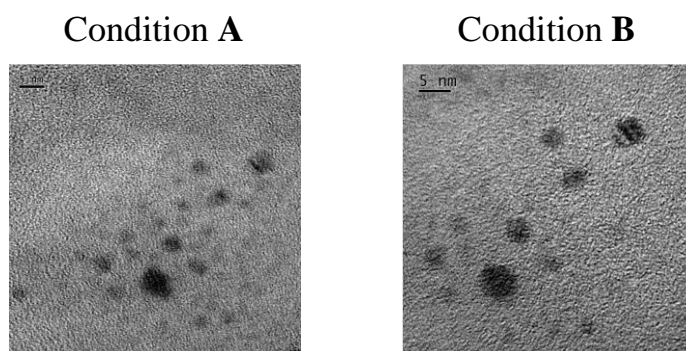


Figure 8. TEM image of recovered catalyst.

Plausible mechanism

From the control and spectroscopic studies, we hypothesised the following as a likely mechanism (Scheme 23). To generate an active methyl radical under “Condition A”, DTBP first goes through homolytic cleavage, then goes through β -methyl scission. One proton is removed from the benzylic position of **1a** by $\cdot\text{CH}_3$, which then emits CH_4 , forming the corresponding benzylic radical species. Gas chromatography of the sample retrieved from the

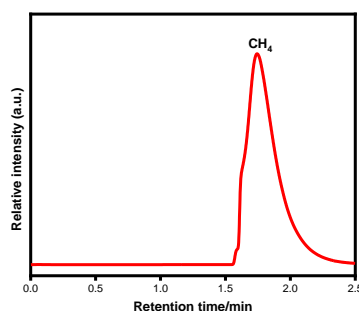
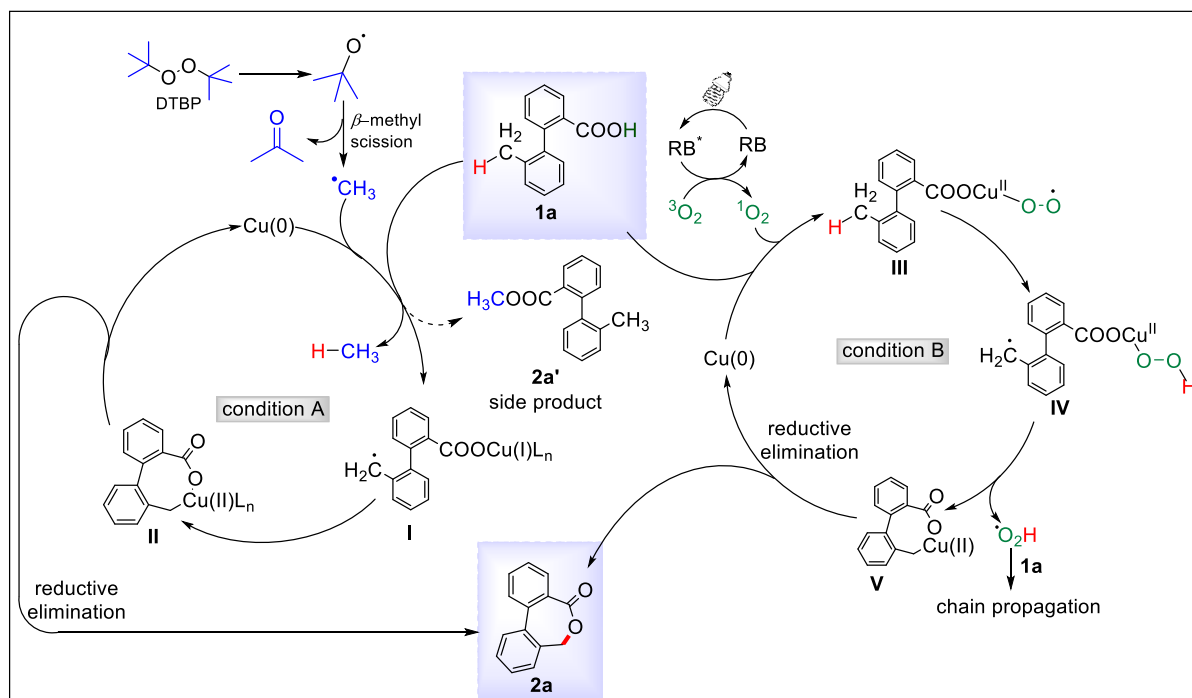


Figure 9. Gas chromatography spectra of headspace gas (under “Condition A”).

reaction vessel verified the development of CH_4 (Figure 9). $\text{Cu}(0)$ then forms a carboxylate to produce reactive intermediate **I**, which is promptly stabilised by the production of an eight-membered copper complex **II**. After that, it proceeds via reductive elimination to produce product **2a** and regenerates $\text{Cu}(0)$, which propels the reaction onward. Additionally, some of the $\cdot\text{CH}_3$ is absorbed by the carboxyl group of the substrate, producing the unwanted **2a'**.

Under “Condition B”, (Scheme 23), the copper-peroxide radical generated from an oxygen molecule by photosensitization is believed to be responsible for the benzylic C-H activation. Under light irradiation, RB (rose bengal) excites and goes to RB^* which produces singlet oxygen ($^1\text{O}_2$) by transferring energy to triplet oxygen ($^3\text{O}_2$).⁴⁸ The $^1\text{O}_2$ is then scavenged by the

Cu(0), which then interacts with the carboxyl group⁴⁹ of **1a** to produce the copper(II)-peroxo intermediate⁵⁰ **III**, which goes through two simultaneous SETs. **III** acts as the active catalyst. The intermediate benzylic radical **IV** is produced when this copper-peroxo radical removes one proton from the proximal benzylic site. After then, an 8-membered Cu(II) complex **V** forms while a hydroperoxyl radical is produced, which propagates the chain⁵¹ to continue to react with another molecules of **1a**. Cu(0) is regenerated from reductive elimination of complex **V** and the final product **2a** is obtained. In either scenario, initial benzylic C–H bond oxidation to benzyl alcohol followed by lactonization under copper catalysis is possible. However, no comparable benzyl alcohol from the reaction mixture could be found either by isolation or by MS characterization. Additionally, under our reaction conditions, the equivalent benzyl alcohol **20**, which was produced by hydrolyzing the lactonized product **2a**, converted back to lactone product **2a** in only 7% yield. As a result, the first step of benzylic oxidation to alcohol might not be possible.

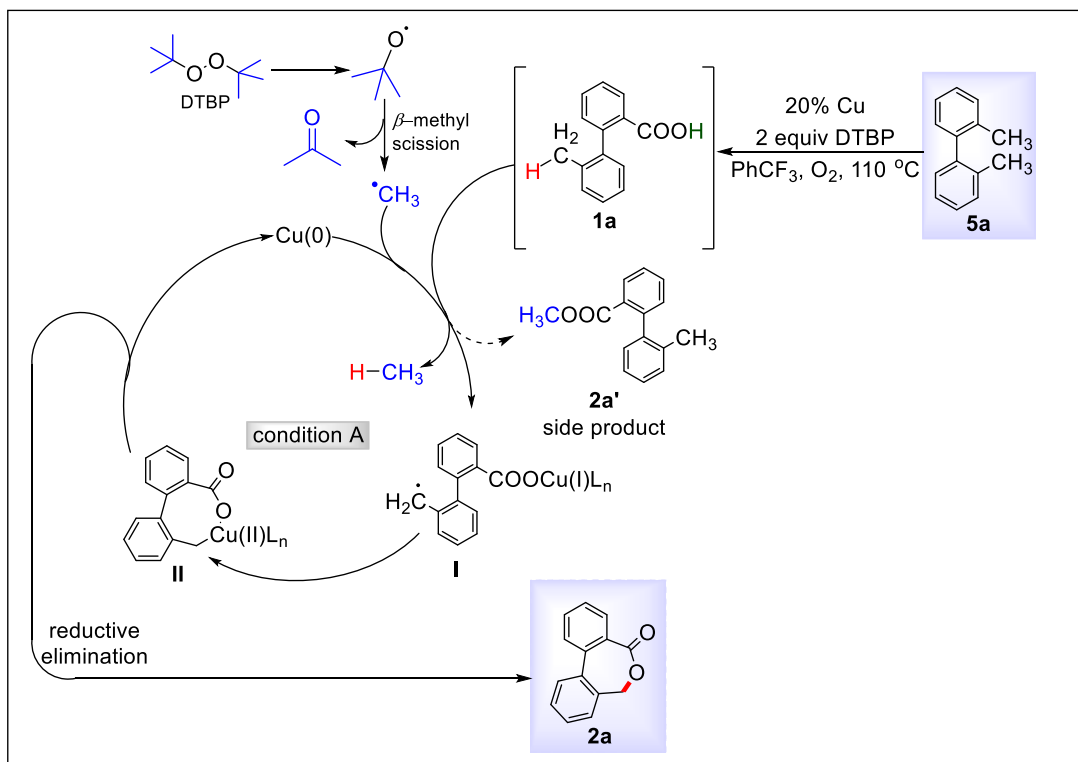


Scheme 23. Plausible mechanism of copper(0) catalyzed benzylic C(sp³)-H activation of 2'-alkyl-[1,1'-biphenyl]-2-carboxylic acids.

In **Scheme 15**, one benzylic C(sp³)-H group of **5a** first undergoes oxidation to provide the equivalent benzoic acid **2a** highly oxidative condition⁵², after which the mechanism consistent with “Condition A” is followed to produce the product **2a** (**Scheme 24**). Notably,

Chemo- and Regioselective Benzylic C(sp³)-H Oxidation Bridging the Gap between Hetero- and Homogeneous Copper Catalysis

the 1° benzylic C(sp³)-H (i.e. CH₃ group) initially oxidises to benzoic acid in the substrates 5p, 5u, and it is followed by the activation of the 2° benzylic C(sp³)-H activation and subsequent cyclization to produce the products.



Scheme 24. Plausible mechanism of copper(0) catalyzed double benzylic C(sp³)-H activation of 2,2'-biaryls.

Further research is required to determine the governing factor of the sequence of oxidation and activation of the two benzylic C(sp³)-H groups when any substitution is present in either ring (**5d-f**).

Recyclability of the catalysts

Gratifyingly, a metallic precipitate formed in each condition once the reaction was finished (**Figure 10**) and the residue was full of dispersed CuNPs (indicated from TEM). So, in order to increase the catalyst's utility, we wanted to recover and recycle it.⁵³ After one batch of the reaction, it was filtered, washed with ethyl acetate and another batch of reaction was set up with the residue. Similarly subsequent four batches were reported in each “Condition A” and the result was satisfactory.



Figure 10. Turbidity after reactions.

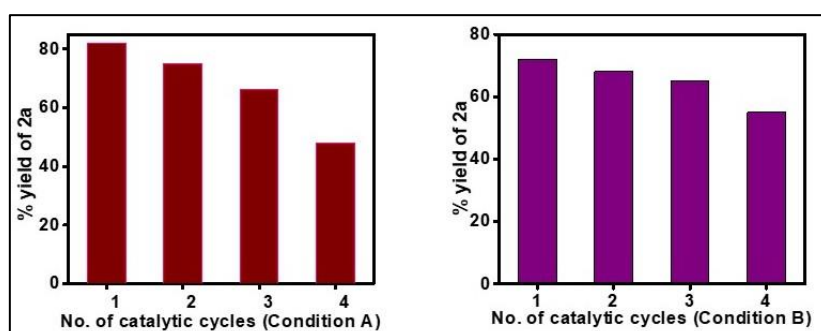


Figure 11. Recyclabilities of the catalytic systems.

For “Condition A”, the yields were 82%, 75%, 66%, and 48% respectively (Figure 11). And the same for “Condition B” were 72%, 68%, 65% and 55% (Figure 11). We were unable to further increase the catalytic activity of the residue by washing it with acetic acid⁵⁴ or organic solvents⁵⁵. Still, the transformation of inexpensive copper powder into a substrate-bound homogeneous catalyst for highly chemoselective benzylic oxidation, and eventual precipitation out to facilitate catalyst recovery, is a unique and fascinating example.

IV.5. Conclusion

Here, we described a low-cost method for chemoselectively activating benzylic C(sp³)-H for the direct synthesis of seven-membered dibenzo[c,e]oxepin-5(7H)-ones. Remarkably, molecular oxygen took the oxidant's role substituting hazardous di-tert-butyl peroxide (DTBP) while merging copper catalysis with organic photosensitizer. Intriguingly, the copper powder is transformed into a highly reactive, substrate-dependent soluble catalyst during the reaction to achieve a high degree of chemoselective benzylic C(sp³)-H oxidation while preventing the synthesis of six-membered lactones via the C(sp²)-H bond activation. Finally, to maximize the advantages of both homogeneous and heterogeneous catalyst, the heterogeneous catalyst is precipitated out and recovered for subsequent runs by easy filtration. The reaction proceeds

through a SET (single electron transfer) mechanism, is scalable and the protocol has been applied to carry out the total synthesis of Alterlactone, a cytotoxic natural product. Further investigations on Cu(0)/photoredox/O₂ catalytic system is being explored in our laboratory.

Limitations of the study: Despite developing sustainable conditions for lactone formation via selective benzylic C(sp³)-H oxidation, it is restricted to 7-membered lactones only. Smiles rearrangement was furnished from the substrate class **3** via 1,5-aryl migration and not afforded 8-membered lactones. And while exploring the substrate scopes, we found that primary amines, aldehydes were not compatible under either condition. After four cycles, it was found that the recovered catalyst had a lower catalytic efficiency, suggesting scope for improvement.

IV.6. Experimental section

IV.6.1. General information

Each air-sensitive reagent handling was done in a dry argon environment. Unless otherwise specified, all commercial chemicals were procured from the chemical manufacturers Sigma Aldrich, TCI, Acros, or Spectrochem and utilised without further purification. Before usage, solvents were distilled and dried using conventional techniques. The spots were visible using UV light (254 and 365 nm) or by charring the plate after dipping it in KMnO₄ or vanillin charring solution. TLC was run on silica gel plates (Merck silica gel 60, f254). In CDCl₃ solvent, ¹³C NMR spectra were recorded at 75 MHz (Bruker-DPX), 100 MHz (JEOL-JNM-ECZ400S/L1), and 150 MHz (Bruker-Avance) frequencies using TMS as the internal standard. ¹H NMR was recorded at 400 MHz (JEOL-JNMECZ400S/L1) and 600 MHz (Bruker-Avance) frequency. Chemical shifts were determined in parts per million (ppm), with tetramethylsilane serving as a reference point at 0.0 ppm. The terms s=singlet, d=doublet, t=triplet, q=quadruplet, m=multiplet, br=broad, and AB_q=AB quartet were all used to describe multiplicities. In Hertz unit, coupling constants, J, were reported (Hz). The ESI technique was used to measure HRMS (m/z) (Q-ToF Micro mass spectrometer). Dichloromethane was used to grow the crystals, and the Bruker D8 Venture with a Photon-III detector instrument was used to record the crystal data. Using a cuvette having length of 1 cm, room temperature absorption spectra were acquired by a Shimadzu UV-Vis spectrophotometer. All the samples' emission spectra were recorded using a FluoroMax-P (HORIBA JobinYvon) luminescence spectrophotometer. A JEOL JEM 2100F transmission electron microscope was used to capture the TEM (transmission electron microscopic) and STEM (scanning transmission electron

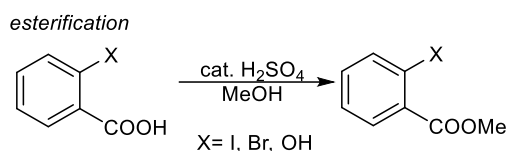
microscopic) images. Equipped with a Scienta Omicron SPHERA analyzer, an Omicron electron spectrometer was used to conduct the X-ray photoelectron spectroscopy (XPS) studies. With a GC instrument with a TCD and the model number 7890B (G3440B), serial no. CN14333203, the in situ evolved gas was detected. A gas tight syringe was used to syringe 500 μL of gas into the GC's inlet from the head space of the H cell's working chamber.

IV.6.2. Preparation of starting materials

IV.6.2.1. General protocol for synthesis of 2'-alkyl-[1,1'-biphenyl]-2-carboxylic acids (1)

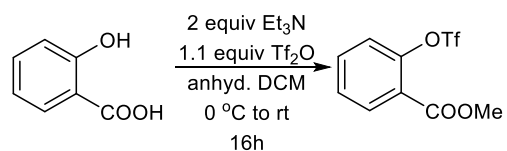
This synthesis was performed following slightly modifying a reported protocol.⁵⁶

Preparation of corresponding ethyl esters of 2-bromo/iodo/hydroxy benzoic acids⁵⁷



In a clean and oven-dried RB, corresponding benzoic acid (5 mmol) was charged and 15 mL MeOH was added to make a solution. 10 drops of conc. H_2SO_4 were added and the mixture was refluxed at 80 $^\circ\text{C}$ overnight. After completion, the solvent was evaporated under reduced pressure and extracted with ethyl acetate (50 mL) after washing with deionized water (50 mL). Finally, the combined organic layer was passed through anhydrous Na_2SO_4 for drying and the mixture was concentrated by evaporating the solvent under reduced pressure. Then, the crude product was purified with column chromatography (eluting with petroleum ether/ethyl acetate) to afford the corresponding ester.

Preparation of methyl 2-(((trifluoromethyl)sulfonyl)oxy)benzoate from methyl salicylates

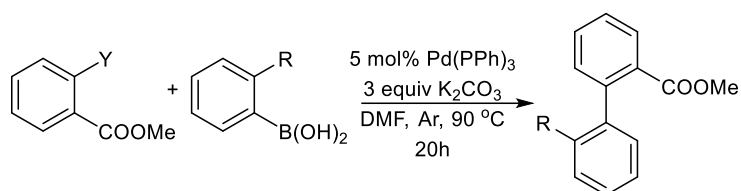


In a clean and oven-dried RB, methyl salicylate (5mmol) was taken dissolving it in anhydrous DCM (10 mL) and was kept for stirring at 0 $^\circ\text{C}$. While stirring, triethylamine (1.4 ml, 2eq) was added to it at 0 $^\circ\text{C}$. Then maintaining 0 $^\circ\text{C}$, trifluoromethanesulfonic anhydride

Chemo- and Regioselective Benzylic C(sp³)-H Oxidation Bridging the Gap between Hetero- and Homogeneous Copper Catalysis

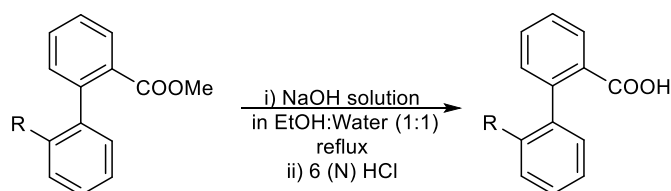
(1 ml, 6 mmol) was added dropwise over 5 min. Thereafter, the resulting clear solution was stirred at room temperature for 16 hours. After completion, water was added to quench the reaction. Therefore, this was extracted with CH₂Cl₂ (5 × 15 mL) and in a separatory funnel, it was washed with deionized water (20 ml) and brine (10 ml). The combined organic layer was filtered through anhydrous sodium sulfate for drying, the solvent was evaporated under reduced pressure to give a liquid. Then, the crude product was purified with column chromatography (eluting with petroleum ether/ethyl acetate) to afford methyl 2-(((trifluoromethyl)sulfonyl)oxy)benzoate as colorless liquid.

Suzuki coupling between 2-bromo/iodo benzoate or methyl 2-(((trifluoromethyl)sulfonyl)oxy)benzoate and 2-alkyl aryl boronic acid



To a solution of The corresponding 2-bromo/iodo benzoate or methyl 2-(((trifluoromethyl)sulfonyl)oxy)benzoate (1 mmol) was taken in a dry 25 mL round-bottom flask and dissolved in anhydrous DMF (5 ml). The corresponding 2-alkyl aryl boronic acid (1.2 equiv., 1.2 mmol), Pd(PPh₃)₄ (5 mol%) and activated K₂CO₃ (3 equiv., 3 mmol) were successively added to it. Then, the reaction mixture was kept for stirring for 20 hours at 90 °C strictly under inert atmosphere. After completion, the mixture was extracted with EtOAc and rinsed with ice-cold water (30 mL) and brine (30 mL). The combined organic layer was filtered through anhydrous sodium sulfate for drying, the solvent was evaporated under reduced pressure to give a liquid. Then, the crude product was purified with column chromatography (eluting with petroleum ether/ethyl acetate) to afford the desired product.

Hydrolysis of methyl esters



Corresponding ester was taken in a round-bottom flask and NaOH (sodium hydroxide) solution in water-ethanol (1:1) was added to dissolve it. Then, the mixture was heated at 60 °C

for overnight with continuous stirring. After completion, the solvent was concentrated under vacuum and 6 (N) HCl was added to neutralize the remaining solution. Thereafter, the mixture was extracted with EtOAc and rinsed with ice-cold water (30 mL) and brine (30 mL). The combined organic layer was filtered through anhydrous sodium sulfate for drying, the solvent was evaporated under reduced pressure to give a liquid. Then, the crude product was purified with column chromatography (eluting with petroleum ether/ethyl acetate) to afford the 2'-alkyl-[1,1'-biphenyl]-2-carboxylic acid **1**.

IV.6.2.2. General protocol for the synthesis of 2-aryloxybenzoic acids (3)

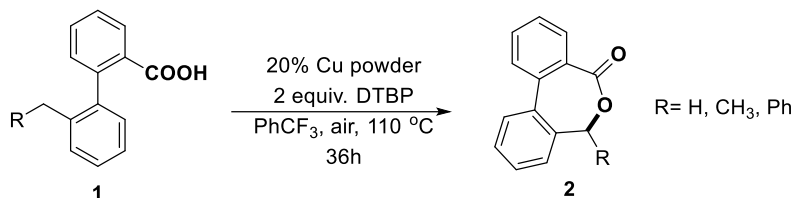
The synthesis was performed following literature procedure^{41a}. 2-halobenzoic acid (1.0 equiv., 6.2 mmol) was taken in a clean and oven-dried 100 mL round bottom flask with magnetic stir bar inside and 50 mL DMF solvent was added to dissolve it. Then subsequently, corresponding phenol (2.0 equiv., 12.4 mmol), copper(I) iodide (0.28 mmol, 53 mg), DBU(1,8-diazabicyclo[5.4.0]undec-7-ene) (3.0 equiv., 18.6 mmol, 2.6 mL), pyridine (0.1 mL) were added to the mixture. The resulting solution was heated under nitrogen atmosphere at 160 °C with continuous stirring. After completion, typically 2 h (indicated by TLC), the reaction mixture was taken in 0 °C, acidified with HCl (3 M). Precipitate formed in acidification process and whole suspension was extracted with DCM (dichloromethane) (70 mL), washed with ice-cold water (60 mL) and brine (30 mL). The combined organic layer was filtered through anhydrous sodium sulfate for drying, the solvent was evaporated under reduced pressure to give a liquid. Then, the crude product was purified with column chromatography (eluting with petroleum ether/ethyl acetate) to afford the solid product.

IV.6.2.3. Protocol for synthesis of 2-alkyl-2'-methyl-1,1'-biphenyls (5)

Successively, the suitable 2-alkyl aryl boronic acid (1.2 equiv., 1.2 mmol), Pd(PPh₃)₄ (5 mol%), and activated K₂CO₃ (3 equiv., 3 mmol) were added to a solution of the appropriate 2-iodo toluene (1 equiv., 1 mmol) in toluene (5 mL) and ethanol (2.5 mL). Then, the reaction mixture was heated at 90 °C under inert atmosphere with continuous stirring for 20 hours. Thereafter, the mixture was extracted with EtOAc and rinsed with water (30 mL) and brine (30 mL). The combined organic layer was filtered through anhydrous sodium sulfate for drying, the solvent was evaporated under reduced pressure to give a liquid. Then, the crude product was purified with column chromatography (eluting with petroleum ether/ethyl acetate) to afford the desired 2-alkyl-2'-methyl-1,1'-biphenyl **5**.

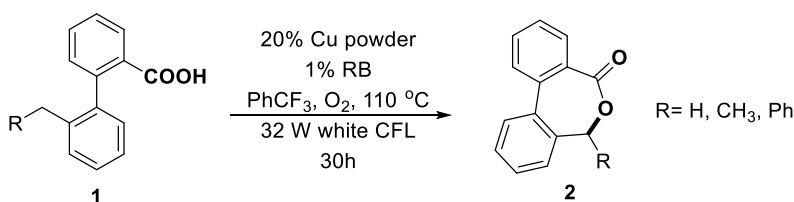
IV.6.3. Experimental protocols for copper(0)-catalyzed chemo- and regioselective intramolecular benzylic C(sp³)-H oxidation of 2'-alkyl-[1,1'-biphenyl]-2-carboxylic acids (1)

IV.6.3.1. General “Condition A”



In a clean and oven-dried pressure tube (15 mL) with magnetic stir-bar inside, substrate **1** (1 equiv., 0.2 mmol), copper powder (20 mol%, 0.04 mmol, 2.54 mg) were taken. Therefore, PhCF₃ (α,α,α -trifluorotoluene (2 mL) was added to it *via* syringe. Then, DTBP (2 equiv., 0.4 mmol, 36.7 μ L) was added with microsyringe and the vessel was sealed. Thereafter, reaction mixture was heated at 110 °C with continuous stirring for 36 hours. Thereafter, after completion, it was allowed to reach room temperature, the mixture was extracted with EtOAc (2 X 30 mL) and rinsed with water (30 mL) and brine (30 mL). The combined organic layer was filtered through anhydrous sodium sulfate for drying, the solvent was evaporated under reduced pressure to give a liquid. Then, the crude product was purified with column chromatography (eluting with petroleum ether/ethyl acetate) to afford the corresponding dibenzo[*c,e*]oxepinones.

IV.6.3.2. General “Condition B”



In a clean and oven-dried pressure tube (15 mL) with magnetic stir-bar inside, substrate **1** (1 equiv., 0.2 mmol), copper powder (20 mol%, 0.04 mmol, 2.54 mg) were taken. Therefore, PhCF₃ (α,α,α -trifluorotoluene (2 mL) was added to it *via* syringe. The vessel was purged with UHP (ultra-high pure) O₂ for 1 minute and sealed promptly. Thereafter, for 30 hours, reaction mixture was heated at 110 °C under continuous irradiation from two white CFLs (each CFL: 32 W and set at 5cm distance from the reaction vessel). Thereafter, after completion, it was

allowed to reach room temperature, the mixture was extracted with EtOAc (2 X 30 mL) and rinsed with water (30 mL) and brine (30 mL). The combined organic layer was filtered through anhydrous sodium sulfate for drying, the solvent was evaporated under reduced pressure to give a liquid. Then, the crude product was purified with column chromatography (eluting with petroleum ether/ethyl acetate) to afford the corresponding dibenzo[*c,e*]oxepinones.

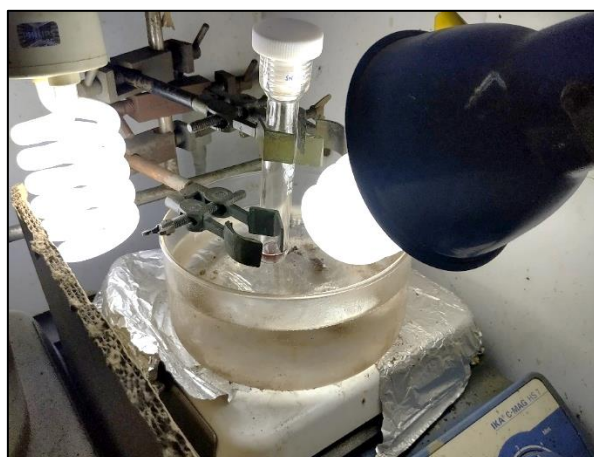
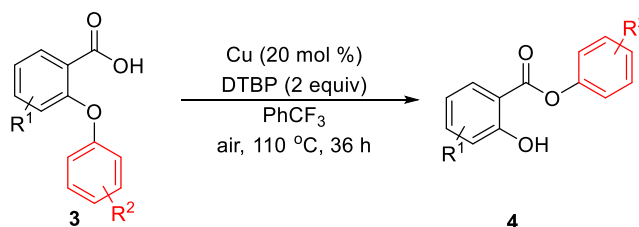


Figure 12. Reaction set up for “Condition B”.

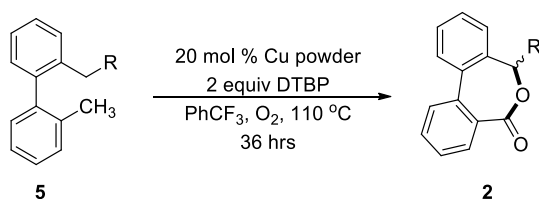
IV.6.4. Experimental protocol for the copper(0)-catalyzed Smiles rearrangement of 2-phenoxybenzoic acids, (Related to Scheme 3)



To an clean and oven-dried pressure tube (15 mL), 2-phenoxybenzoic acids (1.0 equiv., 0.2 mmol), copper(0) powder (20 mol%, 0.04 mmol, 2.54 mg) were charged and PhCF₃ (α,α,α -trifluorotoluene (2 mL) was added to it *via* syringe. Then, DTBP (2 equiv., 0.4 mmol, 36.7 μ L) was added with microsyringe and the vessel was sealed. Thereafter, reaction mixture was heated at 110 °C with continuous stirring for 36 hours. Thereafter, after completion, it was allowed to reach room temperature, the mixture was extracted with EtOAc (2 X 30 mL) and rinsed with water (30 mL) and brine (30 mL). The combined organic layer was filtered through anhydrous sodium sulfate for drying, the solvent was evaporated under reduced pressure to give a liquid. Then, the crude product was purified with column chromatography (eluting with petroleum ether/ethyl acetate) to afford the expected product.

IV.6.5. Experimental protocol for copper(0)-catalyzed double C(sp³)-H activation of 2-alkyl-2'-methyl-1,1'-biphenyls (5)

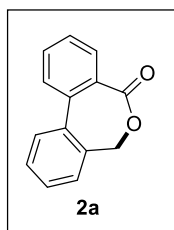
To an clean and oven-dried pressure tube (15 mL) with magnetic bar inside, substrate **5** (1.0 equiv., 0.2 mmol), copper(0) powder (20 mol%, 0.04 mmol, 2.54 mg) were charged and PhCF₃ (α,α,α -trifluorotoluene (2 mL) was added to it *via* syringe. Then, DTBP (2 equiv., 0.4 mmol, 36.7 μ L) was added with microsyringe.



The vessel was purged with UHP (ultra-high pure) O₂ for 1 minute and sealed promptly. Thereafter, reaction mixture was heated at 110 °C with continuous stirring for 36 hours. Thereafter, after completion, it was allowed to reach room temperature, the mixture was extracted with EtOAc (2 X 30 mL) and rinsed with water (30 mL) and brine (30 mL). The combined organic layer was filtered through anhydrous sodium sulfate for drying, the solvent was evaporated under reduced pressure to give a liquid. Then, the crude product was purified with column chromatography (eluting with petroleum ether/ethyl acetate) to afford the corresponding dibenzooxepinones.

IV.6.6. Spectral data

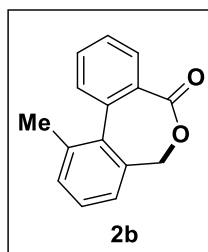
dibenzo[*c,e*]oxepin-5(7H)-one (**2a**)



Following the general procedures A and B, the expected product was obtained using column chromatography (SiO₂, eluting with 97:3 hexane/ethyl acetate) as a white solid, (34.4 mg, 82% with “Condition A” and 30.2 mg, 72% with “Condition B”). mp 98-102 °C. ¹H NMR (600 MHz, CDCl₃): δ 7.99 (d, *J* = 7.8 Hz, 1H), 7.65-7.69 (m, 2H), 7.61 (d, *J* = 7.8 Hz, 1H), 7.51-7.56 (m, 2H), 7.42-7.47 (m, 2H), 5.03 (d(br), *J* = 41.4 Hz, 2H); ¹³C NMR (150 MHz, CDCl₃):

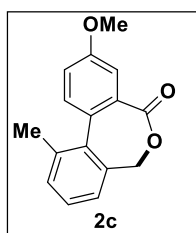
δ 170.23, 138.96, 137.25, 134.81, 132.55, 131.93, 130.65, 130.12, 128.67, 128.65, 128.55, 128.42, 69.18. HRMS (ESI, m/z) calcd. for $C_{14}H_{10}O_2Na [M+Na]^+$: 233.0578; found: 233.0576.

11-methyldibenzo[c,e]oxepin-5(7H)-one (2b)



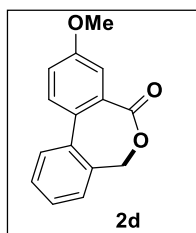
Following the general procedures A and B, the expected product was obtained using column chromatography (SiO_2 , eluting with 97:3 hexane/ethyl acetate) as a white solid, (35.4 mg, 79% with “Condition A” and 31.4 mg, 70% with “Condition B”). mp 110-112 °C. 1H NMR (600 MHz, $CDCl_3$): δ 7.89 (dd, $J_1 = 7.8$ Hz, $J_2 = 1.2$ Hz, 1H), 7.58 (td, $J_1 = 7.8$ Hz, $J_2 = 1.2$ Hz, 1H), 7.48 (dd, $J_1 = 7.2$ Hz, $J_2 = 1.2$ Hz, 1H), 7.38 (dd, $J_1 = 6.6$ Hz, $J_2 = 2.4$ Hz, 1H), 7.27-7.30 (m, 2H), 4.90 (ABq, $J = 8$ Hz, 2H); ^{13}C NMR (150 MHz, $CDCl_3$): δ 170.59, 137.54, 136.62, 135.97, 135.78, 132.87, 131.59, 130.83, 130.76, 130.30, 128.11, 126.23, 70.05, 21.28. HRMS (ESI, m/z) calcd. for $C_{15}H_{13}O_2 [M+H]^+$: 225.1006; found: 225.1205.

3-methoxy-11-methyldibenzo[c,e]oxepin-5(7H)-one (2c)



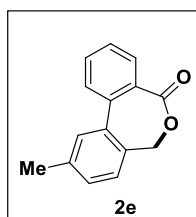
Following the general procedures A and B, the expected product was obtained using column chromatography (SiO_2 , eluting with 95:5 hexane/ethyl acetate) as a white solid, (34.0 mg, 67% with “Condition A” and 27.0 mg, 53% with “Condition B”). mp 118-120 °C. 1H NMR (400 MHz, $CDCl_3$): δ 7.34-7.40 (m, 3H), 7.24-7.26 (m, 2H), 7.12 (dd, $J_1 = 8$ Hz, $J_2 = 4$ Hz, 1H), 4.90 (ABq, $J = 12$ Hz, 2H), 3.89 (s, 3H); ^{13}C NMR (100 MHz, $CDCl_3$): δ 170.54, 159.09, 137.52, 136.53, 135.81, 132.91, 132.81, 131.86, 128.49, 127.69, 126.25, 118.21, 114.30, 70.31, 55.70, 21.40. HRMS (ESI, m/z) calcd. for $C_{16}H_{14}O_3Na [M+Na]^+$: 277.0841; found: 277.0841.

3-methoxydibenzo[c,e]oxepin-5(7H)-one (2d)



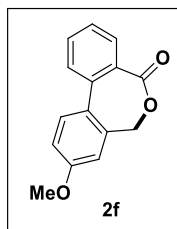
Following the general procedures A and B, the expected product was obtained using column chromatography (SiO₂, eluting with 95:5 hexane/ethyl acetate) as a white solid, (29.4 mg, 61% with “Condition A” and 26.2 mg, 54% with “Condition B”). mp 116-122 °C. ¹H NMR (600 MHz, CDCl₃): δ 7.61 (d, *J* = 7.8 Hz, 1H), 7.51-7.55 (m, 2H), 7.48 (d, *J* = 3 Hz, 1H), 7.45 (dd, *J*₁=7.2 Hz, *J*₂= 1.2 Hz, 1H), 7.39 (td, *J*₁= 7.2 Hz, *J*₂= 1.2 Hz, 1H), 7.22 (dd, *J*₁= 9Hz, *J*₂= 3Hz, 1H), 5.01 (d(br), *J* = 30.6 Hz, 2H), 3.91(s, 3H); ¹³C NMR (150 MHz, CDCl₃): δ 170.06, 159.46, 138.77, 134.32, 131.69, 131.60, 130.16, 130.04, 128.44, 128.16, 127.96, 120.04, 115.20, 69.34, 55.64. HRMS (ESI, *m/z*) calcd. for C₁₅H₁₂O₃Na [M+Na]⁺: 263.0684; found: 263.0690.

10-methyldibenzo[c,e]oxepin-5(7H)-one (2e)



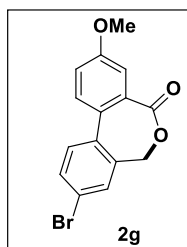
Following the general procedures A and B, the expected product was obtained using column chromatography (SiO₂, eluting with 97:3 hexane/ethyl acetate) as a gummy syrup, (25.8 mg, 58% with “Condition A” and 27.2 mg, 61% with “Condition B”). ¹H NMR (600 MHz, CDCl₃): δ 7.96 (dd, *J*₁ = 7.8 Hz, *J*₂ = 1.2 Hz, 1H), 7.64 (td, *J*₁=7.8 Hz, *J*₂=1.2 Hz, 1H), 7.58-7.59 (m, 1H), 7.49 (td, *J*₁=7.2 Hz, *J*₂=1.2 Hz, 1H), 7.44 (s, 1H), 7.33 (d, *J*=7.8 Hz, 1H), 7.22 (d, *J* = 7.8 Hz, 1H), 5.04 (ABq, *J*= 12 Hz, 2H), 2.43 (s, 3H); ¹³C NMR (150 MHz, CDCl₃): δ 170.36, 140.07, 138.86, 137.39, 132.43, 132.06, 131.89, 130.76, 129.28, 128.55, 128.47, 128.27, 68.93, 21.42. HRMS (ESI, *m/z*) calcd. for C₁₅H₁₃O₂ [M+H]⁺: 225.0916; found: 225.0919.

9-methoxydibenzo[c,e]oxepin-5(7H)-one (2f)



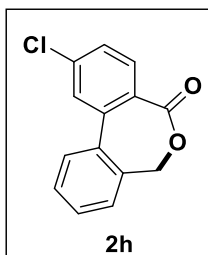
Following the general procedures A and B, the expected product was obtained using column chromatography (SiO₂, eluting with 95:5 hexane/ethyl acetate) as a white solid, (38.0 mg, 79% with “Condition A” and 31.2 mg, 65% with “Condition B”). mp 155-158 °C. ¹H NMR (400 MHz, CDCl₃): δ 7.95 (dd, *J*₁ = 6 Hz, *J*₂ = 1.6 Hz, 1H), 7.62 (td, *J*₁ = 7.6 Hz, *J*₂ = 1.6 Hz, 1H), 7.52-7.57 (m, 1H), 7.45 (td, *J*₁ = 7.6 Hz, *J*₂ = 1.6 Hz, 1H), 7.05 (dd, *J*₁ = 8 Hz, *J*₂ = 1.6 Hz, 1H), 6.97 (d, *J* = 2.4 Hz, 1H), 4.97 (d(br), *J* = 40 Hz, 2H), 3.87 (s, 3H); ¹³C NMR (100 MHz, CDCl₃): δ 170.48, 159.97, 137.35, 136.24, 132.62, 132.13, 131.51, 130.25, 10.02, 128.43, 127.85, 115.70, 113.94, 69.37, 55.62. HRMS (ESI, *m/z*) calcd. for C₁₅H₁₃O₂ [M+H]⁺: 241.0865; found: 241.0870.

9-bromo-3-methoxydibenzo[c,e]oxepin-5(7H)-one (2g)



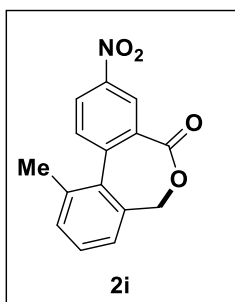
Following the general procedures A and B, the expected product was obtained using column chromatography (SiO₂, eluting with 95:5 hexane/ethyl acetate) as a white solid, (42.6 mg, 67% with “Condition A” and 45.2 mg, 71% with “Condition B”). mp 172-178 °C. ¹H NMR (400 MHz, CDCl₃): δ 8.09 (d, *J* = 2.4 Hz, 1H), 7.73 (dd, *J*₁ = 8.4 Hz, *J*₂ = 2 Hz, 1H), 7.53 (d, *J* = 8.4 Hz, 1H), 7.41 (d, *J* = 8.4 Hz, 1H), 7.05 (dd, *J*₁ = 8.4 Hz, *J*₂ = 1.2 Hz, 1H), 6.97 (d, *J* = 1.4 Hz, 1H), 4.97 (d(br), *J* = 16.8 Hz, 2H), 3.87 (s, 3H); ¹³C NMR (100 MHz, CDCl₃): δ 168.95, 160.25, 136.20, 136.00, 135.65, 134.72, 131.74, 130.43, 130.00, 129.89, 121.77, 115.87, 114.16, 69.40, 55.66. HRMS (ESI, *m/z*) calcd. for C₁₅H₁₂O₃Br [M+H]⁺: 318.9970; found: 318.9978.

2-chlorodibenzo[c,e]oxepin-5(7H)-one (2h)



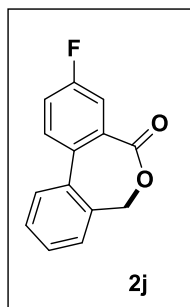
Following the general procedures A and B, the expected product was obtained using column chromatography (SiO₂, eluting with 97:3 hexane/ethyl acetate) as a white solid, (33.2 mg, 68% with “Condition A” and 34.2 mg, 70% with “Condition B”). mp 140-142 °C. ¹H NMR (400 MHz, CDCl₃): δ 7.92 (d, *J* = 12 Hz, 1H), 7.63 (d, *J* = 12 Hz, 1H), 7.60 (d, *J* = 4 Hz, 1H), 7.53-7.57 (m, 1H), 7.45-7.49 (m, 3H), 5.01 (d(br), *J* = 16 Hz, 2H); ¹³C NMR (100 MHz, CDCl₃): δ 167.79, 139.00, 138.98, 137.85, 134.90, 133.68, 129.40, 129.12, 128.72, 128.69, 128.64, 69.22. HRMS (ESI, *m/z*) calcd. for C₁₄H₁₀O₂Cl [M+H]⁺: 245.0369; found: 245.0371.

11-methyl-3-nitrodibenzo[c,e]oxepin-5(7H)-one (2i)



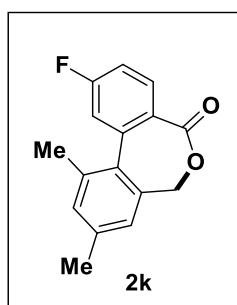
Following the general procedures A and B, the expected product was obtained using column chromatography (SiO₂, eluting with 97:3 hexane/ethyl acetate) as a white solid, (30.1 mg, 57% with “Condition A” and 25.8 mg, 48% with “Condition B”). mp 198-200 °C. ¹H NMR (400 MHz, CDCl₃): δ 8.76 (d, *J* = 2.4 Hz, 1H), 8.41 (dd, *J*₁ = 4.8 Hz, *J*₂ = 2.4 Hz, 1H), 7.67 (d, *J* = 4.8 Hz, 1H), 7.32-7.45 (m, 3H), 4.95 (ABq, *J* = 12.4 Hz, 2H), 2.43 (s, 3H); ¹³C NMR (100 MHz, CDCl₃): δ 168.26, 142.00, 137.08, 135.91, 133.50, 133.16, 131.79, 129.73, 126.87, 126.32, 125.22, 70.13, 21.30. HRMS (ESI, *m/z*) calcd. for C₁₅H₁₂NO₄ [M+H]⁺: 270.0766; found: 270.0769.

3-fluorodibenzo[c,e]oxepin-5(7H)-one (2j)



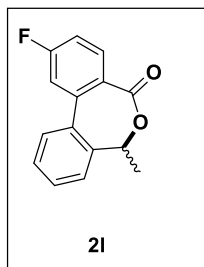
Following the general procedures A and B, the expected product was obtained using column chromatography (SiO₂, eluting with 97:3 hexane/ethyl acetate) as a white solid, (31.0 mg, 68% with “Condition A” and 26.4 mg, 58% with “Condition B”). mp 166-168 °C. ¹H NMR (400 MHz, CDCl₃): δ 7.69 (dd, *J*₁ = 9 Hz, *J*₂ = 3 Hz, 1H), 7.61-7.65 (m, 2H), 7.53 (td, *J*₁ = 7.8 Hz, *J*₂ = 1.8 Hz, 1H), 7.34-7.47 (m, 3H), 5.01 (d(br), *J* = 12 Hz, 2H); ¹³C NMR (100 MHz, CDCl₃): δ 168.93, 162.30 (d, *J*_{C-F} = 248.9 Hz), 138.13, 134.56, 133.65 (d, *J*_{C-F} = 3.5 Hz), 132.56, 132.49, 130.92 (d, *J*_{C-F} = 7.7 Hz), 130.37, 128.80 (d, *J*_{C-F} = 4 Hz), 128.57, 120.14 (d, *J*_{C-F} = 21.3 Hz), 118.61 (d, *J*_{C-F} = 23.6 Hz), 69.41. HRMS (ESI, *m/z*) calcd. for C₁₄H₁₀FO₂ [M+H]⁺: 229.0665; found: 229.0669.

2-fluoro-9,11-dimethyldibenzo[c,e]oxepin-5(7H)-one (2k)



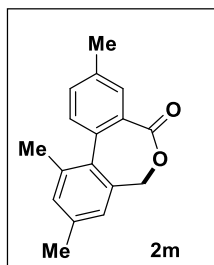
Following the general procedures A and B, the expected product was obtained using column chromatography (SiO₂, eluting with 97:3 hexane/ethyl acetate) as a white solid, (36.8 mg, 72% with “Condition A” and 32.4 mg, 63% with “Condition B”). mp 174-176 °C. ¹H NMR (600 MHz, CDCl₃): δ 7.89-7.91 (m, 1H), 7.20 (s, 1H), 7.13-7.17 (m, 2H), 7.10 (s, 1H), 4.87 (AB_q, *J* = 36 Hz, 2H), 2.38 (s, 3H), 2.37 (s, 3H); ¹³C NMR (150 MHz, CDCl₃): δ 169.72, 163.52 (d, *J*_{C-F} = 251.2 Hz), 138.72, 138.70, 136.43, 135.80, 133.69, 133.47, d, *J*_{C-F} = 9.3 Hz), 127.82, 127.13, 117.05 (d, *J*_{C-F} = 22.3 Hz), 115.1 (d, *J*_{C-F} = 21.4 Hz), 70.03, 21.09, 20.94. HRMS (ESI, *m/z*) calcd. for C₁₆H₁₃FO₂Na [M+Na]⁺: 279.0797; found: 279.0800.

2-fluoro-7-methyldibenzo[c,e]oxepin-5(7H)-one (2l)



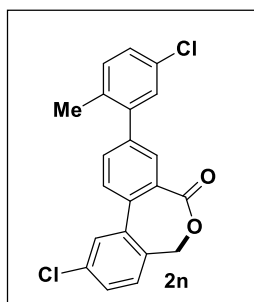
Following the general procedures A and B, the expected product was obtained using column chromatography (SiO₂, eluting with 97:3 hexane/ethyl acetate) as a gummy liquid, (25.6 mg, 53% with “Condition A” and 23.2 mg, 48% with “Condition B”). ¹H NMR (600 MHz, CDCl₃): δ 8.01-8.03 (m, 1H), 7.50-7.59 (m, 4H), 7.29 (dd, *J*₁ = 3.6 Hz, *J*₂ = 2.4 Hz, 1H), 7.51-7.56 (m, 2H), 7.22 (td, *J*₁ = 8.4 Hz, *J*₂ = 2.4 Hz, 1H), 5.29 (q, *J* = 6 Hz, 1H), 1.86 (d, *J* = 6 Hz, 3H); ¹³C NMR (150 MHz, CDCl₃): δ 168.97, 163.12 (d, *J*_{C-F} = 259.5 Hz), 140.16 (d, *J*_{C-F} = 9 Hz), 137.53 (d, *J*_{C-F} = 17 Hz), 134.25 (d, *J*_{C-F} = 9 Hz), 129.71, 129.15, 128.89, 124.10, 115.72 (d, *J*_{C-F} = 22.5 Hz), 115.41 (d, *J*_{C-F} = 22.5 Hz), 73.09, 16.83. HRMS (ESI, *m/z*) calcd. for C₁₅H₁₁O₂F [M+H]⁺: 243.0821; found: 243.0824.

3,9,11-trimethyldibenzo[c,e]oxepin-5(7H)-one (2m)



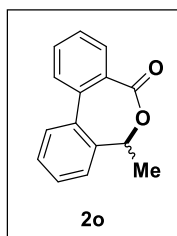
Following the general procedures A and B, the expected product was obtained using column chromatography (SiO₂, eluting with 97:3 hexane/ethyl acetate) as a white solid, (39.2 mg, 78% with “Condition A” and 29.2 mg, 58% with “Condition B”). mp 163-165 °C. ¹H NMR (400 MHz, CDCl₃): δ 7.69-7.70 (m, 1H), 7.32-7.38 (m, 2H), 7.18 (s, 1H), 7.08 (s, 1H), 4.85 (AB_q, *J* = 12 Hz, 2H), 2.43 (s, 3H), 2.37 (s, 3H), 2.36 (s, 3H); ¹³C NMR (100 MHz, CDCl₃): δ 170.98, 137.97, 137.83, 136.47, 135.97, 134.87, 133.58, 133.23, 131.77, 131.48, 131.17, 130.32, 127.01, 70.22, 21.25, 21.06, 21.01. HRMS (ESI, *m/z*) calcd. for C₁₇H₁₆O₂Na [M+Na]⁺: 275.1048; found: 275.1049.

10-chloro-3-(5-chloro-2-methylphenyl)dibenzo[c,e]oxepin-5(7H)-one (2n)



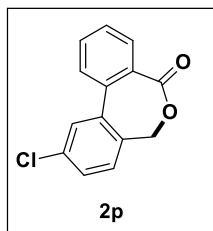
Following the general procedures A and B, the expected product was obtained using column chromatography (SiO₂, eluting with 97:3 hexane/ethyl acetate) as a white solid, (55.2 mg, 75% with “Condition A” and 47.0 mg, 64% with “Condition B”). mp >200 °C. ¹H NMR (600 MHz, CDCl₃): δ 7.96 (d, *J* = 1.2 Hz, 1H), 7.70 (s, 1H), 7.61-7.67 (m, 1H), 7.44 (s, 2H), 7.28-7.29 (m, 2H), 7.25-7.23 (m, 1H), 5.05 (AB_q, *J* = 12.6 Hz, 2H), 2.29 (s, 3H); ¹³C NMR (150 MHz, CDCl₃): δ 169.47, 141.59, 141.06, 140.24, 136.10, 134.83, 133.73, 133.31, 133.19, 132.59, 131.89, 131.58, 130.67, 130.01, 129.43, 128.73, 128.63, 128.56, 128.01, 68.42, 19.88. HRMS (ESI, *m/z*) calcd. for C₂₁H₁₅O₂Cl₂ [M+H]⁺: 369.0449; found: 369.0453.

7-methyldibenzo[c,e]oxepin-5(7H)-one (2o)



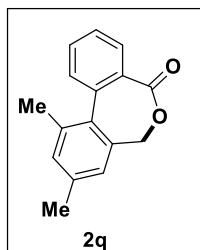
Following the general procedures A and B, the expected product was obtained using column chromatography (SiO₂, eluting with 97:3 hexane/ethyl acetate) as a white solid, (22.8 mg, 51% with “Condition A” and 24.6 mg, 55% with “Condition B”). mp 148-150 °C. ¹H NMR (400 MHz, CDCl₃): δ 7.97 (d, *J* = 8 Hz, 1H), 7.65 (td, *J*₁ = 8 Hz, *J*₂ = 1.2 Hz, 1H), 7.59 (td, *J*₁ = 8 Hz, *J*₂ = 1.2 Hz, 2H), 7.44-7.55 (m, 4H), 5.27 (q, *J* = 6.4 Hz, 1H), 1.84 (d, *J* = 6.4 Hz, 3H); ¹³C NMR (100 MHz, CDCl₃): δ 170.04, 138.77, 137.64, 137.44, 132.58, 131.42, 131.01, 129.66, 129.05, 128.87, 128.64, 128.46, 124.03, 73.19, 16.96. HRMS (ESI, *m/z*) calcd. for C₁₅H₁₃O₂ [M+H]⁺: 225.0916; found: 225.0919.

10-chlorodibenzo[c,e]oxepin-5(7H)-one (2p)



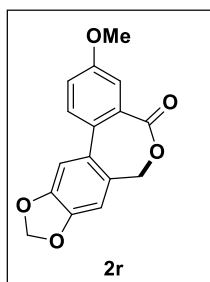
Following the general procedures A and B, the expected product was obtained using column chromatography (SiO₂, eluting with 97:3 hexane/ethyl acetate) as a white solid, (34.6 mg, 71% with “Condition A” and 33.2 mg, 68% with “Condition B”). mp 154-156 °C. ¹H NMR (600 MHz, CDCl₃): δ 8.00 (d, *J* = 12 Hz, 1H), 7.69 (t, *J* = 7.8 Hz, 1H), 7.64 (s, 1H), 7.55-7.60 (m, 2H), 7.41 (s, 2H), 4.99 (d(br), *J* = 24 Hz, 2H); ¹³C NMR (150 MHz, CDCl₃): δ 169.75, 140.61, 136.00, 135.90, 133.22, 132.74, 132.14, 130.67, 129.92, 129.06, 128.60, 128.57, 68.33. HRMS (ESI, *m/z*) calcd. for C₁₄H₁₀O₂Cl [M+Na]⁺: 245.0369; found: 245.0372.

9,11-dimethyldibenzo[c,e]oxepin-5(7H)-one (2q)

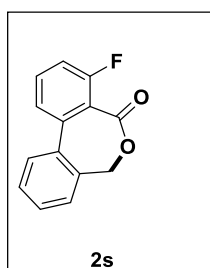


Following the general procedures A and B, the expected product was obtained using column chromatography (SiO₂, eluting with 97:3 hexane/ethyl acetate) as a white solid, (38.4 mg, 81% with “Condition A” and 33.2 mg, 70% with “Condition B”). ¹H NMR (600 MHz, CDCl₃): δ 7.90 (d, *J* = 7.8 Hz, 1H), 7.58 (t, *J* = 6H, 1H), 7.47 (t, *J* = 7.8 Hz, 2H), 7.21 (s, 1H), 7.11 (s, 1H), 4.89 (AB_q, *J* = 12 Hz, 2H), 2.39 (s, 3H), 2.38 (s, 3H); ¹³C NMR (150 MHz, CDCl₃): δ 170.68, 138.04, 136.43, 136.41, 135.92, 135.90, 134.69, 133.53, 131.53, 130.75, 130.25, 127.78, 126.95, 70.09, 21.13, 20.93. HRMS (ESI, *m/z*) calcd. for C₁₆H₁₅O₂ [M+H]⁺: 239.1072; found: 239.1079.

3-methoxy-[1,3]dioxolo[4',5':4,5]benzo[1,2-c]benzo[e]oxepin-5(7H)-one (2r)

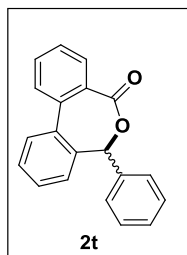


Following the general procedures A and B, the expected product was obtained using column chromatography (SiO₂, eluting with 95:5 hexane/ethyl acetate) as a white solid, (35.2 mg, 62% with “Condition A” and 40.8 mg, 72% with “Condition B”). mp 178-180 °C. ¹H NMR (400 MHz, CDCl₃): δ 7.41-7.43 (m, 2H), 7.17 (dd, *J*₁ = 4.8 Hz, *J*₂ = 2.8 Hz, 1H), 7.03 (s, 1H), 6.03 (s, 2H), 4.87 (AB_q, *J* = 12 Hz, 2H), 3.88 (s, 3H); ¹³C NMR (100 MHz, CDCl₃): δ 170.22, 159.24, 149.25, 147.44, 133.33, 131.44, 130.13, 129.92, 128.45, 120.13, 115.16, 108.79, 108.51, 101.75, 69.11, 55.74. HRMS (ESI, *m/z*) calcd. for C₁₆H₁₂O₅Na [M+Na]⁺: 307.0582; found: 307.0597.

4-fluorodibenzo[*c,e*]oxepin-5(7H)-one (2s)

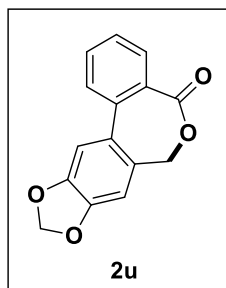
Following the general procedures A and B, the expected product was obtained using column chromatography (SiO₂, eluting with 97:3 hexane/ethyl acetate) as a white solid, (30.6 mg, 67% with “Condition A” and 23.2 mg, 51% with “Condition B”). mp 96-98 °C. ¹H NMR (600 MHz, CDCl₃): δ 7.68 (d, *J* = 12 Hz, 1H), 7.63-7.59 (m, 1H), 7.54-7.57 (m, 1H), 7.46-7.48 (m, 2H), 7.39 (d, *J* = 7.2 Hz, 2H), 7.24-7.27 (m, 1H), 5.04 (AB_q, *J* = 12 Hz, 2H); ¹³C NMR (150 MHz, CDCl₃): δ 169.18, 163.23 (d, *J*_{C-F} = 364.5 Hz), 139.01, 137.93, 137.42, 134.88, 132.92 (d, *J*_{C-F} = 9 Hz), 131.58, 130.28, 129.19, 128.82, 128.54, 124.16 (d, *J*_{C-F} = 3 Hz), 116.11 (d, *J*_{C-F} = 22 Hz), 68.92. HRMS (ESI, *m/z*) calcd. for C₁₄H₁₀O₂F [M+H]⁺: 229.0665; found: 229.0674.

7-phenyldibenzo[*c,e*]oxepin-5(7H)-one (2t)



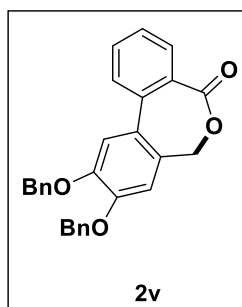
Following the general procedures A and B, the expected product was obtained using column chromatography (SiO₂, eluting with 97:3 hexane/ethyl acetate) as a white solid, (47.0 mg, 82% with “Condition A” and 40.2 mg, 70% with “Condition B”). mp 162-170 °C. ¹H NMR (600 MHz, CDCl₃): δ 8.03 (d, *J* = 7.8 Hz, 1H), 7.65-7.75 (m, 3H), 7.58 (t, *J* = 7.2 Hz, 1H), 7.41-7.52 (m, 6H), 7.29 (t, *J* = 7.2 Hz, 1H), 6.79 (d, *J* = 7.8 Hz, 1H), 6.25 (s, 1H); ¹³C NMR (150 MHz, CDCl₃): δ 169.42, 138.56, 138.46, 137.29, 135.73, 132.68, 131.46, 130.73, 129.54, 128.90, 128.78, 128.55, 128.52, 128.45, 128.40, 127.38, 126.97, 78.99. HRMS (ESI, *m/z*) calcd. for C₂₀H₁₄O₂Na [M+Na]⁺: 309.0891; found: 309.0444.

[1,3]dioxolo[4',5':4,5]benzo[1,2-*c*]benzo[*e*]oxepin-5(7H)-one (2u)



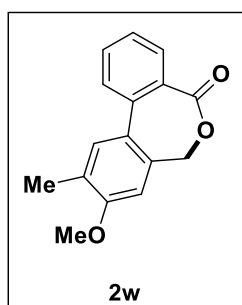
Following the general procedures A and B, the expected product was obtained using column chromatography (SiO₂, eluting with 95:5 hexane/ethyl acetate) as a white solid, (36.2 mg, 71% with “Condition A” and 31.6 mg, 62% with “Condition B”). mp 148-150 °C. ¹H NMR (600 MHz, CDCl₃): δ 7.94 (dd, *J*₁ = 8 Hz, *J*₂ = 1.2 Hz, 1H), 7.62 (td, *J*₁ = 7.6 Hz, *J*₂ = 1.6 Hz, 1H), 7.44-7.51 (m, 2H), 7.07 (s, 1H), 6.90 (s, 1H), 6.04 (s, 1H), 4.88 (AB_q, *J* = 12 Hz, 2H); ¹³C NMR (100 MHz, CDCl₃): δ 170.40, 149.31, 147.96, 137.33, 133.45, 132.59, 131.95, 130.53, 129.13, 128.43, 128.12, 108.90, 108.82, 101.86, 68.94. HRMS (ESI, *m/z*) calcd. for C₁₅H₁₁O₄ [M+H]⁺: 255.0657; found: 255.0659.

9,10-bis(benzyloxy)dibenzo[c,e]oxepin-5(7H)-one (2v)



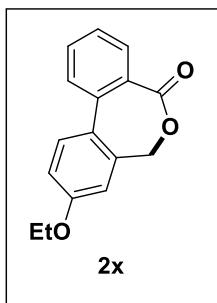
Following the general procedures A and B, the expected product was obtained using column chromatography (SiO₂, eluting with 94:6 hexane/ethyl acetate) as a white solid, (71.6 mg, 85% with “Condition A” and 74.2 mg, 88% with “Condition B”). mp 152-154 °C. ¹H NMR (400 MHz, CDCl₃): δ 7.94 (dd, *J*₁ = 8 Hz, *J*₂ = 1.6 Hz, 1H), 7.59 (td, *J*₁ = 7.6 Hz, *J*₂ = 1.6 Hz, 1H), 7.31-7.46 (m, 12 H), 7.18 (s, 1H), 7.00 (s, 1H), 5.22 (s, 4H), 4.85 (d(br), *J* = 52 Hz, 2H); ¹³C NMR (100 MHz, CDCl₃): δ 170.48, 150.13, 149.33, 137.32, 136.83, 136.76, 132.54, 132.40, 132.09, 130.61, 130.26, 128.72, 128.70, 128.54, 128.46, 128.27, 128.15, 127.98, 127.46, 127.32, 115.39, 114.89, 71.72, 71.52, 68.96. HRMS (ESI, *m/z*) calcd. for C₂₈H₂₃O₄ [M+H]⁺: 423.1596; found: 423.1602.

9-methoxy-10-methyldibenzo[c,e]oxepin-5(7H)-one (2w)



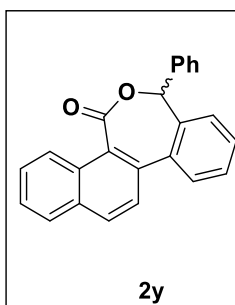
Following the general procedures A and B, the expected product was obtained using column chromatography (SiO₂, eluting with 95:5 hexane/ethyl acetate) as a white solid, (38.0mg, 75% with “Condition A” and 38.6 mg, 76% with “Condition B”). mp 160-164 °C. ¹H NMR (400 MHz, CDCl₃): δ 7.94 (d, *J* = 8 Hz, 1H), 7.61 (t, *J* = 8 Hz, 1H), 7.40-7.46 (m, 2H), 6.87 (s, 1H), 4.96 (d(br), *J* = 48 Hz, 2H), 3.89 (s, 3H), 2.29 (s, 3H); ¹³C NMR (100 MHz, CDCl₃): δ 170.60, 158.10, 137.55, 133.68, 132.50, 132.08, 130.98, 130.91, 130.39, 128.83, 128.37, 127.66, 109.88, 69.39, 55.69, 16.33. HRMS (ESI, *m/z*) calcd. for C₁₆H₁₄O₃ [M]⁺: 254.0943; found: 254.0916.

9-ethoxydibenzo[*c,e*]oxepin-5(7H)-one (2x)



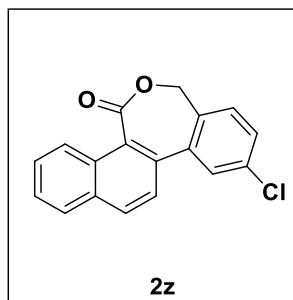
Following the general procedures A and B, the expected product was obtained using column chromatography (SiO₂, eluting with 95:5 hexane/ethyl acetate) as a white solid, (36.0 mg, 71% with “Condition A” and 37.0 mg, 73% with “Condition B”). mp 100-102 °C. ¹H NMR (600 MHz, CDCl₃): δ 7.97 (d, *J* = 7.8 Hz, 1H), 7.63 (td, *J*₁ = 7.8 Hz, *J*₂ = 1.2 Hz, 1H), 7.61 (d, *J* = 7.8 Hz, 1H), 7.49-7.57 (m, 2H), 7.45-7.48 (m, 1H), 6.97-7.06 (m, 2H), 4.97 (d(br), *J* = 7.3 Hz, 2H), 4.11 (q, *J* = 7.2 Hz, 2H), 1.46 (t, *J* = 7.2 Hz, 3H); ¹³C NMR (150 MHz, CDCl₃): δ 170.39, 159.22, 137.29, 136.07, 132.48, 132.00, 131.19, 130.10, 129.86, 128.29, 127.67, 116.08, 114.31, 69.28, 63.77, 14.73. HRMS (ESI, *m/z*) calcd. for C₁₆H₁₅O₃ [M+H]⁺: 255.1021; found: 255.1021.

3-phenylbenzo[*c*]naphtho[2,1-*e*]oxepin-1(3H)-one (2y)



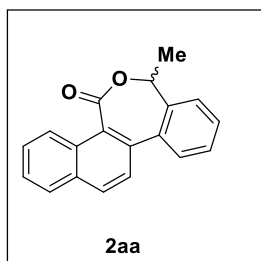
Following the general procedures A and B, the expected product was obtained using column chromatography (SiO₂, eluting with 97:3 hexane/ethyl acetate) as a white solid, (49.0 mg, 73% with “Condition A” and 51.6 mg, 77% with “Condition B”). mp 184-186 °C. ¹H NMR (400 MHz, CDCl₃): δ 8.38 (d, *J* = 8 Hz, 1H), 8.11-8.27 (m, 1H), 7.41-7.79 (m, 9H), 7.31 (td, *J*₁ = 8 Hz, *J*₂ = 1.2 Hz, 1H), 6.81 (d, *J* = 8 Hz, 1H), 6.25 (s, 1H); ¹³C NMR (100 MHz, CDCl₃): δ 167.81, 139.21, 138.76, 135.66, 135.28, 133.19, 132.34, 130.99, 129.23, 128.68, 128.64, 128.38, 128.27, 127.65, 127.26, 126.96, 126.79, 126.09, 124.43, 123.57, 118.92, 117.36, 78.88. HRMS (ESI, *m/z*) calcd. for C₂₄H₁₆O₂Na [M+Na]⁺: 359.1048; found: 359.1057.

6-chlorobenzo[c]naphtho[2,1-e]oxepin-1(3H)-one (2z)



Following the general procedures A and B, the expected product was obtained using column chromatography (SiO₂, eluting with 97:3 hexane/ethyl acetate) as a white solid, (41.6 mg, 71% with “Condition A” and 42.2 mg, 72% with “Condition B”). mp 188-190 °C. ¹H NMR (400 MHz, CDCl₃): δ 8.33 (d, *J* = 8 Hz, 1H), 8.07 (d, *J* = 8 Hz, 1H), 7.91 (d, *J* = 8 Hz, 1H), 7.76 (d, *J* = 1.2 Hz, 1H), 7.67-7.58 (m, 3H), 7.45-7.40 (m, 2H), 4.98 (AB_q, *J* = 12 Hz, 2H); ¹³C NMR (100 MHz, CDCl₃): δ 168.14, 140.95, 136.13, 133.98, 133.93, 133.38, 132.44, 131.18, 129.93, 129.06, 128.80, 128.47, 128.31, 127.92, 127.51, 126.88, 125.42, 68.15. HRMS (ESI, *m/z*) calcd. for C₁₈H₁₂O₂Cl [M+H]⁺: 295.0526; found: 295.0531.

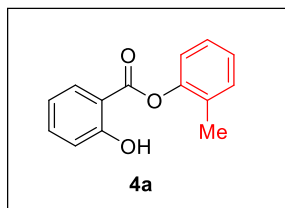
6-chloro-3-methylbenzo[c]naphtho[2,1-e]oxepin-1(3H)-one (2aa)



Following the general procedures A and B, the expected product was obtained using column chromatography (SiO₂, eluting with 97:3 hexane/ethyl acetate) as a white solid, (40.2 mg, 65% with “Condition A” and 33.2 mg, 54% with “Condition B”). mp 160-162 °C. ¹H NMR (600 MHz, CDCl₃): δ 8.42 (d, *J* = 8.4 Hz, 1H), 8.08 (d, *J* = 9 Hz, 1H), 7.93 (d, *J* = 8.4 Hz, 1H), 7.76 (d, *J* = 8.4 Hz, 1H), 7.68-7.64 (m, 2H), 7.56-7.61 (m, 3H), 7.51 (t, *J* = 7.8 Hz, 1H), 5.32 (q, *J* = 6 Hz, 1H), 1.88 (d, *J* = 6.6 Hz, 3H); ¹³C NMR (150 MHz, CDCl₃): δ 168.22, 138.85, 138.05, 135.14, 132.96, 131.99, 130.77, 129.51, 129.29, 128.57, 128.12, 127.69, 127.00, 126.64, 125.93, 123.85, 72.76, 16.53. HRMS (ESI, *m/z*) calcd. for C₁₉H₁₄O₂Na [M+Na]⁺: 297.0891; found: 297.0898.

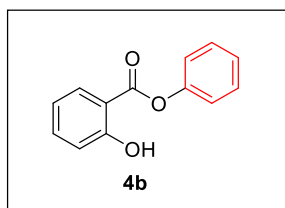
Chemo- and Regioselective Benzylic C(sp³)-H Oxidation Bridging the Gap between Hetero- and Homogeneous Copper Catalysis

o-tolyl 2-hydroxybenzoate (4a)^{41b}



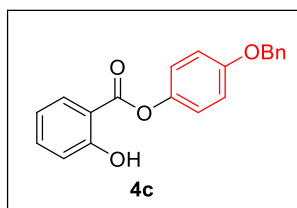
Following the experimental protocol for copper(0)-catalyzed Smiles rearrangement, the expected product was yielded using column chromatography (SiO₂, eluting with 96:4 hexane/ethyl acetate) as a colourless oil, (28.6 mg, 62%). ¹H NMR (400 MHz, CDCl₃): δ 10.56 (s, 1H), 8.12 (dd, *J* = 8.0 Hz, 2.0 Hz, 1H), 7.56 (td, *J* = 8.0 Hz, 1.6 Hz, 1H), 7.27-7.32 (m, 2H), 7.23 (td, *J* = 8.0 Hz, 1.6 Hz, 1H), 7.14 (dd, *J* = 8.0 Hz, 1.2 Hz, 1H), 7.06 (dd, *J* = 8.8 Hz, 1.2 Hz, 1H), 6.99 (td, *J* = 7.6 Hz, 1.2 Hz, 1H), 2.26 (s, 3H); ¹³C NMR (150 MHz, CDCl₃): δ 168.8, 162.3, 148.8, 136.6, 131.5, 130.43, 130.40, 127.2, 126.7, 121.9, 119.6, 117.9, 111.8, 16.3.

Phenyl 2-hydroxybenzoate (4b)^{41b}



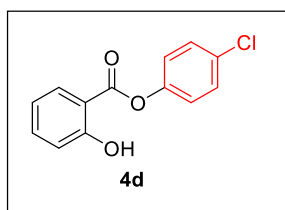
Following the experimental protocol for copper(0)-catalyzed Smiles rearrangement, the expected product was yielded using column chromatography (SiO₂, eluting with 96:4 hexane/ethyl acetate) as a colourless oil, (30.2 mg, 64%). ¹H NMR (600 MHz, CDCl₃): δ 10.53 (s, 1H), 8.10 (d, *J* = 7.8 Hz, 1H), 7.55 (t, *J* = 8.4 Hz, 1H), 7.47 (t, *J* = 8.4 Hz, 2H), 7.33 (t, *J* = 7.2 Hz, 1H), 7.23 (d, *J* = 8.4 Hz, 2H), 7.06 (d, *J* = 8.4 Hz, 1H), 6.99 (t, *J* = 7.2 Hz, 1H); ¹³C NMR (150 MHz, CDCl₃): δ 168.9, 162.2, 150.1, 136.5, 130.3, 129.6, 126.4, 121.6, 119.4, 117.8, 111.8.

4-(Benzyloxy)phenyl 2-hydroxybenzoate (4c)^{41a}



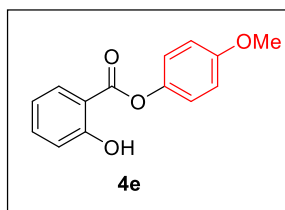
Following the experimental protocol for copper(0)-catalyzed Smiles rearrangement, the expected product was yielded using column chromatography (SiO₂, eluting with 95:5 hexane/ethyl acetate) as a white solid, (40.8 mg, 64%). ¹H NMR (400 MHz, CDCl₃): δ 10.52 (s, 1H), 8.05 (dd, *J* = 8.0 Hz, 1.6 Hz, 1H), 7.52 (td, *J* = 7.8 Hz, 2.0 Hz, 1H), 7.31-7.44 (m, 5H), 7.10-7.14 (m, 2H), 7.01-7.03 (m, 3H), 6.96 (t, *J* = 8.0 Hz, 1H), 5.07 (s, 2H); ¹³C NMR (100 MHz, CDCl₃): δ 169.3, 162.2, 156.9, 143.7, 136.8, 136.5, 130.4, 128.7, 128.2, 127.5, 122.5, 119.5, 117.9, 115.7, 111.9, 70.5.

4-Chlorophenyl 2-hydroxybenzoate (4d)^{41a}



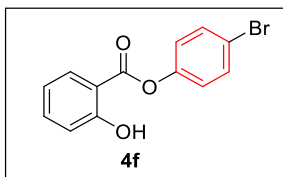
Following the experimental protocol for copper(0)-catalyzed Smiles rearrangement, the expected product was yielded using column chromatography (SiO₂, eluting with 96:4 hexane/ethyl acetate) as a white solid, (28.4 mg, 57%). ¹H NMR (600 MHz, CDCl₃): δ 10.40 (s, 1H), 8.05 (d, *J* = 7.8 Hz, 1H), 7.55 (t, *J* = 7.8 Hz, 1H), 7.42 (d, *J* = 9.0 Hz, 2H), 7.17 (d, *J* = 9.0 Hz, 2H), 7.05 (d, *J* = 8.4 Hz, 1H), 6.98 (t, *J* = 7.8 Hz, 1H); ¹³C NMR (150 MHz, CDCl₃): δ 168.6, 162.2, 148.5, 136.7, 131.8, 130.3, 129.7, 123.0, 119.6, 117.9, 111.5.

4-Methoxyphenyl 2-hydroxybenzoate (4e)^{41b}



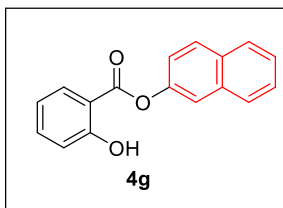
Following the experimental protocol for copper(0)-catalyzed Smiles rearrangement, the expected product was yielded using column chromatography (SiO₂, eluting with 96:4 hexane/ethyl acetate) as a colourless oil, (29.4 mg, 61%). ¹H NMR (400 MHz, CDCl₃): δ 10.51 (s, 1H), 8.05 (dd, *J* = 8.0 Hz, 2.0 Hz, 1H), 7.50-7.54 (m, 1H), 7.09-7.12 (m, 2H), 7.02 (dd, *J* = 8.0 Hz, 0.8 Hz, 1H), 6.93-6.97 (m, 3H), 3.82 (s, 3H); ¹³C NMR (100 MHz, CDCl₃): δ 169.4, 162.2, 157.8, 143.6, 136.5, 130.4, 122.5, 119.5, 117.9, 114.7, 111.9, 55.7.

4-bromophenyl 2-hydroxybenzoate (4f)^{41a}



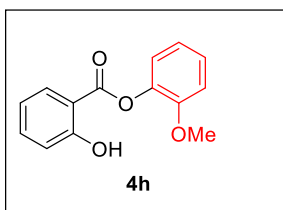
Following the experimental protocol for copper(0)-catalyzed Smiles rearrangement, the expected product was yielded using column chromatography (SiO₂, eluting with 96:4 hexane/ethyl acetate) as a white solid, (28.2 mg, 48%). ¹H NMR (400 MHz, CDCl₃): δ 10.36 (s, 1H), 8.03 (dd, *J* = 8.0 Hz, 1.6 Hz, 1H), 7.51-7.57 (m, 3H), 7.08-7.12 (m, 2H), 7.03 (d, *J* = 8.4 Hz, 1H), 6.99 (t, *J* = 8.0 Hz, 1H); ¹³C NMR (100 MHz, CDCl₃): δ 168.6, 162.3, 149.3, 136.8, 132.7, 130.4, 123.5, 119.6, 119.6, 118.0, 111.6.

Naphthalen-2-yl 2-hydroxybenzoate (4g)^{41a}



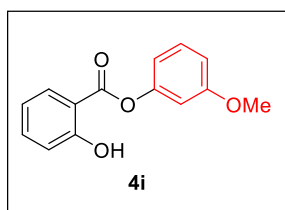
Following the experimental protocol for copper(0)-catalyzed Smiles rearrangement, the expected product was yielded using column chromatography (SiO₂, eluting with 96:4 hexane/ethyl acetate) as a white solid, (34.0 mg, 65%). ¹H NMR (400 MHz, CDCl₃): δ 10.51 (s, 1H), 8.13 (dd, *J* = 8.0 Hz, 1.6 Hz, 1H), 7.92 (d, *J* = 8.8 Hz, 1H), 7.83-7.89 (m, 2H), 7.68 (d, *J* = 2.4 Hz, 1H), 7.49-7.58 (m, 3H), 7.34 (dd, *J* = 8.8 Hz, 2.4 Hz, 1H), 7.05 (dd, *J* = 8.4 Hz, 0.8 Hz, 1H), 6.99 (t, *J* = 8.4 Hz, 1H); ¹³C NMR (100 MHz, CDCl₃): δ 169.2, 162.3, 147.8, 136.6, 133.8, 131.8, 130.5, 129.8, 127.9, 127.8, 126.9, 126.1, 120.9, 119.6, 118.8, 117.9, 111.9.

2-Methoxyphenyl 2-hydroxybenzoate (4h)^{41b}



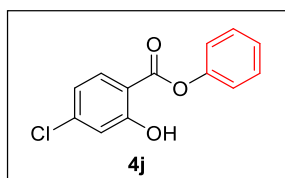
Following the experimental protocol for copper(0)-catalyzed Smiles rearrangement, the expected product was yielded using column chromatography (SiO₂, eluting with 95:5 hexane/ethyl acetate) as a white solid, (26.0 mg, 53%). ¹H NMR (400 MHz, CDCl₃): δ 10.47 (s, 1H), 8.10 (dd, *J* = 8.0 Hz, 1.2 Hz, 1H), 7.50-7.54 (m, 1H), 7.25-7.29 (m, 1H), 7.15 (dd, *J* = 8.0 Hz, 1.6 Hz, 1H), 7.00-7.04 (m, 3H), 6.99-6.94 (m, 1H), 3.82 (s, 3H); ¹³C NMR (100 MHz, CDCl₃): δ 168.5, 162.1, 151.2, 139.2, 136.3, 130.7, 127.5, 122.9, 120.9, 119.5, 117.8, 112.7, 111.9, 56.0.

3-Methoxyphenyl 2-hydroxybenzoate (4i)^{41a}



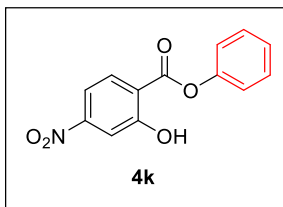
Following the experimental protocol for copper(0)-catalyzed Smiles rearrangement, the expected product was yielded using column chromatography (SiO₂, eluting with 95:5 hexane/ethyl acetate) as a colourless oil, (34.0 mg, 68%). ¹H NMR (400 MHz, CDCl₃): δ 10.48 (s, 1H), 8.06 (dd, *J* = 8.0 Hz, 1.6 Hz, 1H), 7.53 (td, *J* = 8.4 Hz, 1.6 Hz, 1H), 7.34 (t, *J* = 8.0 Hz, 1H), 7.02 (dd, *J* = 8.0 Hz, 0.8 Hz, 1H), 6.96 (td, *J* = 8.0 Hz, 1.2 Hz, 1H), 6.84-6.87 (m, 1H), 6.78-6.81 (m, 1H), 6.76 (t, *J* = 2.4 Hz, 1H), 3.82 (s, 3H); ¹³C NMR (100 MHz, CDCl₃): δ 168.9, 162.3, 160.7, 151.1, 136.5, 130.4, 130.1, 119.5, 117.9, 113.8, 112.3, 111.9, 107.8, 55.58.

phenyl 4-chloro-2-hydroxybenzoate (4j)⁴¹



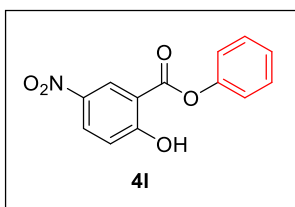
Following the experimental protocol for copper(0)-catalyzed Smiles rearrangement, the expected product was yielded using column chromatography (SiO₂, eluting with 96:4 hexane/ethyl acetate) as a colourless oil, (30.0 mg, 61%). ¹H NMR (400 MHz, CDCl₃): δ 10.62 (s, 1H), 8.03 (d, *J* = 8.8 Hz, 1H), 7.46-7.50 (m, 2H), 7.34 (t, *J* = 7.2 Hz, 1H), 7.22-7.24 (m, 2H), 7.09 (d, *J* = 2.0 Hz, 1H), 6.98 (dd, *J* = 8.4 Hz, 2.0 Hz, 1H); ¹³C NMR (100 MHz, CDCl₃): δ 168.4, 162.7, 150.0, 142.4, 131.4, 129.7, 126.6, 121.6, 120.3, 118.1, 110.6.

Phenyl 2-hydroxy-4-nitrobenzoate (4k)^{41a}



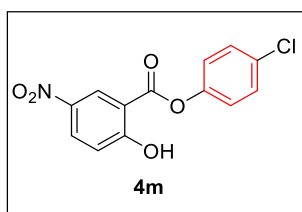
Following the experimental protocol for copper(0)-catalyzed Smiles rearrangement, the expected product was yielded using column chromatography (SiO₂, eluting with 9:1 hexane/ethyl acetate) as a yellowish solid, (25.8 mg, 50%). ¹H NMR (400 MHz, CDCl₃): δ 10.71 (s, 1H), 8.25 (d, *J* = 8.8 Hz, 1H), 7.86 (d, *J* = 2.0 Hz, 1H), 7.78 (dd, *J* = 8.8 Hz, 2.0 Hz, 1H), 7.47 (t, *J* = 7.6 Hz, 2H), 7.34 (tt, *J* = 7.6 Hz, 1.2 Hz, 1H), 7.20-7.23 (m, 2H); ¹³C NMR (100 MHz, CDCl₃): δ 167.7, 162.6, 153.0, 149.7, 131.8, 129.9, 127.0, 121.4, 116.7, 113.8, 113.4.

Phenyl 2-hydroxy-5-nitrobenzoate (4l)^{41a}



Following the experimental protocol for copper(0)-catalyzed Smiles rearrangement, the expected product was yielded using column chromatography (SiO₂, eluting with 9:1 hexane/ethyl acetate) as a yellowish solid, (26 mg, 50%). ¹H NMR (400 MHz, CDCl₃): δ 11.16 (s, 1H), 9.02 (d, *J* = 2.8 Hz, 1H), 8.40 (dd, *J* = 9.2 Hz, 2.8 Hz, 1H), 7.47 (t, *J* = 8.0 Hz, 2H), 7.34 (tt, *J* = 7.2 Hz, 1.2 Hz, 1H), 7.21-7.24 (m, 2H), 7.15 (d, *J* = 9.2 Hz, 1H); ¹³C NMR (100 MHz, CDCl₃): δ 167.8, 166.7, 149.7, 140.3, 131.2, 129.9, 127.1, 127.0, 121.4, 119.0, 111.8.

4-Chlorophenyl 2-hydroxy-5-nitrobenzoate (4m)^{41a}



Following the experimental protocol for copper(0)-catalyzed Smiles rearrangement, the expected product was yielded using column chromatography (SiO₂, eluting with 9:1 hexane/ethyl acetate) as a white solid, (28.2 mg, 45%). ¹H NMR (400 MHz, CDCl₃): δ 11.03 (s, 1H), 8.98 (d, *J* = 2.8 Hz, 1H), 8.41 (dd, *J* = 9.2 Hz, 2.8 Hz, 1H), 7.42-7.45 (m, 2H), 7.17-7.19 (m, 2H), 7.15 (d, *J* = 9.2 Hz, 1H); ¹³C NMR (100 MHz, CDCl₃): δ 167.5, 166.7, 148.1, 140.3, 132.6, 131.4, 130.0, 127.1, 122.8, 119.1, 111.5.

IV.6.7. Step-by-step experimental protocol for total synthesis of Alterlactone (21) (related to Scheme 16)

5,7-dihydroxy-2,2-dimethyl-4H-benzo[d][1,3]dioxin-4-one (7)⁵⁸

This synthesis was performed slightly modifying a previously reported protocol.⁵⁸ In a 250 mL round-bottom flask, 2,4,6-trihydroxybenzoic acid monohydrate **6** (10.0 g, 58.8 mmol) was dissolved in trifluoroacetic acid (100 mL), and cooled to 0 °C. Then, acetone (15 mL) and trifluoroacetic anhydride (70 mL) were added to it. After being gradually warmed to room temperature, the mixture was stirred for 12 hours. Thereafter, after completion, it was allowed to reach room temperature, solvent was evaporated under reduced pressure. Then, saturated aqueous NaHCO₃ solution (200 mL) was added to it and the mixture was extracted with EtOAc (3 × 200 mL) and rinsed with water (2 × 300 mL) and brine (2 × 300 mL). The combined organic layer was filtered through anhydrous sodium sulfate for drying, the solvent was evaporated under reduced pressure to give a liquid. Then, the crude product was purified with column chromatography (eluting with petroleum ether/ethyl acetate 4:1) to afford the corresponding **7** (9.7 g, 79%) as light-yellow solid.

5-Hydroxy-7-methoxy-2,2-dimethyl-4H-benzo[d][1,3]dioxin-4-one (8)⁵⁸

Triphenyl phosphine (PPh₃) (23.5 mmol, 6.2 g), DIAD (23.5 mmol, 4.6 mL) were added to a stirring solution of compound **7** (21.4 mmol, 4.5 g) in methanol (23.5 mmol, 0.9 mL) in dichloromethane (DCM) (50 mL) at 0 °C. After being gradually warmed to room temperature, the mixture was stirred for 3 hours. Thereafter, after completion acc. to TLC, it was allowed to reach room temperature, water (30 mL) was added to the solution for quenching

and was extracted with DCM (2 × 50 mL) and rinsed with water (2 × 60 mL) and brine (2 × 60 mL). The combined organic layer was filtered through anhydrous sodium sulfate for drying, the solvent was evaporated under reduced pressure to give a liquid. Then, the crude product was purified with column chromatography (eluting with petroleum ether/ethyl acetate 9:1) to afford **8** (4.6 g, 95%) as white solid.

7-Methoxy-2,2-dimethyl-4-oxo-4H-benzo[d][1,3]dioxin-5-yl trifluoromethanesulfonate (9**)⁵⁸**

To a solution of **8** (5.0 g, 25.7 mmol) in anhydrous DCM (40 mL), anhydrous pyridine (51.5 mmol, 4.2 mL) and trifluoromethanesulfonic anhydride (38.6 mmol, 6.5 mL) were added at 0 °C. Then the mixture was stirred for 2 hours at 0 °C. After completion, water (50 mL) was added to quench and it was extracted with DCM (3 × 50 mL). The combined organic layer was filtered through anhydrous sodium sulfate for drying, the solvent was evaporated under reduced pressure to give a liquid. Then, the crude product was purified with column chromatography (eluting with petroleum ether/ethyl acetate 3:1) to afford **9** (7.7 g, 92%) as white solid. ¹H NMR (400 MHz, CDCl₃): δ 6.47 (d, *J* = 8 Hz, 2H), 3.84 (s, 3H), 1.69 (s, 6H); ¹³C NMR (100 MHz, CDCl₃): δ 165.70, 158.92, 157.20, 149.93, 123.58, 120.38, 117.19, 114.00, 106.67, 105.42, 105.41, 105.40, 101.20, 100.94, 56.39, 25.53.

4-bromo-5-methylbenzene-1,2-diol (14**)**

This synthesis was performed slightly modifying a previously reported procedure.⁵⁹ 4-methylcatechol (**10**) (1.24 g, 10 mmol, 1 equiv.) was dissolved in acetonitrile (10 mL) and to this solution, a solution of N-bromosuccinimide (NBS) (1.05 equiv., 10.5 mmol, 1.86 g) in MeCN (10 mL) at 0 °C. The solution was then stirred for additional 20 minutes at ambient temperature. After that, water (100 mL) was added to quench it and extracted with EtOAc (3 × 50 mL). The combined organic layer was filtered through anhydrous sodium sulfate for drying, the solvent was evaporated under reduced pressure to yield 4-bromo-5-methylbenzene-1,2-diol (**11**) (2 g, 99%) as a white solid and was used for the next step without further purification.

((4-bromo-5-methyl-1,2-phenylene)bis(oxy))bis(methylene)dibenzene (12**)**

The synthesis was performed by benzylation of **11**. In a 100 mL round-bottom flask closed with guard tube, suspension of compound **11** (1 equiv., 1 g, 5 mmol) and K₂CO₃ (2.5 equiv., 1.7 g, 12.5 mmol) was taken and DMF solvent (20 mL) was added to it. Then, the flask was closed with guard tube and stirred at ambient temperature for 20 minutes. Therefore, BnBr

(benzyl bromide) (12.5 mmol, 2.5 equiv., 1.5 mL) was added to it dropwise. Then again, the mixture was stirred at room temperature after closing the flask-mouth with guard tube for additional 5 hours. After that, the reaction was quenched with 50 mL of ice-cold water and washed three times with 50 mL of ethyl acetate. The combined organic layer was filtered through anhydrous sodium sulfate for drying, the solvent was evaporated under reduced pressure to give a liquid. Then, the crude product was purified with column chromatography (eluting with petroleum ether/ethyl acetate 95:5) to afford (((4-bromo-5-methyl-1,2-phenylene)bis(oxy))bis(methylene))dibenzene (**12**) (1.81 g, 95%) as a colourless gel.

2-(4,5-bis(benzyloxy)-2-methylphenyl)-4,4,5,5-tetramethyl-1,3,2-dioxaborolane (13)

In a clean and dry pressure tube (30 mL), bromo arene **12** (1.15 g, 3 mmol, 1 equiv.), bis(pinacolato)diboron (839 mg, 1.1 equiv.) were charged and dioxane (15 mL) was added. Then, PdCl₂ (palladium chloride) (26.6 mg, 5 mol%), DPPF (1,1'-Ferrocenediyl-bis(diphenylphosphine)) (166.3 mg, 10 mol%), potassium acetate (KOAc) (590 mg, 2 equiv.) was added successively. The pressure-tube was sealed under argon atmosphere and was heated at 110 °C with continuous stirring for 20 hours. After completion, the solution was diluted with deionized water (50 mL) and extracted with EtOAc (3 × 50 mL). The combined organic layer was filtered through anhydrous sodium sulfate for drying, the solvent was evaporated under reduced pressure. Then, the crude product was purified with column chromatography (eluting with petroleum ether/ethyl acetate 95:5) to afford borylated compound **13** (1.16 g, 90 %) as white solid. ¹H NMR (400 MHz, CDCl₃): δ 7.24-7.48 (m, 12H), 5.15 (s, 2H), 5.13 (s, 2H), 2.46 (s, 3H), 1.32 (s, 12H); ¹³C NMR (100 MHz, CDCl₃): δ 151.29, 146.19, 139.91, 137.80, 137.35, 128.52, 127.72, 127.30, 122.90, 116.50, 83.34, 71.92, 70.84, 24.99, 21.82.

5-(4,5-bis(benzyloxy)-2-methylphenyl)-7-methoxy-2,2-dimethyl-4H-benzo[d][1,3]dioxin-4-one (14)

In an oven-dried pressure tube (30 mL), aryl triflate **9** (356 mg, 1.00 mmol), **13** (516 mg, 1.20 mmol), Cs₂CO₃ (cesium carbonate) (813 mg, 2.50 mmol), palladium chloride (PdCl₂) (8.8 mg, 5mol%) and S-Phos (purity 97%, 41.0 mg, 10 mol%) were charged in the glove-box. Then, under Ar atmosphere, dioxane/H₂O (7:1, 10 mL) was added to the vessel. The tube was taken out of the glove box and was heated at 80 °C with continuous stirring for 20 h. After completion, it was cooled to room temperature, quenched with saturated NH₄Cl solution (10 mL) and was extracted with EtOAc (2×30 mL). The combined organic layer was filtered

through anhydrous sodium sulfate for drying, the solvent was evaporated under reduced pressure. Then, the crude product was purified with column chromatography (eluting with petroleum ether/ethyl acetate 9:1) to afford **14** (428.4 mg, 84 %) as colourless gel. ¹H NMR (400 MHz, CDCl₃): δ 7.26-7.48 (m, 10H), 6.83 (s, 1H), 6.72 (s, 1H), 6.43 (d, *J* = 2.4 Hz, 1H), 6.37 (d, *J* = 2.4 Hz, 1H), 5.05-5.20 (m, 4H), 3.81 (s, 3H), 2.03 (s, 3H), 1.72 (s, 6H); ¹³C NMR (100 MHz, CDCl₃): δ 164.67, 158.96, 158.61, 148.64, 146.89, 146.59, 137.65, 133.18, 128.52, 128.50, 128.43, 127.78, 127.70, 127.65, 127.49, 116.43, 113.14, 105.85, 105.11, 100.68, 71.99, 71.40, 55.77, 26.26, 25.32, 19.52. HRMS (ESI, *m/z*) calcd. for C₃₂H₃₁O₆ [M+H]⁺: 511.2121; found: 511.2123.

Benzyl 3,4',5'-tris(benzyloxy)-5-methoxy-2'-methyl-[1,1'-biphenyl]-2-carboxylate (15)

This was synthesized by slightly modifying the literature procedure.⁵⁷ NaH (60 % purity, 30 mg, 1.5 equiv.) was added to a solution of **14** (325 mg, 0.5 mmol, 1 equiv.) in DMF-water (5 mL, 8:1) in a 25 mL round bottom flask with a guard tube and stirred for 10 minutes. After that, BnBr (benzyl bromide) (1.48 mL, 2.5 equiv.) was added dropwise at 0 °C with stirring continuously. The mixture was warmed to room temperature and stirred for 20 hours. Therefore, it was quenched with ice-cold water (20 mL) and extracted with EtOAc (2×30 mL). The combined organic layer was filtered through anhydrous sodium sulfate for drying, the solvent was evaporated under reduced pressure to give the crude product **15**. This was used without further purification at the next step.

3,4',5'-tris(benzyloxy)-5-methoxy-2'-methyl-[1,1'-biphenyl]-2-carboxylic acid (16)

To a KOH (potassium hydroxide) (168 mg, 6 equiv.) solution in water-ethanol (1:1), corresponding crude ester **15** was added. The reaction solution was then refluxed at 100 °C with constant stirring for 24 hours. After that, the solution was concentrated under reduced pressure and neutralized with 6 (N) HCl. Then, the solution was extracted with EtOAc. The combined organic layer was filtered through anhydrous sodium sulfate for drying, the solvent was evaporated under reduced pressure. Then, the crude product was purified with column chromatography (eluting with petroleum ether/ethyl acetate 7:3) to afford **16** (243 mg, 87%) is yielded as white solid. ¹H NMR (400 MHz, CDCl₃): δ 7.27-7.46 (m, 15H), 6.80 (s, 1H), 6.75 (s, 1H), 6.53 (d, *J* = 2.4 Hz, 1H), 6.31 (d, *J* = 2.4 Hz, 1H), 5.07-5.15 (m, 6H), 3.77 (s, 3H), 2.04 (s, 3H); ¹³C NMR (100 MHz, CDCl₃): δ 163.55, 161.63, 157.73, 148.46,

146.22, 144.77, 137.58, 135.79, 133.30, 128.83, 128.52, 128.43, 127.79, 127.65, 127.58, 127.44, 116.50, 116.35, 108.30, 99.17, 71.58, 71.38, 71.32, 55.64, 19.59.

4,9,10-tris(benzyloxy)-2-methoxydibenzo[*c,e*]oxepin-5(7H)-one (**17**)

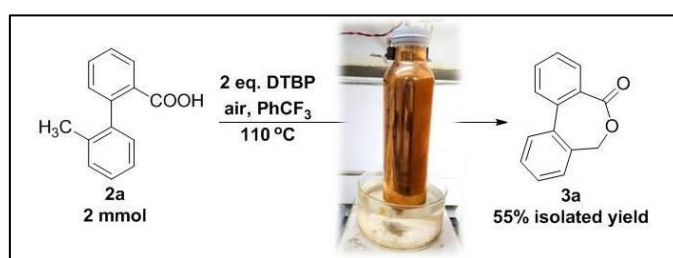
In a clean and oven-dried pressure tube (15 mL) with magnetic stir-bar, **16** (0.1 mmol, 56 mg), copper powder (20 mol %, 0.04 mmol, 1.2 mg) and rose Bengal (RB) (1 mol%, 0.002 mmol, 1 mg) was charged. Then, PhCF₃ (2 mL) was added and the pressure-tube was sealed promptly during purging with UHP O₂. Therefore, the mixture was heated at 110 °C for 30 hours with continuous irradiation from two white CFLs (each CFL: 32 W and set at a distance of 5 cm). After the completion (monitored with TLC), it was allowed to reach room temperature and then water (30 mL) was added. The mixture was extracted with EtOAc (2 x 40 mL). The combined organic layer was filtered through anhydrous sodium sulfate for drying, the solvent was evaporated under reduced pressure. Then, the crude product was purified with column chromatography (eluting with petroleum ether/ethyl acetate 9:1) to afford protected Alterlactone **17** (42.8 mg, 77%) as colourless gel. ¹H NMR (400 MHz, CDCl₃): δ 7.29-7.48 (m, 15H), 7.14 (s, 1H), 6.96 (s, 1H), 6.55 (d, *J* = 2 Hz, 1H), 6.32 (d, *J* = 2 Hz, 1H), 5.11-5.28 (m, 6H), 4.80 (AB_q, *J* = 12 Hz, 2H), 3.77 (s, 3H); ¹³C NMR (100 MHz, CDCl₃): δ 166.67, 162.30, 159.46, 149.73, 149.43, 139.80, 137.01, 136.77, 136.43, 132.14, 130.23, 129.20, 128.74, 128.73, 128.69, 128.67, 128.55, 128.14, 128.04, 127.94, 127.40, 127.32, 127.17, 127.14, 127.13, 115.47, 114.74, 114.03, 104.81, 100.50, 71.74, 71.50, 71.18, 68.22, 55.60. HRMS (ESI, *m/z*) calcd. for C₁₆H₃₁O₆ [M+H]⁺: 559.2121; found: 559.2132.

4,9,10-Trihydroxy-2-methoxydibenzo[*c,e*]oxepin-5(7H)-one, Alterlactone (**18**)⁴²

To a stirred solution of protected alterlactone **17** (27.9 mg, 50.0 μmol) in ethyl acetate-ethanol (1:1), Pd/C (10 mol%, 300 μmol, 32.0 mg) was added. The mixture was stirred under H₂ atmosphere at rt for 7 hours. After completion (indicated by TLC), the whole mixture was filtered. The filtrate was concentrated under reduced pressure to afford alterlactone (**18**) as a colourless solid (14 mg, 50.0 μmol, quant.). ¹H NMR (600 MHz, DMSO-*d*₆): δ 10.21 (brS, 1H), 9.47 (br S, 1H), 9.38 (brS, 1H), 7.04 (s, 1H), 6.91 (s, 1H), 6.51 (d, *J* = 2.4 Hz, 1H), 6.46 (d, *J* = 2.4 Hz, 1H), 4.87-4.79 (m, 2H), 3.82 (s, 3H); ¹³C NMR (100 MHz, DMSO-*d*₆): δ 168.77, 162.26, 159.99, 146.60, 145.91, 140.08, 129.88, 126.65, 115.55, 109.48, 105.08, 100.83, 67.84, 55.41. HRMS (EI, *m/z*) calcd. for C₁₅H₁₂O₆ [M+H]⁺: 288.0634; found: 288.0636. Spectroscopic data is in full accordance with the reported one⁴².

IV.6.8. Protocol for external catalyst-free intramolecular benzylic C(sp³)-H oxidation of 2'-methyl-[1,1'-biphenyl]-2-carboxylic acid in copper bottle

In a clean and dry 500 mL copper bottle (commercially drinking water bottle), substance **1a** (424 mg, 2.0 mmol) was added and dissolved in PhCF₃ (10 mL). Therefore, DTBP (4.0 mmol, 2 equiv.) was added with a microsyringe and vessel was sealed with the cap. Then, the bottle was heated at 110 °C with continuous stirring for 36 hours. After the completion (monitored with TLC), it was allowed to reach room temperature and then water (100 mL) was added.

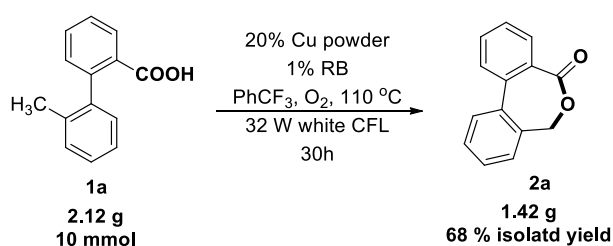


The mixture was extracted with EtOAc (2 x 100 mL). The combined organic layer was filtered through anhydrous sodium sulfate for drying, the solvent was evaporated under reduced pressure. Then, the crude product was purified with column chromatography (eluting with petroleum ether/ethyl acetate 9:1) to afford dibenzo[c,e]oxepin-5(7H)-one **2a** (231 mg, 55%) as white solid.



Figure 13. Experimental set up for reaction in copper bottle.

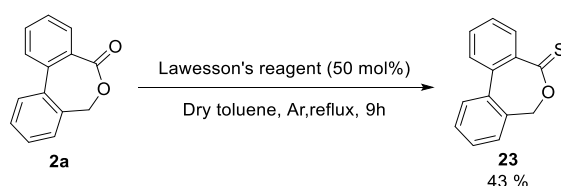
IV.6.9. Experimental protocol for the standard reaction with 1a in “Condition B” in gram-scale



In a clean and oven-dried pressure tube (100 mL) with magnetic stir-bar inside, substrate **1a** (10 mmol, 1 equiv., 2.12 g), copper powder (20 mol %, 2 mmol, 127 mg) were taken. Therefore, PhCF₃ (α,α,α -trifluorotoluene (20 mL) was added to. The vessel was purged with UHP (ultra-high pure) O₂ for 1 minute and sealed promptly. Thereafter, for 30 hours, reaction mixture was heated at 110 °C under continuous irradiation from two white CFLs (each CFL: 32 W and set at 5 cm distance from the reaction vessel). Thereafter, after completion, it was allowed to reach room temperature, the mixture was extracted with EtOAc (2 X 300 mL) and rinsed with water (300 mL) and brine (300 mL). The combined organic layer was filtered through anhydrous sodium sulfate for drying, the solvent was evaporated under reduced pressure to give a liquid. Then, the crude product was purified with column chromatography (eluting with petroleum ether/ethyl acetate 3:97) to afford the dibenzo[*c,e*]oxepin-5(7H)-one **2a** (1.42 g, 68%) as white solid.

IV.6.10. Product derivatization

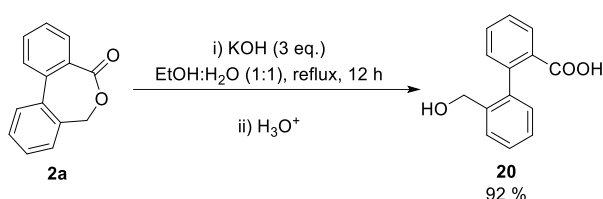
Protocol for synthesis of dibenzo[*c,e*]oxepan-5-thione (DOT, 19)⁴⁴ via thiolation of dibenzo[*c,e*]oxepin-5(7H)-one (2a)



To a solution of dibenzo[*c,e*]oxepan-5-one **2a** (42 mg, 0.2 mmol) in anhydrous toluene (2 mL), Lawesson's Reagent (57 mg, 0.12 mmol, 0.6 equiv.) was added was refluxed for 22 hours. Then, the reaction mixture was concentrated under reduced pressure and purification was performed by column chromatography (SiO₂, hexane–ethyl acetate, 4:1) to afford yellow crystals of **23** (19.43 mg, 43%). ¹H NMR (600 MHz, CDCl₃) δ 8.18 (d, *J* = 8.4 Hz, 1 H), 7.66 (d, *J* = 7.2 Hz, 1 H), 7.62 (t, *J* = 8.4 Hz, 1 H), 7.52-7.57 (m, 2 H), 7.46 (t, *J* = 6.6 Hz, 3 H), 5.20 (AB_q, *J* = 1.2 Hz, 2H); ¹³C NMR (150 MHz, CDCl₃) δ 216.04, 139.06, 134.55, 134.49, 133.93, 132.05, 130.30, 128.74, 128.55, 128.40, 128.07, 73.79.

Protocol for hydrolysis of dibenzo[*c,e*]oxepin-5(7H)-one (2a**) to synthesize of 2'-(hydroxymethyl)-[1,1'-biphenyl]-2-carboxylic acid (**20**)**

The solution of dibenzo[*c,e*]oxepan-5-one **2a** (42 mg, 0.2 mmol) potassium hydroxide (KOH) solution of water-ethanol (1:1) was refluxed for overnight. Then the mixture was concentrated under reduced pressure and was neutralized with 6 (N) HCl. The mixture was extracted with EtOAc and rinsed with water and brine. The combined organic layer was filtered through anhydrous sodium sulfate for drying, the solvent was evaporated under reduced pressure to give a liquid.



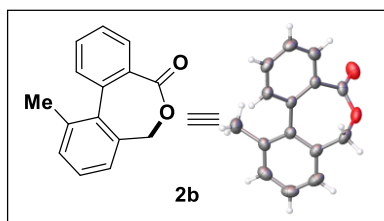
Then, the crude product was purified with column chromatography (eluting with petroleum ether/ethyl acetate) to afford the 2'-(hydroxymethyl)-[1,1'-biphenyl]-2-carboxylic acid (**20**) as white solid

(42 mg, 92%). ¹H NMR (400 MHz, DMSO-*d*₆) δ 7.89 (dd, *J*₁ = 2 Hz, *J*₂ = 1.6 Hz, 1 H), 7.52 (qd, *J*₁ = 8 Hz, *J*₂ = 1.6 Hz, 2 H), 7.43 (td, *J*₁ = 8 Hz, *J*₂ = 1.6 Hz, 1 H), 7.32 (td, *J*₁ = 8 Hz, *J*₂ = 1.6 Hz, 1 H), 7.23 (tt, *J*₁ = 7.2 Hz, *J*₂ = 1.6 Hz, 2 H), 7.02 (dd, *J*₁ = 7.6 Hz, *J*₂ = 1.2 Hz, 1H), 4.80 (brs, 1H), 4.35 (AB_q, *J* = 13.2 Hz, 2H); ¹³C NMR (100 MHz, DMSO-*d*₆) δ 169.76, 141.31, 140.33, 138.35, 131.44, 131.01, 130.90, 129.52, 128.56, 127.19, 127.15, 126.83, 126.39, 61.79.

IV.6.11. Representative crystal structures

Crystal structure of compound **2b**

The crystals were grown in chloroform solvent. The pure compound was dissolved in chloroform and slow evaporation led to the crystal **2b**. The crystal data was collected in X-ray spectroscopy (Bruker D8 Venture with a Photon-III detector), and the data was analyzed using OLEX2 software. The structure is given below.



X-ray determined molecular structure of **2b**, CCDC: 2105616

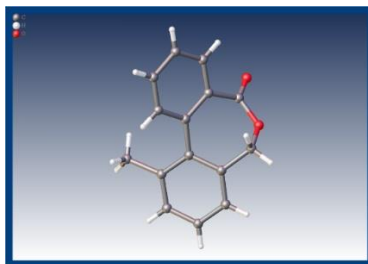


Table 3. Crystal data and structure refinement for **2b**

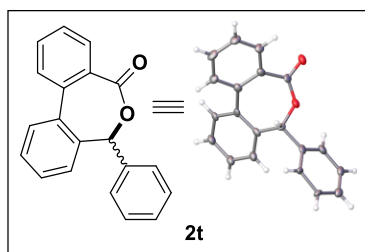
Identification code	SNAN-494_a
Empirical formula	C ₁₅ H ₁₂ O ₂
Formula weight	224.25
Temperature/K	298
Crystal system	monoclinic
Space group	P2 ₁ /n
a/Å	6.761(10)
b/Å	13.096(19)
c/Å	13.88(2)
α/°	90
β/°	103.633(18)
γ/°	90
Volume/Å ³	1194(3)
Z	4
ρ _{calc} /cm ³	1.247
μ/mm ⁻¹	0.082
F(000)	472.0
Crystal size/mm ³	0.45 × 0.35 × 0.25
Radiation	MoKα (λ = 0.71073)
2θ range for data collection/°	4.336 to 49.992
Index ranges	-7 ≤ h ≤ 8, -15 ≤ k ≤ 15, -16 ≤ l ≤ 12

Chemo- and Regioselective Benzylic C(sp³)-H Oxidation Bridging the Gap between Hetero- and Homogeneous Copper Catalysis

Reflections collected	9034
Independent reflections	2089 [$R_{\text{int}} = 0.0438$, $R_{\text{sigma}} = 0.0325$]
Data/restraints/parameters	2089/0/155
Goodness-of-fit on F^2	0.763
Final R indexes [$I \geq 2\sigma(I)$]	$R_1 = 0.0418$, $wR_2 = 0.1195$
Final R indexes [all data]	$R_1 = 0.0457$, $wR_2 = 0.1258$
Largest diff. peak/hole / $e \text{ \AA}^{-3}$	0.24/-0.16

Crystal structure of compound **2t**

The crystals of **2t** were grown, and the data was collected and analyzed at same procedure with that of **2b**.



X-ray determined molecular structure of **2t**, CCDC: 2105617

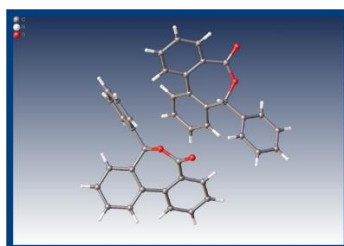
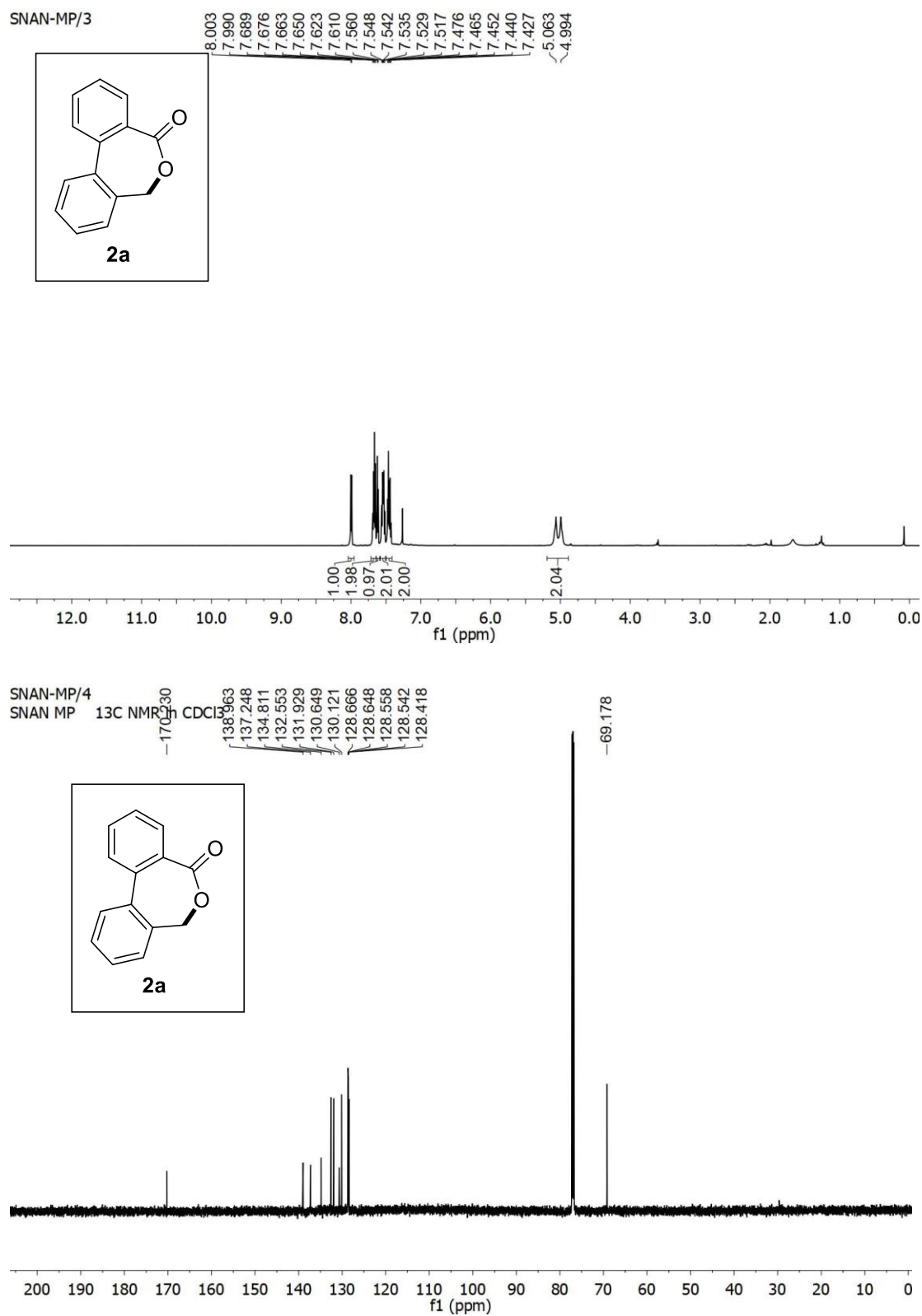


Table 4. Crystal data and structure refinement for **2t**

Identification code	SNAN760_0m_a
Empirical formula	$C_{40}H_{28}O_4$
Formula weight	572.62
Temperature/K	100.0
Crystal system	orthorhombic

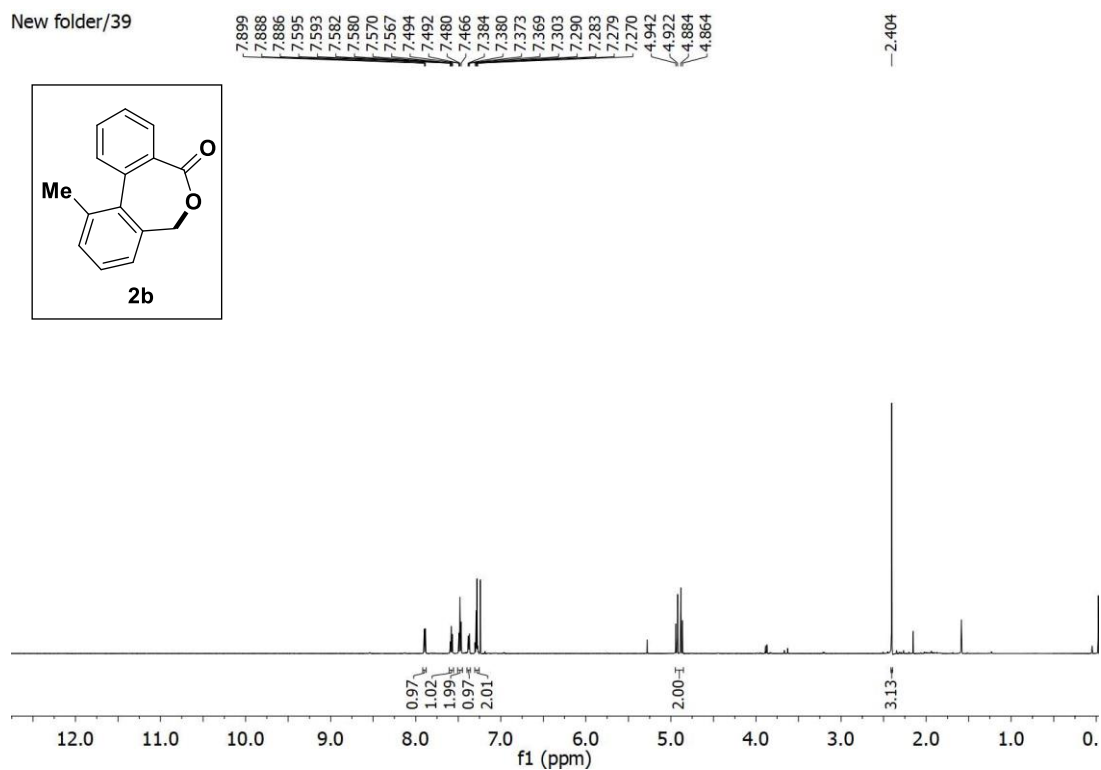
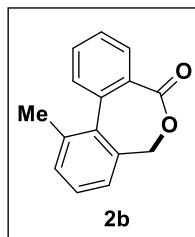
Space group	Pca2 ₁
a/Å	14.9718(4)
b/Å	10.7966(3)
c/Å	17.1600(5)
α/°	90
β/°	90
γ/°	90
Volume/Å ³	2773.82(13)
Z	4
ρ _{calc} /cm ³	1.371
μ/mm ⁻¹	0.697
F(000)	1200.0
Crystal size/mm ³	0.3 × 0.25 × 0.18
Radiation	CuKα (λ = 1.54178)
2Θ range for data collection/°	8.188 to 133.462
Index ranges	-16 ≤ h ≤ 17, -11 ≤ k ≤ 12, -20 ≤ l ≤ 20
Reflections collected	44507
Independent reflections	4862 [R _{int} = 0.0575, R _{sigma} = 0.0309]
Data/restraints/parameters	4862/1/397
Goodness-of-fit on F ²	1.052
Final R indexes [I ≥ 2σ (I)]	R ₁ = 0.0662, wR ₂ = 0.1748
Final R indexes [all data]	R ₁ = 0.0671, wR ₂ = 0.1760
Largest diff. peak/hole / e Å ⁻³	0.74/-0.33
Flack parameter	0.26(8)

IV.7. Representative NMR spectra

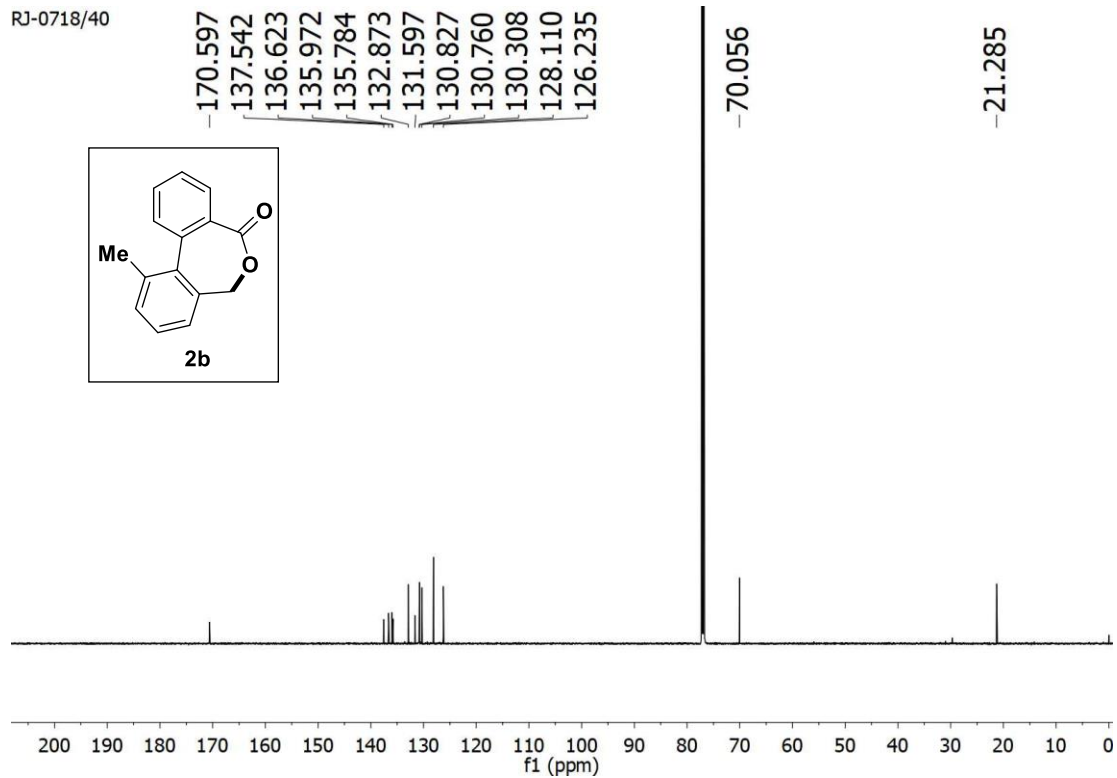
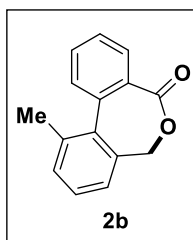


¹H and ¹³C spectra of **2a**

New folder/39

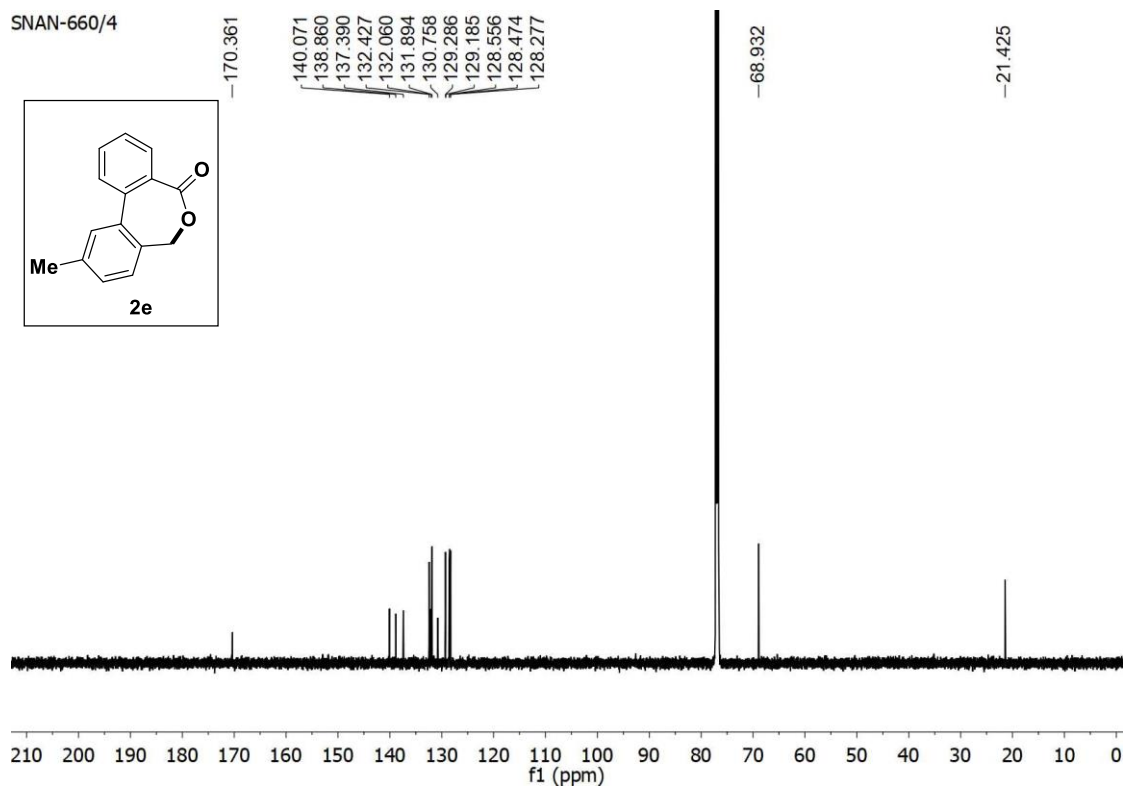
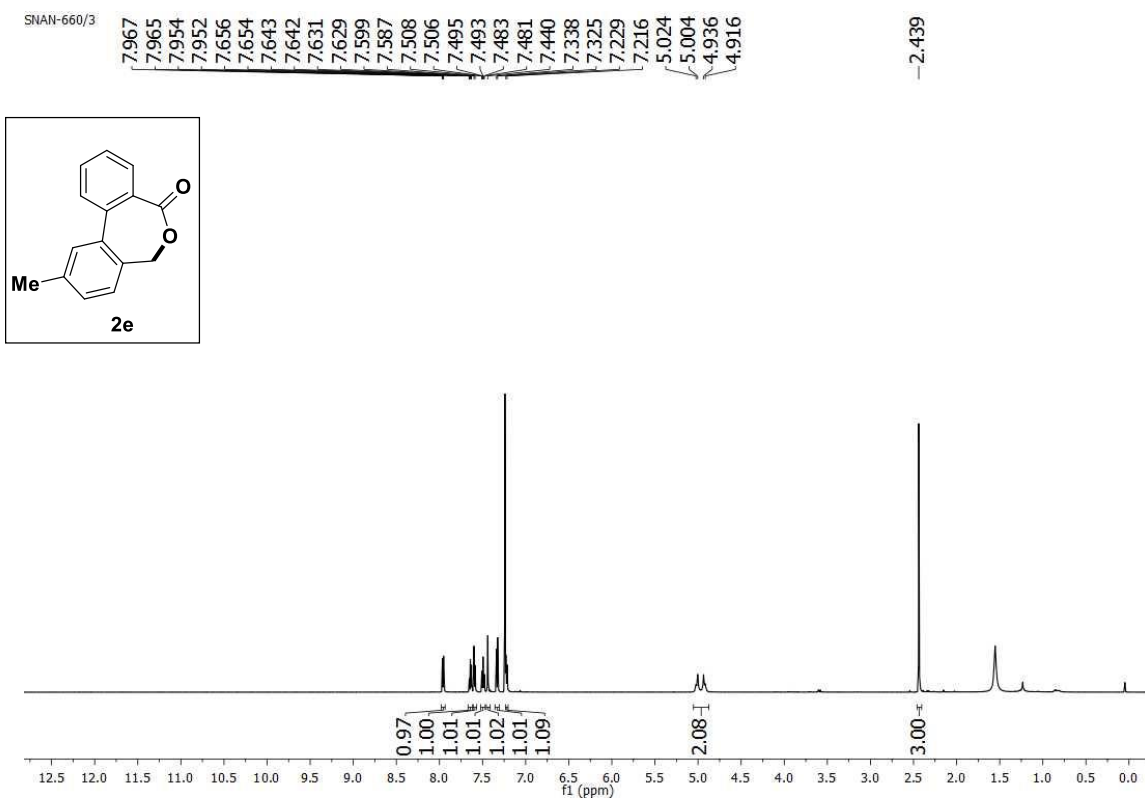


RJ-0718/40



^1H and ^{13}C spectra of **2b**

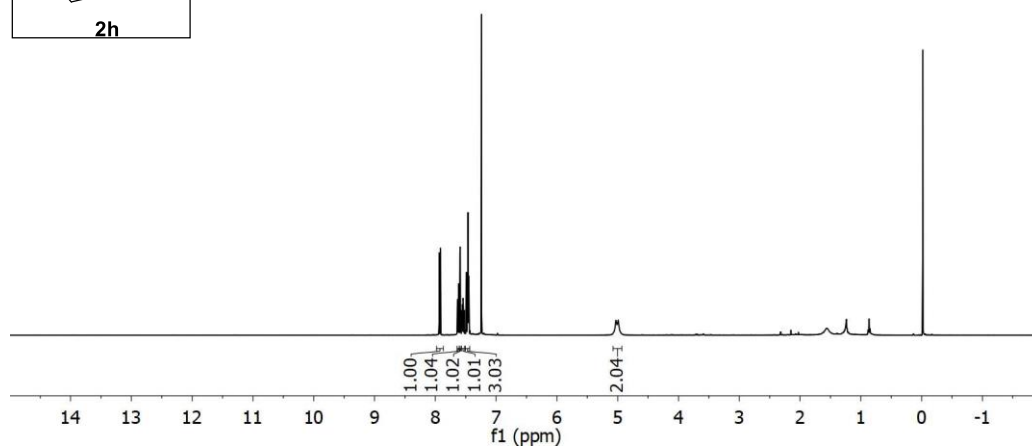
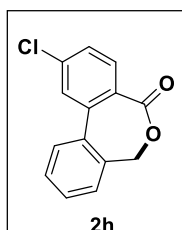
Chemo- and Regioselective Benzylic C(sp³)-H Oxidation Bridging the Gap between Hetero- and Homogeneous Copper Catalysis



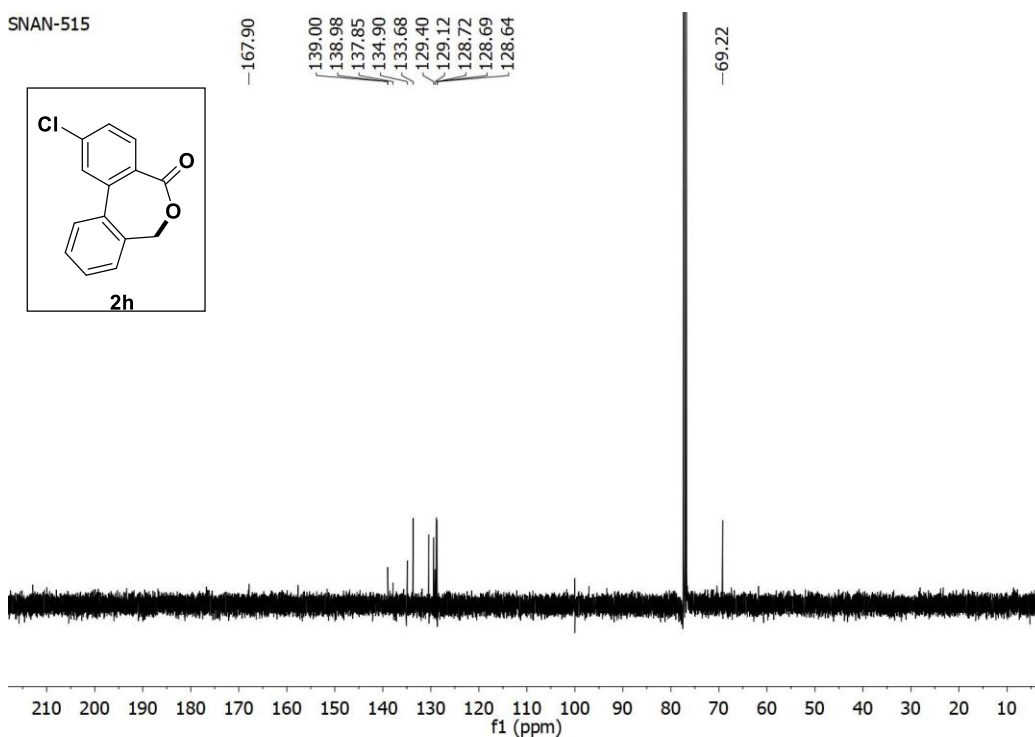
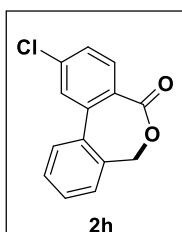
¹H and ¹³C spectra of **2e**

Chapter IV

SNAN-515
single_pulse

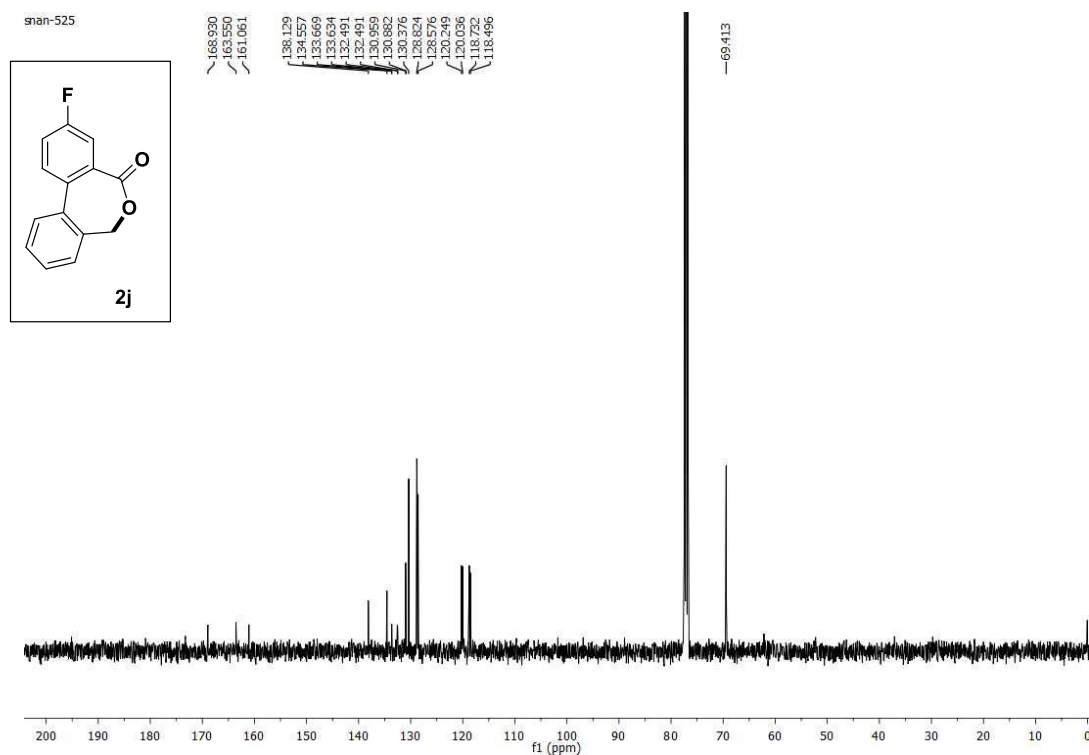
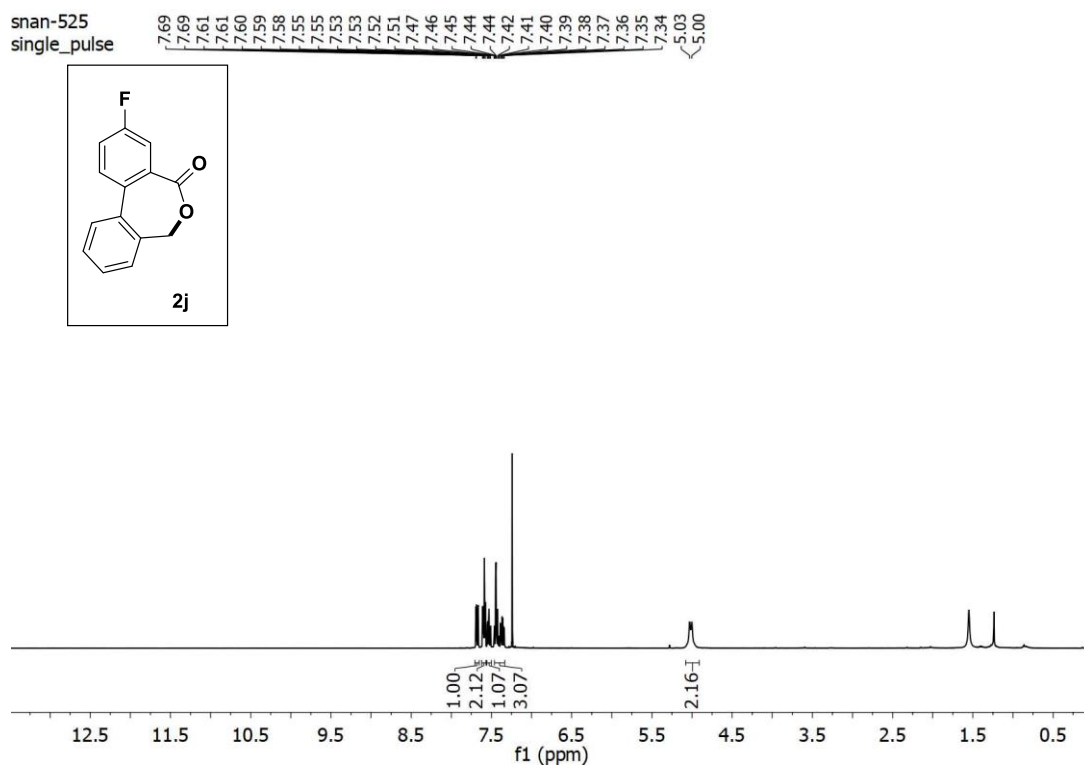


SNAN-515



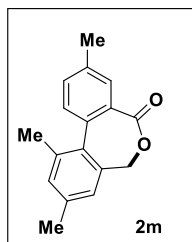
^1H and ^{13}C spectra of **2h**

Chemo- and Regioselective Benzylic C(sp³)-H Oxidation Bridging the Gap between Hetero- and Homogeneous Copper Catalysis

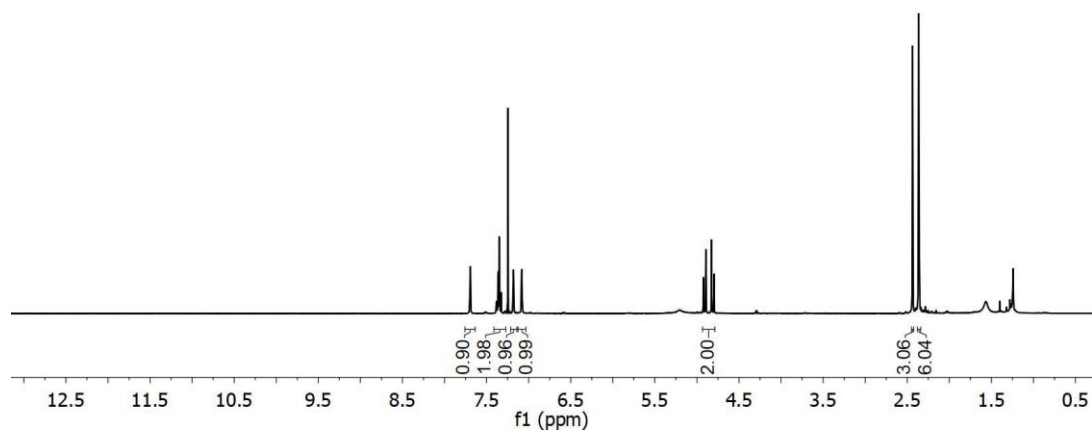


¹H and ¹³C spectra of **2j**

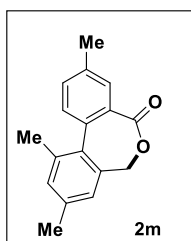
SNAN-709
single_pulse



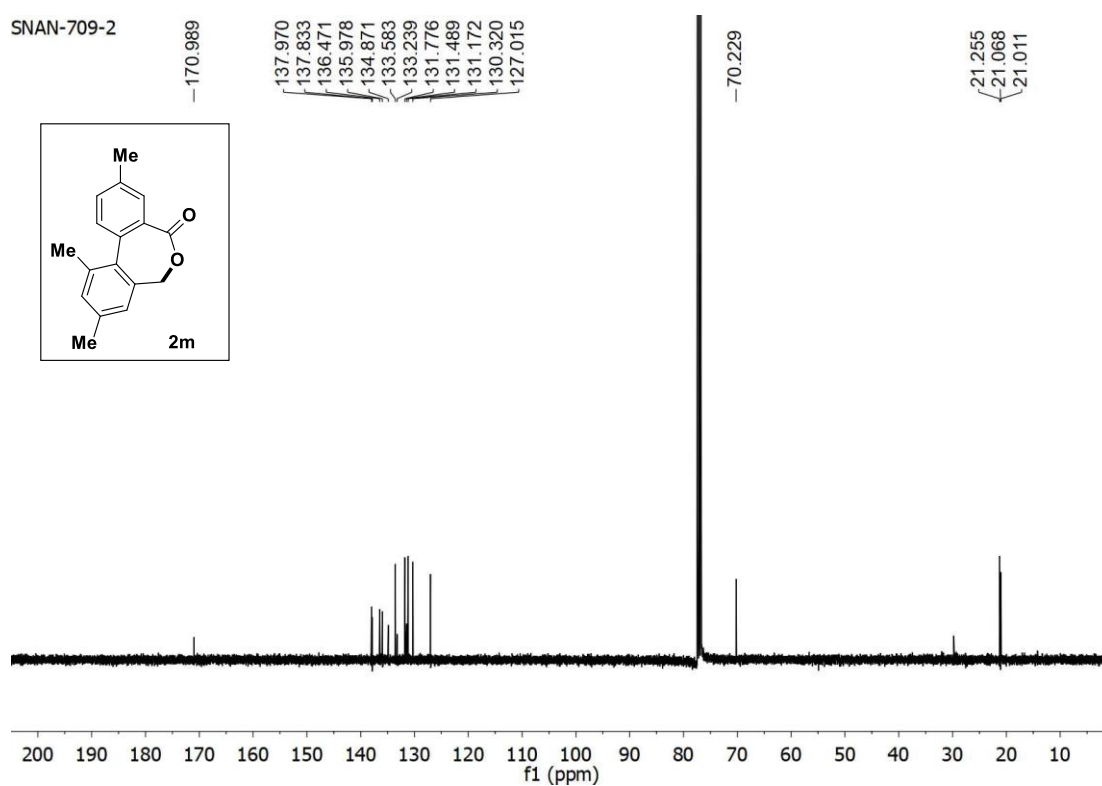
7.699
7.697
7.693
7.691
7.381
7.380
7.363
7.360
7.347
7.327
7.182
7.084
4.923
4.893
4.826
4.796
2.437
2.365
2.361



SNAN-709-2



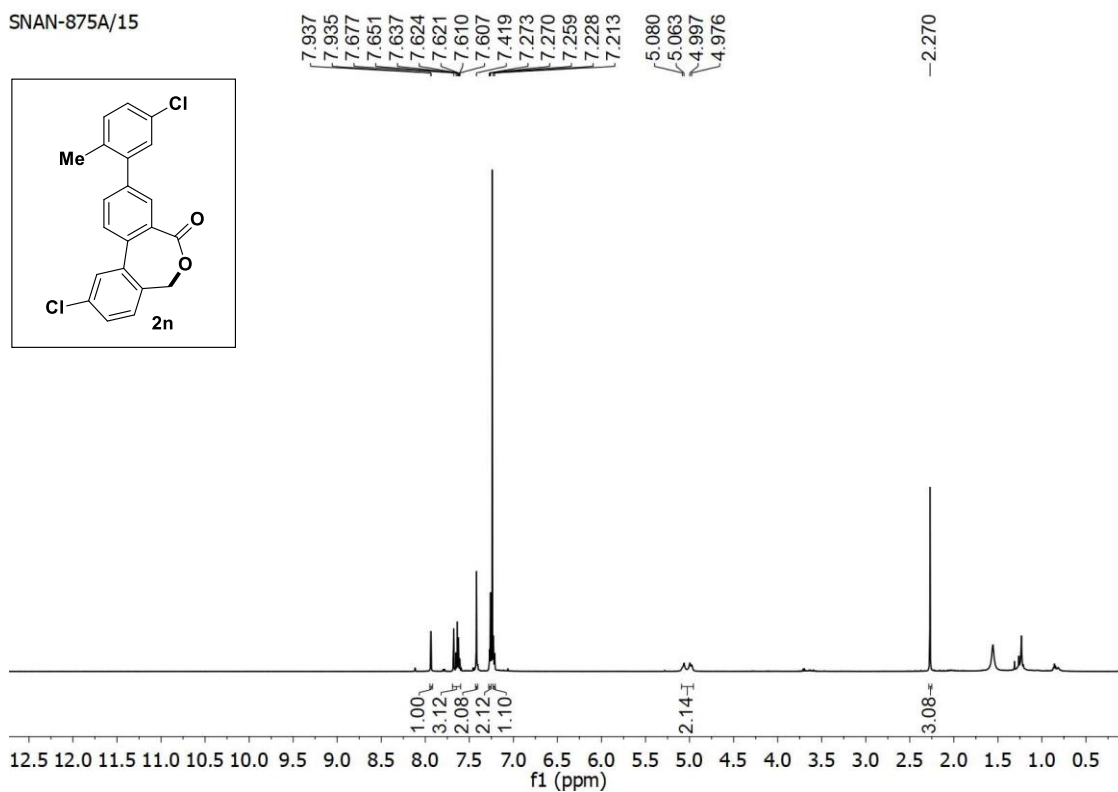
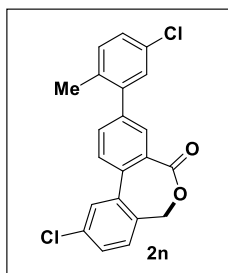
170.989
137.970
137.833
136.471
135.978
134.871
133.583
133.239
131.776
131.489
131.172
130.320
127.015
-70.229
21.255
21.068
21.011



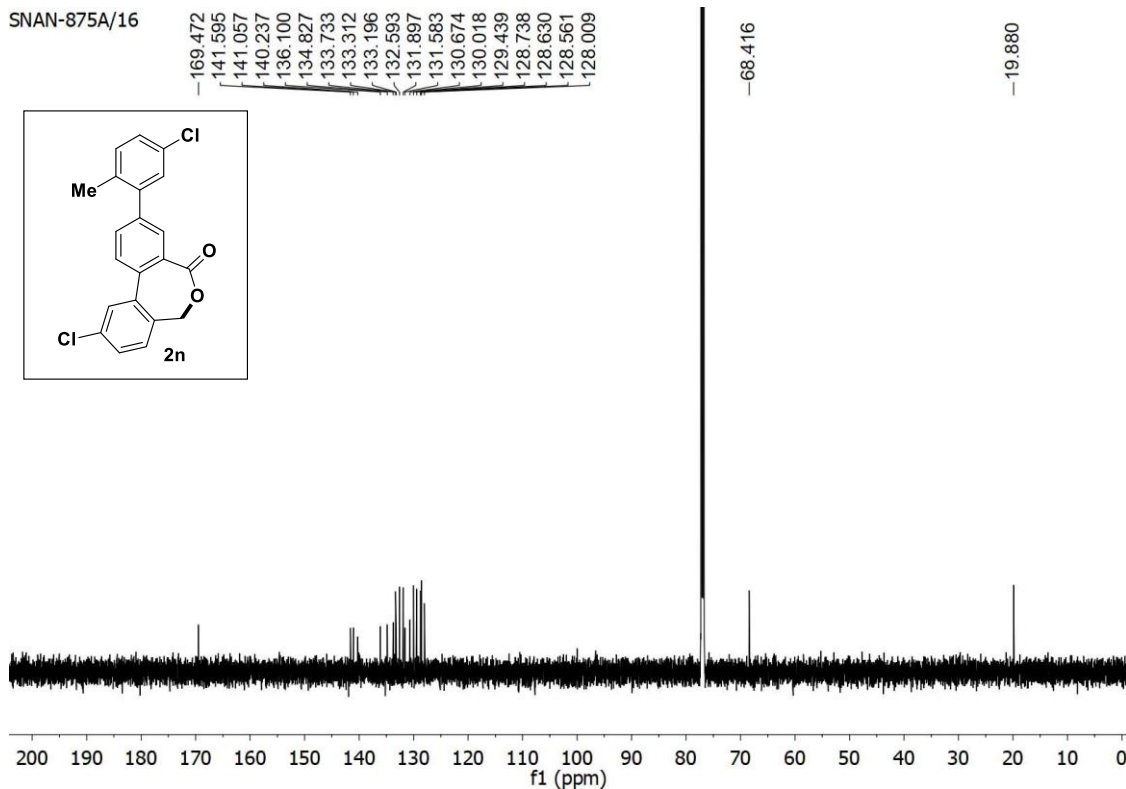
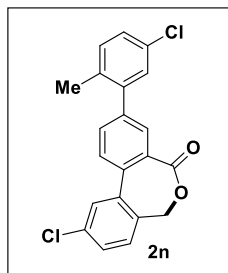
^1H and ^{13}C spectra of **2m**

Chemo- and Regioselective Benzylic C(sp³)-H Oxidation Bridging the Gap between Hetero- and Homogeneous Copper Catalysis

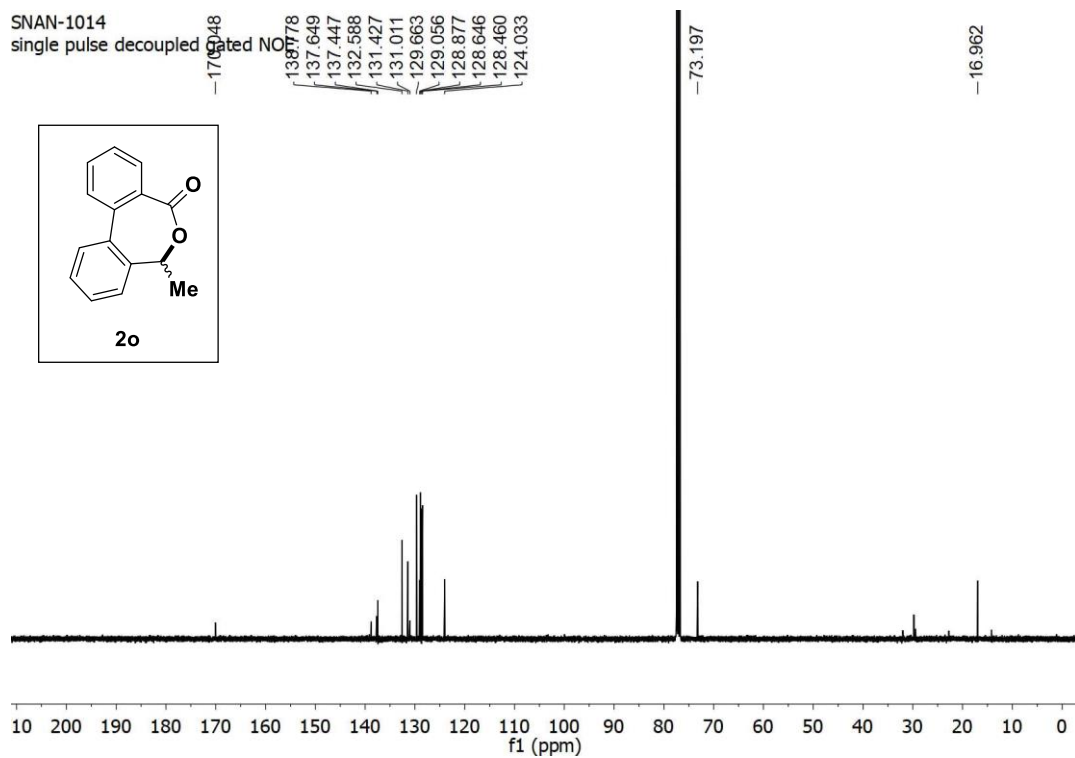
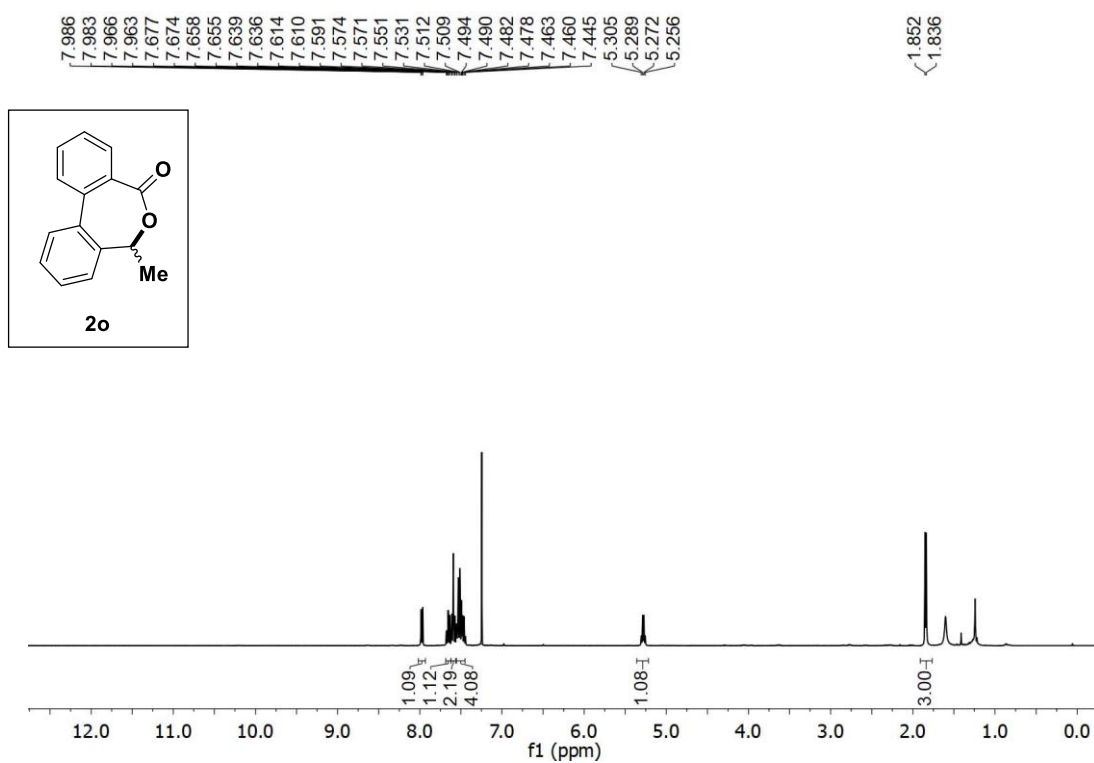
SNAN-875A/15



SNAN-875A/16



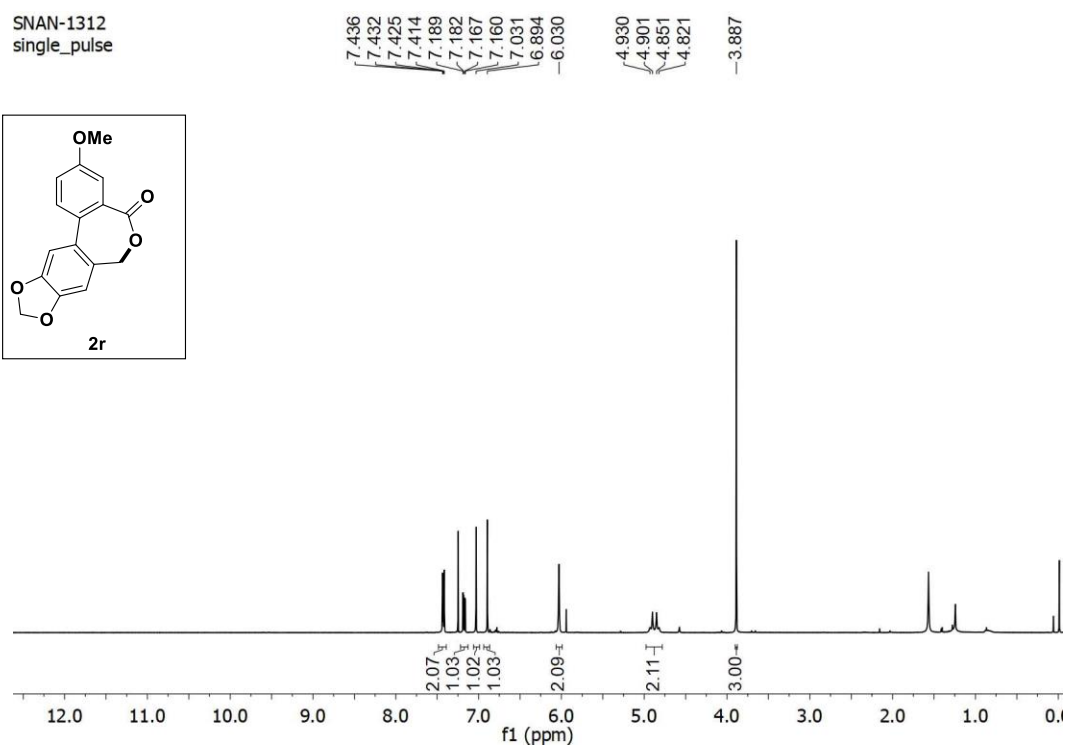
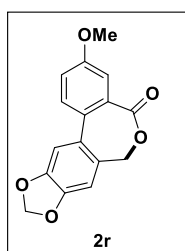
¹H and ¹³C spectra of **2n**



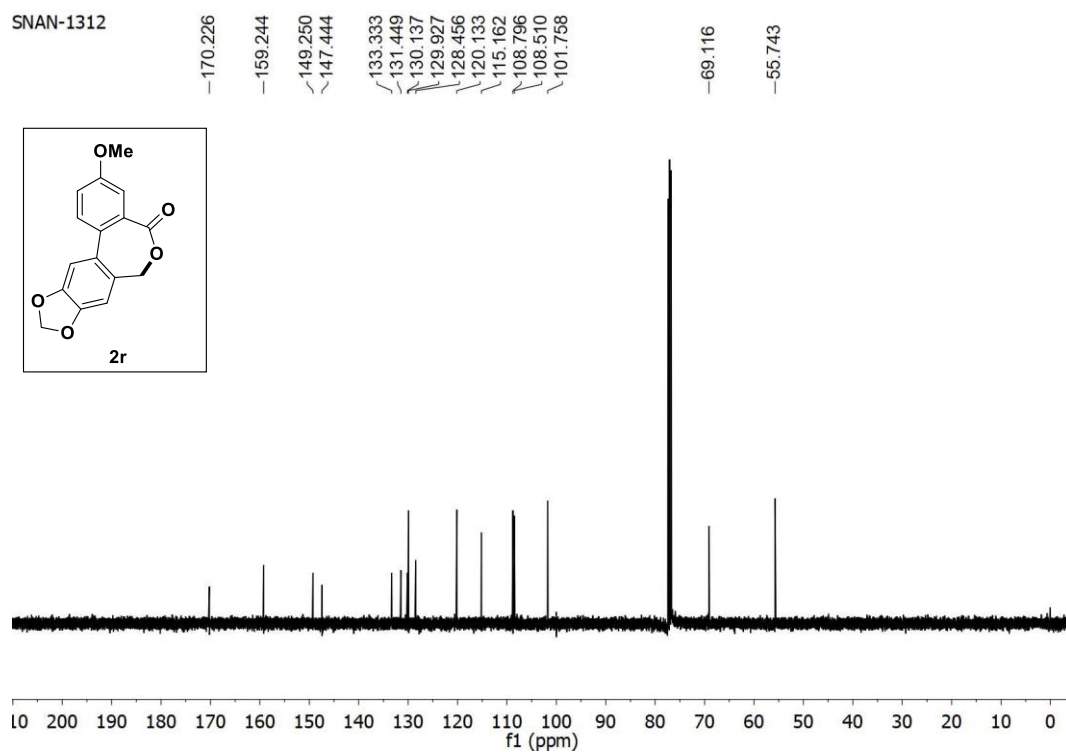
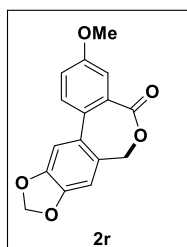
^1H and ^{13}C spectra of **2o**

Chemo- and Regioselective Benzylic C(sp³)-H Oxidation Bridging the Gap between Hetero- and Homogeneous Copper Catalysis

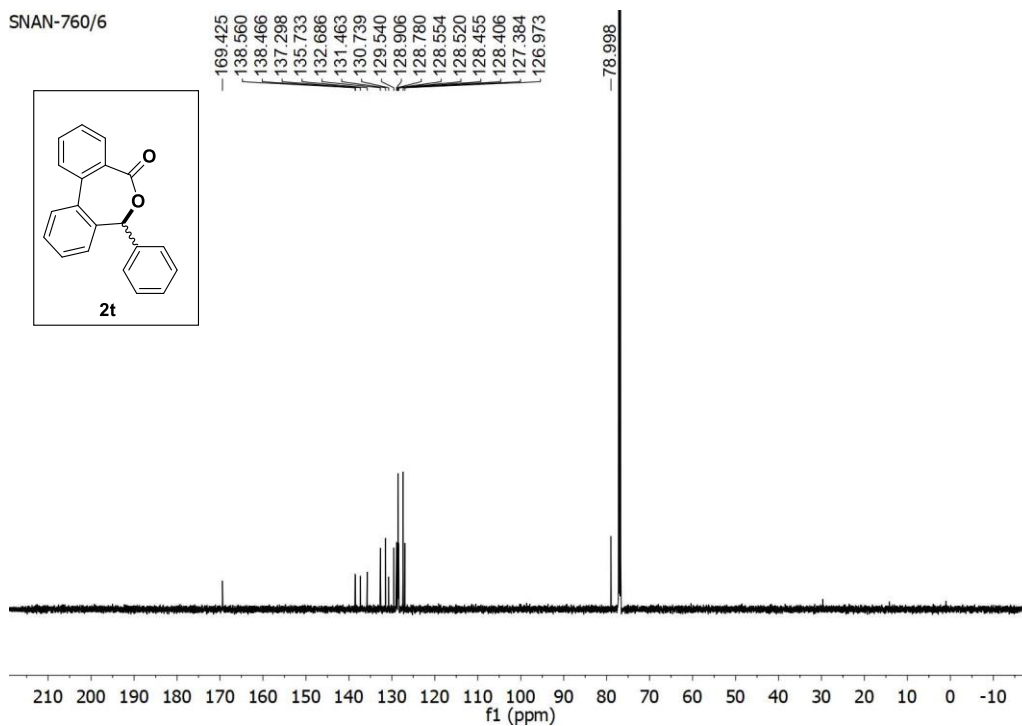
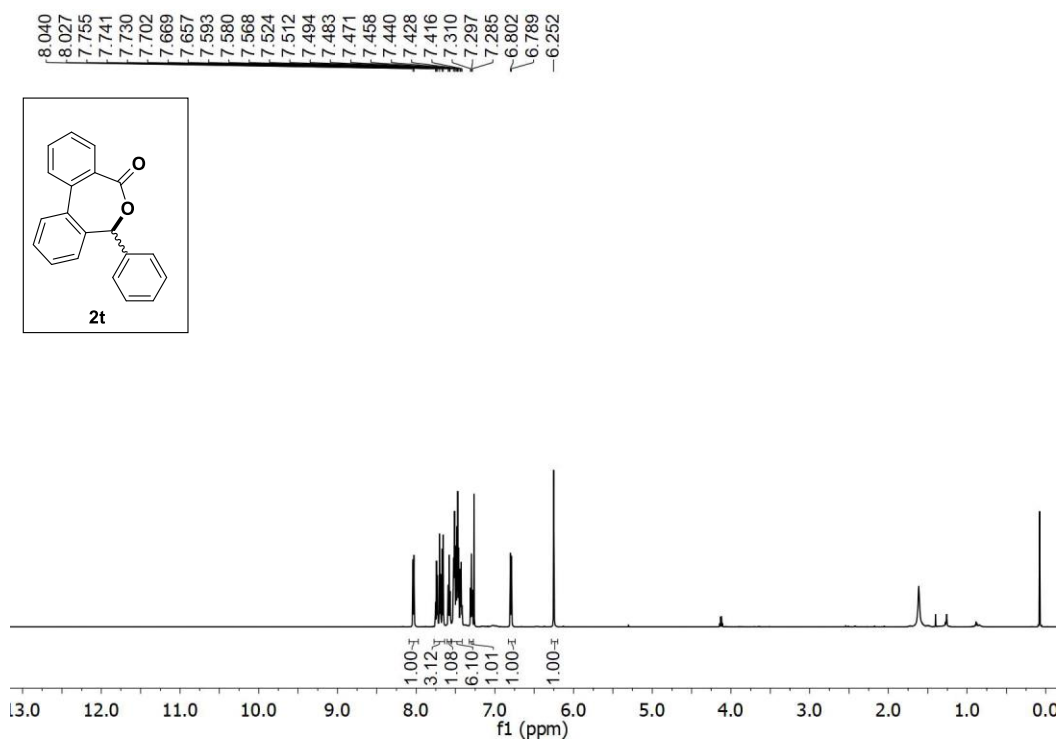
SNAN-1312
single_pulse



SNAN-1312

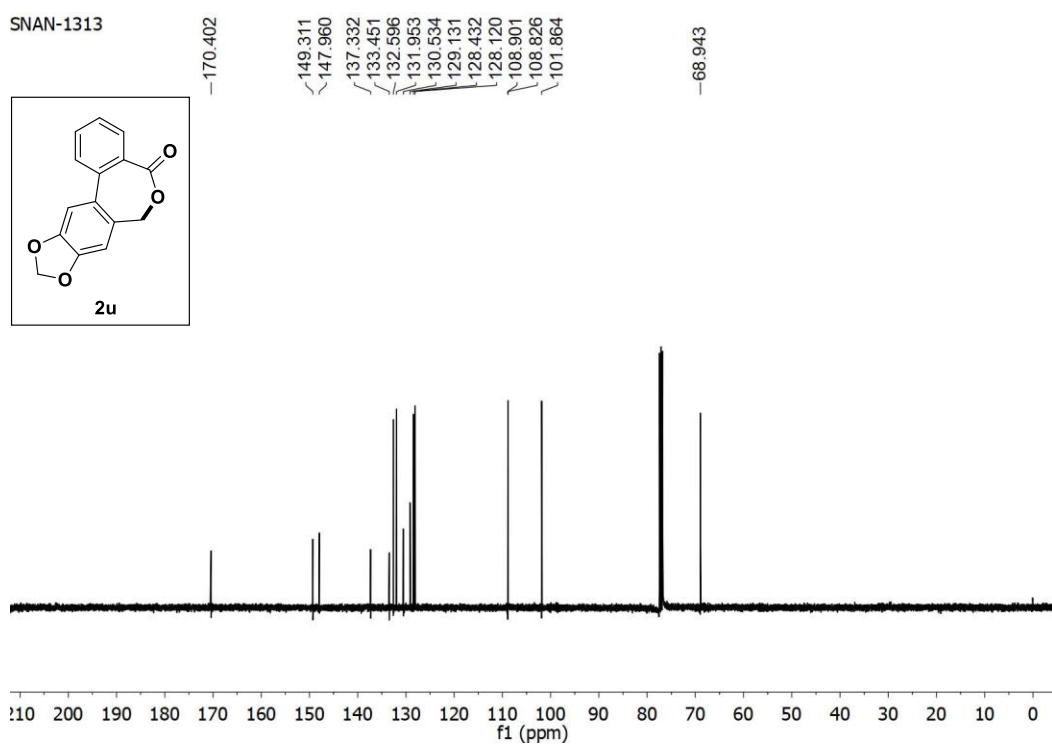
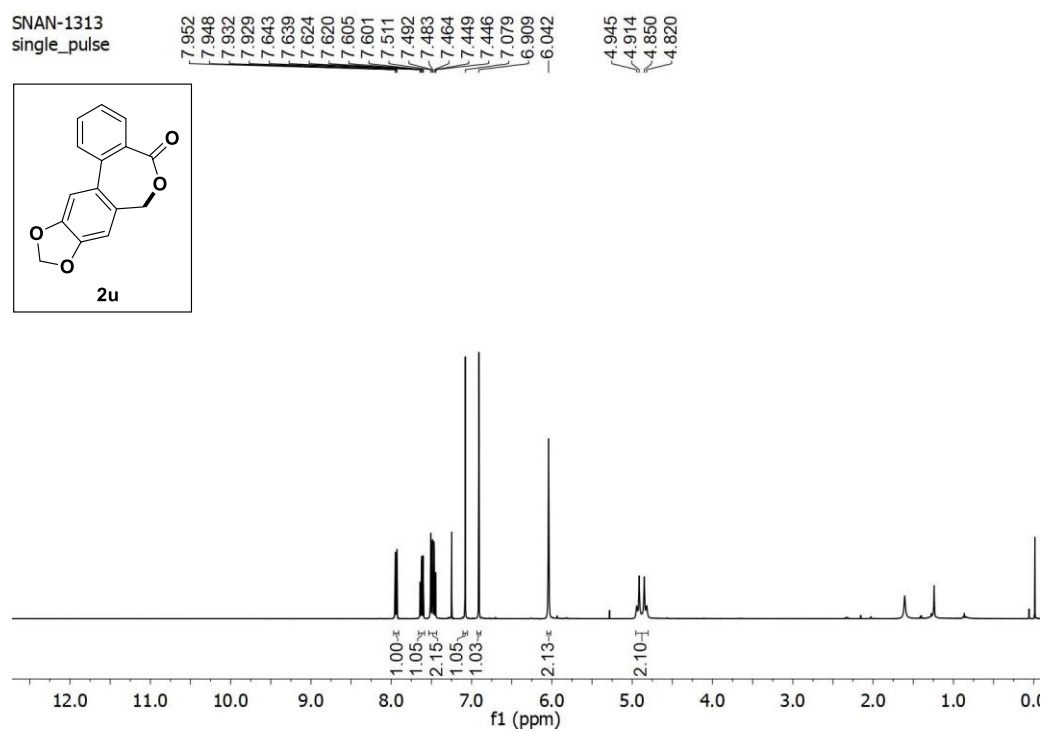


¹H and ¹³C spectra of **2r**

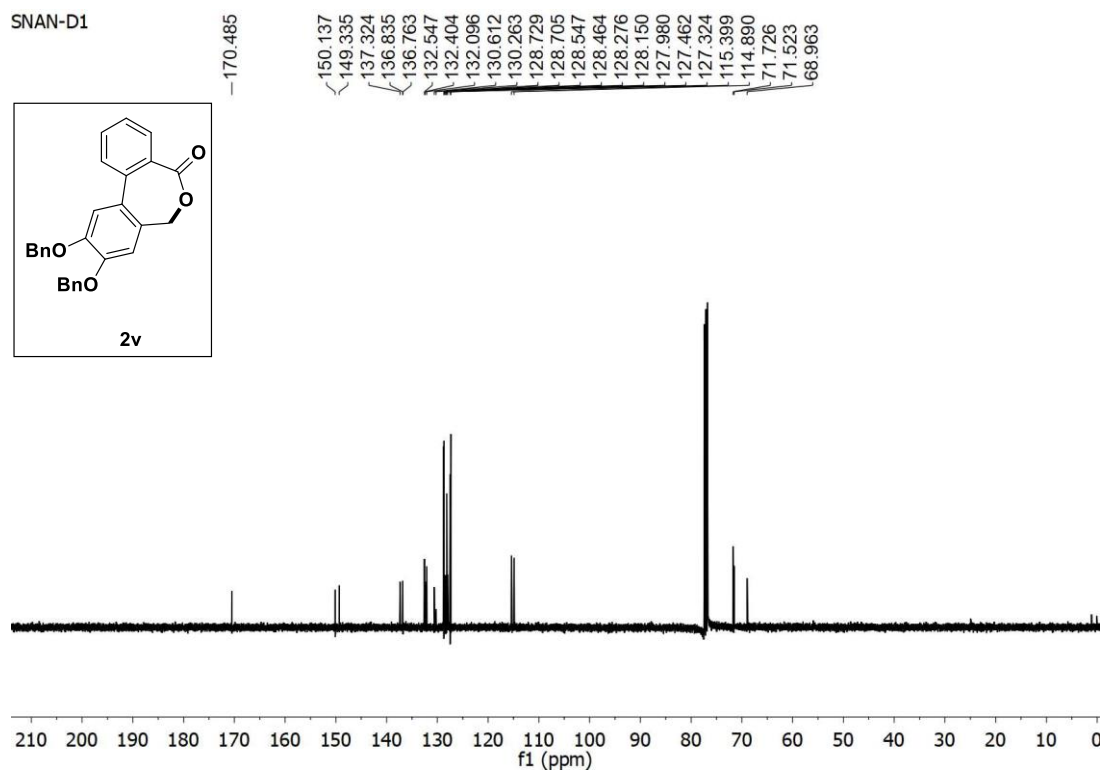
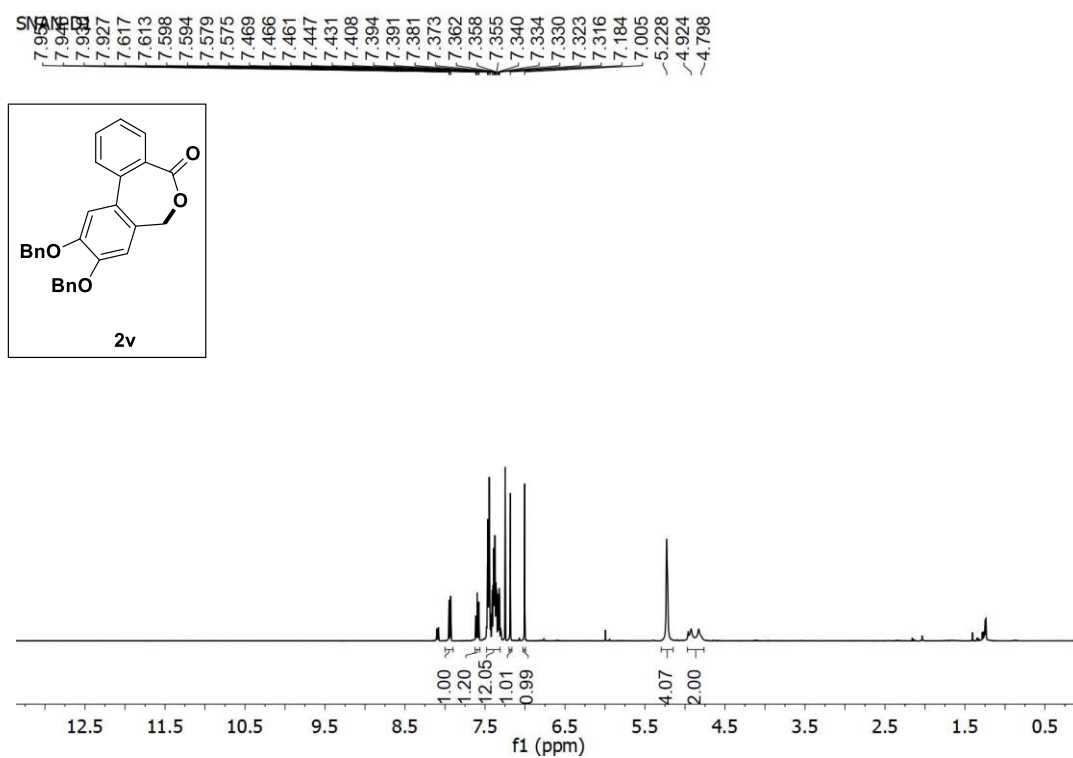


^1H and ^{13}C spectra of **2t**

Chemo- and Regioselective Benzylic C(sp³)-H Oxidation Bridging the Gap between Hetero- and Homogeneous Copper Catalysis

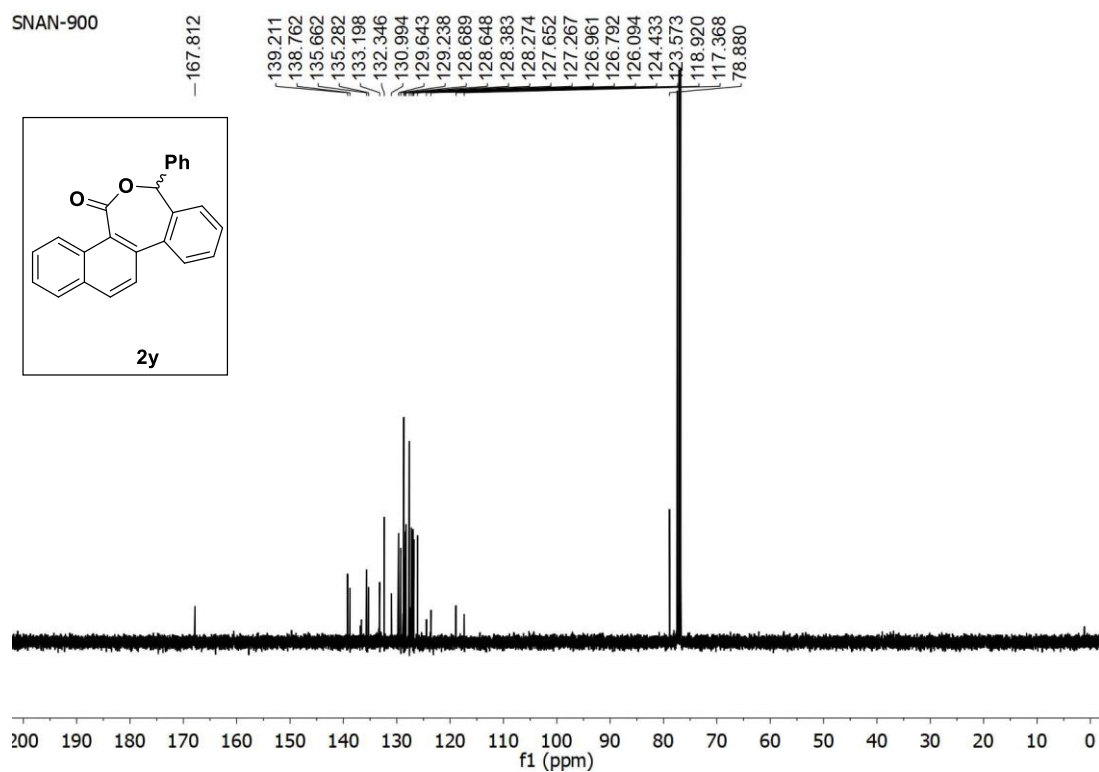
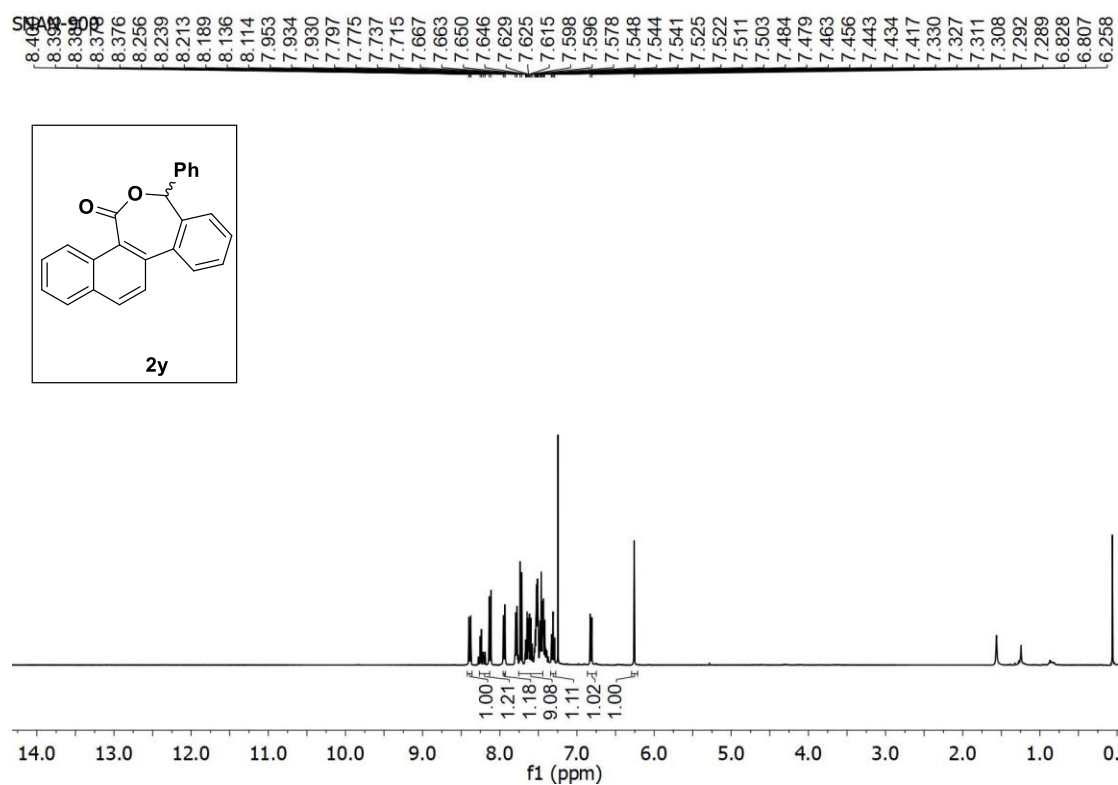


¹H and ¹³C spectra of **2u**

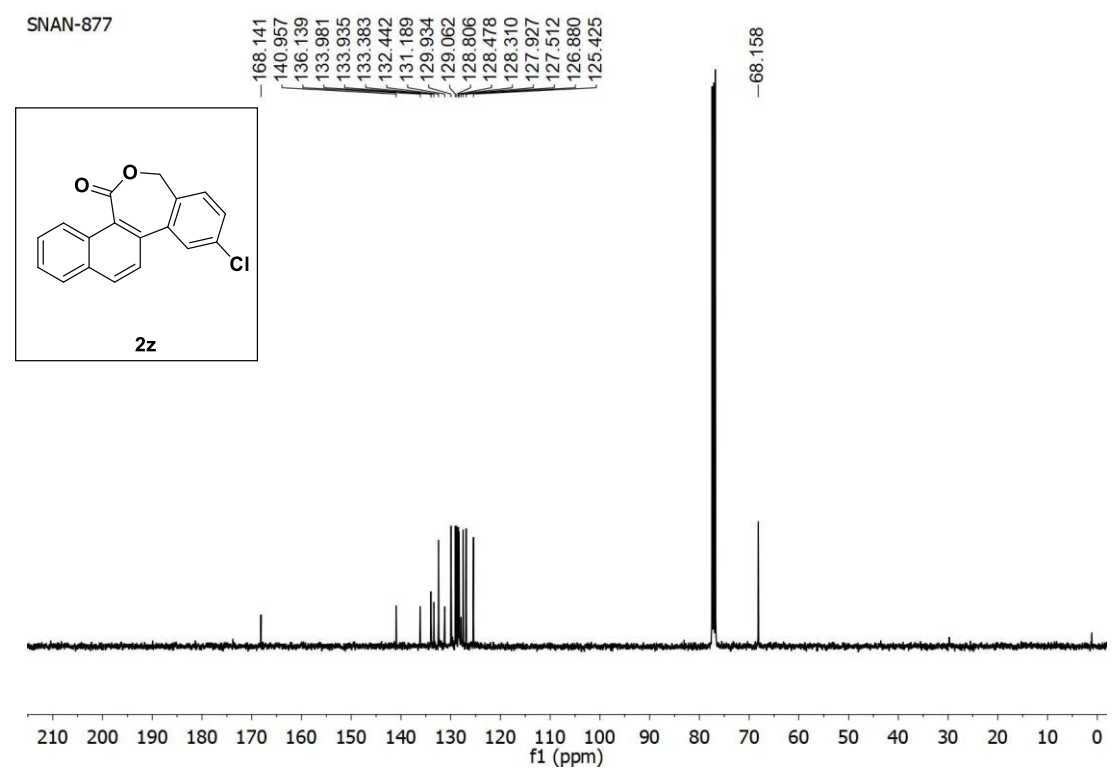
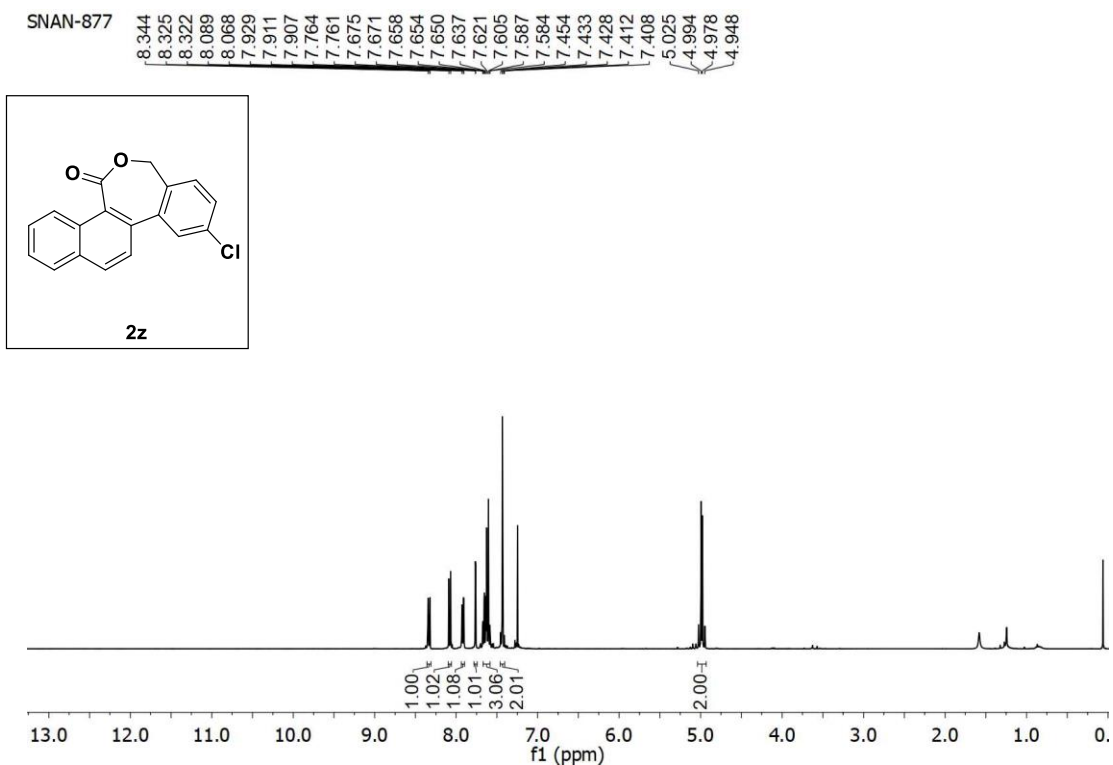


^1H and ^{13}C spectra of 2v

Chemo- and Regioselective Benzylic C(sp³)-H Oxidation Bridging the Gap between Hetero- and Homogeneous Copper Catalysis



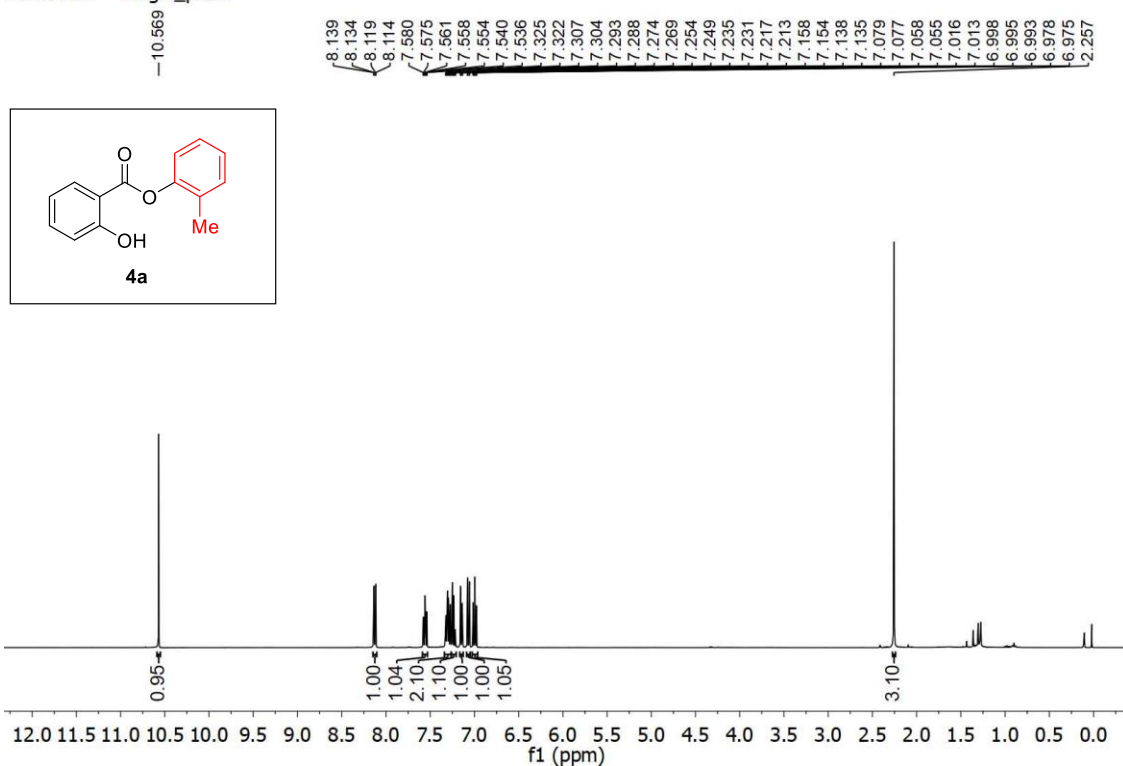
¹H and ¹³C spectra of **2y**



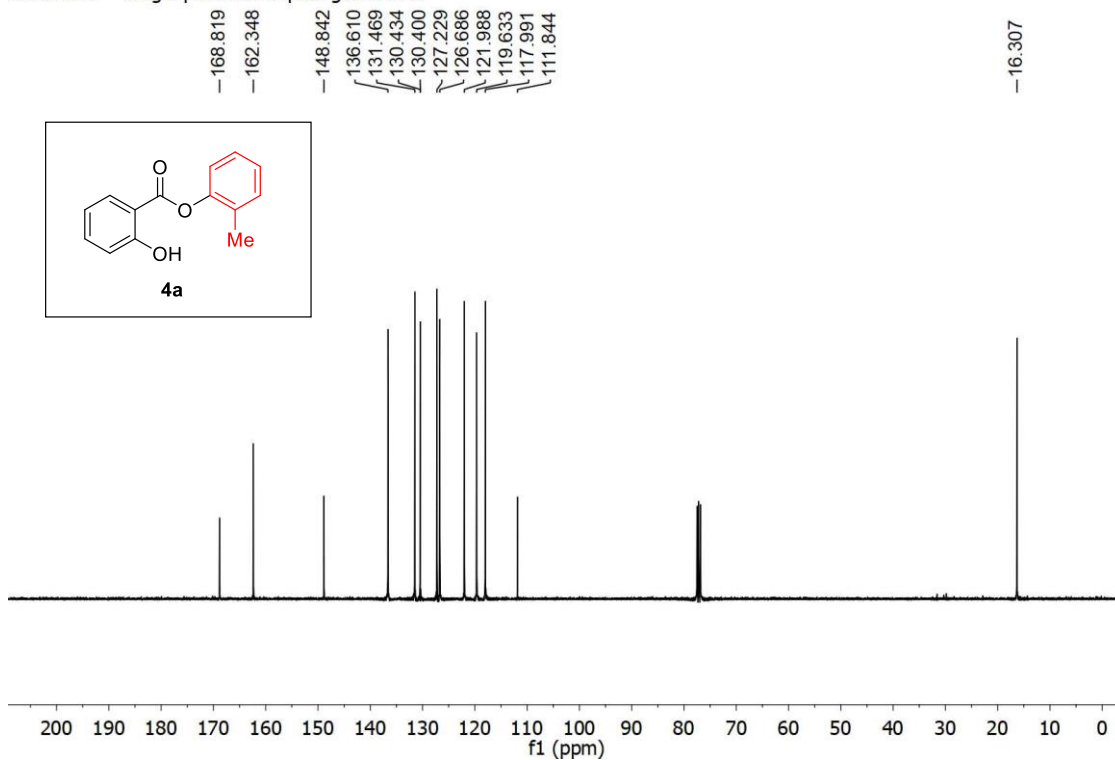
^1H and ^{13}C spectra of **2z**

Chemo- and Regioselective Benzylic C(sp³)-H Oxidation Bridging the Gap between Hetero- and Homogeneous Copper Catalysis

SNAN-705 — single_pulse



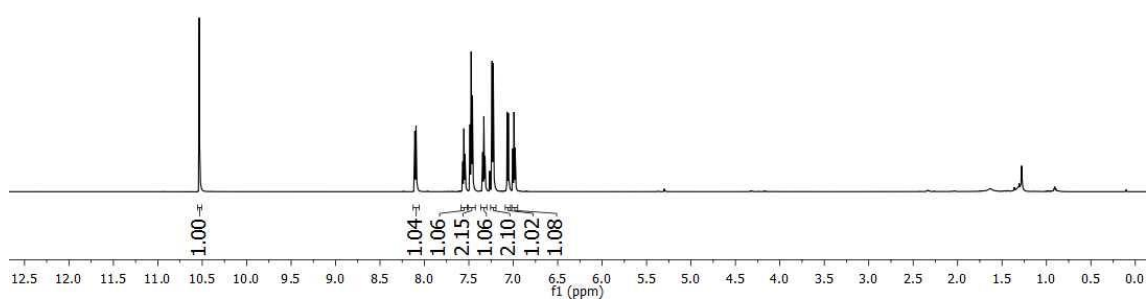
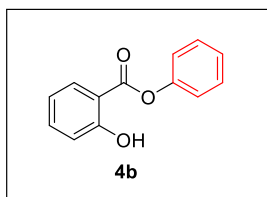
SNAN-705 — single pulse decoupled gated NOE



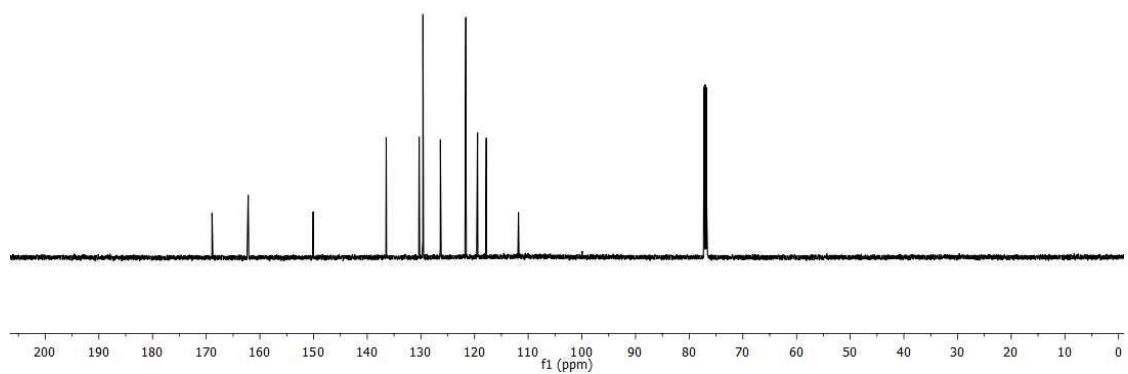
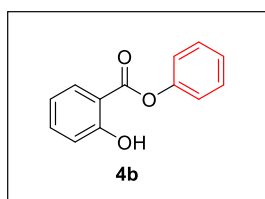
¹H and ¹³C spectra of **4a**

Chapter IV

SNAN-726/5
SNAN 726 $^1\text{H-NMR}$ in CDCl_3



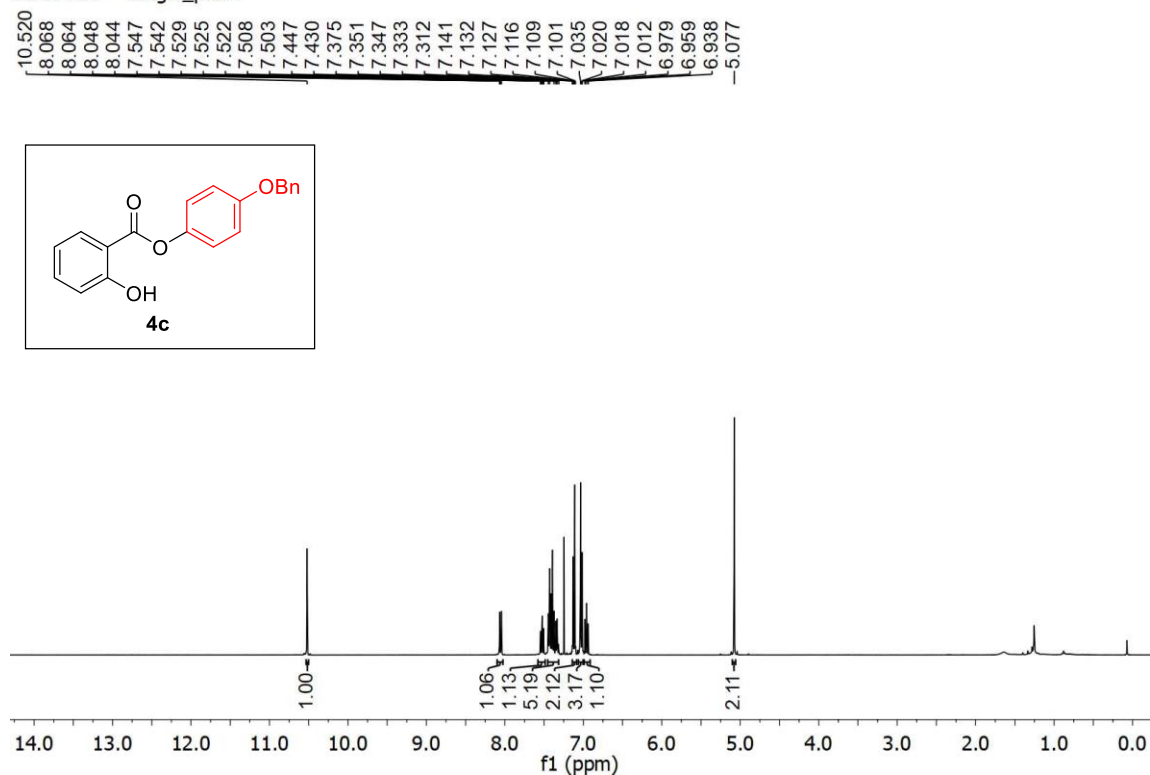
SNAN-726/6
SNAN 726 $^{13}\text{C-NMR}$ in CDCl_3



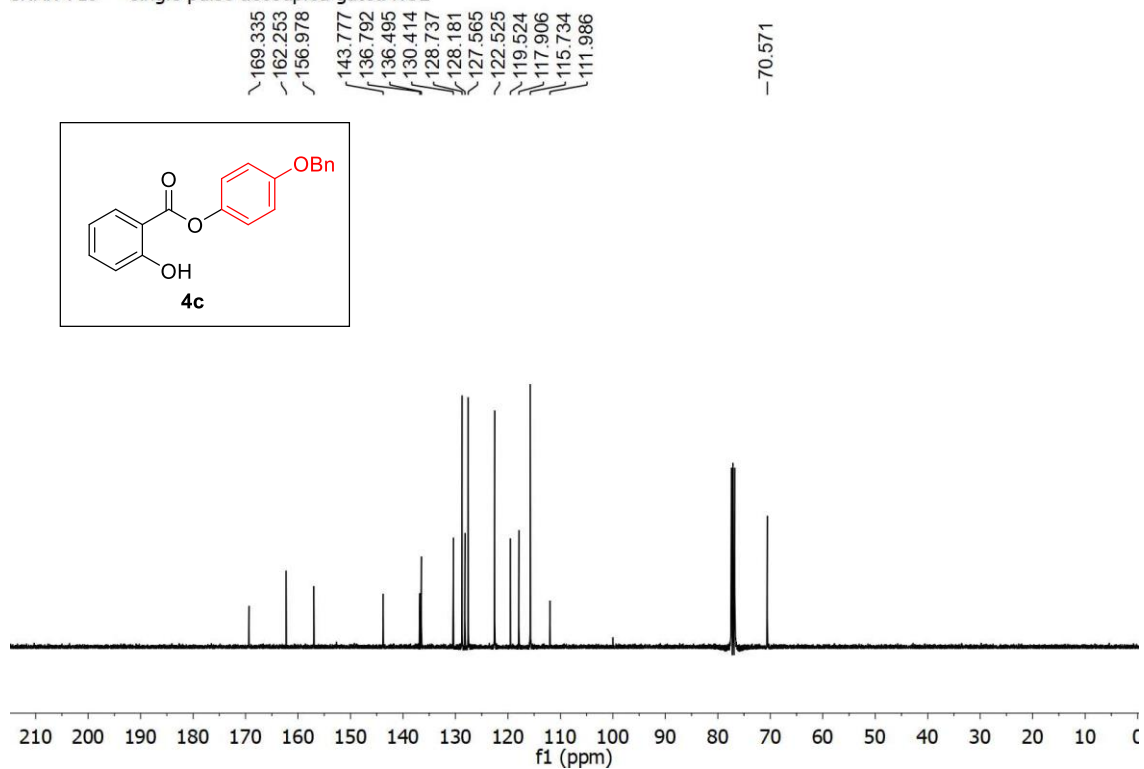
^1H and ^{13}C spectra of **4b**

Chemo- and Regioselective Benzylic C(sp³)-H Oxidation Bridging the Gap between Hetero- and Homogeneous Copper Catalysis

SNAN-719 — single_pulse



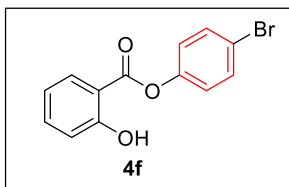
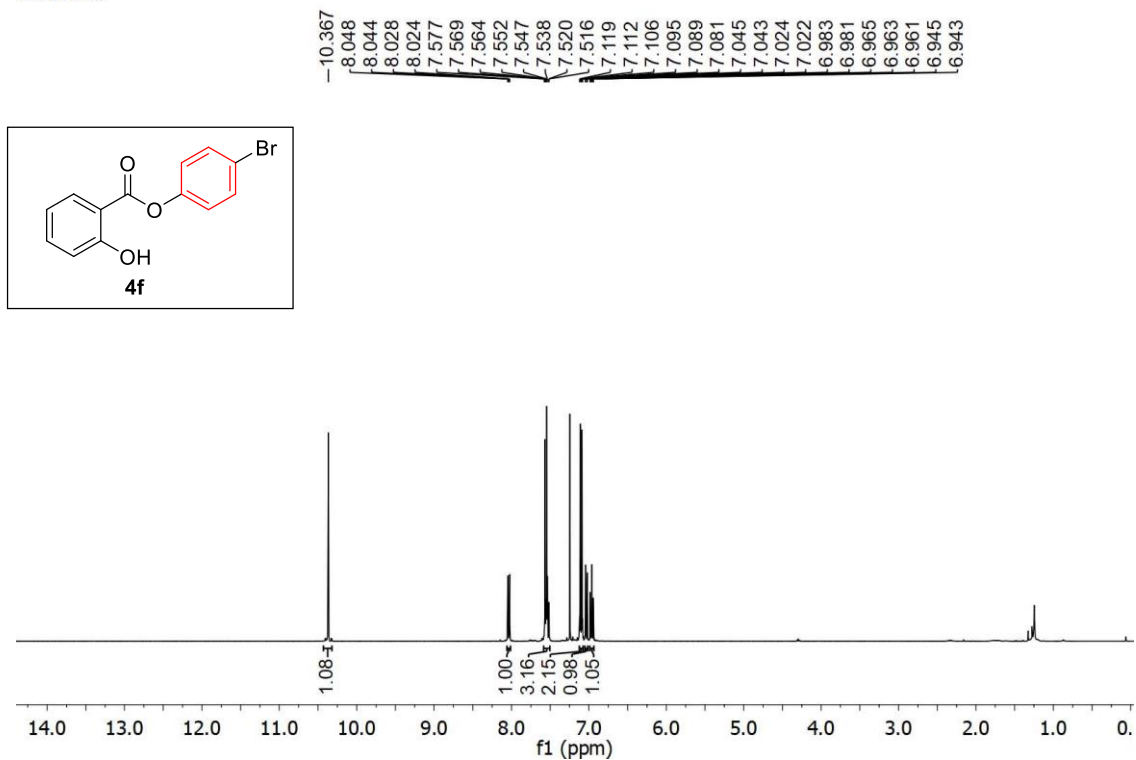
SNAN-719 — single pulse decoupled gated NOE



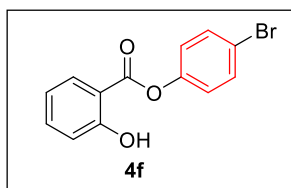
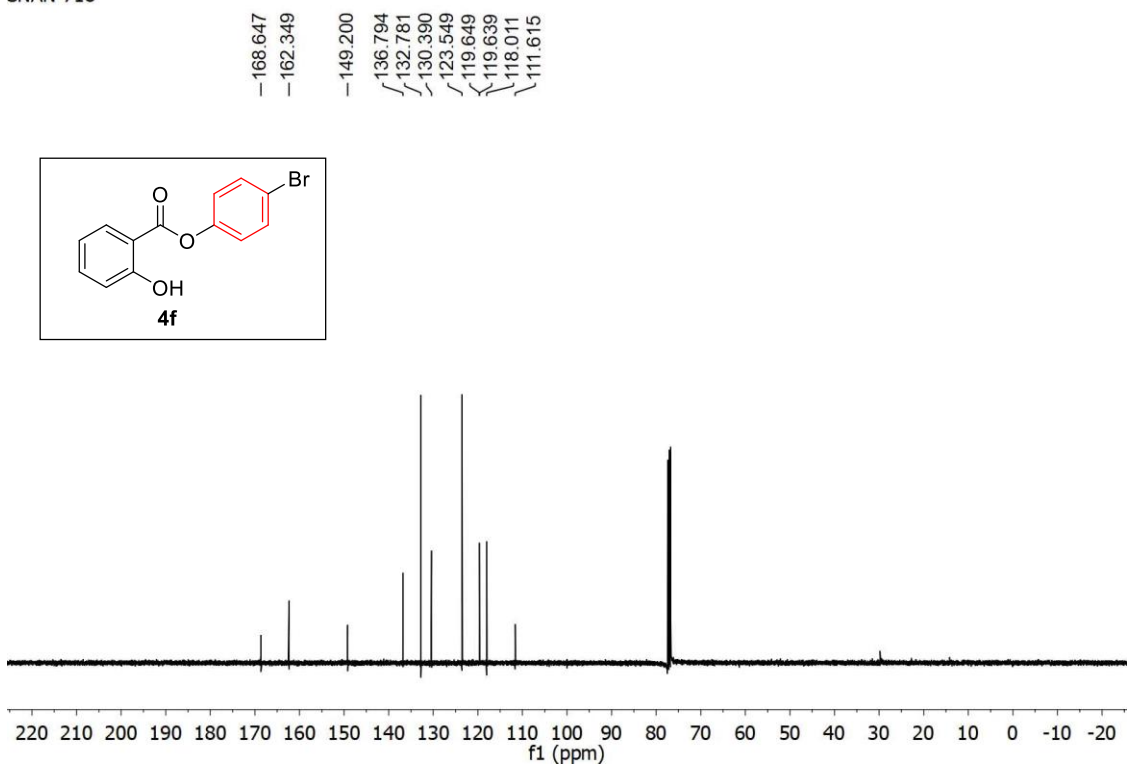
¹H and ¹³C spectra of **4c**

Chapter IV

SNAN-718



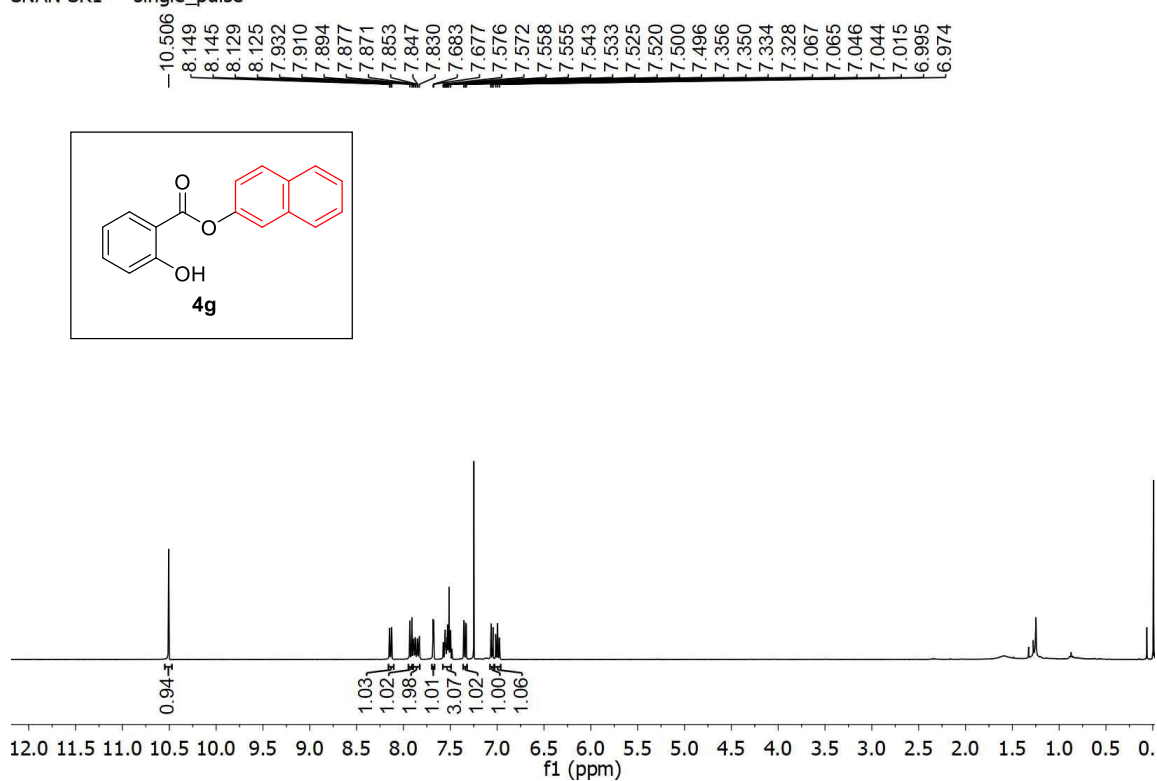
SNAN-718



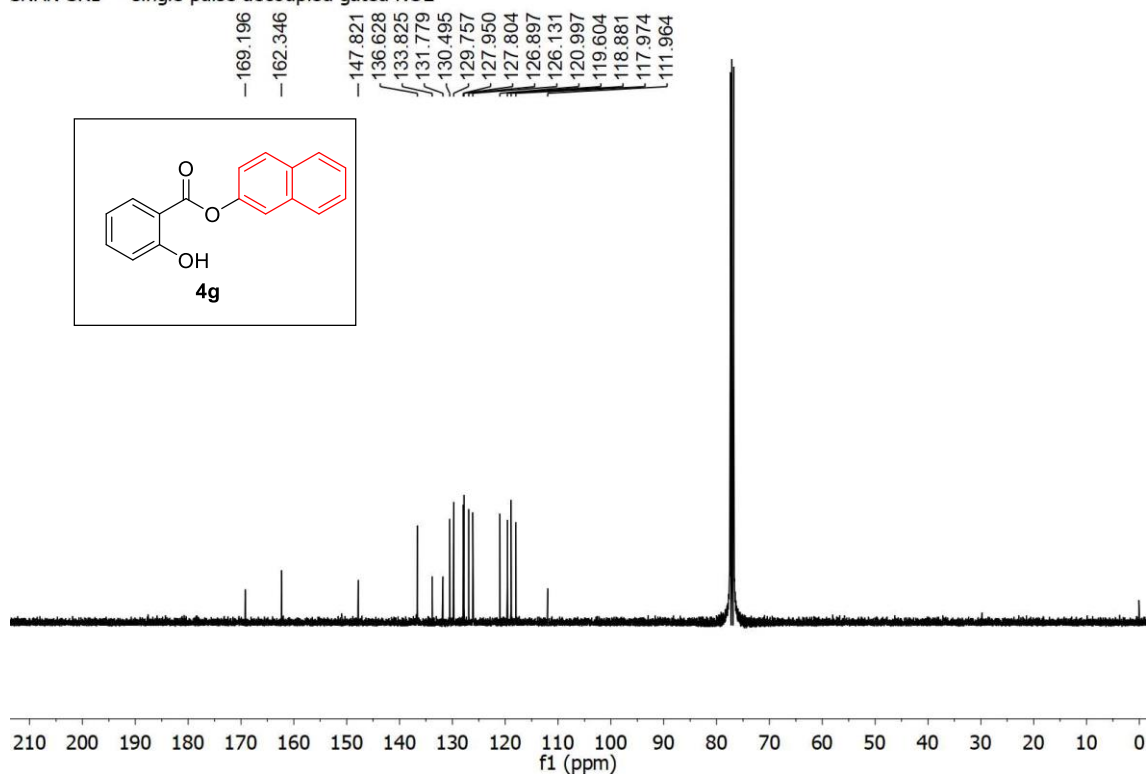
^1H and ^{13}C spectra of **4f**

Chemo- and Regioselective Benzylic C(sp³)-H Oxidation Bridging the Gap between Hetero- and Homogeneous Copper Catalysis

SNAN-SR1 — single_pulse



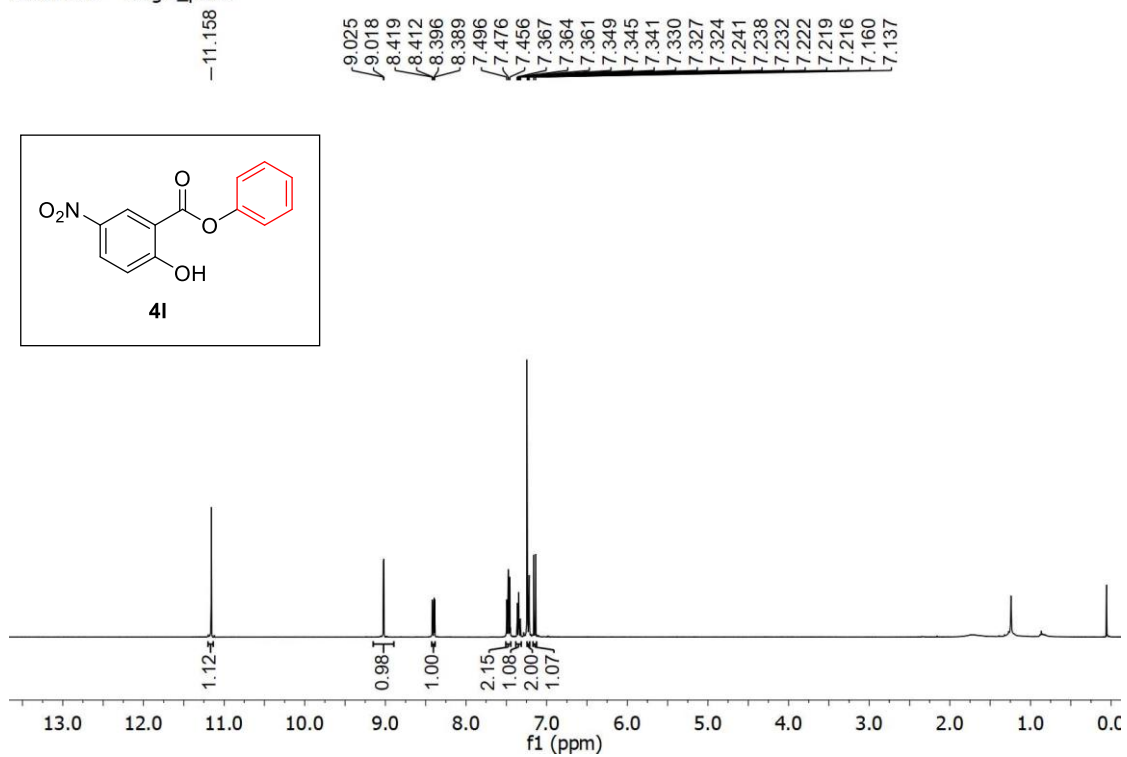
SNAN-SR1 — single pulse decoupled gated NOE



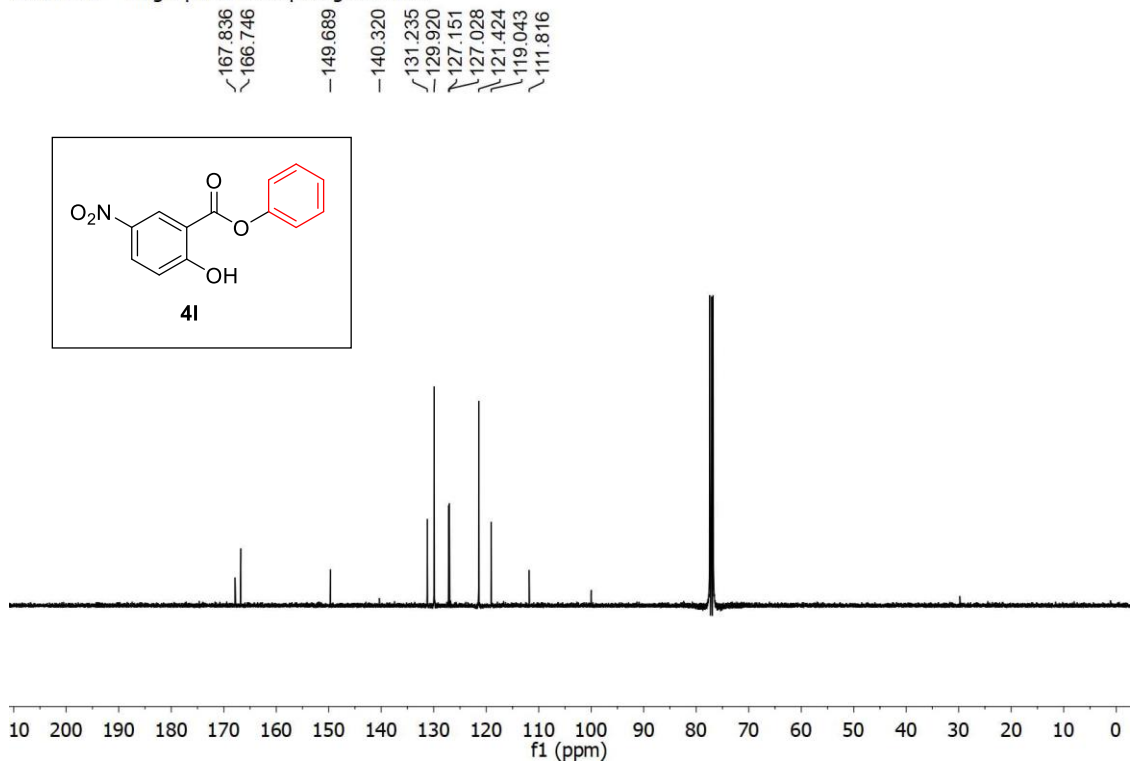
¹H and ¹³C spectra of **4g**

Chapter IV

SNAN-720 — single_pulse



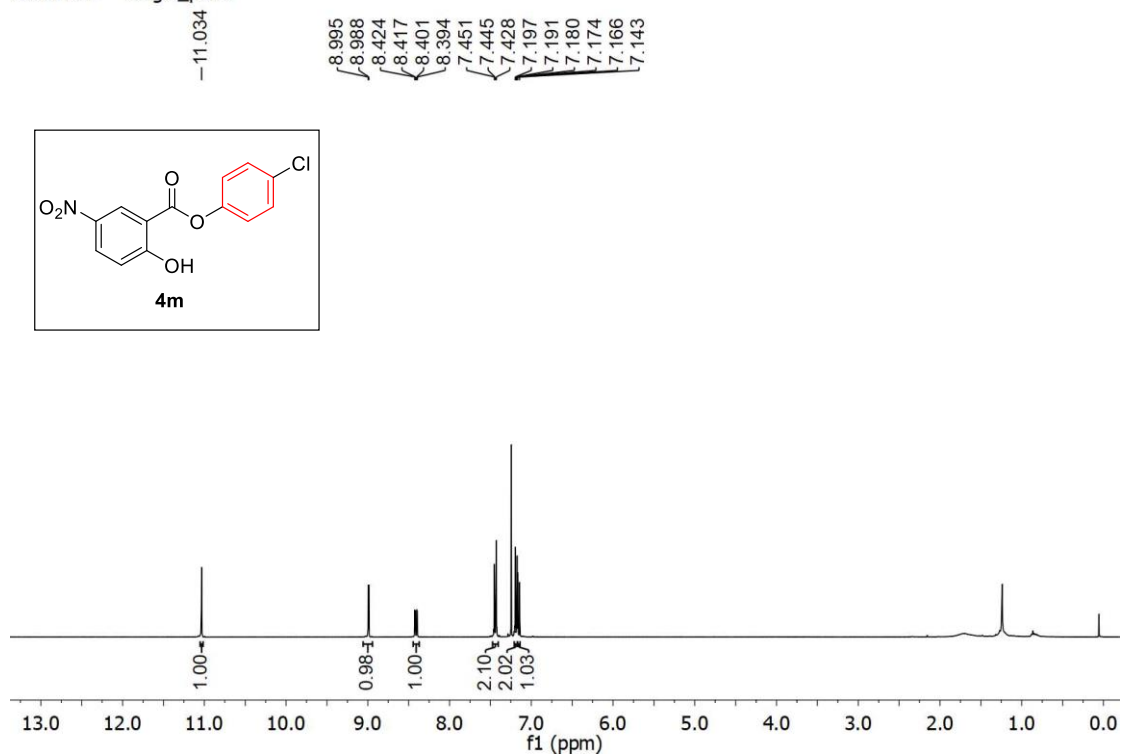
SNAN-720 — single_pulse decoupled gated NOE



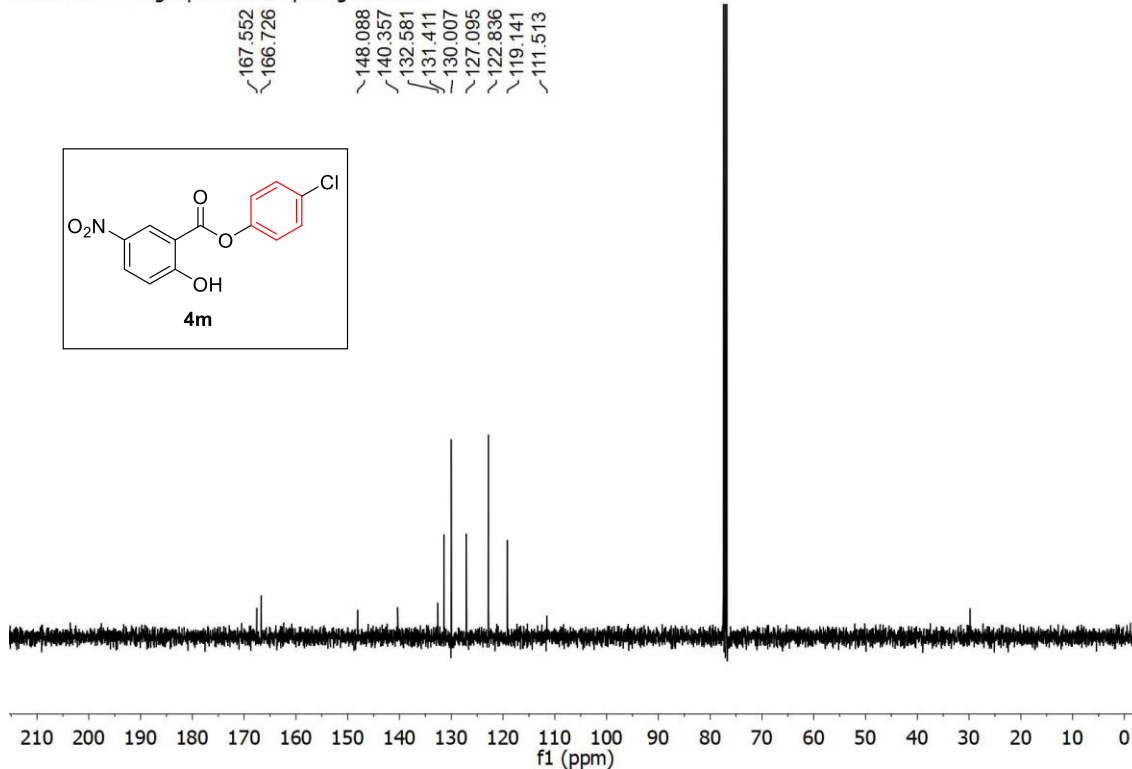
¹H and ¹³C spectra of **4l**

Chemo- and Regioselective Benzylic C(sp³)-H Oxidation Bridging the Gap between Hetero- and Homogeneous Copper Catalysis

SNAN-721 — single_pulse



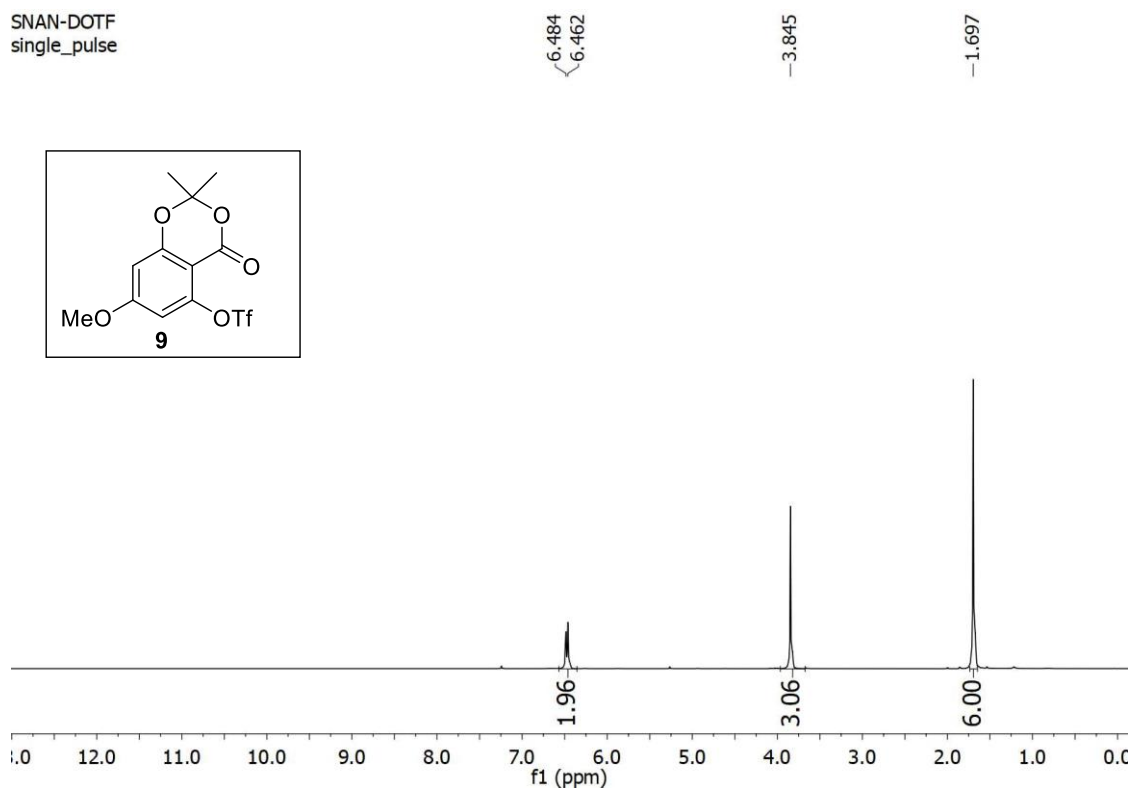
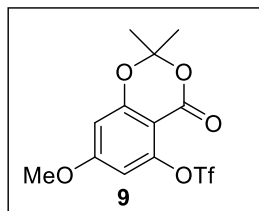
SNAN-721 — single pulse decoupled gated NOE



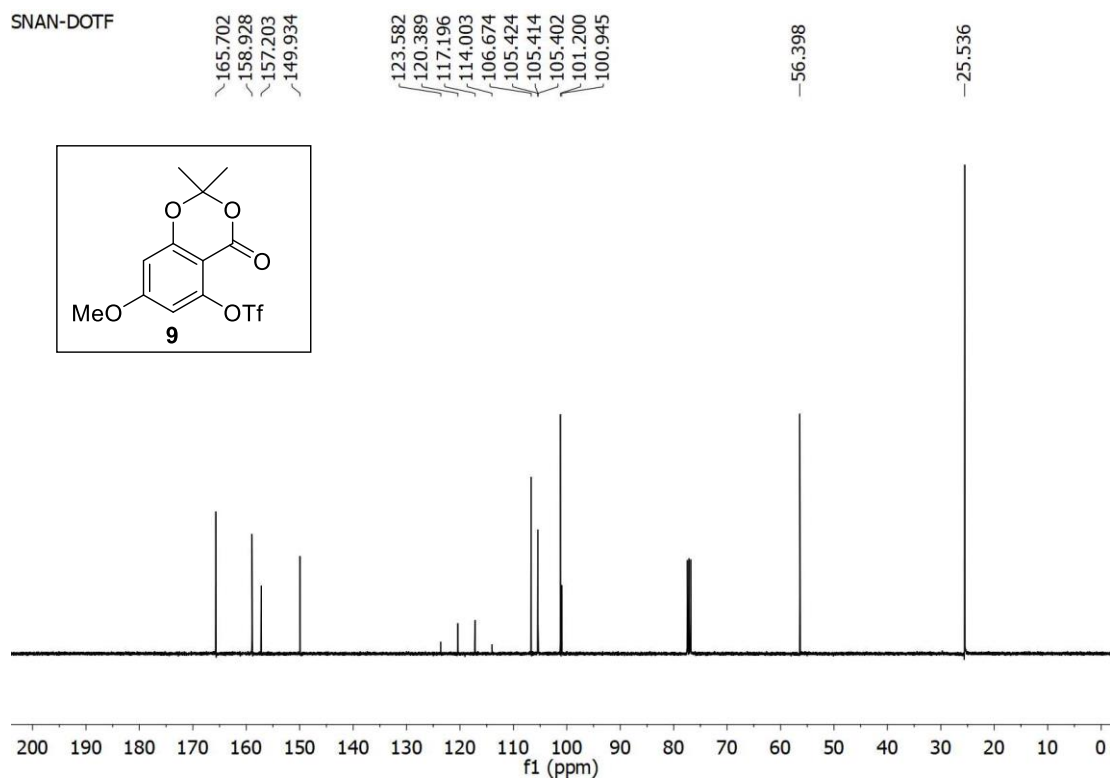
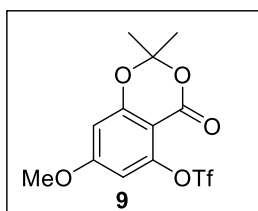
¹H and ¹³C spectra of **4m**

Chapter IV

SNAN-DOTF
single_pulse

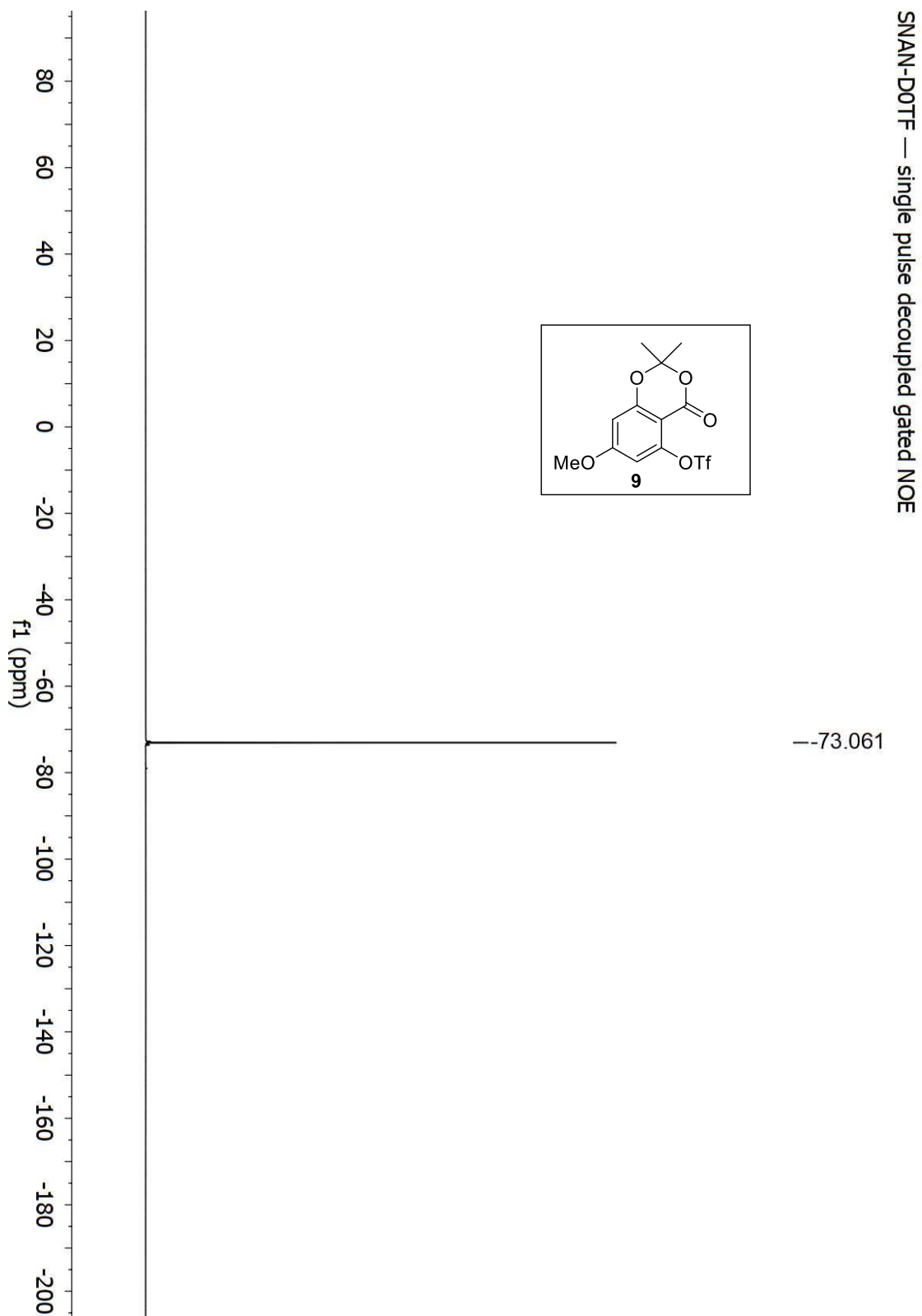


SNAN-DOTF



^1H and ^{13}C spectra of **9**

Chemo- and Regioselective Benzylic C(sp³)-H Oxidation Bridging the Gap between Hetero- and Homogeneous Copper Catalysis



¹⁹F spectra of **9**

Chapter IV

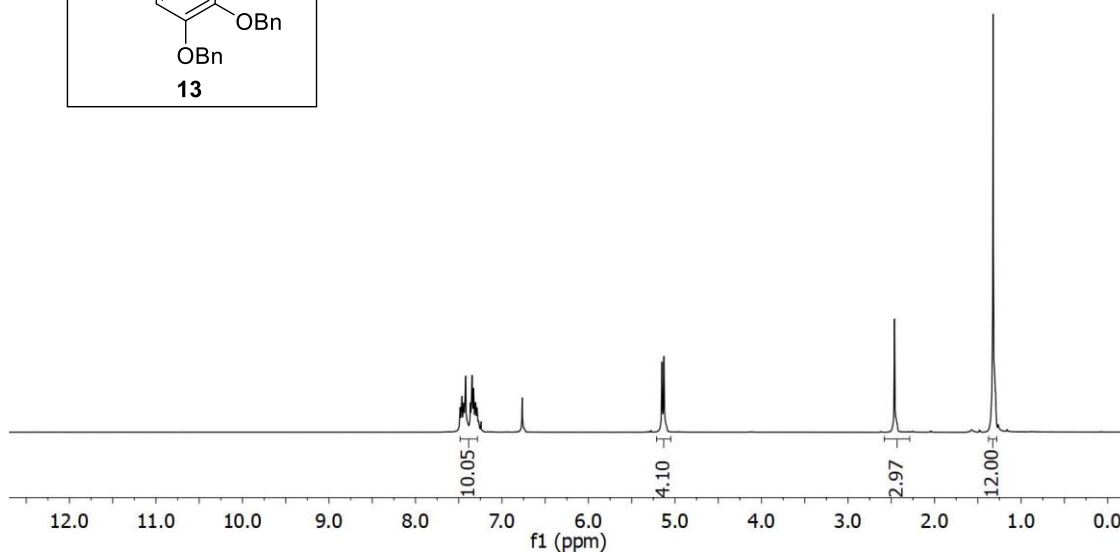
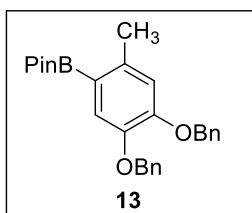
SNAN-999
single_pulse

7.483
7.465
7.444
7.419
7.362
7.347
7.329
7.304
7.290
7.244

5.151
5.128

2.463

1.323



SNAN-999
single pulse decoupled gated NOE

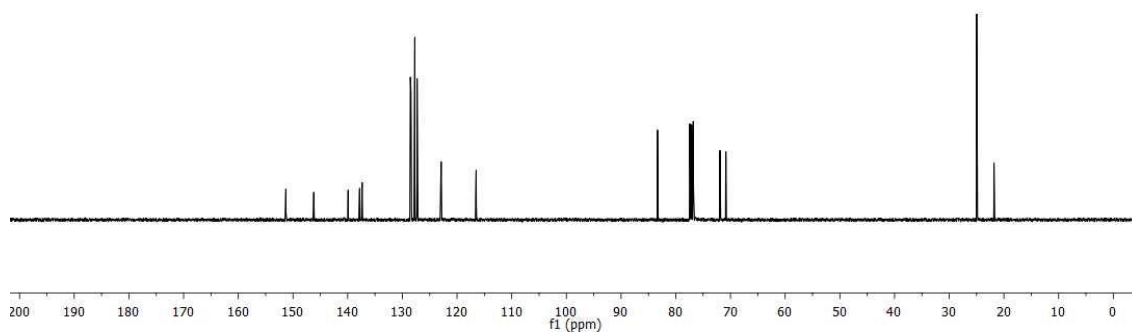
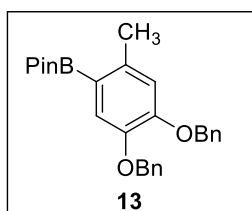
151.290
146.193
139.913
137.809
137.358

128.527
127.718
127.305
122.902
116.502

83.346

71.924
70.845

24.986
21.822

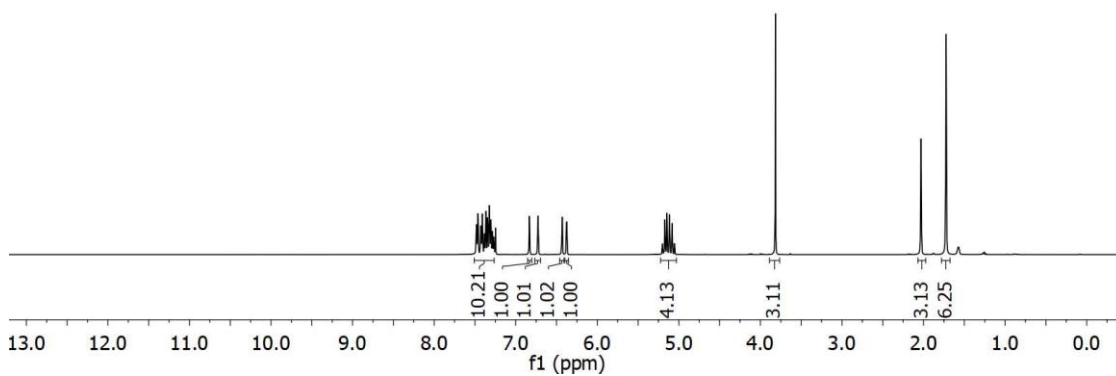
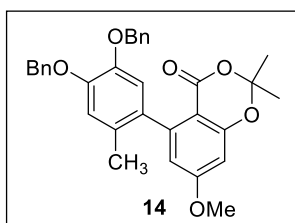


^1H and ^{13}C spectra of **13**

Chemo- and Regioselective Benzylic C(sp³)-H Oxidation Bridging the Gap between Hetero- and Homogeneous Copper Catalysis

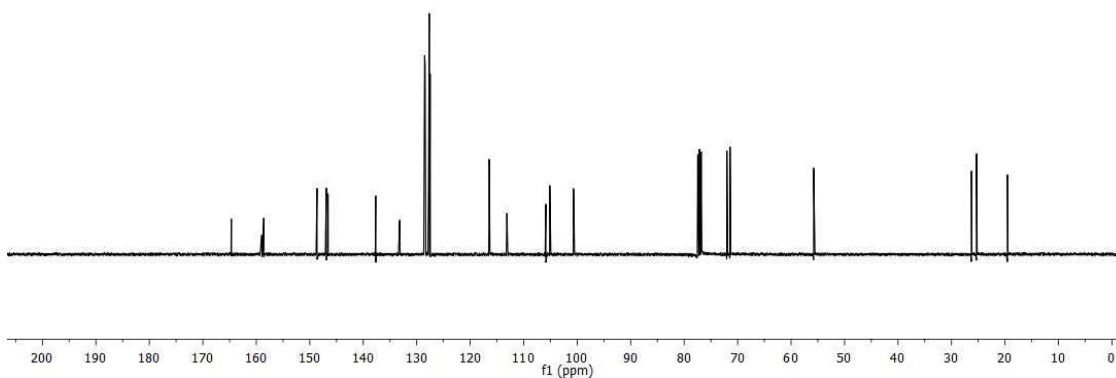
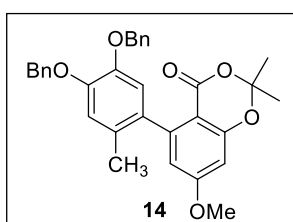
SNAN-1089
single_pulse

7.481
7.463
7.428
7.409
7.385
7.367
7.347
7.325
7.305
7.286
7.268
6.833
6.728
6.435
6.429
6.379
6.373
5.202
5.172
5.147
5.115
5.083
5.053
-3.816
-2.031
-1.724

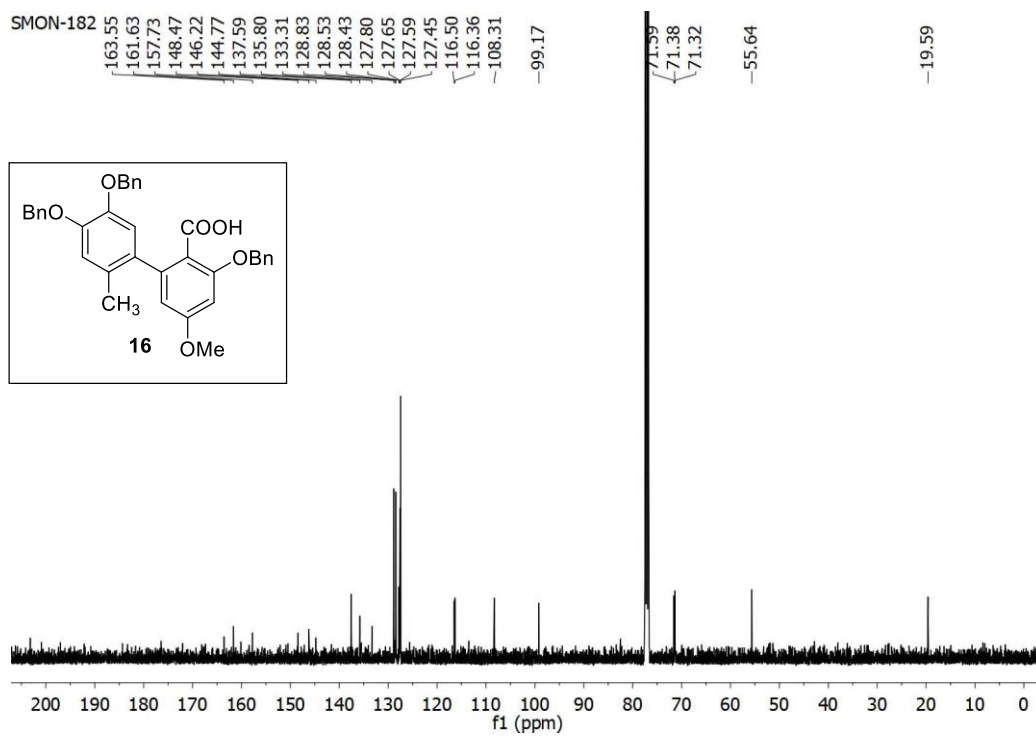
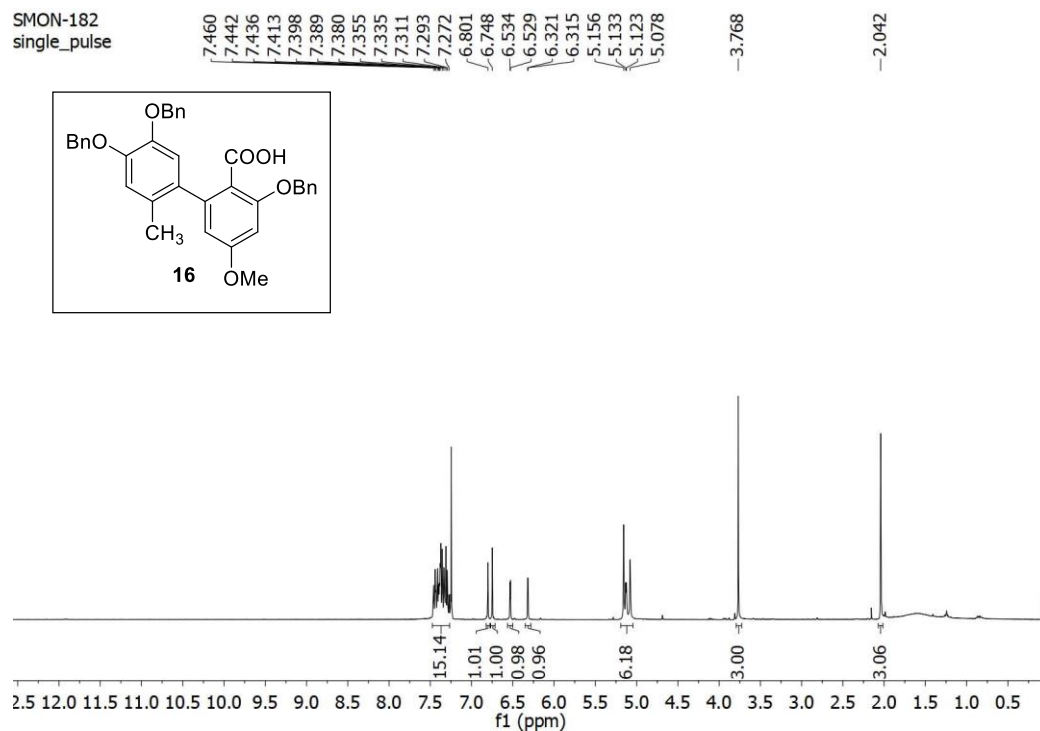


SNAN-1089
single pulse decoupled gated NOE

164.671
158.966
158.611
148.642
146.898
146.591
137.653
133.185
128.527
128.503
128.431
127.788
127.709
127.655
127.490
116.447
116.433
113.144
105.856
105.116
100.683
71.998
71.409
55.778
26.269
25.328
19.528



¹H and ¹³C spectra of **14**

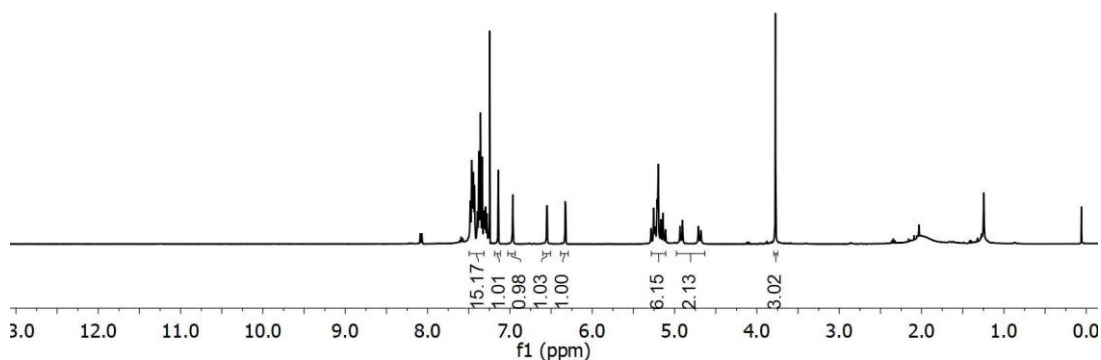
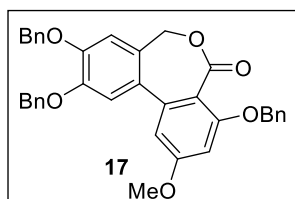


^1H and ^{13}C spectra of **16**

Chemo- and Regioselective Benzylic C(sp³)-H Oxidation Bridging the Gap between Hetero- and Homogeneous Copper Catalysis

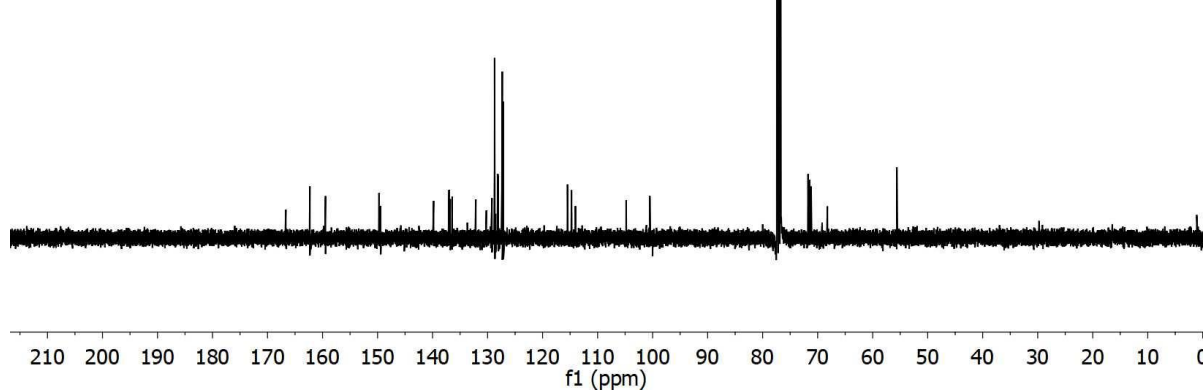
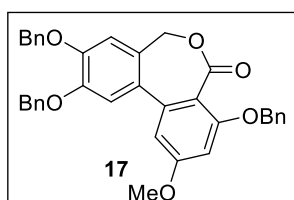
SNAN-NP
single_pulse

7.482
7.463
7.445
7.430
7.396
7.378
7.357
7.338
7.318
7.300
7.295
7.142
6.966
5.285
5.255
5.235
5.213
5.198
5.167
5.142
5.112
4.934
4.904
4.710
4.680
3.776



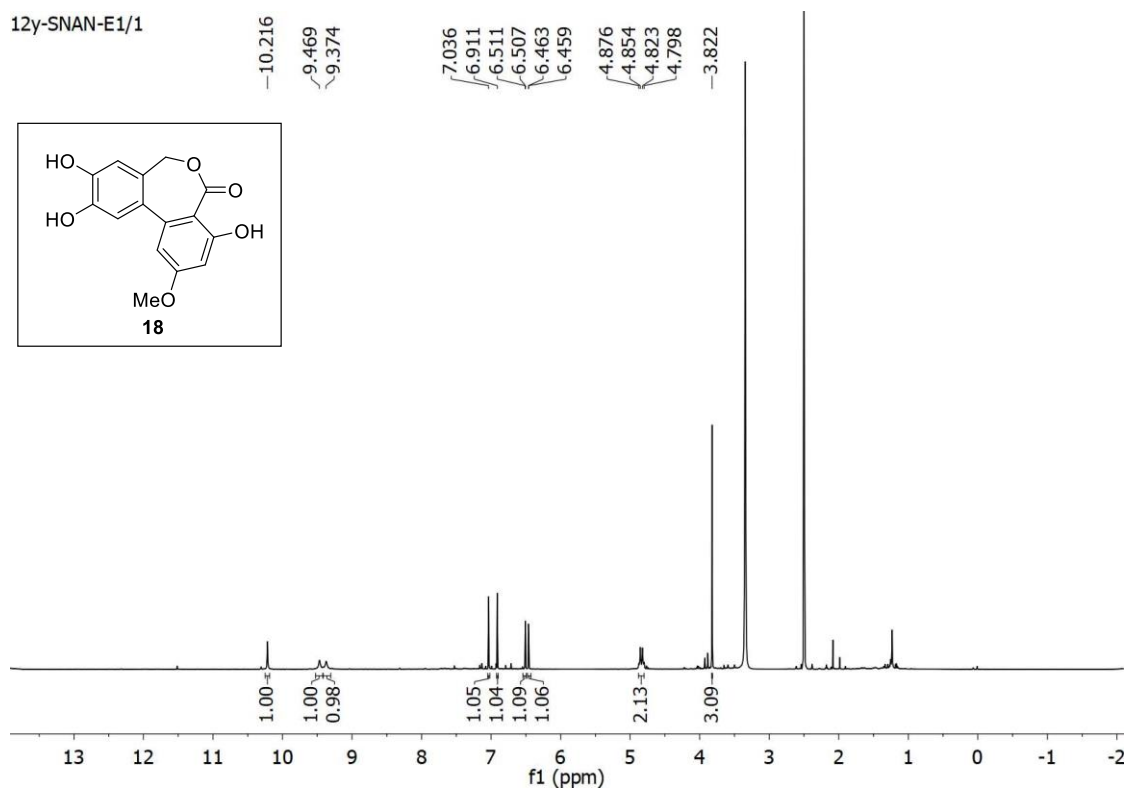
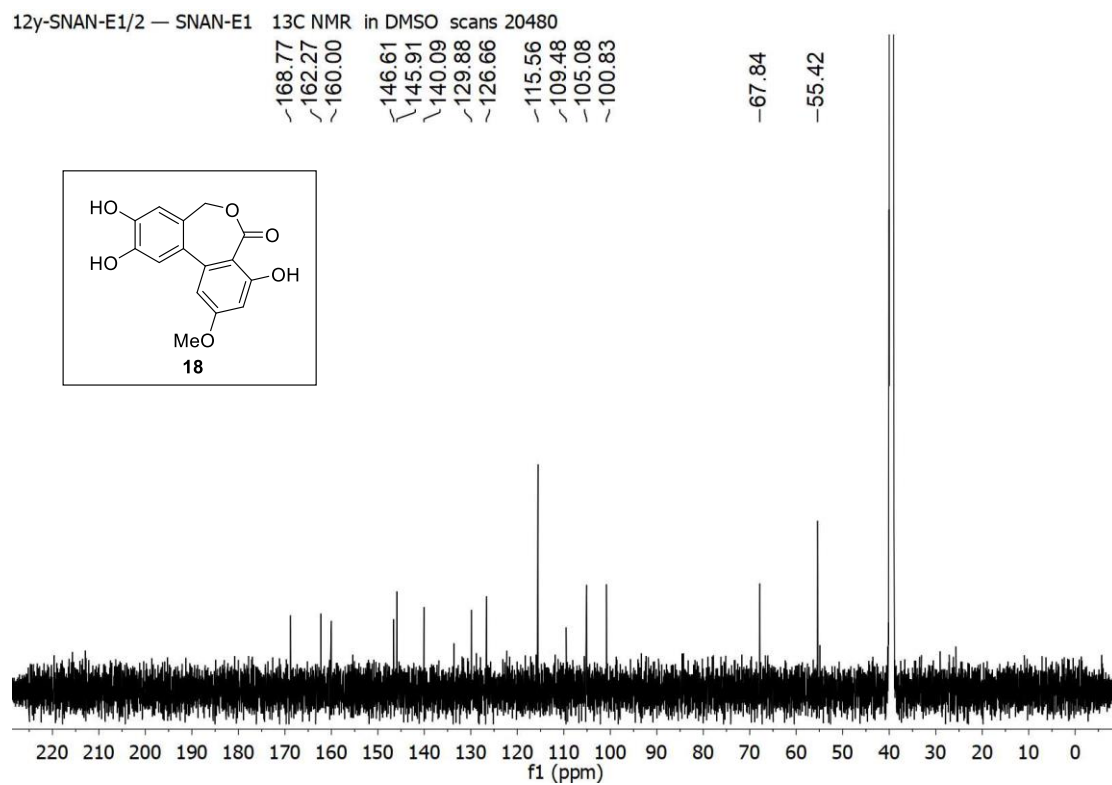
SNAN-NP

166.671
162.302
159.465
149.739
149.431
139.806
137.013
136.776
136.430
132.141
130.230
129.205
128.746
128.734
128.694
128.671
128.552
128.140
128.047
127.945
127.406
127.325
127.175
127.147
127.137
115.477
114.741
114.033
104.813
100.506
71.747
71.501
71.185
68.224
55.608



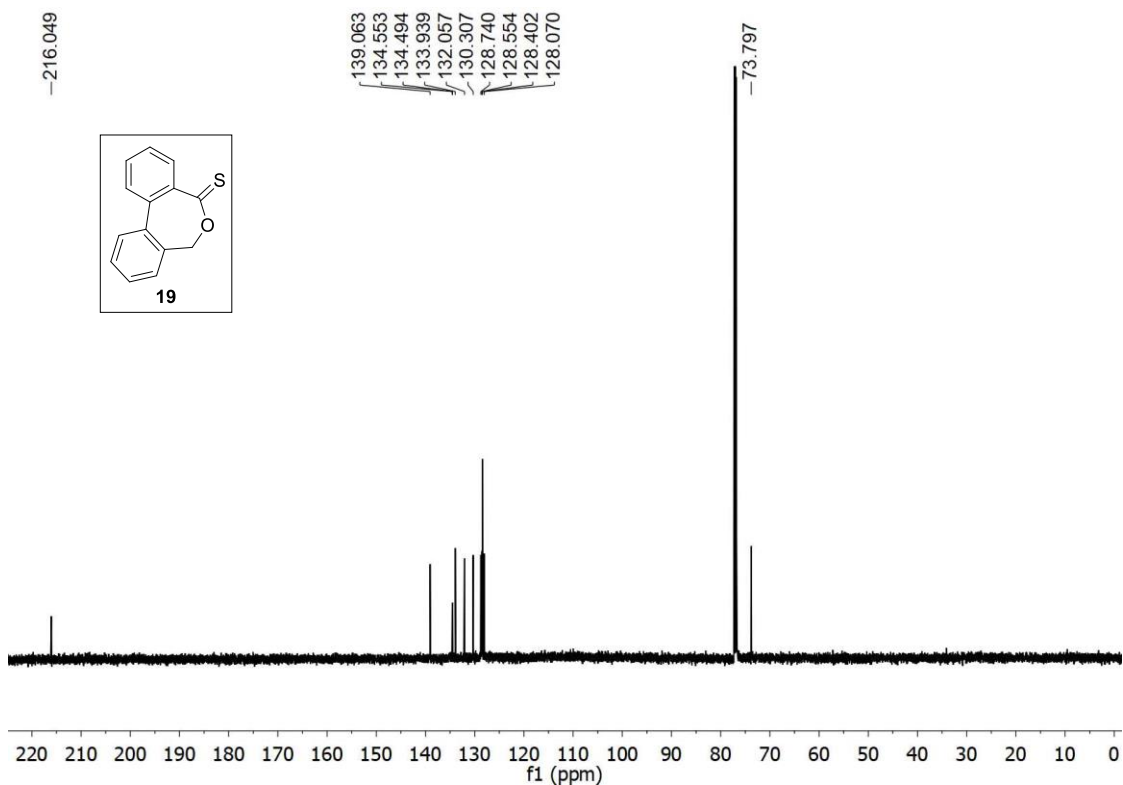
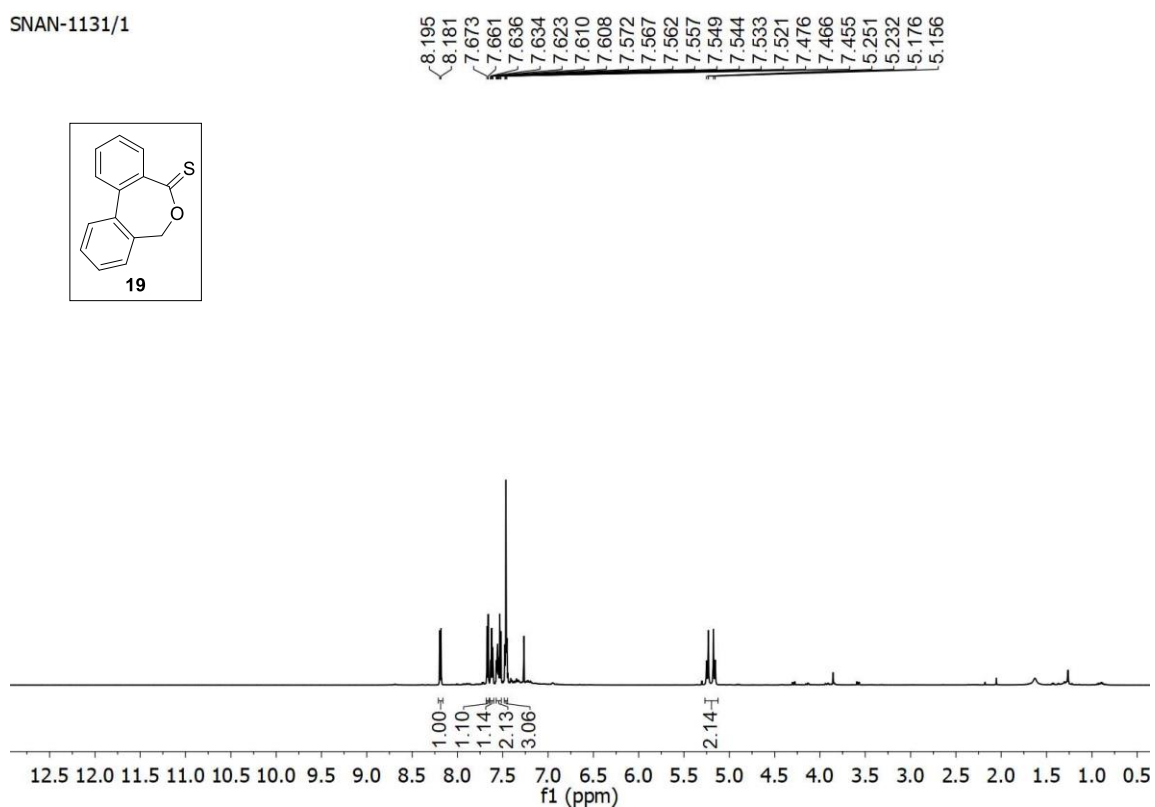
¹H and ¹³C spectra of 17

12y-SNAN-E1/1

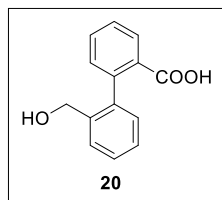
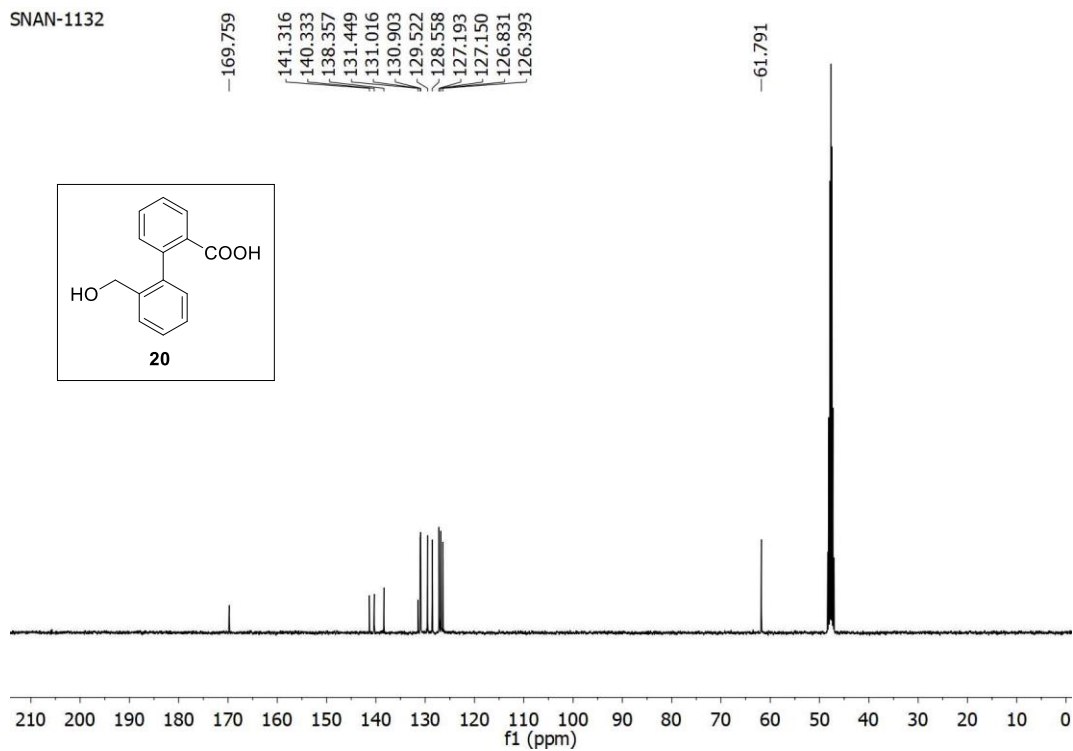
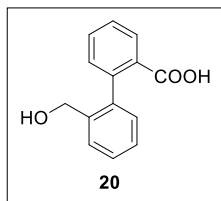
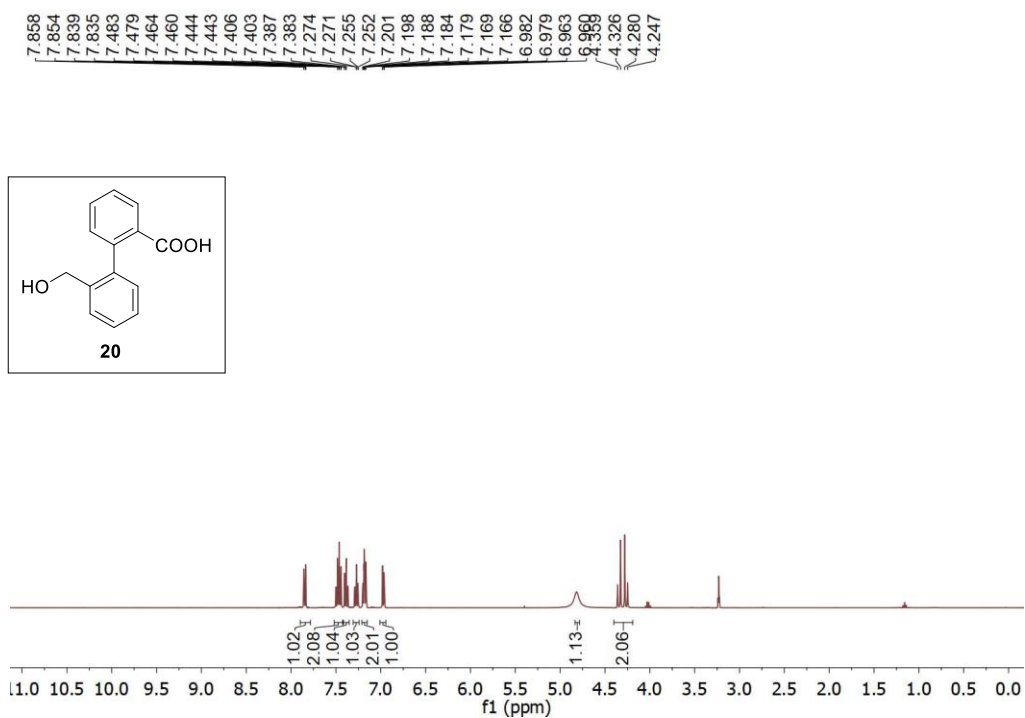
12y-SNAN-E1/2 — SNAN-E1 ^{13}C NMR in DMSO scans 20480 ^1H and ^{13}C spectra of **18**

Chemo- and Regioselective Benzylic C(sp³)-H Oxidation Bridging the Gap between Hetero- and Homogeneous Copper Catalysis

SNAN-1131/1



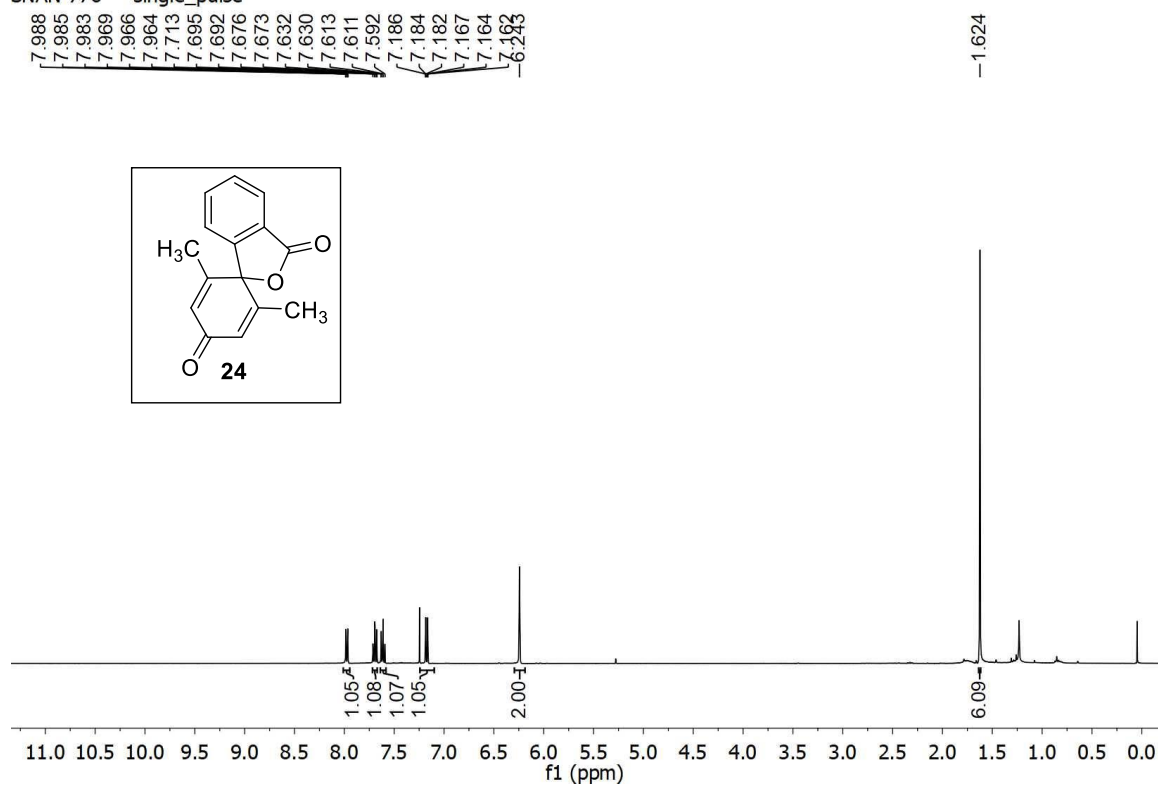
¹H and ¹³C spectra of **19**



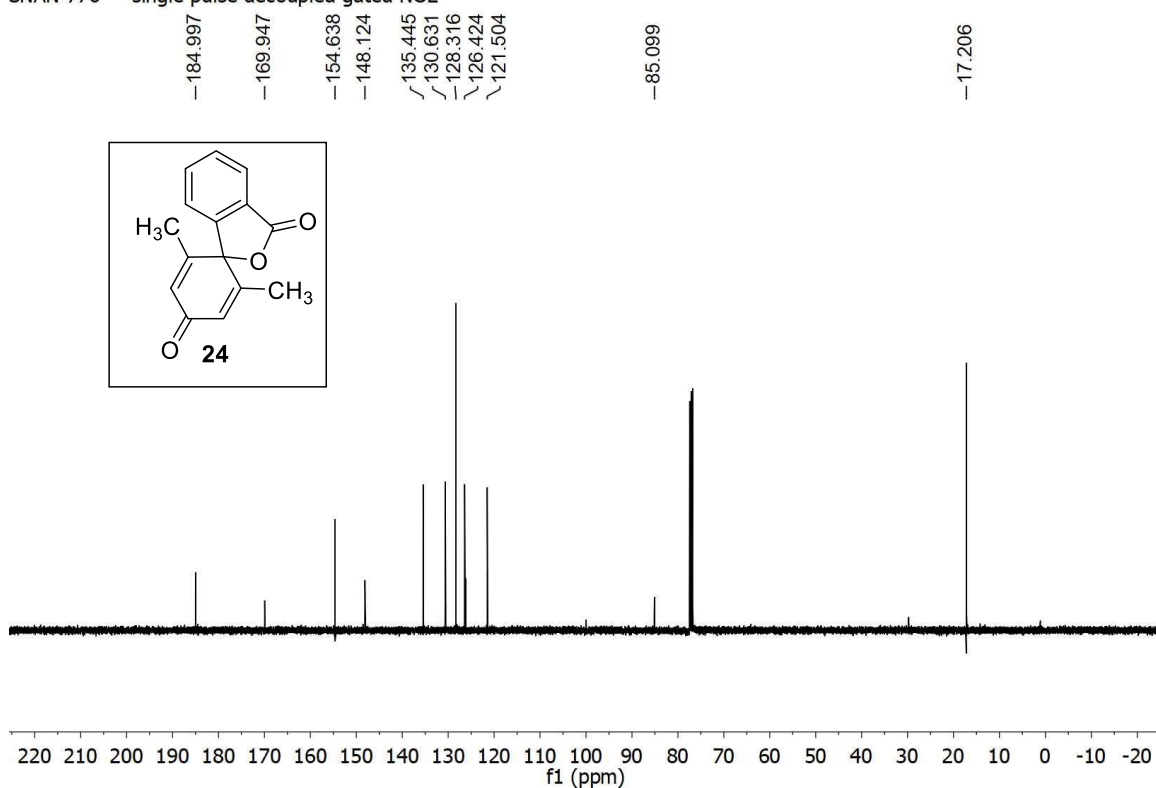
^1H and ^{13}C spectra of **20**

Chemo- and Regioselective Benzylic C(sp³)-H Oxidation Bridging the Gap between Hetero- and Homogeneous Copper Catalysis

SNAN-776 — single_pulse



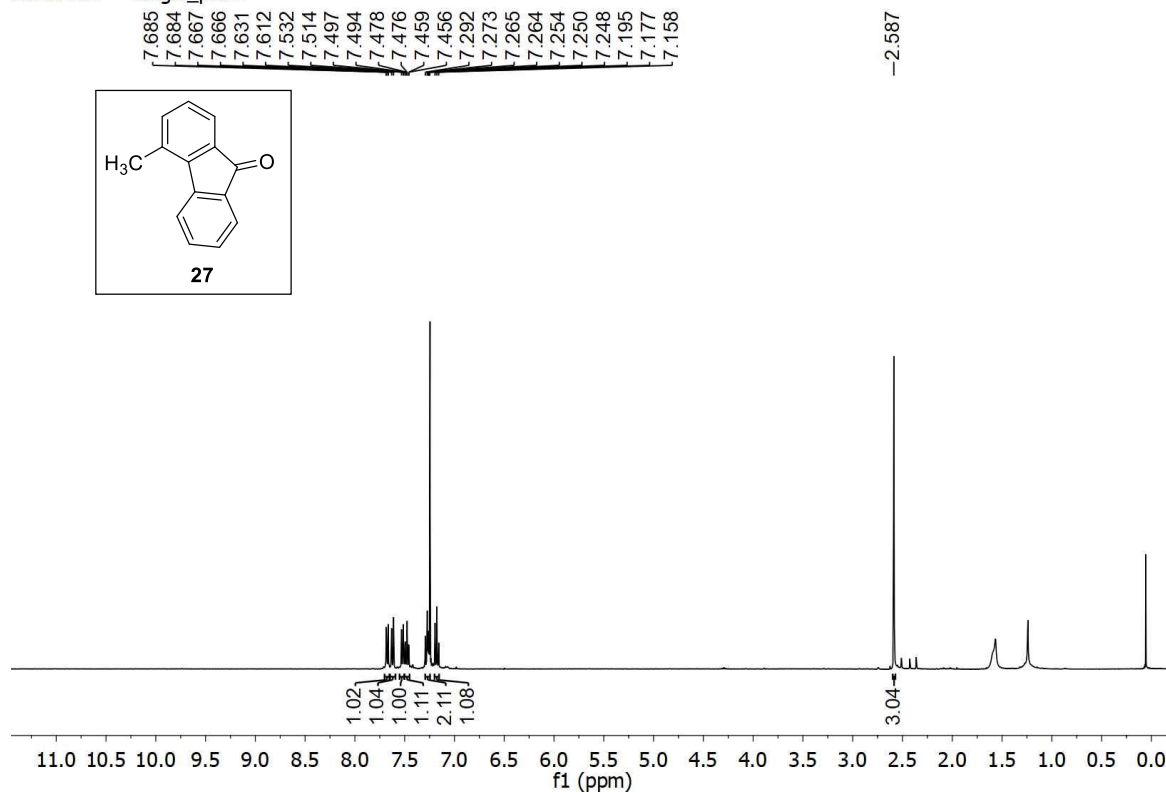
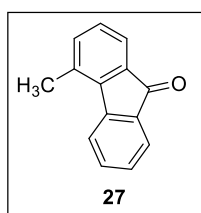
SNAN-776 — single_pulse decoupled gated NOE



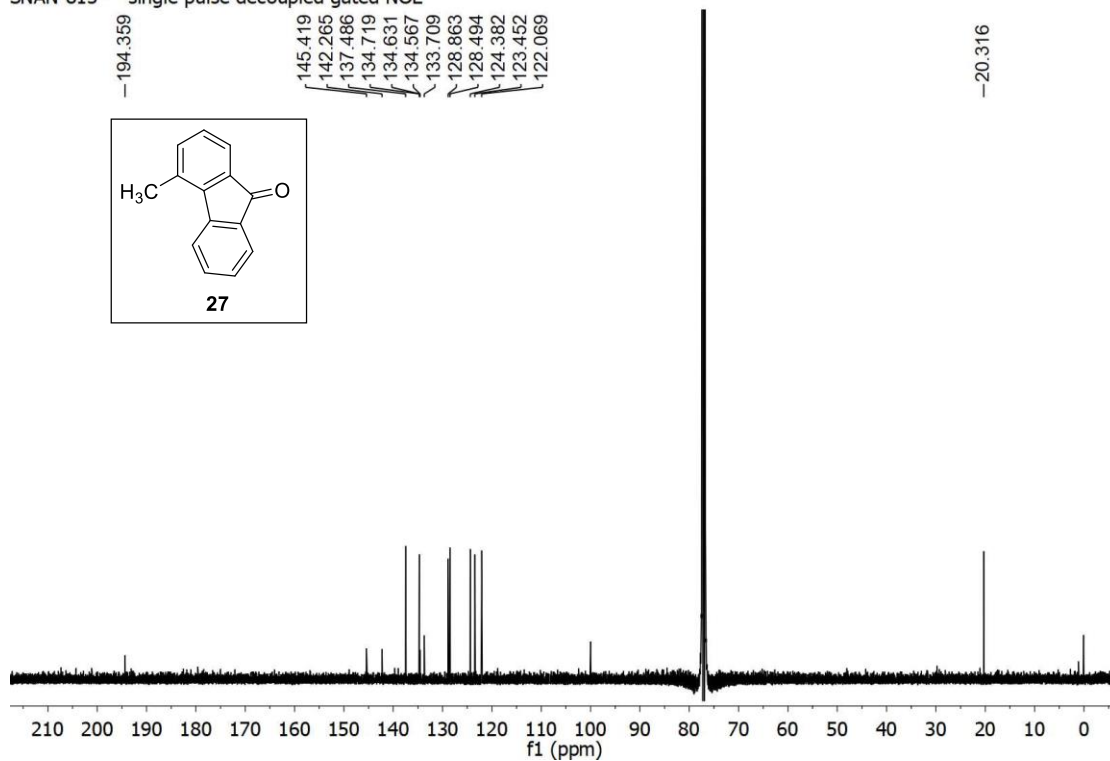
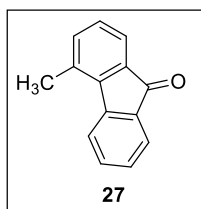
¹H and ¹³C spectra of **24**

Chapter IV

SNAN-815 — single_pulse

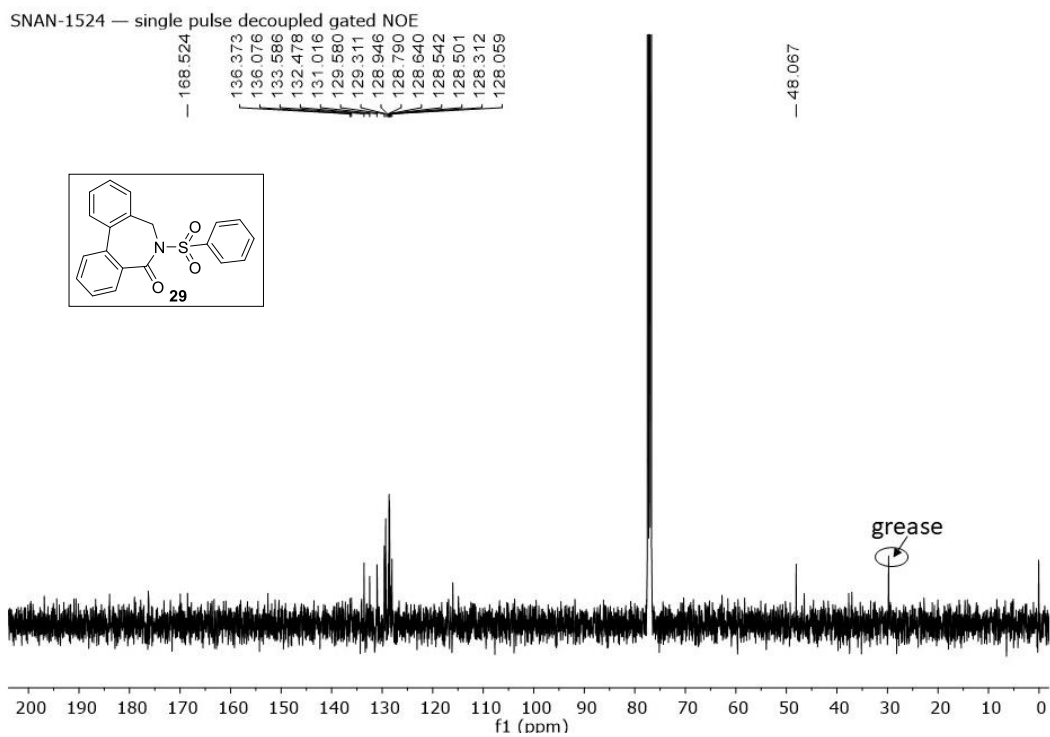
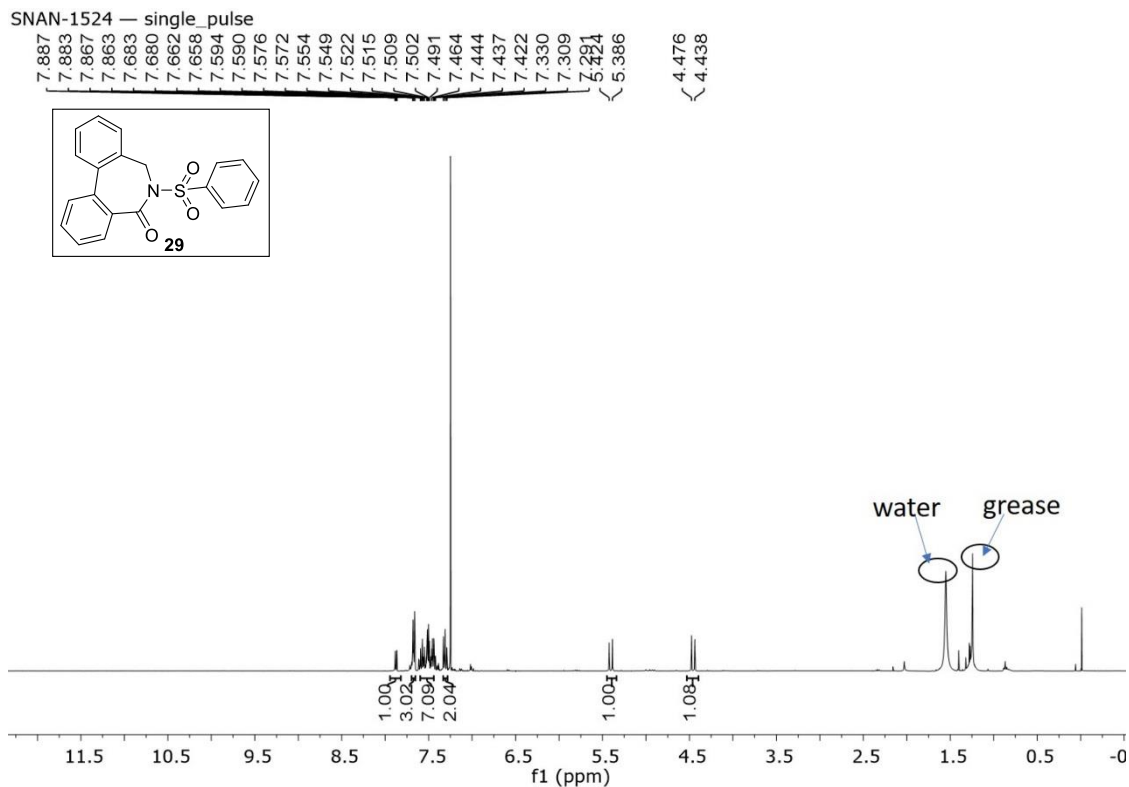


SNAN-815 — single pulse decoupled gated NOE



^1H and ^{13}C spectra of **27**

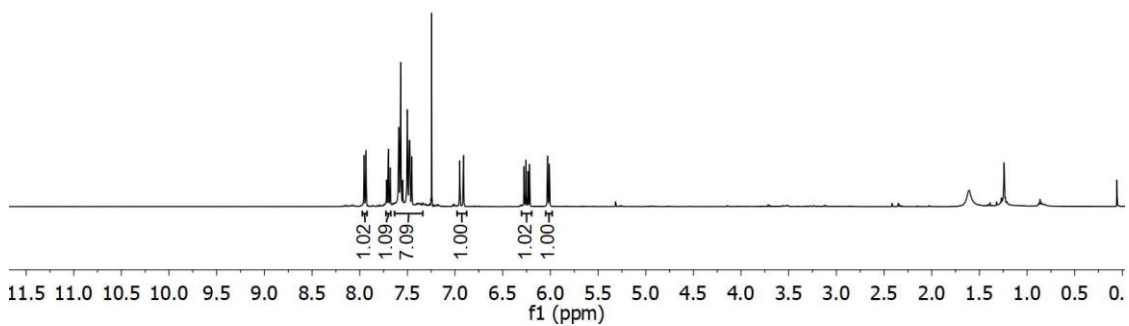
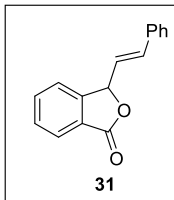
Chemo- and Regioselective Benzylic C(sp³)-H Oxidation Bridging the Gap between Hetero- and Homogeneous Copper Catalysis



¹H and ¹³C spectra of **29**

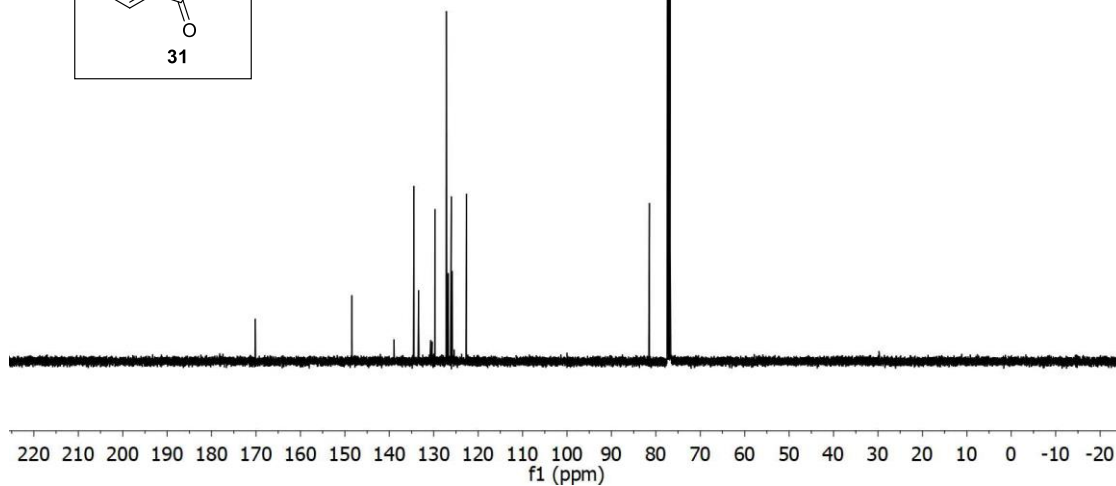
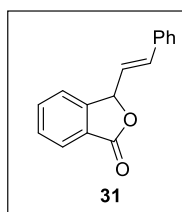
SNAN-1117 — single_pulse

7.953
7.934
7.720
7.718
7.701
7.699
7.683
7.680
7.590
7.570
7.550
7.501
7.480
7.473
7.454
6.951
6.912
6.276
6.258
6.237
6.218
6.029
6.011



SNAN-1117 — single_pulse decoupled gated NOE

170.149
148.421
138.945
134.435
133.406
130.692
130.367
129.731
127.157
126.715
126.045
125.817
125.794
122.644
-81.444



^1H and ^{13}C spectra of **31**

IV.8. References

- (1) (a) Yi, H.; Zhang, G.; Wang, H.; Huang, Z.; Wang, J.; Singh, A. K.; Lei, A. *Chem. Rev.* **2017**, *117*, 9016-9085; (b) Gandeepan, P.; Müller, T.; Zell, D.; Cera, G.; Warratz, S.; Ackermann, L. *Chem. Rev.* **2019**, *119*, 2192-2452; (c) Dalton, T.; Faber, T.; Glorius, F. *ACS Cent. Sci.* **2021**, *7*, 245-261.
- (2) (a) Lerchen, A.; Knecht, T.; Koy, M.; Ernst, J. B.; Bergander, K.; Daniliuc, C. G.; Glorius, F. *Angew. Chem. Int. Ed.* **2018**, *57*, 15248-15252; (b) Khake, S. M.; Chatani, N. *Chem* **2020**, *6*, 1056-1081.
- (3) Ju, L.; Yao, J.; Wu, Z.; Liu, Z.; Zhang, Y. *J. Org. Chem.* **2013**, *78*, 10821-10831.
- (4) Rout, S. K.; Guin, S.; Ghara, K. K.; Banerjee, A.; Patel, B. K. *Org. Lett.* **2012**, *14*, 3982-3985.
- (5) Lu, B.; Zhu, F.; Sun, H.-M.; Shen, Q. *Org. Lett.* **2017**, *19*, 1132-1135.
- (6) Feng, J.; Liang, S.; Chen, S.-Y.; Zhang, J.; Fu, S.-S.; Yu, X.-Q. *Adv. Synth. Catal.* **2012**, *354*, 1287-1292.
- (7) (a) Vasilopoulos, A.; Zultanski, S. L.; Stahl, S. S. *J. Am. Chem. Soc.* **2017**, *139*, 7705-7708; (b) Hu, H.; Chen, S.-J.; Mandal, M.; Pratik, S. M.; Buss, J. A.; Krska, S. W.; Cramer, C. J.; Stahl, S. S. *Nat. Catal.* **2020**, *3*, 358-367; (c) Liu, S.; Achou, R.; Boulanger, C.; Pawar, G.; Kumar, N.; Lusseau, J.; Robert, F.; Landais, Y. *Chem. Commun.* **2020**, *56*, 13013-13016; (d) Chi, H.; Li, H.; Liu, B.; Ye, R.; Wang, H.; Guo, Y.-L.; Tan, Q.; Xu, B. *iScience* **2019**, *21*, 650-663; (e) Wang, C.-Y.; Qin, Z.-Y.; Huang, Y.-L.; Jin, R.-X.; Lan, Q.; Wang, X.-S. *iScience* **2019**, *21*, 490-498.
- (8) Rout, S. K.; Guin, S.; Ali, W.; Gogoi, A.; Patel, B. K. *Org. Lett.* **2014**, *16*, 3086-3089.
- (9) Tanwar, L.; Börgel, J.; Ritter, T. *J. Am. Chem. Soc.* **2019**, *141*, 17983-17988.
- (10) (a) Zhuang, Z.; Yu, J.-Q. *Nature* **2020**, *577*, 656-659; (b) Das, J.; Dolui, P.; Ali, W.; Biswas, J. P.; Chandrashekar, H. B.; Prakash, G.; Maiti, D. *Chem. Sci.* **2020**, *11*, 9697-9702; (c) Cianfanelli, M.; Olivo, G.; Milan, M.; Klein Gebbink, R. J. M.; Ribas, X.; Bietti, M.; Costas, M. *J. Am. Chem. Soc.* **2020**, *142*, 1584-1593.
- (11) Gallardo-Donaire, J.; Martin, R. *J. Am. Chem. Soc.* **2013**, *135*, 9350-9353.
- (12) (a) Dai, J.-J.; Xu, W.-T.; Wu, Y.-D.; Zhang, W.-M.; Gong, Y.; He, X.-P.; Zhang, X.-Q.; Xu, H.-J. *J. Org. Chem.* **2015**, *80*, 911-919; (b) Li, L.; Yang, Q.; Jia, Z.; Luo, S. *Synthesis* **2018**, *50*, 2924-2929; (c) Li, Y.; Ding, Y.-J.; Wang, J.-Y.; Su, Y.-M.; Wang, X.-S. *Org. Lett.* **2013**, *15*, 2574-2577; (d) Ramirez, N. P.; Bosque, I.; Gonzalez-Gomez, J. C. *Org. Lett.* **2015**, *17*, 4550-4553; (e) Shao, A.; Zhan, J.; Li, N.; Chiang, C.-W.; Lei, A. *J. Org. Chem.* **2018**, *83*, 3582-3589; (f) Tao, X.-Z.; Dai, J.-J.; Zhou, J.; Xu, J.; Xu, H.-J. *Chem.*

- Eur. J.* **2018**, *24*, 6932-6935; (g) Wang, X.; Gallardo-Donaire, J.; Martin, R. *Angew. Chem. Int. Ed.* **2014**, *53*, 11084-11087; (h) Yang, Q.; Jia, Z.; Li, L.; Zhang, L.; Luo, S. *Org. Chem. Front.* **2018**, *5*, 237-241; (i) Zhang, M.; Ruzi, R.; Li, N.; Xie, J.; Zhu, C. *Org. Chem. Front.* **2018**, *5*, 749-752; (j) Zhang, S.; Li, L.; Wang, H.; Li, Q.; Liu, W.; Xu, K.; Zeng, C. *Org. Lett.* **2018**, *20*, 252-255; (k) Bhunia, S. K.; Das, P.; Nandi, S.; Jana, R. *Org. Lett.* **2019**, *21*, 4632-4637.
- (13) Wang, Y.; Gulevich, A. V.; Gevorgyan, V. *Chem. Eur. J.* **2013**, *19*, 15836-15840.
- (14) Sathyamoorthi, S.; Du Bois, J. *Org. Lett.* **2016**, *18*, 6308-6311.
- (15) Dangel, B. D.; Johnson, J. A.; Sames, D. *J. Am. Chem. Soc.* **2001**, *123*, 8149-8150.
- (16) Novák, P.; Correa, A.; Gallardo-Donaire, J.; Martin, R. *Angew. Chem. Int. Ed.* **2011**, *50*, 12236-12239.
- (17) Im, H.; Kang, D.; Choi, S.; Shin, S.; Hong, S. *Org. Lett.* **2018**, *20*, 7437-7441.
- (18) Cianfanelli, M.; Olivo, G.; Milan, M.; Klein Gebbink, R. J. M.; Ribas, X.; Bietti, M.; Costas, M. *J. Am. Chem. Soc.* **2020**, *142*, 1584-1593.
- (19) Qian, S.; Li, Z.-Q.; Li, M.; Wisniewski, S. R.; Qiao, J. X.; Richter, J. M.; Ewing, W. R.; Eastgate, M. D.; Chen, J. S.; Yu, J.-Q. *Org. Lett.* **2020**, *22*, 3960-3963.
- (20) Chen, S.; Mu, D.; Mai, P.-L.; Ke, J.; Li, Y.; He, C. *Nat. Commun.* **2021**, *12*, 1249.
- (21) Dohi, T.; Takenaga, N.; Goto, A.; Maruyama, A.; Kita, Y. *Org. Lett.* **2007**, *9*, 3129-3132.
- (22) Wang, X.; Gallardo-Donaire, J.; Martin, R. *Angew. Chem. Int. Ed.* **2014**, *53*, 11084-11087.
- (23) Ramirez, N. P.; Bosque, I.; Gonzalez-Gomez, J. C. *Org. Lett.* **2015**, *17*, 4550-4553.
- (24) Morack, T.; Metternich, J. B.; Gilmour, R. *Org. Lett.* **2018**, *20*, 1316-1319.
- (25) (a) Guo, X.-X.; Gu, D.-W.; Wu, Z.; Zhang, W. *Chem. Rev.* **2015**, *115*, 1622-1651; (b) Aneja, T.; Neetha, M.; Afsina, C. M. A.; Anilkumar, G. *RSC Adv.* **2020**, *10*, 34429-34458.
- (26) (a) Guo, S.; Yuan, Y.; Xiang, J. *New J. Chem.* **2015**, *39*, 3093-3097; (b) Meng, H.; Xu, Z.; Qu, Z.; Huang, H.; Deng, G.-J. *Org. Lett.* **2020**, *22*, 6117-6121.
- (27) (a) Cui, X.; Li, W.; Ryabchuk, P.; Junge, K.; Beller, M. *Nat. Catal.* **2018**, *1*, 385-397; (b) Liu, L.; Corma, A. *Chem. Rev.* **2018**, *118*, 4981-5079; (c) Copéret, C.; Chabanas, M.; Petroff Saint-Arroman, R.; Basset, J.-M. *Angew. Chem. Int. Ed.* **2003**, *42*, 156-181; (d) Van Velthoven, N.; Wang, Y.; Van Hees, H.; Henrion, M.; Bugaev, A. L.; Gracy, G.; Amro, K.; Soldatov, A. V.; Alauzun, J. G.; Mutin, P. H.; De Vos, D. E. *ACS Appl. Mater. Interfaces* **2020**, *12*, 47457-47466.

- (28) (a) Curto, J. M.; Kozlowski, M. C. *J. Am. Chem. Soc.* **2015**, *137*, 18-21; (b) Hong, G.; Nahide, P. D.; Neelam, U. K.; Amadeo, P.; Vijeta, A.; Curto, J. M.; Hendrick, C. E.; VanGelder, K. F.; Kozlowski, M. C. *ACS Catal.* **2019**, *9*, 3716-3724.
- (29) (a) Altemöller, M.; Gehring, T.; Cudaj, J.; Podlech, J.; Goesmann, H.; Feldmann, C.; Rothenberger, A. *Eur. J. Org. Chem.* **2009**, *2009*, 2130-2140; (b) Aly, A. H.; Edrada-Ebel, R.; Indriani, I. D.; Wray, V.; Müller, W. E. G.; Totzke, F.; Zirrgiebel, U.; Schächtele, C.; Kubbutat, M. H. G.; Lin, W. H.; Proksch, P.; Ebel, R. *J. Nat. Prod.* **2008**, *71*, 972-980; (c) Höller, U.; Wright, A. D.; Matthee, G. F.; König, G. M.; Draeger, S.; Aust, H.-J.; Schulz, B. *Mycol. Res.* **2000**, *104*, 1354-1365; (d) Wu, G.; Guo, H.-F.; Gao, K.; Liu, Y.-N.; Bastow, K. F.; Morris-Natschke, S. L.; Lee, K.-H.; Xie, L. *Bioorg. Med. Chem. Lett.* **2008**, *18*, 5272-5276; (e) Colombel, V.; Joncour, A.; Thoret, S.; Dubois, J.; Bignon, J.; Wdzieczak-Bakala, J.; Baudoin, O. *Tetrahedron Lett.* **2010**, *51*, 3127-3129.
- (30) (a) Dana, S.; Chowdhury, D.; Mandal, A.; Chipem, F. A. S.; Baidya, M. *ACS Catal.* **2018**, *8*, 10173-10179; (b) Omura, S.; Fukuyama, T.; Murakami, Y.; Okamoto, H.; Ryu, I. *Chem. Commun.* **2009**, 6741-6743; (c) Tang, Y.; Meador, R. I. L.; Malinchak, C. T.; Harrison, E. E.; McCaskey, K. A.; Hempel, M. C.; Funk, T. W. *J. Org. Chem.* **2020**, *85*, 1823-1834; (d) Miyagawa, M.; Akiyama, T. *Chem. Lett.* **2017**, *47*, 78-81.
- (31) Tang, P.-T.; Shao, Y.-X.; Wang, L.-N.; Wei, Y.; Li, M.; Zhang, N.-J.; Luo, X.-P.; Ke, Z.; Liu, Y.-J.; Zeng, M.-H. *Chem. Commun.* **2020**, *56*, 6680-6683.
- (32) Zhang, X.-S.; Zhang, Y.-F.; Li, Z.-W.; Luo, F.-X.; Shi, Z.-J. *Angew. Chem. Int. Ed.* **2015**, *54*, 5478-5482.
- (33) Blanksby, S. J.; Ellison, G. B. *Acc. Chem. Res.* **2003**, *36*, 255-263.
- (34) (a) Barzanò, G.; Mao, R.; Garreau, M.; Waser, J.; Hu, X. *Org. Lett.* **2020**, *22*, 5412-5416; (b) Zheng, Y.-W.; Narobe, R.; Donabauer, K.; Yakubov, S.; König, B. *ACS Catal.* **2020**, *10*, 8582-8589; (c) Tao, C.; Wang, B.; Sun, L.; Liu, Z.; Zhai, Y.; Zhang, X.; Wang, J. *Org. Biomol. Chem.* **2017**, *15*, 328-332; (d) Shi, Y.; Zhang, T.; Jiang, X.-M.; Xu, G.; He, C.; Duan, C. *Nat. Commun.* **2020**, *11*, 5384.
- (35) Liang, T.; Zhao, H.; Gong, L.; Jiang, H.; Zhang, M. *iScience* **2019**, *15*, 127-135.
- (36) (a) Tran, B. L.; Driess, M.; Hartwig, J. F. *J. Am. Chem. Soc.* **2014**, *136*, 17292-17301; (b) Xia, Q.; Liu, X.; Zhang, Y.; Chen, C.; Chen, W. *Org. Lett.* **2013**, *15*, 3326-3329.
- (37) (a) Maity, A.; Hyun, S.-M.; Powers, D. C. *Nat. Chem.* **2018**, *10*, 200-204; (b) Maity, A.; Hyun, S.-M.; Wortman, A. K.; Powers, D. C. *Angew. Chem. Int. Ed.* **2018**, *57*, 7205-7209.

- (38) Agarwal, N.; Freakley, S. J.; McVicker, R. U.; Althahban, S. M.; Dimitratos, N.; He, Q.; Morgan, D. J.; Jenkins, R. L.; Willock, D. J.; Taylor, S. H.; Kiely, C. J.; Hutchings, G. J. *Science* **2017**, *358*, 223.
- (39) Sushkevich, V. L.; Palagin, D.; Ranocchiari, M.; van Bokhoven, J. A. *Science* **2017**, *356*, 523.
- (40) Fabry, D. C.; Rueping, M. *Acc. Chem. Res.* **2016**, *49*, 1969-1979.
- (41) (a) Hossian, A.; Jana, R. *Org. Biomol. Chem.* **2016**, *14*, 9768-9779; (b) Wang, S.-F.; Cao, X.-P.; Li, Y. *Angew. Chem. Int. Ed.* **2017**, *56*, 13809-13813.
- (42) Cudaj, J.; Podlech, J. *Synlett* **2012**, *2012*, 371-374.
- (43) Hou, Y.; Li, J.; Wu, J.-C.; Wu, Q.-X.; Fang, J. *ACS Chem. Neurosci.* **2021**.
- (44) Bingham, N. M.; Roth, P. J. *Chem. Commun.* **2019**, *55*, 55-58.
- (45) Zhang, G.; Fu, L.; Chen, P.; Zou, J.; Liu, G. *Org. Lett.* **2019**, *21*, 5015-5020.
- (46) Liang, Q.; Walsh, P. J.; Jia, T. *ACS Catal.* **2020**, *10*, 2633-2639.
- (47) Maity, S.; Bain, D.; Chakraborty, S.; Kolay, S.; Patra, A. *ACS Sustainable Chem. Eng.* **2020**, *8*, 18335-18344.
- (48) Wootton, R. C. R.; Fortt, R.; de Mello, A. J. *Org. Proc. Res. Dev.* **2002**, *6*, 187-189.
- (49) Hu, X.-Q.; Liu, Z.-K.; Hou, Y.-X.; Gao, Y. *iScience* **2020**, *23*, 101266.
- (50) (a) Davydov, R.; Herzog, A. E.; Jodts, R. J.; Karlin, K. D.; Hoffman, B. M. *J. Am. Chem. Soc.* **2022**, *144*, 377-389; (b) Kunishita, A.; Ishimaru, H.; Nakashima, S.; Ogura, T.; Itoh, S. *J. Am. Chem. Soc.* **2008**, *130*, 4244-4245.
- (51) Trammell, R.; Rajabimoghadam, K.; Garcia-Bosch, I. *Chem. Rev.* **2019**, *119*, 2954-3031.
- (52) (a) Mohammadpour, P.; Safaei, E. *RSC Adv.* **2020**, *10*, 23543-23553; (b) Sutradhar, M.; Alegria, E. C. B. A.; Roy Barman, T.; Scorcelletti, F.; Guedes da Silva, M. F. C.; Pombeiro, A. J. L. *Molecular Catalysis* **2017**, *439*, 224-232.
- (53) Pla, D.; Gómez, M. *ACS Catal.* **2016**, *6*, 3537-3552.
- (54) Argyle, M. D.; Bartholomew, C. H. *Catalysts* **2015**, *5*.
- (55) Chen, C.-X.; Xu, C.-H.; Feng, L.-R.; Qiu, F.-L.; Suo, J.-S. *J Mol Catal A Chem* **2006**, *252*, 171-175.
- (56) Li, H.; Subbotina, E.; Bunrit, A.; Wang, F.; Samec, J. S. M. *Chem. Sci.* **2019**, *10*, 3681-3686.
- (57) Carrillo-Arcos, U. A.; Rojas-Ocampo, J.; Porcel, S. *Dalton Trans.* **2016**, *45*, 479-483.
- (58) Mallampudi, N. A.; Reddy, G. S.; Maity, S.; Mohapatra, D. K. *Org. Lett.* **2017**, *19*, 2074-2077.
- (59) Zysman-Colman, E.; Arias, K.; Siegel, J. S. *Can. J. Chem.* **2009**, *87*, 440-447.

Summary of the work

Historically, carbon dioxide (CO₂) found many applications in organic chemistry from reaction medium e.g., super critical carbon dioxide (scCO₂) or CO₂-expanded liquid (CXL) system; extraction (natural products), separation (supercritical fluid chromatography); to chemo-, regio-, and stereoselective transformation *via* the formation of transient intermediates i.e., carbonate, carbamate etc. Recently, researchers exploited CO₂ and its reduced form formic acid (HCOOH) as inexpensive, renewable, and non-toxic C1 feedstocks for carboxylation and carbonylation reactions. However, owing to its inherent kinetic and thermodynamic stability of CO₂, most of the transformations require high temperatures, high pressure, and stoichiometric amounts of organometallic reductants that leads to accidental and environmental hazards. Inspired by the natural processes, photocatalytic conversion of CO₂ into value-added products has emerged as a benign and practical approach in organic synthesis.

In addition to CO₂, using HCOOH as C-1 feedstock has also appeared as ever-growing research field. Mainly, carboxylation reactions to synthesize carboxylic acids have been performed using these two benign C-1 source.

Besides, carboxylic acids and its derivatives constitute common units in various natural products, bioactive compounds and synthetic intermediates. Upon successful attempts of producing carboxylic acids, transformation of the same would be performed using sustainable reaction conditions and new catalytic methods to produce library of pharmacophores.

The major objectives of this thesis have been concentrated on photo- or metal catalytic transformation of CO₂ and HCOOH to synthesize diverse range of carboxylic acids and subsequently, transformation of carboxylic acids to achieve various type of potential bioactive compounds using sustainable catalytic methods.

Firstly, a detailed general review has been presented to understand the modern sustainable modes of carboxylation reactions with CO₂ and the mild techniques to convert carboxylic acids to a diverse range of compounds. Although CO₂ is an excellent C1 source, due to its inherent thermodynamic stability and kinetic inertness most of the carboxylation reactions using CO₂ are far from practical as they require high pressure of CO₂, harsh conditions, high energy input etc. To circumvent this, photocatalysis has emerged as state-of-

Conclusion

the-art and promising techniques for carboxylation with CO₂. In this chapter, we presented the chronological development of modern photocarboxylation reactions mainly to synthesize carboxylic acids aiming towards sustainable development. Then, the prime modes of reactions have been discussed to convert carboxylic acids to produce value-added products. Here, we have discussed metal, metal-free, photo-, and electrocatalytic strategies for decarboxylative couplings, carboxyl group directed C–H activations, and C–H activation towards lactone formation starting from carboxylic acid substrates.

Secondly, a visible light mediated, organic photoredox-catalyzed acylative carboxylation of alkene has been developed. The acyl radical is generated from the corresponding α -ketocarboxylic acids through decarboxylation and attacks regioselectively at the β -position of the vinyl arenes. The incipient benzylic radical is further reduced to the corresponding anion by the photoredox-catalyst and reacts with the slightly electrophilic carbon dioxide to furnish 1,2-acylation-carboxylation product. As, decarboxylation to liberate CO₂ and carboxylation to employ CO₂ –these two events are taking place at single operation, the reaction condition has been developed so that it could behave against “Le Chatelier’s principle”. Remarkably, α -ketocarboxylic acids undergo decarboxylation selectively and further decarboxylation was not observed under this reaction condition.

Thirdly, a palladium catalyzed hydroxycarbonylation of aryldiazonium salt has been developed. The method has also been realized on anilines via *in-situ* formation of diazonium salts. For this transformation, convenient carbonyl source carbon monoxide (CO) has been replaced with commonly available formic acid. By doing so, we have been successful to eliminate the toxicity of CO or any special high-pressure equipment. Unlike the previous similar procedures, reaction time is shorter, catalyst loading is low, temperature is lesser and finally the halide groups survive the reaction condition. Remarkably, via this method we have been able to synthesize dicarboxylic acid with different isotopes successfully, which is otherwise hardly possible. Here, common dehydrant DCC has been used as an activator of HCOOH by liberating CO *in-situ*.

Finally, we have presented strategy for expedient synthesis of privileged seven-membered lactones, dibenzo[*c,e*]oxepin-5(7H)-one through a highly chemoselective benzylic C(sp³)–H activation. Selective C–H functionalization in a pool of proximal C–H bonds, predictably altering their innate reactivity is a daunting challenge. Here remarkably, the formation of widely explored six-membered lactone *via* C(sp²)–H activation is suppressed

Conclusion

under the present conditions. Primarily, the reaction proceeded smoothly on use of inexpensive metallic copper catalyst and di-tert-butyl peroxide (DTBP). Owing to the hazards of stoichiometric DTBP, further, we have developed a sustainable metallic copper/rose bengal dual catalytic system to utilize molecular oxygen replacing DTBP. This is a rare and probably the first example where metallic copper has been coupled with photocatalysis to capture gaseous O₂. A 1,5-aryl migration through Smiles rearrangement was realized from the corresponding diaryl ether substrates instead of expected eight membered lactones. The present methodology is scalable, applied to the total synthesis of cytotoxic and neuroprotective natural product Alterlactone. The catalyst is recyclable and the reaction can be performed in a copper-bottle without any added external catalyst. Additionally, using same catalytic condition, a range of different substrates have shown diverse and interesting reaction patterns via C–H activation.

So, in short, we have performed photocatalytic transformation of two gaseous systems – carbon dioxide (CO₂) and oxygen (O₂) to synthesize molecularly complex carboxylic acids and a 7-membered privileged biaryl lactones, respectively. And, we have executed transition-metal catalyzed transformation of HCOOH to synthesize diverse range of carboxylic acids. Transformation of carboxylic acids has been developed to achieve various type of potential bioactive compounds using sustainable catalytic methods.

Scope for the future work

Despite noteworthy developments, the use of renewable and environmentally benign C-1 feedstock like CO₂ or HCOOH in mild and green strategies is still at budding stage. The fantastic breakthroughs over the past few years paved the way. Still, huge improvements are required to be industrially accepted so that the continuous effort towards “low-carbon economy” is paid off.

- In comparison with transition-metal catalyzed C–X carboxylation with CO₂, the substrate variation remains narrow in case of photocarboxylation. Specifically, most of carboxylation of the C–X bonds took place either with the C(sp²)- or benzylic C(sp³)-center which is a stabilized one under visible-light catalysis; on the contrary, photocarboxylation cleaving unbiased C(sp³)–X bonds has not been developed yet.
- Direct carboxylation breaking unactivated C–H bonds has hardly been developed. With simultaneous development of the photocatalyzed directing group (DG)-assisted

Conclusion

or DG-free C–H activation reactions, this major field of unbiased C–H carboxylation drew attention.

- As far as carboxylation reactions of alkenes are concerned, the substrates are mostly limited to styrenes or activated alkenes, as the intermediate radicals or anions at benzylic or α -position are stabilized. So far, the normal unbiased long chain alkenes have never been used for the same. Selective carboxylation of unbiased alkenes demands further improvements and remains a long-cherished goal.
- SET activation of CO₂ has seldom been executed compared to two-electron activation of substrate. Though, the former is achievable occasionally with photocatalysis in selected examples, finding a general method and a wide use of the same has not been discovered till date.
- Continuous-flow techniques have shown the potential to be applicable in large scale. Attention nowadays also is devoted towards further improvement of the strategies so that these could be implemented in strategic sector.
- Metal-free activation of HCOOH has not been performed extensively, though, photocatalysis has been successful to do so in some occasions. A lot of efforts should be concentrated on this strategy to make this more sustainable.
- The metallic-copper/photocatalyzed benzylic C(sp³)–H oxidation with molecular O₂ only led to 7-membered lactones in our case. Access to 8- or 5-membered lactones *via* benzylic C(sp³)–H activation with similar strategy has not been successful. Future work would be devoted to overcome these pitfalls.

Publications/Conferences



List of publications

- 1) **Nandi, S.;** Mondal, S.; Jana, R. A heterogeneous copper powder-catalyzed protocol for chemo- and regioselective benzylic C(sp³)-H activation *en route* to dibenzo[*c,e*]oxepinones. *STAR Protocols*. **2022**, 3, 101781.
- 2) **Nandi, S.;** Jana, R. Toward Sustainable Photo-/Electrocatalytic Carboxylation of Organic Substrates with CO₂. *Asian J. Org. Chem.* **2022**, e202200356. (Featured as Cover) (Part of the “Special Collection on Carbon Dioxide Utilization” by “Wiley Publications”)
- 3) **Nandi, S.;** Mondal, S.; Jana, R. Chemo-and regioselective benzylic C (sp³)-H oxidation bridging the gap between hetero-and homogeneous copper catalysis. *iScience*. **2022**, 25, 104341.
- 4) Begam, H.M.; **Nandi, S.;** Jana, R. A directing group switch in copper-catalyzed electrophilic C-H amination/migratory annulation cascade: divergent access to benzimidazolone/benzimidazole. *Chem. Sci.* **2022**, 13, 5726-5733.
- 5) Bhunia, S.; Das, P.; **Nandi, S.;** Jana, R. Carboxylation of Aryl Triflates with CO₂ Merging Palladium and Visible-Light-Photoredox Catalysts. *Org. Lett.* **2019**, 21, 4632-4637.
- 6) Mukherjee, M. M.; Basu, N.; **Nandi, S.;** Ghosh, R. A metal free mild and green approach for tandem opening of 4,6-*O*-benzylidene acetals to their corresponding 6-*O*-acetyl derivatives: Application in the synthesis of a trisaccharide using one-pot glycosylation reactions. *Carbohydr. Res.* **2019**, 476, 36-43.

Manuscripts communicated/under preparation

- 7) **Nandi, S.;** Das, S.; Mondal, S.; Jana, R. One-pot hydroxycarbonylation of anilines *via* diazonium salt *en route* to benzoic acids: Formic acid as C-1 source. *Manuscript communicated*.
- 8) **Nandi, S.;** Das, P.; Das, S.; Mondal, S.; Jana, R. Unified strategy for photoredox catalyzed acylative dicarbofunctionalization of alkenes: harmony between radical-radical / radical-polar pathways. *Manuscript communicated*.
- 9) **Nandi, S.;** Mondal, S.; Jana, R. Nickel/photoredox dual catalyzed one-pot carboxylation of phenols *via* tosylates with CO₂. *Manuscript under preparation*.

List of attended conferences

- 1) **“Chemical Science Symposium 2022: Sustainable Synthesis and Catalysis”** (Hybrid mode), 10-11 November, 2022, London, UK. (*Presented an online poster on “Bridging between hetero- and homogeneous catalysis: copper powder catalyzed chemo- and regioselective benzylic C(sp³)-H oxidation”*)
- 2) **“International Conference on Chemistry for Human Development (ICCHD-2020)”**, January 9-11, 2020 at HIT, Kolkata organized by University of Calcutta. (*Presented a poster on “Carboxylation of Aryl Triflates with CO₂ Merging Palladium and Visible-Light-Photoredox Catalysts”*).
- 3) **“International Conference on Chemistry for Human Development (ICCHD-2018)”**, January 8-10, 2018 at HIT, Kolkata. (*Presented a poster on “Se-C and Se-P bond formation Via C-H Bond Activation and Cross Dehydrogenative Coupling Under Air”*)
- 4) **“National Seminar on Chemistry of Functional Materials of Current Interest (CFMCI-2016)”**, March 16, 2016 at Jadavpur University.
- 5) **“National Seminar on Emerging Trends in Chemistry (ETC-2017)”**, February 15, 2017 at Jadavpur University.

Reprints of Selected Publications

ASIAN JOURNAL OF ORGANIC CHEMISTRY

www.AsianJOC.org



A Journal of



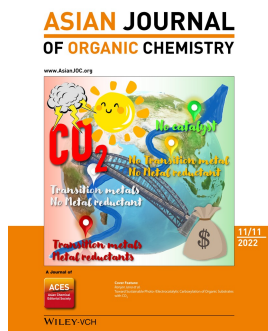
Cover Feature:

Ranjan Jana et al.

Toward Sustainable Photo-/Electrocatalytic Carboxylation of Organic Substrates with CO₂

WILEY-VCH

Owing to the global environmental policies for decarbonization, conversion of waste CO₂ into value-added products is the research focus today. Although CO₂ is an excellent C1 source, due to its inherent thermodynamic stability and kinetic inertness most of the carboxylation reactions using CO₂ are far from practical as they require high pressure of CO₂, harsh conditions, high energy input etc. To circumvent this, photo- and electrocatalysis have emerged as state-of-the-art and promising technique for carboxylation with CO₂. In this review, we chronologically present the development of these modern carboxylation reactions aiming towards sustainable development. More information can be found in the Review by Ranjan Jana et al.



S. Nandi, Dr. R. Jana*

1 – 2

Toward Sustainable Photo-/Electrocatalytic Carboxylation of Organic Substrates with CO₂

Special
Collection

Toward Sustainable Photo-/Electrocatalytic Carboxylation of Organic Substrates with CO₂

Shantanu Nandi and Ranjan Jana*^[a]



Abstract: Historically, carbon dioxide found many applications in organic chemistry from reaction medium e.g., supercritical carbon dioxide (scCO₂) or CO₂-expanded liquid (CXL) system; extraction (natural products), separation (supercritical fluid chromatography); chemo-, regio-, and stereoselective transformation via the formation of transient intermediates i.e., carbonate, carbamate etc. Recently, researchers have exploited CO₂ as an inexpensive, renewable and non-toxic C1 feedstock for carboxylation and carbonylation reactions. However, owing to its inherent kinetic and thermodynamic

stability, most of the transformations require high temperatures, high pressure, and stoichiometric amounts of organometallic reductants that leads to accidental and environmental hazards. Inspired by the natural processes, photo- and electrocatalytic conversion of CO₂ into value-added products has emerged as a benign and practical approach in organic synthesis. Here in this review, we will discuss some recent photo- and electrocatalytic methods and their comparison toward sustainable development.

1. Introduction

Despite non-toxicity, having the most significant contribution to the “greenhouse effect”, carbon dioxide (CO₂) is heavily responsible for global warming.^[1] Moreover, the ever-growing concentration of CO₂ in nature since the industrial revolution due to over-depletion of fossil fuel and other activities result in acceleration of the problem. As, to overlook the industrial benefits and technological advances is not at all an option, the only mission is now to reduce the “carbon footprint”^[2] from the sources. Designing sustainable technologies replacing the troublesome ones and reutilizing the CO₂ to synthesize other value-added products go hand in hand to fulfill this goal. To the synthetic chemist’s community, “waste to wealth” conversion is a long-cherished goal and enormous effort has been dedicated. Due to the stringent pressure from environmental protection agencies (EPA) this field has received renewed interest in recent times.

Although, “circular carbon economy” using CO₂ is an ideal concept in energy research,^[3] from synthetic chemistry point of view, CO₂ is an ideal C-1 source,^[4] for its low-cost, high abundance and non-toxicity compared to its counterpart carbon monoxide (CO). Besides, carboxylic acids and its derivatives constitute common units in various natural products, bioactive compounds^[5] and synthetic intermediates.^[6] Several research groups made significant advancement from concept, catalyst to industrial application of CO₂ utilization reaction for fine chemical synthesis (Figure 1).^[7] With the upsurge of transition-metal catalysis, in the past decade, a huge effort has been put for direct use of CO₂ as C-1 feedstock in organic synthesis mainly using transition metal and environmentally toxic (super)stoichiometric amount of metal reductants.^[8] But the obvious pitfall remained in the fact that huge amount of toxic waste would have generated if these methodologies start to be implemented in industrial scale. As solar energy is the biggest source of energy and natural

photosynthesis utilizes the same to capture CO₂ naturally; mimicking the technology is the ultimate goal.

However, keeping these sugar-coats aside and flipping the coin reveals the actual challenge that hindered to achieve these goals till this long time. The carbon is in the most oxidized state in CO₂ and hence CO₂ molecule is thermodynamically very stable and kinetically inert. So, activating CO₂ is itself a huge task to do. The most traditional approaches deal with the use of nucleophilic organometallic reagents. As stated, substantial work has been done on use of CO₂ to generate new C–C bonds from C–B, C–X or C–H bonds with help of transition metal catalysis. But the toxic and harsh nature of the reaction conditions bar these methods to be applicable to variety of substrates for their low stability under thermal condition.

For the continued effort for green and sustainable developments, carboxylation methods also demand for newer technologies utilizing renewable energy sources. For the last 8–9 years, the photoredox chemistry has surged by storm.^[9] With the quick development, this chemistry has been successful to ease various chemical transformations which were otherwise very challenging. Chemists elegantly merged this with the transition metal catalysis to remove the metal reductants or used photochemistry solely to achieve carboxylation reactions mainly at ambient temperatures. Though, it is relatively newer with respect to time, continuous engagement into utilizing this strategy made it quite explorative and fruitful in this short time too.

Talking about renewable energies, the world is now leaning towards using electrical energy in place of direct combustion of fuel. With the flow, the synthetic chemistry is also experiencing a renaissance of electrochemistry.^[10] Though it is in very early stage to explore the challenges in carboxylation reactions, the indication from the reported procedures proves its potential. Compared to normal transition metal catalysis, both electrochemistry and photochemistry display complementary

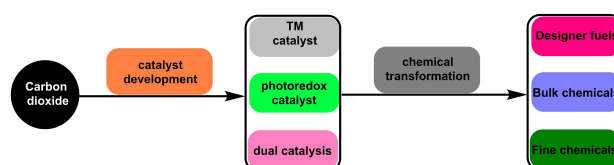


Figure 1. Utilization of Carbon Dioxide (CO₂).

[a] S. Nandi, Dr. R. Jana
Organic and Medicinal Chemistry Division,
CSIR – Indian Institute of Chemical Biology
Raja S. C. Mullick Road, Jadavpur, Kolkata 700032, West Bengal (India)
E-mail: rjana@iicb.res.in

This manuscript is part of a special collection on Carbon Dioxide Utilization in Organic Chemistry

characteristics.^[11] These two strategies have successfully been utilized in direct carboxylation of alkenes, C–X, C–N, C–O or C–H bonds, some very interesting alkene difunctionalization reactions, which would be reviewed here. Though, some interesting reviews are available for photocarboxylation reactions^[12] and couple of reviews are also there for electrocarboxylation,^[13] a comparative discussion of these two state-of-the-art technologies is highly required to understand the future route in this field to attain sustainability.

2. Conceptual framework

Owing to the aforementioned drawbacks of transition metal catalysis, it has become a cherished goal for chemists to transform CO₂ in more sustainable pathways and at atmospheric pressure. Inspired by the natural photosynthesis and the current developments of photoredox catalysis, scientists over the world hypothesized to utilize photocatalysis for the CO₂

Shantanu Nandi received B.Sc and M.Sc in Chemistry from Jadavpur University, Kolkata in 2014 and 2016, respectively. From 2017, he has been continuing his doctoral studies under the supervision of Dr. Ranjan Jana at CSIR – Indian Institute of Chemical Biology. His research interest is mainly focused on development of sustainable carboxylation reactions with benign C-1 feedstocks and transformation of carboxylic acids with C–H activation.



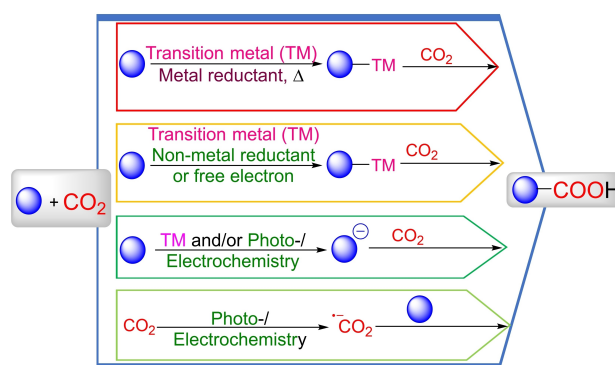
Ranjan Jana received his M.Sc. from Vidyasagar University. After attaining his PhD. in Organic Chemistry from the Indian Association for the Cultivation of Science (IACS) under the supervision of B. C. Ranu, he moved to Israel for postdoctoral studies at Bar-Ilan University under the supervision of Professor S. Braverman. He joined the Tunge group at the University of Kansas in 2008 and moved to University of Utah to join the Sigman group in 2010. He started his independent research career at the CSIR-Indian Institute of Chemical Biology as a senior scientist in 2012. Since 2020, he is working as a Sr. principal scientist at the same institute. His research interest is the divergent synthesis of privileged medicinal scaffolds and active pharmaceutical ingredients (APIs) through tandem C–H activation, alkene difunctionalization, decarboxylative cross-coupling reactions and smart utilization of CO₂. He has received prestigious Ramanujan fellowship and has been elected as the fellow of West Bengal Academy of Science and Technology.



utilization. And electrocatalysis has upsurged as another energy-efficient strategy in the past couple of years. Depending on the precedents, it would be easier to proceed by understanding the possible mechanisms of carboxylation with CO₂. As shown in the 'Scheme 1', the well-developed transition metal catalysis deals with stoichiometric amount of metal reductants. The active organometallic complex can capture CO₂ and insert it to the organic compounds. 2) While the metal reductants are replaced in transition-metal catalysis with non-metallic sacrificial electron donor with synergistic help of photocatalysis, the similar organometallic complex does the job. 3) Being feebly electrophilic, CO₂ is prone towards nucleophilic attack by a suitable anionic intermediate, given that the anion should be strong and stable enough to satisfy HSAB principle. The main challenge of this strategy lies in the fact of CO₂ being thermodynamically very stable. With the help of photocatalysis solely, the stable carbanions are formed which are made to react with CO₂ or a nucleophilic heteroatom containing compound is carboxylated by attacking CO₂ by the heteroatom. 4) SET reduction of CO₂ to produce CO₂ radical anion followed by coupling with another transient but stabilized radical or with unsaturated olefins to form C–C bond. Having said this, the biggest challenge resides in the fact of CO₂ having extremely high reduction potential ($E^{\ominus} = -2.21$ V vs SCE in DMF), which is supplemented by an overpotential of 0.1–0.6 V, generally. For surpassing this high energy barrier in mild way, it demands the use of suitable photocatalysts or high potential externally. We will discuss the developments of CO₂ fixation over the decade coordinating them with this binding fashions.

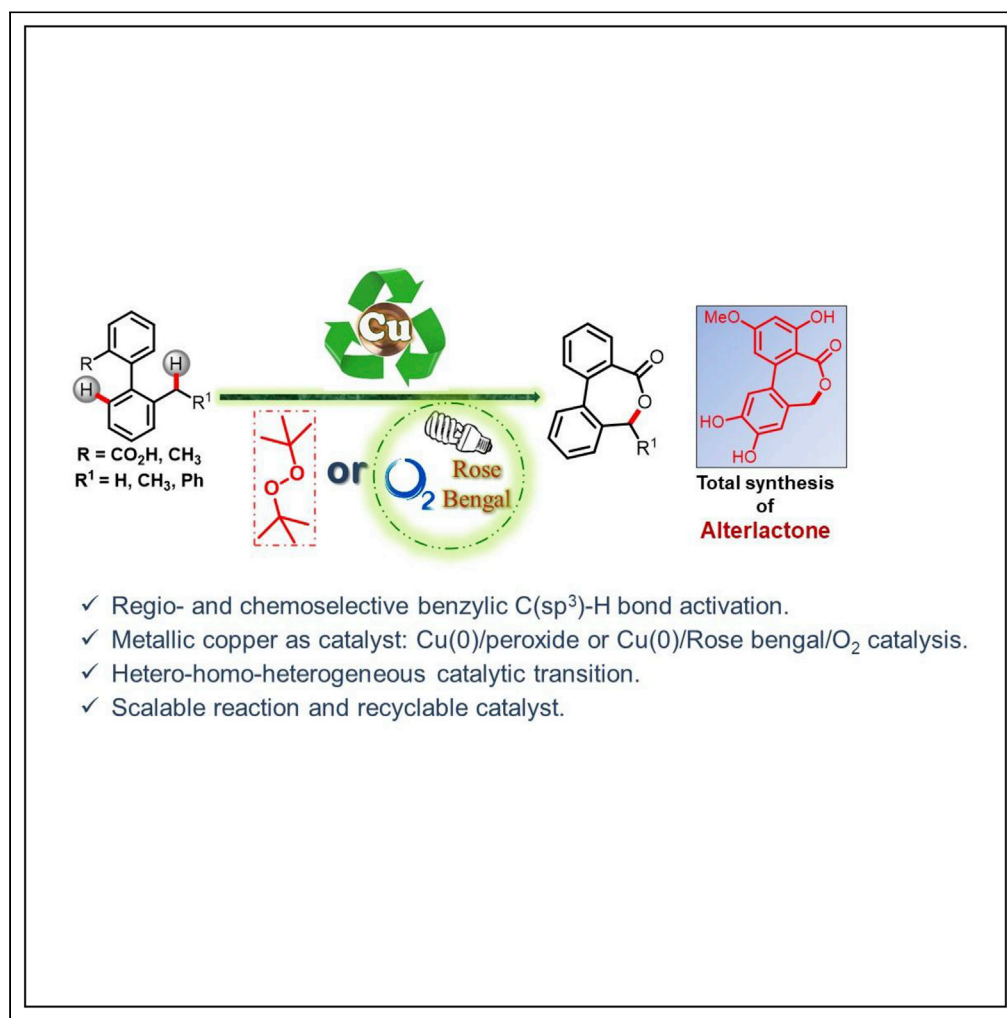
3. Photocarboxylation

During the past decade, in the field of organic synthesis, photoredox catalysis has emerged as a powerful tool when it comes to sustainability as well as versatility. Varying over the challenges, it has been used solely or combining with transition metal catalysis. While talking about carboxylation, it has no exception. We would like to compartmentalize the modes of catalysis and discuss the developments for better understanding. As mentioned earlier, the fashions of carboxylation via



Scheme 1. General Mechanisms for Carboxylation Reactions.

Article

Chemo- and regioselective benzylic C(sp³)-H oxidation bridging the gap between hetero- and homogeneous copper catalysis

Shantanu Nandi,
Shuvam Mondal,
Ranjan Jana

rjana@iicb.res.in

Highlights

Catalytic strategy for chemo- and regioselective benzylic C-H activation

Bulk copper catalysis merging with photocatalysis

Reusable copper catalyst

Reaction demonstrated in commercial copper bottle without external catalyst

Nandi et al., iScience 25, 104341
May 20, 2022 © 2022 The Authors.
<https://doi.org/10.1016/j.isci.2022.104341>

Article

Chemo- and regioselective benzylic C(sp³)-H oxidation bridging the gap between hetero- and homogeneous copper catalysisShantanu Nandi,¹ Shuvam Mondal,¹ and Ranjan Jana^{1,2,*}

SUMMARY

Selective C–H functionalization in a pool of proximal C–H bonds, predictably altering their innate reactivity is a daunting challenge. We disclose here, an expedient synthesis of privileged seven-membered lactones, dibenzo[*c,e*]oxepin-5(7H)-one through a highly chemoselective benzylic C(sp³)-H activation. Remarkably, the formation of widely explored six-membered lactone via C(sp²)-H activation is suppressed under the present conditions. The reaction proceeds smoothly on use of inexpensive metallic copper catalyst and di-*tert*-butyl peroxide (DTBP). Owing to the hazards of stoichiometric DTBP, further, we have developed a sustainable metallic copper/rose bengal dual catalytic system coupled with molecular oxygen replacing DTBP. A 1,5-aryl migration through Smiles rearrangement was realized from the corresponding diaryl ether substrates instead of expected eight-membered lactones. The present methodology is scalable, applied to the total synthesis of cytotoxic and neuroprotective natural product alterlactone. The catalyst is recyclable and the reaction can be performed in a copper bottle without any added catalyst.

INTRODUCTION

Despite an impressive array of C–H functionalization reported in the last decades, maintaining a high degree of chemo-, regio-, and stereoselectivity in a plethora of ubiquitous C–H bonds remains a major challenge (Dalton et al., 2021; Gandeepan et al., 2019; Yi et al., 2017). The chemo- and regioselective transformation in a pool of vulnerable C–H bonds in nondirected fashion through the judicious choice of the catalytic system is a prime research area (Khake and Chatani, 2020; Lerchen et al., 2018). In the past, copper (Rout et al., 2012), iron (Lu et al., 2017), palladium-catalyzed (Ju et al., 2013), or metal-free (Feng et al., 2012) intermolecular acetoxylation of benzylic C–H bonds have been reported where the reaction proceeds through the formation of a putative metal-carboxylate or acyloxy radical species. The Stahl group and others reported copper-catalyzed intermolecular benzylic C–H functionalization for the synthesis of pharmacophores from feedstock chemicals (Chi et al., 2019; Hu et al., 2020a; Liu et al., 2020; Vasilopoulos et al., 2017; Wang et al., 2019). The Ritter group reported a copper (II)-catalyzed synthesis of benzylic alcohols from alkyl arenes employing bis(methanesulfonyl)peroxide as an oxidant followed by hydrolysis (Tanwar et al., 2019). Synthesis of benzyl esters was unveiled by the Patel group using Cu(II)/TBHP and excess amount of methylarenes (Rout et al., 2012, 2014). However, the scope of benzylic activation with equimolar amount of alkylarene as coupling partner is still limited. Alternatively, intramolecular C–H bond oxidation by a tethered carboxylic acid is emerging to provide lactones directly (Cianfanelli et al., 2020; Das et al., 2020; Zhuang and Yu, 2020). A copper-catalyzed five- and six-membered lactone formation through intramolecular benzylic C–H acetoxylation was reported by the Bois group (Sathyamoorthi and Du Bois, 2016). Alternatively, the Martin group accomplished the synthesis of a six-membered lactone from *ortho*-aryl benzoic acid through copper-catalyzed C(sp²)-H bond activation (Gallardo-Donaire and Martin, 2013). Subsequently, this protocol was extrapolated by several groups using other metals or metal-free conditions via the single electron activation of aryl carboxylic acids (Scheme 1A). (Bhunia et al., 2019; Dai et al., 2015; Li et al., 2013, 2018; Ramirez et al., 2015; Shao et al., 2018; Tao et al., 2018; Wang et al., 2014; Yang et al., 2018; Zhang et al., 2018a, 2018b) Although soluble copper complexes or copper nanoparticles (CuNPs) have been used for the C–H functionalization (Aneeja et al., 2020; Guo et al., 2015b), the use of inexpensive bulk Cu catalyst is extremely rare (Guo et al., 2015a; Meng et al., 2020). Recent efforts to bridge the gap between hetero- and homogeneous catalysis for improved catalytic activity, selectivity, and cost efficiency

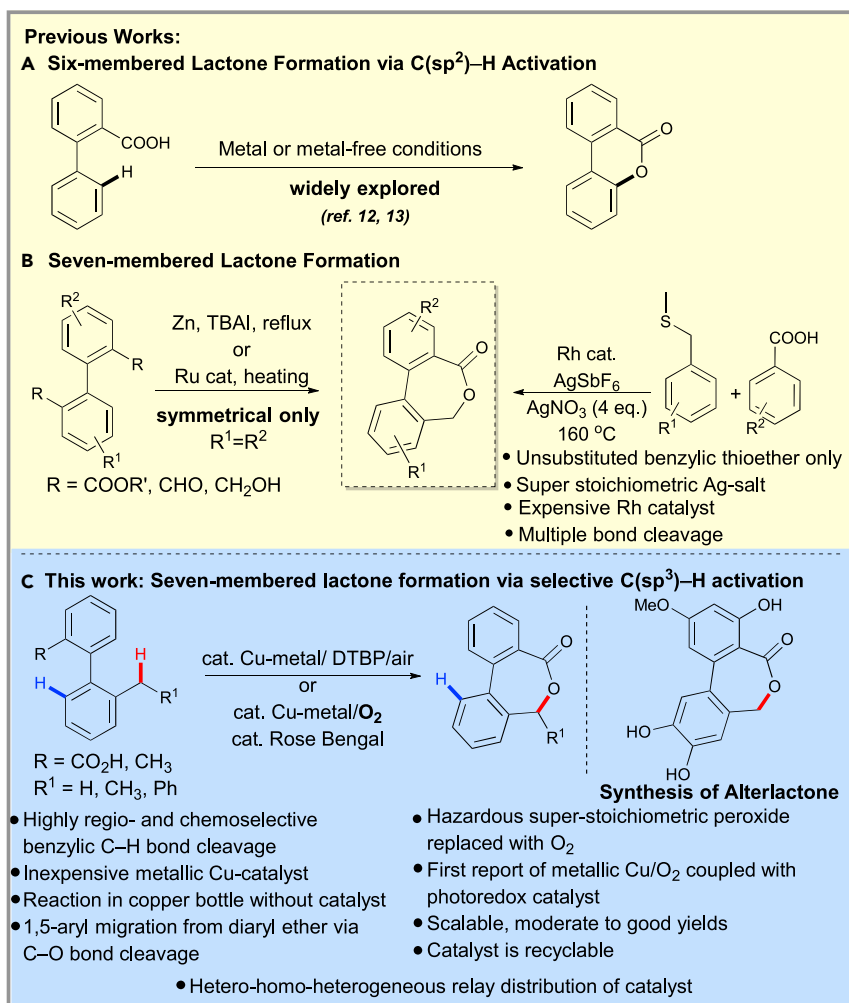
¹Organic and Medicinal Chemistry Division, CSIR-Indian Institute of Chemical Biology, Raja S. C. Mullick Road, Jadavpur, Kolkata 700032, West Bengal, India

²Lead contact

*Correspondence: rjana@iicb.res.in

<https://doi.org/10.1016/j.isci.2022.104341>





Scheme 1. Approaches to access biaryl lactones

is prevailing (Copéret et al., 2003; Cui et al., 2018; Liu and Corma, 2018; Van Velthoven et al., 2020). Particularly, inexpensive bulk copper catalysis for the chemoselective sp³ vs sp² C-H activation has not been explored. Only a palladium-mediated chemoselective sp³ vs sp² C-H activation was disclosed by the Kozłowski group (Curto and Kozłowski, 2015; Hong et al., 2019).

Dibenzo[*c,e*]oxepinones and their analogs are found in natural products and bioactive molecules exhibiting antitumor, tyrosine kinase inhibitor, cytotoxic, and antimicrotubule activity (Figure 1). (Altemöller et al., 2009; Aly et al., 2008; Colombel et al., 2010; Höller et al., 2000; Wu et al., 2008) Typically, this dibenzo [*c,e*]oxepin-5(7*H*)-one motif is constructed by a sequence of biaryl coupling and C-O bond-forming lactonization (Scheme 1B). (Dana et al., 2018; Miyagawa and Akiyama, 2018; Omura et al., 2009; Tang et al., 2020b) However, these methods are either limited to the symmetrical biaryls or prefunctionalized benzyl alcohols for lactone formation. Recently, Tang et al. reported the synthesis of 7-membered biaryl lactones via iodolactonization of electron-deficient olefins (Tang et al., 2020a). A rhodium(III)-catalyzed cross-coupling of benzylic thioethers and aryl carboxylic acids exploiting two directing groups was reported by the Shi group (Scheme 1C). (Zhang et al., 2015) However, synthesis of benzylic thioether from the corresponding bromide was necessary where no benzylic substitution was tolerated. Surprisingly, the formation of seven-membered biaryl lactone through simple intramolecular benzylic C-H oxidation by the carboxylic acid is not explored. This could be attributed to the fact that although benzylic sp³ C-H bond cleavage is energetically favorable compared to sp² C-H bond (85–90 kcal/mol vs 110–115 kcal/mol) (Blanksby and El-lison, 2003; Curto and Kozłowski, 2015), the metal-catalyzed seven-membered ring formation is disfavored

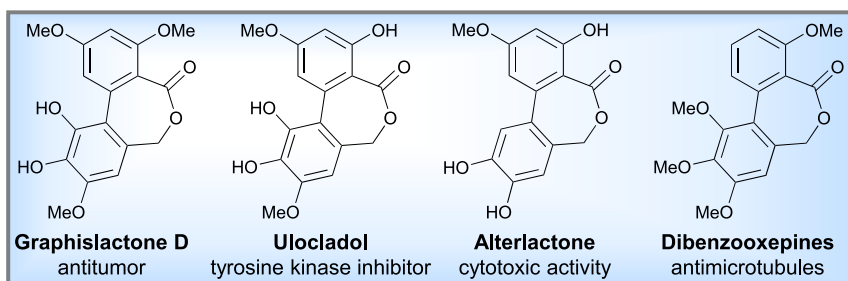


Figure 1. Biologically important dibenzooxepinone core

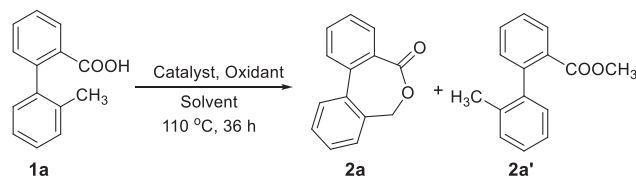
compared to the corresponding six-membered ring due to the involvement of putative eight-membered metallacycle. We hypothesized that contrary to the conventional two-electron pathway, a single electron activation of the aryl carboxylic acid followed by hydrogen atom transfer (HAT) might activate the benzylic C–H bond selectively furnishing seven-membered lactones. If succeeded, a series of dibenzooxepinones could be synthesized via this unusual disconnection approach which is prevalent in natural products and pharmaceuticals. Intrigued by these precedents, we were motivated to explore an orthogonal reaction for the formation of dibenzooxepinone through intramolecular benzylic C–H oxidation of the corresponding 2'-alkyl-[1,1'-biphenyl]-2-carboxylic acid **1**. Furthermore, exploiting the subtle disparity in chemical reactivity of the two alkyl groups, similar dibenzo[c,e]oxepin-5(7H)-ones were obtained from the corresponding 2,2'-dialkyl-substituted biaryls. Remarkably, inexpensive copper powder is used with organic peroxide as an oxidant. Fascinatingly, hazardous peroxide has been replaced with molecular oxygen merging copper powder catalyst with organic photocatalyst, rose bengal. Though there are some reports for copper salt/photoredox (Barzanò et al., 2020; Shi et al., 2020; Tao et al., 2017; Zheng et al., 2020) or copper/O₂ systems (Liang et al., 2019), to the best of our knowledge, this is the first report for bulk metallic copper/photocatalysis to couple with O₂ in benzylic C–H oxidation. Remarkably, a highly reactive, substrate-dependent soluble catalyst is formed from the copper powder during the reaction to achieve high degree of chemoselective sp³ vs sp² C–H oxidation (Scheme 1D). The corresponding diaryl ether undergoes a carboxylic acid radical-assisted 1,5-aryl migration via *ortho* C–O bond cleavage. Finally, the heterogeneous catalyst is precipitated out and recovered for subsequent runs by simple filtration offering dual benefits of homo- and heterogeneous catalyst.

RESULTS AND DISCUSSION

Investigation of reaction conditions

To create a competitive innate C–H activation scenario, we designed 2'-methyl-[1,1'-biphenyl]-2-carboxylic acid **1a** as a model substrate. To our delight, we achieved 52% of our desired product along with the corresponding methyl ester **2a'** using catalytic CuI in combination with di-tert-butyl peroxide (DTBP) (Tran et al., 2014; Xia et al., 2013). Presumably, **2a'** is formed by the radical-radical coupling of methyl radical generated from the DTBP and carboxyl radical. To improve the yield of **2a** and diminish the formation of **2a'** systematically, the metal catalysts, oxidants, and solvents were examined (Table 1). α,α,α -trifluorotoluene was found to be the best solvent. Surprisingly, we found copper(II) catalysts as well as other oxidants such as TBHP, DCP to be inferior to copper(I)/DTBP. Next, we focus to use inexpensive copper(0) metal as a catalyst which eventually oxidized to higher oxidation states *in situ*. Gratifyingly, metallic copper (mesh size 425 μ m) with DTBP furnished **2a** in 82% yield on heating at 110°C for 36 h along with the formation of deleterious product **2a'** (Entry 11, Table 1). We speculated that the addition of an external radical trapping agent might capture the methyl radical to sieve the formation of **2a'**. As hypothesized, the addition of 2.0 equiv of TEMPO suppressed the formation of **2a'** with an improved 83% yield of the desired lactone product **2a** (Entry 12, Table 1). Notably, reaction with commercial CuNPs (25nm particle size) also furnished the reaction in similar yields (Entry 10, Table 1) whereas reaction under argon or oxygen atmosphere did not improve the yield. As despite suppressing the side reaction, TEMPO did not improve the yield of **2a**, we used TEMPO only for few substrates which produced significant amount of the ester product. Inspite of having an acceptable synthetic condition in hand to produce 7-membered lactones, one of the major drawbacks of using super stoichiometric amount of peroxide remained an unsolved problem due to its explosive nature in the large-scale process development. Furthermore, formation of deleterious methyl ester **2a'** could be overcome if we succeed to eliminate DTBP. Intrigued by the captivating works on molecular oxygen by the Powers group (Maity et al., 2018a, 2018b), the Freakley group (Agarwal et al., 2017),

Table 1. Optimization of 7-membered lactone formation^{a,b}



Entry	Catalyst (20 mol%)	Oxidant	Solvent	Yield (%) 2a/2a'
1	CuI	DTBP (2.0 equiv)	DCE	52/25
2	CuI	DTBP (2.0 equiv)	PhCl	60/27
3	CuI	DTBP (2.0 equiv)	PhCF ₃	65/20
4	Cu(OAc) ₂	DTBP (2.0 equiv)	PhCF ₃	46/35
5	Cu(OTf) ₂	DTBP (2.0 equiv)	PhCF ₃	41/32
6	CuO	DTBP (2.0 equiv)	PhCF ₃	35/40
7	CuI	TBHP (2.0 equiv)	PhCF ₃	40/38
8	CuI	BPO (2.0 equiv)	PhCF ₃	20/0
9	CuI	TBPB (2.0 equiv)	PhCF ₃	38/20
10	CuNPs	DTBP (2.0 equiv)	PhCF ₃	80/18
11	Cu(0)	DTBP (2.0 eq)	PhCF ₃	82/12
12 ^c	Cu(0)	DTBP (2.0 equiv)	PhCF ₃	83/0
13 ^d	Cu(0)	DTBP (2.0 equiv)	PhCF ₃	69/0
14 ^e	Cu(0)	DTBP (2.0 equiv)	PhCF ₃	75/18
15 ^f	Cu(0)	DTBP (2.0 equiv)	PhCF ₃	56/27
16	Cu(0)	O ₂ (purged)	PhCF ₃	20/0
17 ^g	Cu(0)	O ₂ (purged)	PhCF ₃	20/0
18 ^h	Cu(0)	O ₂ (purged)	PhCF ₃	ND
19 ⁱ	Cu(0)	O ₂ (purged)	PhCF ₃	10/0
20 ^j	Cu(0)	O ₂ (purged)	PhCF ₃	Trace
21 ^k	Cu(0)	O ₂ (purged)	PhCF ₃	ND
22 ^l	Cu(0)	O ₂ (purged)	PhCF ₃	30/0
23 ^m	Cu(0)/EY	O ₂ (purged)	PhCF ₃	45/0
24 ^m	Cu(0)/RB	O ₂ (purged)	PhCF ₃	72/0
25 ^m	Cu(0)/Ru(bpy) ₃ Cl ₂	O ₂ (purged)	PhCF ₃	35/0
26 ^{l,m}	Cu(0)/RB	O ₂ (purged)	PhCF ₃	50/0

^aAll reactions were carried out in 0.2 mmol scale.

^bYields refer to here are overall isolated yields.

^cadditional amount of 2 equiv TEMPO.

^dadditional 2 equiv BHT.

^eunder Ar atmosphere.

^funder O₂ atmosphere.

^gadditional 30 mol% of Et₃N.

^hadditional 30 mol% of ethylenediamine.

ⁱadditional 30 mol% of pyridine.

^jadditional 30 mol% of Bpy.

^kadditional 30 mol% of terpyridine.

^ladditional 30 mol% of TMEDA was used.

^munder 32 W CFL.

and others (Sushkevich et al., 2017), we envisioned that the coupling of aerial oxygen as a terminal oxidant for this transformation would be synthetically sustainable and attractive. To investigate, a reaction of **1a** with catalytic copper powder under the oxygen atmosphere PhCF₃ afforded 20% of the desired product

(Entry 16, Table 1). The combination of an array of nitrogen-containing ligands did not improve the yield further (Entry 17–22, Table 1). Rueping and others have demonstrated the activation and utilization of molecular oxygen merging visible-light photoredox catalysis in metal-catalyzed C–H activations (Fabry and Rueping, 2016). In this line, we focused our attention to reoptimize the reaction condition under copper/photosensitizer dual catalytic condition. Simply purging the reaction vessel with oxygen and using 1 mol% Eosin Y (EY) furnished the desired product in 45% yield under white CFL (46 W) irradiation at 110°C (Entry 23, Table 1). Gratifyingly, the yield of the desired product was improved to 72% using 1 mol% Rose Bengal (RB) (Entry 24, Table 1) along with the unreacted substrate. Next, we proceeded to examine the substrate scope under this sustainable condition denoted as condition B and the corresponding yields are represented along with previous DTBP condition A.

Substrate scope

The requisite biaryl substrates bearing methyl and carboxylic acid at the 2,2'-position were prepared by Suzuki-Miyaura cross-coupling to examine the scope of this lactonization under these optimized conditions. Gratifyingly, a broad range of substrates underwent benzylic oxidation reaction to provide seven-membered lactones in moderate to good yields as shown in Scheme 2. Electron donating groups such as OMe, Me, OBn, and OEt on both rings A and B afforded moderate to good yields (2b–2g, 2m, 2q, 2r, 2v–2x, Scheme 2). Electron withdrawing groups such as NO₂, Cl, and F bearing substrates also provided moderate to a good yield of the product (2h–2l, 2n, 2p, 2s, 2z, 2aa, Scheme 2). Interestingly, besides methyl group, ethyl and aryl-substituted diarylmethanes also underwent seven-membered lactonization reaction chemo- and regioselectively (2l, 2o, 2t, 2y, 2aa, Scheme 2, Figure S2) which was a limitation in previous C–H activation methods (Dana et al., 2018; Zhang et al., 2015). Diarylmethanes (1t, 1y) provided better yields presumably due to activated benzylic C–H bond by two aryl groups. Notably, substrates bearing more than one methyl groups react at the *ortho* benzyl moiety leaving others intact (2b, 2e, 2i, 2k, 2m, 2n, 2q, 2w, Scheme 2). Hence, carboxylic acid might have a crucial role for intramolecular benzylic C–H activation to the formation of 7-membered lactone.

Attempt toward 8-membered lactone and serendipitous Smiles rearrangement

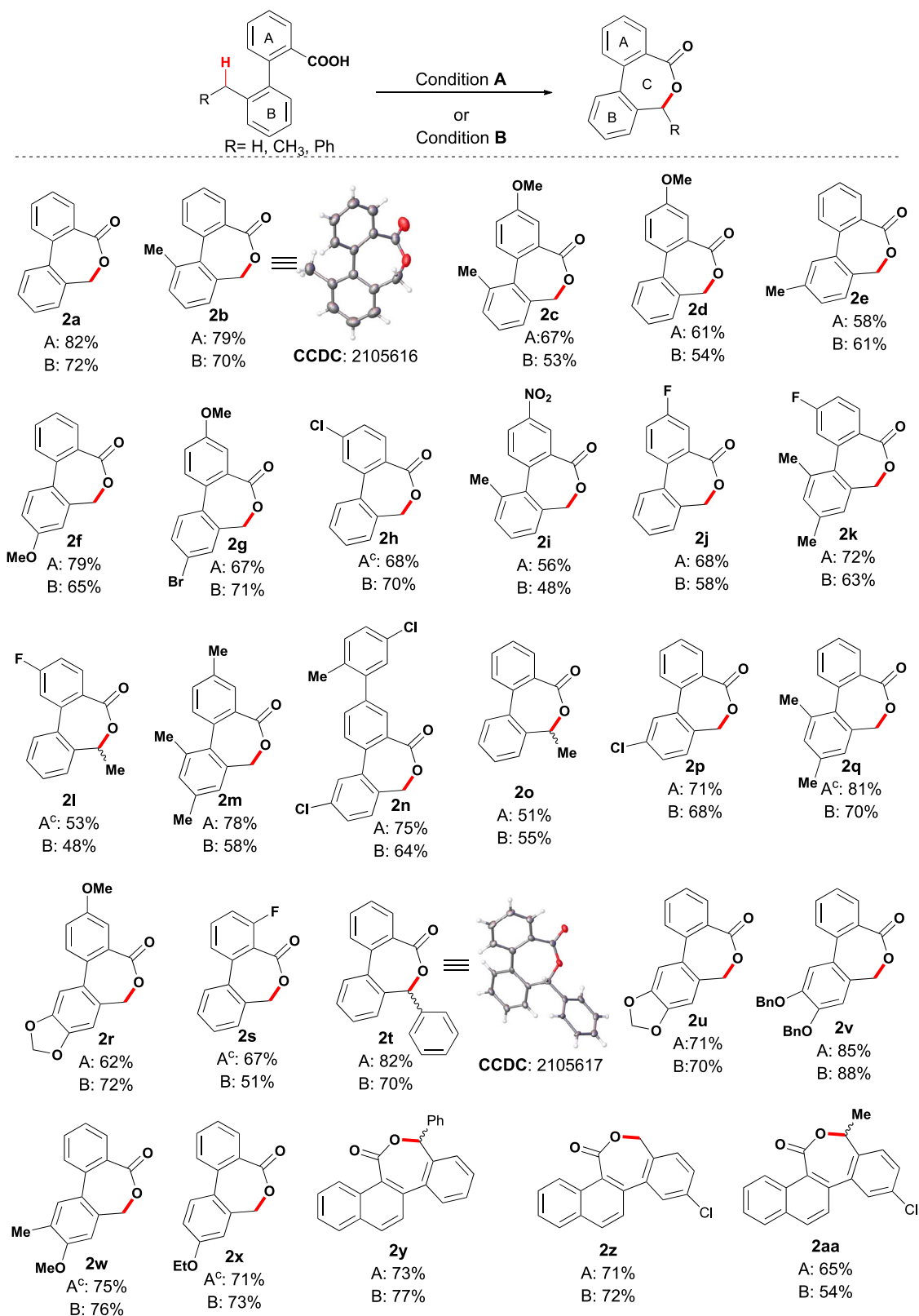
To examine the viability of the formation of 8-membered lactone, we prepared the corresponding diaryl ether 3a and subjected to the reaction condition A. Interestingly, instead of the expected product 4a', 2-hydroxyphenyl 2-methyl benzoate 4a was obtained in 62% yield through C–O bond cleavage and 1,5-aryl migration. The generation and involvement of carboxyl radical in this Smiles-type rearrangement has been reported by our group and others (Hossian and Jana, 2016; Wang et al., 2017). Subsequently, we examined the scope of 2-aryloxybenzoic acids with several substituents on both the phenol and aryl benzoic acid components, which provided moderate to good yields under the reaction condition (Scheme 3). The reaction was also reproduced in 0.5 mmol scale providing comparable yields which was a major limitation under our previous condition (4a, Scheme 3) (Hossian and Jana, 2016).

Double benzyl C–H activation en route to 7-membered lactone

We anticipated that the lactonization product can be obtained from 2,2'-alkyl biaryls by subtle tuning the reactivity between two alkyl moieties where one of them would be oxidized to the corresponding carboxylic acid. Therefore, 2,2'-dimethyl-1,1'-biphenyl (5a) was prepared and subjected to the reaction condition A. Gratifyingly, the desired 7-membered lactone 2a was obtained in 52% yield which is formed through 4-fold benzylic C–H bond cleavage. The yield was further improved to 65% on purging O₂. Besides unsubstituted benzyl, methyl- and phenyl-substituted substrates also furnished the desired product through the selective oxidation of methyl to carboxylic acid. Surprisingly, in case of unsymmetrical biaryls, the corresponding lactone products were obtained in moderate yields through the formation of carboxylic acid of CH₃, Cl, and OMe substituted-aryl methyls (Scheme 4). However, in case of 5d–f, an inseparable mixture presumably due to the lactonization from the other methyl group was observed resulting in lower isolated yields.

Synthetic utility: total synthesis of alterlactone

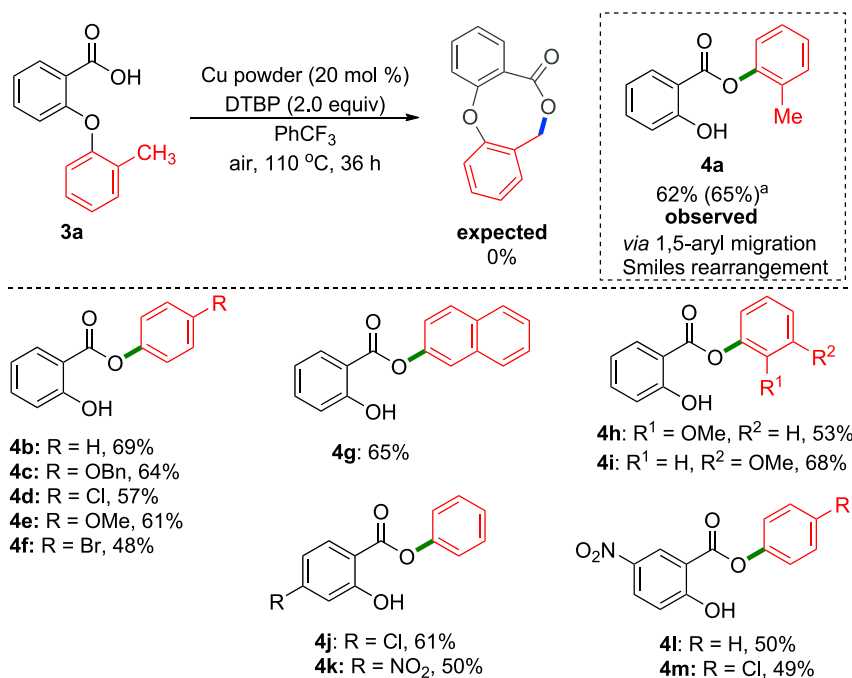
The synthetic utility of the present protocol was demonstrated through the total synthesis of a natural product alterlactone (Cudaj and Podlech, 2012) which was isolated from the extract of endophytic fungi *Alter-naria* sp. It is cytotoxic against L5178Y cells (Aly et al., 2008), neuroprotective, and Nrf2 activator in PC12



Scheme 2. Substrate scope of Dibenzo[c,e]oxepin-5(7H)-ones^{a,b}

Condition A: 20 mol% Cu, 2.0 equiv. DTBP, PhCF₃, 110 °C, air, 36–48 h. Condition B: 20 mol% Cu, 1 mol% Rose Bengal, PhCF₃, 110 °C, O₂, 32 W CFL, 36–48 h.

^aAll reactions were carried out in 0.2 mmol scale. ^bYields refer to the overall isolated yields. ^cAdditionally, 2.0 equiv TEMPO was used.



Scheme 3. Smiles rearrangement

20% Cu, 2 equiv DTBP, PhCF₃, 110 °C, air, 36 h. All reactions were carried out in 0.2 mmol scale. Yields refer to the overall isolated yields. ^ain 0.5 mmol scale.

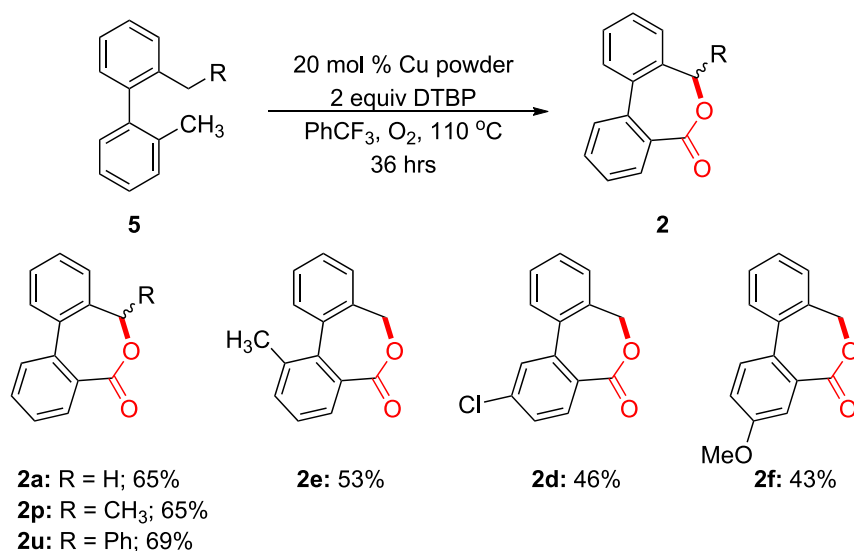
cells (Hou et al., 2021). We have successfully achieved the expected product alterlactone **18** in 10 steps starting from acetal-protected phloroglucinol acid and 3,4-hydroxytoluene (Scheme 5). In this total synthesis, we have applied our methodology at a late-stage under the dual catalytic condition which provided desired alterlactone after global deprotection of benzyl groups. This method is cost effective compared to the previous method (Cudaj and Podlech, 2012).

Practical demonstration and product derivatization

Furthermore, we hypothesized that the reaction might take place by itching the wall of copper vessel without any added copper catalyst. To our delight, the model substrate **2a** underwent the reaction smoothly under condition A in a 2.0 mmol scale furnishing 55% isolated yield of **3a** (Scheme 6A). Then, to check the scalability, model reaction was performed in 10 mmol scale under condition B. Gratifyingly, the reaction is reproducible furnishing 68% of the desired product **3a** (Scheme 6B). A thiolation reaction of dibenzo[*c,e*]oxepan-5-one **2a** with 0.5 equiv Lawesson's reagent afforded dibenzo[*c,e*]oxepan-5-thione **19** in 43% yield (Scheme 6C) which is an initiator for radical polymerization (Bingham and Roth, 2019). Finally, base hydrolysis of **2a** afforded the corresponding benzyl alcohol **20** in 92% yield (Scheme 6D).

Diverse reactivities with different substrates

To explore the suitability of the developed catalytic systems to differently designed substrates, a range of reactions were carried out (Schemes 7 and S1). Interestingly, in both the conditions, substrate **1ab**, which contains OH at the *para* and two CH₃ groups at two *ortho* positions of the second ring, underwent dearomatization to yield spiro lactone **24** instead of giving the eight-membered lactone. When indole **1af** was subjected to condition A, 6-membered lactone forms via C(sp²)-H activation and subsequent oxidation at C-3 position furnished dearomatized indole dione **25**. When benzyl alcohol substrate **26** was taken instead of benzoic acid, oxidation led to the formation of fluorenone **27** in lieu of the seven-membered lactone. Fascinatingly, the benzenesulfonamide **28** underwent the C(sp³)-H activation to yield the seven-membered lactam **29** under condition A. In our trial to expand the scope of eight-membered lactone formation (Chen et al., 2021), we took substrate **30**, which showed a different reactivity to afford five-membered lactone **31** selectively. Thus, a broad scope of diverse reactivities



Scheme 4. Lactonization through double benzylic C-H activation

Reaction condition: 20% Cu, 2 equiv DTBP, PhCF₃, 110 °C, O₂, 36 h. All reactions were carried out in 0.2 mmol scale. Yields refer to the overall isolated yields.

for the formation of seven- and five-membered lactonization via C–H could be opened up using this catalytic system.

Mechanistic study

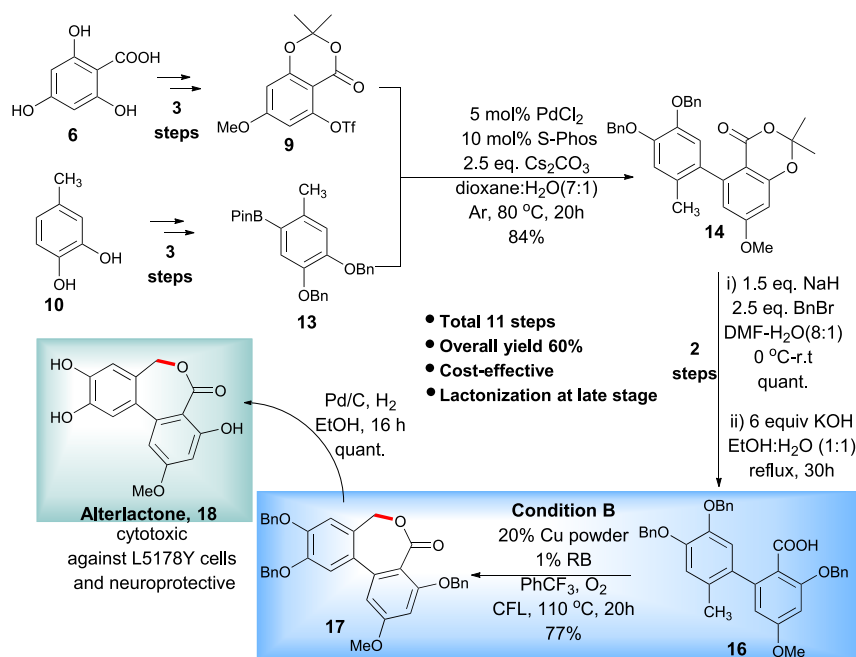
To elucidate the origin of high degree of chemoselectivity, we performed several control and spectroscopic experiments.

a) Radical quenching experiment

During optimization, we observed the formation of methyl ester **3a** by the methyl-radical which is formed through the decomposition of DTBP. This esterification was completely arrested by the addition of 2.0 equiv of TEMPO in the optimized reaction condition leading to the formation of a methyl radical adduct of TEMPO which was detected by the ESI-MS from an aliquot of reaction mixture (Scheme 8A(i)). After the complete suppression of 2.0 equiv methyl radical generated from 2.0 equiv DTBP, excess amount of TEMPO (e. g. 5.0 equiv) completely suppressed the formation of desired lactone **2a** and a TEMPO adduct with **1a** (M⁺–H) at benzylic or carboxylate (**22a** or **22a'**) position was detected in the ESI-MS (Schemes 8A(ii) and S10).

b) Competitive experiment between C(sp²)–H and C(sp³)–H activation

Interestingly, when **1a** was subjected to the Martin's reaction condition (Gallardo-Donaire and Martin, 2013), only the 6-membered lactone **23a** was obtained in 72% yield via C(sp²)–H activation selectively. On the other hand, in our optimized condition A and B, selectively 7-membered lactone **2a** was isolated in 82% and 72% yields, respectively (Scheme 8B). Besides energy difference (benzylic sp³ C–H vs sp² C–H bond; 85–90 vs 110–115 kcal/mol) (Blanksby and Ellison, 2003), the nature of oxidant cum radical initiator might have a crucial role for this chemoselectivity. From thorough control studies (Scheme S11), we observed that external oxidants capable of generating at least 1 equiv of methyl radicals e.g., DTBP, TBHP, and TBPB were effective. Hence, unlike the Martin's condition where BPO was effective oxidant for sp² C–H bond activation, was ineffective in our study. Presumably, the methyl radical generated through β-methyl scission of tert-butyl oxo radical might result in selective weak benzylic C–H bond cleavage and methane formation. Whereas, benzoyl radical or phenyl radical (via decarboxylation) generated *in situ* probably prefers sp² C–H bond activation. However, the origin of chemoselectivity in our developed peroxide-free condition B warrants further studies.



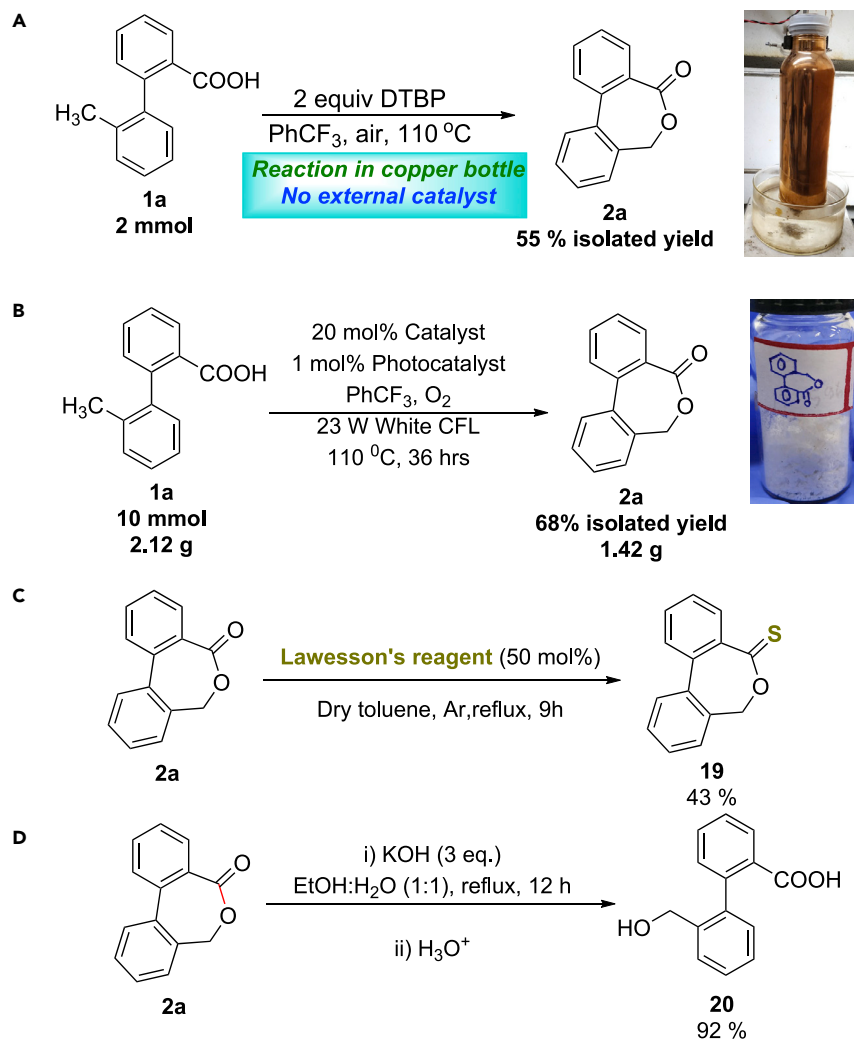
Scheme 5. Total synthesis of alterlactone

c) Addition of external substituted benzoic acids and ligands

To understand whether the reaction proceeds via inner- or outer-sphere copper complex, super stoichiometric (2.0 equiv) amount of benzoic acid was added to the reaction mixture under both conditions A and B. Surprisingly, no intermolecular benzoylation product was obtained except the desired lactonization products in moderate yields. Electron-rich 4-methoxy and electron-deficient 4-nitro benzoic acids also furnished similar results (Schemes 8C and S12). Furthermore, common external ligands such as pyridine, bipyridine, 1,10-phenanthroline, TMEDA etc. affected negatively in the reaction outcome (Scheme 8D) suggesting that copper might generate an inner sphere soluble complex binding with the substrate **1a** which was further supported by the spectroscopic studies.

d) UV and XPS studies of the reaction mixture

Because Cu(0) powder was used as an initial catalyst, we were intrigued to elucidate the formation of active catalyst and its oxidation state. Under the condition A (Figures 2A and S1) (Zhang et al., 2019), visually the insoluble Cu powder was converted to slightly suspended particles and showed light blue coloration after 6 h. Subsequently, it turned into an intense blue clear solution after 12 h indicating the formation of Cu(II) species. Finally, the solution turns into greenish color and turbid again. To check the presence of Cu(II) species unambiguously, UV-vis absorption spectra were recorded from the reaction mixture at 3 h interval. Notably, characteristic peak at 684 nm of Cu(II) appeared after 3 h with increasing intensity with the progress of the reaction (Figures 2B and S2) (Liang et al., 2020). No similar Cu(II) peak was observed in the absence of substrate and/or DTBP (Figures S3 and S4). It indicates that substrates may act as a ligand for the formation and stabilization of Cu(II) species. The UV-vis spectra from condition B also exhibited a similar spectral pattern indicating the formation of Cu(II) species to steer the reaction (Figures 2C and S5) where substrate was essential to stabilize the Cu(II) similarly (Figure S6). Notably, an intense peak of Cu(II) was observed just after 1 h using rose bengal/light (condition B) whereas a weak peak of the same appeared after 8 h without rose bengal/light (Figure S7). Hence, photoredox catalyst under light irradiation may accelerate the formation of active Cu(II) catalyst by molecular oxygen. However, the formation of Cu(III) species was not observed neither under condition A nor condition B. The oxidation state of the copper was further confirmed by XPS analysis. Under the condition B, the characteristic peaks at 931.0 and 950.9 eV are assigned to Cu 2p^{3/2} and 2p^{1/2} of Cu(II). An



Scheme 6. Practical demonstration and product derivatization

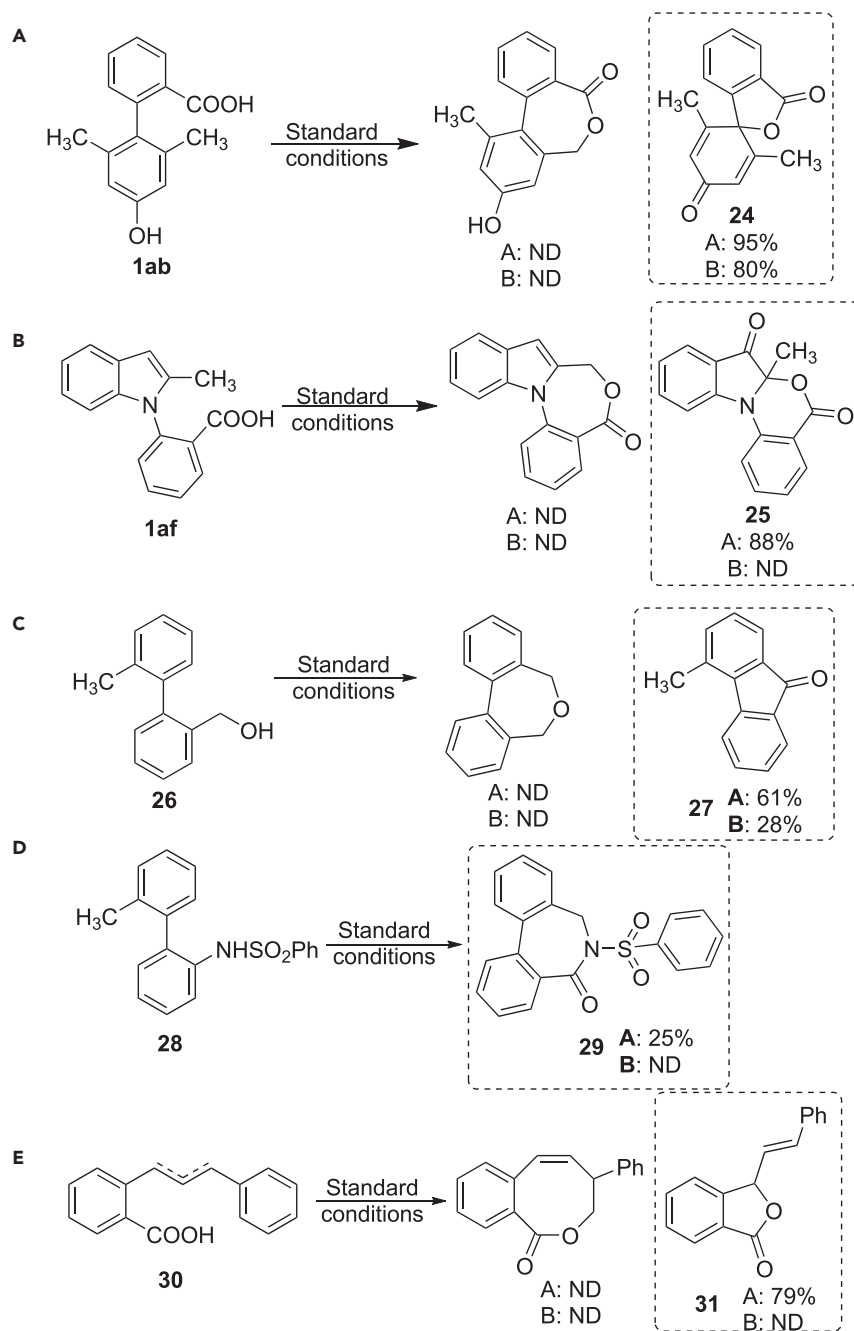
intense satellite peak at 942 eV confirms the presence of Cu(II) species in the reaction mixture (Figure 2D). (Maity et al., 2020) Similar peaks were also appeared in the condition A indicating the involvement of Cu(II) in this reaction (Figure S9).

e) Characterization of the recovered catalyst

Because an almost clear blue solution became turbid after the completion of the reaction (Figure S9), we assumed that copper (oxide or hydroxide) nanoparticles (CuNPs) might form. The transmission electron microscopic (TEM) image of both reaction mixtures indicated the formation of copper nanoparticles of 2–5 nm diameter (Figures 2E and S10). In fact, the reaction also took place using preformed nanoparticles (CuNPs), entry 10, Table 1. However, the size of the particles formed *in situ* from the copper powder may vary beyond the nanometer range.

Plausible mechanism

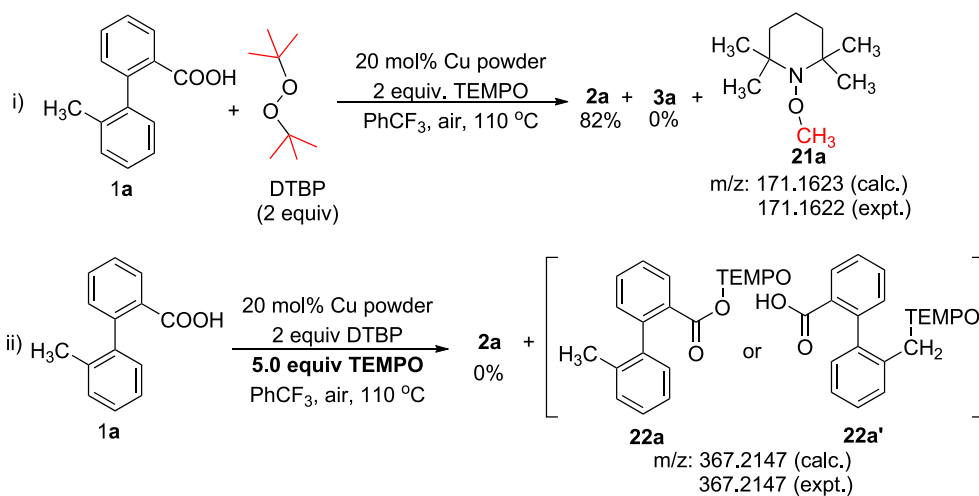
From the control and spectroscopic experiments, we envisioned the plausible mechanism as follows. Under condition A (Scheme 9), first DTBP undergoes homolytic cleavage followed by β -methyl scission to generate active methyl radical $\cdot\text{CH}_3$ and abstracts one proton from benzylic position of **1a** to emit CH_4 and corresponding benzylic radical species are formed. The evolution of CH_4 was

**Scheme 7. Diverse reactivities**

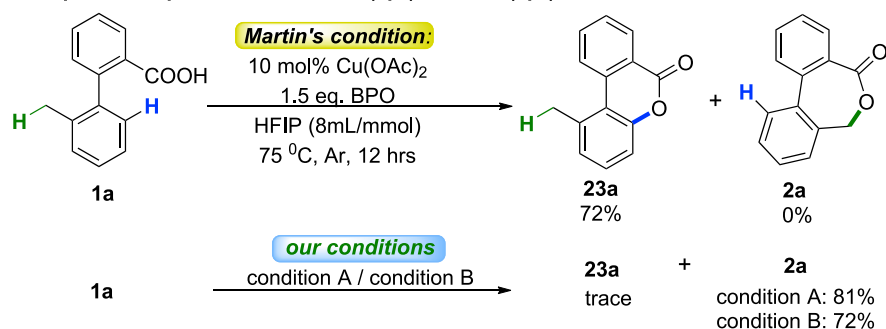
confirmed by gas chromatography of the sample taken from the reaction vessel (Figure S11). Subsequently, Cu(0) forms carboxylate to generate reactive intermediate I which readily gets stabilization by formation of 8-membered copper complex II. Thereafter, it undergoes reductive elimination to yield product 2a and regenerates Cu(0) which continues the reaction in forward direction. Besides, some amount of $\cdot\text{CH}_3$ is captured by the carboxyl group of the substrate to provide undesired 2a'.

Under condition B (Scheme 9), the benzylic C–H activation is believed to be performed by copper-peroxide radical formed from oxygen molecule via photosensitization. The RB is excited to RB* upon

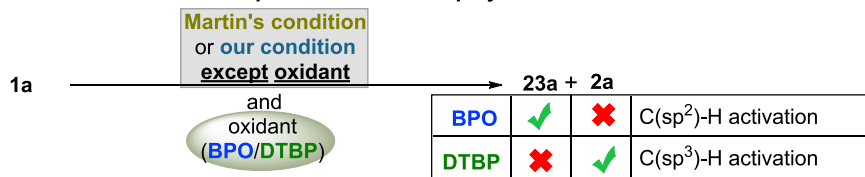
A TEMPO experiment



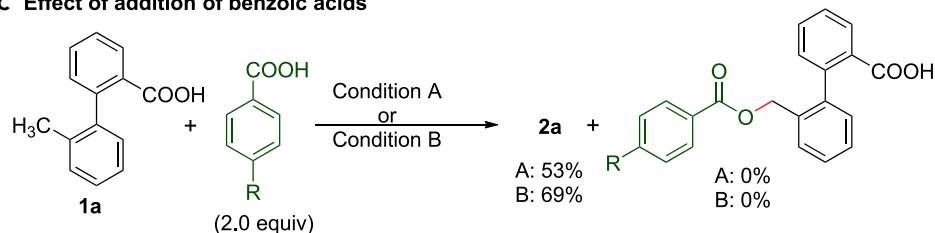
B Competitive experiment between C(sp²)-H and C(sp³)-H activation



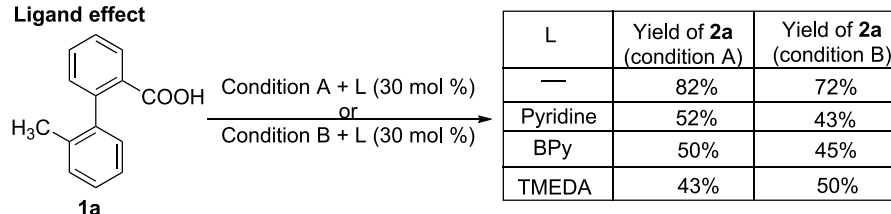
Result after series of control experiments: Oxidant plays the role



C Effect of addition of benzoic acids



D Ligand effect



Scheme 8. Control experiments

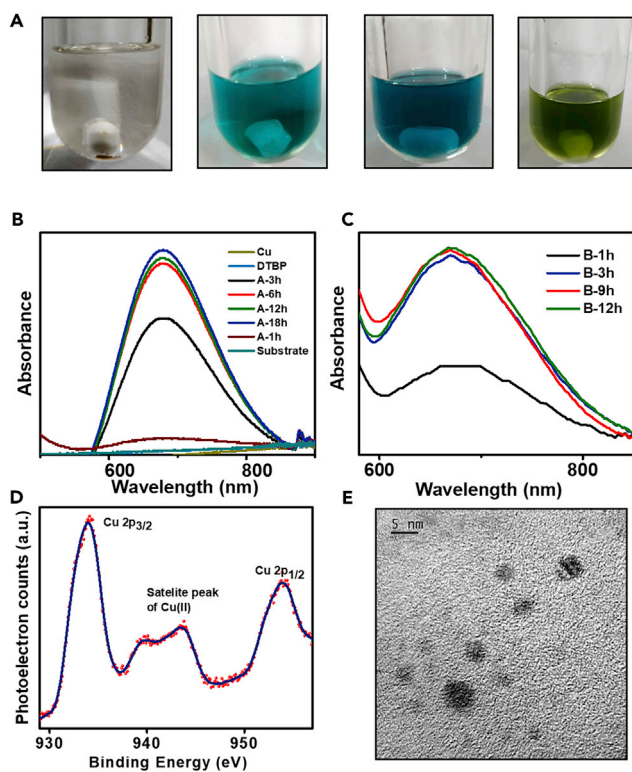
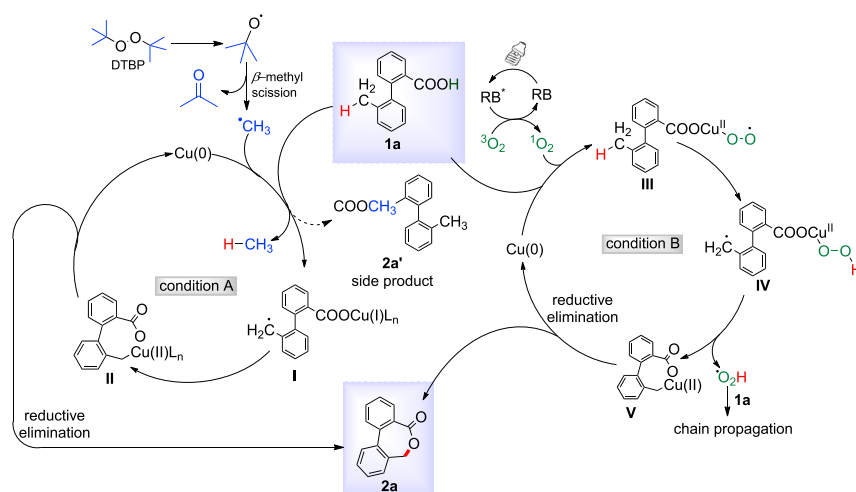


Figure 2. Mechanistic study

- (A) Digital photograph of *in situ* color change of standard reaction with condition A over time.
(B) UV-vis absorption spectra of standard reaction with condition A.
(C) *In situ* UV-vis absorption spectra of standard reaction with condition B.
(D) XPS analysis from condition B.
(E) TEM image of reaction mixture after 36 h from condition B.

irradiation of light and subsequently transfers energy to triplet oxygen ($^3\text{O}_2$) to produce singlet oxygen ($^1\text{O}_2$) (Wootton et al., 2002). Then, the Cu(0) scavenges the $^1\text{O}_2$ and reacts with carboxyl group (Hu et al., 2020b) of **1a** to generate copper(II)-peroxo intermediate (Davydov et al., 2022; Kunishita et al., 2008) **III** undergoing two simultaneous SET. Then, this copper-peroxo radical abstracts one proton from proximal benzylic position to produce benzylic radical intermediate **IV**. Subsequently, 8-membered Cu(II) complex **V** is formed while hydroperoxyl radical is released which may propagate the chain (Trammell et al., 2019) reacting with another molecule of **1a**. Complex **V** undergoes reductive elimination to furnish the final product **2a** and Cu(0) is regenerated. In either cases, copper-catalyzed initial oxidation of benzylic C–H bonds to benzyl alcohol followed by lactonization is plausible. However, neither by isolation nor via MS characterization, corresponding benzyl alcohol was identified from the reaction mixture. Furthermore, the corresponding benzyl alcohol **20**, which was obtained through hydrolysis of the lactonized product **2a**, converted back to lactone product **2a** in only 7% yield under our reaction condition (Scheme S13). Hence, initial benzylic oxidation to alcohol may not be a feasible pathway.

In the case of Scheme 4, one benzylic C(sp³)–H group of **5a** first oxidizes to the corresponding benzoic acid **2a** under the highly oxidative condition (Mohammadpour and Safaei, 2020; Sutradhar et al., 2017) and then follows the mechanism corresponding to the condition A to afford the product **2a** (Scheme S14). Notably, when there is one 2° and another 1° benzylic C(sp³)–H groups in the substrates (**5p**, **5u**), the 1° benzylic C–H (i.e. CH₃ group) first oxidizes to benzoic acid followed by the activation of 2° benzylic C–H activation and subsequent cyclization to achieve the products. And, when any substitution is present in either ring (**5d-f**), the controlling factor of sequence of oxidation and activation of the two benzylic C(sp³)–H groups demand further investigations.



Scheme 9. Plausible mechanism

Recyclability of the catalysts

Fortunately, a metallic precipitation was appeared after the completion of the reaction. Hence, we intended to recover and reuse the catalyst to enhance the practical utility (Pla and Gómez, 2016). After a batch reaction, the catalyst was recovered by simple filtration, washed with ethyl acetate, and subjected to the subsequent batch of reaction. Delightedly, 75% of our desired product **2a** was isolated in the second run. Similarly, a total of subsequent four batches of the same reaction were repeated without further addition of Cu catalyst furnishing 82%, 75%, 66%, and 48% yields, respectively (Figure 3). Similarly, the catalysts including rose bengal were also recycled and reused in the Cu/O₂ system (Condition B) as depicted in Figure 3. Washing the precipitate with organic solvents (Chen et al., 2006) or acetic acid (Argyle and Bartholomew, 2015) to further enhance the catalytic activity went in vain. Still, this is rare and exciting example where inexpensive copper powder is converted to the substrate-bound homogeneous catalyst for highly chemoselective benzylic oxidation and finally, precipitate out facilitating catalyst recovery.

Conclusion

We disclosed here an inexpensive copper powder-catalyzed chemoselective benzylic sp³ C–H activation for the direct synthesis of seven-membered dibenzo[*c,e*]oxepin-5(7H)-ones. Remarkably, hazardous oxidant di-*tert*-butyl peroxide (DTBP) was replaced by molecular oxygen merging with organic photosensitizer. Interestingly, a highly reactive, substrate-dependent soluble catalyst is formed from the copper powder during the reaction to achieve a high degree of chemoselective benzylic sp³ C–H oxidation suppressing the six-membered lactone formation via the sp² C–H bond activation. Finally, the heterogeneous catalyst is precipitated out and recovered for subsequent runs by simple filtration offering maximum benefits of homo- and heterogeneous catalyst. The reaction proceeds through a single electron transfer (SET)

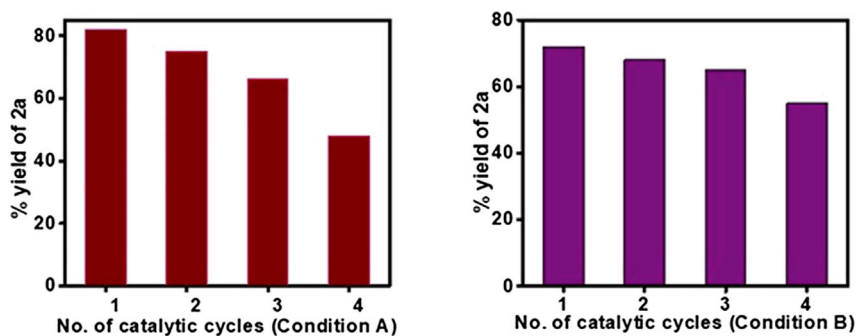


Figure 3. Recyclability of the catalysts

pathway, is scalable and applied to the total synthesis of cytotoxic natural product alterlactone. Further exploration of Cu(0)/photoredox/O₂ is undergoing in our laboratory.

Limitations of the study

Despite advantageous development of sustainable conditions for benzylic C(sp³)-H activation toward lactone formation, it is limited to 7-membered lactones. The substrate class **3** furnished Smiles rearrangement product via 1,5-aryl migration instead of 8-membered lactone formation. Aldehyde, primary amines were incompatible under the reaction conditions. Recovered catalyst was found to be inferior in catalytic efficiency after four runs, which could be a subject of further improvement.

STAR★METHODS

Detailed methods are provided in the online version of this paper and include the following:

- KEY RESOURCES TABLE
- RESOURCE AVAILABILITY
 - Lead contact
 - Materials availability
 - Data and code availability
- METHOD DETAILS
 - General reagent information
 - General analytical information
 - General procedure for preparation of starting materials 2'-alkyl-[1,1'-biphenyl]-2-carboxylic acids (1)
 - General experimental procedure for the preparation of 2-aryloxybenzoic acids (3)
 - Preparation of starting materials 2-alkyl-2'-methyl-1,1'-biphenyls (5)
 - Reaction profile of the standard reaction under condition A and B (Scheme 2)
 - General experimental procedure for the carboxyl radical assisted 1,5-aryl migration through Smiles rearrangement using 2-phenoxybenzoic acids, Scheme 4
 - General experimental procedures for copper-catalyzed chemo- and regioselective double C-H activation of 2-alkyl-2'-methyl-1,1'-biphenyls (5), Scheme 5
 - Experimental procedure for total synthesis of alterlactone (21)
 - Derivatization procedures
 - Practical demonstrations
 - Spectroscopic details

SUPPLEMENTAL INFORMATION

Supplemental information can be found online at <https://doi.org/10.1016/j.isci.2022.104341>.

ACKNOWLEDGMENTS

This work was supported by DST, SERB, Govt. of India Core Research Grant No. CRG/2021/006717. S.N. and S.M. thank DST and CSIR for their respective fellowships.

AUTHOR CONTRIBUTIONS

R.J. and S.N. envisioned and designed the project and wrote the manuscript. S.N. and S.M. conducted the methodology development, synthesis, and characterization of compounds. R.J. supervised the project overall.

DECLARATION OF INTERESTS

The authors declare no competing interests.

Received: January 20, 2022

Revised: April 9, 2022

Accepted: April 26, 2022

Published: May 20, 2022

REFERENCES

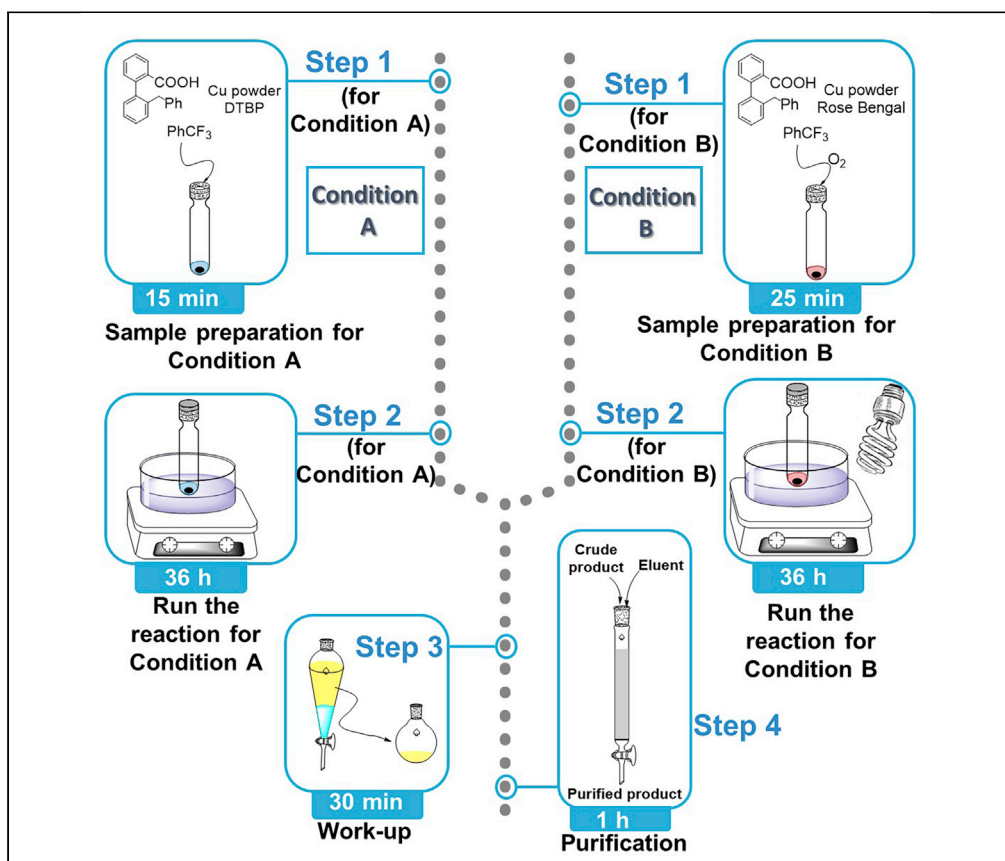
- Agarwal, N., Freakley, S.J., McVicker, R.U., Althabhan, S.M., Dimitratos, N., He, Q., Morgan, D.J., Jenkins, R.L., Willock, D.J., Taylor, S.H., et al. (2017). Aqueous Au-Pd colloids catalyze selective CH₄ oxidation to CH₃OH with O₂ under mild conditions. *Science* 358, 223–227. <https://doi.org/10.1126/science.aan6515>.
- Altemöller, M., Gehring, T., Cudaj, J., Podlech, J., Goesmann, H., Feldmann, C., and Rothenberger, A. (2009). Total synthesis of graphisfalcones A, C, D, and H, of ulocladol, and of the originally proposed and revised structures of graphisfalcones E and F. *Eur. J. Org. Chem.* 2009, 2130–2140. <https://doi.org/10.1002/ejoc.200801278>.
- Aly, A.H., Edrada-Ebel, R., Indriani, I.D., Wray, V., Müller, W.E.G., Totzke, F., Zirrgiebel, U., Schächtele, C., Kubbutat, M.H.G., Lin, W.H., and Proksch, P. (2008). Cytotoxic metabolites from the fungal endophyte *Alternaria* sp. and their subsequent detection in its host plant *Polygonum senegalense*. *J. Nat. Prod.* 71, 972–980. <https://doi.org/10.1021/np070447m>.
- Aneja, T., Neetha, M., Afsina, C.M.A., and Anilkumar, G. (2020). Progress and prospects in copper-catalyzed C–H functionalization. *RSC Adv.* 10, 34429–34458. <https://doi.org/10.1039/d0ra06518h>.
- Argyle, M.D., and Bartholomew, C.H. (2015). Heterogeneous catalyst deactivation and regeneration: a review. *Catalysts* 5, 145–269. <https://doi.org/10.3390/catal5010145>.
- Barzanò, G., Mao, R., Garreau, M., Waser, J., and Hu, X. (2020). Tandem photoredox and copper-catalyzed decarboxylative C(sp³)–N coupling of anilines and imines using an organic photocatalyst. *Org. Lett.* 22, 5412–5416. <https://doi.org/10.1021/acs.orglett.0c01769>.
- Bhunia, S.K., Das, P., Nandi, S., and Jana, R. (2019). Carboxylation of aryl triflates with CO₂ merging palladium and visible-light-photoredox catalysts. *Org. Lett.* 21, 4632–4637. <https://doi.org/10.1021/acs.orglett.9b01532>.
- Bingham, N.M., and Roth, P.J. (2019). Degradable vinyl copolymers through thiocarbonyl addition–ring-opening (TARO) polymerization. *Chem. Commun.* 55, 55–58. <https://doi.org/10.1039/c8cc08287a>.
- Blanksby, S.J., and Ellison, G.B. (2003). Bond dissociation energies of organic molecules. *Acc. Chem. Res.* 36, 255–263. <https://doi.org/10.1002/chin.200324299>.
- Carrillo-Arcos, U.A., Rojas-Ocampo, J., and Porcel, S. (2016). Oxidative cyclization of alkenoic acids promoted by AgOAc. *Dalton Trans.* 45, 479–483. <https://doi.org/10.1039/c5dt03808a>.
- Chen, C.-X., Xu, C.-H., Feng, L.-R., Qiu, F.-L., and Suo, J.-S. (2006). Deactivation and reactivation of copper-containing pentatomic hydroxalate in catalytic hydroxylation of phenol. *J. Mol. Catal. A. Chem.* 252, 171–175. <https://doi.org/10.1016/j.molcata.2006.01.065>.
- Chen, S., Mu, D., Mai, P.-L., Ke, J., Li, Y., and He, C. (2021). Enantioselective construction of six- and seven-membered triorgano-substituted silicon-stereogenic heterocycles. *Nat. Commun.* 12, 1249. <https://doi.org/10.1038/s41467-021-21489-6>.
- Chi, H., Li, H., Liu, B., Ye, R., Wang, H., Guo, Y.-L., Tan, Q., and Xu, B. (2019). From isocyanides to iminonitriles via silver-mediated sequential insertion of C(sp³)–H bond. *iScience* 21, 650–663. <https://doi.org/10.1016/j.isci.2019.10.057>.
- Cianfanelli, M., Olivo, G., Milan, M., Klein Gebbink, R.J.M., Ribas, X., Bietti, M., and Costas, M. (2020). Enantioselective C–H lactonization of unactivated methylenes directed by carboxylic acids. *J. Am. Chem. Soc.* 142, 1584–1593. <https://doi.org/10.1021/jacs.9b12239>.
- Colombel, V., Joncour, A., Thoret, S., Dubois, J., Bignon, J., Wdzieczak-Bakala, J., and Baudoin, O. (2010). Synthesis of antimicrotubule dibenzoxepines. *Tetrahedron Lett.* 51, 3127–3129. <https://doi.org/10.1016/j.tetlet.2010.04.039>.
- Copéret, C., Chabanas, M., Saint-Arroman, R.P., and Basset, J.-M. (2003). Homogeneous and heterogeneous catalysis: bridging the gap through surface organometallic chemistry. *Angew. Chem. Int. Ed.* 42, 156–181. <https://doi.org/10.1002/chin.200316246>.
- Cudaj, J., and Podlech, J. (2012). Total synthesis of altenuin and alterlactone. *Synlett* 23, 371–374. <https://doi.org/10.1055/s-0031-1290135>.
- Cui, X., Li, W., Ryabchuk, P., Junge, K., and Beller, M. (2018). Bridging homogeneous and heterogeneous catalysis by heterogeneous single-metal-site catalysts. *Nat. Catal.* 1, 385–397. <https://doi.org/10.1038/s41929-018-0090-9>.
- Curto, J.M., and Kozłowski, M.C. (2015). Chemoselective activation of sp³ vs sp² C–H bonds with Pd(II). *J. Am. Chem. Soc.* 137, 18–21. <https://doi.org/10.1021/ja5093166>.
- Dai, J.-J., Xu, W.-T., Wu, Y.-D., Zhang, W.-M., Gong, Y., He, X.-P., Zhang, X.-Q., and Xu, H.-J. (2015). Silver-catalyzed C(sp²)–H functionalization/C–O cyclization reaction at room temperature. *J. Org. Chem.* 80, 911–919. <https://doi.org/10.1021/jo5024238>.
- Dalton, T., Faber, T., and Glorius, F. (2021). C–H activation: toward sustainability and applications. *ACS Cent. Sci.* 7, 245–261. <https://doi.org/10.1021/acscentsci.0c01413>.
- Dana, S., Chowdhury, D., Mandal, A., Chipem, F.A.S., and Baidya, M. (2018). Ruthenium(II) catalysis/noncovalent interaction synergy for cross-dehydrogenative coupling of arene carboxylic acids. *ACS Catal.* 8, 10173–10179. <https://doi.org/10.1021/acscatal.8b03392>.
- Das, J., Dolui, P., Ali, W., Biswas, J.P., Chandrashekar, H.B., Prakash, G., and Maiti, D. (2020). A direct route to six and seven membered lactones via γ -C(sp³)–H activation: a simple protocol to build molecular complexity. *Chem. Sci.* 11, 9697–9702. <https://doi.org/10.1039/d0sc03144e>.
- Davydov, R., Herzog, A.E., Jodts, R.J., Karlin, K.D., and Hoffman, B.M. (2022). End-on copper(I) superoxo and Cu(II) peroxo and hydroperoxo complexes generated by cryoreduction/annealing and characterized by EPR/ENDOR spectroscopy. *J. Am. Chem. Soc.* 144, 377–389. <https://doi.org/10.1021/jacs.1c10252>.
- Fabry, D.C., and Rueping, M. (2016). Merging visible light photoredox catalysis with metal catalyzed C–H activations: on the role of oxygen and superoxide ions as oxidants. *Acc. Chem. Res.* 49, 1969–1979. <https://doi.org/10.1021/acs.accounts.6b00275>.
- Feng, J., Liang, S., Chen, S.-Y., Zhang, J., Fu, S.-S., and Yu, X.-Q. (2012). A metal-free oxidative esterification of the benzyl C–H bond. *Adv. Synth. Catal.* 354, 1287–1292. <https://doi.org/10.1002/adsc.201100920>.
- Fukuyama, T., Maetani, S., Miyagawa, K., and Ryu, I. (2014). Synthesis of fluorenones through rhodium-catalyzed intramolecular acylation of biarylcarboxylic acids. *Org. Lett.* 16, 3216–3219. <https://doi.org/10.1021/ol5012407>.
- Gallardo-Donaire, J., and Martin, R. (2013). Cu-Catalyzed Mild C(sp³)–H Functionalization Assisted by Carboxylic Acids en Route to Hydroxylated Arenes. *J. Am. Chem. Soc.* 135, 9350–9353. <https://doi.org/10.1021/ja4047894>.
- Gandeepan, P., Müller, T., Zell, D., Cera, G., Warratz, S., and Ackermann, L. (2019). 3d transition metals for C–H activation. *Chem. Rev.* 119, 2192–2452. <https://doi.org/10.1021/acs.chemrev.8b00507>.
- Guo, S., Yuan, Y., and Xiang, J. (2015a). Copper-catalyzed oxidative alkenylation of C(sp³)–H bonds via benzyl or alkyl radical addition to β -nitrostyrenes. *New J. Chem.* 39, 3093–3097. <https://doi.org/10.1039/c4nj02416h>.
- Guo, X.-X., Gu, D.-W., Wu, Z., and Zhang, W. (2015b). Copper-catalyzed C–H functionalization reactions: efficient synthesis of heterocycles. *Chem. Rev.* 115, 1622–1651. <https://doi.org/10.1021/cr500410y>.
- Höller, U., Wright, A.D., Mathee, G.F., König, G.M., Draeger, S., Aust, H.-J., and Schulz, B. (2000). Fungi from marine sponges: diversity, biological activity and secondary metabolites. *Mycol. Res.* 104, 1354–1365. <https://doi.org/10.1017/s0953756200003117>.
- Hong, G., Nahide, P.D., Kumar Neelam, U., Amadeo, P., Vijeta, A., Curto, J.M., Hendrick, C.E., VanGelder, K.F., and Kozłowski, M.C. (2019). Palladium-catalyzed chemoselective activation of sp³ vs sp² C–H bonds: oxidative coupling to form quaternary centers. *ACS Catal.* 9, 3716–3724. <https://doi.org/10.1021/acscatal.9b00091>.
- Hossian, A., and Jana, R. (2016). Carboxyl radical-assisted 1,5-aryl migration through Smiles rearrangement. *Org. Biomol. Chem.* 14, 9768–9779. <https://doi.org/10.1039/c6ob01758d>.
- Hou, Y., Li, J., Wu, J.-C., Wu, Q.-X., and Fang, J. (2021). Activation of cellular antioxidant defense system by naturally occurring dibenzopyrone derivatives confers neuroprotection against oxidative insults. *ACS Chem. Neurosci.* 12, 2798–2809. <https://doi.org/10.1021/acchemneuro.1c00023>.
- Hu, H., Chen, S.-J., Mandal, M., Pratik, S.M., Buss, J.A., Krška, S.W., Cramer, C.J., and Stahl, S.S. (2020a). Copper-catalyzed benzylic C–H coupling

- with alcohols via radical relay enabled by redox buffering. *Nat. Catal.* 3, 358–367. <https://doi.org/10.1038/s41929-020-0425-1>.
- Hu, X.-Q., Liu, Z.-K., Hou, Y.-X., and Gao, Y. (2020b). Single electron activation of aryl carboxylic acids. *iScience* 23, 101266. <https://doi.org/10.1016/j.isci.2020.101266>.
- Ju, L., Yao, J., Wu, Z., Liu, Z., and Zhang, Y. (2013). Palladium-catalyzed oxidative acetoxylation of benzylic C–H bond using bidentate auxiliary. *J. Org. Chem.* 78, 10821–10831. <https://doi.org/10.1021/jo401830k>.
- Khake, S.M., and Chatani, N. (2020). Nickel-catalyzed C–H functionalization using A non-directed strategy. *Chem* 6, 1056–1081. <https://doi.org/10.1016/j.chempr.2020.04.005>.
- Krätschmar, F., Kaßel, M., Delony, D., and Breder, A. (2015). Selenium-catalyzed C(sp³)–H acyloxylation: application in the expedient synthesis of isobenzofuranones. *Chem. Eur. J.* 21, 7030–7034. <https://doi.org/10.1002/chem.201406290>.
- Kunishita, A., Ishimaru, H., Nakashima, S., Ogura, T., and Itoh, S. (2008). Reactivity of mononuclear alkylperoxo copper(II) complex. O–O bond cleavage and C–H bond activation. *J. Am. Chem. Soc.* 130, 4244–4245. <https://doi.org/10.1021/ja800443s>.
- Lerchen, A., Knecht, T., Koy, M., Ernst, J.B., Bergander, K., Daniliuc, C.G., and Glorius, F. (2018). Non-directed cross-dehydrogenative (Hetero)arylation of allylic C(sp³)–H bonds enabled by C–H activation. *Angew. Chem. Int. Ed.* 57, 15248–15252. <https://doi.org/10.1002/anie.201807047>.
- Li, Y., Ding, Y.-J., Wang, J.-Y., Su, Y.-M., and Wang, X.-S. (2013). Pd-catalyzed C–H lactonization for expedient synthesis of biaryl lactones and total synthesis of cannabidiol. *Org. Lett.* 15, 2574–2577. <https://doi.org/10.1021/ol400877q>.
- Li, L., Yang, Q., Jia, Z., and Luo, S. (2018). Organocatalytic electrochemical C–H lactonization of aromatic carboxylic acids. *Synthesis* 50, 2924–2929. <https://doi.org/10.1055/s-0036-1591558>.
- Li, H., Subbotina, E., Bunrit, A., Wang, F., and Samec, J.S.M. (2019). Functionalized spiro lactones by photoinduced dearomatization of biaryl compounds. *Chem. Sci.* 10, 3681–3686. <https://doi.org/10.1039/c8sc05476b>.
- Liang, T., Zhao, H., Gong, L., Jiang, H., and Zhang, M. (2019). Synthesis of multisubstituted benzimidazolones via copper-catalyzed oxidative tandem C–H aminations and alkyl deconstructive carbonyl functionalization. *iScience* 15, 127–135. <https://doi.org/10.1016/j.isci.2019.04.019>.
- Liang, Q., Walsh, P.J., and Jia, T. (2020). Copper-catalyzed intermolecular difunctionalization of styrenes with thiosulfonates and arylboronic acids via a radical relay pathway. *ACS Catal.* 10, 2633–2639. <https://doi.org/10.1021/acscatal.9b04887>.
- Liu, L., and Corma, A. (2018). Metal catalysts for heterogeneous catalysis: from single atoms to nanoclusters and nanoparticles. *Chem. Rev.* 118, 4981–5079. <https://doi.org/10.1021/acs.chemrev.7b00776>.
- Liu, S., Achou, R., Boulanger, C., Pawar, G., Kumar, N., Lusseau, J., Robert, F., and Landais, Y. (2020). Copper-catalyzed oxidative benzylic C(sp³)–H amination: direct synthesis of benzylic carbamates. *Chem. Commun.* 56, 13013–13016. <https://doi.org/10.1039/d0cc05226d>.
- Lu, B., Zhu, F., Sun, H.-M., and Shen, Q. (2017). Esterification of the primary benzylic C–H bonds with carboxylic acids catalyzed by ionic iron(III) complexes containing an imidazolium cation. *Org. Lett.* 19, 1132–1135. <https://doi.org/10.1021/acs.orglett.7b00148>.
- Maity, A., Hyun, S.-M., and Powers, D.C. (2018a). Oxidase catalysis via aerobically generated hypervalent iodine intermediates. *Nat. Chem.* 10, 200–204. <https://doi.org/10.1038/nchem.2873>.
- Maity, A., Hyun, S.-M., Wortman, A.K., and Powers, D.C. (2018b). Oxidation catalysis by an aerobically generated dess–martin periodinane analogue. *Angew. Chem. Int. Ed.* 57, 7205–7209. <https://doi.org/10.1002/ange.201804159>.
- Maity, S., Bain, D., Chakraborty, S., Kolay, S., and Patra, A. (2020). Copper nanocluster (Cu₂₃ NC)-Based biomimetic system with peroxidase activity. *ACS Sustainable Chem. Eng.* 8, 18335–18344. <https://doi.org/10.1021/acssuschemeng.0c07431>.
- Meng, H., Xu, Z., Qu, Z., Huang, H., and Deng, G.-J. (2020). Copper(0)/PPh₃-Mediated bisheteroannulations of o-nitroalkynes with methylketoximes accessing pyrazo-fused pseudoindoxyls. *Org. Lett.* 22, 6117–6121. <https://doi.org/10.1021/acs.orglett.0c02180>.
- Miyagawa, M., and Akiyama, T. (2018). Tishchenko reaction using substoichiometric amount of metallic Zinc. *Chem. Lett.* 47, 78–81. <https://doi.org/10.1246/cl.170897>.
- Mohammadpour, P., and Safaei, E. (2020). Catalytic C–H aerobic and oxidant-induced oxidation of alkylbenzenes (including toluene derivatives) over VO₂⁺ immobilized on core–shell Fe₃O₄@SiO₂ at room temperature in water. *RSC Adv.* 10, 23543–23553. <https://doi.org/10.1039/d0ra03483e>.
- Omura, S., Fukuyama, T., Murakami, Y., Okamoto, H., and Ryu, I. (2009). Hydrooruthenation triggered catalytic conversion of dialdehydes and keto aldehydes to lactones. *Chem. Commun.* 6741–6743. <https://doi.org/10.1039/b912850f>.
- Pla, D., and Gómez, M. (2016). Metal and metal oxide nanoparticles: a lever for C–H functionalization. *ACS Catal.* 6, 3537–3552. <https://doi.org/10.1021/acscatal.6b00684>.
- Ramirez, N.P., Bosque, I., and Gonzalez-Gomez, J.C. (2015). Photocatalytic dehydrogenative lactonization of 2-arylbenzoic acids. *Org. Lett.* 17, 4550–4553. <https://doi.org/10.1021/acs.orglett.5b02269>.
- Rout, S.K., Guin, S., Ghara, K.K., Banerjee, A., and Patel, B.K. (2012). Copper catalyzed oxidative esterification of aldehydes with alkylbenzenes via cross dehydrogenative coupling. *Org. Lett.* 14, 3982–3985. <https://doi.org/10.1021/ol301756y>.
- Rout, S.K., Guin, S., Ali, W., Gogoi, A., and Patel, B.K. (2014). Copper-catalyzed esterification of alkylbenzenes with cyclic ethers and cycloalkanes via C(sp³)–H activation following cross-dehydrogenative coupling. *Org. Lett.* 16, 3086–3089. <https://doi.org/10.1021/ol5011906>.
- Sathyamoorthi, S., and Du Bois, J. (2016). Copper-catalyzed oxidative cyclization of carboxylic acids. *Org. Lett.* 18, 6308–6311. <https://doi.org/10.1021/acs.orglett.6b03176>.
- Shao, A., Zhan, J., Li, N., Chiang, C.-W., and Lei, A. (2018). External oxidant-free dehydrogenative lactonization of 2-arylbenzoic acids via visible-light photocatalysis. *J. Org. Chem.* 83, 3582–3589. <https://doi.org/10.1021/acs.joc.7b03195>.
- Shi, Y., Zhang, T., Jiang, X.-M., Xu, G., He, C., and Duan, C. (2020). Synergistic photoredox and copper catalysis by diode-like coordination polymer with twisted and polar copper–dye conjugation. *Nat. Commun.* 11, 5384. <https://doi.org/10.1038/s41467-020-19172-3>.
- Sushkevich, V.L., Palagin, D., Ranocchiaro, M., and van Bokhoven, J.A. (2017). Selective anaerobic oxidation of methane enables direct synthesis of methanol. *Science* 356, 523–527. <https://doi.org/10.1126/science.aam9035>.
- Sutradhar, M., Alegria, E.C.B.A., Roy Barman, T., Scorzellotti, F., Guedes da Silva, M.F.C., and Pombeiro, A.J.L. (2017). Microwave-assisted peroxidative oxidation of toluene and 1-phenylethanol with monomeric keto and polymeric enol aroylhydrazone Cu(II) complexes. *Mol. Catal.* 439, 224–232. <https://doi.org/10.1016/j.mcat.2017.07.006>.
- Tang, P.-T., Shao, Y.-X., Wang, L.-N., Wei, Y., Li, M., Zhang, N.-J., Luo, X.-P., Ke, Z., Liu, Y.-J., and Zeng, M.-H. (2020a). Synthesis of seven-membered lactones by regioselective and stereoselective iodolactonization of electron-deficient olefins. *Chem. Commun.* 56, 6680–6683. <https://doi.org/10.1039/c9cc10080f>.
- Tang, Y., Meador, R.I.L., Malinchak, C.T., Harrison, E.E., McCaskey, K.A., Hempel, M.C., and Funk, T.W. (2020b). (Cyclopentadienone) iron-catalyzed transfer dehydrogenation of symmetrical and unsymmetrical diols to lactones. *J. Org. Chem.* 85, 1823–1834. <https://doi.org/10.1021/acs.joc.9b01884>.
- Tanwar, L., Börgel, J., and Ritter, T. (2019). Synthesis of benzylic alcohols by C–H oxidation. *J. Am. Chem. Soc.* 141, 17983–17988. <https://doi.org/10.1021/jacs.9b09496>.
- Tao, C., Wang, B., Sun, L., Liu, Z., Zhai, Y., Zhang, X., and Wang, J. (2017). Merging visible-light photoredox and copper catalysis in catalytic aerobic oxidation of amines to nitriles. *Org. Biomol. Chem.* 15, 328–332. <https://doi.org/10.1039/c6ob02510b>.
- Tao, X.-Z., Dai, J.-J., Zhou, J., Xu, J., and Xu, H.-J. (2018). Electrochemical C–O bond formation: facile access to aromatic lactones. *Chem. Eur. J.* 24, 6932–6935. <https://doi.org/10.1002/chem.201801108>.
- Trammell, R., Rajabimoghadam, K., and Garcia-Bosch, I. (2019). Copper-Promoted functionalization of organic molecules: from biologically relevant Cu/O₂ model systems to organometallic transformations. *Chem. Rev.* 119, 2954–3031. <https://doi.org/10.1021/acs.chemrev.8b00368>.

- Tran, B.L., Driess, M., and Hartwig, J.F. (2014). Copper-catalyzed oxidative dehydrogenative carboxylation of unactivated alkanes to allylic esters via alkenes. *J. Am. Chem. Soc.* *136*, 17292–17301. <https://doi.org/10.1021/ja510093x>.
- Van Velthoven, N., Wang, Y., Van Hees, H., Henrion, M., Bugaev, A.L., Gracy, G., Amro, K., Soldatov, A.V., Alauzun, J.G., Mutin, P.H., and De Vos, D.E. (2020). Heterogeneous single-site catalysts for C–H activation reactions: Pd(II)-Loaded S,O-functionalized metal oxide-bisphosphonates. *ACS Appl. Mater. Inter.* *12*, 47457–47466. <https://doi.org/10.1021/acscami.0c12325>.
- Vasilopoulos, A., Zultanski, S.L., and Stahl, S.S. (2017). Feedstocks to pharmacophores: Cu-catalyzed oxidative arylation of inexpensive alkylarenes enabling direct access to diarylalkanes. *J. Am. Chem. Soc.* *139*, 7705–7708. <https://doi.org/10.1021/jacs.7b03387>.
- Wang, X., Gallardo-Donaire, J., and Martin, R. (2014). Mild ArI-catalyzed C(sp²)-H or C(sp³)-H functionalization/C–O formation: an intriguing catalyst-controlled selectivity switch. *Angew. Chem. Int. Ed.* *53*, 11084–11087. <https://doi.org/10.1002/ange.201407011>.
- Wang, S.-F., Cao, X.-P., and Li, Y. (2017). Efficient aryl migration from an aryl ether to a carboxylic acid group to form an ester by visible-light photoredox catalysis. *Angew. Chem. Int. Ed.* *56*, 13809–13813. <https://doi.org/10.1002/ange.201706597>.
- Wang, C.-Y., Qin, Z.-Y., Huang, Y.-L., Jin, R.-X., Lan, Q., and Wang, X.-S. (2019). Enantioselective copper-catalyzed cyanation of remote C(sp³)-H bonds enabled by 1,5-hydrogen atom transfer. *iScience* *21*, 490–498. <https://doi.org/10.1016/j.isci.2019.10.048>.
- Wootton, R.C.R., Fortt, R., and de Mello, A.J. (2002). A microfabricated nanoreactor for safe, continuous generation and use of singlet oxygen. *Org. Proc. Res. Dev.* *6*, 187–189. <https://doi.org/10.1021/op0155155>.
- Wu, G., Guo, H.-F., Gao, K., Liu, Y.-N., Bastow, K.F., Morris-Natschke, S.L., Lee, K.-H., and Xie, L. (2008). Synthesis of unsymmetrical biphenyls as potent cytotoxic agents. *Bioorg. Med. Chem. Lett.* *18*, 5272–5276. <https://doi.org/10.1016/j.bmcl.2008.08.050>.
- Xia, Q., Liu, X., Zhang, Y., Chen, C., and Chen, W. (2013). Copper-catalyzed N-methylation of amides and O-methylation of carboxylic acids by using peroxides as the methylating reagents. *Org. Lett.* *15*, 3326–3329. <https://doi.org/10.1021/ol401362k>.
- Yang, Q., Jia, Z., Li, L., Zhang, L., and Luo, S. (2018). Visible-light promoted arene C–H/C–X lactonization via carboxylic radical aromatic substitution. *Org. Chem. Front.* *5*, 237–241. <https://doi.org/10.1039/c7qo00826k>.
- Yi, H., Zhang, G., Wang, H., Huang, Z., Wang, J., Singh, A.K., and Lei, A. (2017). Recent advances in radical C–H activation/radical cross-coupling. *Chem. Rev.* *117*, 9016–9085. <https://doi.org/10.1021/acs.chemrev.6b00620>.
- Zhang, X.-S., Zhang, Y.-F., Li, Z.-W., Luo, F.-X., and Shi, Z.-J. (2015). Synthesis of Dibenzo[*c,e*]oxepin-5(7H)-ones from Benzyl Thioethers and Carboxylic Acids: rhodium-Catalyzed Double C–H Activation Controlled by Different Directing Groups. *Angew. Chem. Int. Ed.* *54*, 5478–5482. <https://doi.org/10.1002/ange.201500486>.
- Zhang, M., Ruzi, R., Li, N., Xie, J., and Zhu, C. (2018a). Photoredox and cobalt Co-catalyzed C(sp²)-H functionalization/C–O bond formation for synthesis of lactones under oxidant- and acceptor-free conditions. *Org. Chem. Front.* *5*, 749–752. <https://doi.org/10.1039/c7qo00795g>.
- Zhang, S., Li, L., Wang, H., Li, Q., Liu, W., Xu, K., and Zeng, C. (2018b). Scalable electrochemical dehydrogenative lactonization of C(sp²/sp³)-H bonds. *Org. Lett.* *20*, 252–255. <https://doi.org/10.1021/acs.orglett.7b03617>.
- Zhang, G., Fu, L., Chen, P., Zou, J., and Liu, G. (2019). Proton-coupled electron transfer enables tandem radical relay for asymmetric copper-catalyzed phosphinoylcyanation of styrenes. *Org. Lett.* *21*, 5015–5020. <https://doi.org/10.1021/acs.orglett.9b01607>.
- Zheng, Y.-W., Narobe, R., Donabauer, K., Yakubov, S., and König, B. (2020). Copper(II)-Photocatalyzed N–H alkylation with alkanes. *ACS Catal.* *10*, 8582–8589. <https://doi.org/10.1021/acscatal.0c01924>.
- Zhuang, Z., and Yu, J.-Q. (2020). Lactonization as a general route to β-C(sp³)-H functionalization. *Nature* *577*, 656–659. <https://doi.org/10.1038/s41586-019-1859-y>.

Protocol

Protocol for chemo- and regioselective C(sp³)-H activation using a heterogeneous copper powder-catalyzed reaction



Here, we present a protocol for the synthesis of dibenzo[c,e]oxepin-5(7H)-ones starting from 2'-alkyl-[1,1'-biphenyl]-2-carboxylic acids. This technique uses two copper(0)-catalyzed benzylic C(sp³)-H activation strategies taking either *di*-tertbutyl peroxide or gaseous oxygen as an oxidant. We detail a photocatalytic thermal approach for copper powder-catalyzed reaction with oxygen. We also describe a procedure for catalyst recycling in both the strategies. The product has been successfully synthesized both in mmol and gram scale.

Publisher's note: Undertaking any experimental protocol requires adherence to local institutional guidelines for laboratory safety and ethics.

Shantanu Nandi,
Shuvam Mondal,
Ranjan Jana

shantanunandi.ju@gmail.com (S.N.)
rjana@iicb.res.in (R.J.)

Highlights

Chemo- and regioselective benzylic C(sp³)-H activation

Copper powder is used as recyclable catalyst, no copper salt required

Sustainable copper/rose bengal dual catalysis replacing peroxide with oxygen

Synthesis of dibenzooxepinones: seven-membered biaryl lactones

Nandi et al., STAR Protocols 3, 101781
December 16, 2022 © 2022
The Author(s).
<https://doi.org/10.1016/j.xpro.2022.101781>



Protocol

Protocol for chemo- and regioselective C(sp³)-H activation using a heterogeneous copper powder-catalyzed reactionShantanu Nandi,^{1,2,*} Shuvam Mondal,¹ and Ranjan Jana^{1,3,*}¹Organic and Medicinal Chemistry Division, CSIR-Indian Institute of Chemical Biology, 4 Raja S.C. Mullick Road, Jadavpur, Kolkata, West Bengal 700032, India²Technical contact³Lead contact*Correspondence: shantanunandi.ju@gmail.com (S.N.), rjana@iicb.res.in (R.J.)
<https://doi.org/10.1016/j.xpro.2022.101781>

SUMMARY

Here, we present a protocol for the synthesis of dibenzo[c,e]oxepin-5(7H)-ones starting from 2'-alkyl-[1,1'-biphenyl]-2-carboxylic acids. This technique uses two copper(0)-catalyzed benzylic C(sp³)-H activation strategies taking either *di*-tert-butyl peroxide or gaseous oxygen as an oxidant. We detail a photocatalytic thermal approach for copper powder-catalyzed reaction with oxygen. We also describe a procedure for catalyst recycling in both the strategies. The product has been successfully synthesized both in mmol and gram scale.

For complete details on the use and execution of this protocol, please refer to Nandi et al. (2022).

BEFORE YOU BEGIN

In the last two decades, huge development has been realized in the C-H activation field to ease the direct functionalization of C-H bond avoiding the pre-functionalization step (Crabtree and Lei, 2017; Rogge et al., 2021; Yi et al., 2017). Despite the progress, achieving high chemo-, regio- or stereoselectivity still remains as a tough task in absence of directing groups (Dalton et al., 2021; Lerchen et al., 2018). Thus, for the non-directed C(sp³)-H bond activation, choosing weaker C(sp³)-H bonds (e.g., benzyl, allyl etc.) over unbiased strong alkyl C(sp³)-H bonds have been more fruitful (Feng et al., 2012; Golden et al., 2022; Liu et al., 2013, 2020; Lu et al., 2017; Manna et al., 2020; Nandi and Jana, 2022; Rout et al., 2014; Suh et al., 2020; Vasilopoulos et al., 2017).

Including the aforementioned literatures, plenty of the prior intra-/intermolecular benzylic-C(sp³)-H /C(sp²)-H activation strategies have been developed with copper catalysis (Begam et al., 2022; Guo et al., 2015b; Hu et al., 2020; Liang et al., 2020; Tran et al., 2014; Zhang et al., 2017). The Bois group achieved five- and six-membered lactones through Cu(II) catalyzed intramolecular C(sp³)-H acyloxylolation (Sathyamoorthi and Du Bois, 2016). Besides, following Martin (Gallardo-Donaire and Martin, 2013), other groups (Bhunia et al., 2019; Li et al., 2013, 2018; Ramirez et al., 2015; Shao et al., 2018; Tao et al., 2018) accessed six-membered lactones via intramolecular C(sp²)-H activation of ortho-aryl benzoic acids using metal/metal-free conditions. Though use of bulk copper is worth aspiring (Guo et al., 2015a; Meng et al., 2020) for its low cost and easier handling, different copper salts have been used in most of the cases.

Inspired from these precedents, we hypothesized to synthesize dibenzo[c,e]oxepin-5(7H)-ones from 2'-alkyl-[1,1'-biphenyl]-2-carboxylic acids via C(sp³)-H activation. Dibenzooxepinones, consisting of seven-membered lactone rings are quite prevalent in various natural products, bio-active



Table 1. Preparation of "vessel A" solution

Chemical	Final concentration	Amount
2'-benzyl-[1,1'-biphenyl]-2-carboxylic acid (stored at room temperature)	0.06 M	42.4 mg
Copper powder (stored at room temperature)	0.02 M	2.5 mg
DTBP (stored at 4°C)	0.13 M	74 μ L
α,α,α -Trifluorotoluene	N/A	3 mL

compounds (Altemöller et al., 2009; Aly et al., 2008; Colombel et al., 2010). Recently, we have successfully realized the hypothesis taking copper(0) powder as the catalyst in two related yet distinct methodologies (Nandi et al., 2022), either using di-tertbutyl peroxide (DTBP) as oxidant or by efficiently replacing hazardous DTBP with molecular oxygen (O_2) taking additional help of photocatalysis. For both the strategies, the catalyst is easily recovered by filtration and recycled. Contrary to the previously available reports for synthesizing dibenzooxepinones, (Zhang et al., 2015), we have been able to execute it in fewer steps avoiding the pre-activation of substrate using low-cost copper as catalyst.

Therefore, the current protocol describes the stepwise synthesis of 7-phenyldibenzo[c,e]oxepin-5(7H)-one starting from 2'-benzyl-[1,1'-biphenyl]-2-carboxylic acid utilizing two distinct methodologies, both catalyzed by easily available copper(0) powder. For complete use of this protocol, please refer to (Nandi et al., 2022).

Preparation of the reagents and setting up the equipment

A complete list of reagents and equipment can be found in the "key resources table" and "materials and equipment".

Preparation of reaction vessel for "condition A"

⌚ Timing: 15 min

In this step, reaction vessel for Condition A is get ready. One pressure tube with Teflon cap labeled as "vessel A" containing solution of 2'-benzyl-[1,1'-biphenyl]-2-carboxylic acid, copper powder and di-tert butyl peroxide (DTBP) in α,α,α -Trifluorotoluene.

Note: Reaction vessel needs to be prepared fresh every time.

1. Preparation of "vessel A" (Table 1).
 - a. In one 15 mL pressure tube with Teflon cap, place one magnetic stir-bar.
 - b. Weigh out 42.4 mg (0.2 mmol) of 2'-benzyl-[1,1'-biphenyl]-2-carboxylic acid to the pressure tube.
 - c. Add 2.5 mg of Cu powder (0.04 mmol).
 - d. Add 3 mL of α,α,α -Trifluorotoluene to the pressure tube with a syringe.
 - e. Add 74 μ L (0.4 mmol) of DTBP with a microsyringe.

⚠ CRITICAL: DTBP is potentially explosive in nature. It should be handled with care. However, no such incident took place in our laboratory. Add DTBP at ambient condition in the fume hood promptly. And do not leave the reagent container opened in the air. Unfailingly, assure to close the container soon after taking the reagent.

- f. Seal the tube.

⚠ CRITICAL: All the reactants need to be efficiently put into the vessel so that any of the particle do not adhere to the mouth or inner wall of the pressure tube.

Table 2. Preparation of “vessel B” solution

Chemical	Final concentration	Amount
2'-benzyl-[1,1'-biphenyl]-2-carboxylic acid (stored at room temperature)	0.06 M	42.4 mg
Copper powder (stored at room temperature)	0.02 M	2.5 mg
rose bengal (RB) (stored at room temperature)	0.001 M	2.0 mg
α,α,α -Trifluorotoluene	N/A	3 mL

Preparation of reaction vessel for “condition B”

⌚ Timing: 25 min

In this step, reaction vessel for Condition B is arranged. One Teflon bushing pressure tube labeled as “vessel B” containing solution of 2'-benzyl-[1,1'-biphenyl]-2-carboxylic acid, copper powder, rose bengal (RB) in α,α,α -Trifluorotoluene is prepared.

Note: Reaction vessel needs to be prepared fresh every time.

2. Preparation of “vessel B” (Table 2).
 - a. In one 15 mL pressure tube with Teflon cap, place one magnetic stir-bar.
 - b. Weigh out 42.4 mg (0.2 mmol) of 2'-benzyl-[1,1'-biphenyl]-2-carboxylic acid to the pressure vessel.
 - c. Add 2.5 mg of Cu powder (0.04 mmol).
 - d. Add 2.0 mg of RB (0.002 mmol).
 - e. Add to the pressure tube 3 mL of α,α,α -Trifluorotoluene with a syringe.
 - f. Purge the tube with ultra-high purity (UHP) grade O₂ gas for one minute and readily seal with the cap.

⚠ **CRITICAL:** All the reactants need to be efficiently put into the vessel so that any of the particle do not remain stucked to the mouth or inner wall of the pressure tube.

Instrumental set-up for “condition A” (set-up A)

⌚ Timing: 30 min

Here, beside setting up the heater cum stirrer and clamp to perform the reaction under optimal conditions, some key parameters such as temperature, rotation speed are also set. And this would be denoted as “set-up A”.

3. Set-up the heater cum stirrer.
 - a. Equip the IKA stirrer (IKA WORKS INC. 3581201 C-MAG HS 7 IKAMAG Hot Plate Magnetic Stirrer, Glass Ceramics Heating Plate, 115 V in a fume hood (Figure 1A).
 - b. Take one dry and clean borosilicate glass flat-bottom bowl (1 L) for making the oil bath.
 - c. Fill the bowl with silicone oil.
 - d. Place the oil filled bowl on the magnetic stirrer.
 - e. Set one clamp on the stirrer so that the “vessel A” can be set.
 - f. Hang and dip one thermometer to the oil, vertically. Troubleshooting 2.
4. Digital screen interface of the stirrer.
 - a. Turn on the stirrer.
 - b. Set the temperature so that the oil bath temperature reaches to 110°C. (In our case, setting digital reading of 145 was sufficient) (Figure 1C, yellow box).
 - c. Set the rotation regulator at in between 1 and 2 (500 rpm) (Figure 1C, red box).

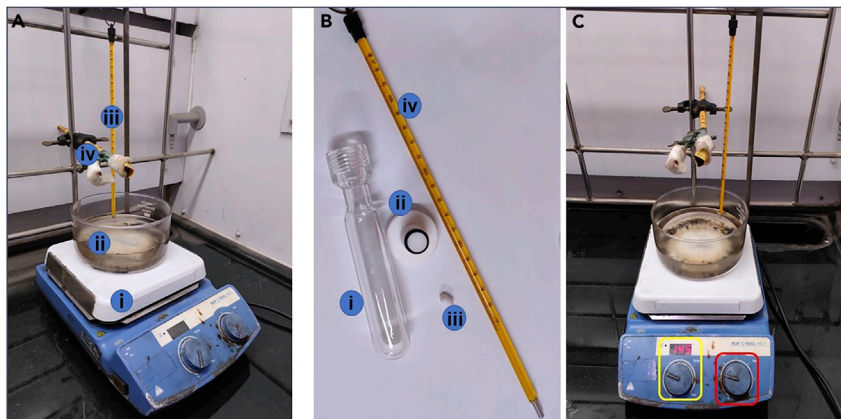


Figure 1. Overview of the "reaction set-up A"

(A) Instrumental set-up: (i) IKA hot plate magnetic stirrer, (ii) oil bath, (iii) clamp, (iv) hanging thermometer dipped in oil.

(B) Zoom in on the required accessories: (i) 15 mL pressure-tube, (ii) Teflon cap of the pressure tube, (iii) magnet bar, (iv) thermometer.

(C) The instrumental "set-up A". Yellow box: temperature interface. Red box: rotation regulator.

Instrumental set-up for "condition B" (set-up B)

⌚ Timing: 30 min

In this step, just like the previous one, beside setting up the magnetic stirrer and clamp to perform the reaction under optimal conditions, some key parameters such as temperature, rotation speed are also set. And this would be denoted as "set-up B".

5. Set-up the heater cum stirrer.

- Equip the IKA stirrer (IKA WORKS INC. 3581201 C-MAG HS 7 IKAMAG Hot Plate Magnetic Stirrer, Glass Ceramics Heating Plate, 115 V) in a fume hood (Figure 2A).
- Place an oil bath on the stirrer, similar to "set-up A".
- Set one clamp on the stirrer so that the "vessel A" can be set.
- Hang and dip one thermometer to the oil, vertically. [Troubleshooting 2](#).

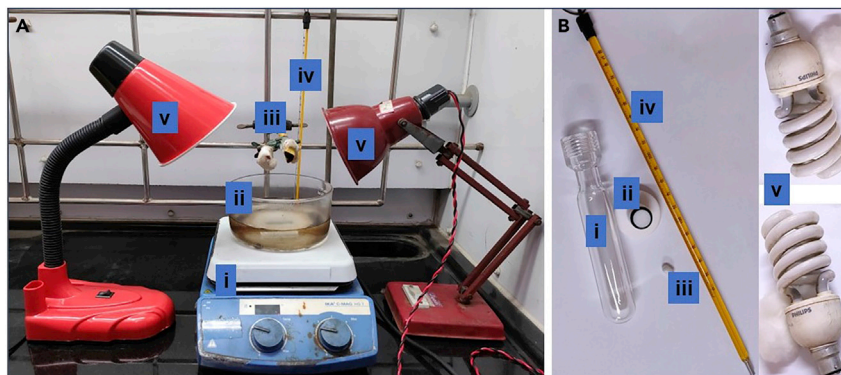


Figure 2. Overview of the "reaction set-up B"

(A) Instrumental set-up: (i) IKA hot plate magnetic stirrer, (ii) oil bath, (iii) clamp, (iv) hanging thermometer dipped in oil, (v) CFL stands.

(B) Zoom in on the required accessories: (i) 15 mL pressure-tube, (ii) Teflon cap of the pressure tube, (iii) magnet bar, (iv) thermometer, (v) CFLs.



Figure 3. The instrumental “set-up B”

Yellow box: temperature interface. Red box: rotation regulator.

- e. Set two white 23 W compact fluorescent lamps (CFLs) (Phillips Tornado T2 23W WW B22 220–240 V 1BC/6) in light-stands.
- f. Place the lamps each at opposite sides of the magnetic stirrer so that the lamps remain headed towards oil bath at 5 cm apart.
6. Digital screen interface of the stirrer.
 - a. Turn on the stirrer (Figure 3).
 - b. Set the temperature so that the oil bath temperature reaches to 110°C. (In our case, setting digital reading of 145 was sufficient (Figure 3, yellow box).
 - c. Set the rotation speed regulator at in between 1 and 2 (500 rpm) (Figure 3, red box).
 - d. Turn on two CFLs.

KEY RESOURCES TABLE

REAGENT or RESOURCE	SOURCE	IDENTIFIER
Chemicals, peptides, and recombinant proteins		
Copper (powder, <425 μm, 99.5% trace metals basis)	Sigma-Aldrich	CAS 7440-50-8
2'-benzyl-[1,1'-biphenyl]-2-carboxylic acid	Synthesized at our lab	(Nandi et al., 2022)
Di-tert-butyl peroxide	Sigma-Aldrich	CAS 110-05-4
Rose bengal	Sigma-Aldrich	CAS 632-69-9
α,α,α-Trifluorotoluene	Sigma-Aldrich	CAS 98-08-8
Other		
IKA WORKS INC. 7 IKAMAG Hot Plate Magnetic Stirrer	IKA	Ident. No. 0003581222
Microsyringe 50 μL, 700 series, removable needle	Hamilton	Cat. No. 20788
Tornado T2 23W WW B22 220–240 V 1BC/6	Philips	Product code: 872790092972001
Oil bath, flat bottom	Pyrex	Item code: 1470/12D
Round bottom flask	Borosil	Product code: 4380A16
Pressure tube, 15 mL	Sigma-Aldrich	Product code: Z181099
Separating funnel	Borosil	Product code: 6400017
Erlenmeyer (conical) flask	Borosil	Product code: 4980021
Reagent bottles	Borosil	Product code: 1501021
Chromatography column	Borosil	Product code: 6100063
Thin layer chromatography using aluminum TLC plate, silica gel coated with fluorescent indicator F254	Supelco	Cat no.: 105554
Silica gel for chromatography, Silica gel 60 (0.040–0.063 mm) for column chromatography (230–400 mesh ASTM)	Millipore	CAS No.: 112926-00-8

(Continued on next page)

Continued

REAGENT or RESOURCE	SOURCE	IDENTIFIER
Elecpto UV Cabinet for Chromatography analysis	Elecpto	Item part number: EO-111 ASIN: B089GNGKCC Buying link: https://www.amazon.in/Elecpto-UV-Cabinet-Chromatography-analysis/dp/B089GNGKCC/ref=sr_1_5?crd=2IK85T9EVYP2Q&keywords=uv+cabinet&qid=1653478071&sprefix=uv+cabinet+%2Caps%2C217&sr=8-5
Bruker-Avance 600 MHz NMR spectrometer	Bruker	N/A

MATERIALS AND EQUIPMENT

Reagents

Reagents	Storage temperature	Maximum time for storage
2'-benzyl-[1,1'-biphenyl]-2-carboxylic acid	room temperature	more than two years
Copper powder	room temperature	more than two years
rose bengal (RB)	room temperature	more than two years
α,α,α -Trifluorotoluene	room temperature	more than two years
Di-tert-butyl peroxide	5°C	two years
Ultra-high purity (UHP) O ₂	room temperature	more than two years

STEP-BY-STEP METHOD DETAILS

Part 1A: Synthesis of 7-phenyldibenzo[c,e]oxepin-5(7H)-one via "condition A"

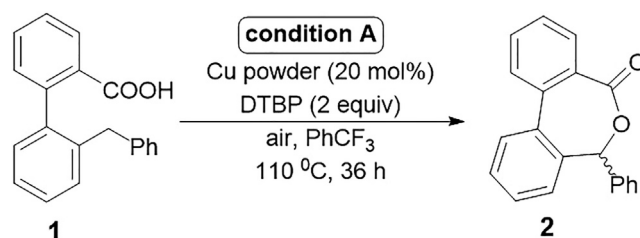
⌚ Timing: 36 h

In this step, the synthesis of 7-phenyldibenzo[c,e]oxepin-5(7H)-one **2** (Scheme 1) has been accomplished within 36 h on heating. As per the previous discussion, 2'-benzyl-[1,1'-biphenyl]-2-carboxylic acid is converted to the product **2** on heating it at 110°C with Cu powder as catalyst and DTBP as oxidant.

- Set up the reaction (Figure 4). [Troubleshooting 1](#).
 - Deal with the "set up A" for the reaction under "condition A".
 - Ensure that the stirrer is on and rotation speed is set at regulator reading 1 and 2.
 - Ensure that the temperature is set rightly.
 - Check the temperature reading in the thermometer. [Troubleshooting 2](#).

⏸ **Pause point:** Once the oil bath temperature reaches at 110°C, the equipment is ready to be run for the reaction and throughout the reaction, this temperature is required to be maintained.

- Run the reaction.
 - Dip the properly capped "vessel A" to the oil bath of "set up A" and attach it to the clamp.



Scheme 1. General scheme of the reaction under "condition A"

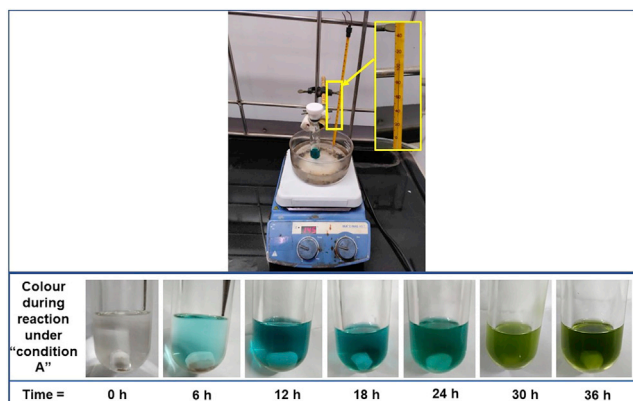


Figure 4. Running the reaction at 110°C and color change time-by-time

△ **CRITICAL:** Ensure that the reaction solvent front inside the “vessel A” is completely under the oil front in such a way that the headspace of the vessel is not immersed into oil either.

- b. Ensure that the magnetic stir-bar is stirring properly.
- c. At the calculated time, to stop the heating, reduce the temperature to 0 (at digital screen) so that the reaction temperature gradually reduces to the room temperature. The progress of the reaction is checked by TLC.

Note: During the reaction under “condition A”, an evident color change of the reaction solution could be observed as depicted in “Figure 4”. As shown, the color changes from colorless to blue to green. At the end of the reaction, green color appears and reaction becomes turbid, which indirectly refers to the reaction completion, additional to TLC.

- d. Check the temperature of the bath using thermometer, hung vertically in the oil bath ([troubleshooting 2](#)). When the temperature reduces to room temperature, raise the pressure vessel from the oil and wash the outer wall with hexane and tissue paper.
- e. Switch off the magnetic stirrer.

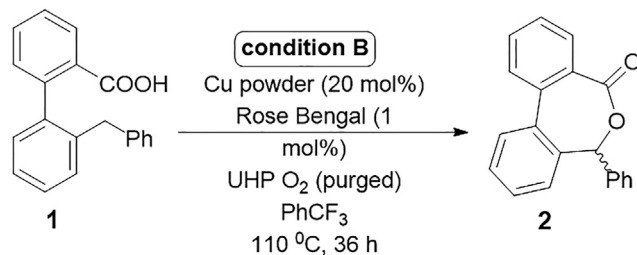
Part 1B: Synthesis of 7-phenyldibenzo[c,e]oxepin-5(7H)-one via “condition B”

⌚ **Timing:** 36 h

In this step, the synthesis of 7-phenyldibenzo[c,e]oxepin-5(7H)-one **2** ([Scheme 2](#)) has been accomplished within 36 h on heating. As per the previous discussion, 2'-benzyl-[1,1'-biphenyl]-2-carboxylic acid is converted to the product **2** on heating it at 110°C with Cu powder as catalyst and DTBP as oxidant.

3. Set up the reaction ([Figure 6](#)). [Troubleshooting 1](#).
 - a. Deal with the “set up B” for the reaction under “condition B”.
 - b. Ensure that the stirrer is on and rotation regulator is set at in between 1 and 2.
 - c. Ensure that the temperature is set rightly.
 - d. Ensure that both the lights are on.
 - e. Check the temperature reading in the thermometer. [Troubleshooting 2](#).

⏸ **Pause point:** Once the oil bath temperature reaches at 110°C, the equipment is ready to be run for the reaction, and throughout the reaction, this temperature is must to be maintained.



Scheme 2. General scheme of the reaction under "condition B"

4. Run the reaction.
 - a. Dip the properly capped "vessel B" to the oil bath of "set up B" and attach it to the clamp.

△ CRITICAL: Ensure that the reaction solvent front inside the "vessel A" is completely under the oil front in such a way that the headspace of the vessel is not immersed into oil either.

- b. Ensure that the magnetic stir-bar is stirring properly.
- c. At the calculated time, reduce the temperature to 0 (at digital screen) so that the reaction temperature gradually reduces to the room temperature.
- d. Switch off the lights.
- e. Check the temperature in thermometer ([troubleshooting 2](#)). When the temperature reduces to room temperature, raise the pressure vessel from the oil and wash the outer wall with hexane and tissue paper.
- f. Switch of the magnetic stirrer.

Part 2A: Catalyst recycling of "condition A"

⌚ Timing: 2 h

As at the end of the reaction, the reaction medium became extremely turbid ([Figure 7A](#)) and full of dispersed CuNPs (indicated from transmission electron microscope image i.e., TEM) ([Nandi et al., 2022](#)), recyclability was checked. After one batch of the reaction, it was filtered, washed with ethyl

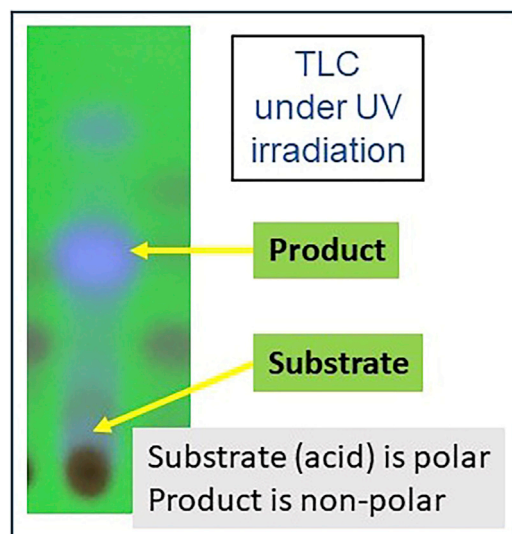


Figure 5. Image of TLC (run with 10% EtOAc in hexane) from reaction mixture

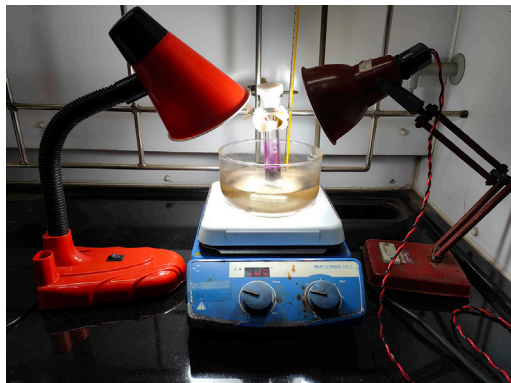


Figure 6. Running the reaction at 110°C under CFL irradiation

acetate and another batch of reaction was set up with the residue. Similarly subsequent four batches were repeated and the result was satisfactory.

5. Filter the residue and set-up a new batch.
 - a. After completion, let the pressure tube settle as that allows the residues to be precipitated better.
 - b. Isolate the precipitate by simple filtration by a funnel under air.
 - c. Wash the filtrand with ethyl acetate for several times (Figure 7A).
 - d. With filtrate, follow steps 3–16 (Part 2A) to isolate the product.
 - e. Let the filtrand dry under air for 1 h. It will be used as catalyst for subsequent batches.
 - f. Take back the recovered catalyst to another clean oven-dried pressure tube (Figure 7A).
 - g. As the filtrand would be used as catalyst, prepare the reaction vessel as discussed earlier except the external addition of copper powder.
 - h. Run the reaction similarly for 36 h.
 - i. Follow steps 5a–5h (Part 2A).

Part 2B: Catalyst recycling of “condition B”

⌚ Timing: 2 h

Similarly, as “condition A”, the catalyst was recycled in case of “condition B”.

6. Filter the residue and set-up a new batch.
 - a. Filter the residue and set-up a new batch of reaction following exactly similar manner as performed for “condition A” following steps 5a–5i (Part 2A).

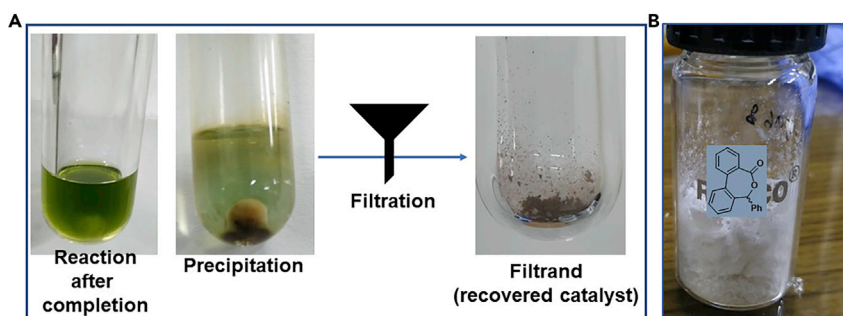


Figure 7. Practical utility of the protocol

(A) Recycling the catalyst, (B) Scale-up reaction under “condition B”

Part 3: Purification of the crude material

⌚ Timing: 1.5 h

Purify the crude material in similar manner for each type of reaction (under “condition A”, “condition B” or “catalyst recycling”).

7. Upon completion of the reaction,
 - a. transfer the reaction mixture to a 125 mL separatory funnel.
 - b. Add 30 mL of deionized water and 30 mL of ethyl acetate (EtOAc).
 - c. Shake the separatory funnel vigorously.
 - d. Let it settle so that the aqueous phase is separated from the organic one.

Note: The thin-layer chromatography (TLC) (run with 10% ethyl acetate in hexane solution) from the reaction mixture looks like [Figure 5](#), under UV irradiation (365 nm).

8. Transfer the separated aqueous phase and organic phase, each in one 250 mL Erlenmeyer flask.
9. Take back the aqueous phase to the separatory funnel and add 30 mL of EtOAc to it.
10. Then,
 - a. Shake the separatory funnel vigorously.
 - b. Let the two phases to separate.
 - c. Transfer those similarly in their corresponding Erlenmeyer flasks.
11. For two times, repeat steps 9 and 10.
12. Transfer the combined organic phase into the separatory funnel and add 30 mL of deionized water to it. Shake the funnel vigorously and let it be stable so that the organic phase is separated from the aqueous one.
13. Take the aqueous phase and discard it in the proper waste container.
14. For additional two times, repeat steps 12 and 13.
15. Now, add 30 mL of Brine to the separatory funnel containing the organic phase and repeat step 14.
16. Take the organic phase in a 100 mL round bottom flask by filtering it through anhydrous sodium sulphate (Na_2SO_4) bed taken in a funnel.
17. Evaporate the solvent under reduced pressure in rotatory evaporator. (45°C, 240 mmHg, ~15 min).
18. Therefore,
 - a. Add 1 mL of dichloromethane (DCM) and 200 mg of silica (mesh size: 230–400) to the dried crude material taken in round bottom flask.
 - b. Swirl the flask gently.
 - c. Evaporate the solvent under reduced pressure (40°C, 800 mbar, ~5 min).
19. Perform column chromatography to purify the crude product (25 cm of silica, \varnothing of the column = 3.0 cm) eluting 97:3 (by volume) mixture of hexane/ethyl acetate (~300 mL).
20. Combine the collected fractions containing pure product and remove the solvent under vacuum to achieve the desired product. [Troubleshooting 3](#).

EXPECTED OUTCOMES

Condition A

7-phenyldibenzo[c,e]oxepin-5(7H)-one **2** appears as a white solid obtained in 82% isolated yield (34.4 mg).

Condition B

7-phenyldibenzo[c,e]oxepin-5(7H)-one **2** appears as a white solid obtained in 72% yield (30.2 mg). [Troubleshooting 4](#).

Catalyst recycling

For condition A, the yields were 82%, 75%, 66%, and 48% from respective batches. [Troubleshooting 5](#).

For "condition B", the yields were 72%, 68%, 65% and 55% from respective batches. [Troubleshooting 5](#).

QUANTIFICATION AND STATISTICAL ANALYSIS

Analytical data

For 7-phenyldibenzo[c,e]oxepin-5(7H)-one (**2**).

^1H NMR (600 MHz, Chloroform- d) δ 8.03 (d, J = 7.8 Hz, 1H), 7.65–7.75 (m, 3H), 7.58 (t, J = 7.2 Hz, 1H), 7.41–7.52 (m, 6H), 7.29 (t, J = 7.2 Hz, 1H), 6.79 (d, J = 7.8 Hz, 1H), 6.25 (s, 1H).

^{13}C NMR (150 MHz, Chloroform- d) δ 169.42, 138.56, 138.46, 137.29, 135.73, 132.68, 131.46, 130.73, 129.54, 128.90, 128.78, 128.55, 128.52, 128.45, 128.40, 127.38, 126.97, 78.99.

HRMS(ESI $^+$): Calculated for $\text{C}_{20}\text{H}_{14}\text{O}_2\text{Na}$ [$\text{M}+\text{Na}$] $^+$: 309.0891; found: 309.0444.

Scaling-up the reaction under "condition B"

Under "condition B", we performed a reaction in 5 mmol scale, and the expected 7-phenyldibenzo[c,e]oxepin-5(7H)-one was isolated in 62% yield (650.2 mg).

Under "condition B", we performed a reaction in 10 mmol scale, and gratifyingly, the expected 7-phenyldibenzo[c,e]oxepin-5(7H)-one was isolated in 68% yield (1.426 g) ([Figure 7B](#)).

LIMITATIONS

The protocol is only limited to 7-membered lactone formation.

TROUBLESHOOTING

Problem 1

Step 1, step 3: The temperature does not fix at 110°C according to thermometer reading.

Potential solution

The magnetic stirrers cum heaters can behave differently on different occasions. While setting 145 digitally was adequate for us to reach oil bath temperature at 110°C, at another environment, it could be insufficient. But the main requirement is reaching the reaction temperature to 110°C. To attain that, set the instrumental temperature (digital reading) accordingly.

Problem 2

Steps 1d, 2d, 3e, 4e: The thermometer reading is fluctuating over time.

Potential solution

Please take care that the thermometer should not touch the bottom of the bath to avoid erroneous temperature measurements.

Problem 3

Step 19: Yield is lower than expected.

Potential solution

Check that the amount of solvent is taken as required. The headspace volume is important for the reaction.

Problem 4

Yield is lower than expected.

Potential solution

Check whether the reaction tube was fully purged with O₂ efficiently and capped. Since, O₂ is the main oxidant here, slight deviation might affect the reaction yield enormously.

Problem 5

Yield is lower than expected.

Potential solution

Be assured to use the filtrand soon after filtration and drying within 1 h. Failing which, resting the residue under air for longer time might affect the reaction outcome.

RESOURCE AVAILABILITY

Lead contact

Further information and requests for resources and reagents should be directed to and will be fulfilled by the lead contact, Ranjan Jana (rjana@iicb.res.in).

Materials availability

This study did not generate new unique reagents.

Data and code availability

All data reported in this paper will be shared by the [lead contact](#) upon request.

This paper does not report original code.

Any additional information required to reanalyze the data reported in this paper is available from the [lead contact](#) upon request.

ACKNOWLEDGMENTS

The authors wish to thank the DST, SERB, Govt. of India Core Research Grant no. CRG/2021/006717 for financial support. S.N. and S.M. thank DST and CSIR for their respective PhD fellowships.

AUTHOR CONTRIBUTIONS

S.N. and R.J. designed and wrote the protocol with inputs from all the authors. S.N. and S.M. performed the experimental data. R.J. supervised the project.

DECLARATION OF INTERESTS

The authors declare no competing interests.

REFERENCES

- Altemöller, M., Gehring, T., Cudaj, J., Podlech, J., Goesmann, H., Feldmann, C., and Rothenberger, A. (2009). Total synthesis of graphislacones A, C, D, and H, of ulocladol, and of the originally proposed and revised structures of graphislacones E and F. *Eur. J. Org. Chem.* 2130–2140.
- Aly, A.H., Edrada-Ebel, R., Indriani, I.D., Wray, V., Müller, W.E.G., Totzke, F., Zirrgiebel, U., Schächtele, C., Kubbutat, M.H.G., Lin, W.H., et al. (2008). Cytotoxic metabolites from the fungal endophyte *alternaria* sp. and their subsequent detection in its host plant *polygonum senegalense*. *J. Nat. Prod.* 71, 972–980.
- Begam, H.M., Nandi, S., and Jana, R. (2022). A directing group switch in copper-catalyzed electrophilic C–H amination/migratory annulation cascade: divergent access to benzimidazolone/benzimidazole. *Chem. Sci.* 13, 5726–5733.
- Bhunia, S.K., Das, P., Nandi, S., and Jana, R. (2019). Carboxylation of aryl triflates with CO₂ merging palladium and visible-light-photoredox catalysts. *Org. Lett.* 21, 4632–4637.
- Colombel, V., Joncour, A., Thoret, S., Dubois, J., Bignon, J., Wdzieczak-Bakala, J., and Baudoin, O. (2010). Synthesis of antimicrotubule dibenzoxepines. *Tetrahedron Lett.* 51, 3127–3129.
- Dalton, T., Faber, T., and Glorius, F. (2021). C–H activation: toward sustainability and applications. *ACS Cent. Sci.* 7, 245–261.
- Feng, J., Liang, S., Chen, S.-Y., Zhang, J., Fu, S.-S., and Yu, X.-Q. (2012). A metal-free oxidative esterification of the benzyl C–H bond. *Adv. Synth. Catal.* 354, 1287–1292.
- Gallardo-Donaire, J., and Martin, R. (2013). Cu-catalyzed mild C(sp²)-H functionalization assisted

by carboxylic acids en route to hydroxylated arenes. *J. Am. Chem. Soc.* **135**, 9350–9353.

Golden, D.L., Suh, S.-E., and Stahl, S.S. (2022). Radical C(sp³)–H functionalization and cross-coupling reactions. *Nat. Rev. Chem.* **6**, 405–427.

Guo, S., Yuan, Y., and Xiang, J. (2015a). Copper-catalyzed oxidative alkenylation of C(sp³)–H bonds via benzyl or alkyl radical addition to β -nitrostyrenes. *New J. Chem.* **39**, 3093–3097.

Guo, X.-X., Gu, D.-W., Wu, Z., and Zhang, W. (2015b). Copper-catalyzed C–H functionalization reactions: efficient synthesis of heterocycles. *Chem. Rev.* **115**, 1622–1651.

Hu, H., Chen, S.-J., Mandal, M., Pratik, S.M., Buss, J.A., Krska, S.W., Cramer, C.J., and Stahl, S.S. (2020). Copper-catalyzed benzylic C–H coupling with alcohols via radical relay enabled by redox buffering. *Nat. Catal.* **3**, 358–367.

Crabtree, R.H., and Lei, A. (2017). Introduction: CH activation. *Chem. Rev.* **117**, 8481–8482.

Lerchen, A., Knecht, T., Koy, M., Ernst, J.B., Bergander, K., Daniliuc, C.G., and Glorius, F. (2018). Non-directed cross-dehydrogenative (hetero) arylation of allylic C(sp³)–H bonds enabled by C–H activation. *Angew. Chem. Int. Ed. Engl.* **57**, 15248–15252.

Luo, S., Li, L., Yang, Q., and Jia, Z. (2018). Organocatalytic electrochemical C–H lactonization of aromatic carboxylic acids. *Synthesis* **50**, 2924–2929.

Li, Y., Ding, Y.-J., Wang, J.-Y., Su, Y.-M., and Wang, X.-S. (2013). Pd-catalyzed C–H lactonization for expedient synthesis of biaryl lactones and total synthesis of cannabiol. *Org. Lett.* **15**, 2574–2577.

Liang, Q., Walsh, P.J., and Jia, T. (2020). Copper-catalyzed intermolecular difunctionalization of styrenes with thiosulfonates and arylboronic acids via a radical relay pathway. *ACS Catal.* **10**, 2633–2639.

Liu, H., Shi, G., Pan, S., Jiang, Y., and Zhang, Y. (2013). Palladium-catalyzed benzylation of carboxylic acids with toluene via benzylic C–H activation. *Org. Lett.* **15**, 4098–4101.

Liu, S., Achou, R., Boulanger, C., Pawar, G., Kumar, N., Lusseau, J., Robert, F., and Landais, Y. (2020). Copper-catalyzed oxidative benzylic C(sp³)–H amination: direct synthesis of benzylic carbamates. *Chem. Commun.* **56**, 13013–13016.

Lu, B., Zhu, F., Sun, H.-M., and Shen, Q. (2017). Esterification of the primary benzylic C–H bonds with carboxylic acids catalyzed by ionic iron(III) complexes containing an imidazolium cation. *Org. Lett.* **19**, 1132–1135.

Manna, K., Begam, H.M., Samanta, K., and Jana, R. (2020). Overcoming the dealylation problem: palladium(II)-Catalyzed chemo-regio- and stereoselective allylic oxidation of aryl allyl ether, amine, and amino acids. *Org. Lett.* **22**, 7443–7449.

Meng, H., Xu, Z., Qu, Z., Huang, H., and Deng, G.-J. (2020). Copper(0)/PPh₃-Mediated bisheteroannulations of o-nitroalkynes with methylketoximes accessing pyrazo-fused pseudoindoxyls. *Org. Lett.* **22**, 6117–6121.

Nandi, S., and Jana, R. (2022). Toward sustainable photo-/electrocatalytic carboxylation of organic substrates with CO₂. *Asian J. Org. Chem.* **2022**, e202200356.

Nandi, S., Mondal, S., and Jana, R. (2022). Chemo- and regioselective benzylic C(sp³)–H oxidation bridging the gap between hetero- and homogeneous copper catalysis. *iScience* **25**, 104341.

Ramirez, N.P., Bosque, I., and Gonzalez-Gomez, J.C. (2015). Photocatalytic dehydrogenative lactonization of 2-arylbenzoic acids. *Org. Lett.* **17**, 4550–4553.

Rogge, T., Kaplaneris, N., Chatani, N., Kim, J., Chang, S., Punji, B., Schafer, L.L., Musaev, D.G., Wencel-Delord, J., Roberts, C.A., et al. (2021). C–H activation. *Nat. Rev. Methods Primers* **1**, 43.

Rout, S.K., Guin, S., Ali, W., Gogoi, A., and Patel, B.K. (2014). Copper-catalyzed esterification of alkylbenzenes with cyclic ethers and cycloalkanes via C(sp³)–H activation following cross-dehydrogenative coupling. *Org. Lett.* **16**, 3086–3089.

Sathyamoorthi, S., and Du Bois, J. (2016). Copper-catalyzed oxidative cyclization of carboxylic acids. *Org. Lett.* **18**, 6308–6311.

Shao, A., Zhan, J., Li, N., Chiang, C.-W., and Lei, A. (2018). External oxidant-free dehydrogenative lactonization of 2-arylbenzoic acids via visible-light photocatalysis. *J. Org. Chem.* **83**, 3582–3589.

Suh, S.-E., Chen, S.-J., Mandal, M., Guzei, I.A., Cramer, C.J., and Stahl, S.S. (2020). Site-selective copper-catalyzed azidation of benzylic C–H bonds. *J. Am. Chem. Soc.* **142**, 11388–11393.

Tao, X.-Z., Dai, J.-J., Zhou, J., Xu, J., and Xu, H.-J. (2018). Electrochemical C–O bond formation: facile access to aromatic lactones. *Chemistry* **24**, 6932–6935.

Tran, B.L., Driess, M., and Hartwig, J.F. (2014). Copper-catalyzed oxidative dehydrogenative carboxylation of unactivated alkanes to allylic esters via alkenes. *J. Am. Chem. Soc.* **136**, 17292–17301.

Vasilopoulos, A., Zultanski, S.L., and Stahl, S.S. (2017). Feedstocks to pharmacophores: Cu-catalyzed oxidative arylation of inexpensive alkylarenes enabling direct access to diarylalkanes. *J. Am. Chem. Soc.* **139**, 7705–7708.

Yi, H., Zhang, G., Wang, H., Huang, Z., Wang, J., Singh, A.K., and Lei, A. (2017). Recent advances in radical C–H activation/radical cross-coupling. *Chem. Rev.* **117**, 9016–9085.

Zhang, J., Shi, D., Zhang, H., Xu, Z., Bao, H., Jin, H., and Liu, Y. (2017). Synthesis of dibenzopyranones and pyrazolobenzopyranones through copper(0)/selectfluor system-catalyzed double CH activation/oxygen insertion of 2-arylbenzaldehydes and 5-arylpyrazole-4-carbaldehydes. *Tetrahedron* **73**, 154–163.

Zhang, X.-S., Zhang, Y.-F., Li, Z.-W., Luo, F.-X., and Shi, Z.-J. (2015). Synthesis of dibenzo[c, e]joxepin-5(7H)-ones from benzyl thioethers and carboxylic acids: rhodium-catalyzed double C–H activation controlled by different directing groups. *Angew. Chem. Int. Ed. Engl.* **54**, 5478–5482.

Carboxylation of Aryl Triflates with CO₂ Merging Palladium and Visible-Light-Photoredox Catalysts

Samir Kumar Bhunia,^{†,‡} Pritha Das,^{†,§} Shantanu Nandi,^{†,§} and Ranjan Jana^{*,†,‡,§}

[†]Organic and Medicinal Chemistry Division, CSIR-Indian Institute of Chemical Biology, 4 Raja S. C. Mullick Road, Jadavpur, Kolkata 700032, West Bengal, India

[‡]Academy of Scientific and Innovative Research (AcSIR), Kolkata 700032, West Bengal, India

Supporting Information

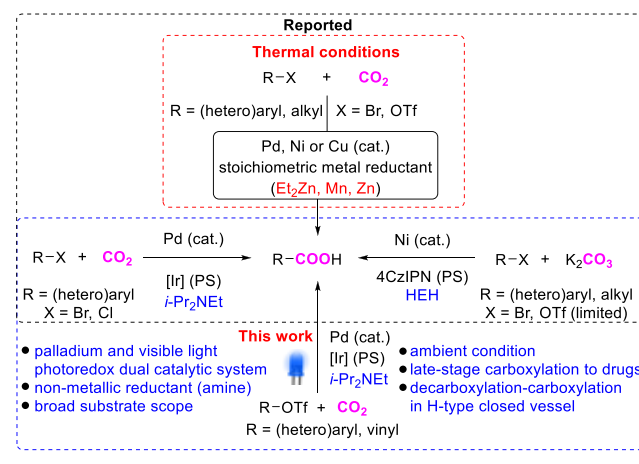
ABSTRACT: We report herein a visible-light-promoted, highly practical carboxylation of readily accessible aryl triflates at ambient temperature and a balloon pressure of CO₂ by the combined use of palladium and photoredox Ir(III) catalysts. Strikingly, the stoichiometric metallic reductant is replaced by a nonmetallic amine reductant providing an environmentally benign carboxylation process. In addition, one-pot synthesis of a carboxylic acid directly from phenol and modification of estrone and concise synthesis of pharmaceutical drugs adapalene and bexarotene have been accomplished via late-stage carboxylation reaction. Furthermore, a parallel decarboxylation–carboxylation reaction has been demonstrated in an H-type closed vessel that is an interesting concept for the strategic sector. Spectroscopic and spectroelectrochemical studies indicated electron transfer from the Ir(III)/DIPEA combination to generate aryl carboxylate and Pd(0) for catalytic turnover.



Due to stringent regulation by the Environmental Protection Agency (EPA), petrochemical industries are being forced to utilize CO₂ that is produced during the processing of fossil fuel.¹ Moreover, carboxylic acids and their derivatives are ubiquitously found in natural products, biologically active compounds, and polymeric materials.² Hence, there is an urgent call for the development of synthetic methods using CO₂ as an abundant, inexpensive, and nontoxic C1 building block.³ An impressive array of transition metal-catalyzed (Pd, Ni, and Cu) carboxylations of aryl, alkyl, alkenyl halides, triflates, or (pseudo)halides has been developed in the past few decades with CO₂.⁴ However, due to the inherent thermodynamic stability of CO₂, most of the transformations require high temperatures, high pressures of CO₂, and stoichiometric amounts of organometallic reductants like Et₂Zn, AlEt₃, Zn or Mn powder, etc. (Scheme 1), which leads to accidental and environmental hazards.⁴ Therefore, to explore the full potential of carboxylation reactions, the development of a mild and practical catalytic protocol without any stoichiometric metal additive is in high demand.

Previously, the group of Nielsen and Jutand reported palladium-catalyzed electrosynthesis of aromatic and α,β -unsaturated carboxylic acids from the corresponding triflates with CO₂.⁵ Deleterious homocoupling, hydrolysis to phenol, and reduced product formation at elevated temperatures lead to the carboxylation products in moderate yields. However, their mechanistic studies are intriguing for the development of transition metal and photoredox dual catalysis.⁶ In recent years, activation of inert CO₂ for the synthesis of carboxylic acids is emerging.⁷ In this vein, the group of Martin and Iwasawa developed an elegant methodology for the carboxylation of aryl bromides and chlorides combining palladium and visible-light-photoredox iridium catalysts.⁸ Subsequently, the group of König reported a nickel and organic photosensitizer dual catalytic approach for the carboxylation of aryl and alkyl bromides and a few aryl triflates using K₂CO₃ as a CO₂ source (Scheme 1).⁹ Thus, we were motivated to develop a general method for carboxylation of aryl triflates using CO₂ directly.

Scheme 1. Carboxylation Reaction with CO₂



In 2015, Murakami and co-workers proposed the carboxylation of *o*-alkylphenyl ketones with CO₂ under ultraviolet-

Received: May 1, 2019
Published: June 12, 2019

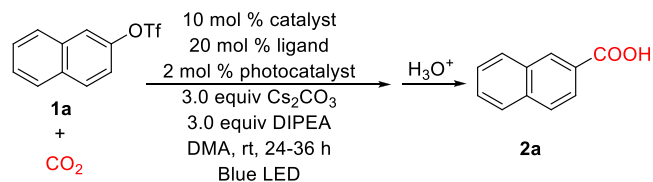
light or solar-light irradiation.^{7a} Jamison and co-workers reported the α -carboxylation of inert amine in a continuous flow via single-electron activation of CO₂ under ultraviolet-light irradiation.^{7c} In 2015, Tsuji and co-workers published cobalt- and nickel-catalyzed carboxylation of alkenyl and sterically hindered aryl triflates utilizing CO₂ with a metallic reductant at elevated temperatures.^{3j} Very recently, Mei and co-workers published nickel-catalyzed carboxylation of aryl and heteroaryl fluorosulfates by CO₂ where 3.0 equiv of manganese has been used as a reducing agent.¹⁰

We report herein a mild and general protocol for the carboxylation of aryl or (hetero)aryl triflates with a balloon pressure of CO₂ combining Pd(OAc)₂ and an iridium(III) photocatalyst and *i*-Pr₂NEt as the nonmetallic reducing agent at room temperature (Scheme 1).

Our initial trials with 2-naphthyl triflate using nickel and photoredox dual catalysts were not effective. Gratifyingly, palladium complexes in combination with electron-rich ligands such as xantphos and photocatalyst **1** provided 25% of the desired carboxylation product in DMA (entry 1, Table 1). The yield was further improved to 45% when photocatalyst Ir(4-F-ppy)₂(dtbpy)(PF₆) **2** was used (entry 2, Table 1). The yield was drastically improved to 82% by using Xphos ligand (entry 7, Table 1), and further screening reveals that 2.0 equiv of *i*-Pr₂NEt and Cs₂CO₃ are optimal reducing agents and bases, respectively. The optimal yield of 89% was obtained with davephos ligand and photocatalyst **3** (entry 12, Table 1). Other organic dyes such as 4CzIPN, 5CzBN, and 3DPAFIPN were found to be inferior compared to Ir catalyst **3**. Our control experiments reveal that all reagents are essential for furnishing the desired product (for details, see the Supporting Information).

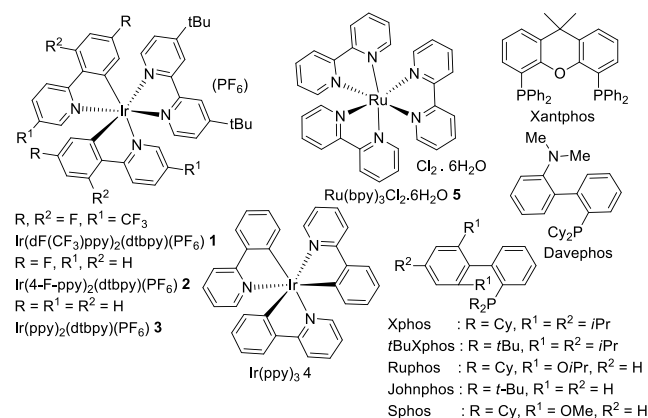
Next, we examined the generality of the reaction with a variety of *ortho*-, *meta*-, and *para*-substituted aryl triflates furnishing corresponding carboxylic acids in excellent to moderate yields (Scheme 2). As shown in Scheme 2, aryl triflates with various functional groups such as cyano (**2j**), trifluoromethoxy (**2k**), fluoro (**2l**), trifluoromethyl (**2m**), ether (**2b**, **2f**, **2h**, **2q**, **2w**, **2ab**, and **2ac**), esters (**2x**), ketone (**2z**), or NBoc or NHBoc (**2y** and **2aa**) groups were well-tolerated under the reaction conditions. This carboxylation reaction took place selectively at the triflate group, leaving chloro (**2g** and **2ac**) and bromo (**2c**) intact for further manipulations, which is a remarkable contrast from Martin's work.⁸ However, DMSO solvent was found to be optimal for **2c**, which may act as a ligand to tune the electronic nature of the palladium complex for selective oxidative addition.¹¹ Gratifyingly, 4-allyl (**2q**)- and 2-allyl (**2r**)-substituted aryl triflates also provided moderate to excellent yields. The sterically demanding substrate also delivered the desired product in good to moderate yields (**2i**, **2n**, **2p**, and **2v**). Overall, electron-rich substrates undergo carboxylation faster than electro-deficient arenes. Interestingly, heterocyclic triflates such as thiophene, indole, and carbazole provided the corresponding carboxylic acids (**2x**, **2y**, and **2ad**) in moderate yields. However, pyridine-3-triflate proved to be unsuccessful for this transformation. Notably, triflate of (+)- δ -tocopherol afforded the corresponding carboxylic acid (**2ae**) in 20% yield with 75% substrate recovery. The carboxylation of a vinyl triflate derived from β -tetralone provided the corresponding carboxylic acid in a 45% yield (**2af**) along with the formation of the homocoupling product. Unfortunately, other -OH derivatives of 2-naphthol such as tosylate, mesylate, nonaflate, and benzylic and allylic triflates provided a very low

Table 1. Optimization of the Reaction Conditions^a



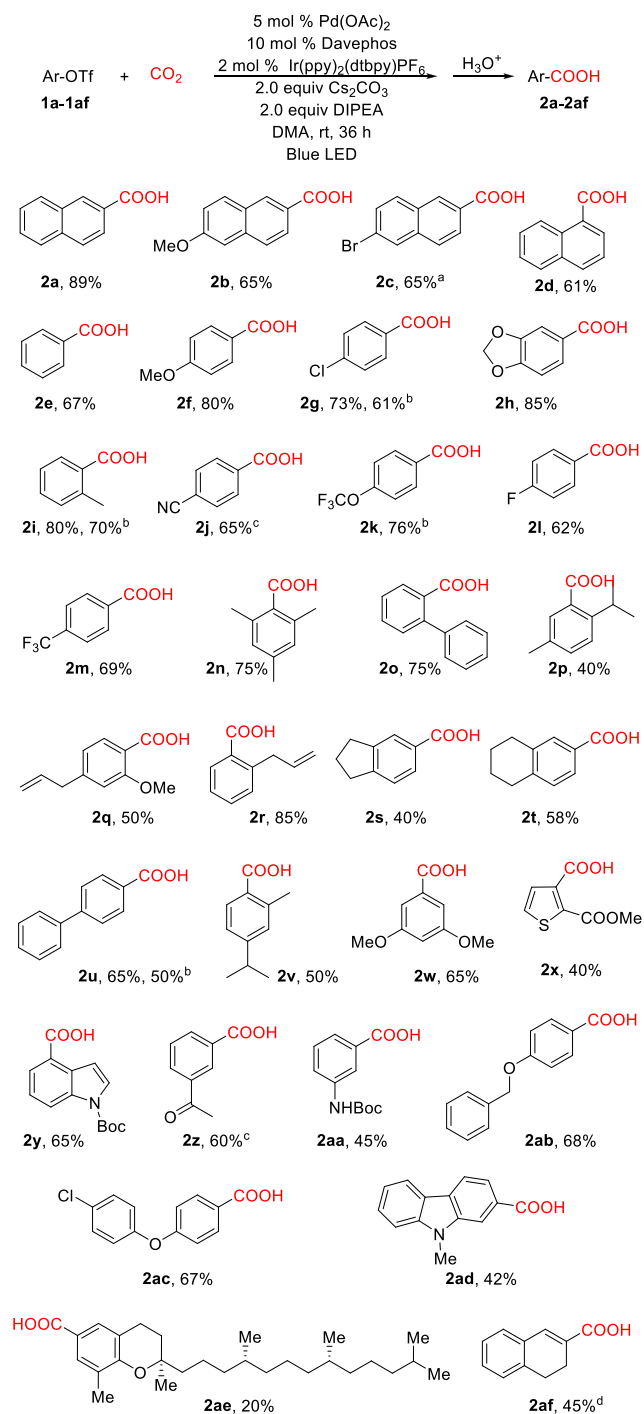
entry	catalyst	ligand	photocatalyst	yield (%)
1	Pd(OAc) ₂	xantphos	1	25
2	Pd(OAc) ₂	xantphos	2	45
3	Pd(OAc) ₂	xantphos	4	not determined
4	Pd(OAc) ₂	xantphos	5	35
5	Pd(OAc) ₂	xantphos	3	50
6	Pd(PPh ₃) ₄	—	2	20
7	Pd(OAc) ₂	xphos	3	82
8	Pd(OAc) ₂	johnphos	3	50
9	Pd(OAc) ₂	ruphos	3	76
10	Pd(OAc) ₂	sphos	3	72
11	Pd(OAc) ₂	<i>t</i> -buxphos	3	50
12	Pd(OAc) ₂	davephos	3	91, 89 ^b
13	Pd(OAc) ₂	davephos	3	80 ^c
14	Pd(OAc) ₂	davephos	3	0, ^d 15 ^e

^aReactions were carried out with naphthyl triflate (0.1 mmol), a catalyst (0.01 mmol), a ligand (0.02 mmol), a photocatalyst (0.002 mmol), Cs₂CO₃ (0.3 mmol), and *i*-Pr₂NEt (0.3 mmol) under a CO₂ atmosphere in 2.0 mL of DMA, followed by irradiation with blue light-emitting diodes at room temperature for 24–36 h. Yields are overall isolated yields. ^bTwo equivalents of Cs₂CO₃ and *i*-Pr₂NEt were used for 36 h. ^cDMSO was used. ^dAny reagent absent from the optimized reaction conditions. ^eWithout Cs₂CO₃.



yield (<10%) of the carboxylation product under the optimized reaction conditions.

To demonstrate the practical utility of this methodology, one-pot carboxylation reaction starting from phenol was performed to provide the desired product in good yield (Scheme 3a). This methodology was applied for the late-stage modification of estrone to provide the corresponding carboxylated estrone in a 40% yield (**2ag**) (Scheme 3b). Interestingly, bis-triflate of the corresponding 2,2'-biphenol provided a lactone product directly through selective monocarboxylation and subsequent lactonization **2ah** (Scheme 3c).¹² The late-stage carboxylation was also applied for an expedient synthesis of adapalene **2ai** (Scheme 3e), a Food and Drug Administration-approved drug for acne treatment.¹³ Inexpensive 6-bromo-2-naphthol was used in this protocol instead of expensive 6-bromo-2-naphthoic acid in earlier methods.¹⁴ Furthermore, an improved synthesis of anticancer

Scheme 2. Substrate Scope of the Carboxylation Reaction^e

^aDMSO was used as a solvent. ^bXphos was used as a ligand. ^ct-Buxphos was used as a ligand. ^dXantphos was used as a ligand. ^eAll reactions are carried out with 0.2 mmol of aryl triflate.

drug bexarotene **2aj** has been accomplished through late-stage carboxylation reaction (Scheme 3f).¹⁵ This late-stage carboxylation reaction is particularly attractive for isotope labeling for metabolomic and imaging studies.¹⁶ Because of the emerging trends in decarboxylative couplings, we have demonstrated this carboxylation reaction in an H-type COgen closed vessel originally designed by the group of Skrydstrup.¹⁷ Thus, CO₂ was generated by metal-free decarboxylative iodination of 2,6-dimethoxybenzoic acid developed by the group of Larrosa¹⁸

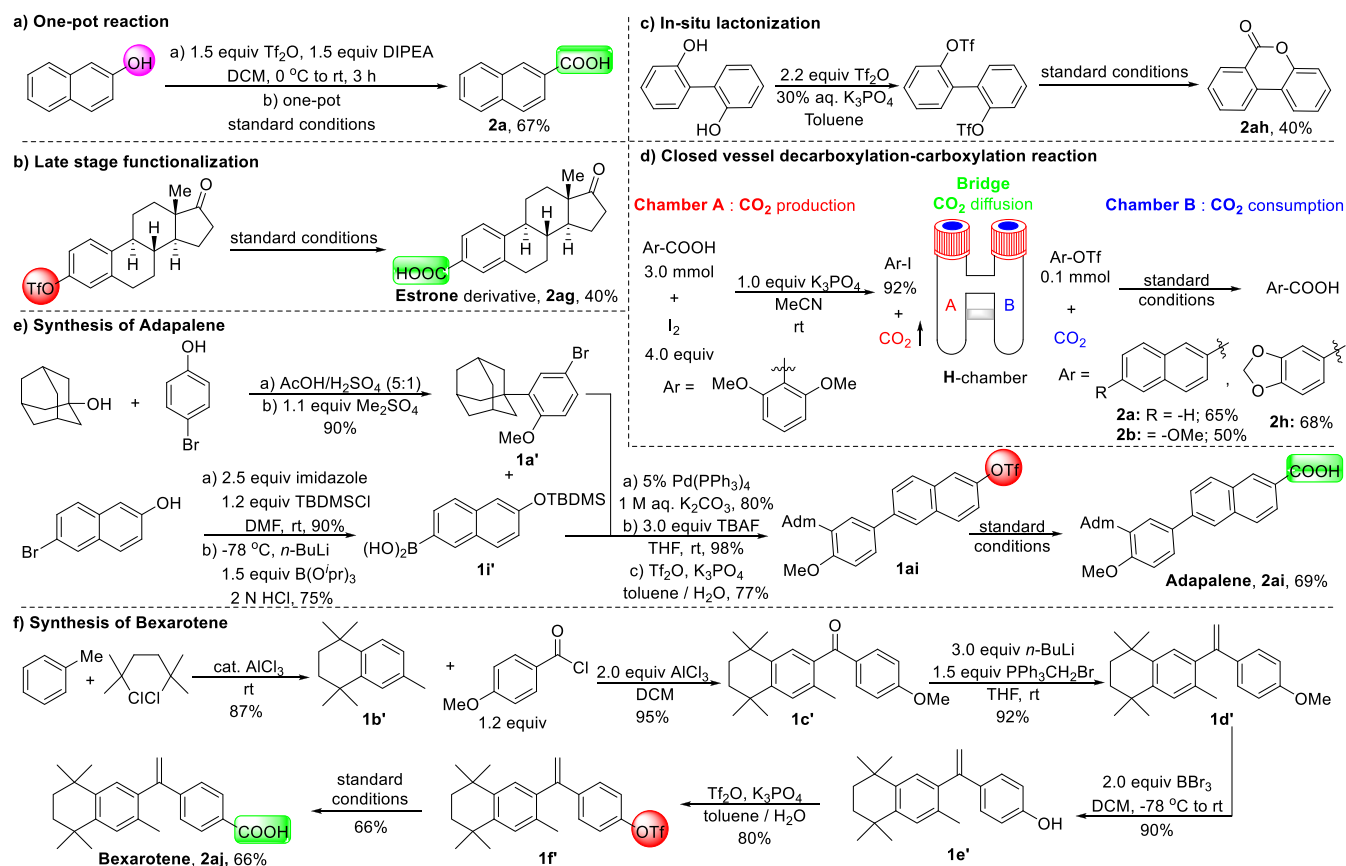
and diffused through the connector to the other arm to realize carboxylation reaction (see the Supporting Information). This demonstration could be useful for the strategic sectors to execute two important classes of reactions without affecting the environment.¹⁹

To elucidate the probable mechanistic pathway, we have performed several control experiments. In the presence of radical scavengers such as BHT and TEMPO, the yield of **2a** was reduced to 65% and 12%, respectively. Hence, TEMPO may interfere with the redox cascade of Pd(II)/Ir(III) dual catalysis. Typically, Pd(0) in the presence of electron-rich ligands is known to undergo oxidative addition to the aryl triflate to generate a Pd complex **B** [detected by HRMS from the reaction mixture (see the Supporting Information)] via a concerted pathway.²⁰ However, from the cyclic voltammetric analysis, the first reduction potentials of the ligated naphthylpalladium triflate complex [(davephos)(2-naphthyl)-(OTf)Pd] **B** (for the synthesis, see the Supporting Information) and its corresponding cationic complex (with BAr_F⁻) were measured as -2.07 V (Figure S6a) and -2.02 V (Figure S6c), respectively, which is much lower than that of the reductant Ir(II) catalyst. Therefore, the reduction of Pd complex **B** by the reduced Ir(II) catalyst is thermodynamically unfavorable, which was also observed by the Martin group.⁸ Surprisingly, when cyclic voltammetry was performed under a CO₂ atmosphere, a new peak at approximately -1.15 V (Figure S6b) appeared, which indicates that a new species may be generated in the presence of CO₂, which can be reduced by the Ir(II) catalyst [with Ir(II) as the reductant, E₁ = -1.51 V vs SCE].²¹ In addition, we have performed fluorescence quenching and electrochemical experiments to elucidate the initial electron transfer process. The fluorescence of the excited state of Ir(ppy)₂(dtbpy)(PF₆) [E_{1/2}(PC^{*}/PC⁻) = +0.66 V vs SCE at λ_{max} = 570 nm in CH₃CN]²² was quenched by DIPEA [E_{ox}(DIPEA) = +0.65 V vs SCE in MeCN]²³ with a rate of 0.69 M⁻¹ (Figure S5). It was also quenched by Pd(OAc)₂ at a rate of 0.14 M⁻¹ (Figure S3). However, the introduction of davephos decreased the rate to 0.11 M⁻¹ (Figure S4). Furthermore, we have performed the emission lifetime measurement of the excited state of Ir(ppy)₂(dtbpy)(PF₆) in the presence of DIPEA, Pd(OAc)₂, and 2-naphthyl triflate. The excited state decay profile was changed in the presence of DIPEA but almost identical with Pd(OAc)₂ and 2-naphthyl triflate, indicating the possibility of photoinduced electron transfer of the ³MLCT excited state, which is reductively quenched by the superior electron donor DIPEA (Figure S7).

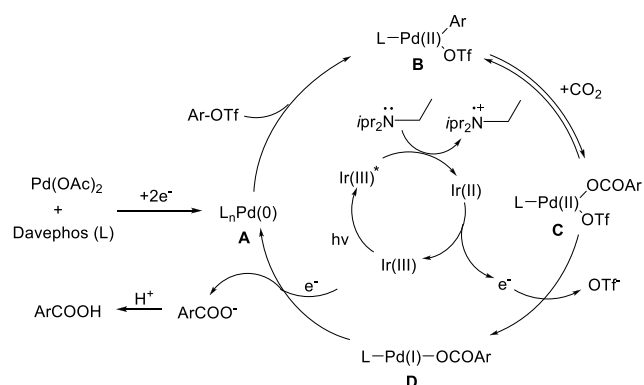
From these control experiments, we propose that the mechanism is closely related to that proposed by Iwasawa and Martin; initially, a Pd(0) species is formed, which undergoes oxidative addition to aryl triflates providing intermediate **B** (Scheme 4). It may undergo carboxylation with CO₂ in a reversible manner to form intermediate **C**.²⁴ Subsequent single-electron reduction by Ir(II) may generate intermediate **D**, which was reduced by one more electron to generate aryl carboxylate and Pd(0) for subsequent runs.

In conclusion, we have developed a practical carboxylation of readily accessible aryl triflates with CO₂ under palladium and visible-light-iridium(III) dual catalysis at ambient temperature and pressure. This mild and highly chemoselective protocol is suitable for the modification of estrone and synthesis of adapalene and bexarotene drugs via late-stage carboxylation. Furthermore, an interesting decarboxylation-carboxylation reaction has been demonstrated in an H-type

Scheme 3. Practical Applications of the Dual Catalytic Carboxylation Reaction



Scheme 4. Plausible Catalytic Cycle



closed vessel that is a novel concept for the strategic sectors in chemical industries for sustainable development.

■ ASSOCIATED CONTENT

S Supporting Information

The Supporting Information is available free of charge on the ACS Publications website at DOI: 10.1021/acs.orglett.9b01532.

Experimental procedures, spectroscopic data, and ¹H, ¹³C, and ¹⁹F NMR spectra of all synthesized compounds (PDF)

■ AUTHOR INFORMATION

Corresponding Author

*E-mail: rjana@iicb.res.in.

ORCID

Ranjan Jana: 0000-0002-5473-0258

Author Contributions

§P.D. and S.N. contributed equally to this work.

Notes

The authors declare no competing financial interest.

■ ACKNOWLEDGMENTS

This work was supported by DST, SERB, Government of India, via the Ramanujan fellowship (Grant SR/S2/RJN-97/2012) and Extramural Research Grant EMR/2014/000469. S.K.B., P.D., and S.N. thank UGC, CSIR, and DST for their fellowships. The authors thank S. Roy and S. Das for their contributions.

■ REFERENCES

- (1) (a) Perera, F. Pollution from Fossil-Fuel Combustion is the Leading Environmental Threat to Global Pediatric Health and Equity: Solutions Exist. *Int. J. Environ. Res. Public Health* **2018**, *15*, 16. (b) *Cost and Performance Baseline for Fossil Energy Plants, Vol. 1: Revision 3*; National Energy Technology Laboratory: Albany, OR, 2015; p 240.
- (2) (a) Patai, S. *The Chemistry of Acid Derivatives*; Wiley: New York, 1992. (b) Goossen, L. J.; Rodríguez, N.; Goßen, K. Carboxylic acids as substrates in homogeneous catalysis. *Angew. Chem., Int. Ed.* **2008**, *47*, 3100–3120. (c) Maag, H. In *Prodrugs: Challenges and Rewards*

Part 1; Stella, V. J., Borchardt, R. T., Hageman, M. J., Oliyai, R., Maag, H., Tilley, J. W., Eds.; Springer: New York, 2007; pp 703–729.

(3) For recent reviews, see: (a) Kielland, N.; Whiteoak, C. J.; Kleij, A. W. Stereoselective Synthesis with Carbon Dioxide. *Adv. Synth. Catal.* **2013**, *355*, 2115–2138. (b) Liu, Q.; Wu, L.; Jackstell, R.; Beller, M. Using carbon dioxide as a building block in organic synthesis. *Nat. Commun.* **2015**, *6*, 5933–5947. (c) Fujihara, T.; Tsuji, Y. Cobalt- and rhodium-catalyzed carboxylation using carbon dioxide as the C1 source. *Beilstein J. Org. Chem.* **2018**, *14*, 2435–2460. (d) Seo, H.; Nguyen, L. V.; Jamison, T. F. Using Carbon Dioxide as a Building Block in Continuous Flow Synthesis. *Adv. Synth. Catal.* **2019**, *361*, 247–264. For selected examples, see: (e) Fujihara, T.; Nogi, K.; Xu, T.; Terao, J.; Tsuji, Y. Nickel-Catalyzed Carboxylation of Aryl and Vinyl Chlorides Employing Carbon Dioxide. *J. Am. Chem. Soc.* **2012**, *134*, 9106–9109. (f) Moragas, T.; Cornella, J.; Martin, R. Ligand-Controlled Regiodivergent Ni-Catalyzed Reductive Carboxylation of Allyl Esters with CO₂. *J. Am. Chem. Soc.* **2014**, *136*, 17702–17705. (g) Liu, Y.; Cornella, J.; Martin, R. Ni-Catalyzed Carboxylation of Unactivated Primary Alkyl Bromides and Sulfonates with CO₂. *J. Am. Chem. Soc.* **2014**, *136*, 11212–11215. (h) Correa, A.; Leon, T.; Martin, R. Ni-Catalyzed Carboxylation of C(sp²)- and C(sp³)-O Bonds with CO₂. *J. Am. Chem. Soc.* **2014**, *136*, 1062–1069. (i) Wang, X.; Liu, Y.; Martin, R. Ni-Catalyzed Divergent Cyclization/Carboxylation of Unactivated Primary and Secondary Alkyl Halides with CO₂. *J. Am. Chem. Soc.* **2015**, *137*, 6476–6479. (j) Nogi, K.; Fujihara, T.; Terao, J.; Tsuji, Y. Cobalt- and Nickel-Catalyzed Carboxylation of Alkenyl and Sterically Hindered Aryl Triflates Utilizing CO₂. *J. Org. Chem.* **2015**, *80*, 11618–11623. (k) Börjesson, M.; Moragas, T.; Martin, R. Ni-Catalyzed Carboxylation of Unactivated Alkyl Chlorides with CO₂. *J. Am. Chem. Soc.* **2016**, *138*, 7504–7507. (l) Rebih, F.; Andreini, M.; Moncomble, A.; Harrison-Marchand, A.; Maddaluno, J.; Durandetti, M. Direct Carboxylation of Aryl Tosylates by CO₂ Catalyzed by In situ-Generated Ni⁰. *Chem. - Eur. J.* **2016**, *22*, 3758–3763. (m) Moragas, T.; Gaydou, M.; Martin, R. Nickel-Catalyzed Carboxylation of Benzylic C-N Bonds with CO₂. *Angew. Chem., Int. Ed.* **2016**, *55*, 5053–5057. (n) Li, Y.; Cui, X.; Dong, K.; Junge, K.; Beller, M. Utilization of CO₂ as a C1 Building Block for Catalytic Methylation Reactions. *ACS Catal.* **2017**, *7*, 1077–1086.

(4) For recent reviews, see: (a) Zhang, L.; Hou, Z. N-Heterocyclic carbene (NHC)-copper-catalyzed transformations of carbon dioxide. *Chem. Sci.* **2013**, *4*, 3395–3403. (b) Tortajada, A.; Juliá-Hernández, F.; Börjesson, M.; Moragas, T.; Martin, R. Transition-Metal-Catalyzed Carboxylation Reactions with Carbon Dioxide. *Angew. Chem., Int. Ed.* **2018**, *57*, 15948–15982. (c) Hou, J.; Li, J.-S.; Wu, J. Recent Development of Light-Mediated Carboxylation Using CO₂ as the Feedstock. *Asian J. Org. Chem.* **2018**, *7*, 1439–1447. For recent selected catalytic carboxylation examples, see: (d) Fujihara, T.; Xu, T.; Semba, K.; Terao, J.; Tsuji, Y. Copper-Catalyzed Hydrocarboxylation of Alkynes Using Carbon Dioxide and Hydrosilanes. *Angew. Chem., Int. Ed.* **2011**, *50*, 523–527. (e) Mizuno, H.; Takaya, J.; Iwasawa, N. Rhodium(I)-Catalyzed Direct Carboxylation of Arenes with CO₂ via Chelation-Assisted C-H Bond Activation. *J. Am. Chem. Soc.* **2011**, *133*, 1251–1253. (f) Li, S.; Yuan, W.; Ma, S. Highly Regio- and Stereoselective Three-Component Nickel-Catalyzed syn-Hydrocarboxylation of Alkynes with Diethyl Zinc and Carbon Dioxide. *Angew. Chem., Int. Ed.* **2011**, *50*, 2578–2582. (g) Sasano, K.; Takaya, J.; Iwasawa, N. Palladium(II)-Catalyzed Direct Carboxylation of Alkenyl C-H Bonds with CO₂. *J. Am. Chem. Soc.* **2013**, *135*, 10954–10957. (h) León, T.; Correa, A.; Martin, R. Ni-Catalyzed Direct Carboxylation of Benzyl Halides with CO₂. *J. Am. Chem. Soc.* **2013**, *135*, 1221–1224. (i) Mita, T.; Higuchi, Y.; Sato, Y. Highly Regioselective Palladium-Catalyzed Carboxylation of Allylic Alcohols with CO₂. *Chem. - Eur. J.* **2015**, *21*, 16391–16394.

(5) For electrochemical carboxylation, see: (a) Amatore, C.; Jutand, A.; Khalil, F.; Nielsen, M. F. Carbon Dioxide as a C1 Building Block. Mechanism of Palladium-Catalyzed Carboxylation of Aromatic Halides. *J. Am. Chem. Soc.* **1992**, *114*, 7076–7085. (b) Jutand, A.; Négri, S. Activation of Aryl and Vinyl Triflates by Palladium and

Electron Transfer-Electrosynthesis of Aromatic and α,β -Unsaturated Carboxylic Acids from Carbon Dioxide. *Eur. J. Org. Chem.* **1998**, *1998*, 1811–1821.

(6) For recent reviews and examples of photoredox/transition metal catalysis, see: (a) Prier, C. K.; Rankic, D. A.; MacMillan, D. W. C. Visible Light Photoredox Catalysis with Transition Metal Complexes: Applications in Organic Synthesis. *Chem. Rev.* **2013**, *113*, 5322–5363. (b) Fabry, D. C.; Rueping, M. Merging Visible Light Photoredox Catalysis with Metal Catalyzed C-H Activations: On the Role of Oxygen and Superoxide Ions as Oxidants. *Acc. Chem. Res.* **2016**, *49*, 1969–1979. (c) Hopkinson, M. N.; Tlahuext-Aca, A.; Glorius, F. Merging Visible Light Photoredox and Gold Catalysis. *Acc. Chem. Res.* **2016**, *49*, 2261–2272. (d) Ye, Y.; Sanford, M. S. Merging Visible-Light Photocatalysis and Transition-Metal Catalysis in the Copper-Catalyzed Trifluoromethylation of Boronic Acids with CF₃I. *J. Am. Chem. Soc.* **2012**, *134*, 9034–9037. (e) Fabry, D. C.; Zoller, J.; Raja, S.; Rueping, M. Combining Rhodium and Photoredox Catalysis for C-H Functionalizations of Arenes: Oxidative Heck Reactions with Visible Light. *Angew. Chem., Int. Ed.* **2014**, *53*, 10228–10231. (f) Fabry, D. C.; Ronge, M. A.; Zoller, J.; Rueping, M. C-H Functionalization of Phenols Using Combined Ruthenium and Photoredox Catalysis: In Situ Generation of the Oxidant. *Angew. Chem., Int. Ed.* **2015**, *54*, 2801–2805. (g) Xie, J.; Zhang, T.; Chen, F.; Mehrkens, N.; Rominger, F.; Rudolph, M.; Hashmi, A. S. K. Gold-Catalyzed Highly Selective Photoredox C(sp²)-H Difluoroalkylation and Perfluoroalkylation of Hydrazones. *Angew. Chem., Int. Ed.* **2016**, *55*, 2934–2938. (h) Xie, J.; Rudolph, M.; Rominger, F.; Hashmi, A. S. K. Photoredox-Controlled Mono- and Di-Multifluoroarylation of C(sp³)-H Bonds with Aryl Fluorides. *Angew. Chem., Int. Ed.* **2017**, *56*, 7266–7270. (i) Marzo, L.; Pagire, S. K.; Reiser, O.; König, B. Visible-Light Photocatalysis: Does It Make a Difference in Organic Synthesis? *Angew. Chem., Int. Ed.* **2018**, *57*, 10034–10072. (j) Yue, H.; Zhu, C.; Rueping, M. Cross-Coupling of Sodium Sulfonates with Aryl, Heteroaryl, and Vinyl Halides by Nickel/Photoredox Dual Catalysis. *Angew. Chem., Int. Ed.* **2018**, *57*, 1371–1375. (k) Zheng, J.; Breit, B. Regiodivergent Hydroaminoalkylation of Alkynes and Allenes by a Combined Rhodium and Photoredox Catalytic System. *Angew. Chem., Int. Ed.* **2019**, *58*, 3392–3397. (l) Kalyani, D.; McMurtrey, K. B.; Neufeldt, S. R.; Sanford, M. S. Room-Temperature C-H Arylation: Merger of Pd-Catalyzed C-H Functionalization and Visible-Light Photocatalysis. *J. Am. Chem. Soc.* **2011**, *133*, 18566–18569. (m) Shu, X.-Z.; Zhang, M.; He, Y.; Frei, H.; Toste, F. D. Dual Visible Light Photoredox and Gold-Catalyzed Arylative Ring Expansion. *J. Am. Chem. Soc.* **2014**, *136*, 5844–5847. (n) Tellis, J. C.; Primer, D. N.; Molander, G. A. Dual catalysis. Single-electron transmetalation in organoboron cross-coupling by photoredox/nickel dual catalysis. *Science* **2014**, *345*, 433–436. (o) Noble, A.; McCarver, S. J.; MacMillan, D. W. C. Merging Photoredox and Nickel Catalysis: Decarboxylative Cross-Coupling of Carboxylic Acids with Vinyl Halides. *J. Am. Chem. Soc.* **2015**, *137*, 624–627. (p) Lang, S. B.; O'Nele, K. M.; Tunge, J. A. Decarboxylative Allylation of Amino Alkanoic Acids and Esters via Dual Catalysis. *J. Am. Chem. Soc.* **2014**, *136*, 13606–13609. (q) Tasker, S. Z.; Jamison, T. F. Highly Regioselective Indoline Synthesis under Nickel/Photoredox Dual Catalysis. *J. Am. Chem. Soc.* **2015**, *137*, 9531–9534. (r) Huang, H.; Jia, K.; Chen, Y. Radical Decarboxylative Functionalizations Enabled by Dual Photoredox Catalysis. *ACS Catal.* **2016**, *6*, 4983–4988. (s) Schwarz, J. L.; Schafers, F.; Tlahuext-Aca, A.; Lückemeier, L.; Glorius, F. Diastereoselective Allylation of Aldehydes by Dual Photoredox and Chromium Catalysis. *J. Am. Chem. Soc.* **2018**, *140*, 12705–12709. (t) Liao, L.-L.; Gui, Y.-Y.; Zhang, X.-B.; Shen, G.; Liu, H.-D.; Zhou, W.-J.; Li, J.; Yu, D.-G. Phosphorylation of Alkenyl and Aryl C-O Bonds via Photoredox/Nickel Dual Catalysis. *Org. Lett.* **2017**, *19*, 3735–3738. (u) Liu, N.-W.; Hofman, K.; Herbert, A.; Manolikakes, G. Visible-Light Photoredox/Nickel Dual Catalysis for the Cross-Coupling of Sulfinic Acid Salts with Aryl Iodides. *Org. Lett.* **2018**, *20*, 760–763. (v) Matsui, J. K.; Molander, G. A. Direct α -Arylation/Heteroarylation of 2-Trifluoroboratochromanones via Photoredox/Nickel Dual Catalysis. *Org. Lett.* **2017**, *19*, 436–439.

(w) Vara, B. A.; Patel, N. R.; Molander, G. A. *O*-Benzyl Xanthate Esters under Ni/Photoredox Dual Catalysis: Selective Radical Generation and $\text{Csp}^3\text{-Csp}^2$ Cross-Coupling. *ACS Catal.* **2017**, *7*, 3955–3959. (x) Karakaya, I.; Primer, D. N.; Molander, G. A. Photoredox Cross-Coupling: Ir/Ni Dual Catalysis for the Synthesis of Benzylic Ethers. *Org. Lett.* **2015**, *17*, 3294–3297. (y) Key, R. J.; Vannucci, A. K. Nickel Dual Photoredox Catalysis for the Synthesis of Aryl Amines. *Organometallics* **2018**, *37*, 1468–1472. (z) Liu, K.; Zou, M.; Lei, A. Aerobic Oxidative Carbonylation of Enamides by Merging Palladium with Photoredox Catalysis. *J. Org. Chem.* **2016**, *81*, 7088–7092.

(7) For photocatalytic carboxylation reactions, see: (a) Masuda, Y.; Ishida, N.; Murakami, M. Light-Driven Carboxylation of *o*-Alkylphenyl Ketones with CO_2 . *J. Am. Chem. Soc.* **2015**, *137*, 14063–14066. (b) Ishida, N.; Masuda, Y.; Uemoto, S.; Murakami, M. A Light/Ketone/Copper System for Carboxylation of Allylic C-H Bonds of Alkenes with CO_2 . *Chem. - Eur. J.* **2016**, *22*, 6524–6527. (c) Seo, H.; Katcher, M. H.; Jamison, T. F. Photoredox activation of carbon dioxide for amino acid synthesis in continuous flow. *Nat. Chem.* **2017**, *9*, 453–456. (d) Murata, K.; Numasawa, N.; Shimomaki, K.; Takaya, J.; Iwasawa, N. Construction of a visible light-driven hydrocarboxylation cycle of alkenes by the combined use of Rh(I) and photoredox catalysts. *Chem. Commun.* **2017**, *53*, 3098–3101. (e) Hou, J.; Ee, A.; Feng, W.; Xu, J.-H.; Zhao, Y.; Wu, J. Visible-Light-Driven Alkyne Hydro-/Carboxylation Using CO_2 via Iridium/Cobalt Dual Catalysis for Divergent Heterocycle Synthesis. *J. Am. Chem. Soc.* **2018**, *140*, 5257–5263. (f) Hou, J.; Ee, A.; Cao, H.; Ong, H.-W.; Xu, J.-H.; Wu, J. Visible-Light-Mediated Metal-Free Difunctionalization of Alkenes with CO_2 and Silanes or $\text{C}(\text{sp}^3)\text{-H}$ Alkanes. *Angew. Chem., Int. Ed.* **2018**, *57*, 17220–17224.

(8) Shimomaki, K.; Murata, K.; Martin, R.; Iwasawa, N. Visible-Light-Driven Carboxylation of Aryl Halides by the Combined Use of Palladium and Photoredox Catalysts. *J. Am. Chem. Soc.* **2017**, *139*, 9467–9470.

(9) Meng, Q.-Y.; Wang, S.; König, B. Carboxylation of Aromatic and Aliphatic Bromides and Triflates with CO_2 by Dual Visible-Light-Nickel Catalysis. *Angew. Chem., Int. Ed.* **2017**, *56*, 13426–13430.

(10) Ma, C.; Zhao, C.-Q.; Xu, X.-T.; Li, Z.-M.; Wang, X.-Y.; Zhang, K.; Mei, T.-S. Nickel-Catalyzed Carboxylation of Aryl and Heteroaryl Fluorosulfates Using Carbon Dioxide. *Org. Lett.* **2019**, *21*, 2464–2467.

(11) Wayland, B. B.; Schramm, R. F. Cationic and Neutral Chloride Complexes of Palladium(II) with the Nonaqueous Solvent Donors Acetonitrile, Dimethyl Sulfoxide, and a Series of Amides. Mixed Sulfur and Oxygen Coordination Sites in a Dimethyl Sulfoxide Complex. *Inorg. Chem.* **1969**, *8*, 971–976.

(12) Ramirez, N. P.; Bosque, I.; Gonzalez-Gomez, J. C. Photocatalytic Dehydrogenative Lactonization of 2-Arylbenzoic Acids. *Org. Lett.* **2015**, *17*, 4550–4553.

(13) (a) Piskin, S.; Uzunali, E. A review of the use of adapalene for the treatment of acne vulgaris. *Ther. Clin. Risk Manage.* **2007**, *3*, 621–624. (b) Rolewski, S. L. Clinical review: topical retinoids. *Dermatology Nursing* **2003**, *15*, 447–450, 459–465.

(14) Liu, Z.; Xiang, J. A High Yield and Pilot-Scale Process for the Preparation of Adapalene. *Org. Process Res. Dev.* **2006**, *10*, 285–288.

(15) (a) Gniadecki, R.; Assaf, C.; Bagot, M.; Dummer, R.; Duvic, M.; Knobler, R.; Ranki, A.; Schwandt, P.; Whittaker, S. The optimal use of bexarotene in cutaneous T-cell lymphoma. *Br. J. Dermatol.* **2007**, *157*, 433–440. (b) Panchal, M. R.; Scarisbrick, J. J. The utility of bexarotene in mycosis fungoides and Sézary syndrome. *Oncotargets Ther.* **2015**, *8*, 367–373.

(16) (a) Rotstein, B. H.; Hooker, J. M.; Woo, J.; Collier, T. L.; Brady, T. J.; Liang, S. H.; Vasdev, N. Synthesis of $[^{11}\text{C}]$ bexarotene by Cu-mediated $[^{11}\text{C}]$ carbon dioxide fixation and preliminary PET imaging. *ACS Med. Chem. Lett.* **2014**, *5*, 668–672. (b) Shibahara, O.; Watanabe, M.; Yamada, S.; Akehi, M.; Sasaki, T.; Akahoshi, A.; Hanada, T.; Hirano, H.; Nakatani, S.; Nishioka, H.; Takeuchi, Y.; Kakuta, H. Synthesis of ^{11}C -Labeled RXR Partial Agonist 1-[(3,5,5,8,8-Pentamethyl-5,6,7,8-tetrahydronaphthalen-2-yl)amino]

benzotriazole-5-carboxylic Acid (CBt-PMN) by Direct $[^{11}\text{C}]$ Carbon Dioxide Fixation via Organolithiation of Trialkyltin Precursor and PET Imaging Thereof. *J. Med. Chem.* **2017**, *60*, 7139–7145.

(17) (a) Lian, Z.; Nielsen, D. U.; Lindhardt, A. T.; Daasbjerg, K.; Skrydstrup, T. Cooperative redox activation for carbon dioxide conversion. *Nat. Commun.* **2016**, *7*, 13782. (b) Nielsen, D. B.; Wahlqvist, B. A.; Nielsen, D. U.; Daasbjerg, K.; Skrydstrup, T. Utilizing Glycerol as an Ex Situ CO -Source in Pd-Catalyzed Alkoxycarbonylation of Styrenes. *ACS Catal.* **2017**, *7*, 6089–6093. (c) Nielsen, D. U.; Hu, X.-M.; Daasbjerg, K.; Skrydstrup, T. Chemically and electrochemically catalysed conversion of CO_2 to CO with follow-up utilization to value-added chemicals. *Nature Catalysis* **2018**, *1*, 244–254.

(18) Perry, G. J. P.; Quibell, J. M.; Panigrahi, A.; Larrosa, I. Transition-Metal-Free Decarboxylative Iodination: New Routes for Decarboxylative Oxidative Cross-Couplings. *J. Am. Chem. Soc.* **2017**, *139*, 11527–11536.

(19) (a) Alper, E.; Yuksel Orhan, O. CO_2 utilization: Developments in conversion processes. *Petroleum* **2017**, *3*, 109–126. (b) Pan, S.-Y.; Chiang, P.-C.; Pan, W.; Kim, H. Advances in state-of-art valorization technologies for captured CO_2 toward sustainable carbon cycle. *Crit. Rev. Environ. Sci. Technol.* **2018**, *48*, 471–534.

(20) For oxidative addition, see: (a) Jutand, A.; Mosleh, A. Rate and Mechanism of Oxidative Addition of Aryl Triflates to Zerovalent Palladium Complexes. Evidence for the Formation of Cationic (σ -Aryl)palladium Complexes. *Organometallics* **1995**, *14*, 1810–1817. (b) Hutt, J. T.; Wolfe, J. P. Synthesis of 2,3-dihydrobenzofurans via the palladium catalyzed carboalkoxylation of 2-allylphenols. *Org. Chem. Front.* **2016**, *3*, 1314–1318. (c) Pye, D. R.; Mankad, N. P. Bimetallic catalysis for C–C and C–X coupling reactions. *Chem. Sci.* **2017**, *8*, 1705–1718.

(21) Xuan, J.; Zeng, T.-T.; Feng, Z.-J.; Deng, Q.-H.; Chen, J.-R.; Lu, L.-Q.; Xiao, W.-J.; Alper, H. Redox-Neutral α -Allylation of Amines by Combining Palladium Catalysis and Visible-Light Photoredox Catalysis. *Angew. Chem., Int. Ed.* **2015**, *54*, 1625–1628.

(22) Lowry, M. S.; Goldsmith, J. I.; Slinker, J. D.; Rohl, R.; Pascal, R. A., Jr.; Malliaras, G. G.; Bernhard, S. Single-Layer Electroluminescent Devices and Photoinduced Hydrogen Production from an Ionic Iridium(III) Complex. *Chem. Mater.* **2005**, *17*, 5712–5719.

(23) (a) Chatterjee, T.; Iqbal, N.; You, Y.; Cho, E. J. Controlled Fluoroalkylation Reactions by Visible-Light Photoredox Catalysis. *Acc. Chem. Res.* **2016**, *49*, 2284–2294. (b) Magallanes, G.; Kärkäs, M. D.; Bosque, I.; Lee, S.; Maldonado, S.; Stephenson, C. R. J. Selective C–O Bond Cleavage of Lignin Systems and Polymers Enabled by Sequential Palladium-Catalyzed Aerobic Oxidation and Visible-Light Photoredox Catalysis. *ACS Catal.* **2019**, *9*, 2252–2260.

(24) For an alternative mechanistic possibility, see the [Supporting Information \(Schemes S1 and S2\)](#).

Cite this: *Chem. Sci.*, 2022, 13, 5726

All publication charges for this article have been paid for by the Royal Society of Chemistry

A directing group switch in copper-catalyzed electrophilic C–H amination/migratory annulation cascade: divergent access to benzimidazolone/benzimidazole†

Hasina Mamataj Begam, Shantanu Nandi and Ranjan Jana *

We present here a copper-catalyzed electrophilic *ortho* C–H amination of protected naphthylamines with *N*-(benzoxy)amines, cyclization with the pendant amide, and carbon to nitrogen 1,2-directing group migration cascade to access *N,N*-disubstituted 2-benzimidazolones. Remarkably, this highly atom-economic tandem reaction proceeds through a C–H and C–C bond cleavage and three new C–N bond formations in a single operation. Intriguingly, the reaction cascade was altered by the subtle tuning of the directing group from picolinamide to thiopicolinamide furnishing 2-heteroaryl-imidazoles *via* the extrusion of hydrogen sulfide. This strategy provided a series of benzimidazolones and benzimidazoles in moderate to high yields with low catalyst loading (66 substrates with yields up to 99%). From the control experiments, it was observed that after the C–H amination an incipient tetrahedral oxyanion or thiolate intermediate is formed *via* an intramolecular attack of the primary amine to the amide/thioamide carbonyl. It undergoes either a 1,2-pyridyl shift with the retention of the carbonyl moiety or H₂S elimination for scaffold diversification. Remarkably, in spite of a positive influence of copper in the reaction outcome, from our preliminary investigations, the benzimidazolone product was obtained in good to moderate yields in two steps under metal-free conditions. The *N*-pyridyl moiety of the benzimidazolone was removed for further manipulation of the free NH group.

Received 10th March 2022
Accepted 13th April 2022

DOI: 10.1039/d2sc01420c

rsc.li/chemical-science

Introduction

At the threshold of an era of automated organic synthesis, the cascade reaction encompassing C–H activation is emerging as a powerful tool for the rapid construction and late-stage diversification of functional molecules in a step- and atom-economic manner.¹ In this cascade process, a command to control chemoselectivity using an inherent chemical reporter enables to achieve rapid molecular diversity.² However, the introduction and removal of directing groups is one of the major drawbacks in chelation-assisted C–H functionalization.³ To circumvent, transient, traceless, and inherent directing group strategies were unveiled.⁴ Very recently, the migration and incorporation of a directing group into the target molecule has emerged as a practical strategy in transition metal-catalyzed C–H functionalization to access rapid molecular complexity maximizing atom-economy.⁵ In this direction, cobalt and rhodium-catalyzed

stereoselective syntheses of tetra-substituted alkenes were reported through the migration of the directing group.⁶ The Ackermann group reported a cobalt-catalyzed pyridine-directing group migration/annulation cascade in C–H activation.⁷ The Wang group reported manganese-catalyzed C–H activation/enaminylation/DG migration cascade in an *N*-pyridyl protected indole system.⁸ The Huang group demonstrated a multitasking directing group strategy for structural diversification in C–H activation cascade.⁹ Very recently, the Li group reported a Pd-catalyzed domino C4-arylation/3,2-carbonyl directing group migration in indoles.¹⁰ To the best of our knowledge, there is no report of a single atom of a directing group (O *vs.* S) switch for scaffold diversification exploiting their innate reactivity in the C–H functionalization/annulation cascade. Benzimidazolone and benzimidazole are prevalent in pharmaceuticals, agrochemicals, pigments, herbicides, and fine chemicals (Fig. 1).¹¹ The synthesis of these privileged scaffolds primarily relies on *ortho*-phenylenediamine or *ortho*-haloanilines.¹² Recently, the oxidative annulation of anilides/aniline is emerging as an attractive strategy for expanding the substrate scope.¹³ The Zhang group reported the copper-catalyzed synthesis of benzimidazolones and benzimidazoles exploiting the SOMO-stabilized radical cation of diarylamines (Scheme 1a).¹⁴ The electrophilic C–H amination has emerged as

Organic and Medicinal Chemistry Division, CSIR-Indian Institute of Chemical Biology, 4 Raja S. C. Mullick Road, Jadavpur, Kolkata-700032, West Bengal, India. E-mail: rjana@iicb.res.in

† Electronic supplementary information (ESI) available: Optimization details, general procedures, spectral data, crystal data, NMR experiments. CCDC 2025266, 2025269, 2025275, 2025279 and 2025280. For ESI and crystallographic data in CIF or other electronic format see <https://doi.org/10.1039/d2sc01420c>



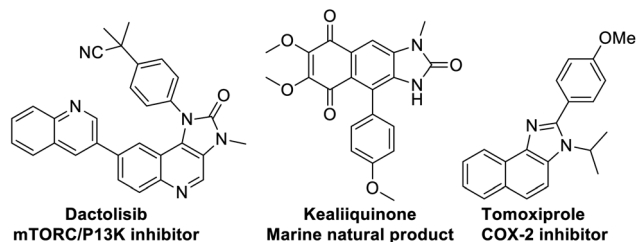
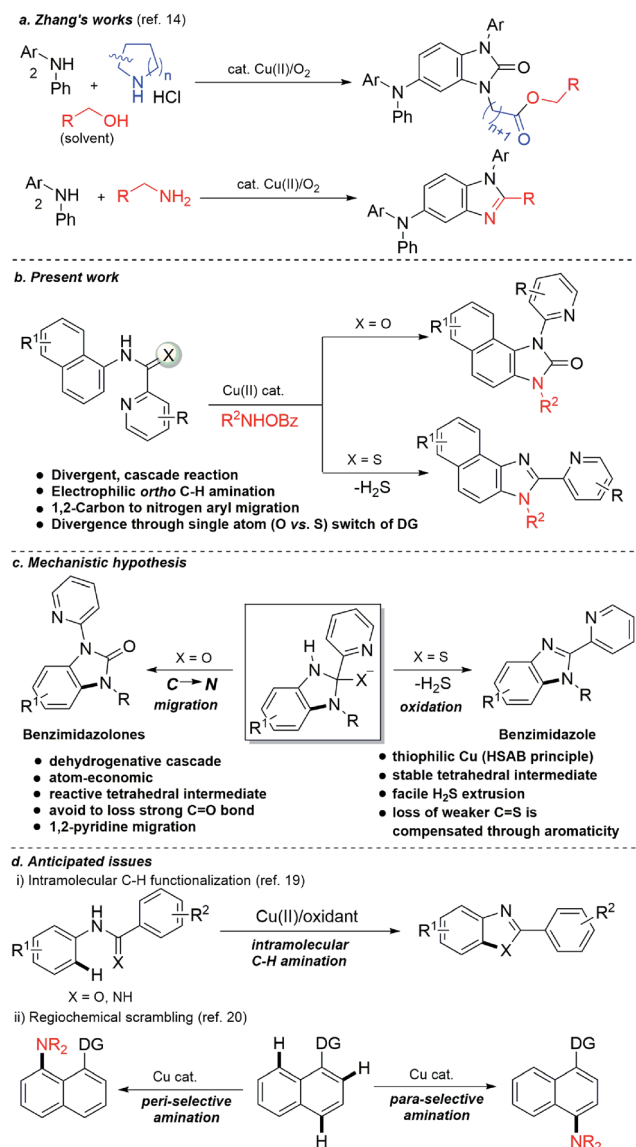


Fig. 1 Biologically important imidazolone/imidazole core.



Scheme 1 Cascade synthesis of benzimidazole and benzimidazolones.

a benign alternative to construct *N*-heterocycles under mild conditions.¹⁵ Although a Ru(II)-catalyzed O → N migration during benzimidazole to benzimidazolone conversion is reported,¹⁶ direct C-2 aryl migration is not reported. We disclose here a novel single atom of a directing group switch strategy for

the chemoselective synthesis of 1,3-dihydro-2*H*-naphtho[1,2-*d*]imidazole-2-one *via* electrophilic *ortho* C-H amination, intramolecular cyclization, C → N 1,2-pyridyl shift or 2-(pyridin-2-yl)-3*H*-naphtho[1,2-*d*]imidazole derivatives through an electrophilic C-H amination/annulation cascade (Scheme 1b).

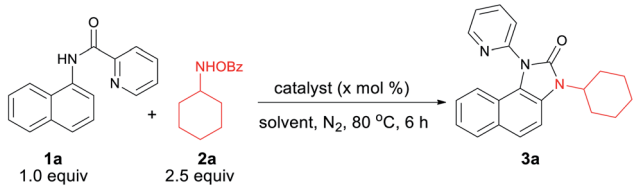
Contrary to the previous procedures, we observed an excellent reactivity of the bicyclic system towards electrophilic *ortho* C-H amination with secondary amines under our optimized reaction condition.¹⁷ We hypothesized that C-H amination with primary amine may initiate an annulation cascade *via* subsequent addition to the picolinamide directing group. The incipient oxyanion may trigger the 1,2-migration of the directing group to provide benzimidazolone. Instead, thiophilic copper may endorse the extrusion of hydrogen sulfide to provide benzimidazole from the corresponding thioamide directing group (Scheme 1c). However, (1) copper-catalyzed C-H amination with a primary amine is a formidable challenge due to the catalyst inhibition;¹⁸ (2) a deleterious intramolecular oxidative cyclization of the corresponding directing group may impede the cascade process¹⁹ (Scheme 1d(i)); (3) competing *peri*- and *para*-C-H amination of naphthalene should be suppressed²⁰ (Scheme 1d(ii)). Furthermore, C-H amination with aliphatic primary amines is challenging and less explored.²¹

Results and discussion

We hypothesized that C-H amination with electrophilic primary amine surrogates may overcome the catalyst inhibition problem. To test our hypothesis, picolinamide-protected 1-naphthylamine **1a**, and 1.0 equiv. of *O*-benzoylhydroxylamine **2a** was subjected to our previous reaction condition to afford the expected imidazolone product **3a** in 44% yield. In the course of further optimization, DMSO was found to be the optimal solvent and excellent yields of this tandem reaction, *e.g.*, 93% and 87% were obtained with just 5.0 and 1.0 mol% catalyst loading, respectively (Table 1). Other copper catalysts, lower reaction temperature, and 1.2 equiv. of **2a** provided inferior results. Free primary amines along with external oxidants such as PIDA, K₂S₂O₈ or Bz₂O₂ were able to furnish the desired product in <5%, 12% and 32% yields, respectively. Using 1.2 equiv. of **2a** along with 1.0 equiv. Bz₂O₂ the yield was dropped to 58%. Other metal catalysts such as Pd(OAc)₂, Co(OAc)₂, Ni(OAc)₂, Mn(OAc)₂, FeCl₂, and FeBr₂ were less or ineffective for this transformation (for detailed optimization, see the ESI†). Other aminating reagents such as anthranil, benzisoxazole, or oxime esters under the same condition could not afford any desired product.

Under the optimized reaction condition, cyclic as well as acyclic primary amines furnished the desired products in good to high yields (Table 2). Cyclohexylamine provided an excellent 93% yield of the desired product (**3a**), whereas cyclopentyl, cycloheptyl, and cyclooctylamines afforded slightly lower 78%, 65%, and 46% yields, respectively (**3b–3d**). In the case of acyclic amines, yields increased with the increase in chain length (**3e–3g**) and steric bulk. Surprisingly, sterically hindered *sec*-butyl (**3i**), *tert*-butyl (**3j**), adamantylamine (**3m**) provided almost quantitative yields exhibiting a positive influence of steric bulk



Table 1 Optimization of the reaction conditions^{a,b}


Entry	Catalyst	X	Oxidant	Solvent	Yield ^b (3a)
1 ^c	Cu(OAc) ₂ · H ₂ O	10	—	DMSO	44
2	Cu(OAc) ₂ · H ₂ O	10	—	H ₂ O	0
3	Cu(OAc) ₂ · H ₂ O	10	—	MeCN	39
4	Cu(OAc) ₂ · H ₂ O	10	—	Dioxane	62
5	Cu(OAc) ₂ · H ₂ O	10	—	DMSO	90
6	Cu(OAc) ₂ · H ₂ O	5	—	DMSO	93
7	Cu(OAc) ₂ · H ₂ O	2.5	—	DMSO	90
8	Cu(OAc) ₂ · H ₂ O	1.0	—	DMSO	87
9	Cu(OAc) ₂ · H ₂ O	0.5	—	DMSO	72
10 ^d	Cu(OAc) ₂ · H ₂ O	0	—	DMSO	0
11 ^e	Cu(OAc) ₂ · H ₂ O	2.5	—	DMSO	56
12	Cu powder	5	—	DMSO	83
13 ^f	Cu(OAc) ₂ · H ₂ O	10	PIDA	DMSO	>5
14 ^g	Cu(OAc) ₂ · H ₂ O	10	Bz ₂ O ₂	DMSO	58
15	Pd(OAc) ₂	10	—	DMSO	>5
16	Co(OAc) ₂	10	—	DMSO	20

^a All reactions were carried out on a 0.2 mmol scale. ^b Yields refer to here are overall isolated yields. ^c 1.0 equiv. **2a** was used. ^d 25% *ortho* aminated product was obtained. ^e Reaction was performed at room temperature. ^f Free amine was used as amine source and 2.5 equiv. PIDA as oxidant. ^g 1.0 equiv. Bz₂O₂ and 1.2 equiv. of **2a** were used.

of amines on the rearrangement cascade. Competition experiment of **1a** with **2m** and **2n** afforded **3m** and **3n** in 70% and 28%, respectively. Several substituted 1-naphthylamines including methyl substitution at the C8 position provided high to excellent yields of the desired products (**3q–3y**). Heterocyclic amino quinoline and isoquinoline provided the rearranged product in excellent yields (**3z**, **3aa**). Delightedly, diverse (2-*N*-heteroaryl) anilides serve as excellent directing groups and are incorporated into the benzimidazolones (**3ac–3ah**). Interestingly, 3-methyl picolinamide provided the corresponding *N*-pyridyl product (**3ac**) *via ipso*-substitution. Similarly, the amides of 5-methyl pyrazinoic (**3ad**, CCDC 2025269), quinaldic (**3ae**), and pyrazinoic acid (**3af**, **3ag**) also furnished in comparable yields. Isoquinoline-1-carbamide provided a mixture of benzimidazolone **3ah** and C–H amination product **3ah'**. This may be the result of an unfavourable tetrahedral intermediate due to steric reasons. 6-Aminoquinoline provided the C–H amination at the C5 position. Furthermore, sterically less hindered methyl amine provided a corresponding 2-pyridylbenzimidazole (**3aj**, CCDC 2025266), imparting the role of steric and trajectory of the C–H amination on the subsequent rearrangement reaction.

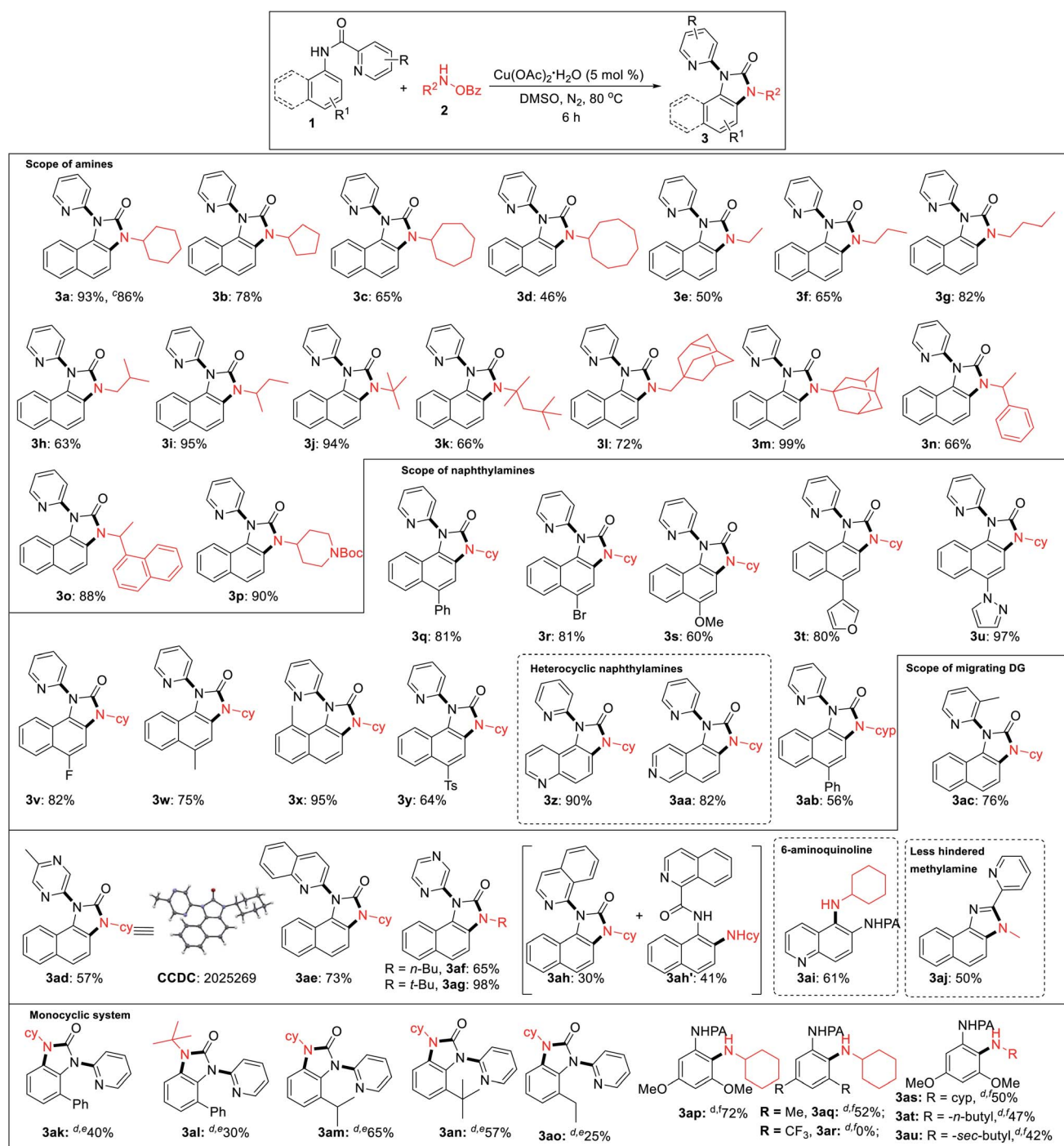
We performed the reaction with various *ortho*, *meta*, *para*-substituted anilines under the same condition and successfully we got 30% rearranged product in 2-phenyl aniline and *ortho* amination product (35%) in a 3,5-dimethoxy aniline system. After getting these results, we turned our attention to optimize

these reactions (for detailed optimization; see the ESI†). After several screenings of solvents, base or acid additives, ligands there was no significant improvement in the rearrangement reaction of 2-phenyl aniline picolinamide. Increasing temperature to 100 °C product yield increased to 40%. Then, we performed the reaction in different *ortho*-substituted anilines (electron-donating bulky groups) to obtain rearranged benzimidazolones in moderate to good yields (**3ak–3ao**). Finally, we were able to get an *ortho* C–H amination product in 3,5-dimethoxy aniline with 72% yield at 90 °C using 2.0 equiv. LiO^tBu (**3ap**). While 3,5-dimethyl substituted picolinamide furnished the C–H amination product in 52% yield, the corresponding 3,5-bis(trifluoromethyl)aniline substrate remained unreactive indicating a profound role of electronic nature (**3aq**, **3ar**). Besides cyclohexylamine, other amines also afforded the *ortho* C–H amination products in moderate yields (**3as–3au**). However, no benzimidazolones were formed even at a low catalyst loading or additives, suggesting that an *ortho* substitution w.r.t. picolinamide is crucial for the subsequent rearrangement reaction.

2-Pyridylbenzimidazoles are an important class of compounds generally used as excellent ligands for metal complexation and glukokinase activator.²² We turned our attention to optimize the reaction for benzimidazole. Initially, we started the optimization of benzimidazole with **1a** and **2a**. All our efforts using different acidic solvents such as AcOH or TFE, acid additives such as BzOH, TsOH, and high temperature (120 °C) to facilitate dehydration after cyclization were in vain. Gratifyingly, the corresponding picolinimidamide afforded the imidazole product in 30% yield in 12 h. Since thioamides have been proved as excellent directing groups in Pd- or Co-catalyzed C–H functionalizations,²³ we hypothesized that thiophilic copper²⁴ may trigger the liberation of hydrogen sulfide from thioamide instead of 1,2-pyridyl migration to furnish the desired benzimidazole product. Hence, examining thio-picolinamide **4a** under the reaction condition resulted in the desired 2-pyridylbenzimidazole exclusively albeit in a low yield. After several screenings (for detailed optimization, see the ESI†), using 3.0 equiv. of **2a**, 20 mol% Cu(OAc)₂ · H₂O and 1.2 equiv. of K₂CO₃ in DMSO at 90 °C under O₂ atmosphere the desired product was obtained in 88% yield. During the optimization, we found K₂CO₃ and O₂ to be crucial otherwise yield dropped significantly.

During the substrate scope studies, we observed a positive influence of the increasing chain length of the linear amines (**5c–5d**, Table 3). Unlike imidazolones, the yields of isomeric acyclic amines decreased with the increase in α -substitution (**5d–5g**). Benzylamine, furylamine, adamantanemethylamine and 4-amino-1-boc piperidine afforded the products in moderate yields (**5h–5k**). Thioamides of 5-methyl pyrazine-2-carboxylic acid and 2-quinaldic acids also provided the imidazole product in moderate yields (**5l**, **5m**). Various substituted 1-naphthylamines at different positions also underwent the reaction providing the desired product in medium to good yields (**5n–5s**). The reaction is also reproducible on a 2.0 mmol scale demonstrating the practicability of this methodology. The



Table 2 Substrate scope of benzimidazolones^{a,b,g}

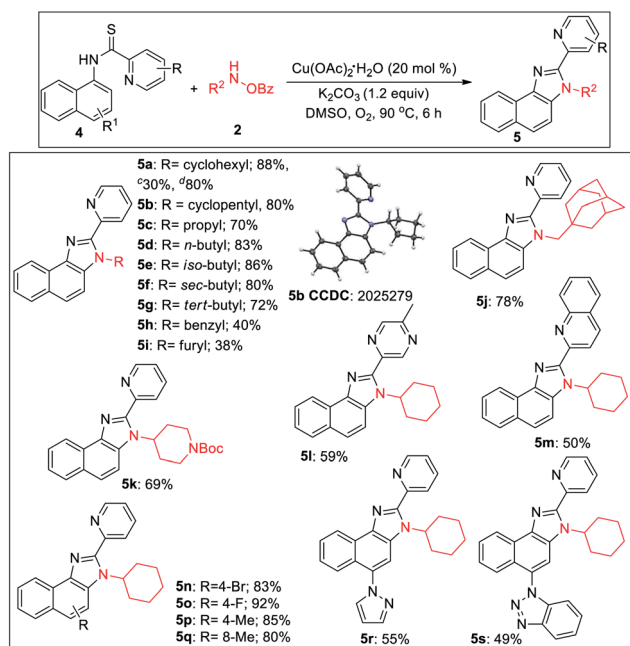
^a All reactions were carried out in 0.2 mmol scale. ^b Yields refer to the overall isolated yields with respect to **1**. ^c 2.0 mmol scale reaction. ^d 10 mol% Cu(OAc)₂·H₂O is used. ^e Reaction temperature was 100 °C. ^f Additional 2.0 equiv. LiO^tBu is used and reaction temperature was 90 °C. In the competition experiment: **1a** (0.20 mmol), **2m** (0.50 mmol), **2n** (0.50 mmol), Cu(OAc)₂·H₂O (0.01 mmol), dry DMSO (2.0 mL), N₂, 80 °C, and 6 h. ^g Reaction conditions: **1** (0.20 mmol), **2** (0.50 mmol), Cu(OAc)₂·H₂O (0.01 mmol), Dry DMSO (2.0 mL), N₂, 80 °C, and 6 h.

thio-picolinamide of monocyclic anilines under the same condition mostly oxidized to picolinamide.

Intrigued by the initial C–H amination product formation under the metal-free conditions (entry 10, Table 1), we

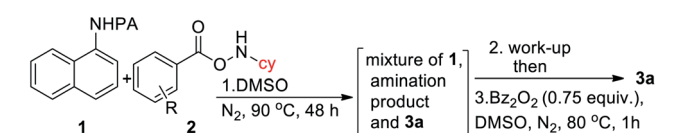
wondered whether it can be re-optimized to achieve the desired benzimidazolones. Initially, a mixture of C–H amination product **1a'**, imidazolone **3a** and unreacted starting material was obtained, which was subjected to the subsequent



Table 3 Substrate scope of benzimidazoles^{a,b,e}

^a All reactions were carried out in 0.2 mmol scale. ^b Yields refer to overall isolated yields with respect to **4**. ^c Picolinimidamide **4a'** used as substrate. ^d Reaction in 2.0 mmol scale. ^e Reaction conditions: **4** (0.20 mmol), **2** (0.60 mmol), Cu(OAc)₂·H₂O (0.04 mmol), K₂CO₃ (0.24 mmol), dry DMSO (2.0 mL), O₂, 90 °C, and 6 h.

cyclization reaction (Table 4). However, the work-up of the reaction mixture and the subsequent addition of benzoyl peroxide converted the C–H amination product to the desired

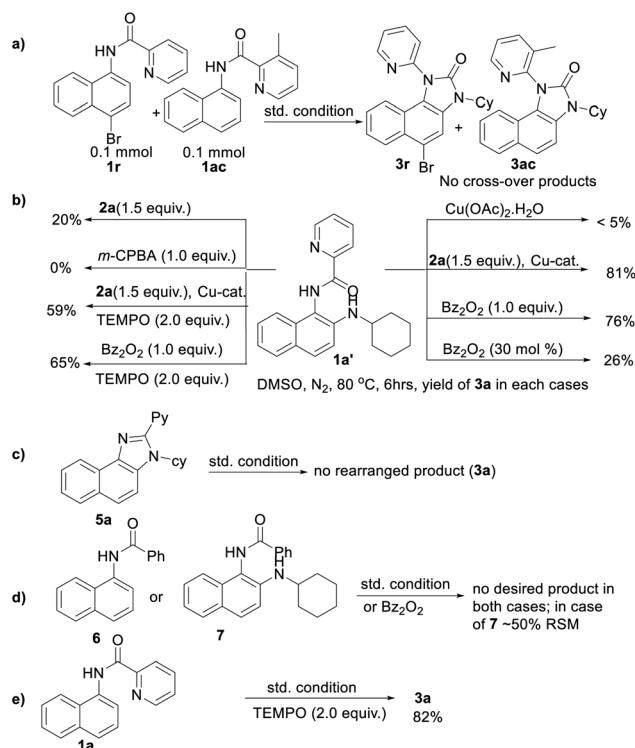
Table 4 Optimization of the metal-free condition^{a,b,e}

Entry	Amine source	Equiv. of 2	Yield ^b (%)
1	2a : R = H	2.5	25
2	2a : R = H	4.0	25
4	2a₂ : R = 4-NMe ₂	4.0	65
5	2a₃ : R = 4-CF ₃	4.0	10
6	2a₄ : R = 4- ^t Bu	4.0	20
7	2a₅ : R = 4-OMe	4.0	41
8	2a₆ : R = 3,5-di Cl	4.0	0
9	2a₇ : R = pentafluoro	4.0	25
10 ^c	2b₂ : R = 4-NMe ₂	4.0	44
11 ^d	2a₂ : R = 4-NMe ₂	4.0	70

^a All reactions were carried out on a 0.1 mmol scale. ^b Yields refer to here are isolated yields after two steps with respect to **1**. ^c Protected cyclopentylamine was used and reaction time was 12 h. ^d Substrate **1r** was used. ^e Reaction conditions: 1st step: **1** (0.10 mmol), **2** (0.40 mmol), dry DMSO (1.0 mL), N₂, 90 °C, and 48 h. 2nd step: Bz₂O₂ (0.75 equiv.), DMSO, N₂, 80 °C, and 1 h.

annulation product. Increasing the amine source **2a** to 4.0 equiv. or temperature to 90 °C did not improve the yield. Gratifyingly, varying different substituents in the phenyl ring of **2**, we observed that 4-NMe₂ substitution furnished the product in 65% yield. Protected cyclopentylamine afforded the desired product in 44% yield in 12 h. Monocyclic substrates were unreactive under metal-free conditions. Notably, the possibility of metal contamination was excluded by using all new glass-ware, freshly distilled solvents, and repeating the reaction at least four times. Although, this metal-free, two-step process has inherent limitations, we anticipate that it has profound mechanistic implications.

To gain insight into the reaction mechanism, when an equimolar mixture of **1r** and **1ac** was treated in our reaction condition, **3r** and **3ac** were formed and no cross-over product was isolated suggesting an intramolecular 1,2-pyridyl migration (Scheme 2a). Unsymmetrically-substituted 5-methyl pyrazine anilide **1ad** afforded the imidazolone product **3ad** exclusively through *ipso* C–N bond formation (Table 2). Either performing the reaction at room temperature for a shorter time or quenching the reaction after 1.5 h, a mixture of the starting material, C–H amination product **1a'**, and rearranged product were observed. Heating a preformed C–H amination product **1a'** in absence of **2a** <5% product was formed. However, a combination of copper catalyst and *O*-benzoylhydroxylamine **2a** (1.5 equiv.) or even benzoylperoxide alone furnished the desired **3a** in high yields (Scheme 2b). Therefore, besides an aminating agent, **2a** also acts as an oxidant for catalytic turnover. Furthermore, the imidazole product **5a** was not converted into the corresponding imidazolone **3a** under the



Scheme 2 Control experiments.

reaction condition, suggesting a plausible concerted cyclization/1,2-pyridyl migration pathway (Scheme 2c). In place of picolinamide **1a**, the corresponding benzanilide **6** or **7** did not furnish any desired product (Scheme 2d). **7** does not undergo any rearrangement even in the presence of Bz_2O_2 , suggesting that the pyridyl-nitrogen is not only involved in the directed C–H amination but also in the subsequent steps. In both conditions, **7** underwent decomposition with 50% starting material recovery. To examine the involvement of radicals in this C–H amination/migratory annulation cascade, we performed the reaction in the presence of 2.0 equiv. of TEMPO. The yield was slightly decreased from 93% to 82% (Scheme 2e). Further, cyclization from a pre-formed amination product **1a'** furnished an almost similar yield in the presence of TEMPO. Hence, the single electron transfer (SET) process may not be involved in the migratory cyclization step. Then, we performed the time-dependent ^1H NMR experiment to get a clue about the intermediate of the rearrangement reaction. We took **1a'** in a NMR tube in DMSO-d_6 and 1.0 equiv. of Bz_2O_2 was added to it for recording the time-dependent ^1H NMR spectra at room temperature (Fig. 2). After 5–7 min, a new peak corresponding to H_b or H_b' appeared at 8.71, which was slowly decreased and finally diminished while the desired product was formed. In this study, the chemical shift of the *ortho* proton of pyridine (H_a) in **1a'** is indicative of the formation of intermediate **VII** or **VIIa'**, which gradually shifted to more upfield in the intermediates and then in the product (H_d). It indicates that the electron-withdrawing effect of the amide-carbonyl is no longer persists in the intermediate pointing either of the intermediates **VII** or **VIIa'** (H_b or H_b'). Since the chemical shift value in the intermediate is closer to the product than the starting material, we assume that the new C–N bond may already have been formed, which is in favor of the intermediate **VIIa'** (for full spectrum, see the ESI †).

A $\text{Cu}^{\text{I}}/\text{Cu}^{\text{III}}$ cycle may be involved in this cascade reaction as reported by the Li, Gaunt, Stahl, and other groups. 25 Based on control experiments and the above literature reports, $\text{Cu}(\text{II})$ salt first undergoes disproportionation to form an active Cu^{I} species, which undergoes oxidative addition to *O*-benzoylhydroxylamine **2**

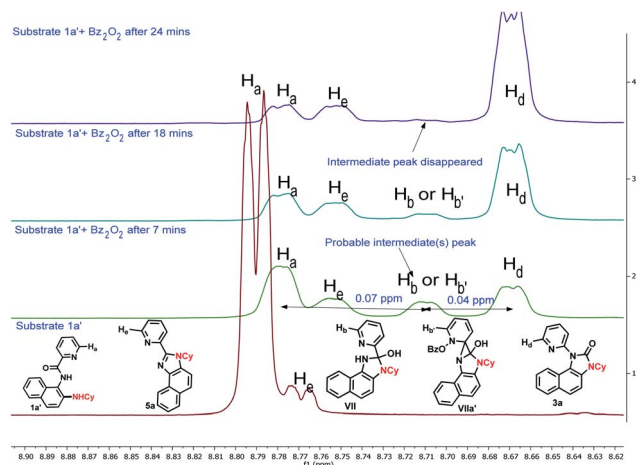
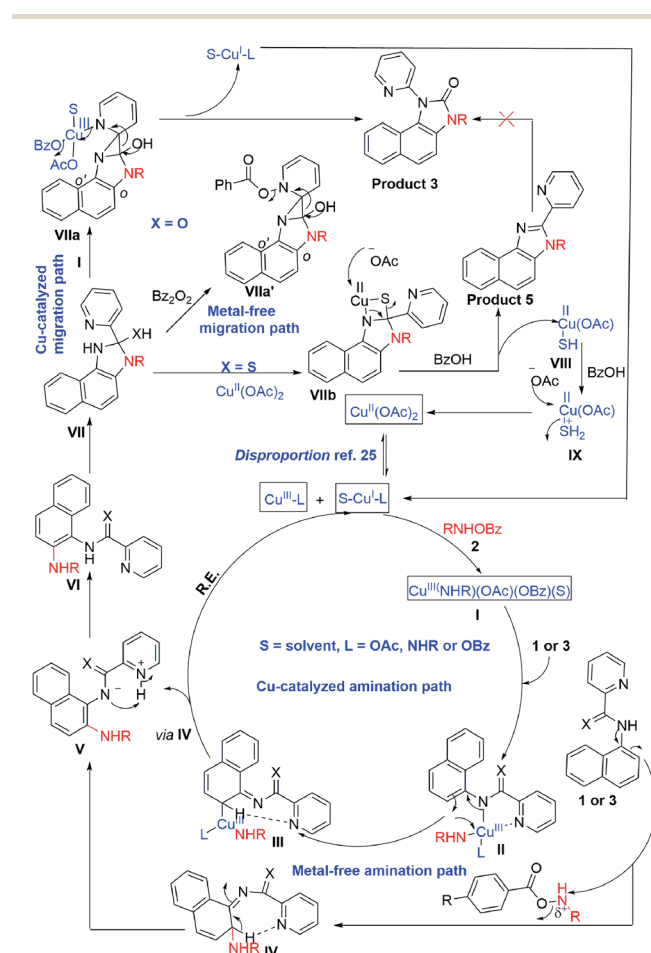


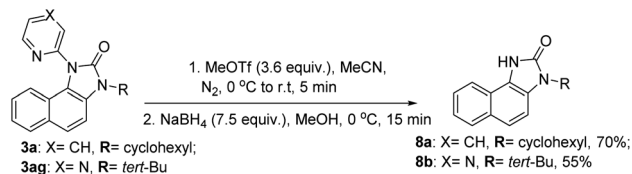
Fig. 2 Time-dependent ^1H NMR experiment.

forming a Cu^{III} complex, **I** (Scheme 3). This complex chelates with the substrate **1** or **3** forming **II**, which then undergoes electrophilic aromatic substitution type reaction generating **III**. Similarly, intermediate **IV** may also form under metal-free conditions. The pyridine of the picolinamide may work as a proton shuttle that abstracts *ortho* proton and delivers to the amide nitrogen during rearomatization through **V** providing *ortho* amination products **VI**. Next, a tetrahedral intermediate **VII** may form through the intramolecular attack of the amine moiety to the amide/thioamide carbonyl group. The nucleophilic nitrogen may attack at the *ipso* position of the pyridine moiety in the presence of the second molecule of the Cu^{III} -complex **I**, forming **VIIa** that explains the need for an excess (2.5 equiv.) amount of *O*-benzoylhydroxylamine. 26 A similar kind of an intermediate, **VIIa'** may generate in the presence of Bz_2O_2 in the metal-free pathway. This kind of a three-membered cyclic intermediate is claimed by the Feng group for aryl migration. 27 A similar $\text{O} \rightarrow \text{C}$ pyridyl migration through the de-aromatization of the pyridine ring was reported. 28 Then, a 1,2-pyridyl migration from $\text{C} \rightarrow \text{N}$ may take place to furnish the corresponding benzimidazolone product **3** and regenerates the active Cu^{I} species. **VIIa'** also furnishes the product in a similar fashion. It is further supported by the fact that electron-donating substitution (*e.g.* ethyl, isopropyl in case of



Scheme 3 Proposed reaction mechanism.





Scheme 4 Deprotection of the *N*-heteroaryls of the benzimidazolone product.

monocyclic anilines) at the *o'*-position has a positive influence in the reaction outcome. However, the *tert*-Bu group may hinder the reaction slightly due to steric inhibition. Owing to the distinct reactivity of thiol than the corresponding oxygen analogue,²⁹ a putative 4-membered cyclic intermediate **VIIb** may form with thiophilic copper from the tetrahedral thiolate intermediate (Scheme 3). Subsequently, the elimination of hydrogen sulphide provides the thermodynamically favourable benzimidazoles (**5**) regenerating Cu(II). However, the exact mechanism is not clear at this moment and warrants further studies.

Our efforts to utilize the pendant pyridine moiety for further C–H functionalization (thioarylation, alkylation) at the *peri*-position remained unsuccessful at this moment. However, to expand the synthetic utility of this migratory annulation cascade, the pyridine and pyrazine moieties were deprotected from the representative benzimidazolones (**3a**, **3ag**) using a reported condition providing **8a** and **8b** in 70% and 55% yield, respectively (Scheme 4).³⁰ The free –NH moiety can be further manipulated to achieve further molecular diversity.

Conclusions

In conclusion, we have demonstrated a directing group-dependent complete switch of product selectivity in copper-catalyzed electrophilic C–H amination with protected primary amines. The benzimidazolones are formed *via* an unprecedented electrophilic *ortho* C–H amination with primary amines, intramolecular cyclization, and 1,2-directing group migration from carbon to the nitrogen center. Remarkably, one C–H and C–C bond cleavage and three new C–N bond formations take place in a single operation in this migratory annulation cascade. Strikingly, by changing the picolinamide directing group to the corresponding thiopicolinamide, the chemoselectivity is switched to form 2-pyridylbenzimidazoles *via* the extrusion of H₂S. Inexpensive copper catalyst, scale-up synthesis, low catalyst loading, and controlled scaffold diversification are some of the practical aspects of this tandem reaction. From the preliminary studies, the benzimidazolone product was also obtained in good to moderate yields in two steps under metal-free conditions. The in-depth mechanistic studies and investigation of metal-free conditions of this divergent tandem reaction is undergoing in our laboratory.

Data availability

All experimental data is available in the ESI.† No computation component is present in this manuscript.

Author contributions

R. J. conceptualized and supervised the project and wrote the manuscript. H. M. B. performed the experiments and wrote the manuscript. S. N. analyzed the crystal structure.

Conflicts of interest

There are no conflicts to declare.

Acknowledgements

This work was supported by DST, SERB, Govt. of India, Core Research Grant No. CRG/2021/006717. HMB and SN thank CSIR and DST-Inspire respectively for their fellowships.

Notes and references

- (a) J. Wencel-Delord and F. Glorius, *Nat. Chem.*, 2013, **5**, 369–375; (b) A. Baccalini, G. Faita, G. Zanoni and D. Maiti, *Chem.–Eur. J.*, 2020, **26**, 9749–9783; (c) L. Song and E. V. Van der Eycken, *Chem.–Eur. J.*, 2021, **27**, 121–144.
- (a) T. A. Davis, T. K. Hyster and T. Rovis, *Angew. Chem., Int. Ed.*, 2013, **52**, 14181–14185; (b) J. Kim, S.-W. Park, M.-H. Baik and S. Chang, *J. Am. Chem. Soc.*, 2015, **137**, 13448–13451; (c) C. Yamamoto, K. Takamatsu, K. Hirano and M. Miura, *J. Org. Chem.*, 2017, **82**, 9112–9118.
- (a) X. Chen, K. M. Engle, D.-H. Wang and J.-Q. Yu, *Angew. Chem., Int. Ed.*, 2009, **48**, 5094–5115; (b) C. Sambigiato, D. Schönbauer, R. Blicke, T. Dao-Huy, G. Pototschnig, P. Schaaf, T. Wiesinger, M. F. Zia, J. Wencel-Delord, T. Besset, B. U. W. Maes and M. Schnürch, *Chem. Soc. Rev.*, 2018, **47**, 6603–6743; (c) R. L. Carvalho, R. G. Almeida, K. Murali, L. A. Machado, L. F. Pedrosa, P. Dolui, D. Maiti and E. N. da Silva Júnior, *Org. Biomol. Chem.*, 2021, **19**, 525–547.
- (a) G. Rani, V. Luxami and K. Paul, *Chem. Commun.*, 2020, **56**, 12479–12521; (b) J. I. Higham and J. A. Bull, *Org. Biomol. Chem.*, 2020, **18**, 7291–7315; (c) M. Font, J. M. Quibell, G. J. P. Perry and I. Larrosa, *Chem. Commun.*, 2017, **53**, 5584–5597; (d) P. Gandeepan and L. Ackermann, *Chem*, 2018, **4**, 199–222.
- (a) J. Zhang, H. Xie, H. Zhu, S. Zhang, M. Reddy Lonka and H. Zou, *ACS Catal.*, 2019, **9**, 10233–10244; (b) Z. He and Y. Huang, *ACS Catal.*, 2016, **6**, 7814–7823; (c) R. Manoharan and M. Jeganmohan, *Org. Biomol. Chem.*, 2018, **16**, 8384–8389; (d) X. Zhou, H. Xu, Q. Yang, H. Chen, S. Wang and H. Zhao, *Chem. Commun.*, 2019, **55**, 8603–8606; (e) J. Sun, G. Wang, L. Hao, J. Han, H. Li, G. Duan, G. You, F. Li and C. Xia, *ChemCatChem*, 2019, **11**, 2799–2802; (f) D. Kalsi, N. Barsu and B. Sundararaju, *Chem.–Eur. J.*, 2018, **24**, 2360–2364; (g) S. Qiu, S. Zhai, H. Wang, C. Tao, H. Zhao and H. Zhai, *Adv. Synth. Catal.*, 2018, **360**, 3271–3276; (h) Y. Wu, C. Pi, Y. Wu and X. Cui, *Chem. Soc. Rev.*, 2021, **50**, 3677–3689.
- (a) H. Ikemoto, R. Tanaka, K. Sakata, M. Kanai, T. Yoshino and S. Matsunaga, *Angew. Chem., Int. Ed.*, 2017, **56**, 7156–



- 7160; (b) X. Wu, Y. Lu, J. Qiao, W. Dai, X. Jia, H. Ni, X. Zhang, H. Liu and F. Zhao, *Org. Lett.*, 2020, **22**, 9163–9168; (c) G. Liu, Y. Shen, Z. Zhou and X. Lu, *Angew. Chem., Int. Ed.*, 2013, **52**, 6033–6037.
- 7 C. Zhu, R. Kuniyil, B. B. Jei and L. Ackermann, *ACS Catal.*, 2020, **10**, 4444–4450.
- 8 X. Zhou, Z. Li, Z. Zhang, P. Lu and Y. Wang, *Org. Lett.*, 2018, **20**, 1426–1429.
- 9 Y. Chen, D. Wang, P. Duan, R. Ben, L. Dai, X. Shao, M. Hong, J. Zhao and Y. Huang, *Nat. Commun.*, 2014, **5**, 4610.
- 10 Y. Cheng, S. Yu, Y. He, G. An, G. Li and Z. Yang, *Chem. Sci.*, 2021, **12**, 3216–3225.
- 11 (a) M. Beesu, S. S. Malladi, L. M. Fox, C. D. Jones, A. Dixit and S. A. David, *J. Med. Chem.*, 2014, **57**, 7325–7341; (b) D. B. Nale and B. M. Bhanage, *Green Chem.*, 2015, **17**, 2480–2486.
- 12 (a) S. W. Youn and Y. H. Kim, *Org. Lett.*, 2016, **18**, 6140–6143; (b) R. Zeng, P.-h. Chen and G. Dong, *ACS Catal.*, 2016, **6**, 969–973; (c) D. Li and T. Ollevier, *Org. Lett.*, 2019, **21**, 3572–3575; (d) A. J. Blacker, M. M. Farah, M. I. Hall, S. P. Marsden, O. Saidi and J. M. J. Williams, *Org. Lett.*, 2009, **11**, 2039–2042; (e) J.-P. Wan, S.-F. Gan, J.-M. Wu and Y. Pan, *Green Chem.*, 2009, **11**, 1633–1637; (f) E. Skolia, M. K. Apostolopoulou, N. F. Nikitas and C. G. Kokotos, *Eur. J. Org. Chem.*, 2021, **2021**, 422–428.
- 13 (a) Y. Park, Y. Kim and S. Chang, *Chem. Rev.*, 2017, **117**, 9247–9301; (b) J. Xia, X. Yang, Y. Li and X. Li, *Org. Lett.*, 2017, **19**, 3243–3246; (c) S. M. Khake and N. Chatani, *Org. Lett.*, 2020, **22**, 3655–3660.
- 14 (a) T. Liang, H. Zhao, L. Gong, H. Jiang and M. Zhang, *iScience*, 2019, **15**, 127–135; (b) T. Liang, Z. Tan, H. Zhao, X. Chen, H. Jiang and M. Zhang, *ACS Catal.*, 2018, **8**, 2242–2246.
- 15 (a) X. Dong, Q. Liu, Y. Dong and H. Liu, *Chem.–Eur. J.*, 2017, **23**, 2481–2511; (b) X. Yan, X. Yang and C. Xi, *Catal. Sci. Technol.*, 2014, **4**, 4169–4177; (c) M.-L. Louillat and F. W. Patureau, *Chem. Soc. Rev.*, 2014, **43**, 901–910; (d) J.-S. Yu, M. Espinosa, H. Noda and M. Shibasaki, *J. Am. Chem. Soc.*, 2019, **141**, 10530–10537.
- 16 (a) C. S. Yeung, T. H. H. Hsieh and V. M. Dong, *Chem. Sci.*, 2011, **2**, 544–551; (b) M. Seki and Y. Takahashi, *Synthesis*, 2021, **53**, 2689–2692.
- 17 H. M. Begam, R. Choudhury, A. Behera and R. Jana, *Org. Lett.*, 2019, **21**, 4651–4656.
- 18 B. K. Singh, A. Polley and R. Jana, *J. Org. Chem.*, 2016, **81**, 4295–4303.
- 19 (a) G. Brasche and S. L. Buchwald, *Angew. Chem., Int. Ed.*, 2008, **47**, 1932–1934; (b) S. Ueda and H. Nagasawa, *Angew. Chem., Int. Ed.*, 2008, **47**, 6411–6413.
- 20 (a) C. Zu, T. Zhang, F. Yang, Y. Wu and Y. Wu, *J. Org. Chem.*, 2020, **85**, 12777–12784; (b) S. Pradhan, P. B. De and T. Punniyamurthy, *J. Org. Chem.*, 2017, **82**, 4883–4890; (c) J. Xu, K. Du, J. Shen, C. Shen, K. Chai and P. Zhang, *ChemCatChem*, 2018, **10**, 3675–3679.
- 21 (a) J. Roane and O. Daugulis, *J. Am. Chem. Soc.*, 2016, **138**, 4601–4607; (b) H. Kim and S. Chang, *ACS Catal.*, 2015, **5**, 6665–6669; (c) P. Patel and S. Chang, *Org. Lett.*, 2014, **16**, 3328–3331; (d) K.-H. Ng, Z. Zhou and W.-Y. Yu, *Chem. Commun.*, 2013, **49**, 7031–7033; (e) Y. Xue, Z. Fan, X. Jiang, K. Wu, M. Wang, C. Ding, Q. Yao and A. Zhang, *Eur. J. Org. Chem.*, 2014, **2014**, 7481–7488; (f) K. Wu, Z. Fan, Y. Xue, Q. Yao and A. Zhang, *Org. Lett.*, 2014, **16**, 42–45.
- 22 (a) D. Mondal, S. Biswas, A. Paul and S. Baitalik, *Inorg. Chem.*, 2017, **56**, 7624–7641; (b) A. Klapars, K. R. Campos, J. H. Waldman, D. Zewge, P. G. Dormer and C.-y. Chen, *J. Org. Chem.*, 2008, **73**, 4986–4993.
- 23 (a) P. W. Tan, A. M. Mak, M. B. Sullivan, D. J. Dixon and J. Seayad, *Angew. Chem., Int. Ed.*, 2017, **56**, 16550–16554; (b) T. Yamauchi, F. Shibahara and T. Murai, *Org. Lett.*, 2015, **17**, 5392–5395; (c) K.-X. Tang, C.-M. Wang, T.-H. Gao, C. Pan and L.-P. Sun, *Org. Chem. Front.*, 2017, **4**, 2167–2169; (d) Y.-H. Liu, P.-X. Li, Q.-J. Yao, Z.-Z. Zhang, D.-Y. Huang, M. D. Le, H. Song, L. Liu and B.-F. Shi, *Org. Lett.*, 2019, **21**, 1895–1899; (e) R.-H. Liu, Q.-C. Shan, X.-H. Hu and T.-P. Loh, *Chem. Commun.*, 2019, **55**, 5519–5522; (f) Z.-Z. Zhang, G. Liao, H.-M. Chen and B.-F. Shi, *Org. Lett.*, 2021, **23**, 2626–2631; (g) Z.-J. Cai, C.-X. Liu, Q. Wang, Q. Gu and S.-L. You, *Nat. Commun.*, 2019, **10**, 4168; (h) A. T. Tran and J.-Q. Yu, *Angew. Chem., Int. Ed.*, 2017, **56**, 10530–10534; (i) A. Modi, P. Sau, N. Chakraborty and B. K. Patel, *Adv. Synth. Catal.*, 2019, **361**, 1368–1375; (j) F. Shibahara, Y. Asai and T. Murai, *Asian J. Org. Chem.*, 2018, **7**, 1323–1326; (k) S. R. Yetra, Z. Shen, H. Wang and L. Ackermann, *Beilstein J. Org. Chem.*, 2018, **14**, 1546–1553.
- 24 (a) K. P. Kepp, *Inorg. Chem.*, 2016, **55**, 9461–9470; (b) K. Sandeep, A. Siva Reddy and K. C. Kumara Swamy, *Org. Biomol. Chem.*, 2019, **17**, 6880–6894; (c) S. N. M. Boddapati, R. Tamminana, R. K. Gollapudi, S. Nurbasha, M. E. Assal, O. Alduhaish, M. R. H. Siddiqui, H. B. Bollikolla and S. F. Adil, *Molecules*, 2020, **25**, 1788.
- 25 (a) B. Chen, X.-L. Hou, Y.-X. Li and Y.-D. Wu, *J. Am. Chem. Soc.*, 2011, **133**, 7668–7671; (b) R. J. Phipps and M. J. Gaunt, *Science*, 2009, **323**, 1593–1597; (c) X. Ribas, C. Calle, A. Poater, A. Casitas, L. Gómez, R. Xifra, T. Parella, J. Benet-Buchholz, A. Schweiger, G. Mitrikas, M. Solà, A. Llobet and T. D. P. Stack, *J. Am. Chem. Soc.*, 2010, **132**, 12299–12306; (d) A. E. King, L. M. Huffman, A. Casitas, M. Costas, X. Ribas and S. S. Stahl, *J. Am. Chem. Soc.*, 2010, **132**, 12068–12073.
- 26 X.-G. Liu, H. Gao, S.-S. Zhang, Q. Li and H. Wang, *ACS Catal.*, 2017, **7**, 5078–5086.
- 27 C.-Q. Wang, Y. Zhang and C. Feng, *Angew. Chem., Int. Ed.*, 2017, **56**, 14918–14922.
- 28 J. Yang and G. B. Dudley, *J. Org. Chem.*, 2009, **74**, 7998–8000.
- 29 K. C. Nicolaou, D. G. McGarry, P. K. Somers, C. A. Veale and G. T. Furst, *J. Am. Chem. Soc.*, 1987, **109**, 2504–2506.
- 30 V. Smout, A. Peschiulli, S. Verbeeck, E. A. Mitchell, W. Herrebout, P. Bultinck, C. M. L. Vande Velde, D. Berthelot, L. Meerpoel and B. U. W. Maes, *J. Org. Chem.*, 2013, **78**, 9803–9814.

